On the Production, Assessment and Usage of Data in Microplastics Research

Kumulative Dissertation

zur Erlangung des Akademischen Grades

Doctor rerum naturalium (Dr. rer. nat.)

der Mathematisch-Naturwissenschaftlichen Fakultät

der Universität Rostock

Robin Lenz, 0000-0003-4156-7380

2025-08-14

https://doi.org/10.18453/rosdok_id00005704


Dieses Werk ist lizenziert unter einer
Creative Commons Namensnennung 4.0 International Lizenz.

"Sometimes, the fastest way to get there is to go slow."

— Tina Dickow

Note

A digital version of this thesis
including supporting information
is available in the accompanying
repository which you can find at
https://doi.org/10.5281/zenodo.15531255.



Supervised by: Prof. Dr. Matthias Labrenz

Reviewers:
Prof. Dr. Matthias Labrenz, University of Rostock;
Prof. Dr. Sonja Herres-Pawlis, RWTH Aachen University

Date of submission: August 14, 2025

Date of defense: November 21, 2025

Table of contents

Summary **1**

Zusammenfassung **3**

List of publications **5**

Synopsis **7**
Preface . . . 7
Introduction and an Appetiser for Microplastics Data Science . . . 9
Existing Knowledge, Gaps and Research Objectives . . . 13
Act I: Producing Data . . . 16
Act II: Assessing Data . . . 18
Act III: Using Data . . . 23
Conclusions and Outlook: Towards FAIRer Microplastics Data . . . 26

References **29**

Publications **45**
Microplastic exposure studies should be environmentally realistic . . . 46
Extraction of microplastic from biota: recommended acidic digestion destroys common plastic polymers . . . 50
Small Microplastic Sampling in Water: Development of an Encapsulated Filtration Device 58
When every particle matters: A QuEChERS approach to extract microplastics from environmental samples . . . 68
High-Throughput Analyses of Microplastic Samples Using Fourier Transform Infrared and Raman Spectrometry . . . 90
A Synthesis of Marine Monitoring Methods With the Potential to Enhance the Status Assessment of the Baltic Sea . . . 105
Combined Approaches to Predict Microplastic Emissions Within an Urbanized Estuary (Warnow, Southwestern Baltic Sea) . . . 123
Identification and quantification of microplastic particles in drinking water treatment sludge as an integrative approach to determine microplastic abundance in a freshwater river . . . 140
Measuring impacts of microplastic treatments via image recognition on immobilised particles below 100 µm . . . 150
A Public Database for Microplastics in the Environment . . . 173
MPX_specDB: MicroPlastiX Spectra Database . . . 190
What Goes Around Should Not Move Around: Immobilizing Microplastics as a New Approach for Analytical Ring Trials . . . 195
Mapping the plastic legacy: Machine-learning enabled microplastic inventory prediction in aquatic sedimentary systems . . . 208

Appendix **239**
Acknowledgements 239
Use of Tools 241
Declaration of Authenticity 243

Summary

Microplastics. Small, inconspicuous particles, basically the dust remaining when plastics fall apart into micron-sized pieces. They embody the remarkable contradiction of the chemical inertness of their poorly degradable macromolecular chains on the one hand, and their perception as a danger to the environment and health, as a chemical cocktail or physical hazard on the other. For about a century, synthetic polymer materials have been on the path to becoming one of the defining drivers of modern civilisation, but it is only in the last two decades that their fragmentation into microparticles and persistence in anthropogenic and natural environments has received attention, making it a dominant topic in environmental sciences and other disciplines. The publications on which this work is based have in common that they extend the methodology of microplastic research. Constant improvement on how microplastics data can be made more useful and accessible is a recurring theme that has motivated much of my work. This is demonstrated in several publications, which emphasise it as a central aspect of the research methodology in order to effectively address this pollutant through data- and knowledge-based decisions. The way to get there means to go through all steps, or acts, required to further our knowledge about microplastics.

In **Act I** (*Producing Data*), I include a study presenting a suspended solids sampler designed to operate well in surface water field campaigns for particles in the lower micron range. We put special emphasis on avoiding sample contamination due to wear of device components or airborne particles. The device features a closed setup and filtration in suction mode, with particles being retained on stainless steel filters before the water passes the pump. Reverse flushing enables the assembled system to be evacuated ahead of sampling. For example, when using 10 µm filters, depending on the suspended matter content in the water, between 100 and 2000 litres can be sampled before a filter change is necessary. A second study presents a collection of modular laboratory protocols for purifying different types of sample material, and serves as a practical decision guide for choosing an appropriate method of separating microplastics from a given matrix. The actual identification and quantification of microplastics, covered by a third study, requires us to be able to locate and measure sometimes hundreds of thousands of particles in a set of samples. The automation of these processes is reflected in the development of a software suite for the microspectroscopic analysis of microplastics.

Act II (*Assessing Data*) focuses on how we can assess and validate the quality of the data produced. Testing the effects of purification protocols on plastics in different size ranges provides insights for secure method application. For larger plastic pieces such investigations are shown using simple experimental setups. However, observing potential changes in the smallest particle fractions (< 100 µm) required the development of new particle immobilisation techniques. The presented method enables comparisons to be made before and after treatment, thus allowing treatment effects on individual particles in the lower micron range to be tracked. Nevertheless, certain limitations of the microscopy-based comparisons remain, which are discussed. A later adaptation of the immobilisation concept is presented for use in an interlaboratory comparison study, in which all participants analyse the same set of immobilised microplastics using their own microspectroscopic

methods. Looking at the variance in particle numbers reported in this serial study design provides a better estimate of specific analytical uncertainties than in the established parallel design, where each participant analyses their own sample specimen, meaning that uncertainties introduced during specimen creation propagate into the results. Finally, an important aspect of data assessment is data management. A relational database scheme is presented that allows microplastics data to be stored in a structured way. Using such a database facilitates the organisation of data inputs and outputs and can be used to enforce data integrity. An instance of the proposed database has been used to store and retrieve particle-related data in the publications of the following and last act.

As data is not yet knowledge, **Act III** (*Using Data*) comprises studies that made use of the outputs from the previous two acts to generate higher-level insights into specific research questions. The first study is a compilation of marine monitoring methods that can improve the assessment of the Baltic Sea's environmental status. It recommends the proposed water sampling device and protocol for sampling microplastics < 300 µm in the upper water layers. Next, with a more local focus on the Baltic estuary of the Warnow river, microplastics are explored in the context of urbanised emission scenarios. Microplastic particle concentrations obtained from a catchment field sampling campaign serve as a reference for microplastic inputs into the estuary and are estimated as the largest source contributing about half of the estuarine discharged microplastics, followed by around 40% from urban stormwater runoff, and minor urban sources of combined sewer overflows and waster water treatment effluents, both well below 10%. The same *in situ* sampling data is then used in another study to calibrate a novel quantification approach involving sludge from a local drinking water treatment plant. Where drinking water is produced from surface water, we hypothesised that the sludge from precipitated suspended solids could be utilised to sample and quantify particulate pollutant loads of the supplying water body. A proof-of-concept study showed that the estimated riverine microplastic particle concentrations did not differ significantly between the two techniques, suggesting the sludge approach as a viable alternative to direct sampling, enabling time-integrated routine monitoring. Shifting focus to another Baltic estuary, microplastics in surface sediments of the Schlei were investigated in the wake of a major pollution event. This study demonstrates how a small precursory microplastics dataset of 26 stations can be used for distribution mapping and estimation of particle- and mass-based inventories. It does so by utilising easier-to-obtain proxy data, such as sediment grain size and hydrodynamic parameters, in empirical predictive modelling. A machine learning pipeline, developed for the typically small sample numbers of microplastics studies, facilitates a data-driven integration of model selection, training and validation, yielding a geospatial regression model with known performance of prediction on unseen data. We show that a simple extrapolation of microplastic concentrations without the granulometric normalisation, which forms the theoretical basis of the model, can lead to substantial over- or underestimation of microplastic inventories.

Zusammenfassung

Mikroplastik. Kleine, unscheinbare Partikel, im Grunde der Staub, der bleibt, wenn Kunststoffe in mikroskopisch kleine Stücke zerfallen. Sie verkörpern den bemerkenswerten Widerspruch zwischen der chemischen Inertheit ihrer schwer abbaubaren makromolekularen Ketten einerseits und ihrer Wahrnehmung als Gefahr für Umwelt und Gesundheit, als Chemiecocktail oder physische Gefahr andererseits. Seit etwa einem Jahrhundert sind synthetische polymere Materialien auf dem Weg, zu einem der bestimmenden Treiber der modernen Zivilisation zu werden, aber erst in den letzten zwei Jahrzehnten wurde ihrer Fragmentierung in Mikropartikel und ihrer Persistenz in der anthropogenen und natürlichen Umwelt Aufmerksamkeit geschenkt, wodurch sie zu einem beherrschenden Thema der Umweltwissenschaften und anderer Disziplinen wurden. Die Veröffentlichungen, auf denen diese Arbeit basiert, haben gemeinsam, dass sie die Methodik der Mikroplastikforschung erweitern. Die ständige Verbesserung der Möglichkeiten, Mikroplastikdaten nützlicher und zugänglicher zu machen, ist dabei ein wiederkehrendes Thema, das einen Großteil meiner Arbeit motiviert hat. In mehreren Veröffentlichungen wird dies als zentraler Aspekt der Forschungsmethodik hervorgehoben, mit dem Ziel, dass durch daten- und wissensbasierte Entscheidungen wirksamer gegen diese Schadstoffe vorgegangen werden kann. Der Weg dorthin bedeutet, die Schritte ("Acts") zu unternehmen, die erforderlich sind, um unser Wissen über Mikroplastik zu erweitern.

In **Act I** (*Datenproduktion*) stelle ich zunächst eine Studie vor, in der ein Probenahmegerät für suspendierte Feststoffe beschrieben wird, das für Feldkampagnen in Oberflächengewässern für Partikel im unteren Mikrometerbereich gut geeignet ist. Besonderen Wert haben wir darauf gelegt, dass die Proben nicht durch den Verschleiß von Gerätekomponenten oder durch Partikel in der Luft verunreinigt werden können. Das Gerät verfügt daher über einen geschlossenen Aufbau und Filtration im Ansaugmodus, wobei die Partikel auf Edelstahlfiltern zurückgehalten werden, bevor das Wasser die Pumpe passiert. Durch Umkehrspülung kann das zusammengesetzte System vor der Probenahme evakuiert werden. Es lassen sich so, zum Beispiel bei Einsatz von 10 µm Filtern, je nach Schwebstoffgehalt im Wasser circa zwischen 100 und 2000 Litern beproben, bevor ein Filterwechsel notwendig ist. Eine zweite Studie stellt eine Sammlung von modularen Laborprotokollen für die Aufreinigung verschiedener Arten von Probenmaterial vor und dient als praktische Entscheidungshilfe für die Wahl einer geeigneten Methode zur Abtrennung von Mikroplastik aus einer bestimmten Matrix. Die eigentliche Identifizierung und Quantifizierung von Mikroplastik, die in einer dritten Studie behandelt wird, setzt voraus, dass wir in der Lage sind, mitunter Hunderttausende von Partikeln in einer Reihe von Proben zu lokalisieren und zu messen. Die Automatisierung dieser Prozesse spiegelt sich in der Entwicklung einer Software-Suite für die mikrospektroskopische Analyse von Mikroplastik wider.

Das Kapitel **Act II** (*Datenbewertung*) konzentriert sich darauf, wie wir die Qualität der erzeugten Daten einschätzen und validieren können. So liefert die Prüfung der Auswirkungen von Aufreinigungsprotokollen auf Kunststoffe in verschiedenen Größenbereichen Erkenntnisse für eine sichere Anwendung der Methoden. Während solche Untersuchungen für größere Plastikstücke in einfachen experimentellen Ansätzen durchführbar sind, erfordert die Beobachtung möglicher Veränderungen in

den kleinsten Partikelfraktionen (< 100 µm) jedoch die Entwicklung neuer Partikelimmobilisierungstechniken. Die vorgestellte Methode ermöglicht Vergleiche der Partikelzustände vor und nach der Behandlung, so dass Auswirkungen auf einzelne Partikel im unteren Mikrometerbereich verfolgt werden können. Dennoch bleiben bestimmte Einschränkungen der auf Mikroskopie basierenden Vergleiche bestehen, die diskutiert werden. Eine spätere Anpassung des Immobilisierungskonzepts wird für die Verwendung in einer Ringversuchsstudie vorgestellt, bei der alle Teilnehmer denselben Satz immobilisierter Mikroplastikpartikel mit ihren eigenen mikrospektroskopischen Methoden analysieren. Die Betrachtung der Varianz der Partikelzahlen, die in diesem seriellen Studiendesign berichtet werden, ermöglicht eine bessere Abschätzung der spezifischen analytischen Unsicherheiten als im etablierten parallelen Design, bei dem jeder Teilnehmer seine eigene Probe analysiert, was bedeutet, dass sich Unsicherheiten, die bei der Probenherstellung eingeführt werden, in den Ergebnissen niederschlagen. Zuletzt wird das Management von Mikroplastik-Forschungsdaten als ein wichtiger Aspekt der Datenbewertung thematisiert. Es wird ein relationales Datenbankschema vorgestellt, mit dem Mikroplastikdaten strukturiert gespeichert werden können. Die Verwendung einer solchen Datenbank erleichtert die Organisation von Dateneingaben und -ausgaben und kann zur Sicherstellung von Datenintegrität verwendet werden. Eine Instanz der vorgeschlagenen Datenbank wurde verwendet, um partikelbezogene Daten in den Veröffentlichungen des folgenden und letzten Kapitels zu speichern und abzurufen.

Da Daten an sich noch kein Wissen sind, umfasst **Act III** (*Datennutzung*) nun Studien, in denen die Ergebnisse der beiden vorangegangenen Kapitel genutzt werden, um übergeordnete Erkenntnisse zu spezifischen Forschungsfragen zu gewinnen. Die erste Studie ist eine Zusammenstellung von marinen Monitoringmethoden, die die Bewertung des Umweltzustands der Ostsee verbessern können. Sie empfiehlt das vorgeschlagene Wasserprobenahmegerät und -protokoll als Methode für die Probenahme von kleinem Mikroplastik. Als nächstes wird Mikroplastik im Zusammenhang mit urbanen Emissionsszenarien am Beispiel der Warnow bei Rostock untersucht. Mikroplastikkonzentrationen, die aus einer Probennahmekampagne im Einzugsgebiet gewonnen wurden, dienen als Referenz für den Eintrag von Mikroplastik in das Ästuar dar. Diese Eintragsart macht etwa die Hälfte des ästuaren Mikroplastiks aus. Etwa 40% entstammen der städtischen Regenentwässerung, gefolgt von kleineren städtischen Quellen wie Mischwasserüberläufen und der Einleitung geklärter Abwässer, die beide deutlich unter 10% liegen. Dieselben *in situ* Mikroplastikkonzentrationsdaten werden dann in einer weiteren Studie zur Kalibrierung eines neuartigen Quantifizierungsansatzes unter Verwendung von Fällungsschlamm einer örtlichen Trinkwasseraufbereitungsanlage eingesetzt. Die Hypothese war, dass der abgetrennte Schlamm der Trinkwassergewinnung aus Oberflächenwasser zur Beprobung und Quantifizierung partikulärer Schadstofffrachten des speisenden Wasserkörpers verwendet werden kann. Eine Machbarkeitsuntersuchung zeigte, dass sich die ermittelten Mikroplastikkonzentrationen im Flusswasser zwischen den beiden Techniken nicht signifikant unterschieden, was darauf hindeutet, dass der Schlammansatz eine praktikable Alternative zur direkten Probennahme darstellt und dabei ein zeitlich integriertes Monitoring ermöglicht. Zuletzt wird der Fokus noch auf ein anderes Ostsee-Ästuar gelegt: Mikroplastik in den Oberflächensedimenten der Schlei wurde nach Bekanntwerden eines signifikanten Plastikeintrags untersucht. Diese Studie zeigt, wie ein kleiner Mikroplastikdatensatz von 26 Stationen für die Verteilungskartierung von Mikroplastik sowie die Abschätzung von partikel- und massenbasierten systemweiten Inventaren eingesetzt werden kann. Dies geschieht durch die Verwendung von leichter zu ermittelnden Proxydaten wie Sedimentkorngrößenverteilungen und hydrodynamischen Parametern in empirischen Modellen. Der Einsatz bestimmter Techniken aus dem Bereich des maschinellen Lernens wird zur Entwicklung einer Modellierungs-Pipeline genutzt, die für die typischerweise kleinen Stichprobenzahlen in Mikroplastikstudien optimiert ist. Sie erleichtert eine datengesteuerte Integration von Modellauswahl, Training und Validierung, wobei ein Regressionsensemble erstellt wird, dessen realistische Vorhersagegüte abgeschätzt werden kann. Wir zeigen, dass eine einfache Extrapolation von Mikroplastikkonzentrationen ohne die granulometrische Normalisierung, die die theoretische Grundlage des Modells bildet, zu einer erheblichen Über- oder Unterschätzung von Mikroplastikbeständen führen kann.

List of publications

This cumulative dissertation comprises ten research articles, one submitted manuscript, one letter and one dataset publication, which are listed here in chronological order. Each publication includes a cover page stating how I and others contributed to the work. There, I provide quantitative estimates of my shares in the 'contributed work' (e.g. writing the paper, data analysis and visualisation) and the 'intellectual contribution' (e.g. idea generation, conceptualisation and methodology).

- [1]: Lenz R, Enders K, Nielsen TG (2016) Microplastic exposure studies should be environmentally realistic. Proceedings of the National Academy of Sciences 113(29):E4121–E4122. DOI: 10.1073/pnas.1606615113
- [2]: Enders K, Lenz R, Beer S, Stedmon CA (2017) Extraction of microplastic from biota: Recommended acidic digestion destroys common plastic polymers. ICES Journal of Marine Science 74:326–331. DOI: 10.1093/icesjms/fsw173
- [3]: Lenz R, Labrenz M (2018) Small Microplastic Sampling in Water: Development of an Encapsulated Filtration Device. Water 10(8):1055. DOI: 10.3390/w10081055
- [4]: Brandt J, Bittrich L, Fischer F, Kanaki E, Tagg A, Lenz R, Labrenz M, Brandes E, Fischer D, Eichhorn K-J (2020) High-Throughput Analyses of Microplastic Samples Using Fourier Transform Infrared and Raman Spectrometry. Applied Spectroscopy 74(9):1185–1197. DOI: 10.1177/0003702820932926
- [5]: Enders K, Lenz R, Ivar do Sul JA, Tagg AS, Labrenz M (2020) When every particle matters: A QuEChERS approach to extract microplastics from environmental samples. MethodsX 7:100784. DOI: 10.1016/j.mex.2020.100784
- [6]: Mack L, Attila J, Aylagas E, Beermann A, Borja A, Hering D, Kahlert M, Leese F, Lenz R, Lehtiniemi M, Liess A, Lips U, Mattila O-P, Meissner K, Pyhälahti T, Setälä O, Strehse JS, Uusitalo L, Wranne AW, Birk S (2020) A Synthesis of Marine Monitoring Methods With the Potential to Enhance the Status Assessment of the Baltic Sea. Frontiers in Marine Science 7. DOI: 10.3389/fmars.2020.552047
- [7]: Piehl S, Hauk R, Robbe E, Richter B, Kachholz F, Schilling J, Lenz R, Fischer D, Fischer F, Labrenz M, Schernewski G (2021) Combined Approaches to Predict Microplastic Emissions Within an Urbanized Estuary (Warnow, Southwestern Baltic Sea). Frontiers in Environmental Science 9. DOI: 10.3389/fenvs.2021.616765
- [8]: Siegel H, Fischer F, Lenz R, Fischer D, Jekel M, Labrenz M (2021) Identification and quantification of microplastic particles in drinking water treatment sludge as an integrative approach to determine microplastic abundance in a freshwater river. Environmental Pollution 286:117524. DOI: 10.1016/j.envpol.2021.117524
- [9]: Lenz R, Enders K, Fischer F, Brandt J, Fischer D, Labrenz M (2021) Measuring impacts of microplastic treatments via image recognition on immobilised particles below 100 µm. Microplastics and Nanoplastics 1(1):12. DOI: 10.1186/s43591-021-00012-0
- [10]: Čerkasova N, Enders K, Lenz R, Oberbeckmann S, Brandt J, Fischer D, Fischer F, Labrenz M, Schernewski G (2023) A Public Database for Microplastics in the Environment. Microplastics 2(1):132–146. DOI: 10.3390/microplastics2010010

- [11]: Lenz R, Fischer F, Arnold M, Fernández-González V, Moscoso Pérez CM, Andrade-Garda JM, Muniategui-Lorenzo S, Fischer D (2023) MPX_specDB: MicroPlastiX Spectra Database. DOI for code: 10.5281/zenodo.8314801. DOI for dataset: 10.22000/1820
- [12]: Lenz R, Enders K, Vizsolyi ÉC, Schumacher M, Lötsch J, Löder MGJ, Eder G, Voronko Y, Andrade-Garda JM, Muniategui-Lorenzo SN, Laforsch C, Fischer D, Labrenz M (2024) What Goes Around Should Not Move Around: Immobilizing Microplastics as a New Approach for Analytical Ring Trials. Environmental Science & Technology. DOI: 10.1021/acs.est.4c09427
- [13]: Enders K, Lenz R, Fischer F, Schwarzer K, Seiß G, Labrenz M (2025 (expected)) Mapping the plastic legacy: Machine-learning enabled microplastic inventory prediction in aquatic sedimentary systems. [submitted manuscript].

The following publications on related topics are not part of this thesis, because they are earlier works [part of a previous thesis 14, 15] or later works [16]:

- [14]: Lenz R, Enders K, Stedmon CA, Mackenzie DMA, Nielsen TG (2015) A Critical Assessment of Visual Identification of Marine Microplastic Using Raman Spectroscopy for Analysis Improvement. Marine Pollution Bulletin 100(1):82–91. DOI: 10.1016/j.marpolbul.2015.09.026
- [15]: Enders K, Lenz R, Stedmon CA, Nielsen TG (2015) Abundance, Size and Polymer Composition of Marine Microplastics 10 µm in the Atlantic Ocean and Their Modelled Vertical Distribution. Marine Pollution Bulletin 100(1):70–81. DOI: 10.1016/j.marpolbul.2015.09.027
- [16]: Maitz M, Lenz R, Winkler S, Abschke M, Werner C, Fischer D (2025) Weathered Microplastics in Human Blood: Unraveling the Effect of Structural Changes at the Particle Surface on Coagulation and Platelet Activation. Microplastics and Nanoplastics [accepted]. DOI: 10.1186/s43591-025-00139-4.

Synopsis

Preface

Around 10 years ago I started my research in microplastics pollution, while, at the same time, the topic started gaining momentum both scientifically as well as in the broader public. There is a growing awareness that substantial fractions of these materials are getting outside of our control and continuously infiltrate our microparticulate surroundings. Thus, they return to us with the air we breath, the water we drink and the food we eat. It evokes the feeling of a diffuse intangible threat without the ability to know the actual risk involved due to an information deficit. While obvious for microplastics, this equally pertains to the plastic items that we use in virtually any aspect of today's civilisation.

Note

I will use text blocks of indented italic style like the one below in several places of this thesis when I want to share some personal ponderings. For me, it makes the document more lively, thought-provoking and engaging, I hope for you too. Feel free to skip them if you enjoy the crisp dryness of classical scholarly prose.
Further, I will use callout boxes like this one (blue) for small topical excursions or to provide capsuled information about a specific aspect.

So how does this information deficit feels like in daily life? Maybe some of these questions sound familiar?

Should I be flipping my pancakes with that black plastic spatula?[1]

Drinking from a plastic bottle surely won't hurt me. Also not if I refill it a few times, right? Or when I use it for hot tea? Or when I leave out in the sun? But if I do it every day for my whole life??

And what is actually in that soft plastic baby toy my child is chewing on? It was not made for food contact, but clearly children will put it in their mouths anyway, so surely someone thought about that before making it! Or not?

[1] [17] got me thinking, however, looking at their corrigendum [18], there has apparently been a calculation error in the study and the actual risk would be lower…

***Another Note:* This thesis is cumulative**

As this is a cumulative thesis, I shall cover all included publications, their contributions, and the overarching narrative that connects them. At the same time, it is probably overzealous to repeat content already included in the publications, their introductions, discussions, etc. Each of them is presented in the synopsis with a callout box like this one (green) that summarises some key points, shows a small representative graphical teaser and, most importantly, provides the perspective of why the study was conducted. For any other details, there is a link to the publication itself.

I believe our increased interest in this topic is fuelled by the upcoming notion that we intimately surround ourselves with materials incompatible to the natural cycles within us and within the environment. So what are the consequences? Well, the 'natural cycles inside us' is what our body maintains throughout its life and what we generally refer to as 'health'. The 'natural cycles within the environment' is what we rely on to provide us with the resources we need. Today, many experience a more or less conscious perception [19], that these materials contain chemical compounds of toxic, endocrine-disruptive or otherwise undesirable effects which are not brought to our attention, e.g. due to intentional producer secrecy [20, 21]. However, this perception is opposed by a decades long legacy of more light-hearted plastic use, encouraged by an empirical collective cognition that applying an out-of-sight-out-of-mind mentality to plastics has usually had no directly observable or attributable adverse effects within the expended span of attention. Now, our trust in these legacy beliefs is more and more eroded by the growing awareness, perhaps supported by upsettingly realising how much time passed since the commence of plastic mass production with little to no attention given to potential long-term effects on human health and wildlife.

Coming back to the questions I posed above, I assume that being able to raise these concerns is a privilege that many around the world do not share. Many face more immediate and pressing problems. If the answers to such questions suggest threats, then the unequal privilege to address them is a fundamental concern in itself.

Being privileged is motivation and obligation alike. I appreciate the initiative and efforts in the development of a United Nations Plastic Treaty as a legal framework to counter the global issue of plastic pollution, despite its challenges and the long time it takes to reach even small steps on draft agreements [22–26]. As researchers, I believe, we can make our best contribution by ensuring that the evidence we provide is meaningful, comparable, and accessible. By viewing all stages of knowledge generation from a data-oriented perspective - from theory and experimental design to methods and interpretations - and applying FAIR data principles [27] throughout, we can enhance the impact of our work. This thesis therefore centres on these data-oriented aspects, outlining the tangible contributions of the constituent publications to producing, assessing, and using microplastics data. The 'A' in FAIR stands for Accessibility, which is not just technical availability. As you probably notice, I deviate here from the traditional writing style of a thesis. I do so because the choice of language is an important part of accessibility. While the included papers may cover niche topics and technical details, I aim to make this synopsis an approachable and interesting read.

> *Ought a thesis to include a preface? This one does and I hope it helps to guide through the remainder of the synopsis.*

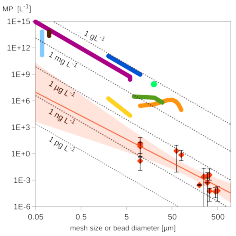
Introduction and an Appetiser for Microplastics Data Science

'Microplastics' is a term used to describe plastic particles in the context of them being a pollution or health concern [28]. Commonly, it includes any particulate matter, insoluble in water and of synthetic polymeric origin with a size in the lower millimetre to micrometre range. For historic reasons 5 mm is often used as a upper size limit, although many studies use 1000 µm. The lower size limit is usually dictated by the capabilities of the analytical methods employed often ranging from 500 µm to 1 µm, below which the term 'nanoplastics' is used. However, such size-based delimitations do not translate well into reality where microplastic particles are highly irregular and malleable. After all, we are observing objects under continuous fragmenting and reaggregating processes.

> *A 5 mm bead used for plastic moulding is a microplastic. But a 6 mm long and 10 µm thin fibre [29] from my fleece blanket is not?*
>
> *The same fibre might be tangled into a 100 µm ball. So is it a microplastic now?*

The issue of particle size is not only a semantic one. It has direct implication to the choice of methods and level of control required for the analysis. It is a central topic for several of the publications included in this thesis, e.g. aiming to develop methods, data collection and reporting practices that mind the requirements of specific microplastic size fractions.

***Letter:* Microplastic exposure studies should be environmentally realistic**



In a brief communication letter [1], we pondered about the apparent mismatch in particle sizes and concentrations between environmental surveys and laboratory studies. We compared studies of both types, i.e. those that sampled and quantified microplastics in the environment and those that exposed different kinds of organisms to microplastics, in a common log-scaled visualisation of particle concentration against size, revealing that over large parts of the size spectrum, concentrations used in laboratory exposures were 2 to 7 orders of magnitude above those found in the environment [1]. The argument that exposures should be environmentally realistic has since been frequently taken up [30]. It is a reminder that the comparability of studies is not only a matter of method harmonisation, but also of the ecological relevance of the data produced.

Go to publication: page 46.

At the time we published this, there was a astounding offset in the concentrations and size ranges of microplastics used in laboratory exposure studies compared to those found in environmental surveys. Despite having been published only as a brief response letter to a previous publication [31], our observation attracted considerable attention, even becoming the most cited letter of PNAS to date.[2] With such a reception, a follow-up investigation appears to be an interesting endeavour to see if and how the situation has changed. I started revisiting the original dataset aiming to extend it to include studies which referenced our letter. The journey evolved into a compelling case exemplifying the need of "FAIRer" data management practices in microplastics research, which is why I find it useful to share it here.

[2] https://www.pnas.org/action/doSearch?field1=AllField&text1=&ConceptID%5B%5D=500101&ConceptID=&publication%5B%5D=pnas&publication=&Ppub=&access=on&sortBy=cited

Revisiting the original papers revealed several inconsistencies in the data presented in our letter. These ranged from unit conversion errors (using diameter instead of radius for several studies [32–34]), citation mistakes, to incomplete concentration values. For instance, we incorrectly reported 100 nm beads for a study that had actually used 27.6 nm beads [33], and citation errors incorrectly referenced Besseling et al. 2012 [35] and [36] instead of Wegner et al. 2012 [33] and [37], respectively. For some studies we reported incomplete or wrong concentration values [32, 38, 39], while others were referenced in the text but missing from the figure [40].

Interestingly, despite being cited around 600 times, these errors seem to have remained undetected by the scientific community. This observation raises important questions about scientific verification practices. The letter was published in a high-impact journal but, as a brief correspondence format, potentially underwent only limited rigor in peer-review which is not directly obvious to the reader. More critically, the data was not available in a machine-readable or FAIR format alongside the publication. Only figure annotations indicated the references for each data point. Verifying our findings would have required others to undertake the same tedious manual process of data extraction that we initially performed.

For the follow-up investigation, I systematically corrected these errors and extended the dataset. Using the OpenAlex.org API [41], I downloaded metadata of all papers citing our letter, manually categorised them as exposures, quantifications, or other studies, and extracted relevant data from a subset of these publications. This process remained highly manual and time-consuming, as data extraction required carefully reading method sections, results, supplementary information, and often performing calculations to standardise reported values. For exposure studies in particular, I frequently needed to calculate particle concentrations from reported mass concentrations and particle sizes and sometimes getting the required data necessitated direct correspondence with study authors. It is clear that this is impractical for several hundred studies, which is why, for the exposure studies (n=*358*), I set the focus to the most cited ones per quarter of the year and only considered exposures in aqueous environments or media (n=*35*). For quantification studies, I included all (n=*15*).

Collected impressions of the use of artificial intelligence tools in scientific literature work

Despite trying, I could not speed up the process of extracting data from the papers using general-purpose artificial intelligence tools like ChatGPT or domain-specific tools like ScienceOS, SciSpace, scite.ai, or ResearchRabbit. While these tools assisted data extraction to some degree, the necessity to read and understand each paper remains in order to verify if the correct data was extracted.

> *On a curious note, my assessment here seem consistent with voices from software engineering.*
> *There, the relevant output is the code, which gets deployed and may perform critical tasks in environments not controlled by the developer. A recent post highlights this [42].*[3]
> *In scientific writing, the relevant outputs are the manuscript, the data and the conclusions drawn from it. Therefore, the question of whether artificial intelligence tools can make a useful contribution to a certain scientific task is less about the tools' capabilities. Rather, it is about whether the resources needed to produce and verify the output can be reduced compared to the manual process. Current research on automation of systematic reviews in medical sciences, however, claims to achieve exactly that [43].*[4] *If rigorous peer-review indicates that these are indeed sensible results, it remains interesting to see if such tools will be meaningfully*

adaptable to other disciplines like environmental science where data and study formats are less standardised and more heterogeneous.

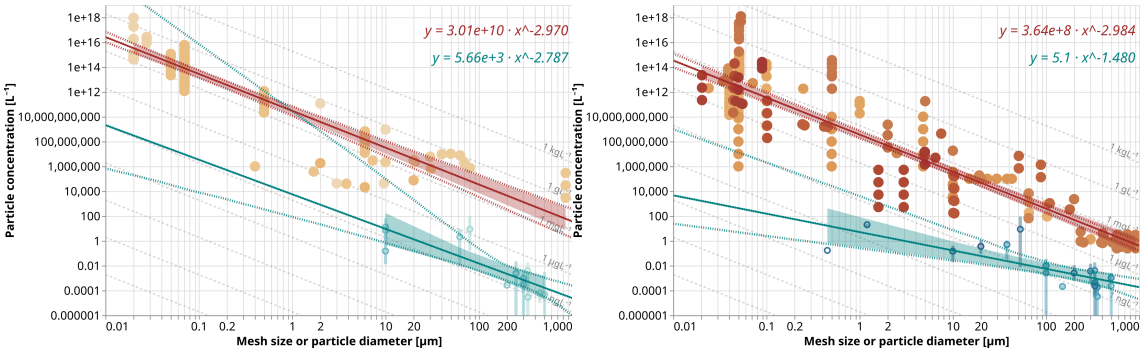
After a few experiments with these tools I resorted to manual data extraction, which was time-consuming but ultimately necessary to ensure accuracy.
In contrast, coding-related tasks in the writing process of this thesis were more successfully aided by tools such as ChatGPT or GitHub Copilot. I primarily used models from Anthropic (Sonnet-3.7-thinking or Sonnet-4), Google (Gemini-2.5-pro), or OpenAI (GPT-4o, GPT-4.1 or GPT-o3) for this purpose. A full documentation of the use of artificial intelligence and other tools in creation of this work is provided in the declaration on the use of tools (page 241) including referrals to the recorded conversations in the supplementary materials [44].

Also after correcting these errors, the fundamental conclusion of our original letter remains valid: there exists a substantial disconnect between the concentrations and size ranges used in laboratory exposure studies compared to those found in environmental surveys (Figure 1A). Studies referencing our letter are shown in Figure 1B (as available end of April 2025), while the combined dataset of all studies is shown in Figure 1C.

At a first glance, the reviewed studies in Figure 1 suggest no significant change in the offset between environmental and laboratory studies, when comparing the earlier studies Figure 1A with those that presumably valued the claim for more realistic exposure scenarios Figure 1B. However, the artificial limitation in this comparison (using only studies related to our letter) means that comprehensive conclusions on the realism in exposure studies in general cannot be drawn. It is an interesting observation, though, that the offset seems to remain similar despite the increased awareness of the issue. For a broader picture it would certainly be worthwhile to include studies that do not relate to our letter and ToMEx, a database on toxicity data for microplastics [103] may be an ideal basis for such an exploration. On a interesting note, there seems to be a few studies of the environmental quantifications type that used a sampling mesh in the mid to lower micron size range (around 40 µm to 80 µm), which show positively deviating concentrations compared to studies targeting smaller or larger particles. This can be observed in both the earlier Figure 1A and the later studies Figure 1B. It is unclear whether this is an artefact due to the low number of studies or a real effect, but it is worth investigating further.

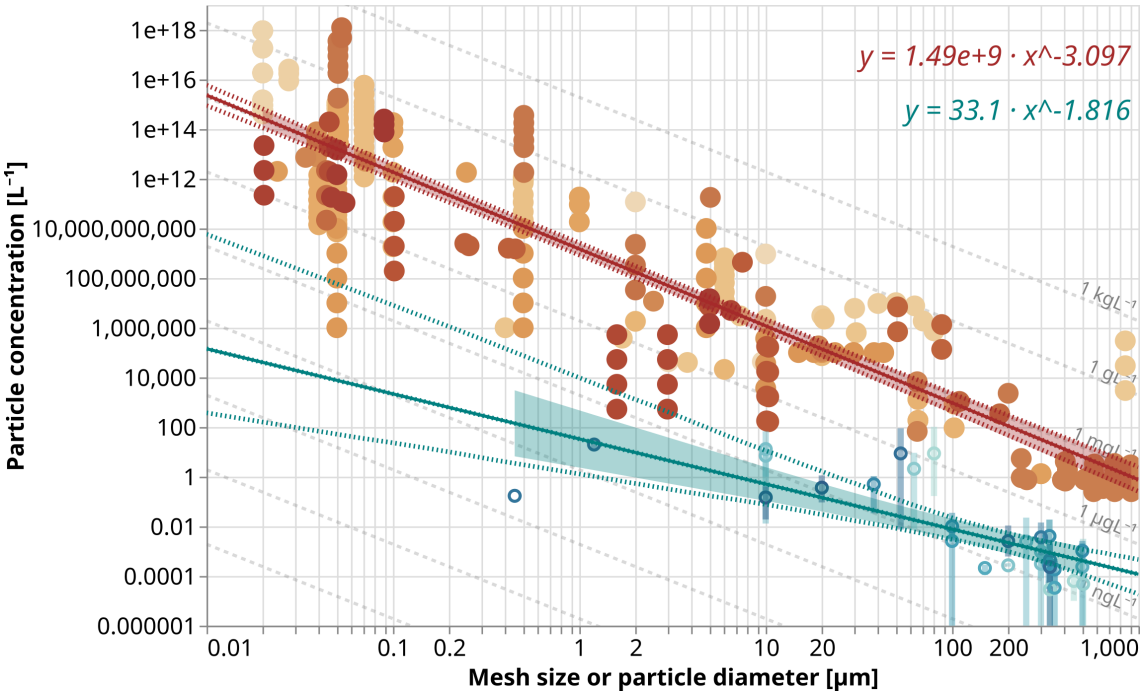
[3]Quote: "Even if we assume that AI coding tools are sophisticated enough (they are not) to fix issues in my projects with little or no supervision, I'm still the bottleneck because all that code has to be reviewed before it can be merged." [42].

[4]In a preprint [43], authors set up an evaluation setting for comparing reproduction of systematic reviews created either by a purpose-built framework using several large language models, a commercial tool or human researchers. They report superior performance of the framework in retrieval of relevant studies and extraction of data from them.



(A) Studies cited by [1]

(B) Studies citing [1]



(C) Cited & citing studies combined

Figure 1: Microplastic particle concentrations and sizes in a comparison of individual studies employing exposure experiments (brown tones) or quantitative environmental surveys (teal tones). Points are at particle size (particle diameter deployed for exposures, or sampling mesh size used for quantifications) and their respective particle concentrations, with same-colored points belonging to the same study. Solid lines show power-law regressions, while shaded areas and hatched lines are parametric and bootstrapped 95% confidence intervals (1000 iterations), respectively. Dashed grey isolines indicate equal mass concentrations for reference (assuming spherical particles with a density of 1 g/cm³). A) revisited data from the original dataset [1] including corrected values and missing studies: quantifications [15, 37, 45–51], exposures [31–35, 38–40, 52, 53]. B) new dataset with studies up to end of April 2025 that referenced the original letter: quantifications [54–68], exposures [63, 69–102]. C) combined dataset with all studies of A and B: quantifications [15, 37, 45–51, 54–68], exposures [31–35, 38–40, 52, 53, 63, 69–102].

Takeaways

Revisiting and extending the dataset highlights some crucial aspects of scientific data management:

1. **Data accessibility**: While our letter was not intended as a data paper, the fact that mistakes were not spotted demonstrates how important it is to make underlying data available in structured formats for every publication.
2. **Reproducibility and extensibility**: Data sharing facilitates not only verification but also the extension of previous work
3. **Reporting standards**: The heterogeneity in how microplastics data and metadata are reported creates unnecessary barriers to data integration and synthesis.
4. **Scientific verification**: The scientific community tends to trust published work, especially in high-impact journals. Without readily accessible data in standardised formats, post-publication verification becomes impractical.
5. **Future-proof reuse**: We cannot know in which ways our data might be used in the future, making comprehensive documentation essential from the outset.

Existing Knowledge, Gaps and Research Objectives

The field of microplastics research is characterised by a high degree of interdisciplinarity and a wide range of research questions. The comparability and reliability of studies are repeatedly questioned, and the need for standardisation and harmonisation of methods often gets emphasised in recent scientific literature and policy advice [104–106].

> *Sometimes, overly repeated calls for more standardisation leave me wondering what such a standard could look like. The diversity of methods in sample purification and analysis are an expression of the ongoing developmental effort.*

> *No single approach is able to sufficiently address the wide range of particle sizes and sample matrices encountered in microplastics research. So instead of having an insufficient standard, we seem better off with less standardised but better adaptable methods as long as the generated data is robust and well-documented: sufficient metadata makes methods traceable and raw data reusable.*

The frequent calls for more standardisation in microplastics research often stem from concerns about the quality and comparability of studies. However, instead of solely focusing on formal standardisation, we should also consider the adoption of FAIR data principles as a means to enhance data quality and accessibility. By prioritising deep documentation, open data formats, and reproducible workflows, we can create an environment where diverse methods can coexist while still allowing for robust data sharing and reuse.

While there is still significant room for improvement in the quality of data and reporting practices in much of the rapidly growing body of scientific literature on microplastics, there are also numerous studies that I find particularly inspiring in terms of introducing a more data-driven approach to microplastics research. These studies have successfully applied FAIR data principles, developed innovative data management practices and provided open-source software tools. They are leading examples of novel data analytical approaches that integrate data science thinking into existing microplastics analytical workflows. The following overview highlights some of these seminal studies that shape the current state of knowledge and influenced the field and the works presented in this thesis.

For instance, there is a growing number of databases providing structured access to various types of microplastics data. The NOAA NCEI marine microplastics database presents and provides access to microplastics abundance data [107]. Similarly, LITTERBASE provides a global viewer of marine litter and microlitter concentrations [108], compiled from a large number of studies. However, direct access to the underlying data is not available. The MP-SED database [109] and the ToMEx database [103] focus on microplastics in sediments and toxicity data, respectively. The PlastChem database [21, 110] provides a collection of chemicals associated with plastics, along with information on their properties and hazards.

Spectral libraries such as OpenSpecy [111], SLoPP/SLoPP-e [112], and FLOPP/FLOPP-e [113] provide access to spectroscopic data for the identification of microplastics. Further examples of spectral data collections include the RDWP/RDSP dataset [114] and the FTIR-Plastics dataset [115, 116].

To reduce uncertainty in measured microplastic abundances, many studies now conduct parallel execution of blank process samples as negative controls. However, how the obtained data is then used varies greatly between studies. Some studies only report that blanks were analysed, while others use different methods to correct the sample data based on the microplastic abundances observed in the blanks. A recent study addressed the question of which of these approaches are recommendable, and its findings may influence future research and produce more comparable results [117]. Another pioneering attempt to increase the harmonisation and reusability of results is the recently presented data integration tool, MaTCH, which offers a drop box interface that can ingest different kinds of microplastics data, performs semantic and qualitative alignment techniques and provides algorithmic presets for certain data conversion, such as count-to-mass approximations [118].

In terms of acquisition, several software tools are now available that target different measurement modes and instrumentation. The open-source TUM ParticleTyper enhances the capabilities of the WITec Raman microspectrometers and their corresponding software suite, ParticleScout (WITec/Oxford Instruments Group), catering specifically to microplastics analysis [119–121]. It is specifically designed for microplastics analysis [119–121]. Its strengths include high-quality automated object outline detection and particle de-agglomeration, and a bootstrapped calculation of the confidence in extrapolated results after a given number of particle measurements. While this high reliance on automation offers advantages in terms of analytical throughput and measurement conformity, it limits the user's options for computer-assisted manual intervention, such as correcting particle attributes or fixing individual cases of artefacts in particle detection (e.g. over- and under-fragmentation or particle halos). Another approach involves identifying and quantifying microplastics using spectroscopic imaging techniques, where pixel-wise spectroscopic information can be used to construct chemical maps. The application of large array detectors in Fourier Transform Infrared (FTIR) spectroscopy enables high sample throughput and resolution. The freeware tool SiMPle is designed for analysing such FTIR imaging data and provides a user-friendly interface for identifying and quantifying microplastics [122]. A similar approach is described by Hufnagl et al. as the basis for a commercially available, closed-source tool [123, 124].

Machine learning models and associated data analytical toolsets are becoming increasingly important in various areas of microplastics research. One of the most prominent use cases is spectroscopic material classification, which has been approached by several recent studies for Raman and FTIR spectra [125–128], as well as for laser-induced fluorescence [129]. These spectroscopic classification methods have the potential to achieve high accuracy if the training material is of sufficient quality and quantity. The large number of spectra and features (i.e. the acquired spectral intensities) result in high data and information density, making spectroscopic problems ideal for machine learning models. In addition to material assignment, machine learning has also been used for spectral

denoising, with an autoencoder being employed to reconstruct low-quality spectra and remove artefacts such as baseline drift, a low signal-to-noise ratio, and interferences from fluorescence and cosmic rays [130]. As high-throughput microplastic measurements do not allow long acquisition times or parameters optimised for individual particles, noisy spectra are a significant issue, and the proposed denoising model can contribute to improved material assignment accuracy.

Other machine learning approaches that rely solely on visual microscopy cues as predictors for the detection of microplastics are more constrained by information content of the data. While this may limit the accuracy of classifications that can be achieved, it enables faster, more cost-efficient applications in use cases where rough estimates suffice or where microplastic isolation is facilitated by other means, such as liquid crystal trapping [131, 132]. In contrast, the number of machine learning models targeting spatial pollution prediction remains limited, with only a few studies using environmental variables for pollution level classification [133–135] or regression [136].

At a more abstract level, it is also important to highlight recent innovative and outstanding work that extends analytical concepts and methodologies in ways that can encourage a more data-science-oriented approach to microplastics research. One example is the concept of unifying particle attribute descriptions by changing them from absolute values (e.g. size) and arbitrary categories (e.g. shape or colour) to continuous probability distributions [137]. Taking this a step further, the concept could be combined with the method of conformal prediction, which has recently been introduced in the field of microplastics for polymer type assignments [138]. In essence, this combination would enable material classifications with known associated uncertainties to be used as the basis for derived probability distributions of material-related properties such as density, surface charge, hydrophobicity, and degradation susceptibility. This can contribute to a more comparable data landscape, providing a valuable foundation for probabilistic risk modelling. However, translating direct measurements and categories of particle properties into parametric probability distributions may come at the cost of reduced intuitive comprehensibility and ease of communication. In this regard, categories that describe particle properties such as shape or colour have value in communicating results and findings. To that end, there have been influential contributions suggesting a nomenclature and methods for harmonised reporting units for microplastics abundance data [139, 140]. This could provide a useful basis for developing a common ontology in microplastics data management.

The publications included in this thesis aim to address open challenges and gaps identified in the existing literature. This is achieved by developing and refining methodologies for sampling and analysing specific parts of microplastics on the microplastic size spectrum, implementing data management practices that facilitate FAIR principles, and providing and employing open-source scientific software code, including machine learning, for use in the microplastics research context.

The objectives that connect the included works are as follows:

1. To develop and refine methodologies for sampling and analysing microplastics through improvements of applicability specifically in the lower micron sizes fractions [3–5].
2. To provide method evaluations of purification techniques for microplastics [2, 5, 9, 12].
3. To use the developed methods to gain new insights into the distribution and impacts of microplastics in the environment [7, 8, 13].
4. To assess comparability of methods and data for recommendation of best practices in microplastics research, potentially providing evidence or guidance for data-driven policy advances [1, 6, 10, 12].
5. To implement FAIR data management and open-source software development, including machine learning applications [4, 9–11, 13].

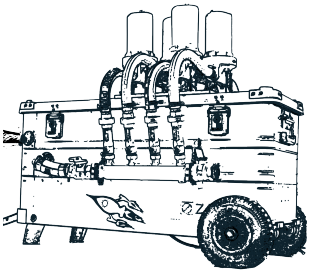
Act I: Producing Data

Despite microplastics research now being an extremely interdisciplinary field, it clearly began as an emerging sub-discipline of marine biology [28, 45, 141–151]. Many of these pioneering studies aimed to quantify microplastic particles using techniques from plankton research. Since then, the field of interest for microplastic analysis has expanded to include all other environmental compartments - notably freshwater [106, 152], soils [153], sediments [154], atmosphere [155–157] and cryosphere [158, 159] - as well as organisms [160–162], human food [163–166], medical [167] and cosmetic products [168]. The core steps common to all such studies are the sampling of particles, their extraction from the sample matrix, and their identification and quantification, which together constitute the act of producing quantitative microplastics data. Interestingly, particle-based microplastic analysis applies principles from the macroscopic world well down to the micrometre scale. Each particle is counted as a single unit of measurement. This may sound reasonable if we were to count and characterise things like trees or furniture. There would be a result, and it would be traceable. But microplastics are handled by operators and devices orders of magnitude larger than themselves. Minor changes in their environment, such as temperature, humidity or electrostatic fields, can cause particles to move or adhere to surfaces, making the process highly susceptible to error. However, it also allows for comparatively high sensitivity of measurement as literally every particle counts. For example, mass-based approaches like pyrolysis gas chromatography / mass spectrometry, in comparison, would not reach their limits of detection with just a few particles in the lower micron range, where individual particle masses are on the order of picograms to nanograms. On the other hand, in particle-based quantifications, the unit 'number of microplastic particles', if reported alone, is problematic due to the wide range of size and materials included under the umbrella term *microplastics*.

> *Consider two samples containing microplastics of the same polymer type in spherical shape.*
>
> *One consists only of particles of 5 mm in diameter, i.e. the largest particle size frequently included in microplastic definitions [139], while the other contains only particles of 1 µm, as an example of a smallest particle size considered as microplastics (though in practice this would be below the measurable size range of most methods).*
>
> *If both samples contained the same polymer mass, their microplastic counts or concentrations would differ by a factor of 125 billion.*

Although the above thought experiment does not reflect a real-world situation, it makes clear the importance of providing rich particle size data and, by extension, sensible conversions to particle volume or mass, together with any particle number data. The same applies to other parameters such as shape or chemical composition. The act of producing quantitative microplastics data is thus a highly sensitive and error-prone process that requires a high level of control to ensure the reliability and comparability of results. A plethora of methods have been described for each of the core steps in the microplastic analysis workflow, reflecting technological advances and the variety of research questions being addressed. The targetted particle size is the key parameter that dictates the experimental design, choice of analytical techniques and control measures required. Smaller particles require highly controlled conditions to avoid contamination or loss, while larger particles can be sampled and analysed with less effort. It is, however, the small fractions of microplastics, i.e. below 100 µm, that are of high concern in terms of causing damage to organisms, due to their higher availability and increased surface to volume ratio, entailing elevated ad- and desorption kinetics of associated toxic chemicals. There is therefore a need for sampling, purification and quantification methods specifically tailored to smaller microplastics. Three publications help to fill these gaps and advance our capabilities in producing microplastics data.

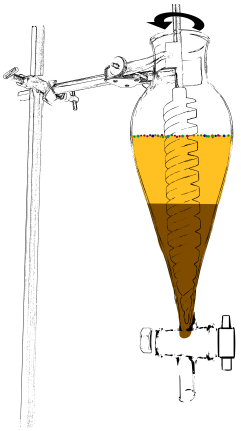
Research Article: **Small Microplastic Sampling in Water: Development of an Encapsulated Filtration Device**



Sampling of microplastics in water can be carried out using towed nets such as the manta net for surface sampling or other plankton nets for subsurface collections. Originating from zooplankton surveys, these nets feature open designs with plastic meshes typically around 300 µm in pore size. At this size range, they are highly effective devices for covering large sample volumes and geographical areas. However, the smaller fractions of the microplastic size spectrum, which are of particular interest because they are easily ingested by many organisms, cannot be efficiently collected by these nets. Simply switching to meshes with much smaller pore sizes is not a viable option due to the rapid clogging and contamination risk of the open design. Therefore, when targeting smaller particles, systemic requirements favour a reduction of potentially contaminating plastics in the sampling gear and closed filtration designs that avoid exposure of the sample to airborne particles. Taking inspiration in other closed-filter sampling prototypes [15, 36], we have developed a pump filtration device that encapsulates the filter in a stainless steel housing, allowing the collection of particles down to 10 µm in samples of approximately 0.2 to 1 m^3 in freshwater systems and wastewater effluent or up to 2 m^3 in coastal waters, depending on site conditions [3]. Its rugged and mobile design makes it suitable for field campaigns and its encapsulation concept, in combination with a suction pump, allows for the inserted filters to be backflushed prior to sampling, reducing the risk of contamination.

Go to publication: page 58.

Research Article: **When every particle matters: A QuEChERS approach to extract microplastics from environmental samples**

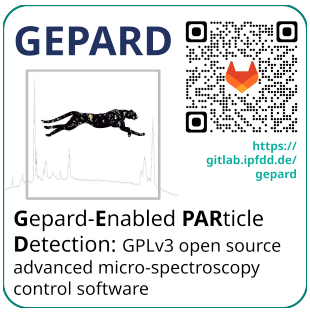


After collection, most samples require some form of extraction protocol to isolate microplastic particles for the analytical methods not to be overloaded. This typically involves steps to separate mineral particles by means of their higher density and chemical digestion steps to remove organic material. Whilst necessary, these steps can have a significant impact on the data produced, potentially removing, introducing or altering particles through aggregation, disaggregation, shrinkage, inflation, erosion or degradation. Based on practical experience with different sample types, we provide decision guidance for the construction of optimal extraction protocols in a comprehensive methods paper [5]. A key recommendation is to sequence method modules according to their matrix removal potential - for instance, performing density separation before chemical digestion for sediment extractions, but reversing this order for biota samples. For large-volume sediment or soil samples, we describe the construction and use of a gentle agitation device that does not grind particles or subject them to turbulent circular flows, which is critical to preserving the shape, size and number of microplastics. Particles are continuously lifted into the liquid separation phase by a conical spiral conveyor, allowing material separation at the density threshold of both larger and smaller particles, thus avoiding

trapping effects.

Go to publication: page 68.

Research Article: **High-Throughput Analyses of Microplastic Samples Using Fourier Transform Infrared and Raman Spectrometry**



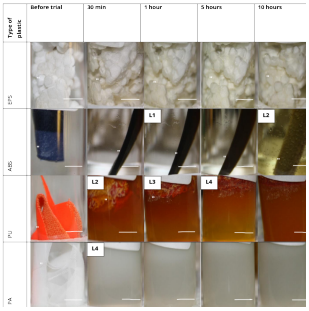
Reliable identification of the polymer type of individual microplastics is enabled by microscopy-coupled vibrational spectroscopy systems that reveal chemical composition at the micrometre scale. While for the larger fractions of microplastics characterisation based on visual appearance alone may be an acceptable compromise for qualification and quantification, small microplastics clearly lack sufficient optical cues to clearly discriminate them from natural debris [14]. Raman and FTIR spectroscopy are two commonly used techniques for particle-based analysis of microplastics that can provide clear chemical fingerprinting of polymer types. However, the acquisition and evaluation of microplastic spectra is a time-consuming process. The open-source software GEPARD [4] has been developed to enable high-throughput measurements of microplastics in a streamlined analytical pipeline. Designed to operate with a range of Raman and FTIR microscopes from different manufacturers, GEPARD's principal workflow is to remotely control instrumental functions and acquire image and spectroscopic data in open accessible formats, avoiding incoherent data in multiple proprietary containers. This makes it well suited for both routine and comparative or correlative measurement applications. The user-guided routines expedite analysis by introducing automation where it makes sense: in large-field image acquisition, vertical resolution for particle height determination, image segmentation for particle outline recognition, spectra acquisition, spectra evaluation and material assignment, as well as post-hoc particle property correction and result reporting.

Go to publication: page 90.

Act II: Assessing Data

There are two equally important aspects contributing to quality of microplastics quantification data: evaluation of fitness for purpose of applied methods and control of quality of method conduct [169]. The former, i.e. quality assurance, is typically part of the method development process. Based on model samples and theoretic considerations, adverse effects of the method on particles can be assessed. However, the size of targeted particles again poses a central challenge for the design of quality assurance experiments. The analytical endpoints are comparison of the relevant particle properties before and after the treatment in question, e.g. a specific matrix digestion protocol. Such experiments are straight forward to setup and analyse for particles in the upper micron range (e.g. > 100 µm) or millimetre size plastic pellets, or by using particles with distinct and readily recognisable properties such as laboratory-purpose microspheres or fluorescent beads. There are several studies evaluating purification methods following these approaches [2, 50, 170–179]. In fact, several aspects such discolouration or dissolution of larger plastic pieces may allow direct conclusions for a method's impacts also on smaller particles.

Research Article: **Extraction of microplastic from biota: Recommended acidic digestion destroys common plastic polymers**



In a study on the extraction of microplastics from fish, we found that a recommended acidic digestion method, using nitric and perchloric acid, destroys common plastic polymers, leading to an underestimation of microplastic concentrations [2]. While this study used centimetre-sized pieces of post-consumer plastic items, the results are suggesting that microplastics of polyamide, polyurethane, acrylonitrile-butadiene-styrene, polymethylmethacrylate, and polyvinylchloride, would not be adequately preserved through the digestion method. A compared digestion protocol combining alkaline and oxidative treatment with potassium hydroxide and sodium hypochlorite was found to be more suitable for the preservation of these polymers and also for a post-digestive Raman-spectroscopic polymer assignment. The study highlights the importance of method validation for the accurate quantification of microplastics in biota samples.

Go to publication: page 50.

However, the situation is more complex for particles measuring less than 100 µm. When using them in suspensions or other mobile states for manipulative experimentation, such as digestion trials, they are more difficult to handle due to their size. They are more likely to aggregate or adhere to surfaces, meaning that observed changes in particle number cannot simply be attributed to the treatment effect itself. There are also methodological limitations due to an unknown level of uncertainty in factors such as handling or analysing the test sample, which may add to or counteract the treatment effects. If the focus is on effects such as surface appearance or crack formation, these limitations are exacerbated by the lack of traceability, as the particles appear fungible and direct observation of changes becomes challenging.

> *The idea almost suggests itself: it would of course be much easier to study these particles if it were only possible to make them less mobile in some way.*

By immobilising the particles on a plain carrier, they can be observed or manipulated in ways that would be impossible with freely moving microplastics. This allows for comparative studies on the same particles, e.g. before and after being exposed to a chemical digestive treatment. Two publications in this act explore immobilisation methods to assess microplastics in the size range below 100 µm.

Research Article: **Measuring impacts of microplastic treatments via image recognition on immobilised particles below 100 µm**

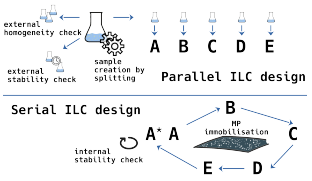


During purification from matrix residues microplastics are exposed to aggressive chemicals and conditions potentially damaging their integrity. The measurement of such impacts on microplastics is therefore an important part of quality assurance and method validation. For microplastic particles below 100 µm, we developed a new method for particle immobilisation and provide required image recognition software to measure the effects of different treatments on the particles [9]. Plain and smooth silicon wafers serve as a carrier on which an epoxy resin layer is added with even thickness by spin coating, acting as an adhesive to immobilise microplastics. A short initial curing period allows the resin to become hard enough to avoid deformation. Particles are scattered on to the pre-hardened adhesive leading to their downward-facing side being permanently attached to the resin after completed curing. Particles immobilised by this technique will have their upward-facing side free from adhesive and available for exposures to chemicals to be tested. The method allows for the rapid and accurate assessment of the impacts, providing valuable information for the development of new methods. One key advantage is that high numbers of particles can be immobilised and analysed in parallel, allowing for better statistical power and more robust conclusions. For example, we applied the method to assess the impacts of different digestion protocols, finding that for most of the tested polymers, the microplastic particle loss was not significantly different from the control. However, acrylonitrile-butadiene-styrene particles were vulnerable to acidic treatments at pH 3 and acrylic and epoxy-based paint resins suffered from oxidative H_2O_2 treatments.

Go to publication: page 150.

In addition to quality assurance studies, there are other areas of application that can benefit from surface-attached plastics. These include the production of reference materials, benchmarking, long-term storage and archiving of samples or correlative microscopy. One particular application is the use of immobilised microplastics in analytical ring trials. Also known as interlaboratory comparisons, they are important tools for measuring the proficiency or result variation between different laboratories or analytical techniques. They rely on having a basis of measurement that theoretically allows each participant to obtain the same result. A number of such studies have been carried out recently, comparing different techniques of microplastic analysis [180–184]. They approached achieving the common basis of measurement by providing participants with sample specimens created by finely tuned homogenisation and stabilisation methods for the fabrication and splitting of microplastic samples. However, the remaining unknown uncertainty in degree of homogeneity of microplastic content between the distributed samples propagates into the result comparison. As a complementary approach, we describe a novel ring-trial design relying on the immobilisation of microplastics, which allows for the direct comparison of the same particles between different participants as measurements are performed sequentially by all participants on the same sample specimen.

Research Article: **What Goes Around Should Not Move Around: Immobilizing Microplastics as a New Approach for Analytical Ring Trials**



Interlaboratory comparisons are a common method to assess the comparability and reliability of analytical methods. We have developed a new method for the immobilisation of microplastics that allows a serial design of interlaboratory comparisons [12]. The applied filtration immobilisation technique differs from the aforementioned spin-coating method in that it avoids the use of an organic adhesive and is directly compatible with the filtration step of microplastic extraction protocols. By injecting a dilute potassium silicate solution into the filtration process - followed by curing - we obtain samples that are sufficiently robust for repeated measurements and transport.
With its purpose in enabling serial interlaboratory comparisons, the method is not yet readily transferable to the creation of long-term stable sample archives. Some particles may remain unattached directly after immobilisation. The procedure described here includes several rinses to remove any loose particulates, leaving only firmly attached particles as part of the final sample. Obviously, this would not be a sensible approach for archiving environmental samples, for example, where the original particle content is the important quantity to preserve. It does, however, directly enable the creation of benchmark or reference material samples. As the prospect of this application has attracted industry interest, the filtration immobilisation technique required has been filed for patent and will be available for licensing for commercial application.

Go to publication: page 195.

Unlike quality assurance, the quality control is a process-oriented perspective that aims to ensure that any changes in respect to the measurand are documented and accounted for. In practice, this is implemented as control measurements. Controls may be positive, i.e. artificial samples containing microplastics of known quantity and quality, or negative, i.e. containing no microplastics. Controls undergo the identical procedural steps as a sample under the same conditions. The deviation from the expected result informs about the loss (positive controls) or contamination (negative controls) of microplastics by the applied methods.

> *Experience tells that negative controls will only contain negligible amounts of microplastics if the targeted particle sizes exclude the lower micron range. For studies targeting particles below 50 µm, and even more so below 10 µm, negative controls are unlikely to be free of microplastics under state-of-the-art laboratory working conditions.*

Even under the most stringent measures to prevent contamination, microparticulate introductions through airborne dust and wear of equipment is unavoidable without the use of certified clean room facilities, which is, however, not practically affordable for most research laboratories. Consequently, controls must cover the full range of processes to which the actual samples were exposed, and a valid correction method is required to adjust microplastic counts accordingly. There is no consensus in the published literature on how such corrections should be made. Methods range from 'no correction' to 'subtraction of the total microplastic control count from the sample counts' to 'subtraction of the mean control count from the mean sample count', as well as 'limit of detection' or 'limit of quantification' based corrections or statistical models, all with varying degrees of variation and effectiveness [117].

At this point it is worth clarifying the value of particle-based data. The most prominent param-

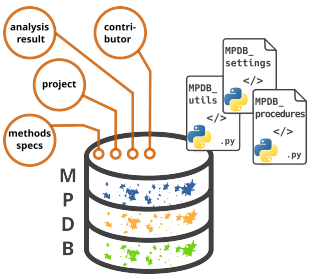
eter reported by environmental microplastic surveys is 'number of microplastic particles', or its concentration with respect to a given matrix quantity. This is a datum in the sample domain because its frame of reference is one sample. The actual raw datum, or unit of measurement, is the individual particle with its observed properties. Retaining data in the particle domain facilitates a match-based data correction, where particle properties can be utilised to group particles with similar phenotypic appearance. This is a more accurate approach than a simple subtraction of control counts at sample level. The description of phenotypes depends on the available particle properties.

> *Polymer type, colour and certain distinct shape categories (e.g. fibres and irregulars) may allow for a differential correction of only blue polyamide fibres assuming a certain number of those had been identified in a blank control. This procedure would not alter the counts of red polyamide fibres, nor blue polyamide irregulars.*
>
> *But, as we are still in the particle data domain, we need a way to facilitate matches of individuals between control and sample data within each phenotype. Here, the continuous particle properties, such as particle size, volume or mass would be suited to always remove the most similar sized particle for every particle in a control.*

The provision of raw data at the particle level is well in line with FAIR data principles and should therefore be applied wherever possible and appropriate. By use of reproducibly executable algorithms, aggregated results needed for interpretation and discussion can then be produced from the raw data in a transparent manner. The above concept of blank corrections was part of the design thinking behind a microplastics particle-dedicated database scheme, which is described in the following publication. Its application and algorithmic implementation are part of a later publication and are available in the corresponding code repository [13].

***Research Article:* A Public Database for Microplastics in the Environment.**

Running high-throughput microplastic analyses [4] generates large amounts of data and the need for a structured data management infrastructure. The 'Marine Plastic Database' (MPDB) is a SQL-based database scheme for the storage of microplastic data, including metadata, images and spectroscopic data [10]. It accounts for the data structure typical for microplastic particle quantification studies, such as the need for particle-level data, the importance of rich particle properties for data interpretation, and the necessary linkage to aggregated sample data. Since publication the MPDB scheme has been adapted and implemented for several other projects including microplastic analyses in food, beverages and air samples. The database scheme and its later modifications can be found in the accompanying repository.



With a built-in possibility for particle flagging, MPDB enables both the storage of raw data and the application of correction algorithms for control data. Flags may be created for any reason that requires a particle to be treated differently from others, such as having been marked for exclusion due to a blank correction procedure. Any particles carrying this flag will still be part of the dataset but data analysis can make an informed choice on whether to exclude them from calculations.

Go to publication: page 173.

Act III: Using Data

The use of microplastics data is essential for answering research questions, informing policy decisions, and guiding management actions. It involves integrating data from different sources, synthesising data into knowledge, and communicating knowledge to different audiences. Four publications contribute to the use of microplastics data by developing new methods for predicting microplastic emissions, identifying microplastic particles in drinking water treatment sludge, and synthesising marine monitoring methods to enhance the status assessment of the Baltic Sea.

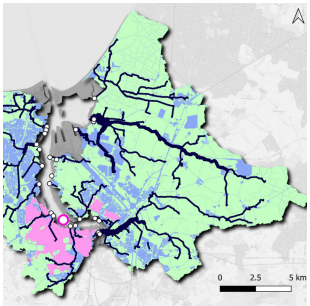
Research Article: **A Synthesis of Marine Monitoring Methods With the Potential to Enhance the Status Assessment of the Baltic Sea**



In a synthesis of marine monitoring methods for the Baltic Sea addresses the need for observation of microplastic pollution by recommending three methods, taking into account the different technical requirements of different compartments and different microplastic size fractions [6]. A Manta trawl is recommended for monitoring microplastics in surface waters in the size range above 300 µm. For smaller microplastics, or in areas inaccessible or impractical for trawling, the synthesis paper suggests the encapsulated filtration device described in one of the above publications [3], for use in monitoring programmes. The third method, a combination of sediment coring and density separation, is recommended for monitoring microplastics in sediments. The synthesis provides a comprehensive overview of the methods available for environmental monitoring task in the Baltic Sea region and their technological readiness.

Go to publication: page 105.

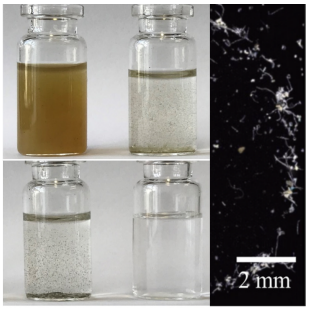
Research Article: **Combined Approaches to Predict Microplastic Emissions Within an Urbanized Estuary (Warnow, Southwestern Baltic Sea)**



Samples, collected from the Warnow River (Rostock, Germany) using the encapsulated filtration device [3], purified according to the recommended H_2O~2 extraction protocol for water samples [5], analysed by Raman microspectroscopy in the GEPARD environment [4], and with the resulting microplastics data stored in the MPDB [10], were used to predict microplastic emissions within the urbanised estuary [7]. While the available quantitative data on microplastics are scarce due to the highly laborious nature of the analysis, this study demonstrates the assessment of microplastic emissions by combining data from different sources such as hydrological catchment discharge, stormwater runoff and combined sewer overflows, land use and population density. It concludes on the order of magnitude of the different emission sources with the largest contributions coming from the catchment and stormwater runoff, while combined sewer overflow events and effluent emissions from the local wastewater treatment plant are considerably lower.

Go to publication: page 123.

Research Article: **Identification and quantification of microplastic particles in drinking water treatment sludge as an integrative approach to determine microplastic abundance in a freshwater river**



Another approach to the problem that environmental microplastic data are typically spatially and temporally sparse snapshots is the use of integrative processes that can be exploited to quantify accumulated microplastics. Here, we explore how flocculation sludge from a surface water supplied drinking water plant can be used as an integrative sample to determine microplastic abundance in a freshwater river [8]. As a reference, microplastic data from the same sampling [3], processing [5] and chemical analysis pipeline [4, 10] described for the above publication are used. They are compared to the microplastic abundance of the sludge, which is converted according to the corresponding raw water influent volumes. The compared datasets show mean microplastic concentrations in the same order of magnitude with only insignificant differences. The concept is transferable to other stationary facilities using surface reservoirs for drinking or process water production. Their continuous operation, high process stability and longer integration times compared to typical snapshot sampling offer good prospects for establishing a reliable and continuous microplastics monitoring network.

Go to publication: page 140.

The last article, which I include in this act, demonstrates the use of microplastics data in an advanced, highly integrative workflow. Again, the basis is the MPDB [10], storing particle data together with all relevant parameters from sampling, processing and spectroscopic quantification. This time the goal is empirical predictive modelling of microplastic distribution in estuarine sediments, for which we provide an open-source Python-based analysis routine that relies on machine learning concepts for model selection and validation (Figure 2).

Techniques from machine learning and data science are now being applied in many areas of environmental and geoscience research [185, 186]. However, these applications tend to address data-rich scenarios involving abundant observations and a large number of features, as in remote sensing or climate modelling. In the field of microplastics, machine learning approaches have been successfully applied in areas such as spectroscopic classification and image analysis, building on the large amounts of data generated by high-throughput analytical methods ([124]; [128]; [125]; [126] and others as reviewed in [187]; [188] and [189]). In contrast, the distribution of environmental microplastics is characterised by data scarcity, as the number of observations available in an area is typically in the lower tens due to the labour-intensive process of producing high-quality microplastics data. Consequently, few studies have attempted to leverage machine learning techniques in this context [189]. We demonstrate that elements of machine learning, such as nested cross-validation for model selection and optimisation, sample stratification and ensembling of multiple models, can be adapted and applied to small datasets to create and validate modelling pipelines for the spatial prediction of microplastics, optimising the use of available data.

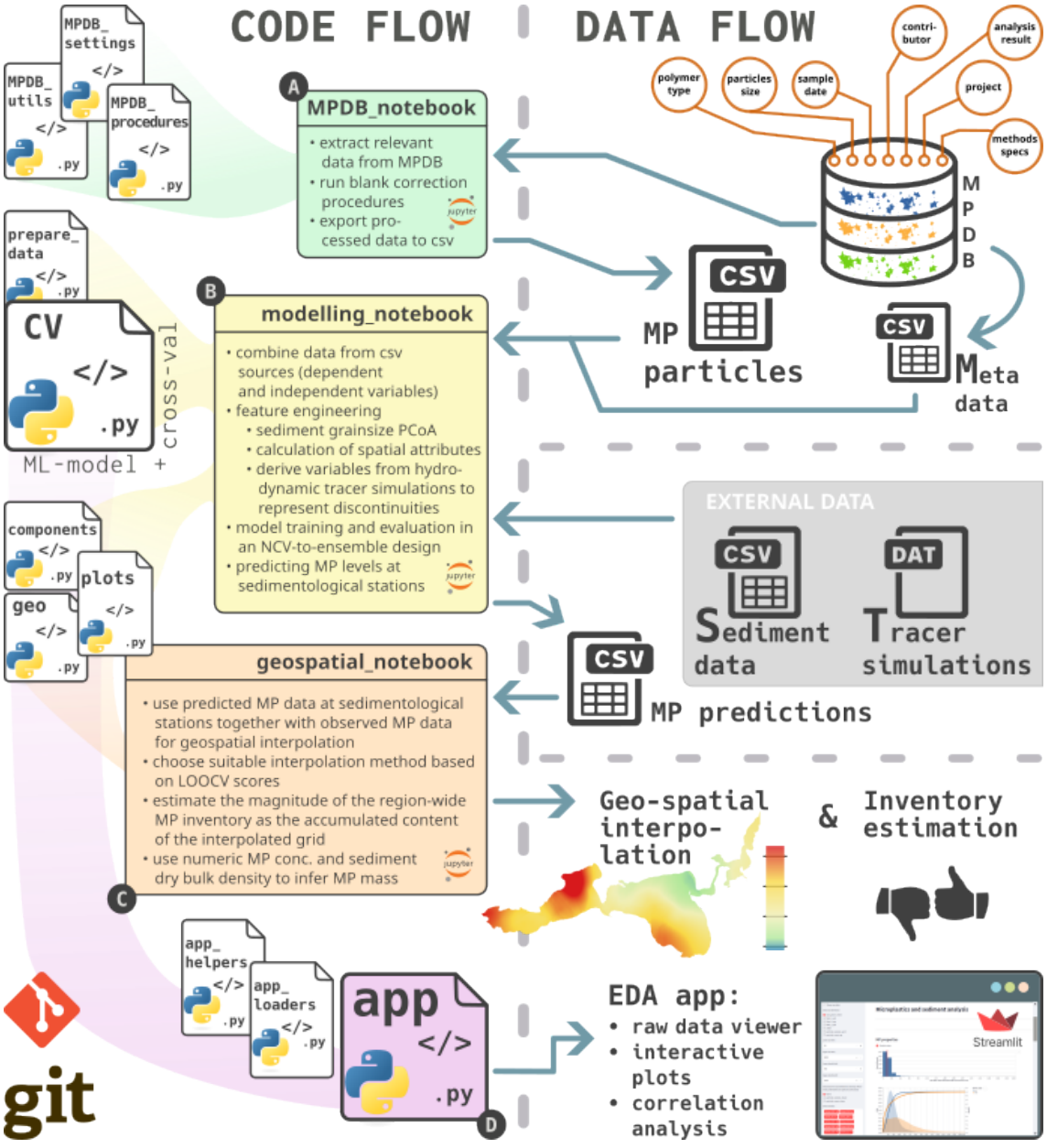
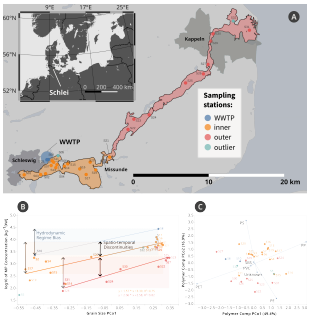


Figure 2: Data processing, analysis and prediction workflow [13]. An implementation of the shown workflow can be found in the accompanying code repository including the web app for exploratory data analysis.

Research Article: **Mapping the plastic legacy: Machine-learning enabled microplastic inventory prediction in aquatic sedimentary systems**



Natural sedimentation and sediment dynamics present an opportunity to observe long-term microplastic distribution. Based on the insights from a previous study in the Warnow estuary [190], which established correlations between certain microplastic properties and sediment grain size characteristics, we developed a machine-learning enabled microplastic inventory prediction model for aquatic sedimentary systems [13]. The model is trained on a dataset of microplastic particle data from the MPDB [10], combined with sediment grain size data from the same sampling campaign. The model is able to predict the microplastic distribution in the sedimentary system based on the sediment grain size distribution and other hydrodynamic proxies, utilising data from an earlier extensive sediment survey [191]. The model is implemented in an open-source Python-based analysis routine Figure 2 that is available for download and use. The routines are designed to be easily adaptable to other sedimentary systems and can be used to predict microplastic distribution in aquatic sediments based on sediment grain size data.

Go to publication: page 208.

Conclusions and Outlook: Towards FAIRer Microplastics Data

Over the preceding sections, I examined how the production, assessment, and usage of microplastic data was advanced by the presented publications. The research objectives were addressed by developing new methods for sampling, extraction, and identification of microplastics, as well as by proposing new approaches for quality assurance and control of microplastic data. Policy initiatives may find support in the developed methods for predicting microplastic emissions and distribution [7] and synthesising marine monitoring methods to enhance the status assessment of the Baltic Sea [6]. Data management practises may be improved by applying the developed versatile MPDB database scheme for microplastics particle data [10], enabling the storage of raw data and the application of correction algorithms for control data. The last publication [11, 192] to describe here for this thesis is special as it is purely a dataset publication, not a classical article. The value of alternative publication formats, is slowly gaining recognition in the scientific community, as they can facilitate direct insight, validation and reuse of the data by others.

> *Actually, not just by others. For me, trying to adopt the FAIR mindset, an important realisation has been that in many cases it's me who is going to have the biggest benefit of having the data FAIR. Simply for the fact that there is one clear documented source of truth for the data.*

> *It just takes a little rethinking that the public repository is the place where I will go to access my own data, just like anyone else would do. No matter how old, I can always go back to the original data and check my assumptions, reproduce my results, or even reanalyse the data with new methods. Over time this can save days of work trying to relocate or understand data that should have been somewhere on that old harddrive…*

Beside datasets these alternative publication formats also include reproducibly executable data

analysis workflows and research-supporting interactive content [9, 11, 13].

***Dataset:* MicroPlastiX SpecDB**



The MicroPlastiX SpecDB project addresses the challenge of microplastic spectroscopic assignment in the presence of degraded spectra. While existing spectral reference libraries predominantly contain pristine polymer spectra, environmental microplastics often show significant alterations due to weathering. The MicroPlastiX project conducted natural weathering experiments at several European coastal sites to generate much-needed reference material. However, the spectroscopic data collection at different institutes was done in a non-standardised way. Here I developed a solution by transferring diverse source data into a common data-language, creating a structured document-oriented database that organises spectroscopic content and associated metadata in machine-readable yet human-friendly file formats [11]. I provide the code for programmatic data access and running a web interface for browsing and searching the database. The chemical data (spectra with metadata) is hosted on the chemical research data repository RADAR$_4$Chem [192]. This database publication was awarded the FAIR4chem award 2024 by the NFDI4Chem [193, 194], for its application of FAIR data principles in chemical research. The database code repository remains open for contributions and serves as a valuable resource for training and validating machine learning models for microplastic identification.

Go to publication: page 190.

Looking ahead, the widespread adoption of FAIR principles in microplastics research would benefit from coordinated infrastructure development. As often, there are already great tools and technical solutions available, but incentives for and knowledge of their application remain limited. As an example, Electronic Laboratory Notebook and Laboratory Information Management Systems (ELN-LIMS) can assist researchers in collecting, managing, and sharing their data in a structured way.

> *Due to large automation potentials of ELN-LIMS, there is a lot of time to be saved on documentation tasks in the long run. However, implementing the required routines or just standing in front of a steep learning curve of yet another tool can feel discouraging at times.*
>
> *This is especially the case when there are communication barriers between those who develop, deploy and use such a system.*

Currently, many research institutes experiment with implementing data management tools from simple electronic notebook solutions to highly automated, hardware-integrated systems documenting all steps of the research process. While understandable from an institutional perspective, this approach can lead to hardly interoperable data silos and introduce friction as researchers of different disciplines need to be included who have very different workflows and views on data management. Instead, field-specific public ELN-LIMS instances can be a way to foster some more natural growth, with new users taking advantage of a certain familiarism when peers are already active on the platform. Examples of possible frameworks are NOMAD [195] or openBIS [196, 197]. Configured for microplastics research, such platform could provide data capture and processing workflows

based on common data formats and reporting schemes tailored to the specific needs of microplastics researchers. National or international research data infrastructure programs such as German National Research Data Infrastructure initiative NFDI, the Dutch SURF, the European Open Science Cloud EOSC, or the Research Data Alliance RDA, are well-positioned to host and support such field-specific instances. However, inter-institutional and discipline-specific instances may be less efficient for graphing multidisciplinary research contributions across different groups at the same institute and make potential gains through automation such as instrument integration or raw material tracking more difficult to achieve. Optimally, using open data exchange protocols through application programming interfaces (APIs) with the possibility for federated data access and search across institutional instances would a direction worth pursuing. Independent of the scope of a instance's setup and technical capabilities of the ELN-LIMS system, I would also regard the inclusion of social community-tools (e.g. on-platform user communication, project management, training resources) as useful for smoother onboarding and adoption of such systems.

References

[1] Lenz R, Enders K, Nielsen TG (2016) Microplastic exposure studies should be environmentally realistic. *Proceedings of the National Academy of Sciences* 113(29):E4121–E4122. https://doi.org/10.1073/pnas.1606615113

[2] Enders K, Lenz R, Beer S, Stedmon CA (2016) Extraction of microplastic from biota: Recommended acidic digestion destroys common plastic polymers. *ICES Journal of Marine Science* 74(1):326–331. https://doi.org/10.1093/icesjms/fsw173

[3] Lenz R, Labrenz M (2018) Small microplastic sampling in water: Development of an encapsulated filtration device. *Water* 10(8):1055. https://doi.org/10.3390/w10081055

[4] Brandt J, Bittrich L, Fischer F, Kanaki E, Tagg A, Lenz R, Labrenz M, Brandes E, Fischer D, Eichhorn K-J (2020) High-throughput analyses of microplastic samples using fourier transform infrared and raman spectrometry. *Applied Spectroscopy* 74(9):1185–1197. https://doi.org/10.1177/0003702820932926

[5] Enders K, Lenz R, Ivar do Sul JA, Tagg AS, Labrenz M (2020) When every particle matters: A QuEChERS approach to extract microplastics from environmental samples. *MethodsX* 7:100784. https://doi.org/10.1016/j.mex.2020.100784

[6] Mack L, Attila J, Aylagas E, Beermann A, Borja A, Hering D, Kahlert M, Leese F, Lenz R, Lehtiniemi M, Liess A, Lips U, Mattila O-P, Meissner K, Pyhälahti T, Setälä O, Strehse JS, Uusitalo L, Willstrand Wranne A, Birk S (2020) A synthesis of marine monitoring methods with the potential to enhance the status assessment of the baltic sea. *Frontiers in Marine Science* 7. https://doi.org/10.3389/fmars.2020.552047

[7] Piehl S, Hauk R, Robbe E, Richter B, Kachholz F, Schilling J, Lenz R, Fischer D, Fischer F, Labrenz M, Schernewski G (2021) Combined approaches to predict microplastic emissions within an urbanized estuary (warnow, southwestern baltic sea). *Frontiers in Environmental Science* 9. https://doi.org/10.3389/fenvs.2021.616765

[8] Siegel H, Fischer F, Lenz R, Fischer D, Jekel M, Labrenz M (2021) Identification and quantification of microplastic particles in drinking water treatment sludge as an integrative approach to determine microplastic abundance in a freshwater river. *Environmental Pollution* 286:117524. https://doi.org/10.1016/j.envpol.2021.117524

[9] Lenz R, Enders K, Fischer F, Brandt J, Fischer D, Labrenz M (2021) Measuring impacts of microplastic treatments via image recognition on immobilised particles below 100 µm. *Microplastics and Nanoplastics* 1(1):12. https://doi.org/10.1186/s43591-021-00012-0

[10] Čerkasova N, Enders K, Lenz R, Oberbeckmann S, Brandt J, Fischer D, Fischer F, Labrenz M, Schernewski G (2023) A public database for microplastics in the environment. *Microplastics* 2(1):132–146. https://doi.org/10.3390/microplastics2010010

[11] Lenz R, Fischer F, Arnold M, Fernández-González V, Moscoso Pérez CM, Andrade-Garda JM, Muniategui-Lorenzo S, Fischer D (2023) MPX_specDB: MicroPlastiX spectra database. https://doi.org/10.5281/zenodo.12511025

[12] Lenz R, Enders K, Vizsolyi EC, Schumacher M, Lötsch J, Löder MGJ, Eder G, Voronko Y, Andrade-Garda JM, Muniategui-Lorenzo S, Laforsch C, Fischer D, Labrenz M (2024) What goes around should not move around: Immobilizing microplastics as a new approach for analytical ring trials. *Environmental Science & Technology*:acs.est.4c09427. https://doi.org/10.1021/acs.est.4c09427

[13] Enders K, Lenz R, Fischer F, Schwarzer K, Seiß G, Labrenz M (2025 (expected)) Mapping the plastic legacy: Machine-learning enabled microplastic inventory prediction in aquatic sedimentary systems.

[14] Lenz R, Enders K, Stedmon CA, Mackenzie DMA, Nielsen TG (2015) A critical assessment of visual identification of marine microplastic using raman spectroscopy for analysis improvement. *Marine Pollution Bulletin* 100(1):82–91. https://doi.org/10.1016/j.marpolbul.2015.09.026

[15] Enders K, Lenz R, Stedmon CA, Nielsen TG (2015) Abundance, size and polymer composition of marine microplastics ≥ 10 μm in the atlantic ocean and their modelled vertical distribution. *Marine Pollution Bulletin* 100(1):70–81. https://doi.org/10.1016/j.marpolbul.2015.09.027

[16] Maitz M, Lenz R, Winkler S, Abschke M, Werner C, Fischer D (2025) Weathered microplastics in human blood: Unraveling the effect of structural changes at the particle surface on coagulation and platelet activation. *Microplastics and Nanoplastics* [accepted]. https://doi.org/10.1186/s43591-025-00139-4

[17] Liu M, Brandsma SH, Schreder E (2024) From e-waste to living space: Flame retardants contaminating household items add to concern about plastic recycling. *Chemosphere* 365:143319. https://doi.org/10.1016/j.chemosphere.2024.143319

[18] Liu M, Brandsma SH, Schreder E (2025) Corrigendum to "from e-waste to living space: Flame retardants contaminating household items add to concern about plastic recycling" [chemosphere 365 (2024) 143319]. *Chemosphere* 370:143903. https://doi.org/10.1016/j.chemosphere.2024.143903

[19] Koelmans AA, Besseling E, Foekema E, Kooi M, Mintenig S, Ossendorp BC, Redondo-Hasselerharm PE, Verschoor A, van Wezel AP, Scheffer M (2017) Risks of plastic debris: Unravelling fact, opinion, perception, and belief. *Environmental Science & Technology* 51(20):11513–11519. https://doi.org/10.1021/acs.est.7b02219

[20] Law KL, Sobkowicz MJ, Shaver MP, Hahn ME (2024) Untangling the chemical complexity of plastics to improve life cycle outcomes. *Nature Reviews Materials* 9(9):657–667. https://doi.org/10.1038/s41578-024-00705-x

[21] Monclús L, Arp HPH, Groh KJ, Faltynkova A, Løseth ME, Muncke J, Wang Z, Wolf R, Zimmermann L, Wagner M (2025) Mapping the chemical complexity of plastics. *Nature* 643(8071):349–355. https://doi.org/10.1038/s41586-025-09184-8

[22] United Nations Environment Programme (2014) Resolutions and decisions adopted by the united nations environment assembly of the united nations environment programme at its first session on 27 june 2014. (United Nations Environment Assembly), pp 1–40. Available at https://wedocs.unep.org/bitstream/handle/20.500.11822/17285/K1402364.pdf (Accessed June 30, 2025)

[23] United Nations Environment Programme (2016) United nations environment assembly of the united nations environment programme second session - marine plastic litter and microplastics. (Nairobi), UNEP/EA.2/Res.11, pp 1–4. Available at https://docs.un.org/en/UNEP/EA.2/Res.11 (Accessed June 30, 2025)

[24] United Nations Environment Programme (2017) United nations environment assembly of the united nations environment programme third session - draft resolution on marine litter and microplastics. (United Nations Environment Assembly, Nairobi), UNEP/EA.3/L.20, pp 1–4. Available at https://docs.un.org/en/UNEP/EA.3/L.20 (Accessed June 30, 2025)

[25] United Nations Environment Programme (2022) United nations environment assembly of the united nations environment programme fifth session - resolution adopted by the united nations environment assembly on 2 march 2022 - end plastic pollution: Towards an international legally binding instrument. (United Nations Environment Programme, Nairobi), UNEP/EA.5/Res.14, pp 1–4. Available at https://docs.un.org/en/UNEP/EA.5/Res.14 (Accessed June 30, 2025)

[26] United Nations Environment Programme (2025) Intergovernmental negotiating committee to develop an international legally binding instrument on plastic pollution, including in the marine environment fifth session - draft report of the intergovernmental negotiating committee to develop an international legally binding instrument on plastic pollution, including in the marine environment, on the work of the first part of its fifth session. UNEP/PP/INC.5/8. (United Nations Environment Programme, Busan, Republic of Korea), UNEP/PP/INC.5/8, pp 1–33. Available at https://docs.un.org/en/UNEP/PP/INC.5/8 (Accessed June 22, 2025)

[27] Wilkinson MD, Dumontier M, Aalbersberg IjJ, Appleton G, Axton M, Baak A, Blomberg N, Boiten J-W, Da Silva Santos LB, Bourne PE, Bouwman J, Brookes AJ, Clark T, Crosas M, Dillo I, Dumon O, Edmunds S, Evelo CT, Finkers R, Gonzalez-Beltran A, Gray AJG, Groth P, Goble C, Grethe JS, Heringa J, Hoen PAC 'T, Hooft R, Kuhn T, Kok R, Kok J, Lusher SJ, Martone ME, Mons A, Packer AL, Persson B, Rocca-Serra P, Roos M, Van Schaik R, Sansone S-A, Schultes E, Sengstag T, Slater T, Strawn G, Swertz MA, Thompson M, Van Der Lei J, Van Mulligen E, Velterop J, Waagmeester A, Wittenburg P, Wolstencroft K, Zhao J, Mons B (2016) The FAIR guiding principles for scientific data management and stewardship. *Scientific Data* 3(1):160018. https://doi.org/10.1038/sdata.2016.18

[28] Thompson RC, Olsen Y, Mitchell RP, Davis A, Rowland SJ, John AWG, McGonigle D, Russell AE (2004) Lost at sea: Where is all the plastic? *Science* 304(5672):838–838. https://doi.org/10.1126/science.1094559

[29] Pirc U, Vidmar M, Mozer A, Kržan A (2016) Emissions of microplastic fibers from microfiber fleece during domestic washing. *Environmental Science and Pollution Research* 23(21):22206–22211. https://doi.org/10.1007/s11356-016-7703-0

[30] De Ruijter VN, Redondo-Hasselerharm PE, Koelmans AA (2025) A brief history of microplastics effect testing: Guidance and prospect. *Environmental Pollution* 368:125711. https://doi.org/10.1016/j.envpol.2025.125711

[31] Sussarellu R, Suquet M, Thomas Y, Lambert C, Fabioux C, Pernet MEJ, Le Goïc N, Quillien V, Mingant C, Epelboin Y, Corporeau C, Guyomarch J, Robbens J, Paul-Pont I, Soudant P, Huvet A (2016) Oyster reproduction is affected by exposure to polystyrene microplastics. *Proceedings of the National Academy of Sciences* 113(9):2430–2435. https://doi.org/10.1073/pnas.1519019113

[32] Besseling E, Wang B, Lürling M, Koelmans AA (2014) Nanoplastic affects growth of *S. obliquus* and reproduction of *D. magna*. *Environmental Science & Technology* 48(20):12336–12343. https://doi.org/10.1021/es503001d

[33] Wegner A, Besseling E, Foekema EM, Kamermans P, Koelmans AA (2012) Effects of nanopolystyrene on the feeding behavior of the blue mussel (*Mytilus edulis* l.). *Environmental Toxicology and Chemistry* 31(11):2490–2497. https://doi.org/10.1002/etc.1984

[34] von Moos N, Burkhardt-Holm P, Köhler A (2012) Uptake and effects of microplastics on cells and tissue of the blue mussel *Mytilus edulis* l. After an experimental exposure. *Environmental Science & Technology* 46(20):11327–11335. https://doi.org/10.1021/es302332w

[35] Besseling E, Wegner A, Foekema EM, van den Heuvel-Greve MJ, Koelmans AA (2012) Effects of microplastic on fitness and PCB bioaccumulation by the lugworm *Arenicola marina* (l.). *Environmental Science & Technology* 47(1):593–600. https://doi.org/10.1021/es302763x

[36] Norén F, Naustvoll L-J (2010) Survey of microscopic anthropogenic particles in skagerrak. (N-research and Havforskningsinstituttet, Lysekil, Sweden), TA-2779-2011, p 22. Available at https://www.researchgate.net/publication/309900873_Survey_of_microscopic_anthropogenic_particles_in_skagerrak (Accessed June 22, 2025)

[37] Norén F, Noren K, Magnusson K (2014) Marint mikroskopiskt skräp – undersökning längs svenska västkusten 2013 och 2014. (Länsstyrelsen i Västra Götalands län, vattenvårdsenheten), 2014:52, p 24. Available at https://www.lansstyrelsen.se/download/18.8cd5a1b19362fb4fc2506/1732533661284/Marint%20mikroskopiskt%20skr%C3%A4p%20%E2%80%93%20unders%C3%B6kning%20l%C3%A4ngs%20svenska%20v%C3%A4stkusten%202013%20och%202014.pdf (Accessed June 22, 2025)

[38] Browne MA, Dissanayake A, Galloway TS, Lowe DM, Thompson RC (2008) Ingested microscopic plastic translocates to the circulatory system of the mussel, *Mytilus edulis* (l.). *Environmental Science & Technology* 42(13):5026–5031. https://doi.org/10.1021/es800249a

[39] Lee K-W, Shim WJ, Kwon OY, Kang J-H (2013) Size-dependent effects of micro polystyrene particles in the marine copepod *Tigriopus japonicus*. *Environmental Science & Technology* 47(19):11278–11283. https://doi.org/10.1021/es401932b

[40] Bhattacharya P, Lin S, Turner JP, Ke PC (2010) Physical adsorption of charged plastic nanoparticles affects algal photosynthesis. *The Journal of Physical Chemistry C* 114(39):16556–16561. https://doi.org/10.1021/jp1054759

[41] Priem J, Piwowar H, Orr R (2022) OpenAlex: A fully-open index of scholarly works, authors, venues, institutions, and concepts. https://doi.org/10.48550/ARXIV.2205.01833

[42] Grinberg M (2025) Why generative AI coding tools and agents do not work for me. Available at https://blog.miguelgrinberg.com/post/why-generative-ai-coding-tools-and-agents-do-not-work-for-me (Accessed June 16, 2025)

[43] Cao C, Arora R, Cento P, Manta K, Farahani E, Cecere M, Selemon A, Sang J, Gong LX, Kloosterman R, Jiang S, Saleh R, Margalik D, Lin J, Jomy J, Xie J, Chen D, Gorla J, Lee S, Zhang K, Ware H, Whelan M, Teja B, Leung AA, Ghosn L, Arora RK, Detsky AS, Noetel M, Emerson DB, Boutron I, Moher D, Church G, Bobrovitz N (2025) Automation of systematic reviews with large language models. https://doi.org/10.1101/2025.06.13.25329541

[44] Lenz R (2025) [Data and supplemental materials for a doctoral thesis] on the production, assessment and usage of data in microplastics research. (Universität Rostock). Available at https://doi.org/10.5281/zenodo.15531255

[45] Lattin GL, Moore CJ, Zellers AF, Moore SL, Weisberg SB (2004) A comparison of neustonic plastic and zooplankton at different depths near the southern california shore. *Marine Pollution Bulletin* 49(4):291–294. https://doi.org/10.1016/j.marpolbul.2004.01.020

[46] Norén F (2007) Small plastic particles in coastal swedish waters. (KIMO, Lysekil, Sweden), pp 1–11. Available at https://www.researchgate.net/publication/284312290_Small_plastic_particles_in_Coastal_Swedish_waters (Accessed June 22, 2025)

[47] Law KL, Morét-Ferguson S, Maximenko NA, Proskurowski G, Peacock EE, Hafner J, Reddy CM (2010) Plastic accumulation in the north atlantic subtropical gyre. *Science* 329(5996):1185–1188. https://doi.org/10.1126/science.1192321

[48] Doyle MJ, Watson W, Bowlin NM, Sheavly SB (2010) Plastic particles in coastal pelagic ecosystems of the northeast pacific ocean. *Marine Environmental Research* 71(1):41–52. https://doi.org/10.1016/j.marenvres.2010.10.001

[49] Desforges J-PW, Galbraith M, Dangerfield N, Ross PS (2014) Widespread distribution of microplastics in subsurface seawater in the NE pacific ocean. *Marine Pollution Bulletin* 79(1–2):94–99. https://doi.org/10.1016/j.marpolbul.2013.12.035

[50] Cole M, Webb H, Lindeque PK, Fileman ES, Halsband C, Galloway TS (2014) Isolation of microplastics in biota-rich seawater samples and marine organisms. *Scientific Reports* 4(1):4528. https://doi.org/10.1038/srep04528

[51] Lusher AL, Burke A, O'Connor I, Officer R (2014) Microplastic pollution in the northeast atlantic ocean: Validated and opportunistic sampling. *Marine Pollution Bulletin* 88(1–2):325–333. https://doi.org/10.1016/j.marpolbul.2014.08.023

[52] Cole M, Lindeque P, Fileman E, Halsband C, Goodhead R, Moger J, Galloway TS (2013) Microplastic ingestion by zooplankton. *Environmental Science & Technology* 47(12):6646–6655. https://doi.org/10.1021/es400663f

[53] Cole M, Lindeque P, Fileman E, Halsband C, Galloway TS (2015) The impact of polystyrene microplastics on feeding, function and fecundity in the marine copepod *Calanus helgolandicus*. *Environmental Science & Technology* 49(2):1130–1137. https://doi.org/10.1021/es504525u

[54] Cózar A, Martí E, Duarte CM, García-de-Lomas J, Van Sebille E, Ballatore TJ, Eguíluz VM, González-Gordillo JI, Pedrotti ML, Echevarría F, Troublè R, Irigoien X (2017) The arctic ocean as a dead end for floating plastics in the north atlantic branch of the thermohaline circulation. *Science Advances* 3(4):e1600582. https://doi.org/10.1126/sciadv.1600582

[55] Beer S, Garm A, Huwer B, Dierking J, Nielsen TG (2018) No increase in marine microplastic concentration over the last three decades – a case study from the baltic sea. *Science of The Total Environment* 621:1272–1279. https://doi.org/10.1016/j.scitotenv.2017.10.101

[56] Kroon F, Motti C, Talbot S, Sobral P, Puotinen M (2018) A workflow for improving estimates of microplastic contamination in marine waters: A case study from north-western australia. *Environmental Pollution* 238:26–38. https://doi.org/10.1016/j.envpol.2018.03.010

[57] Kapp KJ, Yeatman E (2018) Microplastic hotspots in the snake and lower columbia rivers: A journey from the greater yellowstone ecosystem to the pacific ocean. *Environmental Pollution* 241:1082–1090. https://doi.org/10.1016/j.envpol.2018.06.033

[58] Saliu F, Montano S, Leoni B, Lasagni M, Galli P (2019) Microplastics as a threat to coral reef environments: Detection of phthalate esters in neuston and scleractinian corals from the faafu atoll, maldives. *Marine Pollution Bulletin* 142:234–241. https://doi.org/10.1016/j.marpolbul.2019.03.043

[59] Jensen LH, Motti CA, Garm AL, Tonin H, Kroon FJ (2019) Sources, distribution and fate of microfibres on the great barrier reef, australia. *Scientific Reports* 9(1):9021. https://doi.org/10.1038/s41598-019-45340-7

[60] Lindeque PK, Cole M, Coppock RL, Lewis CN, Miller RZ, Watts AJR, Wilson-McNeal A, Wright SL, Galloway TS (2020) Are we underestimating microplastic abundance in the marine environment? A comparison of microplastic capture with nets of different mesh-size. *Environmental Pollution* 265:114721. https://doi.org/10.1016/j.envpol.2020.114721

[61] Jian M, Zhang Y, Yang W, Zhou L, Liu S, Xu EG (2020) Occurrence and distribution of microplastics in china's largest freshwater lake system. *Chemosphere* 261:128186. https://doi.org/10.1016/j.chemosphere.2020.128186

[62] Rodrigues D, Antunes J, Otero V, Sobral P, Costa MH (2020) Distribution patterns of microplastics in seawater surface at a portuguese estuary and marine park. *Frontiers in Environmental Science* 8:582217. https://doi.org/10.3389/fenvs.2020.582217

[63] Magni S, Nigro L, Della Torre C, Binelli A (2021) Characterization of plastics and their ecotoxicological effects in the lambro river (n. italy). *Journal of Hazardous Materials* 412:125204. https://doi.org/10.1016/j.jhazmat.2021.125204

[64] Cabanilles P, Acle S, Arias A, Masiá P, Ardura A, Garcia-Vazquez E (2022) Microplastics risk into a three-link food chain inside european hake. *Diversity* 14(5):308. https://doi.org/10.3390/d14050308

[65] Simantiris N, Vardaki MZ, Koralli P, Chochos CL, Gregoriou VG, Kourkoumelis N, Avlonitis M (2022) Seasonal evaluation of floating microplastics in a shallow mediterranean coastal lagoon: Abundance, distribution, chemical composition, and influence of environmental factors. *Estuarine, Coastal and Shelf Science* 272:107859. https://doi.org/10.1016/j.ecss.2022.107859

[66] Gunaalan K, Nielsen TG, Rodríguez Torres R, Lorenz C, Vianello A, Andersen CA, Vollertsen J, Almeda R (2023) Is zooplankton an entry point of microplastics into the marine food web? *Environmental Science & Technology* 57(31):11643–11655. https://doi.org/10.1021/acs.est.3c02575

[67] Deakin K, Savage G, Jones JS, Porter A, Muñoz-Pérez JP, Santillo D, Lewis C (2024) Sea surface microplastics in the galapagos: Grab samples reveal high concentrations of particles <200 μm in size. *Science of The Total Environment* 923:171428. https://doi.org/10.1016/j.scitotenv.2024.171428

[68] Ugwu K, Vianello A, Almeda R, Iordachescu L, Rotander A (2024) Comparison of two pump-based systems for sampling small microplastics (>10 μm) in coastal waters. *Environmental Pollution* 363:125192. https://doi.org/10.1016/j.envpol.2024.125192

[69] Green DS, Boots B, O'Connor NE, Thompson R (2016) Microplastics affect the ecological functioning of an important biogenic habitat. *Environmental Science & Technology* 51(1):68–77. https://doi.org/10.1021/acs.est.6b04496

[70] Zhao L, Qu M, Wong G, Wang D (2017) Transgenerational toxicity of nanopolystyrene particles in the range of μg l^{-1}in the nematode*Caenorhabditis elegans*. *Environmental Science: Nano* 4(12):2356–2366. https://doi.org/10.1039/C7EN00707H

[71] Bergami E, Pugnalini S, Vannuccini ML, Manfra L, Faleri C, Savorelli F, Dawson KA, Corsi I (2017) Long-term toxicity of surface-charged polystyrene nanoplastics to marine planktonic species dunaliella tertiolecta and artemia franciscana. *Aquatic Toxicology* 189:159–169. https://doi.org/10.1016/j.aquatox.2017.06.008

[72] Chae Y, Kim D, Kim SW, An Y-J (2018) Trophic transfer and individual impact of nano-sized polystyrene in a four-species freshwater food chain. *Scientific Reports* 8(1):284. https://doi.org/10.1038/s41598-017-18849-y

[73] Mao Y, Ai H, Chen Y, Zhang Z, Zeng P, Kang L, Li W, Gu W, He Q, Li H (2018) Phytoplankton response to polystyrene microplastics: Perspective from an entire growth period. *Chemosphere* 208:59–68. https://doi.org/10.1016/j.chemosphere.2018.05.170

[74] Caruso G, Pedà C, Cappello S, Leonardi M, La Ferla R, Lo Giudice A, Maricchiolo G, Rizzo C, Maimone G, Rappazzo AC, Genovese L, Romeo T (2018) Effects of microplastics on trophic parameters, abundance and metabolic activities of seawater and fish gut bacteria in mesocosm conditions. *Environmental Science and Pollution Research* 25(30):30067–30083. https://doi.org/10.1007/s11356-018-2926-x

[75] Al-Sid-Cheikh M, Rowland SJ, Stevenson K, Rouleau C, Henry TB, Thompson RC (2018) Uptake, whole-body distribution, and depuration of nanoplastics by the scallop *Pecten maximus* at environmentally realistic concentrations. *Environmental Science & Technology* 52(24):14480–14486. https://doi.org/10.1021/acs.est.8b05266

[76] Bosker T, Bouwman LJ, Brun NR, Behrens P, Vijver MG (2019) Microplastics accumulate on pores in seed capsule and delay germination and root growth of the terrestrial vascular plant lepidium sativum. *Chemosphere* 226:774–781. https://doi.org/10.1016/j.chemosphere.2019.03.163

[77] Coppock RL, Galloway TS, Cole M, Fileman ES, Queirós AM, Lindeque PK (2019) Microplastics alter feeding selectivity and faecal density in the copepod, calanus helgolandicus. *Science of The Total Environment* 687:780–789. https://doi.org/10.1016/j.scitotenv.2019.06.009

[78] Wang J, Li Y, Lu L, Zheng M, Zhang X, Tian H, Wang W, Ru S (2019) Polystyrene microplastics cause tissue damages, sex-specific reproductive disruption and transgenerational effects in marine medaka (oryzias melastigma). *Environmental Pollution* 254:113024. https://doi.org/10.1016/j.envpol.2019.113024

[79] Liu Z, Cai M, Wu D, Yu P, Jiao Y, Jiang Q, Zhao Y (2020) Effects of nanoplastics at predicted environmental concentration on daphnia pulex after exposure through multiple generations. *Environmental Pollution* 256:113506. https://doi.org/10.1016/j.envpol.2019.113506

[80] Amereh F, Babaei M, Eslami A, Fazelipour S, Rafiee M (2020) The emerging risk of exposure to nano(micro)plastics on endocrine disturbance and reproductive toxicity: From a hypothetical scenario to a global public health challenge. *Environmental Pollution* 261:114158. https://doi.org/10.1016/j.envpol.2020.114158

[81] Yan W, Hamid N, Deng S, Jia P-P, Pei D-S (2020) Individual and combined toxicogenetic effects of microplastics and heavy metals (cd, pb, and zn) perturb gut microbiota homeostasis and gonadal development in marine medaka (oryzias melastigma). *Journal of Hazardous Materials* 397:122795. https://doi.org/10.1016/j.jhazmat.2020.122795

[82] Cole M, Liddle C, Consolandi G, Drago C, Hird C, Lindeque PK, Galloway TS (2020) Microplastics, microfibres and nanoplastics cause variable sub-lethal responses in mussels (mytilus spp.). *Marine Pollution Bulletin* 160:111552. https://doi.org/10.1016/j.marpolbul.2020.111552

[83] Yang X, He Q, Guo F, Sun X, Zhang J, Chen M, Vymazal J, Chen Y (2020) Nanoplastics disturb nitrogen removal in constructed wetlands: Responses of microbes and macrophytes. *Environmental Science & Technology* 54(21):14007–14016. https://doi.org/10.1021/acs.est.0c03324

[84] Zhang X, Wen K, Ding D, Liu J, Lei Z, Chen X, Ye G, Zhang J, Shen H, Yan C, Dong S, Huang Q, Lin Y (2021) Size-dependent adverse effects of microplastics on intestinal microbiota and metabolic homeostasis in the marine medaka (oryzias melastigma). *Environment International* 151:106452. https://doi.org/10.1016/j.envint.2021.106452

[85] Liang B, Zhong Y, Huang Y, Lin X, Liu J, Lin L, Hu M, Jiang J, Dai M, Wang B, Zhang B, Meng H, Lelaka JJJ, Sui H, Yang X, Huang Z (2021) Underestimated health risks: Polystyrene micro- and nanoplastics jointly induce intestinal barrier dysfunction by ROS-mediated epithelial cell apoptosis. *Particle and Fibre Toxicology* 18(1):20. https://doi.org/10.1186/s12989-021-00414-1

[86] Lee Y, Yoon D-S, Lee YH, Kwak JI, An Y-J, Lee J-S, Park JC (2021) Combined exposure to microplastics and zinc produces sex-specific responses in the water flea daphnia magna. *Journal of Hazardous Materials* 420:126652. https://doi.org/10.1016/j.jhazmat.2021.126652

[87] Liang B, Huang Y, Zhong Y, Li Z, Ye R, Wang B, Zhang B, Meng H, Lin X, Du J, Hu M, Wu Q, Sui H, Yang X, Huang Z (2022) Brain single-nucleus transcriptomics highlights that polystyrene nanoplastics potentially induce parkinson's disease-like neurodegeneration by causing energy metabolism disorders in mice. *Journal of Hazardous Materials* 430:128459. https://doi.org/10.1016/j.jhazmat.2022.128459

[88] Teng M, Zhao X, Wang C, Wang C, White JC, Zhao W, Zhou L, Duan M, Wu F (2022) Polystyrene nanoplastics toxicity to zebrafish: Dysregulation of the brain–intestine–microbiota axis. *ACS Nano* 16(5):8190–8204. https://doi.org/10.1021/acsnano.2c01872

[89] Medriano CA, Bae S (2022) Acute exposure to microplastics induces metabolic disturbances and gut dysbiosis in adult zebrafish (danio rerio). *Ecotoxicology and Environmental Safety* 245:114125. https://doi.org/10.1016/j.ecoenv.2022.114125

[90] Deng Y, Chen H, Huang Y, Zhang Y, Ren H, Fang M, Wang Q, Chen W, Hale RC, Galloway TS, Chen D (2022) Long-term exposure to environmentally relevant doses of large polystyrene microplastics disturbs lipid homeostasis via bowel function interference. *Environmental Science & Technology* 56(22):15805–15817. https://doi.org/10.1021/acs.est.1c07933

[91] Bandekar M, Abdolahpur Monikh F, Kekäläinen J, Tahvanainen T, Kortet R, Zhang P, Guo Z, Akkanen J, Leskinen JTT, Gomez-Gonzalez MA, Krishna Darbha G, Grossart H-P, Valsami-Jones E, Kukkonen JVK (2022) Submicron plastic adsorption by peat, accumulation in sphagnum mosses and influence on bacterial communities in peatland ecosystems. *Environmental Science & Technology* 56(22):15661–15671. https://doi.org/10.1021/acs.est.2c04892

[92] Wu H, Liu Q, Yang N, Xu S (2023) Polystyrene-microplastics and DEHP co-exposure induced DNA damage, cell cycle arrest and necroptosis of ovarian granulosa cells in mice by promoting ROS production. *Science of The Total Environment* 871:161962. https://doi.org/10.1016/j.scitotenv.2023.161962

[93] Ding P, Xiang C, Li X, Chen H, Shi X, Li X, Huang C, Yu Y, Qi J, Li AJ, Zhang L, Hu G (2023) Photoaged microplastics induce neurotoxicity via oxidative stress and abnormal neurotransmission in zebrafish larvae (danio rerio). *Science of The Total Environment* 881:163480. https://doi.org/10.1016/j.scitotenv.2023.163480

[94] Liu Z, Hua X, Zhao Y, Bian Q, Wang D (2024) Polyethylene nanoplastics cause reproductive toxicity associated with activation of both estrogenic hormone receptor NHR-14 and DNA damage checkpoints in c. elegans. *Science of The Total Environment* 906:167471. https://doi.org/10.1016/j.scitotenv.2023.167471

[95] Xu H, Wang J, Wang Q, Tu W, Jin Y (2024) Co-exposure to polystyrene microplastics and cypermethrin enhanced the effects on hepatic phospholipid metabolism and gut microbes in adult zebrafish. *Journal of Hazardous Materials* 465:133051. https://doi.org/10.1016/j.jhazmat.2023.133051

[96] Li L, Lv X, He J, Zhang L, Li B, Zhang X, Liu S, Zhang Y (2024) Chronic exposure to polystyrene nanoplastics induces intestinal mechanical and immune barrier dysfunction in mice. *Ecotoxicology and Environmental Safety* 269:115749. https://doi.org/10.1016/j.ecoenv.2023.115749

[97] Shao Y, Hua X, Li Y, Wang D (2024) Comparison of reproductive toxicity between pristine and aged polylactic acid microplastics in caenorhabditis elegans. *Journal of Hazardous Materials* 466:133545. https://doi.org/10.1016/j.jhazmat.2024.133545

[98] Li W, Zeng J, Zheng N, Ge C, Li Y, Yao H (2024) Polyvinyl chloride microplastics in the aquatic environment enrich potential pathogenic bacteria and spread antibiotic resistance genes in the fish gut. *Journal of Hazardous Materials* 475:134817. https://doi.org/10.1016/j.jhazmat.2024.134817

[99] Wu J, Shao Y, Hua X, Wang Y, Wang D (2024) Nanoplastic at environmentally relevant concentrations induces toxicity across multiple generations associated with inhibition in germline g protein-coupled receptor CED-1 in caenorhabditis elegans. *Chemosphere* 364:143011. https://doi.org/10.1016/j.chemosphere.2024.143011

[100] Liu S, Huang X, Han J, Yao L, Li H, Xin G, Ho S-H, Zhao J, Xing B (2024) Genome-wide molecular adaptation in algal primary productivity induced by prolonged exposure to environmentally realistic concentration of nanoplastics. *ACS Nano* 18(43):29820–29831. https://doi.org/10.1021/acsnano.4c09709

[101] Liu L, Ma Y, Xu Y, Liu B, Wang C, Feng J, Li M, Yin H, Sun L, Li P, Li Z-H (2024) Mechanisms of eco-corona effects on micro(nano)plastics in marine medaka: Insights into translocation, immunity, and energy metabolism. *Journal of Hazardous Materials* 480:136236. https://doi.org/10.1016/j.jhazmat.2024.136236

[102] Xiong Z, Kong Q, Hua J, Chen Q, Wang D (2025) Cardiotoxicity of polystyrene nanoplastics and associated mechanism of myocardial cell injury in mice. *Ecotoxicology and Environmental Safety* 290:117712. https://doi.org/10.1016/j.ecoenv.2025.117712

[103] Thornton Hampton LM, Lowman H, Coffin S, Darin E, De Frond H, Hermabessiere L, Miller E, De Ruijter VN, Faltynkova A, Kotar S, Monclús L, Siddiqui S, Völker J, Brander S, Koelmans AA, Rochman CM, Wagner M, Mehinto AC (2022) A living tool for the continued exploration of microplastic toxicity. *Microplastics and Nanoplastics* 2(1):13. https://doi.org/10.1186/s43591-022-00032-4

[104] SAPEA (2019) *A scientific perspective on microplastics in nature and society* (SAPEA, DE). Available at https://doi.org/10.26356/microplastics (Accessed August 9, 2025)

[105] Hermsen E, Mintenig SM, Besseling E, Koelmans AA (2018) Quality criteria for the analysis of microplastic in biota samples: A critical review. *Environmental Science & Technology* 52(18):10230–10240. https://doi.org/10.1021/acs.est.8b01611

[106] Koelmans AA, Nor NHM, Hermsen E, Kooi M, Mintenig S (2019) Microplastics in freshwaters and drinking water: Critical review and assessment of data quality. *Water Research* 155:410–422. https://doi.org/10.1016/j.watres.2019.02.054

[107] Nyadjro ES, Webster JAB, Boyer TP, Cebrian J, Collazo L, Kaltenberger G, Larsen K, Lau YH, Mickle P, Toft T, Wang Z (2023) The NOAA NCEI marine microplastics database. *Scientific Data* 10(1):726. https://doi.org/10.1038/s41597-023-02632-y

[108] Bergmann M, Tekman MB, Walter A, Gutow L (2018) Tackling marine litter—LITTERBASE. *Building Bridges at the Science-Stakeholder Interface*, ed Krause G (Springer International Publishing, Cham), pp 85–92. https://doi.org/10.1007/978-3-319-75919-7_13

[109] Wilkens JL, Calomeni-Eck AJ, Boyda J, Kennedy A, McQueen AD (2024) Microplastic in dredged sediments: From databases to strategic responses. *Bulletin of Environmental Contamination and Toxicology* 112(5):72. https://doi.org/10.1007/s00128-024-03878-x

[110] Wagner M, Monclús L, Arp HPH, Groh KJ, Løseth ME, Muncke J, Wang Z, Wolf R, Zimmermann L (2025) State of the science on plastic chemicals - identifying and addressing chemicals and polymers of concern. (Zenodo). https://doi.org/10.5281/ZENODO.10701705

[111] Cowger W, Steinmetz Z, Gray A, Munno K, Lynch J, Hapich H, Primpke S, De Frond H, Rochman C, Herodotou O (2021) Microplastic spectral classification needs an open source community: Open specy to the rescue! *Analytical Chemistry* 93(21):7543–7548. https://doi.org/10.1021/acs.analchem.1c00123

[112] Munno K, De Frond H, O'Donnell B, Rochman CM (2020) Increasing the accessibility for characterizing microplastics: Introducing new application-based and spectral libraries of plastic particles (SLoPP and SLoPP-e). *Analytical Chemistry* 92(3):2443–2451. https://doi.org/10.1021/acs.analchem.9b03626

[113] De Frond H, Rubinovitz R, Rochman CM (2021) μATR-FTIR spectral libraries of plastic particles (FLOPP and FLOPP-e) for the analysis of microplastics. *Analytical Chemistry* 93(48):15878–15885. https://doi.org/10.1021/acs.analchem.1c02549

[114] Luo Z (2020) A raman database of microplastics weathered under natural environments. https://doi.org/10.17632/KPYGRF9FG6.1

[115] Villegas-Camacho O, Alejo-Eleuterio R, Francisco-Valencia I, Granda-Gutiérrez E, Martínez-Gallegos S, Illescas J (2024) FTIR-plastics: A fourier transform infrared spectroscopy dataset for the six most prevalent industrial plastic polymers. *Data in Brief* 55:110612. https://doi.org/10.1016/j.dib.2024.110612

[116] Villegas Camacho O, Alejo Eleuterio R, Francisco Valencia I, Granda Gutiérrez E, Mártinez Gallegos S, Illescas J (2024) FTIR-plastics: A fourier transform infrared spectroscopy dataset for the six most prevalent industrial plastic polymers. https://doi.org/10.5281/ZENODO.10736650

[117] Dawson AL, Santana MFM, Nelis JLD, Motti CA (2023) Taking control of microplastics data: A comparison of control and blank data correction methods. *Journal of Hazardous Materials* 443:130218. https://doi.org/10.1016/j.jhazmat.2022.130218

[118] Hapich H, Cowger W, Gray AB (2024) Microplastics and trash cleaning and harmonization (MaTCH): Semantic data ingestion and harmonization using artificial intelligence. *Environmental Science & Technology* 58(46):20502–20512. https://doi.org/10.1021/acs.est.4c02406

[119] Jacob O, Ramírez-Piñero A, Elsner M, Ivleva NP (2023) *TUM-ParticleTyper 2*: Software and documentation. https://doi.org/10.14459/2023MP1707179.001

[120] Jacob O, Ramírez-Piñero A, Elsner M, Ivleva NP (2023) TUM-ParticleTyper 2: Automated quantitative analysis of (microplastic) particles and fibers down to 1 $${\upmu }$$m by raman microspectroscopy. *Analytical and Bioanalytical Chemistry* 415(15):2947–2961. https://doi.org/10.1007/s00216-023-04712-9

[121] Von Der Esch E, Kohles AJ, Anger PM, Hoppe R, Niessner R, Elsner M, Ivleva NP (2020) TUM-ParticleTyper: A detection and quantification tool for automated analysis of (microplastic) particles and fibers. *PLOS ONE* 15(6):e0234766. https://doi.org/10.1371/journal.pone.0234766

[122] Primpke S, Cross RK, Mintenig SM, Simon M, Vianello A, Gerdts G, Vollertsen J (2020) Toward the systematic identification of microplastics in the environment: Evaluation of a new independent software tool (siMPle) for spectroscopic analysis. *Applied Spectroscopy* 74(9):1127–1138. https://doi.org/10.1177/0003702820917760

[123] Hufnagl B, Steiner D, Renner E, Löder MGJ, Laforsch C, Lohninger H (2019) A methodology for the fast identification and monitoring of microplastics in environmental samples using random decision forest classifiers. *Analytical Methods* 11(17):2277–2285. https://doi.org/10.1039/C9AY00252A

[124] Hufnagl B, Stibi M, Martirosyan H, Wilczek U, Möller JN, Löder MGJ, Laforsch C, Lohninger H (2022) Computer-assisted analysis of microplastics in environmental samples based on μFTIR imaging in combination with machine learning. *Environmental Science & Technology Letters* 9(1):90–95. https://doi.org/10.1021/acs.estlett.1c00851

[125] Ramanna S, Morozovskii D, Swanson S, Bruneau J (2023) Machine learning of polymer types from the spectral signature of raman spectroscopy microplastics data. *Advances in Artificial Intelligence and Machine Learning* 03(01):647–668. https://doi.org/10.54364/AAIML.2023.1144

[126] Yan X, Cao Z, Murphy A, Ye Y, Wang X, Qiao Y (2023) FRDA: Fingerprint region based data augmentation using explainable AI for FTIR based microplastics classification. *Science of The Total Environment* 896:165340. https://doi.org/10.1016/j.scitotenv.2023.165340

[127] Williams WA, Aravamudhan S (2025) Reliability testing of machine learning model prediction capability towards unidentifiable microplastic spectral data: Triple battery and colorant investigation. *Microplastics and Nanoplastics* 5(1):1. https://doi.org/10.1186/s43591-024-00107-4

[128] Li F, Liu D, Guo X, Zhang Z, Martin FL, Lu A, Xu L (2024) Identification and visualization of environmental microplastics by raman imaging based on hyperspectral unmixing coupled machine learning. *Journal of Hazardous Materials* 465:133336. https://doi.org/10.1016/j.jhazmat.2023.133336

[129] Merlemis N, Drakaki E, Zekou E, Ninos G, Kesidis AL (2024) Laser induced fluorescence and machine learning: A novel approach to microplastic identification. *Applied Physics B* 130(9):168. https://doi.org/10.1007/s00340-024-08308-8

[130] Brandt J, Mattsson K, Hassellöv M (2021) Deep learning for reconstructing low-quality FTIR and raman spectra-a case study in microplastic analyses. *Analytical Chemistry*. https://doi.org/10.1021/acs.analchem.1c02618

[131] Mukherjee F, Shi A, Wang X, You F, Abbott NL (2022) Liquid crystals as multifunctional interfaces for trapping and characterizing microplastics. https://doi.org/10.48550/ARXIV.2209.15440

[132] Phan S, Torrejon D, Furseth J, Mee E, Luscombe C (2023) Exploiting weak supervision to facilitate segmentation, classification, and analysis of microplastics (<100 μm) using raman microspectroscopy images. *Science of The Total Environment* 886:163786. https://doi.org/10.1016/j.scitotenv.2023.163786

[133] Priyanto A, Hapidin DA, Edikresnha D, Aji MP, Khairurrijal K (2025) Predicting microplastic quantities in indonesian provincial rivers using machine learning models. *Science of The Total Environment* 961:178411. https://doi.org/10.1016/j.scitotenv.2025.178411

[134] Zhen Y, Wang L, Sun H, Liu C (2023) Prediction of microplastic abundance in surface water of the ocean and influencing factors based on ensemble learning. *Environmental Pollution* 331:121834. https://doi.org/10.1016/j.envpol.2023.121834

[135] Chen B, Zhang Z, Wang T, Hu H, Qin G, Lu T, Hong W, Hu J, Penuelas J, Qian H (2023) Global distribution of marine microplastics and potential for biodegradation. *Journal of Hazardous Materials* 451:131198. https://doi.org/10.1016/j.jhazmat.2023.131198

[136] Tran H-T, Hadi M, Nguyen TTH, Hoang HG, Nguyen M-K, Nguyen KN, Vo D-VN (2023) Machine learning approaches for predicting microplastic pollution in peatland areas. *Marine Pollution Bulletin* 194:115417. https://doi.org/10.1016/j.marpolbul.2023.115417

[137] Kooi M, Koelmans AA (2019) Simplifying microplastic via continuous probability distributions for size, shape, and density. *Environmental Science & Technology Letters* 6(9):551–557. https://doi.org/10.1021/acs.estlett.9b00379

[138] Clough ME, Ochoa Rivera E, Parham RL, Ault AP, Zimmerman PM, McNeil AJ, Tewari A (2024) Enhancing confidence in microplastic spectral identification via conformal prediction. *Environmental Science & Technology* 58(49):21740–21749. https://doi.org/10.1021/acs.est.4c05167

[139] Hartmann NB, Hüffer T, Thompson RC, Hassellöv M, Verschoor A, Daugaard AE, Rist S, Karlsson T, Brennholt N, Cole M, Herrling MP, Hess MC, Ivleva NP, Lusher AL, Wagner M (2019) Are we speaking the same language? Recommendations for a definition and categorization framework for plastic debris. *Environmental Science & Technology* 53(3):1039–1047. https://doi.org/10.1021/acs.est.8b05297

[140] Koelmans AA, Redondo-Hasselerharm PE, Mohamed Nor NH, Kooi M (2020) Solving the nonalignment of methods and approaches used in microplastic research to consistently characterize risk. *Environmental Science & Technology* 54(19):12307–12315. https://doi.org/10.1021/acs.est.0c02982

[141] Carpenter EJ, Smith KL (1972) Plastics on the sargasso sea surface. *Science* 175(4027):1240–1241. https://doi.org/10.1126/science.175.4027.1240

[142] Carpenter EJ, Anderson SJ, Harvey GR, Miklas HP, Peck BB (1972) Polystyrene spherules in coastal waters. *Science* 178(4062):749–750. https://doi.org/10.1126/science.178.4062.749

[143] Morris AW, Hamilton EI (1974) Polystyrene spherules in the bristol channel. *Marine Pollution Bulletin* 5(2):26–27. https://doi.org/10.1016/0025-326X(74)90311-7

[144] Shaw DG (1977) Pelagic tar and plastic in the gulf of alaska and bering sea: 1975. *Science of The Total Environment* 8(1):13–20. https://doi.org/10.1016/0048-9697(77)90058-4

[145] Gregory MR (1978) Accumulation and distribution of virgin plastic granules on new zealand beaches. *New Zealand Journal of Marine and Freshwater Research* 12(4):399–414. https://doi.org/10.1080/00288330.1978.9515768

[146] Shaw DG, Mapes GA (1979) Surface circulation and the distribution of pelagic tar and plastic. *Marine Pollution Bulletin* 10(6):160–162. https://doi.org/10.1016/0025-326X(79)90421-1

[147] Gregory MR (1983) Virgin plastic granules on some beaches of eastern canada and bermuda. *Marine Environmental Research* 10(2):73–92. https://doi.org/10.1016/0141-1136(83)90011-9

[148] Shaw DG, Day RH (1994) Colour- and form-dependent loss of plastic micro-debris from the north pacific ocean. *Marine Pollution Bulletin* 28(1):39–43. https://doi.org/10.1016/0025-326X(94)90184-8

[149] Gregory MR (1996) Plastic "scrubbers" in hand cleansers: A further (and minor) source for marine pollution identified. *Marine Pollution Bulletin* 32(12):867–871. https://doi.org/10.1016/S0025-326X(96)00047-1

[150] Moore CJ, Moore SL, Leecaster MK, Weisberg SB (2001) A comparison of plastic and plankton in the north pacific central gyre. *Marine Pollution Bulletin* 42(12):1297–1300. https://doi.org/10.1016/S0025-326X(01)00114-X

[151] Moore CJ, Moore SL, Weisberg SB, Lattin GL, Zellers AF (2002) A comparison of neustonic plastic and zooplankton abundance in southern california's coastal waters. *Marine Pollution Bulletin* 44(10):1035–1038. https://doi.org/10.1016/S0025-326X(02)00150-9

[152] Triebskorn R, Braunbeck T, Grummt T, Hanslik L, Huppertsberg S, Jekel M, Knepper TP, Krais S, Müller YK, Pittroff M, Ruhl AS, Schmieg H, Schür C, Strobel C, Wagner M, Zumbülte N, Köhler H-R (2019) Relevance of nano- and microplastics for freshwater ecosystems: A critical review. *TrAC Trends in Analytical Chemistry* 110:375–392. https://doi.org/10.1016/j.trac.2018.11.023

[153] Möller JN, Löder MGJ, Laforsch C (2020) Finding microplastics in soils: A review of analytical methods. *Environmental Science & Technology* 54(4):2078–2090. https://doi.org/10.1021/acs.est.9b04618

[154] Yang L, Zhang Y, Kang S, Wang Z, Wu C (2021) Microplastics in freshwater sediment: A review on methods, occurrence, and sources. *Science of The Total Environment* 754:141948. https://doi.org/10.1016/j.scitotenv.2020.141948

[155] Zhang Y, Kang S, Allen S, Allen D, Gao T, Sillanpää M (2020) Atmospheric microplastics: A review on current status and perspectives. *Earth-Science Reviews* 203:103118. https://doi.org/10.1016/j.earscirev.2020.103118

[156] Allen D, Allen S, Abbasi S, Baker A, Bergmann M, Brahney J, Butler T, Duce RA, Eckhardt S, Evangeliou N, Jickells T, Kanakidou M, Kershaw P, Laj P, Levermore J, Li D, Liss P, Liu K, Mahowald N, Masque P, Materić D, Mayes AG, McGinnity P, Osvath I, Prather KA, Prospero JM, Revell LE, Sander SG, Shim WJ, Slade J, Stein A, Tarasova O, Wright S (2022) Microplastics and nanoplastics in the marine-atmosphere environment. *Nature Reviews Earth & Environment* 3(6):393–405. https://doi.org/10.1038/s43017-022-00292-x

[157] O'Brien S, Rauert C, Ribeiro F, Okoffo ED, Burrows SD, O'Brien JW, Wang X, Wright SL, Thomas KV (2023) There's something in the air: A review of sources, prevalence and behaviour of microplastics in the atmosphere. *Science of The Total Environment* 874:162193. https://doi.org/10.1016/j.scitotenv.2023.162193

[158] Hamilton BM, Jantunen L, Bergmann M, Vorkamp K, Aherne J, Magnusson K, Herzke D, Granberg M, Hallanger IG, Gomiero A, Peeken I (2022) Monitoring microplastics in the atmosphere and cryosphere in the circumpolar north: A case for multi-compartment monitoring. *Arctic Science*:AS-2021-0054. https://doi.org/10.1139/AS-2021-0054

[159] Aves AR, Revell LE, Gaw S, Ruffell H, Schuddeboom A, Wotherspoon NE, LaRue M, McDonald AJ (2022) First evidence of microplastics in antarctic snow. *The Cryosphere* 16(6):2127–2145. https://doi.org/10.5194/tc-16-2127-2022

[160] Wang L, Nabi G, Yin L, Wang Y, Li S, Hao Z, Li D (2021) Birds and plastic pollution: Recent advances. *Avian Research* 12(1):59. https://doi.org/10.1186/s40657-021-00293-2

[161] Müller C (2021) Not as bad as it seems? A literature review on the case of microplastic uptake in fish. *Frontiers in Marine Science* 8:672768. https://doi.org/10.3389/fmars.2021.672768

[162] Leslie HA, Van Velzen MJM, Brandsma SH, Vethaak AD, Garcia-Vallejo JJ, Lamoree MH (2022) Discovery and quantification of plastic particle pollution in human blood. *Environment International* 163:107199. https://doi.org/10.1016/j.envint.2022.107199

[163] Cox KD, Covernton GA, Davies HL, Dower JF, Juanes F, Dudas SE (2019) Human consumption of microplastics. *Environmental Science & Technology* 53(12):7068–7074. https://doi.org/10.1021/acs.est.9b01517

[164] Hernandez LM, Xu EG, Larsson HCE, Tahara R, Maisuria VB, Tufenkji N (2019) Plastic teabags release billions of microparticles and nanoparticles into tea. *Environmental Science & Technology* 53(21):12300–12310. https://doi.org/10.1021/acs.est.9b02540

[165] Mortensen NP, Fennell TR, Johnson LM (2021) Unintended human ingestion of nanoplastics and small microplastics through drinking water, beverages, and food sources. *NanoImpact* 21:100302. https://doi.org/10.1016/j.impact.2021.100302

[166] Jin M, Wang X, Ren T, Wang J, Shan J (2021) Microplastics contamination in food and beverages: Direct exposure to humans. *Journal of Food Science* 86(7):2816–2837. https://doi.org/10.1111/1750-3841.15802

[167] Passos RS, Davenport A, Busquets R, Selden C, Silva LB, Baptista JS, Barceló D, Campos LC (2023) Microplastics and nanoplastics in haemodialysis waters: Emerging threats to be in our radar. *Environmental Toxicology and Pharmacology* 102:104253. https://doi.org/10.1016/j.etap.2023.104253

[168] Napper IE, Bakir A, Rowland SJ, Thompson RC (2015) Characterisation, quantity and sorptive properties of microplastics extracted from cosmetics. *Marine Pollution Bulletin* 99(1–2):178–185. https://doi.org/10.1016/j.marpolbul.2015.07.029

[169] Cowger W, Gray AB, Christiansen S, DeFrond H, Deshpande AD, Hermabessiere L, Lee E, Mill L, Munno K, Ossmann BE, Pittroff M, Rochman CM, Sarau G, Tarby S, Primpke S (2020) Critical review of processing and classification techniques for images and spectra in microplastic research. *Applied Spectroscopy* 74(9):989–1010. https://doi.org/10.1177/0003702820929064

[170] Al-Azzawi MSM, Mohammed S. M. Al-Azzawi, Kefer S, Weisser J, Weißer J, Reichel J, Schwaller C, Glas K, Knoop O, Knoop O, Drewes JE (2020) Validation of sample preparation methods for microplastic analysis in wastewater matrices—reproducibility and standardization. *Water* 12(9):2445. https://doi.org/10.3390/w12092445

[171] Budimir S, Stjepan Budimir, Setälä O, Lehtiniemi M (2018) Effective and easy to use extraction method shows low numbers of microplastics in offshore planktivorous fish from the northern baltic sea. *Marine Pollution Bulletin* 127:586–592. https://doi.org/10.1016/j.marpolbul.2017.12.054

[172] Claessens M, Van Cauwenberghe L, Vandegehuchte MB, Janssen CR (2013) New techniques for the detection of microplastics in sediments and field collected organisms. *Marine Pollution Bulletin* 70(1–2):227–33. https://doi.org/10.1016/j.marpolbul.2013.03.009

[173] Dehaut A, Cassone A-L, Frère L, Hermabessiere L, Himber C, Rinnert E, Rivière G, Lambert C, Soudant P, Huvet A, Duflos G, Paul-Pont I (2016) Microplastics in seafood: Benchmark protocol for their extraction and characterization. *Environmental Pollution* 215:223–233. https://doi.org/10.1016/J.ENVPOL.2016.05.018

[174] Hurley RR, Lusher AL, Olsen M, Nizzetto L (2018) Validation of a method for extracting microplastics from complex, organic-rich, environmental matrices. *Environmental Science & Technology* 52(13):7409–7417. https://doi.org/10.1021/acs.est.8b01517

[175] Kühn S, van Werven B, van Oyen A, Meijboom A, Bravo Rebolledo EL, van Franeker JA (2017) The use of potassium hydroxide (KOH) solution as a suitable approach to isolate plastics ingested by marine organisms. *Marine Pollution Bulletin* 115(1–2):86–90. https://doi.org/10.1016/j.marpolbul.2016.11.034

[176] Lares M, Ncibi MC, Markus Sillanpää, Sillanpää M, Sillanpää M (2019) Intercomparison study on commonly used methods to determine microplastics in wastewater and sludge samples. *Environmental Science and Pollution Research* 26(12):12109–12122. https://doi.org/10.1007/s11356-019-04584-6

[177] Löder MGJ, Imhof HK, Ladehoff M, Löschel LA, Lorenz C, Mintenig S, Piehl S, Primpke S, Schrank I, Laforsch C, Gerdts G (2017) Enzymatic purification of microplastics in environmental samples. *Environmental Science & Technology* 51(24):14283–14292. https://doi.org/10.1021/acs.est.7b03055

[178] Munno K, Helm PA, Jackson DA, Rochman C, Sims A (2018) Impacts of temperature and selected chemical digestion methods on microplastic particles. *Environmental Toxicology and Chemistry* 37(1):91–98. https://doi.org/10.1002/etc.3935

[179] Pfeiffer F, Elke Kerstin Fischer, Fischer EK (2020) Various digestion protocols within microplastic sample processing—evaluating the resistance of different synthetic polymers and the efficiency of biogenic organic matter destruction. *Frontiers in Environmental Science* 8. https://doi.org/10.3389/fenvs.2020.572424

[180] De Frond H, Thornton Hampton L, Kotar S, Gesulga K, Matuch C, Lao W, Weisberg SB, Wong CS, Rochman CM (2022) Monitoring microplastics in drinking water: An interlaboratory study to inform effective methods for quantifying and characterizing microplastics. *Chemosphere* 298:134282. https://doi.org/10.1016/j.chemosphere.2022.134282

[181] Langknecht T, Lao W, Wong CS, Kotar S, El Khatib D, Robinson S, Burgess RM, Ho KT (2023) Comparison of two procedures for microplastics analysis in sediments based on an interlaboratory exercise. *Chemosphere* 313:137479. https://doi.org/10.1016/j.chemosphere.2022.137479

[182] van Mourik LM, Crum S, Martinez-Frances E, van Bavel B, Leslie HA, de Boer J, Cofino WP (2021) Results of WEPAL-QUASIMEME/NORMANs first global interlaboratory study on microplastics reveal urgent need for harmonization. *Science of The Total Environment* 772:145071. https://doi.org/10.1016/j.scitotenv.2021.145071

[183] Thornton Hampton LM, De Frond H, Gesulga K, Kotar S, Lao W, Matuch C, Weisberg SB, Wong CS, Brander S, Christansen S, Cook CR, Du F, Ghosal S, Gray AB, Hankett J, Helm PA, Ho KT, Kefela T, Lattin G, Lusher A, Mai L, McNeish RE, Mina O, Minor EC, Primpke S, Rickabaugh K, Renick VC, Singh S, van Bavel B, Vollnhals F, Rochman CM (2023) The influence of complex matrices on method performance in extracting and monitoring for microplastics. *Chemosphere* 334:138875. https://doi.org/10.1016/j.chemosphere.2023.138875

[184] Wagner J, Robberson W, Allen H (2022) Analytical precision assessment for microplastic analyses. *Chemosphere* 304:135295. https://doi.org/10.1016/j.chemosphere.2022.135295

[185] Zhu M, Wang J, Yang X, Zhang Y, Zhang L, Ren H, Wu B, Ye L (2022) A review of the application of machine learning in water quality evaluation. *Eco-Environment & Health* 1(2):107–116. https://doi.org/10.1016/j.eehl.2022.06.001

[186] Bergen KJ, Johnson PA, De Hoop MV, Beroza GC (2019) Machine learning for data-driven discovery in solid earth geoscience. *Science* 363(6433):eaau0323. https://doi.org/10.1126/science.aau0323

[187] Coleman BR (2025) An introduction to machine learning tools for the analysis of microplastics in complex matrices. *Environmental Science: Processes & Impacts* 27(1):10–23. https://doi.org/10.1039/D4EM00605D

[188] Su J, Zhang F, Yu C, Zhang Y, Wang J, Wang C, Wang H, Jiang H (2023) Machine learning: Next promising trend for microplastics study. *Journal of Environmental Management* 344:118756. https://doi.org/10.1016/j.jenvman.2023.118756

[189] Zhao B, Richardson RE, You F (2024) Advancing microplastic analysis in the era of artificial intelligence: From current applications to the promise of generative AI. *Nexus* 1(4):100043. https://doi.org/10.1016/j.ynexs.2024.100043

[190] Enders K, Käppler A, Biniasch O, Feldens P, Stollberg N, Lange X, Fischer D, Eichhorn K-J, Pollehne F, Oberbeckmann S, Labrenz M (2019) Tracing microplastics in aquatic environments based on sediment analogies. *Scientific Reports* 9(1). https://doi.org/10.1038/s41598-019-50508-2

[191] Schwarzer K, Ricklefs K, Höft D (2019) Sediment inventory and hydromorphology of the schlei, (original: Sedimentinventar und hydromorphologie der schlei). (Institute of Geosciences, Kiel University), p 114. Available at https://www.schleswig-holstein.de/DE/fachinhalte/M/meeresschutz/Downloads/Bericht_SedimentinventarHydromorphologieSchlei.pdf (Accessed August 8, 2025)

[192] Lenz R, Fischer F, Arnold M, Fernández-González V, Moscoso Pérez CM, Andrade-Garda JM, Muniategui-Lorenzo S, Fischer D (2023) MicroPlastiX SpecDB: Database of raman and ATR-FTIR spectra of weathered and biofouled polymers. 127, 8 MB. https://doi.org/10.22000/1820

[193] Lenz R (2024) MPX_specDB: A FAIR data approach to understanding microplastic pollution through spectroscopy.

[194] NFDI4Chem, Lenz R (2024) MPX_specDB - a FAIR data approach to understanding microplastic pollution through spectroscopy. Available at https://youtu.be/_n7I1Gr9LTM (Accessed December 21, 2024)

[195] Scheidgen M, Himanen L, Ladines AN, Sikter D, Nakhaee M, Fekete Á, Chang T, Golparvar A, Márquez JA, Brockhauser S, Brückner S, Ghiringhelli LM, Dietrich F, Lehmberg D, Denell T, Albino A, Näsström H, Shabih S, Dobener F, Kühbach M, Mozumder R, Rudzinski JF, Daelman N, Pizarro JM, Kuban M, Salazar C, Ondračka P, Bungartz H-J, Draxl C (2023) NOMAD: A distributed web-based platform for managingmaterials science research data. *Journal of Open Source Software* 8(90):5388. https://doi.org/10.21105/joss.05388

[196] Bauch A, Adamczyk I, Buczek P, Elmer F-J, Enimanev K, Glyzewski P, Kohler M, Pylak T, Quandt A, Ramakrishnan C, Beisel C, Malmström L, Aebersold R, Rinn B (2011) openBIS: A flexible framework for managing and analyzing complex data in biology research. *BMC Bioinformatics* 12(1):468. https://doi.org/10.1186/1471-2105-12-468

[197] Barillari C, Ottoz DSM, Fuentes-Serna JM, Ramakrishnan C, Rinn B, Rudolf F (2016) openBIS ELN-LIMS: An open-source database for academic laboratories. *Bioinformatics* 32(4):638–640. https://doi.org/10.1093/bioinformatics/btv606

Publications

> **Note**
>
> Each publication is prepended by a cover page providing an overview of the publication's metadata. Only the main body of each publication is embedded. A version including all supporting information is available in the accompanying repository [44].

Microplastic exposure studies should be environmentally realistic

by Robin Lenz, Kristina Enders, Torkel Gissel Nielsen

- **Date published**: July 12, 2016
- **Type**: Letter
- **Published in**: Proceedings of the National Academy of Sciences, National Academy of Sciences

- **License**: © PNAS (free access)

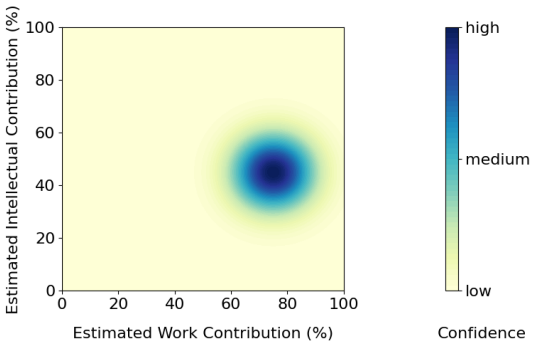
- **DOI**: 10.1073/pnas.1606615113, **Reference**: [1]
- **Citations**: 619 (Crossref/DOI, 2025-11-18)

Contributions

K.E. and T.G.N. designed research | R.L. performed research | T.G.N. provided scientific leadership | R.L. and K.E. wrote the paper.

Quantitative own contributions based on self-assessment

In the dimensions of expended work effort and intellectual contribution, I consider my shares are likely to be between 70% and 80% and between 40% and 50% respectively. This is visualised below as an interpolated histogram of 500 samples from Gaussian distributions with the aforementioned estimates at plus/minus two standard deviations.



LETTER

Microplastic exposure studies should be environmentally realistic

Robin Lenz[a,1], Kristina Enders[a], and Torkel Gissel Nielsen[a]

To understand the impact of microplastic (MP) pollution to aquatic ecosystems, it is important to identify the mechanisms of interaction with organisms. Exposure experiments, like the study of Sussarellu et al. (1) recently published in PNAS, may provide such insights. However, the results of dose–response experiments must always be interpreted in light of environmental concentrations, and the experimental concentrations examined by Sussarellu et al. (1) and several others (2–8) are orders-of-magnitude higher than those reported from field studies (Fig. 1).

Experimental studies on effects of MP on mussels (2, 3), lugworms (4), copepods (5–7), and oysters (1) have documented reduced feeding, survival, and fecundity, as well as promoted polychlorinated biphenyl bioaccumulation linked to MP uptake. In addition, nano-sized plastic particles may reduce body size and lead to reproductive malfunctioning in *Daphnia* (8), and to reduced CO_2 uptake and enhanced production of reactive oxygen species in algae (9).

All of these experimental studies use MP concentrations far above the levels documented in the marine environment (Fig. 1). Many of those studies used MP beads smaller than those reported from the field, but even if one extrapolates field-measured concentrations of MP particles to the size range used in experiments, experimental and expected field concentrations are very far apart. Studies that determined concentrations for micro-bead exposures from field measurements of larger-sized MP assumed a mass-conserving fragmentation (Fig. 1), which compares to a theoretical 3D fragmentation process, where numbers of particles will scale inversely with the particle radius to the power of 3. In contrast, the environmental concentrations documented in studies appear to follow a slightly lower exponent (2.67) (Fig. 1), possibly caused by size-dependent removal processes, lower dimensional breakdown (i.e., of flakes, sheets, and fibers), or considerable influence of new MP input of larger sizes. Additionally, decreased detection accuracy of applied sampling methods in their respective lower size ranges might play a role.

Experimental exposure concentrations tend to be between two to seven orders-of-magnitude higher than environmental levels. The most recent study (1) used concentrations closest to those found in nature. However, Sussarellu et al. calculate their MP concentrations based on sediment data from a pollution hot-spot area close to a ship-breaking yard in India (8, 10); thus, these data are unlikely to be representative of general concentrations beyond the local area.

Microplastic research is an emerging field, and there is a lot of misunderstanding and in some cases overreaction or misinterpretation of results from MP science in the public. We therefore strongly suggest that future studies of MP impact on marine ecosystems should also include concentrations that have been documented in the environment to yield more realistic estimates of sublethal effects.

Acknowledgments

The authors thank Thomas Kiørboe and Mary Wisz for helpful comments on this letter.

[a]Section for Marine Ecology and Oceanography, National Institute of Aquatic Resources, Technical University of Denmark, 2920 Charlottenlund, Denmark

Author contributions: K.E. and T.G.N. designed research; R.L. performed research; T.G.N. provided scientific leadership; and R.L. and K.E. wrote the paper.

The authors declare no conflict of interest.

Data deposition: A fully referenced version of the data review has been deposited at figshare.com, accessible under: https://figshare.com/articles/Size_and_concentration_comparison_for_microplastics_between_reported_environmental_levels_and_laboratory_exposure_studies/3206449.

[1]To whom correspondence should be addressed. Email: roble@aqua.dtu.dk.

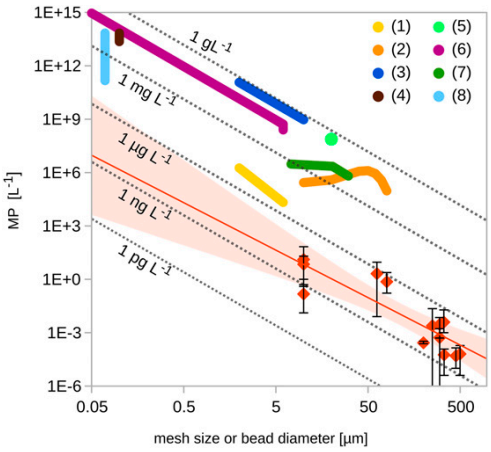


Fig. 1. Comparison between MP concentrations used in exposure studies (fat colored lines) and observed environmental levels (red diamonds: average concentrations; error bars: minimum and maximum concentration). The red line extrapolates the field data with best fit using a power law regression ($y = 3{,}188 \cdot x^{-2.67}$; 95% confidence intervals as pale red areas). The dotted gray isolines show equal mass concentrations for particles density = 1.04 g · cm^{-3}. The *x*-axis scale is the diameter of the micro beads in exposure experiments and the mesh size used in environmental studies, respectively.

1 Sussarellu R, et al. (2016) Oyster reproduction is affected by exposure to polystyrene microplastics. *Proc Natl Acad Sci USA* 113(9):2430–2435.
2 von Moos N, Burkhardt-Holm P, Koehler A (2012) Uptake and effects of microplastics on cells and tissue of the blue mussel *Mytilus edulis* L. after an experimental exposure. *Environ Sci Technol* 46(20):11327–11335.
3 Browne MA, Dissanayake A, Galloway TS, Lowe DM, Thompson RC (2008) Ingested microscopic plastic translocates to the circulatory system of the mussel, *Mytilus edulis* (L). *Environ Sci Technol* 42(13):5026–5031.
4 Besseling E, Wegner A, Foekema EM, van den Heuvel-Greve MJ, Koelmans AA (2012) Effects of microplastic on fitness and PCB bioaccumulation by the lugworm *Arenicola marina* (L.). *Environ Sci Technol* 47(1):593–600.
5 Cole M, Lindeque P, Fileman E, Halsband C, Galloway TS (2015) The impact of polystyrene microplastics on feeding, function and fecundity in the marine copepod *Calanus helgolandicus*. *Environ Sci Technol* 49(2):1130–1137.
6 Lee KW, Shim WJ, Kwon OY, Kang JH (2013) Size-dependent effects of micro polystyrene particles in the marine copepod *Tigriopus japonicus*. *Environ Sci Technol* 47(19):11278–11283.
7 Cole M, et al. (2013) Microplastic ingestion by zooplankton. *Environ Sci Technol* 47(12):6646–6655.
8 Besseling E, Wang B, Lürling M, Koelmans AA (2014) Nanoplastic affects growth of *S. obliquus* and reproduction of *D. magna*. *Environ Sci Technol* 48(20): 12336–12343.
9 Bhattacharya P, Lin S, Turner JP, Ke PC (2010) Physical adsorption of charged plastic nanoparticles affects algal photosynthesis. *J Phys Chem C* 114(39): 16556–16561.
10 Reddy MS, Basha S, Adimurthy S, Ramachandraiah G (2006) Description of the small plastics fragments in marine sediments along the Alang-Sosiya ship-breaking yard, India. *Estuar Coast Shelf Sci* 68(3-4):656–660.

This is the end of the publication

Microplastic exposure studies should be environmentally realistic

by Robin Lenz, Kristina Enders, Torkel Gissel Nielsen

You might want to continue reading the synopsis at page 9, or jump back to the start of this publication at page 46.

Extraction of microplastic from biota: recommended acidic digestion destroys common plastic polymers

by Kristina Enders, Robin Lenz, Sabrina Beer, Colin A. Stedmon

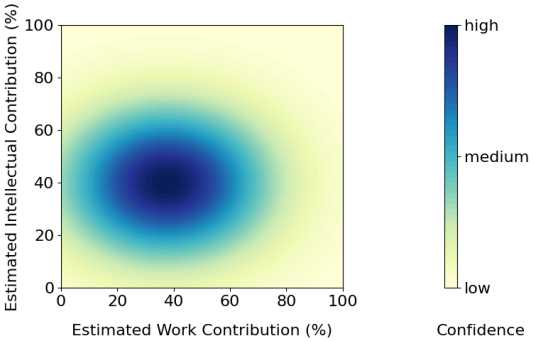
- **Date published**: October 26, 2016
- **Type**: Research Article
- **Published in**: ICES Journal of Marine Science, ICES / OUP
- **License**: © ICES / OUP (free access)
- **DOI**: 10.1093/icesjms/fsw173, **Reference**: [2]
- **Citations**: 221 (Crossref/DOI, 2025-11-18)

Contributions

[**Note**: *No author contribution statement is available for this publication. The following partial contribution statement is created for this thesis only to the best of my knowledge and belief.*] RL contributed to planning and conduction of the experiments, data analysis and writing of the manuscript.

Quantitative own contributions based on self-assessment

In the dimensions of expended work effort and intellectual contribution, I consider my shares are likely to be between 25% and 50% and between 30% and 50% respectively. This is visualised below as an interpolated histogram of 500 samples from Gaussian distributions with the aforementioned estimates at plus/minus two standard deviations.



ICES Journal of Marine Science

ICES Journal of Marine Science (2017), 74(1), 326–331. doi:10.1093/icesjms/fsw173

Original Article

Extraction of microplastic from biota: recommended acidic digestion destroys common plastic polymers

Kristina Enders[1,*], Robin Lenz[1], Sabrina Beer[2] and Colin A. Stedmon[1]

[1]*National Institute of Aquatic Resources, Technical University of Denmark, DTU, Kavalergården 6, Charlottenlund 2920, Denmark*
[2]*Copenhagen University, Nørregade 10, København 1165, Denmark*

**Corresponding author: tel: +4591940467; e-mail: kren@aqua.dtu.dk*

Enders, K., Lenz, R., Beer, S. and Stedmon, C. A. Extraction of microplastic from biota: recommended acidic digestion destroys common plastic polymers. – ICES Journal of Marine Science, 74: 326–331.

Received 1 April 2016; revised 6 September 2016; accepted 7 September 2016; advance access publication 26 October 2016.

The chemical digestion of tissue from marine biota for microplastic analysis is currently conducted following a variety of protocols published in scientific literature. Often there is a lack of information on whether and to which degree the applied chemicals are destructive to microplastic particles of various polymer types. In the present study we report that a digestion protocol recently recommended by ICES using nitric and perchloric acid has strong detrimental effects on several common plastic polymers, in particular polyamide and polyurethane and to a lesser degree acrylonitrile butadiene styrene, polymethyl methacrylate and polyvinylchloride. Raman spectroscopic measurements revealed changes in peak occurrence and intensity for several polymers that did not otherwise show visual macroscopic changes. We developed and tested an alkaline digestion protocol in order to preserve small microplastic particles while removing organic tissue material. We recommend this method for the development of guidelines for plastic microplastic monitoring in biota.

Keywords: digestion, method development, microplastic, stomach samples.

Introduction

Plastic is accumulating in the oceans (Eriksen *et al.*, 2014) where as a result of exposure to various environmental stressors (e.g. Ultra Violet light and abrasion), it breaks down to ever-smaller fragments resulting in microplastic. Plastic of all sizes is of potential harm to marine life overlapping with the feeding size spectrum of a wide range of organisms (Enders and Lenz, 2015). The quantification of microplastic in the stomachs of various biota is central to assessing the impact and extent of plastic pollution and to determining its pathways through food webs and sinks (Setälä *et al.*, 2014). The development of techniques to isolate and characterize microplastic is, however, still in progress and methodologies across different studies are barely standardized. The monitoring of plastics in fish has been integrated into the European Union Marine Strategy Framework Directive (Galgani *et al.*, 2013) and Oslo-Paris Commission (OSPAR) guidelines. OSPAR has requested a common monitoring protocol for plastic particles in fish stomachs, which was provided through a special advice report (ICES, 2015).

Before microplastic distribution and impacts can be systematically assessed standardized sampling and laboratory techniques are required. A major challenge is the removal of organic matter that is often associated with microplastic particles. This can be both detrital organic matter or in the form of tissue or secretion in the case of samples from living biota. Due to the hydrophobic nature of many plastics organic matter in environmental samples will aggregate on its surfaces to form biofilms. Before microplastic can be characterized, either visually or spectroscopically, the organic matrix must be removed. Various approaches have been developed including: enzymes (Cole *et al.*, 2014); bases such as sodium hydroxide (NaOH; Claessens *et al.*, 2013; Cole *et al.*, 2014) or potassium hydroxide (KOH; Foekema *et al.*, 2013); alkaline cleaning agents (Strand and Tairova, 2015); concentrated acids such as nitric acid or hydrochloric acid (HNO_3, HCl; Claessens *et al.*, 2013), or perchloric acid ($HClO_4$; Zoeter Vanpoucke, 2015); oxidants such as hydrogen peroxide (H_2O_2; Nuelle *et al.*, 2014); or other bleaching agents such as sodium hypochlorite (NaClO; Sørensen *et al.*, 2013).

© International Council for the Exploration of the Sea 2016. All rights reserved.
For Permissions, please email: journals.permissions@oup.com

Downloaded from https://academic.oup.com/icesjms/article/74/1/326/2418179 by guest on 03 January 2023

Table 1. Description of the four digestions solutions tested.

Acid mix (ICES)	4:1 (v:v) HNO_3 69% (AnalR, VWR International S.A.S.) + $HClO_4$ 70% (Rectapur, VWR International S.A.S.), procedure: Addition of 5 ml/g and digestion for 5 hours and subsequent heating in a laboratory oven for 10 min in 80 °C.
KOH	Solution of KOH pellets (Emsure, Merck) in microfiltrated H_2O 1120 g/L, procedure: refer to "Methods" section.
NaClO	NaClO solution, 14% active chlorine (VWR International S.A.S.), procedure: refer to "Methods" section.
Industrial CIP agent	VIP 1 (Novadan Aps, Kolding, Denmark), ready solution containing ~3% Potassium hydroxide, ~1% Potassium tripolyphosphate, ~1% Potassium silicate, and ~7% Sodium hypochlorite, procedure: refer to "Methods" section.

A preliminary protocol for the digestion of organic matter in conjunction with microplastic isolation and sample preparation has been issued by ICES. The procedure recommends the usage of a mixture of HNO_3:$HClO_4$ (4:1) as digestive agents (ICES, 2015) and had the goal of contributing towards the standardization of current methods. During preparations for national monitoring activities for microplastics in fish stomachs (Lenz *et al.*, 2016) it was decided to follow the ICES recommendations as they aim to harmonize microplastic protocols. During the course of the sample preparations we found indications that the recommended acid combinations had severe effects on a range of common polymers. An assessment of the suitability of the different digestion chemicals used for microplastic isolation was therefore initiated. In this study, we report the results of tests run on a set of 21 common plastic polymers that underwent the tissue digestion treatment following the ICES protocol. For comparison parallel digestions with KOH, NaClO, and a commercially available alkaline cleaning agent were also carried out.

Methods

Plastic resistance to test chemicals

Polymer samples were chosen from a selection of consumer plastic items of which the material or recycling label was visible. Several pieces of roughly 0.5 × 1 cm in size but with varying thicknesses (~1 mm) were cut and transferred into a separate 8 ml laboratory glass vials with a black butyl/PTFE screw top lid. Further effort to standardize the plastic samples was hindered by the variable properties of the materials such as densities, pliability, and structure (e.g. compact, expanded, or fibrous). A 5-ml aliquot of digestion reagent was added to each vial and the vials were stored upright and unshaken during the testing period. Four different digestion solutions were compared: the recommended acid mix (ICES, 2015); a KOH solution; a NaClO solution; and a commercially available industrial cleaning-in-place (CIP) agent (Table 1). The effects of the different treatments were documented photographically before the addition of chemicals and after 30 min, 1 h, and 5 h. Following this treatment period at room temperature all samples were exposed to 80 °C for 20 min, while still submerged in the digesting agent, as recommended in the ICES advice guidelines (ICES, 2015) and observed changes were documented in the same manner. In the case of the ICES treatment an extra image series was recorded after 10 h to better screen for subtle changes. Observed effects were categorized by severity into four levels (Table 2).

Raman micro-spectrometry

In order to better evaluate weak chemical changes on the outer matrix of the polymer a selection of samples was measured with Raman micro-spectroscopy after the digestive treatments (5 h plus 20 min at 80 °C). The spectra were compared with a spectral library of the same polymers in original condition.

Table 2. Definition of the four different impact levels that the outcome of the digestions was classified into.

Level of impact	Description
L1	Initial visually recognizable changes (colour, surface morphology)
L2	Morphological changes and early stages of dissolution
L3	Strong morphological disintegration and change of bulk structure
L4	Complete dissolution or disintegration

Testing tissue digestion effectiveness

A comparison study was conducted in order to test for digestion effectiveness of fish stomachs among the treatments with: (i) KOH, (ii) NaClO; (iii) KOH and NaClO in combination; and (iv) VIP1. VIP1 is a ready-made solution which contains both KOH (3%) and NaClO (7%) as the main ingredients. This is also the reason for selecting to test each individually for their digestive power first and then later in combination. The cod stomachs tested in this study were caught in the Baltic Sea (Lenz *et al.*, 2016) and weighed between 8 and 22 g. For each gram of tissue, 5 ml test solution (i–iv) was added to the sample respectively contained in a laboratory glass bottles. All treatments were first subjected to a 15 min ultrasonic bath followed by two hours of thorough shaking. The most effective digestion solution was then further diluted to find an optimum i.e. most economical concentration.

Results

ICES acid mix treatment

Examples of the observations from the ICES exposure are shown in Figures 1–4 and are summarized in Table 3. More comprehensive photographic documentation is presented in the Supplementary Material S1. The strongest effects were observed for polyamide (PA), polyurethane (PU), and a black tire rubber elastomer, all of which were completely dissolved by the acidic treatment. In the case of PA6 the complete dissolution (L4) was observed within seconds to minutes after submersion in the acid mix. Other structurally affected polymers were acrylonitrile butadiene styrene (ABS), polymethyl methacrylate (PMMA), and polyvinyl chloride (PVC). The latter being affected in moderation, mainly colour leaching and softening (L2–L3). The structure of polymer samples of polycarbonate (PC), expanded and solid polystyrene (EPS, PS) and polyethylene terephthalate (PET) was only slightly affected resulting in staining or colour loss (L1). No effects were observed for polypropylene (PP), high- and low-density polyethylene (HDPE, LDPE), ethylene-vinyl acetate (EVA), and polytetrafluoroethylene

Downloaded from https://academic.oup.com/icesjms/article/74/1/326/2418179 by guest on 03 January 2023

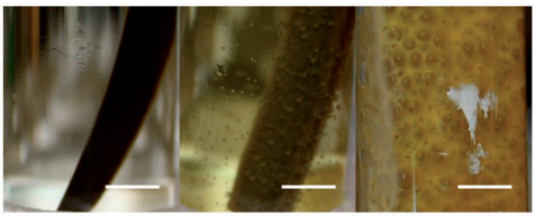


Figure 1. ABS bloating by acidic treatment after 5 h (left), 10 h (middle), and additional heating to 80 °C (right). Scale bar = 0.5 cm. Note: The White spot is a reflection on the glass vial. The entire picture series can be found under Supplementary Material S1.

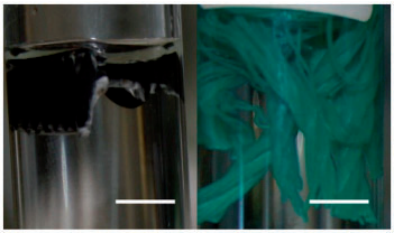


Figure 2. No observable changes after acidic treatment of polyolefins (PP left, HDPE right). Scale bar = 0.5cm.

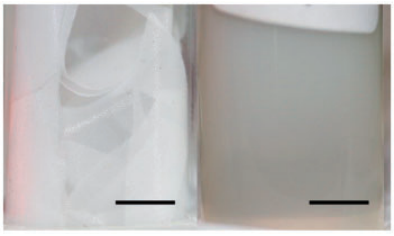


Figure 3. PA-6 before (left) and after first contact with acidic treatment. Scale bar = 0.5cm.

(PTFE). Heating to 80 °C after the digestion period was found to have an exacerbating effect on the polymer destruction in all cases where an initial effect was observed. Raman micro-spectroscopy measurements were performed on all polymer samples, which did not show severe visible changes after the acid mixture treatment. The spectra revealed that apart from ABS (Supplementary Material S2) all remaining polymers had spectra similar to that of the original polymers although some showed signs of degradation or peak shifts (Table 4).

Alkaline treatments

All tested polymers were unaffected by the alkaline treatments according to the defined levels (Table 2) during both the individual and combined reagent treatments. The characteristics of acquired Raman spectra, however, differed between treatments (Table 4). Minimal changes were seen for the 30% dilution 1:1 combined KOH:NaClO solution which was the found optimized protocol.

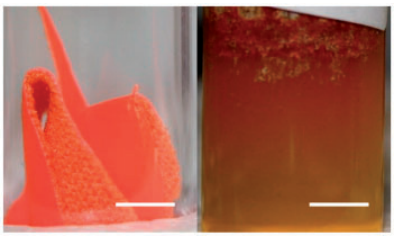


Figure 4. PU before (left) and after 5 h of acidic treatment. Scale bar = 0.5cm.

Table 3. Tested polymer types in the acid test treatment with observed impact levels corresponding to the classification in Table 2.

	0.5 h	1 h	5 h	10 h	80 °C	No change
PP						x
LDPE						x
HDPE						x
PS					L1	
EPS					L1	
ABS		L1	L2		L3	
PU	L2	L3	L4			
PA 1	L4					
PA 2	L2		L3			
EVA						x
PET			L1			
PC	L1					
Nitrile	L1		L3	L4		
PVC 1			L1		L2	
PVC 2			L1		L2	
PVC 3						x
PMMA		L2	L3			
PTFE (Teflon)						x
RE 1- Rubber elastomer	L3	L4				
RE 2- Rubber elastomer	L2	L3			L4	
RE 3- Rubber elastomer	L1	L2	L3		L4	

Results are shown for different digestion time incubations at room temperature and for after an additional 20 minutes at 80 °C. The final column indicates polymers where no change was evident.

The polymer samples treated with.pure and saturated KOH solutions exhibited larger spectral deviations and lower quality spectra (Table 4, Supplementary Material S2). Despite these alterations to the Raman spectra as a result of the digestions all polymer types could still be recognized by comparison with the library of clean spectra from the untreated polymers.

Testing tissue digestion effectiveness

Table 5 shows that among all chemicals tested KOH in combination with NaClO had the most satisfactory effect, dissolving sample tissue completely. Either KOH or NaClO alone were not as effective. The VIP1 treatment was nearly comparable although some mucoid sediment remained undissolved. The KOH:NaClO mixture was then tested in three different proportions (IIIa, IIIb, IIIc) of which IIIc (1:1) was found to be optimal. Higher

Downloaded from https://academic.oup.com/icesjms/article/74/1/326/2418179 by guest on 03 January 2023

Table 4. Evaluation of Raman spectra changes after chemical treatments with the acid mix, saturated KOH and KOH:NaClO 30% solution
Colour legend:

Recognizable, largely identical
Recognizable, with noted peak changes if applicable
Not recognizable
n/a: not measured

	Acid mixture	KOH, saturated solution	30% KOH: NaClO
PP			
LDPE			
HDPE			
PS	slightly noisy, florescence		
EPS	n/a	n/a	
ABS	not recognizable, change in peak positions and fluorescence. 1605 cm^{-1} peak remains	higher noise level than in spectrum of untreated ABS	higher noise level than in spectrum of untreated ABS
PA	n/a	missing peak at 147 cm^{-1}	peak at 147 cm^{-1} weakened
PET		peak at 3080 cm^{-1} and 861 cm^{-1} enhanced, new peaks at 1418 cm^{-1} and 1132 cm^{-1}	
PC		new peak at 1065 cm^{-1}	
PVC	fluorescence, weaker main peaks at 704 and 637 cm^{-1} indicating degradation processes	weaker main peaks at 704 and 637 cm^{-1} indicating degradation processes	
PMMA	new peak at 1054 and 1308 cm^{-1}	new peak at 1070 cm^{-1}	
PTFE	n/a	n/a	

The spectra measured are presented in the Supplementary Materials. Grey shadings symbolize the degree of spectral matching compared to spectra of the untreated clean polymer.

Table 5. Descriptive test results for digestion effectiveness of KOH (I), NaClO (II), KOH: NaClO (III), and VIP1 (IV).

	Treatment	Post treatment
I	100% KOH	Layer of black/brown slime afloat, no big pieces remain.
IIa	30% NaClO	Milky solution, fish stomach still floating as one piece.
IIb	100% NaClO	Only half of mixture added because of very strong foam formation, risk of spillage
III	**1:1 (KOH:NaClO)**	**Sample tissue completely dissolved**
IVa	30% VIP1	Sample mostly dissolved, slimy sediment remaining.
IVb	100% VIP1	Sample dissolved better, less slimy sediment remaining.

a and b indicate when different concentrations were applied. The most effective treatment is highlighted in bold.

Table 6. Results of testing different proportions of KOH:NaClO as a digestion reagent.

	Treatment	Post treatment
IIIa	2:1 (KOH:NaClO)	Numerous small items afloat: undigested stomach content, many of visible biological origin (food items).
IIIb	1:2 (KOH:NaClO)	Foam formation (minimized by cooling glass bottle in cold water), few small pieces (food remaining)
IIIc	**1:1 (KOH:NaClO)**	**Foam formation (slightly less than above). Sample tissue completely dissolved**

The most effective one is marked in bold.

proportions of NaClO caused foam formation, while lower NaClO concentrations reduced the digestion effectiveness (Table 6). Finally a diluted version (30%) of the 1:1 KOH:NaClO mixture was tested and found to still be capable of full digestion and offer a more economical working reagent.

Discussion and recommendations

The tests performed here were carried out on macroscopic plastic fragments and one can assume that the detrimental effects documented for the ICES treatment are likely more severe for microplastics due to the comparatively larger surface area and more fragile nature. This is particular relevant for studies investigating microplastic below 300 µm in size. Raman spectroscopic results revealed that several of the treatments had negative effects on the quality of the spectra obtained and therefore could potentially influence the spectral matching of environmental samples to pure polymer spectra. In particular, the spectra of ABS were greatly influenced.

Several of the other tested polymers lost dyes when exposed to the acid mix treatment. Although this was classified only as low

Downloaded from https://academic.oup.com/icesjms/article/74/1/326/2418179 by guest on 03 January 2023

impact level L1, this increases the likelihood that discoloured microplastics of the concerned polymers are overlooked during visual analyses. The fact that marine microplastics are usually exposed to environmental weathering for extended periods before eventual sampling and isolation (in contrast to the new polymers used in this study) may result in the digestion having more adverse effects than documented here. Environmental weathering from UV degradation is already known to impair microplastic identification (Lenz *et al.*, 2015).

Various studies have already applied the recommended acid mixture (De Witte *et al.*, 2014; Vandermeersch *et al.*, 2015; Zoeter Vanpoucke, 2015) or nitric acid alone (Van Cauwenberghe and Janssen 2014) and are therefore likely to systematically underestimate microplastic abundance and documented polymer diversity. Therefore abundances based on the use of the ICES protocol (ICES, 2015) should be interpreted as a conservative estimate with some bias with respect to polymer detection. The results of this study show the importance of conducting chemical resistance tests prior to a wide application of any microplastic sample digestion protocols and further study on other spectroscopic techniques is warranted.

Another study (Strand and Tairova, 2015) successfully used VIP1 for sediment and tissue digestion purposes. The main digestive ingredients in VIP1 are the same as in the KOH-NaClO-mixture and in order to test the VIP1 solution a small quantity of the same batch that the authors originally work with was obtained (J. Strand and Z. Tairova, pers. comm.). Hence, VIP1 used in the present study was already several months old and has been opened before which makes it likely that active chlorine has deteriorated to some extent. This would mean that the effectiveness was limited and perhaps better results can be obtained when using a fresh VIP1 solution. However, its widespread availability to the scientific community is limited and its actual composition is unknown and this makes it an inappropriate choice for a community-standardized method. The results presented here suggest that due to the widespread availability and effective digestion ability the usage of a 30% KOH:NaClO mixture is the most appropriate and we recommend it therefore as a fast, inexpensive and effective digestion method. For 1 L of reagent 150 ml of saturated KOH solution (1120 g/L) and 150 ml NaClO solution (14% active chlorine) is mixed into 700 ml micro-filtrated water. Although not tested in this study it is likely that this solution is similarly appropriate to remove biofilms, algae, flocculated organic particles and other protein and lipid rich materials of biological origin. The success of the reagent combination also aligns with findings by Strand and Tairova (2015) and Cole *et al.* (2014) which suggest that the KOH and NaClO are useful as active compounds in digestion protocols for sediment and tissue microplastic samples, as well as biota-rich sea water samples.

The alkaline treatments, both KOH and the optimized 30% KOH:NaClO solution did not impair the identification of the tested polymers by Raman micro-spectrometry. Occurring chemical alterations produced minor peak changes in spectra or elevated background noise levels which however did not mask the original polymer signal. We therefore argue that the presented solution can also be applied for the analysis of small microplastic particles (<300 μm). We recommend it being further compared with enzymatic digestion protocols under aspects of economy, digestion effectiveness and plastic resistance. Having evidenced the complete dissolution of sample tissue in reasonable work time while not impairing the integrity of the most common plastic polymer groups, we argue for the described method being considered in international guidelines targeting the standardization of protocols.

Supplementary data

Supplementary material is available at the ICESJMS online version of the article.

Acknowledgements

We thank Jakob Strand for valuable input on digestive solutions.

Funding

This study received funding from the Danish Nature Agency (Naturstyrelsen).

References

Claessens, M., Van Cauwenberghe, L., Vandegehuchte, M. B., Jansenn, C. R. 2013. New techniques for the detection of microplastics in sediments and field collected organisms. Marine Pollution Bulletin, 70: 227–233. http://www.ncbi.nlm.nih.gov/pubmed/23601693 (las accessed 20 January 2014).

Cole, M., Webb, H., Lindeque, P. K., Fileman, E.S., Halsband, C., and Galloway, T. S. 2014. Isolation of microplastics in biota-rich seawater samples and marine organisms. Scientific Reports, 4: 4528. http://www.ncbi.nlm.nih.gov/pubmed/24681661 (last accessed 1 April 2014).

De Witte, B., Devriese, L., BeKaert, K., Hoffman, S., Vandermeersch, G., Cooreman, K., and Robbens, J. 2014. Quality assessment of the blue mussel (Mytilus edulis): comparison between commercial and wild types. Marine Pollution Bulletin 85: p146–155. http://linkinghub.elsevier.com/retrieve/pii/S0025326X14003671.

Enders, K., and Lenz, R. 2015. How to find the small plastic in the big sea - the identification and characterisation of microplastic ≥10 μm from the Atlantic Ocean (Master Thesis). DTU Aqua. http://findit.dtu.dk/en/catalog/2292736934.

Eriksen, M., Lebreton, L. C., Carson, H. S., Thiel, M., Moore, C. J., Borerro, J. C., Galgani, F., *et al.* 2014. Plastic Pollution in the World's Oceans: More than 5 Trillion Plastic Pieces Weighing over 250,000 Tons Afloat at Sea H. G. Dam, ed. PLoS One, 9: e111913. http://dx.plos.org/10.1371/journal.pone.0111913 (last accessed 10 December 2014).

Foekema, E. M., De Gruijter, C., Mergia, M. T., van Franeker, J. A., Murk, A. J., and Koelmans, A. A. 2013. Plastic in north sea fish. Environmental Science and Technology, 47: 8818–8824. http://www.ncbi.nlm.nih.gov/pubmed/23777286.

Galgani, F., Hanke, G., Werner, S., Oosterbaan, L., Nilsson, P., Fleet, D., Kinsey, S., *et al.*, 2013. Guidance on Monitoring of Marine Litter in European Seas Contact information.

ICES. 2015. ICES Special Request Advice Northeast Atlantic and Arctic Ocean. OSPAR request on development of a common monitoring protocol for plastic particles in fish stomachs and selected shellfish on the basis of existing fish disease surveys. IICES Advice 2015, Book 1 (June), 1–6.

Lenz, R., Enders, K., Stedmon, C. A., Mackenzie, D. M., Nielsen, T. G. 2015. A critical assessment of visual identification of marine microplastic using Raman spectroscopy for analysis improvement. Marine Pollution Bulletin, 100: 82–91. http://dx.doi.org/10.1016/j.marpolbul.2015.09.026.

Lenz, R., Enders, K., Beer, S., Søresen, T. K., Stedmon, C. 2016. Analysis of microplastic in the stomachs of herring and cod from the North Sea and Baltic Sea. Naturstyrelsen. http://naturstyrelsen.dk/publikationer/2016/apr/analyse-af-mikroplast-i-torske-og-sildemaver.

Nuelle, M. T., Dekiff, J. H., Remy, D., and Fries, E. 2014. A new analytical approach for monitoring microplastics in marine sediments. Environmental Pollution (Barking, Essex: 1987), 184: 161–169. http://www.ncbi.nlm.nih.gov/pubmed/24051349 (last accessed 21 January 2014).

Downloaded from https://academic.oup.com/icesjms/article/74/1/326/2418179 by guest on 03 January 2023

Setälä, O., Fleming-Lehtinen, V., and Lehtiniemi, M. 2014. Ingestion and transfer of microplastics in the planktonic food web. Environmental Pollution (Barking, Essex: 1987), 185: 77–83. http://www.ncbi.nlm.nih.gov/pubmed/24220023 (last accessed 21 January 2014).

Søresen, T. K., Stedmon, C. A., Enders, K., Henriksen, O. 2013. Analyse af marint affald i sild og hvilling fra det nordlige Storebìlt.

Strand, J., and Tairova, Z. 2015. Microplastic particles in North Sea sediments.http://dce2.au.dk/pub/SR178.pdf.

Van Cauwenberghe, L., and Janssen, C. R. 2014. Microplastics in bivalves cultured for human consumption. Environmental Pollution (Barking, Essex: 1987), 193: 65–70. Available at: http://www.sciencedirect.com/science/article/pii/S0269749114002425.

Vandermeersch, G., Van Cauwenberghe, L., Janssen, C. R., Marques, A., Granby, K., Fait, G., Kotterman, M. J. *et al.* 2015. A critical view on microplastic quantification in aquatic organisms Environment Research, 143: 46–55.

Zoeter Vanpoucke, M. 2015. Impact of microplastic uptake: contamination in sprat and microplastic-mediated uptake of PAHs by European shore crab. Master thesis. Institute for Agricultural and Fisheries Research (ILVO), Ghent.

Handling editor: Howard Browman

Downloaded from https://academic.oup.com/icesjms/article/74/1/326/2418179 by guest on 03 January 2023

This is the end of the publication

Extraction of microplastic from biota: recommended acidic digestion destroys common plastic polymers

by Kristina Enders, Robin Lenz, Sabrina Beer, Colin A. Stedmon

You might want to continue reading the synopsis at page 19, or jump back to the start of this publication at page 50.

Small Microplastic Sampling in Water: Development of an Encapsulated Filtration Device

by Robin Lenz, Matthias Labrenz

- **Date published**: August 08, 2018
- **Type**: Research Article
- **Published in**: Water, MDPI

- **License**: CC-BY

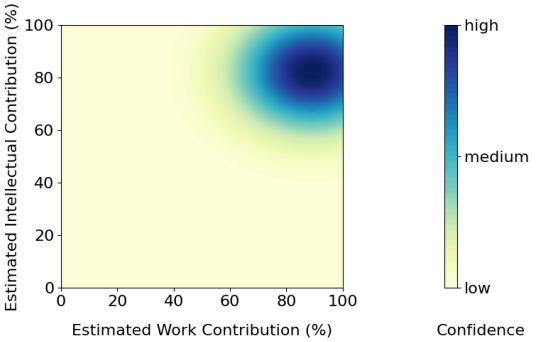
- **DOI**: 10.3390/w10081055, **Reference**: [3]
- **Citations**: 51 (Crossref/DOI, 2025-11-18)

Contributions

Conceptualization: R.L., M.L. | Methodology: R.L. | Validation: R.L., M.L. | Formal Analysis: R.L. | Investigation: R.L. | Resources: M.L. | Data Curation: R.L. | Writing—Original Draft Preparation: R.L. | Writing—Review and Editing: M.L. | Visualization: R.L., M.L. | Supervision: M.L. | Project Administration: M.L. | Funding Acquisition: M.L.

Quantitative own contributions based on self-assessment

In the dimensions of expended work effort and intellectual contribution, I consider my shares are likely to be between 80% and 98% and between 75% and 90% respectively. This is visualised below as an interpolated histogram of 500 samples from Gaussian distributions with the aforementioned estimates at plus/minus two standard deviations.



water

MDPI

Communication

Small Microplastic Sampling in Water: Development of an Encapsulated Filtration Device

Robin Lenz and Matthias Labrenz *

Leibniz Institute for Baltic Sea Research Warnemünde (IOW), Seestraße 15, 18119 Rostock, Germany; robin.lenz@io-warnemuende.de

* Correspondence: matthias.labrenz@io-warnemuende.de; Tel.: +49-381-519-7378

Received: 21 June 2018; Accepted: 2 August 2018; Published: 8 August 2018



Abstract: A variety of microplastic sampling instrumentation is currently used for water pollution studies. Plankton net-based approaches have been the most adopted techniques for water column and surface sampling. When applied to microplastics (MP) in the lower µm size range these methods, however, introduce non-negligible risks of sample contamination and loss due to instrument and procedure design. Based on the first principles of systems engineering design we have developed a mobile sampling platform for field application that fulfils the needs of producing usable MP samples with a lower size limit of 10 µm using an encapsulated flow-through filtration concept. Here, we explain the requirements, development, and construction of the device for others to replicate and improve.

Keywords: microplastics; field work; pollution monitoring; engineering design

1. Introduction

The sampling of microplastics (MP) from surface waters or in the water column is dominated by towed net sampling techniques inherited from plankton research. These include, foremost, Manta trawls [1] that skim a film of surface water of constant depth for floating matter and retain the mesh-size-defined particulate filtrate in a cod-end [2–4]. Bongo nets, WP-2 nets, as well as special constructions for layered profiling have been applied alike [5–8]. Single or staggered open sieve constructions, as well as encapsulated flow-through filtration devices are approaches that have been utilised by other studies [9–11]. Additionally, sampling of MP has been accomplished by means of density separation in continuous flow centrifuges used in suspended matter analysis [12].

Common for all methods is the extraction of suspended particulate matter from the sampled water compartment. An obtained sample has to be removed from the device and stored for transport in a quantitatively complete manner, while procedural contamination with fibres or particles of synthetic polymers has to be excluded. The assurance of these two conditions is the crux for standard plankton net-based approaches. The equipment itself commonly consists of a variety of plastic polymers, such as monofilament polyamide meshes, synthetic textiles, like ropes, seams, and reinforcing fabrics, for instance, made of spun micro-fibrous polyethylene terephthalate (PET). Frames, connectors, and cod-ends can include hard plastic parts where polyethylene (LDPE or HDPE), polypropylene (PP), or polyvinylchloride (PVC) would be common suspects. Usage-related wear is bound to occur under such setups, i.e., as parts are moving against each other or metals included in the construction. Samples are often exposed to airborne contamination during handling and transfer time on board. Together these drawbacks render plankton nets inadequate for small microplastics (S-MP) sampling, while larger size fractions (L-MP) alone might still be investigated by these techniques with reasonable accuracy. Most studies used mesh sizes between 300 and 390 µm [13], which seems a reasonable cut-off to yield acceptable and meaningful samples under open net sampling conditions, whereas MP below

this size would necessitate techniques that appropriately address these constructional vulnerabilities. That it is, however, important to adequately cover the lower microplastic size ranges in surveys that estimate current pollution levels, and has been highlighted by recent research articles and reports [10,11,14], reviews [13], and legislative policy advice [15–17]. Typical sources of small MP size fractions, such as tyre wear or intentionally added abrasive MP in products, are named as points of concern by the latter.

The precision of net sampling relies on the volume counting usually done by mechanical flow meters in front of, or inside, the net's mouth. With pressure building up inside the net due to the tow velocity, and depending on the mouth size and shape, as well as the net and mesh size, the apparent volume passing through the net can vary from what is received by the mechanical counter [18,19]. Another factor, which applies to all mesh-based sampling approaches is the diminishing apparent mesh size with an advancing fill level and clogging of pores [20], leading to increased hydraulic head loss of the unit. Two resulting consequences are the diminished volume flow and a change of the retained particle size spectrum towards smaller sizes.

2. Technical Development

Starting from formulating and narrowing down the problem a user would want to solve with the system we commenced to develop a set of system requirements needed to fulfil the user's demands. Based on first principles of engineering design a range of component concepts was then evaluated against the criteria set by the user and system requirements in light of achieving the wanted result with the simplest design or lowest number of potential points of failure possible.

The overarching premise of the user in the present case is to be able to sample microplastics of any kind suspended in the water column or on the surface where the lower size limit of 10 µm is the single most influential factor dictating the subsequently determined requirements of contamination prevention and quantitative sample retention. A closed filter design, the avoidance of plastic polymers in the equipment parts that are in contact with the sample, as well as a filtration pump setup operated in suction mode, are seen as the most important constructional features to overcome the problems known from other available sampling equipment described above, which is predominantly used for larger MP. An overview of the development process from user and system requirements, the selected solution and testing results thereof are illustrated in the scheme below (Figure 1).

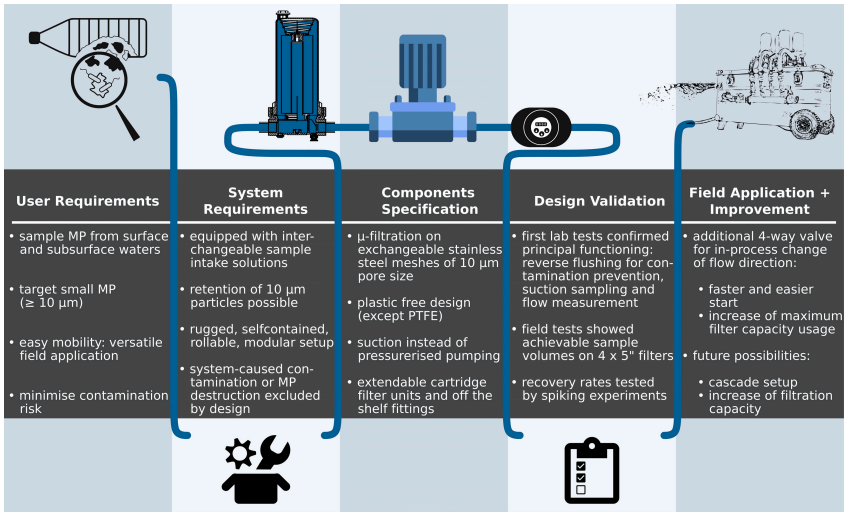


Figure 1. Development of the sampling device from requirements design to field application.

The device is built in and around a movable aluminium storage container (K 424 XC, Zarges, Weilheim, Germany) which acts as a transport vehicle, an operation platform, and as a container for long-term storage in between sampling campaigns (Figure 2a). To avoid unnecessary exposure to plastic polymers the sample is only in contact with the following materials: metals (i.e., stainless steel, aluminium), silicone in O-rings, and polytetrafluoroethylene (PTFE). The latter is applied as a sealant in ball valves and fittings, as well as an inner lining of the sampling hose (TuFlour Chem PTFE, 32 mm inner diameter, TuDerTechnica Chemours Company, Saccolongo, Italy). The hydraulic setup can be seen in Figure 3. Although PTFE belongs to the synthetic carbon-based thermoplastic polymers it was chosen to facilitate the sample transport with minimised loss due to particles settling out of the flowing liquid and sticking to the walls. For this reason PTFE is excluded from the results if found in the spectroscopic analysis that all samples undergo. Based on the comparably low production volume of PTFE [21], which is ~0.05% of the major commodity plastic types [22], and its high wear resistance and chemical stability, very low, to no, particles are practically expected in environmental samples at the targeted size range $\geq$10 µm. We argue for, and assume that, the above reasons for the exclusion of PTFE does not introduce any non-negligible error in MP particle concentrations measured. It should be noted that if smaller sizes are targeted this assumption should be critically evaluated as PTFE has found applications as micrometre-sized particles in dry lubrication aerosol sprays (0.1–1 µm) [23] and as nano-particles in surface coatings [24].

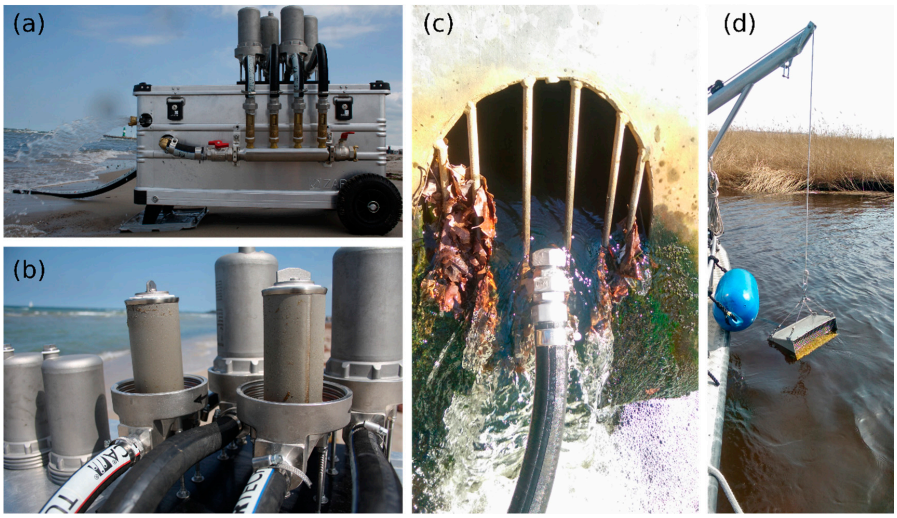


Figure 2. Field assembled configuration of the sampling device: (**a**) overview of the system during sampling; (**b**) the 10 µm cartridge modules in closed housing, opened and partly covered with sample; (**c**) inlet options for water column sampling applied at a waste water treatment plant (WWTP) outlet; and (**d**) water surface sample intake by aluminium funnel applied on board a boat.

The sampling which has a 32 mm inner diameter is built in two parts of ca. 7 m length each that can be connected by a metal quick coupling (CamLock fittings according to EN14420-7, by Schwer Fittings GmbH, Denkingen, Germany) to give flexibility for varying sampling site conditions. The ends of the sampling hose are likewise equipped with quick connectors where one side mounts to a distributor for four individual filtration lines, and the other one holding a mouthpiece of choice depending on the sampled compartment (Figure 3).

Past the distributor the sample is retained as the flow traverses through stainless steel cartridge filters at 10 µm mesh size (01WTGD, with 124 mm (4 7/8") filters, Wolftechnik Filtersysteme GmbH and Co. KG, Weil der Stadt, Germany). The individual filter elements consist of a perforated inner support sheet metal and a top and bottom plate which confine and hold the mesh screen without any adhesive

or cementing material. They are held in place tight inside the unit by a screw pole and a stainless steel tightening cap which presses against PTFE ring seals on each side of the double open-end (DOE) element (see also Figure 2b). The combined filter surface area amounts to 975 cm^2. Larger filter elements, such as cartridges of 5, 10 or 20 inches could be mounted together with their corresponding housings. This way the total filter area and, hence, the sample volume capacity, can be increased, however, at the cost of more demanding sample processing and larger equipment to be handled. At the outlet after each filter housing a see-through observation chamber with a built-in flow rate meter gives an indication of the degree of blocking of the respective filter. The four lines enter into a collector opposite the distributor which passes the water on towards the pump. We applied a centrifugal jet pump (type Jimg 12, Tellarini Pompe S.n.c., Lugo, Italy) which was chosen for its properties of high capacity of nominal 3.6 m^3 h^{-1} and wet self-priming functionality with up to 8 m elevation. It has no dry self-priming capability, meaning that an initial fill is needed before a flow can be established. An impeller pump could be used instead to overcome this necessity, however, at the cost of higher wear during operation and reduced resistance to dry running break down. The addition of a four-way valve with an double L-shaped bore (also referred to as the X port valve) between the two pump ports in one axis, and the collector outlet and discharge port along the other, creates the possibility to promptly reverse the direction of the flow through the system. This allows for an easy priming of the pump and, at the same time, enables a reverse flushing of the filter parts after the cartridge units have been assembled and closed for operation at a sampling site. The flushing procedure eliminates potential airborne contamination which might have settled on the filters during mounting and is used to rinse out the distributor and sampling hose to avoid site cross-contamination in consecutive activities on a sampling campaign.

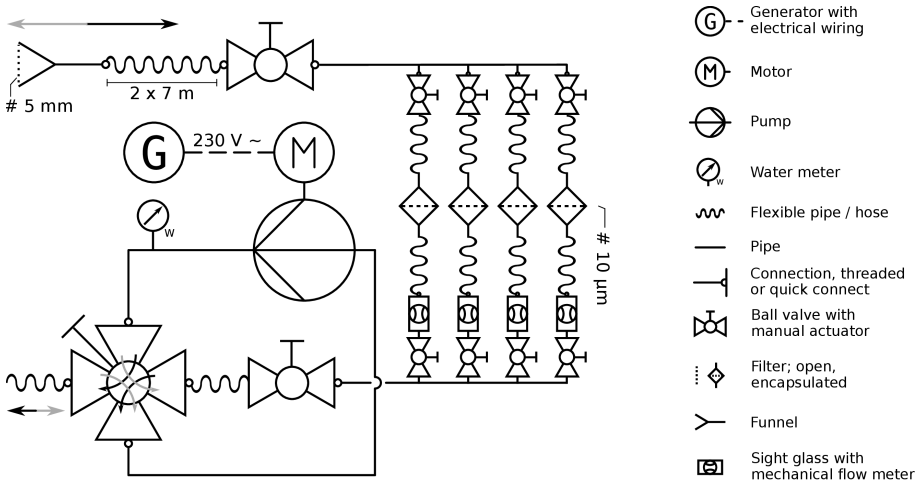


Figure 3. Piping and instrumentation diagram (P&ID) for the microplastic water sampler. Black arrows indicate main flow direction through the system during sampling. Grey arrows show operation in reverse flushing mode.

3. Experimental Work and Validation Results

The volume that passed the system is accurately measured using a standard sanitary water meter (8ZR100, Zenner International, Saarbrücken, Germany). These devices are calibrated according to local legislation, i.e., for the EU, following Annex III of the Directive 2014/32/EU demanding volume measurement errors of 2% or less [25]. Generally, the functioning of such water meters is based on an impeller rotating as water passes by and driving a counter on the display side. Due to this design it has to be assumed that water–air mixtures can lead to positive, as well as negative, misreading.

The former may occur as air-enriched water will take up a larger volume compared to the same water when degassed and, thus, move the counter further, while the latter can be a result of temporary break-down of the flow inside the impeller chamber due to high air entrainment with the remaining passing water volume being too small to adequately spin the rotor. Cases of water–air mixtures could be expected during field sampling due to short-term accidental air intake or leaks in the system. To quantify the error margin two setups were tested under laboratory conditions: a known water volume was passed through the device where, in one case, a deliberate leak was introduced by a thin silicone tubing inserted into the otherwise submerged sample intake, fixed with the open end above the water surface, creating a minor air entraining situation. In the other case the mouth of the sample intake itself was held only half submerged creating a repeatedly breaking down and recovering flow. Readings after the small air entrainment differed from the real water volume by up to 5%, while the larger air intake resulted in ca. 20% difference. The perpetual submersion and a proper check for tightness of all connections are, therefore, a requirement for accurate volume readings. An addition of an air separator prior to the volume meter could be a way to overcome this limitation.

In order to evaluate MP retention we ran the filter system by feeding tap water which had been pre-filtered on 10 µm and inserted pre-counted batches of 1000 pieces per replicate (n = 3) of light red polyamide particles (PA6, fine pre-production nurdles). The cylindrical granules had an average size of 450 and 480 µm in length and diameter, respectively. After each run the filter set was removed and handled in exactly the same way as environmental samples would have been processed. The recovered particles were quantified under a stereomicroscope using a Bogorov counting chamber (custom build at own scientific workshop facility). The achieved recovery rate for the three independent replicates averaged 98.9% with a standard deviation of 0.89%.

From first applications in field studies we are able to draw some conclusions on the functioning of the sampling system and provide a proof of principle. Most remarkably, however, not surprisingly, the achievable sample volumes varied vastly depending on the suspended matter loadings. While turbid river waters in agricultural areas during spring snow melt often allowed ca. 200–300 L to be sampled on one set of filters (location and time data of field applications where achievable sample volumes have been estimated from are provided in the supplementary material: Table S1), clearer rivers were on the order of 200 to 700 L total sample volume. The premature clogging in turbid river waters is attributed to the settling of fine sediment load in between the stainless steel webbing of the filters.

Table 1. Summarising comparison of properties, advantages, and limitations of the presented method and two alternative approaches. Costs are denoted as relative estimates ranging from "+" (lowest costs) to "+++" highest costs as actual costs may vary depending on supplier and chosen design specifics.

Criterion	Encapsulated Flow-through Device (Present System)	Plankton Nets	Continuous Flow Centrifuge
Compartment	Surface and water column	Surface and water column	Surface and water column
Primary sampling zone	Rivers, wetland drainages, WWTP outflows, small lakes/ponds	Open ocean, coastal waters/estuaries, large lakes	Rivers, wetland drainages, WWTP outflows, small lakes/ponds
Additional sampling zone, suitable to limited extent	Coastal waters/estuaries, open ocean, larger lakes	Large rivers	Coastal waters/estuaries, open ocean, larger lakes
Recommendable size range focus	≥10 µm	≥300 µm	Any
Targeted MP types	Any	Any	HD-MP *
One-time expenses	++	+	+++
Running costs	+	+++ if ship time is required + if applied from bridge in streams	+

Table 1. *Cont.*

Criterion	Encapsulated Flow-through Device (Present System)	Plankton Nets	Continuous Flow Centrifuge
Major advantages	S-MP can reliably be sampled with minimized contamination risk	High volume capacity and ease of use	Size independent sampling (no filtration)
Major limitations	Lower sample volume capacity e.g., 1 m^3, might be too low for L-MP statistical analysis	Not practical for S-MP due to open design and higher contamination risk Ship time required (except for rivers)	LD-MP ** is not sampled by design Large equipment restricts sampling site access and handling requires trained personnel
References of method application	[10,11], present study	[2–8]	[12]

* = high density polymers (i.e., denser than water); ** = low density polymers (i.e., lighter than water).

This effect could be counteracted by choosing a larger mesh size (if compatible with the respective research question) or increasing the deployed filter surface area. Wastewater treatment plant (WWTP) outflow water could be sampled with ca. 600 L to 1 m^3, tested at two facilities. The latter was chosen as the desired maximum volume per sample and was not caused by clogging of the filters. In coastal marine waters during winter conditions up to 2 m^3 have been sampled before the filter capacity was exhausted.

The sampling time may vary due to water quality and terrain. Up to four sampling stations per day are deemed realistic for a two- or three-person field work team.

4. Discussion and Conclusions

We have developed a water sampling system to be used for environmental surveys of microplastic contamination in surface and sub-surface waters. The major problems addressed with this new development are the difficulty of sampling small-sized MP from water and the contamination risk associated. The benefits in the current stage of development can be summarised as:

- Minimised contact to plastic polymers: only PTFE and non-plastic materials;
- Closed design: minimised sample exposure time; and
- No handling on site required: samples are transported in the replaceable unit of the cartridge filters.

The primary intended use-case is the sampling of S-MP (i.e., the size fraction below 300 µm) in source areas, such as rivers, inland wet areas and drainages, WWTP outflows, and estuarine and near-shore coastal waters. L-MP will, by design, also be sampled quantitatively, however, the nominal sample volume of 1 m^3 is too low to allow for statistically sound analysis as typical abundances are often below one particle per m^3 and methods of higher volume throughput are needed. On the contrary, open ocean surface concentration data from studies which included S-MP were frequently on the order of 100–200 m^{-3} [10,11], which implies that sample sizes of 1 m^3 may produce meaningful data under these conditions. In Table 1 we summarise the advantages and drawbacks of the current and alternative methods.

On-going work will improve the system in terms of usability and achievable sample volumes. In the current state we applied the four filtering channels in parallel for maximised sampling capacity. If a lower sample volume is acceptable or if longer filter cartridges are used and operated separately, the system seems suitable for streamlined sampling of replicates, e.g., in short time intervals or at different positions at the same location. A recent study on MP monitoring underpinned the importance of replicated sampling throughout a river cross-section [5]. This is just one possible modification to adapt the system to specific sampling scenarios and we encourage others to contact us for requests or comments and to replicate or improve upon the suggested design.

Supplementary Materials: The following are available online at http://www.mdpi.com/2073-4441/10/8/1055/s1, Table S1. Locations, dates and sample volumes from a first sampling campaign in the Warnow river system (Mecklenburg-Vorpommern, Germany).

Author Contributions: Conceptualization: R.L., M.L.; Methodology: R.L.; Validation: R.L., M.L.; Formal Analysis: R.L.; Investigation: R.L.; Resources: M.L.; Data Curation: R.L.; Writing—Original Draft Preparation: R.L.; Writing—Review and Editing: M.L.; Visualization: R.L., M.L.; Supervision: M.L.; Project Administration: M.L.; Funding Acquisition: M.L.

Funding: This research was funded by BmBF project MicroCatch_Balt, grant number 03F0788A.

Acknowledgments: The authors gratefully appreciate the help of L.M., J.G., A.T. and K.E. in conducting laboratory test runs and field work trials of the system. For constructional assembly we thank K.R., and for fruitful discussions on technical practicalities, G.G., C.L. and M.L.

Conflicts of Interest: The authors declare no conflict of interest. The funders had no role in the design of the study; in the collection, analyses, or interpretation of data; in the writing of the manuscript, and in the decision to publish the results.

References

1. Brown, D.; Cheng, L. New Net for Sampling the Ocean Surface. *Mar. Ecol. Prog. Ser.* **1981**, *5*, 225–227. [CrossRef]
2. Tamminga, M.; Hengstmann, E.; Fischer, E.K. Microplastic analysis in the South Funen Archipelago, Baltic Sea, implementing manta trawling and bulk sampling. *Mar. Pollut. Bull.* **2018**, *128*, 601–608. [CrossRef] [PubMed]
3. Gewert, B.; Ogonowski, M.; Barth, A.; MacLeod, M. Abundance and composition of near surface microplastics and plastic debris in the Stockholm Archipelago, Baltic Sea. *Mar. Pollut. Bull.* **2017**, *120*, 292–302. [CrossRef] [PubMed]
4. Setälä, O.; Magnusson, K.; Lehtiniemi, M.; Norén, F. Distribution and abundance of surface water microlitter in the Baltic Sea: A comparison of two sampling methods. *Mar. Pollut. Bull.* **2016**, *110*, 177–183. [CrossRef] [PubMed]
5. Liedermann, M.; Gmeiner, P.; Pessenlehner, S.; Haimann, M.; Hohenblum, P.; Habersack, H. A Methodology for Measuring Microplastic Transport in Large or Medium Rivers. *Water* **2018**, *10*, 414. [CrossRef]
6. Norén, F.; Naustvoll, L. *Survey of Microscopic Anthropogenic Particles in Skagerrak*; N-Research, Lysekil & Institute for Marine Research: Flødevigen, Sweden, 2010.
7. Reisser, J.; Slat, B.; Noble, K.; du Plessis, K.; Epp, M.; Proietti, M.; de Sonneville, J.; Becker, T.; Pattiaratchi, C. The vertical distribution of buoyant plastics at sea: An observational study in the North Atlantic Gyre. *Biogeosciences* **2015**, *12*, 1249–1256. [CrossRef]
8. Leslie, H.A.; van der Meulen, M.D.; Kleissen, F.M.; Vethaak, A.D. *Microplastic Litter in the Dutch Marine Environment—Providing Facts and Analysis for Dutch Policymakers Concerned with Marine Microplastic Litter*; Deltares: Amsterdam, The Netherlands, 2011.
9. Schmidt, L.K.; Bochow, M.; Imhof, H.K.; Oswald, S.E. Multi-temporal surveys for microplastic particles enabled by a novel and fast application of SWIR imaging spectroscopy—Study of an urban watercourse traversing the city of Berlin, Germany. *Environ. Pollut.* **2018**, *239*, 579–589. [CrossRef] [PubMed]
10. Desforges, J.P.W.; Galbraith, M.; Dangerfield, N.; Ross, P.S. Widespread distribution of microplastics in subsurface seawater in the NE Pacific Ocean. *Mar. Pollut. Bull.* **2014**, *79*, 94–99. [CrossRef] [PubMed]
11. Enders, K.; Lenz, R.; Stedmon, C.A.; Nielsen, T.G. Abundance, size and polymer composition of marine microplastics $\geq$10 μm in the Atlantic Ocean and their modelled vertical distribution. *Mar. Pollut. Bull.* **2015**, *100*, 70–81. [CrossRef] [PubMed]
12. Leslie, H.A.; Brandsma, S.H.; van Velzen, M.J.M.; Vethaak, A.D. Microplastics en route: Field measurements in the Dutch river delta and Amsterdam canals, wastewater treatment plants, North Sea sediments and biota. *Environ. Int.* **2017**, *101*, 133–142. [CrossRef] [PubMed]
13. Hidalgo-Ruz, V.; Gutow, L.; Thompson, R.C.; Thiel, M. Microplastics in the marine environment: A review of the methods used for identification and quantification. *Environ. Sci. Technol.* **2012**, *46*, 3060–3075. [CrossRef] [PubMed]
14. Norén, F. *Small Plastic Particles in Coastal Swedish Waters*; N-Research: Lysekil, Sweden, 2007.

15. *Communication from the Commission to the European Parliament, the Council, the European Economic and Social Committee and the Committee of the Regions: A European Strategy for Plastics in a Circular Economy*; European Union: Brussels, Belgium, 2018.
16. United Nations Environment Programme (UNEP). Draft resolution on marine litter and microplastics. In Proceedings of the United Nations Environment Assembly, Nairobi, Kenya, 5 December 2017.
17. Peter, J.K. *Marine Plastic Debris and Microplastics-Global Lessons and Research to Inspire Action and Guide Policy Change*; United Nations Environment Programme: Nairobi, Kenya, 2016.
18. Hernroth, L. Sampling and filtration efficiency of two commonly used plankton nets. A comparative study of the Nansen net and the Unesco WP 2 net. *J. Plankton Res.* **1987**, *9*, 719–728. [CrossRef]
19. Smith, P.E.; Counts, R.C.; Clutter, R.I. Changes in filtering efficiency of plankton nets due to clogging under tow. *ICES J. Mar. Sci.* **1968**, *32*, 232–248. [CrossRef]
20. Evans, M.S.; Sell, D.W. Mesh size and collection characteristics of 50-cm diameter conical plankton nets. *Hydrobiol.* **1985**, *122*, 97–104. [CrossRef]
21. Polytetrafluoroethylene (PTFE)—A Global Market Overview. Available online: https://www.reportlinker.com/p03769747/Polytetrafluoroethylene-PTFE-A-Global-Market-Overview.html (accessed on 2 July 2018).
22. *Plastics Europe Plastics—the Facts 2017—An Analysis of European Plastics Production, Demand and Waste Data*; Plastics Europe (the Association of Plastics Manufacturers in Europe) and EPRO (the European Association of Plastics Recycling and Recovery Organisations): Brussels, Belgium, 2017.
23. Weißbach, W.; Dahms, M.; Jaroschek, C. *Werkstoffkunde*; Springer Fachmedien Wiesbaden: Wiesbaden, Germany, 2015.
24. Basu, B.J.; Dinesh Kumar, V. Fabrication of Superhydrophobic Nanocomposite Coatings Using Polytetrafluoroethylene and Silica Nanoparticles. *ISRN Nanotechnol.* **2011**, *2011*, 1–6. [CrossRef]
25. *2014/32/EU of the European Parliament and of the Council of 26 February 2014 on the Harmonisation of the Laws of the Member States Relating to the Making Available on the Market of Measuring Instruments (Recast)*; European Union: Brussels, Belgium, 2014.



© 2018 by the authors. Licensee MDPI, Basel, Switzerland. This article is an open access article distributed under the terms and conditions of the Creative Commons Attribution (CC BY) license (http://creativecommons.org/licenses/by/4.0/).

This is the end of the publication

Small Microplastic Sampling in Water: Development of an Encapsulated Filtration Device

by Robin Lenz, Matthias Labrenz

You might want to continue reading the synopsis at page 17, or jump back to the start of this publication at page 58.

When every particle matters: A QuEChERS approach to extract microplastics from environmental samples

by Kristina Enders, Robin Lenz, Juliana A. Ivar do Sul, Alexander S. Tagg, Matthias Labrenz

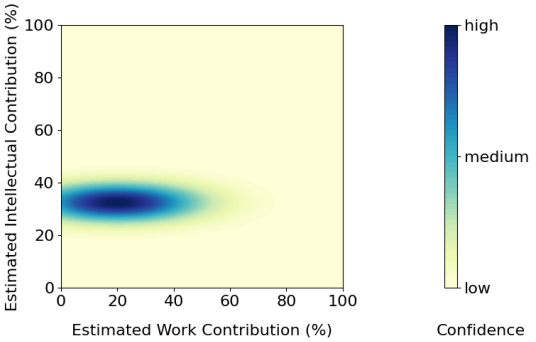
- **Date published**: January 15, 2020
- **Type**: Research Article
- **Published in**: MethodsX, Elsevier
- **License**: CC-BY-NC-ND
- **DOI**: 10.1016/j.mex.2020.100784, **Reference**: [5]
- **Citations**: 79 (Crossref/DOI, 2025-11-18)

Contributions

[**Note**: *No author contribution statement is available for this publication. The following partial contribution statement is created for this thesis only to the best of my knowledge and belief.*] RL contributed to the development of the presented laboratory methods including the sprial conveyor, conceptualisation, writing and illustration of the manuscript.

Quantitative own contributions based on self-assessment

In the dimensions of expended work effort and intellectual contribution, I consider my shares are likely to be between 10% and 30% and between 30% and 35% respectively. This is visualised below as an interpolated histogram of 500 samples from Gaussian distributions with the aforementioned estimates at plus/minus two standard deviations.



MethodsX 7 (2020) 100784

Contents lists available at ScienceDirect

MethodsX

journal homepage: www.elsevier.com/locate/mex

Method Article

When every particle matters: A QuEChERS approach to extract microplastics from environmental samples

Kristina Enders*, Robin Lenz, Juliana A. Ivar do Sul, Alexander S. Tagg, Matthias Labrenz

Leibniz Institute for Baltic Sea Research, Seestraße 15, 18119 Rostock, Germany

A B S T R A C T

The identification of microplastics (MP), especially small (<500 μm) MP, using automated surface-chemistry approaches requires the best possible reduction of natural particles whilst preserving the integrity of the targeted synthetic polymers particles. In general, both natural and synthetic particles can be highly diverse physically and chemically and MP extraction, particularly from complex matrices such as sediments, sludge and soils, requires efficient method pipelines. Our paper presents a universal framework of modular protocols (presented in a decision tree) that fulfil predefined user requirements (QuEChERS: Quick, Easy, Cheap, Effective, Rugged, Safe) as well as providing best practises for reasonable MP working conditions within a standard laboratory. New procedures and technical innovations for density separation of particle-rich matrices are presented, such as a spiral conveyor developed and validated for MP recovery. In sharing such best-practice protocols, we aim to help in the push towards MP quantification method standardisation.

- Publication of protocols of an entire MP extraction (10 μm – 5 mm) pipeline for particle-based analysis of various environmental matrices
- Modularity: Optimised quantitative sample preparation adapted to particle sizes and sample matrices
- New protocols and technical innovations (e.g. spiral conveyor) optimise MP extraction

© 2020 Published by Elsevier B.V. This is an open access article under the CC BY-NC-ND license (http://creativecommons.org/licenses/by-nc-nd/4.0/).

Abbreviations: QuEChERS, Quick, Easy, Cheap, Effective, Rugged, Safe; MP, microplastics; μFTIR, micro Fourier transform infrared; ATR, attenuated total reflection; MPF, microplastic free; SPT, sodium polytungstate; QA, quality assurance; QC, quality control; PTFE, polytetrafluoroethylene; UR, user requirements; SR, system requirements; TS, technical solution; SI, supplementary information; MQ (water), MilliQ (water)/ ultrapure water; SOPs, standard operation procedures.

* Corresponding author.

E-mail addresses: kristina.enders@io-warnemuende.de (K. Enders), robin.lenz@io-warnemuende.de (R. Lenz), juliana.ivardosul@io-warnemuende.de (J.A. Ivar do Sul), alexander.tagg@io-warnemuende.de (A.S. Tagg), matthias.labrenz@io-warnemuende.de (M. Labrenz).

http://dx.doi.org/10.1016/j.mex.2020.100784
2215-0161/© 2020 Published by Elsevier B.V. This is an open access article under the CC BY-NC-ND license (http://creativecommons.org/licenses/by-nc-nd/4.0/).

ARTICLE INFO
Keywords: Sequential protocol, Purification technique, Chemical digestion, Handbook for laboratory work, Manual for good practices on microplastic extraction, Contamination prevention, Recovery rates, Wastewater, Particle-rich
Article history: Accepted 30 December 2019; Available online 15 January 2020

Specification Table

Subject Area:	Environmental Science
More specific subject area:	Microplastic pollution
Method name:	A QuEChERS approach to extract microplastics from environmental samples
Name and reference of original method:	- ***Sieving***: Moore, C.J., Moore, S.L., Weisberg, S.B., Lattin, G.L., Zellers, A.F.A comparison of neustonic plastic and zooplankton abundance in southern California's coastal waters. Mar. Pollut. Bull. 2002, 44, 1035–1038 [27] - ***Density separation***: Thompson, R.C., Olsen, Y., Mitchell, R.P., Davis, A., Rowland, S.J., John, A.W.G., McGonigle, D., Russell, A.E., 2004. Lost at sea: Where is all the plastic? Science 304, 838. doi: https://doi.org/10.1126/science.1094559 [28] - ***Chemical digestion (H_2O_2)***: Liebezeit, G. Dubaish, F. 2012. Microplastics in beaches of the East Frisian islands Spiekeroog and Kachelotplate. Bull. Environ. Contam. Toxicol. 89, 213-217 [26] - **(KOH/ NaOCl)**: Enders, K., Lenz, R., Beer, S., Stedmon, C.A., 2017. Extraction of microplastic from biota: Recommended acidic digestion destroys common plastic polymers. ICES Journal of Marine Science 74, 326–331. https://doi.org/10.1093/icesjms/fsw173 [12]
Resource availability:	**Solutions/liquids/reagents** • Sodium polytungstate (SPT) solution, density 1800 kg m^{-3} (CAS Number 12141-67-2, TC-Tungsten Compunds) • Sodium polytungstate, crystalline (CAS Number 12141-67-2, TC-Tungsten Compunds) • 30% Hydrogen peroxide (CAS Number 7722-84, Carl Roth) • 30% Hydrochloric acid (CAS Number 7647-01-0, Merck) • Potassium hydroxide pellets (CAS Number 1310-58-3, Roth) • Sodium hypochlorite solution, 14% active chlorine (CAS Number 7681-52-9, VWR) • Acetic acid 100% (CAS Number 64-19-7, VWR) • Ethanol 99% (CAS Number 64-17-5, VWR) • Pentane (CAS Number 109-66-0, VWR) • Tween80 (CAS Number 9005-65-6, Merck) **Lab equipment** *Devices* • Laminar flow bench, "Clean bench" (S2020 1.8, Thermo Scientific) • Pump (Model 412721, Welch) • Freeze dryer (Delta 1-24 LSCplus, Christ) • Water purification system (Milli-Q Reference A+with Q-POD dispenser, Merck Millipore) • Sieve shaker (AS200 control, Retsch) • Stereoscope microscope (Stema 2000, Carl Zeiss) • Ultrasonic bath (Sonorex Super, Bandelin) • Muffle oven (L15/11/B170, Nabatherm GmbH) • Freezer (−20 °C) • Fridge (4 °C) • Fine particulate air filter (Vita Shield IPS, Philips) • pH meter (WTW Ingold, Mettler Toledo) • Analytical balance (EMB 2000-2, Kern) • Stain steel filtration device for tap water filtration (01WTGD05, Wolftechnik Filtersysteme GmbH & Co) equipped with stainless steel stand and handle (custom-made: IOW workshop) • Electrical overhead stirrer (Heidolph, RZR 1) *Appliances* • All-Glass Vacuum-filter device (ø 47 mm, metal clamp; Sartorius stedium GmbH) • Large stainless steel sieves (ø 20 cm, different mesh sizes; Retsch) • Small stainless steel sieves (ø 47 mm, different mesh sizes; VWR) • Separation funnels, 250 ml (Squibb, Lenz Laborglas GmbH)

- Separation funnel with extra wide opening (50 mm) and valve outlet (10 mm), 500 ml, 1000 ml, (Squibb, custom-made: Hellbach Glasbläserei)
- Stainless steel (ø 20 mm) and brass (ø 35 mm) spiral conveyors (custom-made: IOW workshop)
- Stainless steel filter (ø 47 mm, 10 μm; Spörl KG)
- Stainless steel filter (200 μm; F. Carl Schröter)
- Glass fibre filter (ø 47 mm; Whattman 934-AH)
- Glass syringes (variable volumes (i.e. 20 ml, 50 ml); FORTUNA® OPTIMA®)
- Glass beakers (VWR, variable volumes i.e. 250 ml, 600 ml, 1 l)
- Glass Erlenmeyer flasks with ground glass lid and metal clamp (50 ml, 100 ml; Labsolute)
- Ceramic bowls (varying sizes, Jizerská porcelánka s.r.o.)
- Aluminium foil (30 μm thickness; Roth)
- Stainless steel tweezers (Dumont)/spoons/spatulas
- Glass Petri dishes (VWR)
- Microscopic glass slides (VWR)
- Fluorescent Green Polyethylene Microspheres (UVPMP-BG-1.025 125-150 μm, Cospheric)

Method details

Protocols background

Microplastics (MP) are particulate synthetic polymerised hydrocarbons which are foreign to natural cycles and act as persistent pollutants if occurrent in the environment. It is to be expected that globally rising production volumes induce rinsing levels of this environmental pollutant if the development of waste management systems do not keep pace and non-circular economic practices persist. Commonly reported sizes of MP range between 1 μm to 5 mm. In contrast to many other environmental pollutants (e.g. heavy metals, pesticides), MP act as dispersed or suspended solid particles and their number and size determine distribution patterns and possible encounter and interaction rates with biota. Therefore, reliable techniques determining numbers and sizes of MP in various environmental matrices are greatly needed.

MP research has intensified considerably since being first scientifically described. Sampling, extraction and analysis methods have been developed and improved continuously to reach higher accuracies. However, the extraction of especially small MP (<500 μm) from various environmental matrices remains very time consuming and a general lack of standards persists. Especially particle-rich matrices such as sediments, sludge and soils require more efficient MP extraction pipelines. Ongoing developmental processes in this research field (see recent review by Zarfl [1]) produce a large variety of protocols which usually depend on the conditions and resources of the laboratories, as well as the sample type and research questions involved. There are numerous scientific publications on MP extraction of a specific sample matrix [2–5], which can be disadvantageous, both in terms of additional costs and required expertise when diversifying the MP extraction work between several sample types.

Objectives

We present a comprehensive compilation of both modified and new methods for MP purification, organised into individual methodological modules designed to be adaptable to the sample type proposed for analysis, and flexible enough to be implemented in a general-purpose research laboratory. Although an optimal working condition for MP sample treatment would require a purpose-built clean lab facility (see SI.1 for further information), the de facto condition for many researchers is to work in a standard laboratory, often used by several other research disciplines simultaneously. Yet some adaptations to a general lab are highly encouraged, the most important of which is the installation of a laminar flow bench to be used exclusively as an MPF zone for all steps involving work on open MP samples. Within the proposed protocol modules are also novel technical steps to further improve both accuracy and efficiency of MP purification. This is especially important given the increasing shift from visual analysis of large MP only towards a focus on the full spectrum of MP size

and type using highly-precise, automated, particle-based analysis approaches. Therefore, the overarching aim of this paper is to enable and encourage an adoption of MP-suitable working conditions. To pursue this goal, the following objectives are satisfied:

- a set of coordinated protocols and devices are presented
- a technical solution to density separations is demonstrated that addresses shortcomings of existing methods
- advise is given to the reader on how to construct a full workflow from the provided protocols, which is adapted to the specific sample properties

Analytical requirements: when every particle counts

The endpoint of automated particle-based analyses, i.e. via micro Fourier transform infrared (μFTIR) or Raman spectroscopy, is the quantification of MP particles based on their chemical compositions or fingerprints without prior visual inspection. Independent of the sample type, the analysis time is mainly dependent on the final number of particles that has to be measured. Thus, when extracting MP from environmental samples, the overarching goal is the best possible reduction of natural particles while preserving the targeted synthetic polymers in numbers, sizes, shapes as well as their chemical composition. The final particle number also greatly depends on the particle size limit. While a common definition of the lower MP size is not yet established, the presented protocols are designed and applied for MP of 10 μm to 5 mm. It should be noted, that MP cover a size range differing up to 500-fold. An analysis attempt in one go would lead to restricted efficiency and quality in the analysis, i.e. by larger particles eclipsing smaller ones. We suggest several options to size-fractionate large, manually handleable particles from smaller MP and prepare them for single particle analysis, e.g. attenuated total reflection (ATR) FTIR (personal communication with Fischer) [6].

All the methods proposed here have been developed with the "QuEChERS" (quick, easy, cheap, effective, rugged and safe) approach in mind [7,8], and are presented in a way reminiscent of systems engineering [9,10]. Fig. 1 visually demonstrates how these approaches have been applied to the presented MP methodology; giving users the methods to achieve their desired goals whilst meeting QuECheERS standards.

In order to analyse a variety of sample matrices, which can differ markedly in composition (i.e. water vs soil), different methodological steps may be needed. By segmenting the methods into modules, certain procedures can be included or omitted as required by the sample type in question, greatly increasing the flexibility of the proposed methods. In order to ascertain which modules should be combined and in what order for a given sample matrix, a decision tree is an ideal way to guide a user to what specific methods they require.

The protocol tree: a decision tree for the protocol modules

We used a decision tree to visualise the complete workflow of connectible protocol modules (see section Protocol modules m0–m6), referred to as the protocol tree (Fig. 2).

How to use the protocol tree and modules?

The sample matrix and the numbers and the sizes of targeted MP determine the route through the tree. They define the optimal protocol pipeline along the tree structure adapted for a given individual case. Essential advancements of the presented methods originate from newly developed equipment applied in the protocols and are described in the respective section (New Equipment). All other materials needed are listed in the beginning of the paper. General MP laboratory procedures, including the cleaning of equipment and laboratory, MPF-filtration of solutions, etc. are described in the general module (m0). Further general measures of quality assurance and control (QA/QC) are described in the respective SI section (SI.2). To cover the diversity of samples in volume and composition some protocol modules contain different optional paths to follow, indicated by an arrow (↦).

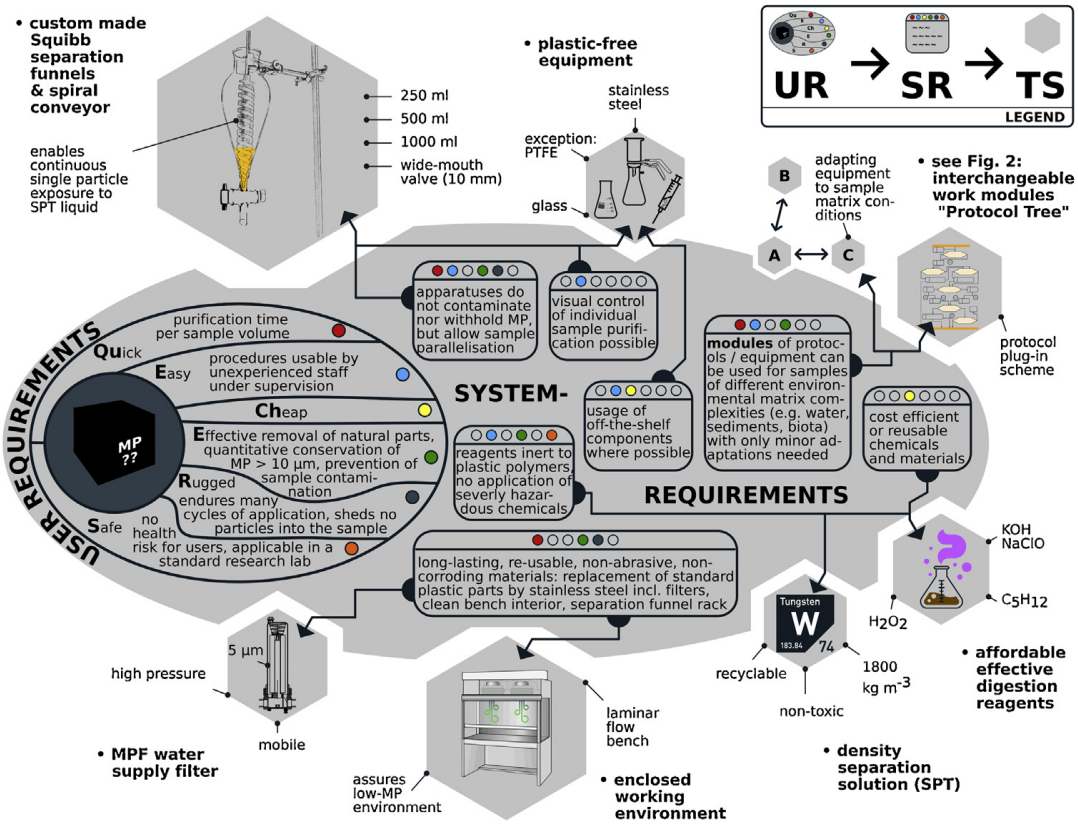


Fig. 1. The scheme detailing the three main components of a system engineering approach is meant to be read from the kernel (the "black box") of a yet to be analysed MP sample. Under the overall goal of enabling a sample to be submitted for efficient microspectroscopic particle identification, the main objectives are the near-complete reduction of natural substances and the preservation of the contained MP. Users requirements (UR, placed around the kernel) formulate typical considerations of MP researchers working under these objectives. They are summarised here by the targets of a QuEChERS approach. One or more UR define a system requirement (SR, in rounded boxes) that specifies what a solution must provide in order to achieve the UR targets. The coloured circles indicate which SR are derived from which UR. Finally, the approach culminates in technical specifications (TS) that satisfy the previously defined requirements. Part of the solutions are the equipment (chemicals, laboratory set up, devices) and procedures used, presented here together as protocols or manuals ready for MP laboratory work (m0–m6).

Modularity and variations due to sample composition

The two widely used techniques to extract MP for a particle-based analysis are a separation by particle density (MP typically range from 900 to 1600 kg m^{-3}) which primarily eliminates the mineral fraction (e.g. quartz, ρ = 2650 kg m^{-3}), and chemical destruction i.e. digestion of particulate organic matter (see e.g. review by [11]). Covering the entire range of possible sample matrices (conceivably substances like honey, household dust, food waste, construction rubble, etc.) would make the decision tree increasingly complex. The focus of the presented protocol workflows is on environmental samples, such as water, soils, sludge, sediments and biota. Biota, for instance, comprise a large range of different biogenic material compositions (chitin, keratin, lipids, etc.) ranging from small zooplankton to stomach contents of birds, some of which may require a repetition or skipping of modules. In most of these cases a freeze drying step may be omitted if the dry weight is not required. Besides, freeze drying facilitates the following digestion step by breaking up cell walls (i.e. in samples rich in plant-based material). In case of a sample being largely made of animal tissue, this time-consuming step may be left out and still yields readily digestible samples. Also, a density separation module might not be necessary, if only negligible amounts of dense non-MP particles remain after digestion. Generally, fewer treatment modules, hence less sample manipulation, is preferential when dealing with

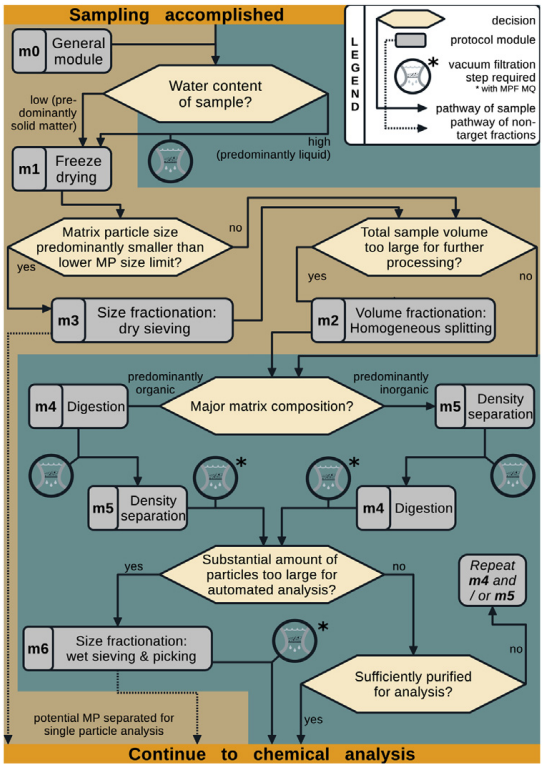


Fig. 2. The decision tree comprises the procedural steps involved in the preprocessing of environmental samples for later particle-based MP chemical analysis. The decision tree starts after accomplished sampling with the sample being transferred from the sampling device, if applicable. It consists of a number of protocol modules equipped with indices (m0–m6) each of them referring to the detailed protocols. The digestion module m4 is further subdivided by specific treatments in a scheme below. These protocol modules are linked through various decisional paths that have to be taken for a complete pretreatment. The background colours indicate whether the sample is in dry (brown) or wet (blue) condition. Vacuum-filtration often finalises wet modules and is included in the respective protocol modules. As filtration is an important intermediate step, it is indicated by a respective symbol (close up of a filter unit, see legend).

potentially small numbers of MP. The required minimum particle size determines parts of the procedural details (e.g. m3 or m6) to assure that also the smallest targeted MP can be reliably quantified.

Digestion modules (m4.1–m4.3) more often necessitate a case-by-case adaptation and are therefore a good example of methodological variation based on sample type. While a purely oxidative treatment with hydrogen peroxide can successfully be applied for purification of water or sediment samples (m4.1), it often fails to degrade animal tissues in reasonable time [2]. A combined alkaline-oxidative treatment based on diluted potassium hydroxide and sodium hypochlorite [12,13] serves as a more appropriate choice for many biota samples (m4.2). The high fat, oil or wax content that can be present in biota samples can in principal be broken up by simple alkaline hydrolysis. However, this process may require longer reaction times or higher temperatures than what is desirable for MP purifications. Therefore, remaining lipid constituents are recommended here to be removed by an additional n-pentane based washing module instead (m4.3). In contrast to the other digestion and density separation modules, the application of a *n*-pentane based treatment has not yet been described for MP sample purification. The effectiveness of the proposed method in terms of achieving better spectral qualities in Raman or μFTIR analysis is promising for sample matrices where lipids could not be sufficiently removed by the other protocols. Apart from biota samples, the application of the n-pentane treatment was preliminarily tested for primary sludge samples from waste water treatments plants that contain potentially high levels of fats and oils, partly due to artificial substitution. This is especially challenging during MP extraction as fats and oils enclose sample

material and this way reduce the effectiveness of the other treatments. A proposed digestion pipeline for these specific sample matrices is a treatment with n-pentane enclosed by repeated hydrogen peroxide digestions. However, the n-pentane module is presented here as a preliminary method, as its inertness to targeted polymers is currently being evaluated (R. Lenz, unpublished data). The general principle is based on classic organic chemistry procedures to dissolve or extract emulsified or deposited lipids from a sample and was applied before in a similar manner e.g. in infant milk fat extraction protocols [14,15]. Fischer and Scholz-Böttcher, 2017 [16] used petroleum ether to prepare greasy fish stomach samples for a mass-based MP analysis (Pyrolysis-Gas Chromatography - Mass-Spectrometry). Compared to n-pentane, use of petroleum can reduce operating costs but has higher health risk due to its hexane contents. The lipid removal potential and resistance of polymers can be expected to be comparable between the two chemicals. The following section presents all protocol modules that build the protocol tree.

Protocol modules

m0 – General module

▸ Irrespective of the protocol pathway selected it is recommended to read the general module as a prerequisite for many other modules as it covers overarching procedural steps when working with MP. It only contains procedures that are specific for the here applied protocols and materials and/or are not yet exhaustively covered in the MP literature and/or are not standard laboratory routines.[1]

Clean bench SOPs: Ensure to keep all surfaces in the laminar flow bench MPF and ready to use. Solely use tissues made of non-disintegrating natural fibres. All water used to clean surfaces should be MPF water. Before use, make sure to rinse all materials with MPF water or muffle at 500 °C. Before muffling, cover with aluminium foil and open again only inside the clean bench to avoid contamination. All sample containers should be rinsed with MPF water when entering the clean bench coming from non-MPF conditions (such as field sampling or cold storage). Additionally, vessels like beakers or Erlenmeyer flasks which hold samples inside the bench are to be thoroughly rinsed with MPF water or MPF MQ before being poured into a filtration or another container. This is important, as a complete separation of droplets from the inner and outer walls cannot be guaranteed during pouring and rinsing procedures. Contamination should also be prevented by entering the bench with arms and hands when working in it. Always wear a 100% cotton lab coat and nitrile gloves kept over the lab coat sleeves to protect the skin and avoid contamination by synthetic clothes. Before entering always use abundant MPF water to wash your hands/gloves.

Cleaning fine stainless steel filters (e.g. 10 µm): After usage, rinse all stainless steel filters with MPF water from the tap to remove coarse dirt. Put the filters in a glass beaker, fill with MPF water and cover with aluminium foil (at all times). Apply repetitive ultrasonic bath sessions with changing power values (50–100%).[2] Recommended are 10 min at 35 kHz and 225 W (for a volume of the ultrasonic bath of 18.7 l). In the initial session, diluted H_2O_2 can be added if the filters contain organic matter. Alternatively few drops of MPF Tween80 can be added. Rinse the beaker and filters and renew the MPF water in between subsequent baths to make sure that all particles are removed from the both the filters and the residual water. It is advisable to apply a minimum of 3 repetitions. However, if the water in the beaker remains cloudy or hazy after sonification the procedure should be repeated. After the final treatment, discard the water from the beaker, rinse and fill up with fresh MPF water. At this point, the MPF filters are ready to be used. Keep them inside the bench in a beaker. Just before use, rinse again with MPF water using tweezers and a syringe.

[1] Note: This document does not include a complete health and safety evaluation of the laboratory procedures. Please carry out a risk assessment for all field and lab work activities and adhere to the health and safety guidelines at your institute or organisation.

[2] It was observed that changing the power resulted in a more efficient removal of matter.

MPF solutions: It is essential when working with MP to ensure that all solutions which get in contact with the sample and/or are used in the clean bench are MPF. Use a vacuum filtration system to filter all solutions (apart from tap water, see tap water filter in the SI.3). Use a filter below your minimum size threshold to ensure a complete removal, e.g. the presented protocols predominantly use 10 μm as the minimum size threshold, a 1.5 μm glass fibre filter (cleaned beforehand[3]) is used for the last filtration. Make sure that the solutions are filtered in pre-cleaned MPF glass bottles and are covered with aluminium foil inside the bench. Appropriate labelling of samples and solutions is part of standard laboratory routines. During MP-extraction it can help to consistently label all the MPF solutions accordingly with "MPF". Inside the clean bench, keep one glass syringe for each specific solution in use and avoid cross-over.

SPTrecovery: The SPT solution can be used for many density separation cycles either by recycling at the manufacturer (if available) or by vacuum filtration in the laboratory. After usage of the SPT solution leave it to settle in a collection flask (>24 h). Pour the supernatant into a separate collection flask. As soon as stirred up particles appear, leave the remaining solution to completely settle again for later recovery. Check pH of recovered SPT before use and adjust to pH 3 if necessary by adding droplets of HCl (10%). Check the density by weighing a defined volume (e.g. 100 ml) and adjust to 1800 kg m^{-3} by dissolving the required amount of crystalline SPT salt in the recovered solution. Vacuum-filter the SPT solution onto a MPF glass fibre filter as explained in the MPF solution section above. In case of high particle content, a pre-filtration on a filter with larger pore sizes (e.g. on 10 μm stainless steel filters) may be applied beforehand to expedite the process. Reconfirm pH and density again after filtration.

Explanatory remarks

► **Starting condition**: Any sampling equipment or specific pretreatment step, such as the removal of sample material from a given sampling device, must be completed beforehand. The assumed sample condition for the following protocols begins with the sample material in a dedicated vessel (e.g. glass beaker).

► **Finishing condition**: The aspiration of a complete pipeline is to bring an environmental MP sample from any possible compartment to an acceptable condition for particle-based chemical analysis. The presented protocols assume that there is a temporal or spatial discontinuity between the sample purification and the analysis, which is why treatments end with readily purified MP particles suspended in MPF MQ water, stored in a sealed MPF glass container (e.g. Erlenmeyer flasks with ground glass joint). This specific procedure is described in detail below (Final Filtration) and is to be conducted at the end of a protocol pipeline. As it would be repetitive to include them in every respective section they are stated here as a general instruction. In case the sample will be submitted to chemical analysis instantly within the same lab, the finalising filtration may be conducted directly onto the desired analysis substrate.



Filtration: Vacuum-filtration often finalises wet modules and is described in detail in the respective protocol modules. The symbol is to be found in the protocol tree (Fig. 2). Additional ultrasonification: Depending on filter pore size and sample composition, removing the sample particles from the filter by rinsing may be non-exhaustive[4] . In such cases the filter should be additionally cleaned in an ultrasonic bath for minimum 2 minutes and residues added to the sample[5]. Check if additional ultasonification is needed to remove all sample particles from the filter.



Final Filtration: The "Final Filtration" symbol is included as an optional path in the respective protocol modules where applicable. This is your last step before chemical analysis. Flush your filtering sample again using MPF MQ water to remove all solutes from the sample[6] (it is marked in the protocol tree with the filtration symbol and an asterisk). At the end of a filtration the filter is removed from the apparatus using tweezers.

[3] To MPF-clean glass-fibre filters, transfer them to a clean petri dish and cover it with aluminium foil. Bake all filters at 500 °C for 5 h. Only remove the filters from the petri dish inside the bench.
[4] Check filter after rinsing step under a binocular microscope for remaining material.
[5] The use (or avoidance) of an ultra-sonification should be conducted in a systematic way within one study.
[6] Remaining solutes can influence spectroscopic results.

If you see >3 MP particles too large for microspectroscopic analysis, apply the module "Size-fractionation: wet sieving & picking" (m6).

Then rinse off the remaining sample particles from the filter into the same final Erlenmeyer flask using MPF MQ water. Place the filter in a clean beaker and cover it with MPF MQ water and sonicate for 2 min to remove all particles from the filter. Then rinse the filter off and add the residues into the same Erlenmeyer flask that containes the bulk of the sample. Close with glass stopper and secure with metal clip. Once the filter is cleaned without residues it can be removed. The sample should be stored in a fridge (4 °C).[7]

m1 – Freeze-drying

▸ Freeze drying is usually performed for one or several of the following three reasons: a) reduction of water in the sample and breakage of particle conglomerates (resulting in a "fluffy" texture) to allow unrestricted performance of the next processing steps (e.g. digestion or density separation), b) determination of the dry weight and c) breakage of cell walls and membranes during the freezing step to increase later digestion efficiency.

1. **Filter**: If the sample is predominantly liquid, filter it in the vacuum filtration set up on a stainless steel filter of the lowest size threshold (e.g. 10 μm). Replace filters if clogged. Make sure to properly rinse all walls, including the sample vessel and the vacuum filtration funnel that the sample was in contact with. Depending on the sample matrix, it may be appropriate to use a diluted detergent solution (e.g. Tween80) to remove sample adherences from the glass ware. Collect all filters (containing sample material) in a glass beaker and add the sample rinsate of the filtration funnels. Cover with aluminium foil.

2. **Freeze**: Freeze the sample at −20 °C (~24 h).[8]

3. **Cover**: Cover sample with an air-permeable MPF membrane with a mesh size smaller than that of the lowest detection size (dust-free tissue paper is ideal for most applications). Fix coverings firmly in place (elastic bands are appropriate). It is recommended to perform the uncovered part near an air filtration device or within an MPF clean bench to avoid contamination.

4. **Freeze-dry**: Freeze-dry the sample according to machine manufacturer's guidelines until the sample is completely dry.

5. **Weigh**: If the sample is not further split, the dry weight is now to be determined.

m2 – Volume-fractionation (homogeneous splitting)

▸Depending on the initial sample volume, a volume fractionation can be necessary to reduce the amount of sample that is treated, or split into several sub-fractions (e.g., for method comparison purposes). If this step is used as sub-sampling (i.e. not all split parts are to be further processed) an effective homogenisation of the sample is most critical for a successful volume fractionation.

1. **Mix**: For freeze-dried samples, shake the sample with the lid closed for minimum 2 min. Then wait until all particles settled. Open the lid and mix the sample with a clean MPF long metal spoon for further minimum 2 min[9] within the MPF clean bench or, if not possible, near an air filtration device. If mixing in the available sample container is restricted, transfer the sample to a MPF-cleaned bowl (i.e. ceramic or stainless steel) and proceed with the homogenisation process.

[7] Cooling the extracted MP sample prevents new biofilms to establish, which would hamper spectroscopic analysis.

[8] If the sample is in a glass container, there is a risk of the glassware breaking as a function of the increasing volume. Placing the sample at a <45° angle can improve matters as this increases the expandable surface area. However, the use of non-breakable MPF containers, such as stainless steel or aluminium, is an ideal alternative for large water volumes.

[9] Mixing times need to be adjusted depending on sample volume and container.

2. **Split**: Transfer the required sample (dry) weight directly into a separate glass beaker, tarred on a scale. If required, several replicate sub-fractions can be obtained in this way.

m3 – Size-fractionation (dry sieving)

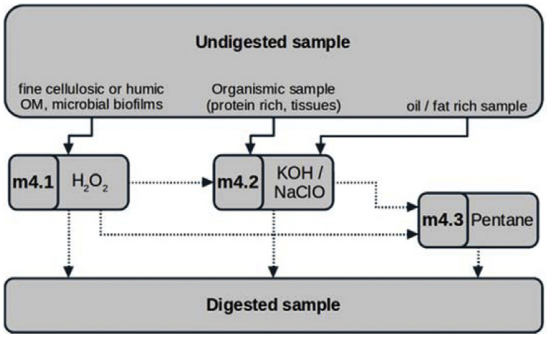
► To further ease processing and analysis of samples where the predominant particle size is substantially smaller than the lower MP size limit, the sample volume can be reduced by sifting out a lower particle size fraction by dry sieving. In principle, this method can also be applied to compartmentalise the sample into a variety of sample fractions of differing particle size, e.g., for differing analytical approaches (visual, surface chemistry, chromatography).[10]

1. **Prepare**: Select sieve sizes appropriate to the size-fractions desired and form a stack. Use a close-fitting stainless steel lid, alternatively thick aluminium foil, to cover the sieve(s) from the top and the bottom. Then slowly add the sample (ideally freeze-dried) to the top sieve, in an MPF clean bench or near an air filtration device. Close the sieve stack making sure there are no gaps where sample material may escape (or contaminated air may enter).

2. **Sieve**: Secure sieve stack in shaker. The amplitude and time can be adjusted according to how easily the sample sieves. We suggest, however, to start with lower amplitudes and shake times and document progress. Two rounds of 5–10 min at 0.75–1.5 mm amplitudes have been found to be sufficient for a variety of soil samples.

m4 – Digestion

► Chemical digestion is a major step to reduce the organic matter content of a sample. A set of different digestion sub-modules are provided that are to be applied for different sample matrices (see scheme below).[11]



m4.1 – Hydrogen peroxide (H_2O_2) digestion

► Hydrogen peroxide (H_2O_2) at 30% is a strong oxidizer. Typically, it is the primary choice for digesting water, sediment, soil, waste water and sludge samples. However, in certain cases the sample matrix might contain substances that are highly resistant to the treatment in which cases other subsequent digestion steps may be added.

1. **Add**: Depending on the nature of the sample, i.e. organic matter content and presence of iron ions, the reaction after the addition of H_2O_2 can be very energetic (bubble formation and temperature rise).

[10] Dry sieving should only be applied if unavoidable as it comes at the risk of losing small particles either during the transfer processes or due to adherence on larger particle surfaces. If applied, use it consistently for the entire data set.

[11] None of the chemicals proposed here are listed under “severely hazardous” (class 3) in the water hazard class (German Water Hazard Classification).

Because of that, it has to be added very carefully and in small amounts. With a glass syringe, add up to 5 ml of H_2O_2 to the sample. For unknown sample matrix even smaller amounts (~2 ml) should be added initially and observed.[12] To anticipate heat generation or an overflow event, the beaker can be kept in a second MPF container (e.g. larger beaker or ceramic bowl) with cold MPF water to avoid temperature rise to more than 40 °C. When working in a fume hood without appropriate MPF conditions an aluminium foil lid should cover the sample at all times and only shortly opened to insert the tip of the glass syringe.

2. **Proceed**: Add more H_2O_2 with a syringe until it completely covers the whole sample. Shake the sample and rinse the walls with H_2O_2 to allow all particles to be in contact with the digestion solution. The beaker should be kept closed in a fume hood for minimum 24 h. Generally, additional H_2O_2 should be added or replaced (filter sample and add new H_2O_2) for as long as the digestion process continues or organic matter remains visible.[13]

⟶ If the sample remains with large indigestible non-MP debris manually pick each item, rinse off adherent smaller particles into the sample and discard. It is recommended to cut very large pieces (e.g. blades of grass, leaves, braches) into smaller ones to allow a more efficient disintegration of biofilms and particle conglomerates during the digestion process.

3. **Filter**: To endthe digestion, filter the digested sample in the vacuum filtration set up on a stainless steel filter of the lowest size threshold (e.g. 10 μm). Carefully rinse the stainless steel filter that remained in H_2O_2 from the previous filtration step from all sides using MPF water, hold it withtweezers and/or a gloved hand. Replace filters if clogged. Once the filter is cleaned without residues it can be removed. Make sure to properly rinse all walls, including the beaker and the vacuum filtration funnel that the sample was in contact with. Depending on the sample matrix, it may be appropriate to use a diluted detergent solution (e.g. Tween80) to remove sample adherences from the glassware.



m4.2 – Potassium hydroxide (KOH) digestion

▸ This protocol module may be applied for samples high in protein content like animal tissue (e.g. stomach analysis). It can also be applied for environmental samples with a challenging matrix composition, that do not sufficiently digest in H_2O_2.

1. **Prepare**: A saturated KOH stock solution is prepared by dissolving 1120 g/l of dry KOH salt (pellets) in water inside a tightly-closed glass bottle. Shake well until complete dissolution. Beware of heat generation, it may be advisable to reduce the temperature with a water bath. The digestion solution is prepared according to the below recipe:

Per 1 l of digestion solution to add to a glass bottle: 700 ml of water (tap water or MilliQ)
150 ml NaClO (14% active chlorine)
150 ml KOH stock solution

After adding the active chlorine, re-seal the bottle and shake well for homogenisation. The ready digestion solution can now be MPF filtered (see General Module m0).

2. **Digest**: Add 5 ml of MPF-filtered digestion solution per gram wet-weight of sample[14] into the sample vessel, however at least so much that the sample is completely covered with solution. Shake

[12] Bubbles indicate that the oxidation of the organic matter started (CO_2 is formed as a result of the chemical reaction between H_2O_2 and organic C). Bubble formation can be delayed by several minutes to hours after addition.
[13] This recommendation aims to provide H_2O_2 in excess to the available digestible OM.
[14] To estimate the required amount of digestion solution measure the wet weight of the samples.

gently to allow the solution to reach all parts of the sample. Leave for 5 h incubation at room temperature.

3. **Filter**: To stop the digestion, filter the digested sample in the vacuum filtration set up on a stainless steel filter of the lowest size threshold (e.g. 10 μm). Carefully rinse the stainless steel filter(s) that remained in the digestive solution from the previous filtration step from all sides using MPF water, hold it by tweezers and/or gloved hand. Replace filters if clogged. Once the filter is cleaned without residues it can be removed. Make sure to properly rinse all walls, including the beaker and the vacuum filtration funnel that the sample was in contact with. Depending on the sample matrix, it may be appropriate to use a diluted detergent solution (e.g. Tween80) to remove sample adherences from the glass ware.



m4.3 – n-*Pentane (C_5H_{12}) digestion*

► Oil and fat constituents in sample matrices can sometimes remain in the digested sample and hinder a successful spectroscopic analysis.[15] Possible use-cases of n-pentane[16] include digested animal tissues (e.g. in fish stomach analysis) post-KOH digestion and primary sludge samples from waste water treatment facilities post-H_2O_2 digestion. The procedure requires extended times with the sample exposed to air and should therefore be conducted inside the MPF clean bench. Check if your work safety regulations require wearing a gas mask (filter type “AX”).

1. **Solubilise**: As a precondition, the digested sample should be contained in a tightly sealed vessel (e.g. Erlenmeyer flasks with ground glass joint) and must be suspended in MPF water or MPF MQ. To better solubilise the fatty constituents, hold the sample in a 35 °C water bath during the procedure. Wait for the sample to warm up to approx. 35 °C, then add 10 ml of the acidified ethanol (pH ∼ 3.0, acidified with acidic acid) per 50 ml of sample. Close and shake the sample for 1 min. Place in the warm water bath again.

2. **Wash**: When the ethanol is fully mixed in the sample continue by adding 10 ml of n-pentane per 50 ml of sample. Close the lid tightly and shake for 2 min. Stop shaking and open the flask periodically to release pressure.[17] Return the sample to the warm water bath and allow the phases to separate for 5 min, with a loosely-closed lid.

3. **Remove**: Remove the pentane phase from the top of the sample using a glass pipette.[18] Stop just before the pentane layer disappears to avoid sucking the sample.[19] Repeat the above steps a further two times.

4. **Filter**: To remove any remaining dissolved fats and pentane continue with a vacuum filtration. Filter the sample in the vacuum filtration set up onto a stainless steel filter of the lowest size threshold (e.g. 10 μm). Make sure to properly rinse all walls, including the Erlenmeyer flask and the vacuum filtration funnel that the sample was in contact with. Check if additional ultasonification is needed to remove all sample particles from the filter (see Filtration above). Once the filter is cleaned without

[15] Droplets of fat or oily remains may or may not be visible, but fatty acids, their salts or alcohol combinations can be identified by spectroscopic analysis if present in the sample.
[16] Based on theoretical chemical considerations, it is not expected that the protocol could impact the integrity, numbers or spectral recognisability of common plastic polymers. However, a detailed test on actual MP is yet to be completed.
[17] Pentane has a boiling point of 36 °C, pressure may build up in the tightly closed containers.
[18] The pentane phase should not contain any MP due to a lower density (630 kg m^{-3}) than that of plastics and low surface tension. This was checked by observing the behaviour of standard fluorescent PE spheres mixed in a water/pentane dispersion.
[19] Low density MP particles might float directly in the phase boundary.

residues it can be removed. Make sure to properly rinse all walls, including the beaker and the vacuum filtration funnel that the sample was in contact with. Depending on the sample matrix, it may be appropriate to use a diluted detergent solution (e.g. Tween80) to remove sample adherences from the glass ware.



m5 – Density separation

▸ Density separation is a major step to reduce the inorganic matter content of a sample.

1. **Transfer**: Choose a separation funnel of appropriate volume.[20] Transfer the sample (dry or suspended in SPT) from a beaker or filter to the separation funnel.

⟶ **Size fractionation**: If the sample contains particles >5 mm or larger than the outlet valve, manually pick (if just very few larger particles) or sieve the sample during transfer to prevent blockage in the outlet valve or during the stirring of the sample. Sieving: Place a glass or metal funnel[21] in the top of the separation funnel with a small sieve (e.g. 4 mm pore size) inside and pass the entire sample (preferably dry) through with help of a metal spatula. Thoroughly rinse the large particles that remained on the sieve with SPT to rinse all adhering smaller particles into the sample. Optionally, retained particles can also be transferred to a beaker with a few droplets of H_2O_2 and SPT to ensure a complete detachment of adhering particles. The detachment process might take some minutes. The rinsate is then added to the separation funnel.

Fill approximately 10% of the separation funnel (valve closed!) with MPF SPT (1800 kg m^{-3}).

Add a first fraction of the sample (maximum up to 5 cm high from the lower tip of the separation funnel) and shake thoroughly to ensure that all particles in the lowest tip of the separation funnel are coated by the SPT solution. Then gently swing/shake the separation funnel inclining it ~45°.

⟶ If the sample does not contain more than approximately 5 g of solids (e.g. water samples) repeat gentle swinging of the separation funnel every 15 min during the first hour to resuspend the settled material and disintegrate agglomerates.

⟶ If the sample does not allow for digestion before density separation, add a few droplets of H_2O_2 solution during the shaking process to initiate the disintegration of particle conglomerates, wait for the reaction to proceed.[22]

2. **Upwell**: If the sample material exceeds a volume where shaking of the separation funnel becomes insufficient in freeing possible overlays of particles (as often the case for sediment and soil samples) continue with the following steps. Firstly, prefill a part of the required SPT solution into the separation funnel followed by a small amount of the sample material. Subsequently add the remaining sample material and SPT solution. Top up with a minimum of 5 cm SPT solution to form the separation phase. Thoroughly rinse all equipment that was in contact with the sample material with SPT, such as the beaker, funnel and sieve and add it to the separation funnel. Insert the spiral conveyor to the sample and mount it to the electrical overhead stirrer. Centre and place

[20] Maximum filling level of the separation funnels should not exceed 2/3 of the total volume. If samples with high matter content (e.g. sediment, soils, etc.) are treated and the application of the spiral conveyor is needed, use the appropriate separation funnels equipped with a wider neck and wider outlet valve (see section: Modified separation funnels - a versatile application for particle-rich samples).

[21] The here-presented set up also allows for sieving without a funnel, as the neck of the separation funnel fits the size of the small sieves applied. However, using a funnel potentially prevents loss of material.

[22] Be careful when adding H_2O_2 to the density separation. Always add only a few droplets to prevent the risk of strong foam formation and loss of sample material. Consider that the addition of H_2O_2 dilutes the density of the solution, therefore adjust or use an initially higher density.

it as low as possible but make sure it does not touch the walls of the separation funnel. Run it at relatively low speed (~35–60 rpm) for approximately 2 h. The time needed to allow sufficient reshuffling of the material depends on sample composition, amount and dimensions of the separation funnel and spiral conveyor.[23] After conveying, stop the spiral conveyor and thoroughly rinse adhering material into the separation funnel with ample MPF SPT while slowly lifting it out of the separation funnel. Release the lower tip (approximately 3 cm) of the separation funnel into a beaker and re-add to the separation solution.[24]

3. **Wait**: Rinse the inner walls of the separation funnel to ensure that all particles are in the separation solution. Leave it to separate for 1.1 h per 1 cm rising distance in the fluid separation phase.[25]

4. **Divide**: Slowly (no stirring up of particles) release the sedimented fraction into a MPF beaker placed below the separation funnel and shut the valve securely before any surface floating particles could be flushed out.

5. **Repeat ($^{*}X_{DS}$)**: Depending on the sediment composition (especially fine/organic rich samples) the density separation (DS) cycle has to be repeated (X_{DS} times) to reach a higher purification efficiency. Therefore, refill some MPF SPT, shake and leave it again to settle for 15 h. After this, evaluate whether you need to repeat again. As a rule, apply as many separation cycles until no further material has settled.

6. **Filter**: When the separation is finished, rinse the supernatant upside down from the separation funnel into the vacuum filtration apparatus equipped with a stainless steel filter of the lowest size threshold (e.g. 10 μm). Replace filters if clogged. Recover the undiluted SPT solution by transferring it from the filtration apparatus to a dedicated SPT recovery container (see General module m0). Then continue to thoroughly rinse the content of the separation funnel (incl. walls and glass stopper if used) into the vacuum filtration funnel using MPF water and a syringe. Take care not to lose any droplet or particle. Rinse all walls of the top part of the vacuum filter apparatus. Once the filter is cleaned without residues it can be removed. Depending on the sample matrix, it may be appropriate to use a diluted detergent solution (e.g. Tween80) to remove sample adherences from the glass ware.



m6 – Size-fractionation (wet sieving or visual sorting)

▸ Samples which remain relatively rich in larger particles (>500 μm) even after passing the treatment pipeline should be size-compartmentalised to ease later chemical analysis.

⟶ The sorting and picking process should always be conducted in a very conservative manner, meaning that only particles with clear indications of natural origin may be discarded and any other particle is to be picked and retained for analysis. This is important to minimise researcher bias.

[23] The time reported here is based on sufficient extraction results based on test MP particles (125–150 μm) in very fine sediments (40–70 μm) in a 500 ml separation funnel (see section: Conical spiral conveyor - a gentle way to separate particles). Larger volumes or more complex sample compositions may require longer time. If in doubt, test the specific sediment matrix with recovery particles.

[24] In order to recover potential MP that have become trapped close to the outlet of the separation funnel.

[25] The required rising time (waiting time) is calculated based on a spherical 10 μm particle of a density of 1.7 g cm^{-3} that travels a certain distance measured between the bottom to the top of the separation phase in SPT of 1.8 g cm^{-3} (Stokes law). Example: For a distance of 13.5 cm (maximum height experienced by the authors) this particle needs 13.7 h to rise to the top (1.1 h for 1 cm).

Whether to use 0.5 or 1 mm as a cut-off size should be decided according to the following criteria table:

	Situations suggesting a cut-off size of 0.5 mm	1 mm
Experience level of the separator	High: picking of 500 μm particles in a conservative manner is only possible with an experienced eye and hand	Low: only for particles larger 1 mm, can an inexperienced user conduct a conservative separation after a basic introduction
Number of particles in 500–1000 μm and >1000 μm size range	Particles potentially disturbing the microspectroscopic analysis are numerous in the 0.5–1 mm range	Particles potentially disturbing the microspectroscopic analysis are predominantly in the >1 mm range
Size cut-off predefined by sampling technique	Lower than 300 μm (e.g. sediment samples, flow-through filtration water samples)	300 μm and larger (e.g. Manta samples)

It should be noted that a 500 μm cut-off size should preferably be used in all cases where possible and meaningful, as it will be more beneficial to ease and expedite the microspectroscopic analysis of the remaining small fraction.

⟶ Depending on the number of particles, a case by case decision needs to be taken whether wet sieving is applied before visual sorting. In general, when more then 10 particles are above the chosen upper size limit for microspectrosopic analysis, it is advisable to first wet sieve the particles according to the below steps:

Optional wet sieving prior to visual sorting and picking

1. **Set up**: Prepare a filtration set-up as usual (e.g. 10 or 200 μm filter depending on minimum size limit) and place an additional 1 mm[26] stainless steel sieve into the vacuum filtration apparatus.

2. **Rinse**: Turn on the vacuum pump and transfer the sample by using ample MPF water, rinse the sample container and the filtrate thoroughly.[27] Finish this step by rising the sample and all relevant walls with MPF MQ water.

3. **Conserve**: Stop the pump and place the 1 mm filter into a petri dish and observed it under a binocular microscope. Particles on the smaller filter (e.g. 200 μm) are filled (back) into the Erlenmeyer beakers by using MPF MQ water.

Visual sorting and picking

1. **Sort on sieve**: If applicable, firstly check the larger (i.e. >0.5 mm or >1 mm) fraction on the sieve (or on the original vacuum filter, if no wet sieving was applied) for prominent plastic suspects,[28] separate them using fine tweezers and rinse off potentially adhering smaller particles with MPF MQ above the sample. Sandwich the separated particle between two MPF microscopy glass slides using tweezers. These “sandwiches” can then be closed with two small stripes of paper tape and labelled with a running number (e.g.: [station name]_[sample number/ ID]_[consecutive number of the plastic suspect (starting with 001)]). It is advisable to mark the location of the particle in the sandwich by circling it with a permanent marker on the outside.

⟶ If the possibility exists, particles may be directly transferred to the analysis stage of an ATR-FTIR instead of “sandwiching”.

[26] The pore size of the filter used here is 1 mm, which is based on the experiences made by the authors especially when treating Manta net samples. However, this needs to be evaluated case by case and filters can be changed or substituted with additional filters depending on the specific sample compositions.

[27] The step of flushing and rinsing the filters/sieves used to perform size-compartmentalisation of the sample must be executed exhaustively in order to prevent smaller particles remaining within the larger size fractions as they may otherwise be lost for analysis.

[28] The pre-analysis of plastic suspects should be executed in a conservative manner, which increases the number of false-positives, however, this also prevents false-negative particles and thus the loss of particles. False-positives will be identified and eliminated in the later chemical analysis.

2. **Sort in petri dish**: When further picking on the sieve is limited (due to the dark background and/or a high number of particles overlaying each other) rinse the sieve content into a petri dish using MPF MQ[29] water and continue picking all MP suspects. Ensure to assess all particles, so none remain on the filter.

3. **Creation of particle groups**: In case of a high number (>>40) of particles of identical morphological characteristics (i.e. colour, size class and surface structure) only transfer a subsample of 40 particles into individual sandwiches, labelled with an additional consecutive index number (e.g.: [. . .].[1–40]). Count all other particles of the same kind (e.g. using a click counter) and place together into an additional glass slide sandwich or petri dish, name accordingly (e.g.: [. . .].rest:[remaining total particle number]).[30]

New equipment

Within the postulated protocols, the required work effort is reduced and extraction efficiency is increased by the conception and application of new equipment. The technical advancements are explained and validated in the following section. Minor accessory equipment, namely simple and mobile tap water filters is presented in the SI.3, Fig. SI.1 which provides ample MPF water supply in the laboratory and thus contribute to QA measures.

Modified separation funnels – a versatile application for particle-rich samples

The application of glass separation funnels for density separation was applied previously [17–19]. They exhibit many advantages as such that they fulfil all relevant system requirements previously defined (Figs. 1 and 3). Firstly, glass allows for visual control of the status and quality of the separation process. Secondly, by having a steep sloping wall, the Squibb-form separation funnels was chosen in order to prevent particle adherence to walls when rising while still having an acceptable volumetric capacity that allow handling in standard laminar flow benches. Furthermore, separation funnels are off-the-shelf, long-lasting products of little cost. The previous problem of only fitting small amounts of sample material [19,20] is overcome by using the newly developed conical spiral conveyor, presented in the respective section below, which allows for efficient MP extraction despite an enormous overlay of particles. Some modifications on the separation funnels were required for matter-rich samples, for instance, to overcome the problem of clogging [17] when using very fine or very coarse materials. Standard outlet valves of all separation funnels, especially those intended for particle-rich samples, were replaced by larger ones (ø 10 mm) to ease the release of sedimented particles. To satisfy the non-contaminating system requirement, plastic handles and nuts were replaced by stainless steel parts. Furthermore, a widening of the standard neck size (ø 25 mm) was necessary to allow the installation of the larger spiral conveyor (ø 35 mm, Fig. 3). We decided that 50 mm was the optimum size as this also fits the sieves potentially used for particle fractionation (m5). While custom equipment can be costly, these adaptations typically come at a low cost and constitute a one-time investment, fulfilling QuEChERS requirements (Fig. 1). All customisations of glass ware can be provided by a glass blower. Protocol modularity can limit costs, simplify the procedures and equalise extraction effectiveness when working with various sample matrices. Hence, the modular use of equipment is of advantage and is implemented by the universal application of the separation funnels for samples from water, sediments, beaches, soils, waste water, etc.

Conical spiral conveyor – a gentle way to separate particles

During density separation, it has to be ensured that particles get in contact with the liquid phase of the density separation solution in order to prevent trapping of particles by overlaying material.

[29] MPF MQ is recommended here, to dilute and wash out solutes in and on the picked particles, as they are subjected to spectroscopic analysis thereafter.

[30] Based on the subsample of 40 particles which undergo chemical analysis, the remaining particles will be extrapolated for plastic/non-plastic origin, as well as polymer type distribution. If the analysed fraction of particles is too diverse, a larger subsample can be compiled.

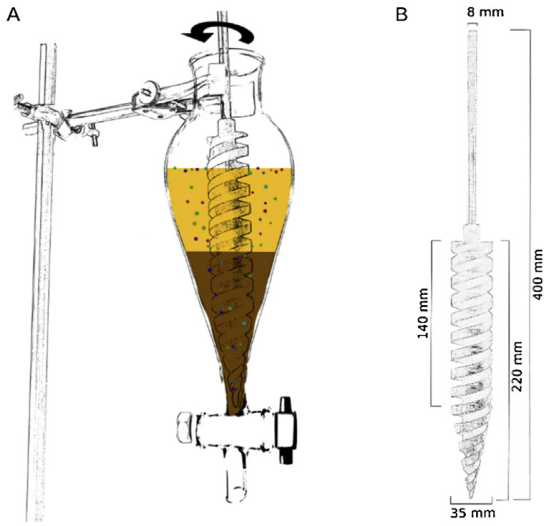


Fig. 3. A) Sketch showing the custom-made conical spiral conveyor, which improves the extraction efficiency of MP in a density separation despite being buried by particulate matter. The spiral conveyor is operated within a separation funnel (Squibb form). The particles of the sample are transported upwards and released in a fountain-like manner into the density separation solution above, where they can freely separate. A video (picture sequence over 2 hours) visualising the efficiency of the density separation process by means of the conical spiral conveyor is provided as supplementary material to the paper. Approximately 0.5 g of test MP i.e. fluorescent green polyethylene microspheres (125–150 μm, $\rho = 1025\ kg\ m^{-3}$) were added initially in the lower part of the sediment fraction (glass particles, 40–70 μm). SPT ($\rho = 1800\ kg\ m^{-3}$) is added as the density separation solution. When starting the spiral conveyor, it can be observed that the test MP are being transported upwards and partially rise to the top. Some test MP cannot be freed in the first cycle and are covered again by sediments. After several cycles (after ~2 h) all particles are extracted and float on the top of the density solution (supernatant). B) The technical drawing of the large spiral conveyor (ø 35 mm) with details on the physical dimensions. Other sizes can be up or down-scaled accordingly.

Different approaches were applied in previous studies, such as shaking or stirring the sample (e.g. [4,13]). However, shaking (by hand or machine) is efficient only on relatively small sample amounts and stirring blades, such as those implemented in the MicroPlastic Sediment Separator (MPSS; [4]), are prone to disintegrate MP particles by grinding sample matter directly against a hard (i.e. stainless steel) surface and thus falsify results [21]. To increase the extraction efficiency of MP from particle-rich samples whilst overcoming these potential limitations, we developed a custom-made spiral conveyor that allows for gentle and sufficient separation of the particles (Fig. 3A). Instead of uncontrolled mixing, particles from the bottom of the separation vessel are gently transported upwards and released in a fountain-like manner to the liquid separation phase above. Once freely suspended, particles can separate based on their physical features and either float to the top, stay in suspension or settle again to the sedimented solid phase. A side effect of the gentle movement is the disintegration of material conglomerates which contributes to an efficient separation process. The conical shape reduces the bottom-facing area of the rotating spiral conveyor to just a fine tip. Compared to other stirring procedures described in the literature which use flat rotor blades or rods (e.g. Imhof, 2012 [4]) this is an important improvement, as it minimises the area and thus the possibility of grinding and squeezing particles between the rotating element and the vessel walls.

The principal functioning of the spiral conveyor is based on the widely-used industrial screw conveyors. In the lower 80 mm, the spiral conveyor fits the conical shape of the Squibb form separation funnels with a 5 mm wide gap in between. As different sample volumes are required depending on the sample type and research question, two different conveyor sizes were built that allow sufficient mobilisation of the particle phase. The smaller one (ø 20 mm) is designed for the application in 250 ml separation funnels, the larger one (ø 35 mm) for 500–1000 ml separation funnels. The spatial dimensions of the larger spiral conveyor are given in Fig. 3B. Other sizes could be simply scaled up or down or adapted to other types of separation vessels. It is important to note, that the screw conveyor part is designed to protrude into the separation solution above the sedimented particles for an efficient separation process to work. The shaft fits into a drill chuck of a typical electrical overhead stirrer for quick (dis)mounting. Due

to the corrosive nature of most separation media, stainless steel is considered the optimal material. In the case of the larger conveyor, brass was used due to limitations of the available lathe machine. The presented set up for particle-rich matrices has a volumetric capacity of up to 1 l, appropriated to fit approximately 500 ml of particulate matter. By experience, this is a reasonable amount to achieve robust MP numbers. This volumetric capacities compares to other methods like the elutriation approach [22], though requiring less space and less steps involved in the separation process to reach reasonable extraction efficiencies. There are few, such as the MPSS, that have a larger sample capacity (~6 kg, [4]), however, most other separators hold substantially smaller volumes [17,20].

Method validations and comparison

Recovery and reduction rates

A first semi-quantitative validation test was given by the video sequence shown above (link, Fig. 3A) demonstrating the efficiency of the density separation process by means of the conical spiral conveyor. Additionally, we performed recovery tests as a measure of extraction efficiency of the entire MP extraction procedure based on beach sediment samples (n = 7, d50 ~ 300 μm). The recovery tests followed the respective pathway though the protocol tree including the operation of the spiral conveyor to separate particle-rich matrices. Test particles were visually identified using a microscope by their specific morphological characteristics. Polyamide particles (PA-6) of 450 μm (n = 20) in size were used and resulted in recovery rate of 95 ± 6%. This value is within the higher margin of other available recovery rates of other MP extraction methods, e.g. modified decanting, elutriation, MP sediment separator, sequential density extraction, oil extraction (see Table 1 in [17] or [19,23] for comparison). However, recovery rates are known to decrease with MP size [20] and most studies lack sufficient tests [24], especially in the size range below 300 μm (longest dimension). We determined the recovery rate of smaller MP using PE fluorescent particles of 125–150 μm (n = 60–80) in size resulting in 78 ± 6%. In this size class, however, reasonable comparisons to other studies are difficult as insufficient data is available. Not all study designs in the available literature (keyword search Web of Science: microplastics, recovery, sediment/soil/sludge) were technically able to extract the full range of polymer types (e.g. ρ = 900–1400 kg m^{-3}). Of those that were, only very few studies tested the distinct size range of small MP from real, particle-rich environmental matrices (e.g. soils, sediments, sludge), whilst applying particle-based analytics and reporting sufficient information on the recovery test to allow a comparison. For instance, Imhof et al. [4] and Claessens et al. [22] tested particles between 40–309 μm and ~250 μm respectively, resulting in a recovery rate above 95%. However, a comparison of our recovery rates to the two mentioned is in question for several reasons. These studies used sediments that underwent several cleaning steps (sequential density separation, elutriation) before performing recover tests which ultimately results in a test matrix of very low conglomeration potential and thus not a realistic sample matrix. It is expected that several factors such as the sediment composition, i.e. grain size and/ or organic matter content influence the extraction efficiency, potentially to a significant degree. This is a current knowledge gap that needs to be investigated in detail in a separate study. Further, when testing such small MP it is important to ensure that the size remained unchanged after the treatment as some techniques are prone to disintegrate MP [21] and thus potentially falsely increase the MP number. This remained unclear in some cases [4]. Hengstmann et al. [25] performed tests in a comparable size range (63–200 μm) to our study acquiring smaller recovery rates of 66 ± 17%. However, they used MP test particles with a higher density which often show reduced recovery rates compared to lighter once. Inconsistencies between recovery test designs exist as some studies tested the entire MP extraction pipeline (present, [23]), while others determined the recovery rates of the separation step solely [4,25]. The latter is likely to achieve higher values. The use of large MP size class ranges (e.g. 100–500 μm, [20]) without determining the size distribution (e.g. median, mean value) complicates a comparison to more narrow size ranges, such as those used in the present study, as the size-dependency of extraction efficiency remains disregarded. For a reasonable comparison of extraction methods, standards on the test material and procedure are needed. To date, a comparison of recovery rates of small MP (<500 μm) between different studies is not reliable due to the listed reasons.

Another measure of method validation is the mass reduction, i.e. the weight difference between the initial and treated dry weight sample. The mass reduction of exemplary sediment samples, ranging

from beach sand (low in organics, coarse sediment) to estuary sediments (high in organics, fine sediment) was 99.98 ± 0.03% (n = 6) on average (SI.4, Table SI.1). Neither the initial sample mass nor the different sample matrix complexities could entirely account for the variability in the amount of material left in a sample after treatment. It can be assumed that the final number of particles also depends on the instruments and procedures used as well as on the operator.

Process time

While selecting the best methodological steps is critical for final accuracy of results, improvements must also be time-efficient. The time consuming nature of MP extraction was often reported in the past (e.g. Zarfl, 2019 [1]), however, without documentation of the concrete time measurements [24]. We report estimated procedural time for exemplary protocol pipelines, conducted by an experienced person, for better comparability of methods and planning of treatment procedures (SI.5, Table SI.2).

This paper presents a compilation of all methods necessary to fully process any given environmental sample ready for automated surface chemistry analysis. These methods are presented in a modular way which can be adapted to what a special sample requires. New equipment has also been described which, combined with the presented methods, significantly improve the methods for extracting both large (>0.5 mm) and small (<0.5 mm) MP from environmental samples.

Funding

This work resulted from the BONUS MICROPOLL project supported by BONUS (Art 185), funded jointly by the European Union and Federal Ministry of Education and Research (BMBF) (03F0775A), the BMBF project MicroCatch_Balt (03F0788A) and the BMBF project PLASTRAT (02WPL1446 J).

Acknowledgements

We thank the IOW workshop for the construction of the spiral conveyor and the clean bench setup, and Dr. Klaus-Jochen Eichhorn (Leibniz-Institute for Polymer Research), as well as Jakob Strand (Aarhus University) for the helpful advice on the development of the pentane protocol for improved spectroscopic analysis. Thanks also to Franziska Fischer and Dieter Fischer for their assistance in method validation.

Declaration of Competing Interest

The authors declare that there are no conflicts of interest.

Appendix A. Supplementary data

Supplementary material related to this article can be found, in the online version, at doi:https://doi.org/10.1016/j.mex.2020.100784.

References

[1] C. Zarfl, Promising techniques and open challenges for microplastic identification and quantification in environmental matrices, Anal. Bioanal. Chem. 411 (2019) 3743–3756, doi:http://dx.doi.org/10.1007/s00216-019-01763-9.
[2] M. Cole, H. Webb, P.K. Lindeque, E.S. Fileman, C. Halsband, T.S. Galloway, Isolation of microplastics in biota-rich seawater samples and marine organisms, Sci. Rep. 4 (2014) 4528, doi:http://dx.doi.org/10.1038/srep04528.
[3] A. Dehaut, L. Hermabessiere, G. Duflos, Current frontiers and recommendations for the study of microplastics in seafood, TrAC Trends Anal. Chem. 116 (2019) 346–359, doi:http://dx.doi.org/10.1016/j.trac.2018.11.011.
[4] H.K. Imhof, J. Schmid, R. Niessner, N.P. Ivleva, C. Laforsch, A novel, highly efficient method for the separation and quantification of plastic particles in sediments of aquatic environments, Limnol. Oceanogr. Methods 10 (2012) 524–537, doi:http://dx.doi.org/10.4319/lom.2012.10.524.
[5] A.L. Lusher, N.A. Welden, P. Sobral, M. Cole, Sampling, isolating and identifying microplastics ingested by fish and invertebrates, Anal. Methods 9 (2017) 1346–1360, doi:http://dx.doi.org/10.1039/C6AY02415G.
[6] D. Fischer, Personal Communication, Leibniz-Institute for Polymer Research (IPFDD), 2019.

[7] D.B. Alcântara, T.S.M. Fernandes, H.O. Nascimento, A.F. Lopes, M.G.G. Menezes, A.C.A. Lima, T.V. Carvalho, P. Grinberg, M.A.L. Milhome, A.H.B. Oliveira, H. Becker, G.J. Zocolo, R.F. Nascimento, Diagnostic detection systems and QuEChERS methods for multiclass pesticide analyses in different types of fruits: an overview from the last decade, Food Chem. 298 (2019)124958, doi:http://dx.doi.org/10.1016/j.foodchem.2019.124958.
[8] M. Anastassiades, S.J. Lehotay, D. Štajnbaher, F.J. Schenck, Fast and Easy Multiresidue Method Employing Acetonitrile Extraction/Partitioning and "Dispersive Solid-Phase Extraction" for the Determination of Pesticide Residues in Produce 21, (2003) .
[9] D.M. Buede, W.D. Miller, The Engineering Design of Systems: Models and Methods, Wiley Series in Systems Engineering and Management, Wiley, 2016.
[10] R. Marshall, P.G. Leaney, A systems engineering approach to product modularity, Proc. Inst. Mech. Eng. Part B: J. Eng. Manuf. 213 (1999) 847–851, doi:http://dx.doi.org/10.1243/0954405991517272.
[11] V. Hidalgo-Ruz, L. Gutow, R.C. Thompson, M. Thiel, Microplastics in the marine environment: a review of the methods used for identification and quantification, Environ. Sci. Technol. 46 (2012) 3060–3075, doi:http://dx.doi.org/10.1021/es2031505.
[12] K. Enders, R. Lenz, S. Beer, C.A. Stedmon, Extraction of microplastic from biota: recommended acidic digestion destroys common plastic polymers, ICES J. Mar. Sci. 74 (2017) 326–331, doi:http://dx.doi.org/10.1093/icesjms/fsw173.
[13] J. Strand, Z. Tairova, Microplastic Particles in North Sea Sediments (No. No. 178), Aarhus University, DCE – Danish Centre for Environment and Energy, 2015.
[14] S. Albalá-Hurtado, L.E. Pascual-Sastre, M.C. Vidal-Carou, A. Mariné-Font, J. Permanyer-Fàbregas, Comparison of two fat extraction methods in powdered infant milks, J. Food Compos. Anal. 12 (1999) 333–337, doi:http://dx.doi.org/10.1006/jfca.1999.0837.
[15] A. Dieffenbacher, B. Lüthi, Die Direkte Kolorimetrische Bestimmung der Peroxidzahl (POZ) in Milchprodukten, Mitteilungen aus dem Gebiete der Lebensmitteluntersuchung und Hygiene 77 (1986) 544–553.
[16] M. Fischer, B.M. Scholz-Böttcher, Simultaneous trace identification and quantification of common types of microplastics in environmental samples by pyrolysis-gas chromatography-mass spectrometry, Environ Sci Technol. 51 (9) (2017) 5052–5060, doi:http://dx.doi.org/10.1021/acs.est.6b06362.
[17] R.L. Coppock, M. Cole, P.K. Lindeque, A.M. Queirós, T.S. Galloway, A small-scale, portable method for extracting microplastics from marine sediments, Environ. Pollut. 230 (2017) 829–837, doi:http://dx.doi.org/10.1016/j.envpol.2017.07.017.
[18] E. Fries, J.H. Dekiff, J. Willmeyer, M.-T. Nuelle, M. Ebert, D. Remy, Identification of polymer types and additives in marine microplastic particles using pyrolysis-GC/MS and scanning electron microscopy, Environ. Sci. Process. Impacts 15 (2013) 1949–1956, doi:http://dx.doi.org/10.1039/c3em00214d.
[19] T. Mani, S. Frehland, A. Kalberer, P. Burkhardt-Holm, Using castor oil to separate microplastics from four different environmental matrices, Anal. Methods 11 (2019) 1788–1794, doi:http://dx.doi.org/10.1039/C8AY02559B.
[20] R. Nakajima, M. Tsuchiya, D.J. Lindsay, T. Kitahashi, K. Fujikura, T. Fukushima, A new small device made of glass for separating microplastics from marine and freshwater sediments, PeerJ 7 (2019) e7915, doi:http://dx.doi.org/10.7717/peerj.7915.
[21] M.B. Zobkov, E.E. Esiukova, Evaluation of the Munich Plastic Sediment Separator efficiency in extraction of microplastics from natural marine bottom sediments, Limnol. Oceanogr. Methods 15 (2017) 967–978, doi:http://dx.doi.org/10.1002/lom3.10217.
[22] M. Claessens, L. Van Cauwenberghe, M.B. Vandegehuchte, C.R. Janssen, New techniques for the detection of microplastics in sediments and field collected organisms, Mar. Pollut. Bull. 70 (2013) 227–233, doi:http://dx.doi.org/10.1016/j.marpolbul.2013.03.009.
[23] R.R. Hurley, A.L. Lusher, M. Olsen, L. Nizzetto, Validation of a method for extracting microplastics from complex, organic-rich, environmental matrices, Environ. Sci. Technol. 52 (2018) 7409–7417, doi:http://dx.doi.org/10.1021/acs.est.8b01517.
[24] M.E. Miller, F.J. Kroon, C.A. Motti, Recovering microplastics from marine samples: a review of current practices, Mar. Pollut. Bull. 123 (2017) 6–18, doi:http://dx.doi.org/10.1016/j.marpolbul.2017.08.058.
[25] E. Hengstmann, M. Tamminga, C. vom Bruch, E.K. Fischer, Microplastic in beach sediments of the Isle of Rügen (Baltic Sea)—implementing a novel glass elutriation column, Mar. Pollut. Bull. 126 (2018) 263–274, doi:http://dx.doi.org/10.1016/j.marpolbul.2017.11.010.
[26] G. Liebezeit, F. Dubaish, Microplastics in beaches of the East Frisian islands Spiekeroog and Kachelotplate, Bull. Environ. Contam. Toxicol. 89 (2012) 213–217, doi:http://dx.doi.org/10.1007/s00128-012-0642-7.
[27] C.J. Moore, S.L. Moore, S.B. Weisberg, G.L. Lattin, A.F. Zellers, A comparison of neustonic plastic and zooplankton abundance in southern California's coastal waters, Mar. Pollut. Bull. 44 (2002) 1035–1038, doi:http://dx.doi.org/10.1016/S0025-326X(02)00150-9.
[28] R.C. Thompson, Y. Olsen, R.P. Mitchell, A. Davis, S.J. Rowland, A.W.G. John, D. McGonigle, A.E. Russell, Lost at sea: where is all the plastic? Science 304 (2004) 838, doi:http://dx.doi.org/10.1126/science.1094559.

This is the end of the publication

When every particle matters: A QuEChERS approach to extract microplastics from environmental samples

by Kristina Enders, Robin Lenz, Juliana A. Ivar do Sul, Alexander S. Tagg, Matthias Labrenz

You might want to continue reading the synopsis at page 18, or jump back to the start of this publication at page 68.

High-Throughput Analyses of Microplastic Samples Using Fourier Transform Infrared and Raman Spectrometry

by Josef Brandt, Lars Bittrich, Franziska Fischer, Elisavet Kanaki, Alexander Tagg, Robin Lenz, Matthias Labrenz, Elke Brandes, Dieter Fischer, Klaus-Jochen Eichhorn

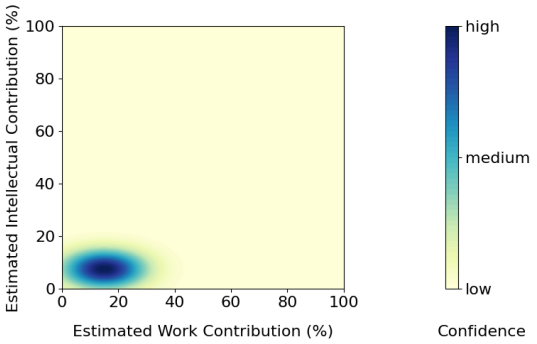
- **Date published**: March 21, 2020
- **Type**: Research Article
- **Published in**: Applied Spectroscopy, SAGE
- **License**: © SAGE
- **DOI**: 10.1177/0003702820932926, **Reference**: [4]
- **Citations**: 55 (Crossref/DOI, 2025-11-18)

Contributions

[**Note**: *No author contribution statement is available for this publication. The following partial contribution statement is created for this thesis only to the best of my knowledge and belief.*] RL provided samples for testing and calibration of the developed software and contributed to writing and revision of the manuscript.

Quantitative own contributions based on self-assessment

In the dimensions of expended work effort and intellectual contribution, I consider my shares are likely to be between 10% and 20% and between 5% and 10% respectively. This is visualised below as an interpolated histogram of 500 samples from Gaussian distributions with the aforementioned estimates at plus/minus two standard deviations.



Special Issue: Microplastics

Applied Spectroscopy

Applied Spectroscopy
2020, Vol. 74(9) 1185–1197
© The Author(s) 2020
Article reuse guidelines:
sagepub.com/journals-permissions
DOI: 10.1177/0003702820932926
journals.sagepub.com/home/asp
SAGE

High-Throughput Analyses of Microplastic Samples Using Fourier Transform Infrared and Raman Spectrometry

Josef Brandt[1,2], Lars Bittrich[1,3], Franziska Fischer[1], Elisavet Kanaki[1], Alexander Tagg[4], Robin Lenz[4], Matthias Labrenz[4], Elke Brandes[5], Dieter Fischer[1], and Klaus-Jochen Eichhorn[1]

Abstract

Determining microplastics in environmental samples quickly and reliably is a challenging task. With a largely automated combination of optical particle analysis, Fourier transform infrared (FT-IR), and Raman microscopy along with spectral database search, particle sizes, particle size distributions, and the type of polymer including particle color can be determined. We present a self-developed, open-source software package for realizing a particle analysis approach with both Raman and FT-IR microspectroscopy. Our software GEPARD (Gepard Enabled PARticle Detection) allows for acquiring an optical image, then detects particles and uses this information to steer the spectroscopic measurement. This ultimately results in a multitude of possibilities for efficiently reviewing, correcting, and reporting all obtained results.

Keywords

Microplastics, Raman, Fourier transform infrared, FT-IR, microspectroscopy, Open Source

Date received: 8 November 2019; accepted: 29 April 2020

Introduction

Microplastic particles (MP) have become a very intensively discussed and highly visible topic in both scientific and mainstream media.[1,2,3–10,11] Of the 8.3 billion tons of plastic produced worldwide by 2015, 6.3 billion tons of plastic waste produced are offset in the same period.[12] Plastics are estimated to remain in the environment for 100–500 years, depending on the type of plastic.[13] By 2015, only 9% of the plastic waste produced worldwide was recycled, just 12% of the plastic waste was incinerated and recycled for energy with 79% of the plastic waste was landfilled or emitted into the environment, mostly in the sea and seabed. According to estimates, approximately eight million tons of plastic waste find their way into the sea every year via rivers, wind, wastewater, etc. This waste accumulates in the environment, mostly in the sea and in the seabed.[13] These plastics can then fragment into MP by wind, waves, and solar radiation. Microplastics are solid and insoluble plastic particles smaller than 5 mm and larger than 1 μm.[14] To reduce the load of MP in the environment, there is a considerable need for research into the main sources, transport routes, and whereabouts, as well as their distribution in the environment. Decisive for future evaluation is the knowledge of how much MP, which MP types, and which sizes are present in different environmental compartments (e.g., oceans, sediments, rivers, soils, atmosphere).

A key issue of current MP studies is to gather greater and more comprehensive knowledge of MP occurrence in the environment and use this to reliably ascertain sources and sinks of MP, as well as to evaluate potential environmental impacts (i.e., effect on biota and humans).[15,16] The

[1]Leibniz-Institut für Polymerforschung Dresden e.V., Dresden, Germany
[2]Department of Marine Sciences, University of Gothenburg, Fiskebäckskil, Sweden
[3]Complex Fiber Structures GmbH, Dresden, Germany
[4]Leibniz-Institut für Ostseeforschung Warnemünde, Rostock, Germany
[5]Johann Heinrich von Thünen-Institut, Braunschweig, Germany

Corresponding Authors:
Josef Brandt, University of Gothenburg, Department of Marine Sciences, Kristineberg 566 SE-451 78 Fiskebäckskil, Sweden
Email: josef.brandt@gu.se
Dieter Fischer, Leibniz Institute for Polymer Research, Hohe Str. 6, Dresden, 01069, Germany
Email: fisch@ipfdd.de

currently employed methods for MP determination in environmental samples are still too time-consuming to be used as monitoring techniques. Hence, significant efforts have been made by numerous research groups to facilitate and harmonize MP analysis procedures.[5–7,17–19]

Determining the MP content of any environmental sample requires three steps: (i) a suitable procedure for actually obtaining the sample has to be found, depending whether a sample is to be taken from, e.g., air, water, biota, or soil.[1,4,20–22] (ii) An adequate protocol for sample processing has to be applied. Depending on the type of analysis, this can be, e.g., sample homogenization or removing as much organic and/or inorganic matter as possible. In particle-based analyses, increasing the MP to non-MP particles ratio significantly reduces analysis time, as a lower number of potential MP particles has to be measured. Commonly employed procedures entail density separation to remove inorganic compounds,[23,24] and Fenton's reagent ($H_2O_2 + Fe^{2+}$)[25] or enzymatic digestion to remove organic residues.[26] (iii) The previously purified MP sample has to be analyzed in detail by an appropriate analysis technique. All three steps are equally important and have to be carried out with extreme care in order to avoid contamination from MP from either equipment used or simply the laboratory air itself. Taking and evaluating blind samples (i.e., samples without any MP that undergo the exact same procedure) for assessing the level of contamination is critical.

Our work focuses on the third part of the aforementioned procedure, the chemical analysis of the purified sample. Numerous works can be found throughout literature that suggest different procedures for MP assessment in environmental samples.[19,27] Notable examples are: Selecting single particles under a microscope for Fourier transform infrared (FT-IR) measurements in attenuated total reflection (ATR),[28–30] transmission[31–33] or reflection,[34–36] FT-IR imaging,[6,31,37,38] Raman microspectroscopy,[7,37,39] pyrolysis–gas chromatography–mass spectrometry (py-GC-MS),[40–42] or thermoextraction and desorption coupled with gas chromatography–mass spectroscopy (TED-GC-MS).[41,43–45] The current key challenge is to streamline suitable methods into easy to apply tools that do not require a team of scientists to be performed. The future of MP analyses lies in scaling up the number of samples, thereby obtaining more comprehensive datasets. Only by significantly expanding campaigns to sample environments at higher frequency both spatially and temporally, effective measures against MP pollution can be derived. Thus, the methods we develop have to be fast, affordable, and easy to learn and use, while not sacrificing information, accuracy, or reliability.

In general, the MP content of any sample can be determined in terms of mass or number of MP. Mass-based techniques, such as py-GC-MS or TED-GC-MS, report total mass but cannot infer from how many individual MP this mass is derived. However, when using a particle-based approach, mass ratios (e.g., milligrams MP per kilogram dry weight of sample) can only be assumed by estimating particle volumes and applying bulk density values.[5] On the other hand, particle-based techniques measure each particle individually to obtain both the chemical composition and size, thereby providing more detailed information. The most frequently employed techniques for that approach employ FT-IR or Raman microspectroscopy.[17,37] Therein, MP samples are filtered onto suitable substrates and then analyzed spectroscopically to determine size and chemical nature of each particle.

Both analytical approaches, thermoanalysis and vibrational spectroscopy, come with their advantages and caveats. The huge advantage of a mass-based technique is its high sample throughput. For example, state of the art py-GC-MS or TED-GC-MS takes only a few hours to process 100 mg of an environmental sample that does not need specific treatment other than careful homogenization.[41,45] This makes these techniques very promising candidates for widespread environmental monitoring in routine operation. In contrast, the spectroscopic techniques require elaborate sample purification and can take significantly longer for measurement and data processing. Their main benefit, however, is that the analysis happens on the particle level, i.e., each particle is registered individually with information on shape, size, chemical classification and, in most cases, even color. This information is currently of high relevance for elucidating sources and sinks of MP particles. Additionally, knowledge of polymer type and particle size/shape is also critical for modeling pathways of MP,[46–48] as well as for assessing potential MP impacts.[15,16] Given the importance of this information, spectroscopic particle analysis is currently widely preferred for MP studies, despite the lack of efficiency compared to mass spectrometry. Therefore, improving the efficiency of these approaches is of paramount importance for the future of MP research.

This study contributes significantly to this issue by enabling the microspectroscopic particle analyses to be employed far more efficiently.

Microplastic Analysis Using FT-IR and Raman Microscopy: State of the Art

Both methods of vibrational spectroscopy can generally be used in two inherently different modes (Fig. 1). The first one is the imaging approach, which entails complete spectroscopic measurement of the entire sample surface in order to obtain an individual spectrum for each "pixel". After evaluation of all spectra, a chemical image is obtained in which each pixel is assigned to a certain material class. Neighboring pixels of the same class are then considered one particle. In contrast to that, the second approach is to first acquire an optical image of the entire filter and to run an automated particle recognition algorithm that identifies all present particles. Spectra then need only to be acquired where particles were found.

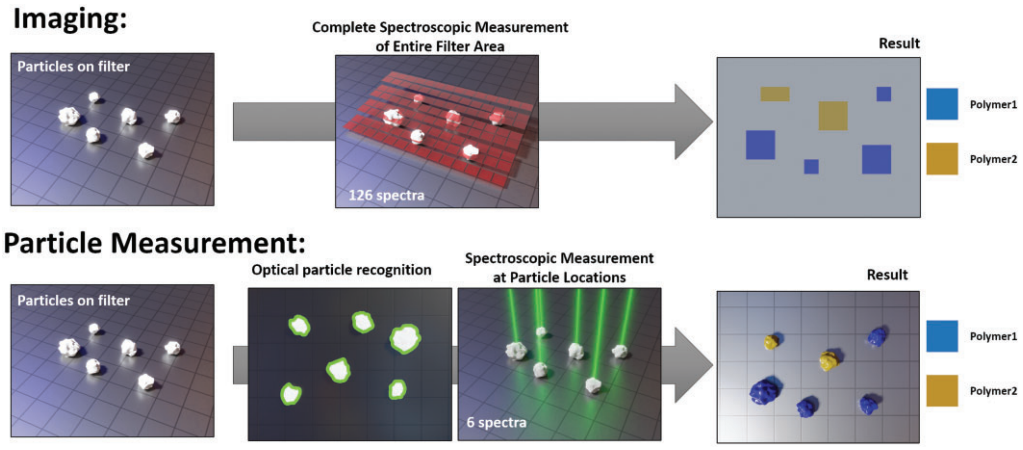


Figure 1. Imaging and particle measurement as two different approaches for analyzing particles on a filter substrate.

The first and most obvious difference between both approaches is the number of acquired spectra. Considering 10 000 particles on a filter of 10 mm × 10 mm, the imaging approach requires acquiring 10^6 spectra in a resolution of 10 μm, whereas only 10^4 have to be taken for the particle recognition approach. Requiring 100 times more spectra for imaging renders both data acquisition and evaluation, a particular challenge. Spectra acquisition can only be done in reasonable time scales, when array detectors are used, such as the focal plane array (FPA) detector, which is capable of acquiring up to 128 × 128 (=16 384) spectra simultaneously.[49] Unfortunately, such detectors are only available for FT-IR spectroscopy, which makes Raman spectroscopy not feasible for high-resolution imaging of larger surfaces. The imaging approach is also more challenging regarding data evaluation.[6,50] Conventional correlation of the measured spectra to databases is becoming either very slow with very high spectra numbers or requires very high computational power. Chemometric tools, such as classification by random decision forest, can significantly speed up analysis, but are far from trivial to set up and are limited in the number of substance classes they can distinguish.[18]

In contrast, the approach using optical image recognition to identify particles requires less sophisticated hardware and allows for a higher flexibility in choosing the evaluation strategy. Both chemometric classification and "conventional" database evaluation are readily applicable. Furthermore, FT-IR and/or Raman microscopy can be used similarly to perform the chemical identification, which is advantageous as Raman, unlike FT-IR, can analyze particles below 10 μm. The practically achievable lower limit strongly depends on instrumental setup and type of sample, the theoretically possible value is 0.4 μm. On our routine setup (20 × objective), we can confidently work down to a size of 2–3 μm. The main challenge remains the particle recognition step, as finding and tuning a suitable image segmentation algorithm is anything but trivial. However, once a reliable particle recognition has been achieved, additional information about particle color or morphology can be derived from the optical image.

To draw a conclusion from this short comparison of imaging and particle recognition approaches, the initial perspective of making MP analysis techniques more suitable for large-scale monitoring strategies has again to be considered. Considering this perspective, the imaging approach has distinct disadvantages, namely costly equipment (FPA detector), less flexible spectra evaluation, and finally the practical limitation to FT-IR, thus excluding Raman measurements for MP particles < 10 μm. Thus, we believe that pushing forward the particle recognition approach is the strategy of choice for greatly expanding the scale in which MP analyses are performed, not only by highly trained MP analysis teams but also by a broader community.

As stated in the Introduction, the key challenge is to decrease the required measurement time for a given particle analysis. Considering the complex nature of the environmental samples on the one side, but also of the respective spectroscopic workflows on the other side, clearly shows that there cannot be a universally valid formula to decrease measurement time. Instead, an analysis procedure should offer the user the highest possible freedom in designing and performing the particle analysis, respecting the constraints coming from the nature of the samples and the accessible laboratory equipment.

Herein, we present our realization for MP analysis using the optical particle detection approach that can be combined with both FT-IR and Raman spectroscopy. We developed a new software for bundling all steps in the analysis pipeline in an easy to use package while providing the highest possible flexibility. Gepard Enabled PARticle Detection

(GEPARD) is an open-source project under the GNU General Public License. It can be downloaded from a GitLab repository and used freely.[51] Moreover, the software is designed in a modular way and can be modified and extended by others for further increasing its usability in the field. In this manuscript, we describe the application of GEPARD in combination with Raman and FT-IR microspectroscopy and present first results in the field of MP analysis.

Materials and Methods

Instruments

The Raman imaging microscope (WITec alpha 300R) was equipped with 532 and 785 nm lasers together with dedicated detectors. Spectra are acquired with gratings of 600 or 1200 l/mm. For typical instruments, we use the 532 nm laser on the 600 l/mm grating, which allows acquiring the entire spectral range (150–3600 cm^{-1}) with one shot, at a spectral resolution of ~3.5 cm^{-1}. Image acquisition can be done in brightfield (BF) and darkfield (DF) at magnifications of 5, 20, 50, and 100×. The step size of the motorized stage is 100 nm. The entire microscope can be remote-controlled through a component object model (COM) interface (interprocess communication developed by Microsoft) to the WITec control software.

The Raman microscope (Renishaw inVia Qontor) can irradiate with lasers of wavelengths of 532, 633, and 785 nm. The switching of lasers and gratings (600 l/mm, 1200 l/mm, or 1800 l/mm) is fully automated. By default, the combination of 532 nm laser and 600 l/mm grating is used, resulting in a spectral range from 150 to 3600 cm^{-1} at a spectral resolution of approx. 7 cm^{-1}. Optical image acquisition works in both DF and BF at magnifications of 5, 20, 50, and 100×. The automated stage has a step size of 100 nm. The liveTrack feature allows for an automated focus tracking in real time. The microscope can be remote controlled via a network interface.

The FT-IR microscope (PerkinElmer Spotlight 400) features a mercury–cadmium–telluride (MCT) line-detector for imaging and an MCT single-detector. Spectra can be acquired in transmission, reflection, or micro-ATR with visual autofocus. The microscope cannot be remote controlled, but allows importing seed-point lists for predefined measuring layouts. The seed-lists contain information about location (*x,y,z*) and aperture configuration (with, height, rotation angle) of each particle. In default operation, we acquire spectra with eight scans per acquisition at a spectral resolution of 4 cm^{-1}.

The optical microscope (Zeiss Imager.Z2m) allows rapid acquisition of optical images at very high fidelity at magnifications of 5, 10, or 20× in either BF or DF. Multiple *z*-levels can be acquired for obtaining an image, with optimal depth-of-field and height map being extracted. Both images can be imported into GEPARD to create a project file that can be used for subsequent particle recognition and spectral measurement. The Zeiss software itself features manifold image segmentation and processing modules.

MP Analysis Pipeline with GEPARD

GEPARD is designed to cover all steps in the analysis pipeline from optical image acquisition over spectra acquisition, combination of particle and chemical data to generation of final reports, both visually and in spreadsheet form. The software currently supports importing images from Zeiss microscopes, controlling Raman microscopes from WITec and Renishaw to allow for image acquisition and particle measurement. Furthermore, particle position data can be exported to FT-IR microscopes from PerkinElmer. Each step is developed to minimize the need for human adjustments, thus keeping human bias and required time at the lowest possible limit.

GEPARD is designed around a particular analysis workflow, as summarized in Table I. First, a full image of the filter is acquired during an optical scan. That image is used to run a particle recognition for identifying particles, determining their size, shape, and color and to set the coordinates for the subsequent spectroscopic measurement. In the spectroscopic scan, a spectrum is acquired for each particle. All acquired spectra are then evaluated to obtain a chemical classification (i.e., particle type) to each spectrum. All spectroscopic classifications are then combined with the already determined particle characteristics. The results can then be reviewed and edited, if necessary. Finally, the results can be displayed graphically and exported into different formats.

Table I. Individual steps of the analysis pipeline using GEPARD.

Step 1	Step 2	Step 3	Step 4	Step 5	Step 6
Image acquisition	Particle recognition	Spectroscopic measurement	Spectra evaluation	Review/edit results	Data output
GEPARD, Zeiss	GEPARD	WITec, Renishaw, PerkinElmer	TrueMatch (refer to the Spectra Evaluation section)	GEPARD	GEPARD

The lower row in Table 1 indicates that most tasks are directly integrated into GEPARD. The following sections will review the individual steps in detail.

Image Acquisition/Optical Scan

The first step is to acquire an optical image of the filter. In the case of a WITec or Renishaw instrument, the optical scan can be done either with the Raman microscope or with a dedicated optical microscope. In the case of the PerkinElmer FT-IR microscope, the optical scan must be performed on an external microscope, as there is no technical possibility to control the instrument from an external software. By using a dedicated optical microscope, such as the Zeiss Imager.Z2m, this allows for reducing image acquisition time while providing a higher fidelity of the acquired image. The use of an external microscope requires using a sample tray with fixed position markers to transfer the coordinate systems from the optical to the Raman/FT-IR microscope. The mathematical error of the coordinate transfer can be at 1 μm for each marker or even less. However, when bringing a sample from one instrument to another, also the precision of the microscopy stages has to be considered, which can be about a few μm. Further deviations can occur when the filter is not fully fixed on the microscope tray or if particles can move on the table. Having image acquisition and particle measurement on different instruments requires very careful sample handling and should only be considered for larger particles (>10 μm) and only after thorough testing.

The GEPARD interface offers a variety of parameters for controlling the image acquisition procedure. The user can set three to five positions that define the border of the region of interest, in which images will be acquired. The z-focus of all initial positions is adjusted by the user to define a surface tilt for the filter in the microscope frame. A background-removal option is integrated to account for brightness gradients within each tile, resulting from non-constant illumination of the respective filter area. Next, a number of z-levels for a so-called focus stacking approach are defined. The number of z-levels and the maximum focus height relative to the tilted filter determine how many focus steps are done and at what z-levels. The focus stacking gives two advantages: First, an image with highest possible depth of field is obtained, which is beneficial for the particle recognition step. Second, a height map of the filter and particles is calculated and stored that allows for focusing the laser during the Raman scan on the surface of the particles. A detailed breakdown on the image acquisition options is given in the supporting information (Image Acquisition with GEPARD section, Supplemental Material).

The optical scan procedure is tailored to minimize the required image acquisition time but also to retrieve height information of the sample. Consequently, elsewhere-described procedures for artificially pressing fibers on the filters to force them into the focal plane are not necessary.[6] The image is contained in full resolution and can be interactively reviewed within the GEPARD sample view.

Particle Recognition

After having obtained the full optical image, the actual particle recognition step has to be performed. Effective and reliable image segmentation is highly challenging, and the employed algorithms have to be chosen and configured carefully. The challenge for GEPARD is to process images of very different natures (i.e., MP samples from drinking water are much cleaner than MP samples from wastewater treatment sludge, even after sample treatment). As all images are stored and processed in full resolution, typical image sizes for 10×10 mm filter acquired with $20\times$ magnification are in the range of $17\,000 \times 17\,000$ pixels. Significant progress was achieved throughout the past years using semantic image segmentation (i.e., using machine learning) on challenging images to achieve very convenient segmentation results.[52–54] Despite their high capability in recognizing complex particle patterns, semantic image segmentation techniques require training procedures that are both difficult to set up and computationally expensive. Consequently, they are usually restricted to images of rather low-resolution images, with 8192×4096 pixels are already considered very large and need to be handled with particular approaches.[55] Conversely, simple segmentation by thresholding the image into fore- and background is very fast but only works well for non-overlapping particles, which is often not the case.

We decided to implement an interactively controllable watershed segmentation to find a compromise between quality of segmentation and computation time/expense. Watershed segmentation allows separating adjacent or overlapping particles and works by flooding the image from marker points that represent particle centers. Particle borders are defined by adjacent water basins that meet during the flooding process.[56] As already demonstrated in a recently published article, watershed segmentation can easily lead to strong over-segmentation, i.e., many particles are fragmented into numerous small particles.[56–58]

A detailed description of all parameters can be found in the Particle Detection with GEPARD section in the Supplemental Material, and shall be skipped here. Instead, the most important features are briefly summarized in the following list:

(i) Contrast adjustments of the acquired image by a user-defined contrast curve or adaptive histogram equalization (contrast limited adaptive histogram equalization, or CLAHE, for compensating local inhomogeneity of image brightness).

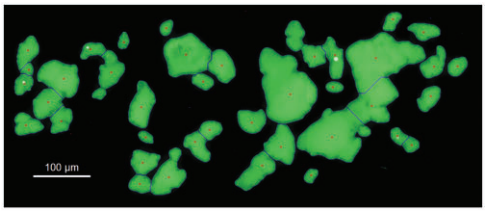


Figure 2. Example results of particle recognition on cryo-milled polymer particles. The necessity and potential of watershed segmentation is demonstrated by touching particle boundaries in several cases. Red spots mark Raman measurement spots, white points are user-defined seed points for guiding the watershed algorithm.

(ii) Thresholding to define particles that are above or below a certain brightness, but also in between two set brightness values or vice versa.
(iii) Size filtering to exclude very small and/or very large particles.
(iv) Manual corrections to split particles or to recombine over-segmented particles.

Our particle recognition leads to good results in a broad variety of cases, as shown in Fig. 2. However, the method frequently leads to over-segmentation, which results in more than one measurement per particle, thus increasing measurement time. However, having more than one spectrum per particle increases the confidence in the spectroscopic identification of the respective particle. Segmented particles that are too heavily segmented can be recombined in the final particle evaluation step (Particle Evaluation section) to obtain reliable particle size information. These manual corrections only have to be done for the relevant MP particles (usually about 1% of the particles), which makes the post-processing possible in little time. Particle count and size distributions of all other particles, though, will be biased by over- or under-segmentation. However, the interpretation of size and count of non-MP particles is highly questionable anyways, as already the previous sample workup steps (e.g., density separation or digestion) make these values not representative for the environmental sample.

Spectroscopic Measurement

After completing the particle detection, the actual spectroscopic scan can be initiated. GEPARD allows for controlling the measurement directly through the instrument interface to the Raman microscopes. A device-specific window prompts measurement parameters, such as number of accumulations, integration time, or laser power. The order in which all particles are measured is optimized by solving the traveling salesman problem through a simulated annealing approach,[59] thus reducing the distance the stage has to move by approx. 20% compared to an intuitive meandering line scan technique. For measuring particle amounts in the thousands to ten of thousands, we chose relatively short Raman scan times per particle, such as five accumulations with 0.5 s integration time. Both an increasing number of accumulations or longer integration times would improve the signal-to-noise ratios of the acquired spectra at the cost of accordingly longer experiment time and, thus, less sample throughput. Balancing out spectrum quality and sample throughput is a delicate endeavor and has to be done carefully for each analytical task. A way to improve the spectral quality is to increase the number of z-levels during the optical scan for increasing the accuracy of the z-focus during measurement. Alternatively, instrument specific hardware options for tracking focus height (i.e., Renishaw Qontor Live Track) can be a great benefit for increasing focus accuracy without significantly impacting the overall measurement time.

We currently measure the entire filter surface with all particles and do not make use of any aliquotation approach. Measuring only a fraction of the filter decreases overall measurement time, thus increasing sample throughput. Alternatively, keeping the overall measurement time constant, the acquisition time for each spectrum can be increased for this fraction of the filter, thus increasing the quality of the performed measurements. GEPARD only allows for the definition of a fraction of particles to be measured currently. Any other subsampling approach can be integrated on demand, due to the open-source nature of GEPARD.

The workflow for using GEPARD for FT-IR measurements on the Perkin Elmer instrument is currently implemented in a workflow that requires acquisition of the optical image on the Zeiss light microscope (LM). A sample tray with position markers in the micrometer size is used to transfer the coordinates to the FT-IR instrument. GEPARD needs to import three files from the LM: (i) the color image, (ii) the height map, and (iii) an extensible markup language (XML) file with all metadata about the sample, such as the exact coordinates of the position markers. Before importing these files into GEPARD, the sample tray has to be mounted into the FT-IR microscope and the coordinates of all position markers have to be determined manually. When importing the LM files into GEPARD, the user is prompted to input the position marker coordinates, which allows GEPARD to transfer the coordinate system from LM to FT-IR microscope. After having performed the particle recognition as described in the previous step, a script is run to determine the FT-IR aperture configurations for all detected particles. Therefore, an algorithm finds the largest rectangle fitting on each particle without leaving its respective boundary. Ultimately, a *.slf-file is generated and exported that can be imported from the FT-IR microscope's Spectrum software to set up a measurement with all detected particles (Figs. 6a and 6b show an example of that setup). The FT-IR measurement is entirely configured

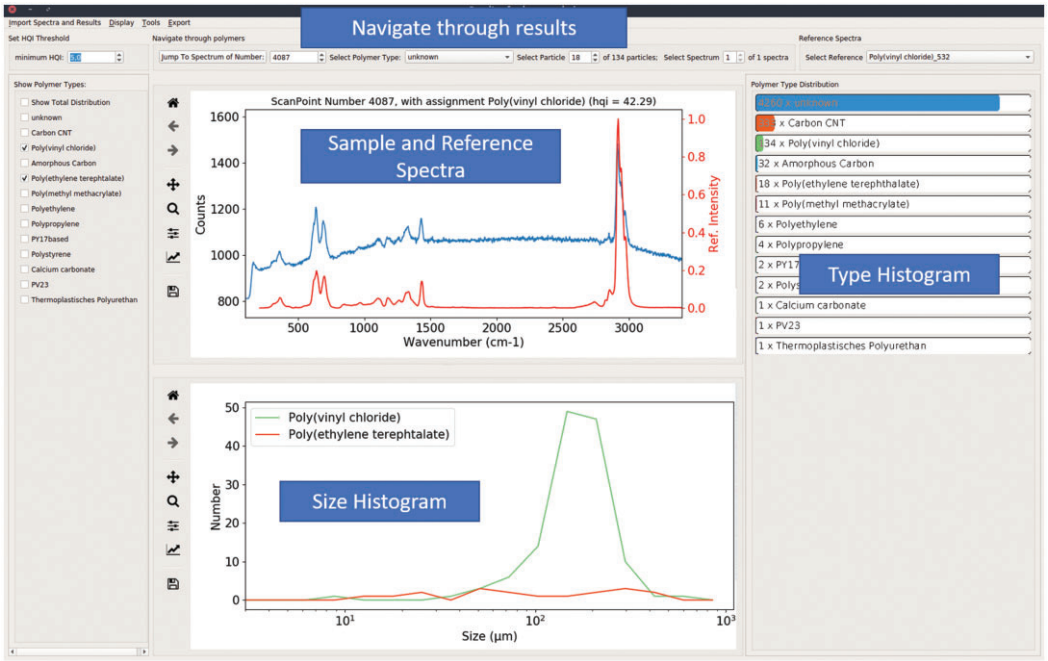


Figure 3. Overview of the particle analysis interface using a Raman microscope. The sample is a soil sample (see Figure 5 and Supplemental Material). All spectra with a hit quality index (HQI) below a given threshold (min HQI = 5 in this example) are labeled as "unknown".

in the Spectrum software. After finishing the measurement, the acquired spectra are exported into a *.csv file to be processed in the following spectra evaluation step.

Spectra Evaluation

All spectra have to be evaluated to determine each particle's chemical nature. The spectra evaluation is the only step, which is currently not yet implemented in GEPARD. Instead, we use the commercial software TrueMatch (WITec) for batch spectra correlation and import the results back to GEPARD. We created dedicated databases containing relevant selections of standard polymers, additives, and other substances that are likely to be found in environmental samples (e.g., fish scales, mussel shells). Each database contains 50 to 100 spectra, thus making the spectra correlation very quick and restricting the results to reasonable entries. We perform background subtraction and take the first derivative of the spectra.

The main challenge is to handle spectra that were acquired in short time and, consequently, are characterized by a low signal-to-noise ratio. As every spectra correlation process can lead to wrong classifications, all automatically obtained results can be revised and checked. The TrueMatch software allows quickly browsing through the results and setting flags to each spectrum. By such an approach, the automatic results can be overwritten, thus increasing the overall result confidence.

Choosing appropriate settings for the database search is critical for obtaining meaningful results. In most cases, we use the build in shape background subtraction with a shape size of 200 points, use the first derivative for correlation and set the hit quality index (HQI) to represent the correlation coefficient (ranging from 0 to 100). After sorting the search results according to their HQI, we manually revisit all spectra down to an HQI of 5 to exclude false classifications. That threshold parameter strongly depends on all chosen database search parameters and, for reproducibility of results, keeping these fixed is important. The list of results and their respective HQIs is then saved to a text file which can be opened in GEPARD. There, the final HQI threshold can be set to determine from which HQI on a particle is considered as "unknown". We usually keep this threshold at an HQI of 5 as well.

Particle Evaluation

GEPARD offers rich possibilities to review and edit particle results after having imported the spectra results. Each detected particle is assigned with a specific color for easy visual identification of particles on the filter surface. A second additional window displays statistics about found

particle types and sizes. Figure 3 shows the analysis window that readily allows for the extracting information about:

Particle type histogram: How many MP particles were found of which polymer type?
Particle size histogram: What is the size distribution of these MP particles?
For each individual particle: Size, classification, color, shape and spectrum or spectra of each MP particle.
Each MP particle spectrum can be overlaid with reference polymer spectra that can be imported from ASCII formatted text files.

The analysis window is linked to the particle image of the main window. Clicking on any particle in the main window displays the corresponding particle information in the analysis window and vice versa, selecting a particular particle in the analysis window makes the main window focus on the corresponding particle.

GEPARD's analysis interface is designed with the same philosophy as the previously described particle detection. We implemented algorithms that process all particles automatically and derive parameters, such as size, shape, and color. However, given the vast diversity of particles in environmental samples, these algorithms can lead to wrong results in some cases. The user has not only the opportunity to review all results but also to check and override them in detail accordingly.

It is highly recommended to perform a critical review of the relevant results. The term "relevant" relates to actual MP particles in our scope. Given that MP usually amount to less than 1% of all particles, this greatly reduces the number of particles that have to be reviewed, which makes the post-processing relatively quick.

The wide array of reviewing options of GEPARD (refer to the Reviewing Particle Measurement Results section; Supplemental Material) is a major strength of our particle analysis approach. We combine and display information from the optical image, particle recognition and spectral analysis. Making it intuitive and quick to review "relevant particles" (here: MP) greatly increases the confidence of the generated results, thus improving their scientific quality.

GEPARD currently offers two ways of exporting the particle results. First, an excel spreadsheet can be generated, containing the information of each individual particle, together with a summarized table listing the number of particles in certain size classes of each particle type. Second, an interface to connect to an SQL database is included. Uploading all particles to a central database is beneficial for making results accessible to all project partners and allows storing all required metadata, which assists in tracking the history of each individual particle from sampling to final analysis.

Assessment of Measurement Quality

Confirming the reliability of any MP analysis is an important, yet challenging step. Preparing a sample of known MP content is still a major challenge for MP round robin test, where the performance across different methodologies and laboratories is compared.

We decided to perform a simple experiment with artificially prepared samples for asserting correct function of our method. We used commercially available spherical particles of polyethylene (PE) and poly(methyl methacrylate) (PMMA) with narrow size distribution and different average sizes. For PE, two batches were used with sphere diameter ranging from 10 to 27 μm and from 106 to 125 μm, respectively. The size of the PMMA particles was indicated to be in between 53 and 63 μm. Particles of each of the three batches were put on a silicon filter and the filter was subjected to the herein described particle analysis procedure using GEPARD with the Renishaw inVia Raman microscope. Figures 4a and 4b show the outcome of the measurement. The size-distribution plot clearly shows that the originally employed particle types and sizes are reproduced correctly. The photo of the filter with false-color overlay shows that also aggregated particles of different types are distinguished correctly.

GEPARD in Routine Operation

The herein proposed analysis procedure has been used by the microplastics group of IPF Dresden in routine operation for more than a year, on over 80 environmental samples; originating from air, water, sediment, beaches, or soil. Having routine operation and method development run in parallel allows for effectively identifying tasks that can be improved and/or accelerated by automatization. The diverse nature of the samples we process confronts us with new challenges in all aspects of not just image acquisition, but also particle detection, spectra evaluation, revision, and final compilation of results.

Figure 5 shows the result of a soil sample from an agricultural area close to Speyer, Germany. Details about sampling and sample workup can be found in the Investigation of a Soil Sample section (Supplemental Material) together with example spectra. The final filtration was done on silicon filters with 50 μm pore size. Due to the relatively large pitch of 100 μm, also smaller particles can be found on the filter, but their number cannot be considered to be quantitative. Image acquisition was done directly within the Raman microscope and took approximately 1.7 h per filter. On the filter shown in Fig. 5, a total of 4862 particles was detected and the Raman measurement took 4.9 h. In addition, approximately 4 h of manual work was required for setting up the measurement and thoroughly reviewing the results as described in the previous sections. The presented sample is a complex soil sample with many fibers but also particle agglomerations. Both are a particular challenge

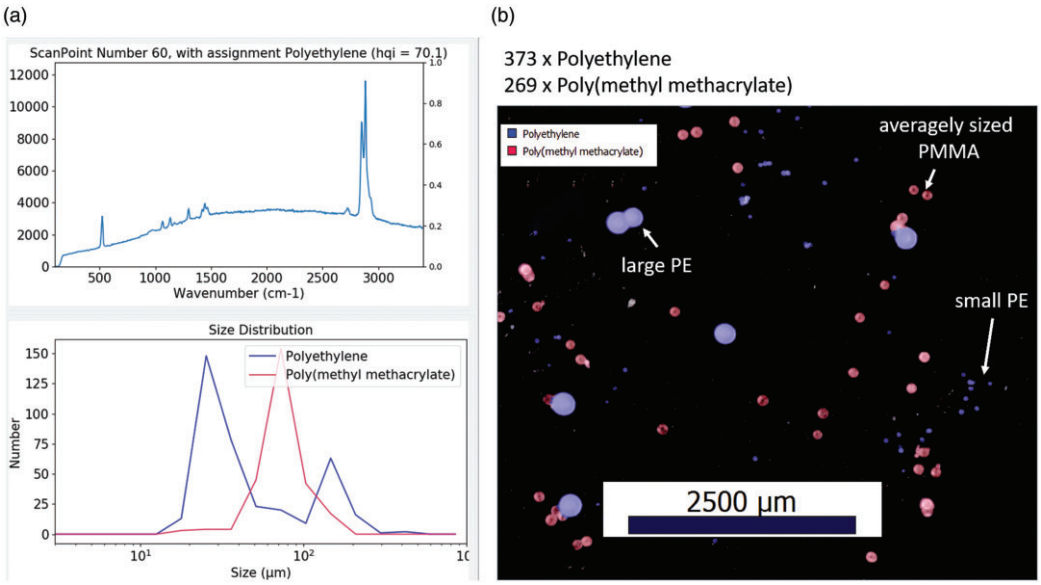


Figure 4. Evaluation of the test sample, clearly showing the two different size distributions of polyethylene and the average sized poly(methyl methacrylate). Image acquisition and Raman scan were performed on the Renishaw inVia microscope. (a) Example spectrum and size distributions. (b) Representative section of the filter with color assignment of PE (blue) and PMMA (purple).

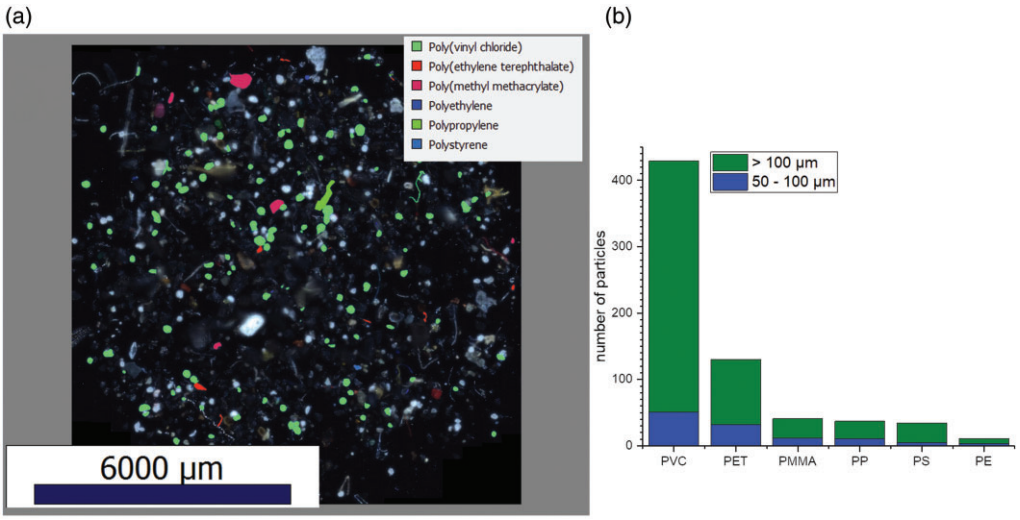


Figure 5. Results of the soil sample. (a) Example photo of one out of a total of nine filters from the complete 500 g (w/w) sample. (b) Summary of MP from a total of 32 211 particles/fibers from all nine filters combined (measurement time: 1.3 d), of which 682 were MP particles.

for the particle recognition, so we very critically review the automated results. In simpler cases, the needed time for that reviewing can be substantially lower. The Investigation of a Soil Sample section (Supplemental Material) gives a complete overview over measurement times of all filters belonging to that sample, together with details of the particle recognition and the obtained spectra.

The example shows that approximately 2% of the measured particles were identified as MP particles, which, according to our experience, is a relatively high value. It

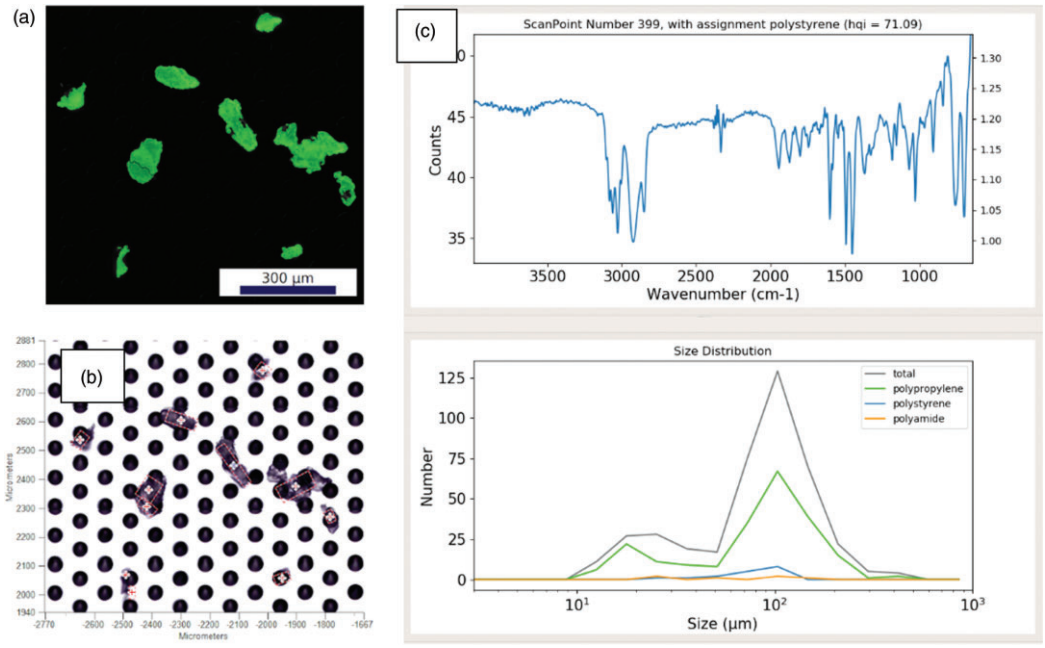


Figure 6. FT-IR measurement of a model sample containing polypropylene and polystyrene on a 50 µm silicon filter. (a) Detail of particle recognition in GEPARD based on dark field image recorded with Zeiss Imager. (b) Preview image in FT-IR microscope of the same position showing imported aperture shapes. (c) Analysis of the FT-IR results in GEPARD.

is interesting to observe that the distribution of the particles on the filter is neither homogenous nor does it follow any distinct pattern. This type of unpredictable particle distribution makes reliable subsampling, i.e., selection of small but representative regions, difficult. We currently measure each detected particle in order not to omit any MP particle, which results in relatively short measurement times per particle. Typical Raman setups use a laser power of 5 mW and the acquisition of five accumulations with 0.5 s integration time per particle. Consequently, it is necessary to handle many spectra with a low signal-to-noise ratio. The current database approach does not always seem to yield ideal results. Chemometric models based on spectral descriptors could probably improve the overall quality,[18] but are not yet implemented in the program.

Several methods for subsampling are described in literature to reduce the number of particles to measure without significantly increasing the uncertainty of the measurement result.[39,60] Their validity, however, was not yet assessed practically on the example of environmental samples. We now start evaluating the suitability of different subsampling methods retrospectively on the base of real-world samples. The results to be published soon.

An example of the analysis of a water sample is shown in the Investigation of a River Water Sample section (Supplemental Material). The water sample was prepared by fractionated filtration on both 50 µm and 10 µm silicon filters. Due to the large hole-to-hole distance of 55 µm on the 10 µm filters, also smaller particles can be found. Their number, however, cannot be considered quantitative. The example shows that the vast majority of particles is found on the 10 µm filters, due to the exponential increase in particle number with decreasing particle size. Eighty-five percent of a total of almost 68 000 particles were found on the 10 µm filters, which shows the importance of including smaller particle sizes, if possible. As a result, 407 MP particles were found, which corresponds to approx. 0.6%. Again, approx. 85% of these MP particles were found on the 10 µm filters.

Figure 6 shows the result of a model sample measured by FT-IR in transmission (resolution 4 cm^{-1}, eight scans per spectrum). For the model sample, cryo-milled particles of polypropylene, polystyrene and polyamide were dispersed in water and filtered onto our silicon filters, as described in the Filtration onto Silicon Filters section of the Supplemental Material. The capability to work with FT-IR and Raman seamlessly is a key advantage of GEPARD and helps in optimizing the general analysis strategy. For instance, large particles can be measured by FT-IR and smaller particles can be measured by Raman. Previous works by Käppler et al. showed that there is no clearly preferable method between FT-IR and Raman to identify MP particles.[37] Thus, being able to measure with one method, identify particles with unclear result and measure them

with the other technique, is a promising approach that becomes accessible with GEPARD.

Conclusion

Spectroscopic methods are still key for a deeper understanding of the occurrence of MP particles in the environment. We portrayed our contribution to improve both the analysis speed and reliability of these methods. We developed a software to cover an analysis pipeline, which is compatible with not just Raman, but also with FT-IR-microspectroscopy. The GEPARD package follows the concept of particle analyses in four main steps:

(i) Optical image acquisition
(ii) Particle recognition
(iii) Spectroscopic measurement
(iv) Data evaluation and reporting.

Size, shape, color, and chemical classification are registered for each detected particle. GEPARD allows for the reviewing and correcting of all results at any time via a user-friendly interface, thereby increasing confidence in the final result. All results can be visualized graphically in the form of false-color overlays on the optical image as well as various other diagrams, exported as Excel tables or uploaded into an SQL database. Integrating all required steps into one software package makes consistent data handling significantly easier and reduces the required time to process a sample.

GEPARD not only gives great flexibility in setting up and performing MP measurements but also allows for the use of different instruments, making GEPARD compatible with a greater number of analyses laboratories.

We successfully applied our approach on a variety of environmental samples from various different compartments, ranging from air to soil samples. As such, we assert that all included steps are not only designed to work on prepared model samples, but can also be (and have successfully been) applied to real-world samples. The continuous and critical evaluation of all analysis steps assists in the ascertaining of areas where further improvements can be made. Main aspects to improve are: (i) a more powerful particle recognition, especially in the case of overlapping particles, and (ii) a fully implemented spectral evaluation that can work, both by correlating spectra with databases and by applying chemometric tools. Random decision forests proved to be efficient in classifying noisy spectra of environmental MP samples in relatively short time[18] and thus, there is the potential to increase both confidence and speed of the spectra evaluation. Additionally, we have further improved the analysis tool by enabling it to process multiple measurements simultaneously. This facilitates the consolidation of data in cases where multiple filters belong to a single sample. Moreover, comprehensive statistics on particle occurrence across multiple samples are useful to identify point contaminations.

The GEPARD package is open source and free to use and edit. Thus, it can be extended and modified by any researcher whom requires particular adjustments for specific objectives.

Acknowledgments

The authors thank Dr. Martin Armbruster at LUFA Speyer for providing soil samples from their experimental fields.

Declaration of Conflicting Interests

The author(s) declared no potential conflicts of interest with respect to the research, authorship, and/or publication of this article.

Funding

This research was funded by the Federal Ministry of Education and Research (BmBF) project MicroCatch_Balt grant number 03F0788A and the BONUS MICROPOLL project supported by BONUS (Art 185), funded jointly by the European Union and BmBF (03F0775A).

Supplemental Material

The supplemental material mentioned in the text, consisting of figures and tables, is available in the online version of the journal.

ORCID iDs

Josef Brandt https://orcid.org/0000-0002-3434-4771
Elisavet Kanaki https://orcid.org/0000-0001-7714-0536
Robin Lenz https://orcid.org/0000-0003-4156-7380

References

1. R. Lenz, M. Labrenz. "Small Microplastic Sampling in Water: Development of an Encapsulated Filtration Device". Water. 2018. 10(8): 1055.
2. A. Käppler, F. Windrich, M.G.J. Löder, et al. "Identification of Microplastics by FTIR and Raman Microscopy: a Novel Silicon Filter Substrate Opens the Important Spectral Range Below 1300 cm^{-1} for FTIR Transmission Measurements". Anal. Bioanal. Chem. 2015. 407(22): 6791–6801.
3. S. Ghosal, M. Chen, J. Wagner, et al. "Molecular Identification of Polymers and Anthropogenic Particles Extracted from Oceanic Water and Fish Stomach: A Raman Micro-Spectroscopy Study". Environ. Pollut. 2017. 233: 1113–1124.
4. A.L. Lusher, N.A. Welden, P. Sobral, et al. "Sampling, Isolating and Identifying Microplastics Ingested by Fish and Invertebrates". Anal. Methods. 2017. 9(9): 1346–1360.
5. M. Simon, N. van Alst, J. Vollertsen. "Quantification of Microplastic Mass and Removal Rates at Wastewater Treatment Plants Applying Focal Plane Array (FPA)-Based Fourier Transform Infrared (FT-IR) Imaging". Water Res. 2018. 142: 1–9.
6. S. Primpke, P.A. Dias, G. Gerdts. "Automated Identification and Quantification of Microfibres and Microplastics". Anal. Methods. 2019. 11(16): 2138–2147.
7. D. Schymanski, C. Goldbeck, H.U. Humpf, et al. "Analysis of Microplastics in Water by Micro-Raman Spectroscopy: Release of

Plastic Particles from Different Packaging into Mineral Water". Water Res. 2018. 129: 154–162.
8. S.M. Mintenig, I. Int-Veen, M.G.J. Löder, et al. "Identification of Microplastic in Effluents of Waste Water Treatment Plants Using Focal Plane Array-Based Micro-Fourier-Transform Infrared Imaging". Water Res. 2017. 108: 365–372.
9. M. Bergmann, V. Wirzberger, T. Krumpen, et al. "High Quantities of Microplastic in Arctic Deep-Sea Sediments from the HAUSGARTEN Observatory". Environ. Sci. Technol. 2017. 51(19): 11000–11010.
10. J. Bertling, L. Hamann, M. Hiebel. "Mikroplastik und Synthetische Polymere in Kosmetikprodukten Sowie Wasch-, Putz-, und Reinigungsmitteln". Fraunhofer Umsicht. 2018. http://publica.fraunhofer.de/eprints/urn_nbn_de_0011-n-4907737.pdf [accessed May 19 2020].
11. J. Bertling, R. Bertling, L. Hamann. "Kunststoffe in der Umwelt: Mikro- und Makroplastik. Ursachen, Mengen, Umweltschicksale, Wirkungen, Lösungsansätze, Empfehlungen. Kurzfassung der Konsortialstudie". Fraunhofer Umsicht. 2018. https://www.umsicht.fraunhofer.de/content/dam/umsicht/de/dokumente/publikationen/2018/kunststoffe-id-umwelt-konsortialstudie-mikroplastik.pdf [accessed May 19 2020].
12. R. Geyer, J.R. Jambeck, K.L. Law. "Production, Use, and Fate of all Plastics Ever Made". Sci. Adv. 2017. 3(7): e1700782.
13. Ellen MacArthur Foundation. The New Plastics Economy: A Circular Economy for Plastic in Which it Never Becomes Waste. 2016. https://www.ellenmacarthurfoundation.org/our-work/activities/new-plastics-economy [accessed May 19 2020].
14. N.B. Hartmann, T. Hüffer, R.C. Thompson, et al. "Are We Speaking the Same Language? Recommendations for a Definition and Categorization Framework for Plastic Debris". Environ. Sci. Technol. 2019. 53(3): 1039–1047.
15. E.R. Zettler, T.J. Mincer, L.A. Amaral-Zettler. "Life in the 'Plastisphere': Microbial Communities on Plastic Marine Debris". Environ. Sci. Technol. 2013. 47(13): 7137–7146.
16. M. Masó, E. Garcés, F. Pagès, et al. "Drifting Plastic Debris as a Potential Vector for Dispersing Harmful Algal Bloom (HAB) Species". Sci. Mar. 2003. 67(1): 107–111.
17. L. Cabernard, L. Roscher, C. Lorenz, et al. "Comparison of Raman and Fourier Transform Infrared Spectroscopy for the Quantification of Microplastics in the Aquatic Environment". Environ. Sci. Technol. 2018. 52(22): 13279–13288.
18. B. Hufnagl, D. Steiner, E. Renner, et al. "A Methodology for the Fast Identification and Monitoring of Microplastics in Environmental Samples Using Random Decision Forest Classifiers". Anal. Methods. 2019. 11(17): 2277–2285.
19. A.M. Elert, R. Becker, E. Duemichen, et al. "Comparison of Different Methods for MP Detection: What Can We Learn from Them, and Why Asking the Right Question Before Measurements Matters?". Environ. Pollut. 2017. 231: 1256–1264.
20. O. Setälä, K. Magnusson, M. Lehtiniemi, et al. "Distribution and Abundance of Surface Water Microlitter in the Baltic Sea: A Comparison of Two Sampling Methods". Mar. Pollut. Bull. 2016. 110(1): 177–183.
21. H.R. Kricheldorf, G. Schwarz. "Cyclic Polymers by Kinetically Controlled Step-Growth Polymerization". Macromol. Rapid Commun. 2003. 24(56): 359–381.
22. D. Brown, L. Cheng. "New Net for Sampling the Ocean Surface". Mar. Ecol. Prog. Ser. 1981. 5: 225–227.
23. H.K. Imhof, J. Schmid, R. Niessner, et al. "A Novel, Highly Efficient Method for the Separation and Quantification of Plastic Particles in Sediments of Aquatic Environments". Limnol. Oceanogr. Methods. 2012. 10: 524–537.
24. B. Quinn, F. Murphy, C. Ewins. "Validation of Density Separation for the Rapid Recovery of Microplastics from Sediment". Anal. Methods. 2017. 9(9): 1491–1498.
25. A.S. Tagg, J.P. Harrison, Y. Ju-Nam, et al. "Fenton's Reagent for the Rapid and Efficient Isolation of Microplastics from Wastewater". Chem. Commun. 2017. 53(2): 372–375.
26. M.G.J. Löder, H.K. Imhof, M. Ladehoff, et al. "Enzymatic Purification of Microplastics in Environmental Samples". Environ. Sci. Technol. 2017. 51(24): 14283–14292.
27. C. Schwaferts, R. Niessner, M. Elsner, et al. "Methods for the Analysis of Submicrometer- and Nanoplastic Particles in the Environment". TrAC, Trends Anal. Chem. 2019. 112: 52–65.
28. A. Käppler, M. Fischer, B.M. Scholz-Böttcher, et al. "Comparison of μ-ATR-FTIR Spectroscopy and py-GCMS as Identification Tools for Microplastic Particles and Fibers Isolated from River Sediments". Anal. Bioanal. Chem. 2018. 410(21): 5313–5327.
29. J. Wagner, Z.M. Wang, S. Ghosal, et al. "Novel Method for the Extraction and Identification of Microplastics in Ocean Trawl and Fish Gut Matrices". Anal. Methods. 2017. 9(9): 1479–1490.
30. I.R. Comnea-Stancu, K. Wieland, G. Ramer, et al. "On the Identification of Rayon/Viscose as a Major Fraction of Microplastics in the Marine Environment: Discrimination between Natural and Manmade Cellulosic Fibers Using Fourier Transform Infrared Spectroscopy". Appl. Spectrosc. 2017. 71(5): 939–950.
31. M.G.J. Löder, M. Kuczera, S. Mintenig, et al. "Focal Plane Array Detector-Based Micro-Fourier-Transform Infrared Imaging for the Analysis of Microplastics in Environmental Samples". Environ. Chem. 2015. 12(5): 563–581.
32. M.A. Browne, T.S. Galloway, R.C. Thompson. "Spatial Patterns of Plastic Debris along Estuarine Shorelines". Environ. Sci. Technol. 2010. 44(9): 3404–3409.
33. M. Compa, A. Ventero, M. Iglesias, et al. "Ingestion of Microplastics and Natural Fibres in *Sardina pilchardus* (Walbaum, 1792) and *Engraulis encrasicolus* (Linnaeus, 1758) Along the Spanish Mediterranean Coast". Mar. Pollut. Bull. 2018. 128: 89–96.
34. A. Vianello, A. Boldrin, P. Guerriero, et al. "Microplastic Particles in Sediments of Lagoon of Venice, Italy: First Observations on Occurrence, Spatial Patterns, and Identification". Estuar. Coast. Shelf Sci. 2013. 130: 54–61.
35. A.S. Tagg, M. Sapp, J.P. Harrison, et al. "Identification and Quantification of Microplastics in Wastewater Using Focal Plane Array-Based Reflectance Micro-FT-IR Imaging". Anal. Chem. 2015. 87(12): 6032–6040.
36. M. Poulain, M.J. Mercier, L. Brach, et al. "Small Microplastics as a Main Contributor to Plastic Mass Balance in the North Atlantic Subtropical Gyre". Environ. Sci. Technol. 2019. 53(3): 1157–1164.
37. A. Käppler, D. Fischer, S. Oberbeckmann, et al. "Analysis of Environmental Microplastics by Vibrational Microspectroscopy: FTIR, Raman, or both?". Anal. Bioanal. Chem. 2016. 408(29): 8377–8391.
38. S. Primpke, C. Lorenz, R. Rascher-Friesenhausen, et al. "An Automated Approach for Microplastics Analysis Using Focal Plane Array (FPA) FTIR Microscopy and Image Analysis". Anal. Methods. 2017. 9(9): 1499–1511.
39. P.M. Anger, E. von der Esch, T. Baumann, et al. "Raman Microspectroscopy as a Tool for Microplastic Particle Analysis". TrAC, Trends Anal. Chem. 2018. 109: 214–226.
40. L. Hermabessiere, C. Himber, G. Duflos, et al. "Pyrolysis–GC/MS: A Powerful Tool for Microplastics Identification". Paper presented at: ECsafeSEAFOOD Conference: Industrial Stakeholder Meeting and Final Conference: 'Seafood Safety: New Findings and Innovation Challenges'. Brussels, Belgium; January 25–26, 2017.
41. M. Fischer, B.M. Scholz-Böttcher. "Microplastics Analysis in Environmental Samples-Recent Pyrolysis–Gas Chromatography–Mass Spectrometry Method Improvements to Increase the Reliability of Mass-Related Data". Anal. Methods. 2019. 11(18): 2489–2497.
42. G. Dierkes, T. Lauschke, S. Becher, et al. "Quantification of Microplastics in Environmental Samples via Pressurized Liquid

Extraction and Pyrolysis-Gas Chromatography". Anal. Bioanal. Chem. 2019. 411(26): 6959–6968.
43. E. Dümichen, A.-K. Barthel, U. Braun, et al. "Analysis of Polyethylene Microplastics in Environmental Samples, Using a Thermal Decomposition Method". Water Res. 2015. 85: 451–457.
44. E. Duemichen, U. Braun, R. Senz, et al. "Assessment of a New Method for the Analysis of Decomposition Gases of Polymers by a Combining Thermogravimetric Solid-Phase Extraction and Thermal Desorption Gas Chromatography Mass Spectrometry". J. Chromatogr. A. 2014. 1354: 117–128.
45. E. Dümichen, P. Eisentraut, C.G. Bannick, et al. "Fast Identification of Microplastics in Complex Environmental Samples by a Thermal Degradation Method". Chemosphere. 2017. 174: 572–584.
46. E. Besseling, J.T.K. Quik, M. Sun, et al. "Fate of Nano- and Microplastic in Freshwater Systems: A Modeling Study". Environ. Pollut. 2017. 220: 540–548.
47. M. Siegfried, A.A. Koelmans, E. Besseling, et al. "Export of Microplastics from Land to Sea. A Modelling Approach". Water Res. 2017. 127: 249–257.
48. H. Zhang. "Transport of Microplastics in Coastal Seas". Estuar. Coast. Shelf Sci. 2017. 199: 74–86.
49. K.M. Dorling, M.J. Baker. "Rapid FTIR Chemical Imaging: Highlighting FPA Detectors". Trends Biotechnol. 2013. 31(8): 437–438.
50. F. Liu, K.B. Olesen, A.R. Borregaard, et al. "Microplastics in Urban and Highway Stormwater Retention Ponds". Sci. Total Environ. 2019. 671: 992–1000.
51. L. Bittrich, J. Brandt. GEPARD: Gepard-Enabled PARticle Detection for Raman Microscopes. 2018. gitlab.ipfdd.de/gepard/gepard [accessed May 19 2020].
52. G. Papandreou, L.-C. Chen, K.P. Murphy, et al. "Weakly and Semi-Supervised Learning of a Deep Convolutional Network for Semantic Image Segmentation". In: 2015 IEEE International Conference on Computer Vision (ICCV). Santiago, Chile: December 7–13, 2015. Pp. 1742–1750.
53. L.-C. Chen, G. Papandreou, I. Kokkinos, et al. "DeepLab: Semantic Image Segmentation with Deep Convolutional Nets, Atrous Convolution, and Fully Connected CRFs". IEEE Trans. Pattern Anal. Mach. Intell. 2018. 40(4): 834–848.
54. V. Badrinarayanan, A. Kendall, R. Cipolla. "SegNet: A Deep Convolutional Encoder-Decoder Architecture for Image Segmentation". IEEE Trans. Pattern Anal. Mach. Intell. 2017. 39(12): 2481–2495.
55. J. Wang, B. Liu, K. Xu. "Semantic Segmentation of High-Resolution Images". Sci. China Inf. Sci. 2017. 60(12): 123101.
56. S. Beucher. "The Watershed Transformation Applied to Image Segmentation". Paper presented at: 10th Pfefferkorn Conference, Signal and Image Processing in Microscopy and Microanalysis. Scanning Microsc. Int. 1991. Supplement 6: 1–26.
57. P.M. Anger, L. Prechtl, M. Elsner, et al. "Implementation of an Open Source Algorithm for Particle Recognition and Morphological Characterisation for Microplastic Analysis by Means of Raman Microspectroscopy". Anal. Methods. 2019. 11(27): 3483–3489.
58. H.P. Ng, S.H. Ong, K.W.C. Foong, et al. "Medical Image Segmentation Using K-Means Clustering and Improved Watershed Algorithm". In: Proceedings of the 2006 IEEE Southwest Symposium on Image Analysis and Interpretation. 2006. Pp. 61–65..
59. V. Cerny. "Thermodynamical Approach to the Traveling Salesman Problem: An Efficient Simulation Algorithm I". J. Optim. Theory Appl. 1985. 45(l): 41–51.
60. S. Huppertsberg, T.P. Knepper. "Instrumental Analysis of Microplastics: Benefits and Challenges". Anal. Bioanal. Chem. 2018. 410(25): 6343–6352.

This is the end of the publication

High-Throughput Analyses of Microplastic Samples Using Fourier Transform Infrared and Raman Spectrometry

by Josef Brandt, Lars Bittrich, Franziska Fischer, Elisavet Kanaki, Alexander Tagg, Robin Lenz, Matthias Labrenz, Elke Brandes, Dieter Fischer, Klaus-Jochen Eichhorn

You might want to continue reading the synopsis at page 18, or jump back to the start of this publication at page 90.

A Synthesis of Marine Monitoring Methods With the Potential to Enhance the Status Assessment of the Baltic Sea

by Leoni Mack, Jenni Attila, Eva Aylagas, Arne Beermann, Angel Borja, Daniel Hering, Maria Kahlert, Florian Leese, Robin Lenz, Maiju Lehtiniemi, Antonia Liess, Urmas Lips, Olli-Pekka Mattila, Kristian Meissner, Timo Pyhälahti, Outi Setälä, Jennifer S. Strehse, Laura Uusitalo, Anna Willstrand Wranne, Sebastian Birk

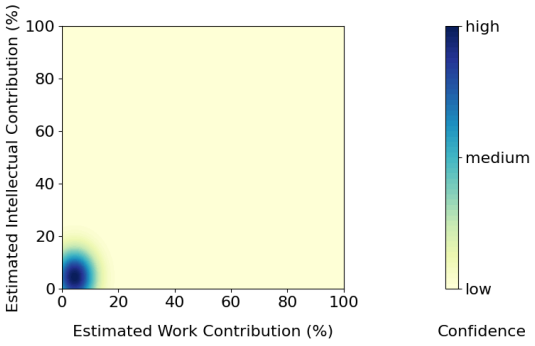
- **Date published**: November 12, 2020
- **Type**: Research Article
- **Published in**: Frontiers in Marine Science, Frontiers
- **License**: CC-BY
- **DOI**: 10.3389/fmars.2020.552047, **Reference**: [6]
- **Citations**: 18 (Crossref/DOI, 2025-11-18)

Contributions

LM designed the approach to conduct this study, coordinated the data acquisition, carried out the rating of methods and wrote the manuscript | SB supervised the approach and data acquisition and contributed to the rating of methods and the writing of the manuscript | KM and DH contributed to the design of the study, the coordination of data acquisition and revised the manuscript | JA, EA, ABe, ABo, MK, FL, RL, ML, AL, UL, O-PM, TP, OS, JS, LU and AW provided data and knowledge about specific methods and revised the manuscript | All authors contributed to the article and approved the submitted version.

Quantitative own contributions based on self-assessment

In the dimensions of expended work effort and intellectual contribution, I consider my shares are likely to be between 2% and 7% and between 1% and 8% respectively. This is visualised below as an interpolated histogram of 500 samples from Gaussian distributions with the aforementioned estimates at plus/minus two standard deviations.



frontiers in Marine Science

ORIGINAL RESEARCH
published: 12 November 2020
doi: 10.3389/fmars.2020.552047

A Synthesis of Marine Monitoring Methods With the Potential to Enhance the Status Assessment of the Baltic Sea

Leoni Mack[1], Jenni Attila[2], Eva Aylagas[3], Arne Beermann[1], Angel Borja[4], Daniel Hering[1], Maria Kahlert[5], Florian Leese[1], Robin Lenz[6], Maiju Lehtiniemi[2], Antonia Liess[7], Urmas Lips[8], Olli-Pekka Mattila[2], Kristian Meissner[2], Timo Pyhälahti[2], Outi Setälä[2], Jennifer S. Strehse[9], Laura Uusitalo[2], Anna Willstrand Wranne[10] and Sebastian Birk[1]*

[1] Faculty of Biology, University of Duisburg-Essen, Essen, Germany, [2] Finnish Environment Institute (SYKE), Helsinki, Finland, [3] Red Sea Research Center, King Abdullah University of Science and Technology, Thuwal, Saudi Arabia, [4] AZTI, Marine Research Division, Pasaia, Spain, [5] Department of Aquatic Sciences and Assessment, Swedish University of Agricultural Sciences, Uppsala, Sweden, [6] Leibniz Institute for Baltic Sea Research Warnemünde, Rostock, Germany, [7] Rydberg Laboratory of Applied Science, Halmstad University, Halmstad, Sweden, [8] Department of Marine Systems, Tallinn University of Technology, Tallinn, Estonia, [9] Institute of Toxicology and Pharmacology for Natural Scientists, University Medical School Schleswig-Holstein, Kiel, Germany, [10] Swedish Meteorological and Hydrological Institute, Gothenburg, Sweden

A multitude of anthropogenic pressures deteriorate the Baltic Sea, resulting in the need to protect and restore its marine ecosystem. For an efficient conservation, comprehensive monitoring and assessment of all ecosystem elements is of fundamental importance. The Baltic Marine Environment Protection Commission HELCOM coordinates conservation measures regulated by several European directives. However, this holistic assessment is hindered by gaps within the current monitoring schemes. Here, twenty-two novel methods with the potential to fill some of these gaps and improve the monitoring of the Baltic marine environment are examined. We asked key stakeholders to point out methods likely to improve current Baltic Sea monitoring. We then described these methods in a comparable way and evaluated them based on their costs and applicability potential (i.e., possibility to make them operational). Twelve methods require low to very low costs, while five require moderate and two high costs. Seventeen methods were rated with a high to very high applicability, whereas four methods had moderate and one low applicability for Baltic Sea monitoring. Methods with both low costs and a high applicability include the Manta Trawl, Rocket, Sediment Corer, Argo Float, Artificial Substrates, Citizen Observation, Earth Observation, the HydroFIA® pH system, DNA Metabarcoding and Stable Isotope Analysis.

Keywords: Baltic Sea Action Plan, Marine Strategy Framework Directive, Water Framework Directive, data acquisition, marine management

OPEN ACCESS

Edited by:
Michelle Jillian Devlin, Centre for Environment, Fisheries and Aquaculture Science (CEFAS), United Kingdom

Reviewed by:
Bo Gustafsson, Stockholm University, Sweden
Thanos Dailianis, Institute of Marine Biology, Biotechnology & Aquaculture, Greece
Agnes M. L. Karlson, Stockholm University, Sweden

****Correspondence:***
Leoni Mack
leoni.mack@uni-due.de

Specialty section:
This article was submitted to Marine Ecosystem Ecology, a section of the journal Frontiers in Marine Science

Received: *15 April 2020*
Accepted: *07 September 2020*
Published: *12 November 2020*

Citation:
Mack L, Attila J, Aylagas E, Beermann A, Borja A, Hering D, Kahlert M, Leese F, Lenz R, Lehtiniemi M, Liess A, Lips U, Mattila O-P, Meissner K, Pyhälahti T, Setälä O, Strehse JS, Uusitalo L, Willstrand Wranne A and Birk S (2020) A Synthesis of Marine Monitoring Methods With the Potential to Enhance the Status Assessment of the Baltic Sea. Front. Mar. Sci. 7:552047. doi: 10.3389/fmars.2020.552047

HIGHLIGHTS

- We rated novel methods regarding their ability to improve the Baltic Sea monitoring.
- Methods were assessed with respect to their costs and applicability.
- All methods can potentially increase data resolution or monitor novel ecosystem elements.
- We recommend several novel methods for the Baltic status assessment.

INTRODUCTION

The unique Baltic Sea ecosystem is in critical condition due to strong anthropogenic pressures, therefore, it urgently requires protection and restoration (Andersen et al., 2015; HELCOM, 2017). As one of the largest brackish water bodies worldwide, the Baltic Sea's most distinguishing feature is a pronounced salinity gradient. Marine and freshwater species coexist and interact, creating a unique but sensitive biological community (HELCOM, 2016). The Baltic Sea is shallow with a low water exchange rate with other marine water bodies, which makes it especially vulnerable to human impacts (Szymczychta et al., 2019). Due to effluents draining from nine countries into its basin, main environmental pressures include eutrophication and contamination. In consequence, areas with low oxygen or even anoxic conditions are expanding (Gustafsson et al., 2012; Carstensen et al., 2014). In addition, the ecosystem is highly impaired by marine litter, non-indigenous species, underwater noise, fishing, as well as habitat disturbance and loss (Andersen et al., 2015). Climate change already reduces the extent and duration of ice cover in the Northern parts, as well as increases riverine freshwater inflow (HELCOM, 2018a). The critical condition of the Baltic Sea calls for profound mitigation actions as stipulated by the present environmental legislation.

Several European directives and international conventions address the protection of the Baltic Sea. The most important directives are the Marine Strategy Framework Directive (MSFD; European Commission, 2008) and the Water Framework Directive (WFD; European Commission, 2000). The common aim of these directives is to achieve a good status of the Baltic Sea. "Status" refers to the qualitative condition of the ecosystem, which is classified as good if it deviates only slightly from near-natural conditions (European Commission, 2000, 2008). Further relevant legislations are the Habitats Directive (92/43/EEC), the Birds Directive (2009/147/EC), the Common Fisheries Policy (Regulation EU No 1380/2013) and the regulation on invasive alien species (Regulation EU No 1143/2014). The implementation of the directives is regionally coordinated by the Baltic Marine Environment Protection Commission HELCOM (i.e., "Helsinki Commission"). This intergovernmental organisation has the aim to protect the Baltic Sea, conserve its habitats and biodiversity and ensure sustainable use of its resources (HELCOM, 2018a). Working with an ecosystem-based approach, the understanding of anthropogenic pressures and their impacts on the marine environment and human well-being are fundamental (Söderström and Kern, 2017). HELCOM established the Baltic Sea Action Plan (BSAP; Backer et al., 2010) as a joint programme to protect the Baltic Sea and restore the good status of its marine environment by 2021 (HELCOM, 2007).

For an efficient protection and restoration of the Baltic Sea, comprehensive monitoring of all its ecosystem elements is of fundamental importance. Monitoring comprises the acquisition of biological, chemical, physical, hydrological and morphological data of the ecosystem to assess its status (Mack et al., 2019). The assessment of the Baltic Sea's status is following an indicator-based approach (HELCOM, 2018a). Indicators address specific measurable attributes of selected ecosystem elements, allowing to monitor spatial or temporal changes of these elements. Several indicators are defined and grouped into eleven thematic categories addressing characteristic ecosystem features and functions, so-called "descriptors" within the MSFD (Zampoukas et al., 2012).

The current monitoring of the Baltic Sea, however, reveals significant gaps, which conceivably prevent a holistic assessment and impede adequate conservation of the Baltic Sea. Five main gaps were identified by Emmerson et al. (2019) and Kahlert et al. (2020), three of which relate to insufficiently monitored and lacking indicators (i–iii), while two relate to regulation and coordination (iv–v):

(i) Insufficient monitoring of existing indicators in space and time, which especially applies to oxygen conditions, phytoplankton, zooplankton, benthic habitats and species, and the monitoring of mobile species.
(ii) The lack of indicators that adequately reflect the descriptors of the MSFD, including food webs, sea-floor integrity, contaminants, marine litter, and underwater noise/energy.
(iii) Ecosystem elements and drivers of change, which are not monitored so far, including climate change and ecosystem services.
(iv) Insufficient regulations on data handling or storage, in particular regarding some descriptors such as biodiversity (i.e., benthic habitats and species), non-indigenous species, bycatch, hazardous substances, and marine litter.
(v) The lack in coordination of the monitoring between countries, which especially applies for the descriptors mentioned in the previous gap.

These gaps arise from various circumstances: Traditional methods require relatively high efforts regarding costs and time, and therefore cannot be conducted as often as necessary to meet the data requirements regarding spatio-temporal resolution and coverage. These traditional methods include manual water/sediment sampling from research vessels, sampling and observation by trained divers, manned aircraft surveys or the morphological identification of sampled organisms. An insufficient development of measurable attributes of existing and emerging ecosystem threats leads to a lack in indicators, ecosystem elements or descriptors monitoring. For instance, food webs are currently assessed by proxies like nutritional

state, growth rate and size structure of specific organisms, but a straightforward indicator describing the food web length and stability was not developed so far. Technological advances and associated high data volumes evolve faster than data management strategies, resulting in the lack of central data management systems. Furthermore, a lack of coordination results from differing national and international legislation (Birk et al., 2012).

To fill these gaps, novel monitoring methods can be implemented. In this investigation, we define as "novel" those methods which are not yet in general use or applied to some Baltic Sea regions, as well as methods which have been developed recently. Several novel methods have been developed to facilitate autonomous acquisition of real-time data, increased spatial and temporal data resolution and the assessment of novel indicators, ecosystem elements or descriptors (Danovaro et al., 2016). A good example for the integration of novel methods is the use of the HELCOM chlorophyll-a indicator for the assessment of eutrophication status (HELCOM, 2018b). The indicator combines data from traditional research vessel-based sampling with Earth Observation and FerryBox systems. It was used in the latest status report to assess the eutrophication effects in the off-shore areas of the Baltic Sea (HELCOM, 2018c). Another example is Earth Observation (EO) that provides near real-time information on water quality parameters and surface water temperature. Some Baltic countries, e.g. Finland, already utilise these observations on daily level in monitoring programmes and also as complementary material for WFD reporting (Attila et al., 2018). The efforts by several EU countries for advancing the use of EO for WFD were summarised in a recent White Paper (Papathanaopoulou et al., 2019). However, to make a monitoring method operational, it should be operationally feasible and at a reasonable cost. Yet, sometimes a new method is not always transferable to routine monitoring contexts due to several constraints such as the inaccessibility to the equipment required for sample collection or preservation. Also, the study of the cost-efficiency of monitoring methods is not very usual (Abramic et al., 2014; Bellanger and Levrel, 2017; Aylagas et al., 2018).

In this context, as part of the BONUS FUMARI project ("Future marine assessment and monitoring of the Baltic"; 2018–2020)[1], which aims to propose a renewed monitoring system of the Baltic Sea marine environment, we reviewed novel methods with the potential to enhance the HELCOM monitoring of the Baltic. We identified methods suited to fill the monitoring gaps (i)– (iii) listed above (as these gap types are directly related to monitoring practices) and rated their costs and applicability potential (i.e., possibility to make them operational) for the Baltic Sea monitoring. The methods offer an improvement in comparison to the traditional methods and might replace or supplement them in a future monitoring system. In the methodology section, we describe the procedure of method identification and rating. In the results and discussion section, each method is classified, shortly described and rated based on its costs and applicability for the marine monitoring. In conclusion, the ability of methods to fill the main gaps is assessed. The results from this research can be applied to other regional seas worldwide.

[1]https://www.syke.fi/BONUS_FUMARI/

MATERIALS AND METHODS

Identification of Novel Methods

To increase the overall impact, our BONUS FUMARI project follows an end-user-centric approach, integrating suggestions from key stakeholders in environmental management (i.e., academic researchers, monitoring coordinators or field biologists). Novel monitoring methods were identified by scanning scientific projects, publications and conducting stakeholder surveys. This comprehensive collation was then examined to retain only methods, which fulfilled the following five criteria: (1) technology readiness level of seven or higher (European Commission, 2014), (2) comprehensive and stand-alone techniques (excluding sensors or analysers depending on a deployment system), (3) filling a gap in the current monitoring, (4) "novel" and not in general use, and (5) evaluated as cost-efficient in terms of their cost-benefit-ratio. For this compilation we considered scientific research projects [all BONUS projects since 2010 and the finished and ongoing projects listed in the Technical guidance on monitoring for the MSFD (JRC, 2014)], scientific publications (JRC, 2013; Danovaro et al., 2016; Filipe et al., 2019; Lehikoinen et al., 2019), and stakeholder suggestions. Stakeholders working in the field of environmental management and research in the Baltic countries were asked for shortcomings in the Baltic monitoring to assess the good status of the region regarding the directives MSFD, WFD and BSAP, and for novel methods with the potential to fill these. This was done during two enquiries from October 2018 to May 2019 and we received 42 responses (see **Supplementary Material A**).

Description and Rating of Novel Methods

All methods were described and evaluated in a standardised way. We specified their potential to add to a reference framework/programme (MSFD, BSAP and WFD), the monitored quality elements and the traditional methods potentially replaced or supplemented by the novel method. Furthermore, we described the general operating principle of the method and its application for the routine monitoring.

For evaluating the costs of a method, we differentiated between *investment costs* and *monitoring costs*. For evaluating a methods' applicability, we assessed *reliability, environmental impact, added value, limitations* and *required expertise*. These criteria were developed including approaches of JRC (2013), Nygård et al. (2016), and Hering et al. (2018). The novel methods were rated by assigning scores ranging from "−−." i.e., "very low" to "++," i.e., "very high" to each of the evaluation criteria. It should be notes that different evaluation criteria were rated using a different range of these scores, depending on their feasibility (**Table 1**). For instance, the criterion "added value" could not score negative and "limitations" could not score positive. Overall cost and applicability rating was done by averaging the grades for the single ratings. Monitoring costs were given a higher weight (2:1) than investment costs to emphasise annual running costs

TABLE 1 | Evaluation criteria and rating scores of the novel methods.

Rating	Investment costs (in k€)	Monitoring costs (in k€)	Reliability	Environmental impact	Added value	Limitations	Required expertise
++	≤ 1	≤ 1			Very high		
+	1–10	1–50	High	Beneficial	High		Low
0	10–50	50–100		None		None	Moderate
−	50–100	100–150	Low	Low		Moderate	High
−−	> 100	> 50		Moderate		High	

In the first column, the quantitative rating is shown, assigned to scores from "++" as best to "−−" as worst rating.

over one-time investments. The final rating of the methods can be found in **Table 2**.

Investment costs were defined as one-time investments for equipment and personnel training. This comprised the costs for the monitoring device or deployment system, including necessary equipment like standard sensors or sampling devices, and the expenses for personnel training (personnel costs were set to 70 € per hour). For *citizen observations* this included costs to start web services and management activities. For *remote sensing* methods, we also included the costs for the development of a data management system. Since the *investment costs* of most methods depended on several parameters, like number and type of included sensors or the place of application, the costs were mainly estimated based on expert knowledge. Cost assignments followed criteria put forth by the Joint Research Centre (JRC, 2013; **Table 1**).

Monitoring costs were defined as the running costs of monitoring, i.e., costs incurring after the initial set up. They include consumables, personnel working time, maintenance and, in case of *citizen observations* and *remote sensing* methods, data handling. Due to data availability, we first collected monitoring costs in various dimensions, ranging from the costs for a single monitoring campaign to the costs for an annual monitoring of a specific transect/area. Based on these, we estimated the annual *monitoring costs* for the whole Baltic Sea. These depend on the monitoring objective and therefore, the costs are given under specific assumptions (see **Supplementary Material B**). Since most of the methods collect data on multiple quality elements at the same time, we calculated the monitoring costs for a single quality element to allow for cost comparisons between methods. For research vessel-dependent methods, we did not include ship costs like fuel or rent.

In our cost analysis, we did not take the possibility of sharing facilities/instruments or cooperating the execution among institutes into account. This can potentially reduce investment and monitoring costs and efforts by maximising the use of resources. Furthermore, analysis protocols can be homogenised, which reduces the need for interlaboratory calibrations (JRC, 2013).

Reliability was assessed based on the failure safety of the method itself and the precision of acquired data in comparison to the traditional methods (see **Supplementary Material B**). Reliability of the methods was "high," when resulting data had an improved *reliability*. This also applied, when the precision of acquired data is comparable to data acquired with the traditional method, but due to the greater amount of data, the reliability can be regarded higher. A high default rate and therefore low *reliability* of the method was assessed as "low."

Environmental impact of the methods was rated ranging from "beneficial" to "moderate." Hereby, "beneficial" means a positive impact on the environment, e.g., by removing litter from the beaches. A "low" impact is caused by small organismic sample sizes and damages to the physical habitats, e.g., by anchoring devices to the sea floor. Methods causing damages of the physical habitats or/and lethal sample treatment of a relatively big sample size were rated with a "moderate" impact.

Added value describes the type of novelty, which a method adds to the routine monitoring. It was rated as "high" for methods with higher spatial and/or temporal data resolution, e.g., due to their autonomous measurement, and therefore, filling gap (i). A "very high" *added value* was assigned to methods including the monitoring of novel quality elements, ecosystem elements or descriptors and therefore, filling gaps (ii) and (iii). Furthermore, methods with an added social or environmental value, e.g., by rising the environmental awareness of the population, were rated as "very high."

Limitations describe disadvantages and shortcomings of a method. We rated *limitations* as "none," i.e., having no or an easily manageable effect on method applicability, or "moderate," i.e., causing slight restrictions to method applicability. Methods that scored "high," i.e., limited method applicability, require further research to improve method applicability.

Required expertise describes the level of expertise needed to conduct field *sampling/surveying* or *sample analysis*. It was rated following categories proposed by JRC (2013): "Low" indicates the need for trained personnel without specific professional education, "moderate" requires trained personnel with specific professional education and "high" requires special skills.

RESULTS AND DISCUSSION

Method Classification

Monitoring typically comprises three steps: (1) *field sampling/surveying* in which *in situ* or remote samples/data are gathered; (2) *sample analysis*, which refers to the treatment of gathered samples/data to extract quantitative or qualitative information; and (3) *data analysis*, the treatment of quantitative and qualitative information to interpret the resulting data, e.g., by calculating metrics or applying class boundaries. We classify methods for *field sampling/surveying* as either *in situ research vessel-dependent* (sampling within the water, the

TABLE 2 | Overall rating of the costs and applicability of novel methods.

Step in monitoring	Classification	Method	Investment costs	Monitoring costs	Overall costs	Reliability	Environmental impact	Added value	Limitations	Required expertise	Applicability
Field sampling/surveying	*In situ*, research vessel-dependent	Moving Vessel Profiler	– –			+	0	+	–	0	+
		Remotely Operated Towed Vehicle	– –			+	0	++	–	0	++
		Manta Trawl	+	+	+	+	–	++	– –	+	+
		Rocket	+	+	+	+	–	++	–	+	++
		GEMAX	0	+	+	+	–	++	0	+	++
	In situ, research vessel–independent	Argo Float	0	+	+	+	0	+	–	0	+
		Glider	– –	0	–	–	0	++	–	0	0
		FerryBox	–	+	0	+	0	+	0	+	++
		Profiling Buoy	– –	+	0	+	0	+	–	+	++
		Bottom-mounted Profiler	– –	+	0	+	0	+	–	+	++
		Active Biomonitoring using Blue Mussels	++	+	+	+	– –	++	–	0	0
		Passive Samplers: Chemcatcher and POCIS	+	0	0	+	–	++	0	0	++
		Artificial Substrates: ARMS and ASU	++	+	+	+	–	++	–	0	+
	Citizen Observations	Citizen Observations	+	++	++	+	+	++	–	0	++
	Remote sensing	Unmanned Aerial Vehicles	0			+	–	+	– –	0	–
		Earth Observation	+	+	+	+	0	++	0	–	++
		Remote Electronic Monitoring	0	– –	–	+	0	+	– –	+	+
Sample analysis	Field analysis	HydroFIA®pH	0	+	+	+	0	+	–	+	++
		Imaging Flow Cytometry Platform	– –	+	0	+	0	+	–	–	0
	Laboratory analysis	DNA Metabarcoding	0	+	+	+	–	++	–	0	+
		Stable Isotope Analysis	++	0	+	+	–	++	0	0	++
		Computer–based Identification	0	+ +	+	+	0	+	–	–	0

Overall costs are divided into investment and monitoring costs, whereas applicability comprises reliability, environmental impact, added value, limitations and required expertise. "++" indicates a very high, "+" a high, "0" a moderate, "–" a low and "––" a very low rating.

whole deployment time is depending on the operation of a (research) vessel), *in situ research vessel-independent* (operation is independent of a research vessel, though devices may be deployed and recovered using one), *citizen observation* or *remote sensing*. Methods for *sample analysis* comprise both *field* and *laboratory analysis*. Methods for data analysis were not included in this work.

Method Descriptions

We identified twenty-two methods to be reviewed, half of the methods were mentioned in both the stakeholder survey and literature, half by stakeholders only. In the following, we give a short description of each novel monitoring method. Furthermore, we list the MSFD descriptor(s), as they can provide information on and highlight the gaps the respective methods can fill (**Table 3**). Comprehensive method descriptions can be found in the **Supplementary Material B** or on the BONUS FUMARI methods database[2].

Methods for Field Sampling/Surveying

In situ, Research Vessel-Dependent

The **Moving Vessel Profiler (MVP)** is a free-falling "fish," which generates near-vertical high-resolution profiles of the water column. The fish is attached to a winch on board of a research vessel and operated while the vessel is moving (**Figure 1A**; Furlong et al., 2006). In marine monitoring the MVP can be operated between stations, and therefore increase the number of profiles generated during a monitoring cruise. These additional data can be used for a more comprehensive assessment of eutrophication and hydrographical conditions due to the enhanced spatio-temporal resolution and coverage of monitoring data.

The **Remotely Operated Towed Vehicle (ROTV)** is a towed profiler, which is deployed from a research vessel and can be operated in three dimensions in the water column (**Figure 1B**; Floeter et al., 2017). In marine monitoring ROTVs enhance the spatio-temporal resolution and coverage of monitoring data used to assess eutrophication and hydrographical conditions. Furthermore, it can be used to obtain high-resolution data or additional information in a specific area of interest, when steered manually. For instance, ROTVs can be operated for the detection and identification of warfare relicts dumped in the sea, and sampling of contaminated water and sediment (Beldowski et al., 2018).

A **Manta Trawl** is a net-based sampling device to collect marine surface microlitter bigger than 300 μm (**Figure 1C**). While being dragged on the water surface, it collects water with its opening. The water is filtered through a fine net and the litter is stored in the cod end, a removable collecting bag (Setälä et al., 2016; Tamminga et al., 2018). In marine monitoring the Manta Trawl can be deployed between monitoring stations to routinely collect data on microlitter in surface waters. In particular, the possibility for a standardised monitoring of microplastics, which is not included in the current monitoring directives (HELCOM, 2018a; Kahlert et al., 2020), gives the Manta a high relevance for the Baltic Sea monitoring.

The **Rocket** is an example for an encapsulated through-flow filtration device used to sample waterborne microplastics in the upper water layers (**Figure 1D**; Lenz and Labrenz, 2018). The concept is based on suction of water through fine stainless-steel cartridge filters to retain any suspended particulate matter larger than the applied pore size (i.e., 10 μm). The mobile design allows for application at field sites, as well as application aboard a vessel to take open water samples. The Rocket is a valuable tool for addressing monitoring needs for pollution of smaller microplastic particles (i.e., < 300 μm) and to cover locations where the application of trawling systems is impractical or impossible.

A **Sediment Corer** like the GEMAX is a gravity corer to sample soft sediments (**Figure 1E**). It is deployed from a research vessel and when released, the corer falls down the water column and vertically cuts into the sediment (Charrieau et al., 2018). A closing mechanism automatically locks the sediment in the system when recovering the corer. The GEMAX is an efficient sampler for monitoring purposes as it takes two sediment cores at the same time doubling the sampled volume of the sediment compared to the more common single-core corers. In marine monitoring it can be deployed at sampling stations with soft sediment to sample microlitter deposited in sediments. The Corer is especially valuable since it offers a standardised method for the monitoring of microplastics.

In situ, Research Vessel-Independent

The **Argo Float** is a free-floating platform, which generates vertical profiles of the water column (**Figure 1F**). Since it floats freely, its horizontal range and path is defined by the currents. It frequently surfaces by changing buoyancy due to an oil filled bladder. In general, an Argo Float profiles at 10-day intervals, but intervals can also be programmed to generate, for instance, multiple profiles a day (Roiha et al., 2018; Siiriä et al., 2019). In marine monitoring Argo Floats can be deployed to autonomously obtain high-resolution vertical profiles of the water column to assess eutrophication and hydrographical conditions.

The **Glider** is an autonomous underwater vehicle used to generate horizontal profiles of the physico-chemical and biological state variables along its route being defined by an operator (**Figure 1G**). It can move down to 1,500 m by changing buoyancy due to an oil-filled bladder (Liblik et al., 2016). Since Gliders can autonomously move underwater, they can also be operated in ice-covered areas and under harsh conditions (Brito et al., 2014; Meyer et al., 2018). Obtained water quality data can be used for a more comprehensive assessment of eutrophication and hydrographical conditions and Gliders can also be used for the detection of warfare relicts dumped in the sea.

A **FerryBox** is an automatic flow-through system for the continuous measurement of water parameters (**Figure 1H**). This system is specifically developed for the permanent operation on non-research vessels like ferries, which regularly ship their transit routes (Petersen, 2014; EuroGOOS, 2017). Regarding the marine monitoring, the FerryBox enables the acquisition of long-term time series on a constant route and, therefore, the

[2]http://freshwaterplatform.eu/fumari/

TABLE 3 | Novel methods and the Marine Strategy Framework Directive descriptor(s), which these methods can be used to monitor.

	Biodiversity	**Non-indigenous species**	**Commercial fish and shellfish**	***Food webs***	***Eutrophi-cation***	***Sea-floor integrity***	***Hydro-graphical conditions***	***Conta-minants***	**Seafood contamination**	***Marine litter***	***Underwater noise/energy***
Moving Vessel Profiler					○		○				
Remotely Operated Towed Vehicle					○		○	○/●			○
Manta Trawl										○/●	
Encapsulated Filtration Device										○/●	
Sediment Corer								○		○/●	
Argo Float					○		○				○
Glider					○		○	○/●			○
FerryBox				○	○		○				
Profiling Buoy	○				○		○				
Bottom-moored Profiler	○				○		○				
Active Biomonitoring					○			○/●	○		
Chemcatcher and POCIS								○/●			
Artificial Substrates: ARMS and ASU	○/●	○			○	○					
Citizen Observations		○			○		○			○	
Unmanned Aerial Vehicles	○		○		○		○	○		○	
Earth Observation	○				○		○			○/●	
Remote Electronic Monitoring	○		○	○							
HydroFIA®pH	○				○		○				
Imaging Flow Cytometry Platform	○	○		○	○						
(e)DNA Metabarcoding	○/●	○/●	○/●		○/●	○/●					
Stable Isotope Analysis				○	○						
Computer-based Identification	○	○	○								

"○" indicates methods that can fill a gap type (i), "●" indicates methods that can fill a gap type (ii), methods with the potential to fill a gap type (iii) (in this case: Climate Change and Ecosystem Services) are highlighted using italic font. The descriptors with main gaps identified by Emmerson et al. (2019) and **Kahlert et al. (2020)** *are also highlighted using italic font.*

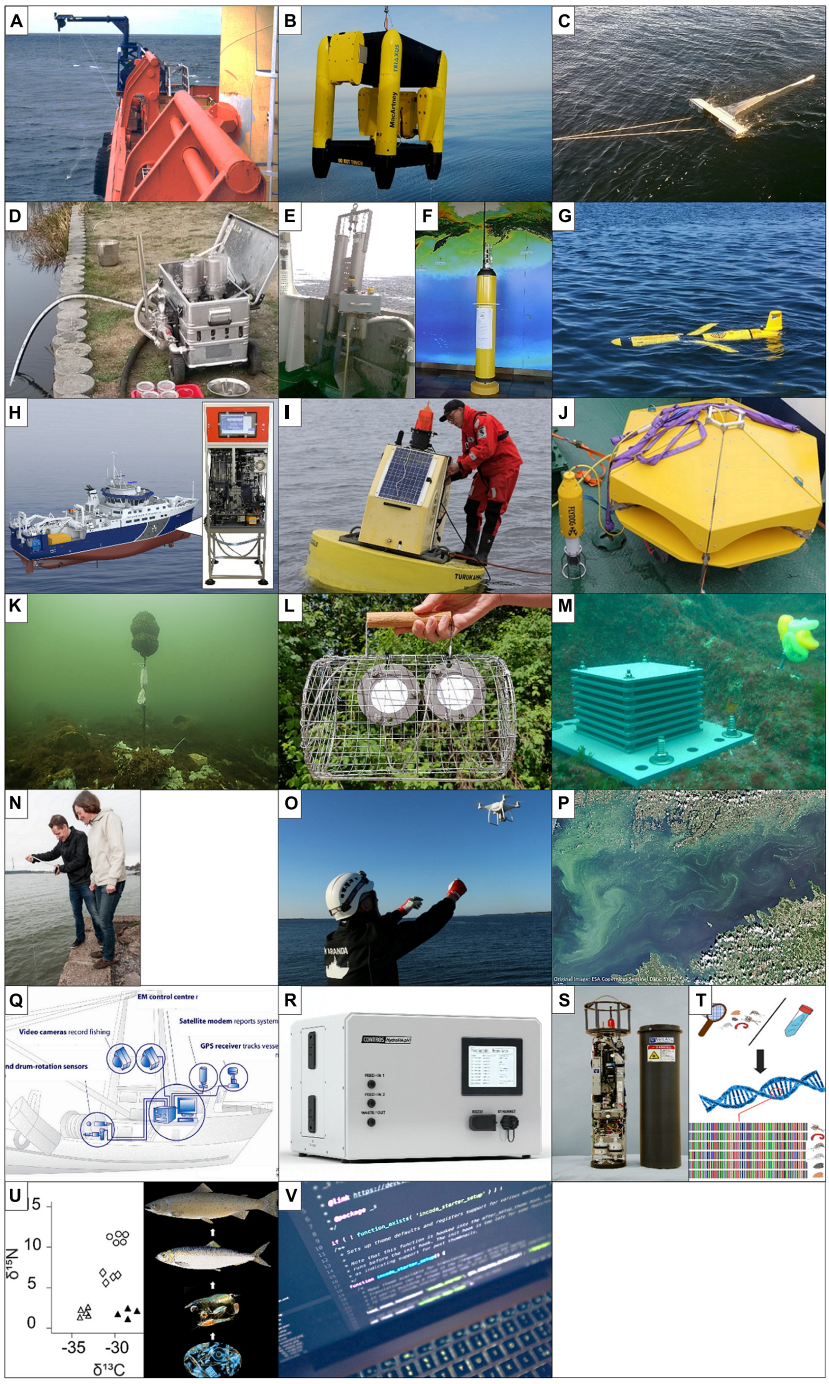


FIGURE 1 | (A) Moving Vessel Profiler © AML Oceanographic; **(B)** Remotely Operated Towed Vehicle © MacArtney; **(C)** Manta Trawl © Maiju Lehtiniemi, SYKE; **(D)** Rocket © Robin Lenz, IOW; **(E)** GEMAX Corer © Maiju Lehtiniemi, SYKE; **(F)** Argo Float © www.argo.uscd.edu; **(G)** Glider © Kimmo Tikka, FMI; **(H)** FerryBox © modified after 4HJena and SLU; **(I)** Profiling Buoy © Tiina Sojakka, UTU; **(J)** Bottom-mounted Profiler © Siim Juuse; **(K)** Active Biomonitoring using Blue Mussels © Jana Ulrich, CAU; **(L)** POCIS © Heidi Ahkola, SYKE; **(M)** ARMS (left) and ASU (right) © AZTI Tecnalia; **(N)** Citizen Observations © Vanessa Riki, SYKE; **(O)** Unmanned Aerial Vehicle © Jan Eric Bruun, SYKE; **(P)** Earth Observation © ESA Copernicus Sentinel Data **(Q)** Remote Electronic Monitoring © Archipelago Marine Research; **(R)** HydroFIA®pH © Kongsberg Maritime Contros; **(S)** Imaging Flow CytoBot © McLane Research Laboratories; **(T)** DNA Metabarcoding © Leoni Mack, UDE; **(U)** Stable Isotope Analysis © Leoni Mack, UDE; **(V)** Computer-based Identification of Organisms © Luca Bravo.

monitoring of temporal changes in food webs, eutrophication and hydrographical conditions like ocean acidification (Lips and Lips, 2017; Schneider and Müller, 2018).

Profiling Buoys for the automatic measurement of water quality profiles are moored platforms, floating on the water surface (**Figure 1I**). For profiling, a multi-parameter probe is lowered in the water column to conduct measurements either continuously or stopping at specific heights. Profiling frequency, intermediate profiling steps and the maximal depth can be programmed (Liu et al., 2019; Venkatesan et al., 2019). Due to the generation of frequent profiles at a given station, the changes in water conditions within the day can be recorded over long periods and, therefore, Profiling Buoys can be used to assess biodiversity, eutrophication and hydrographical conditions (Lips et al., 2011).

Bottom-mounted Profilers for the automatic measurement of water quality profiles are platforms moored to the sea bed (**Figure 1J**). For profiling, either the whole platform or the multi-parameter probe is rising. With profiling frequencies of 3–8 h, the changes in biological and physico-chemical water conditions within the day can be recorded over long periods. Thus, bottom-mounted profilers can be used for an enhanced assessment of biodiversity, eutrophication and hydrographical conditions (Prien and Schulz-Bull, 2016; Stoicescu et al., 2019).

For **Active Biomonitoring with Blue Mussels**, the bivalves are used as sentinel species in the monitoring of bioavailable pollutants (**Figure 1K**). Mussels enable monitoring the pollution of a specific location, as they accumulate environmental chemicals in their tissues. Therefore, mussels without former pollution are translocated to a specific area of interest (Schöne and Krause, 2016; Strehse et al., 2017). For marine monitoring purposes, this method enables a more comprehensive monitoring of eutrophication and contamination due to the collection of time-weighted average concentrations of bioavailable pollutants, including nutrient and carbon isotopes (Briant et al., 2018) and dumped munitions (Strehse et al., 2017; Appel et al., 2018).

Passive Samplers like the **Chemcatcher®** and **Polar Organic Chemical Integrative Sampler (POCIS)** are collecting contaminants based on molecular diffusion and sorption to a binding agent (**Figure 1L**). They are deployed at a specific location and accumulate the contaminants in the surrounding environment over time (Vrana et al., 2005). The Chemcatcher® collects in-/organic substances of polar or non-polar nature (Charriau et al., 2016), while the POCIS is selective for polar organic chemicals (Harman et al., 2012). Passive Samplers can be used to enhance the monitoring of contaminants, including dumped munitions, due to the collection of time-weighted water concentrations of pollutants (Belden et al., 2015; Lotufo et al., 2019).

Artificial Substrates are sampling devices mimicking complex habitats to collect biological communities over years (**Figure 1M**). The **Autonomous Reef Monitoring Structure (ARMS)** mimics the complex structure of hard benthic habitats like rocks or coral reefs, while the **Artificial Substrate Unit (ASU)** resembles soft corals or sponges (DEVOTES, 2013; Cahill et al., 2018). The analysis for community characterisation can be coupled to molecular techniques such as DNA metabarcoding. The applicability of both ARMS and ASUS in marine monitoring is highly valuable, since they enable a standardised sampling of the hard-bottom benthic communities across countries and therefore comparable monitoring data (DEVOTES, 2013).

Citizen Observations

In **Citizen Observations**, voluntary observations are made by non-professional observers (**Figure 1N**). Coordinated by researchers, engaged citizens are integrated into environmental science, including the observation of various environmental phenomena, which are transmitted to specific platforms using the smartphone or computer. Several programmes have been established at local scale (Palacin-Silva et al., 2016), including the monitoring of Secchi depth[3], non-indigenous species[4], phytoplankton[5], and several local, national and European wide campaigns for the prevention of marine litter near the shore and in the coastal waters[6,7]. Besides added value for the acquisition of monitoring data, the integration of citizens into the environmental monitoring can strongly increase the societal environmental awareness.

Remote Sensing

Unmanned Aerial Vehicles (UAVs), commonly known as "drones," are measurement platforms collecting data while flying over the area of interest (**Figure 1O**). For operations in marine and coastal environments, different types of UAVs are used with varying flight duration and modes of operation (autonomous or manual; Colefax et al., 2017; Setlak and Kowalik, 2019). In marine monitoring UAVs can be used to increase the spatio-temporal resolution and coverage of monitoring data for parameters used to assess biodiversity, eutrophication, commercial fish and shellfish, hydrological conditions, contaminants and marine litter.

In a monitoring context, **Earth Observation** means the use of satellites for the remote sensing of biological and physico-chemical properties of the upper water layer (**Figure 1P**). Europe-wide satellite missions are performed by the European and North American Space Agencies, which are offering free access to their satellite images (Harvey et al., 2015; Attila et al., 2018). In marine monitoring Earth Observation profoundly increases the temporal resolution and spatial coverage of data on water quality parameters, giving a more comprehensive picture on environmental conditions related to biodiversity, eutrophication and hydrographical conditions (Anttila et al., 2018; Attila et al., 2018).

In **Remote Electronic Monitoring (REM)**, video and sensor technology are combined to provide a comprehensive overview on the fishing activity and catch handling on fishing trawlers (**Figure 1Q**; WWF, 2015, 2017). The analysis of the REM data can be coupled to computer-based identification and quantification of organisms. In marine monitoring REM can be used to enhance data acquisition on all activities of fishing trawlers,

[3]https://www.havaintolahetti/

[4]https://www.invasive-alien-species-finland

[5]https://Levätbarometri

[6]https://www.siistibiitsi.fi/

[7]https://www.eea.europa.eu/marine-litterwatch

enabling a more comprehensive monitoring of biodiversity, commercial fish and shellfish, and food webs (Kindt-Larsen et al., 2012). Furthermore, fishing practices might become more sustainable due to the continuous surveillance on board of the trawlers (WWF, 2017).

Methods for Sample Analysis

Field Analysis

The CONTROS **HydroFIA®pH** system is autonomously conducting flow injection analysis (FIA) to determine the pH of water (Müller et al., 2018; **Figure 1R**). The system was developed for the continuous long-term measurement of pH of the surface water and is therefore suitable for both the operation on research vessels and non-research vessels like ferries (Aßmann et al., 2011; Müller et al., 2018). In marine monitoring the system can be deployed independently or in combination with a FerryBox to obtain pH long time series for locations along a set route. This enables spatial and temporal monitoring of ocean acidification (Müller et al., 2018).

Imaging Flow Cytometry (IFC) platforms are used to analyse phytoplankton communities (**Figure 1S**) by combining traditional flow cytometry and automated imaging to analyse large sample sizes with high speed (Karlson et al., 2016). The different instruments include laboratory applications, instruments included into a FerryBox, or autonomous *in situ* platforms at fixed stations. Machine Learning algorithms can be used for analysing the acquired images (González et al., 2019). IFC platforms enhance the assessment of biodiversity, non-indigenous species, food webs and eutrophication, and can also be important components early-warning-systems for harmful algal blooms (Anderson et al., 2019).

Laboratory Analysis

(e)DNA Metabarcoding is a molecular-based methodology that allows the simultaneous identification of several species within a sample using high-throughput sequencing technologies (**Figure 1T**). To attain species lists of complete biological communities simultaneously, DNA metabarcoding can be applied. In addition, metabarcoding can be used to detect species inhabiting a certain habitat using environmental DNA (eDNA) extracted from water or sediments (Pawlowski et al., 2018; Zhang et al., 2020). In marine monitoring DNA metabarcoding has the potential to improve the monitoring of biodiversity, non-indigenous species, commercial fish and shellfish and eutrophication indicators (Jeunen et al., 2019).

Stable Isotope Analysis (SIA) can be performed to derive food web structures and energy pathways within communities (Michener and Kaufman, 2007; **Figure 1U**). The stepwise enrichment of ^{15}N compared to ^{14}N with increasing trophic level enables the estimation of the food chain lengths (of number of trophic transfer steps within the food web). The stability of the food web can be monitored by comparing the $^{13}C/^{12}C$ isotopic ratios of predatory fish among years (Michener and Kaufman, 2007; Jardine et al., 2017). So far, parameters to assess food webs are still under development (Rombouts et al., 2013) and the monitoring of food webs can be improved using the proposed novel indicator "food web length and stability" and assessed using SIA. Furthermore, the assessment of eutrophication can be supported by identifying anthropogenic nitrogen and carbon inputs (Briant et al., 2018; Ziółkowska et al., 2018).

For the **computer-based identification and quantification of organisms**, computer systems are trained to autonomously identify and count sampled organisms using algorithms ("Machine Learning"; **Figure 1V**; Kelleher et al., 2015). For the identification of larger organisms (e.g., fish), an algorithm can be trained based on an image recognition system. After successful training, the algorithm can be used to identify and quantify caught species/bycatch (Williams et al., 2012) or evaluate indicator-related metrics (Uusitalo et al., 2016). For marine monitoring, computer-based identification of organisms offers an automated method to increase the speed and accuracy of data acquisition (Osterloff et al., 2019).

Rating of Methods

Costs of Novel Monitoring Methods

Two thirds of the analysed novel methods require very low to low overall costs, while four methods require moderate and two high overall costs (**Table 2**). There is no clear pattern between the different categories of monitoring methods. Citizen Observations is the only method with very low overall costs. This is due to the voluntary field sampling of citizens (data acquisition at no cost) with only the web services and management activities requiring personnel time. Gliders and REM have high overall costs. For Gliders, this is due to very high investment costs (100,000 € for purchasing a Glider). Regarding REM, the installation and maintenance of the system on a single trawler is of low costs with 17,000 €. However, to create equal economic conditions between the trawlers, according to WWF (2017) the system needs to be installed on at least all big sized (> 12 m) trawlers of the Baltic Sea. In the whole area, there are 558 registered big sized trawlers (ICES, 2018), resulting in the high overall costs of REM. It should be noted that the sharing of facilities and instruments offers the possibility to reduce investment and monitoring costs. For instance, Gliders are such instruments, and their investment costs could be reduced by splitting them between institutions.

There is a broad range of costs across the different methods, which also reflects the diversity of methods addressed. Investment costs of 80,000 € on average are required for the initial set up of a novel method. With about 500 €, the Artificial Substrates require the lowest investments, while the ROTV and MVP require about 350,000 and 400,000 €, respectively. This wide range in costs is also reflected in the monitoring costs: Based on the assumptions made (see **Supplementary Material B**), the use of a method for the annual monitoring of the whole Baltic Sea requires on average 93,000 €. Using computer-based identification and Citizen Observations have the lowest costs with 300 and 600 € annually, while the use of Gliders and REM require 85,000 and 1,116,000 €, respectively.

Monitoring costs could not be assessed for three methods. For the MVP, the extrapolation of monitoring costs on Baltic-wide coverage could not be estimated. These costs depend on the total number of installed devices on research vessels, as well

as the frequency, at which these are deployed. Other methods can be used for various different applications, including the ROTV and UAV. The ROTV can be deployed automatically to receive profiles, or in manual mode, steering it in three dimensions to monitor a small area at a very high resolution. Especially the manual deployment is very specific in its time, area and frequency. In case of UAVs, the monitoring costs heavily depend on the kind of vehicle (fixed-wing or multi-rotor and size of vehicle), the place of deployment (open sea or coastal), the mode of operation (manual or automatic operation) and monitoring objective (long-term deployment of a specific area or occasional snapshots). All these variables cannot be estimated for all countries of the Baltic Sea.

We could compare the monitoring costs using novel methods to the costs using traditional methods only for DNA metabarcoding and REM. Regarding metabarcoding, the costs for the molecular identification per sample are decreasing with an increasing number of samples, while the morphological approach has a fixed price (and waiting time) per sample (Aylagas et al., 2018). Metabarcoding is thus most cost-efficient when a sufficiently high number of samples is analysed, which is met under the assumptions made (**Supplementary Material B**). This also applies when identifying hard-bottom benthic macroinvertebrate communities sampled by ARMS and ASU in the Baltic Sea. Assuming that three replicates of ARMSs and ASUs are deployed per southern sub-basin (11 stations, since in the southern Baltic mainly soft bottom is prevalent) and three replicates per northern WFD water body (32 stations, since in the northern Baltic hard substrate is more common), this adds up to 43 sites and 260 samples. Based on these assumptions, the annual costs for DNA metabarcoding sum up to about 45,000 €. The traditional morphological identification of ARMS and ASU samples costs 455 € per sample, summing up to about 118,000 €. See Aylagas et al. (2018) for a detailed calculation of the costs for metabarcoding and traditional identifications. If eDNA metabarcoding is applied rather than bulk sample analysis, the whole costs decrease further for eDNA because no sorting is needed but DNA is directly extracted from water or sediment. Furthermore, WWF (2017) made comprehensive analyses on different methods for the monitoring of fisheries and concluded that REM is the most cost-efficient method for this purpose.

For the remaining methods, the costs could not be compared to the traditional methods due to various reasons. For traditional methods that are research-vessel based, monitoring costs could not be determined due to the case-specific costs (e.g., number of sampled stations per cruise; length of cruise; personnel on board). Methods like ROTV, MVP, FerryBox, or EO collect data on multiple parameters and, therefore, could replace or supplement more than one traditional method. Methods like the Manta Trawl, Rocket, Sediment Corer or SIA collect data on novel quality parameters and, therefore, there is no traditional method to be compared to. This is a common problem when assessing cost efficiency of novel methods (Hyvärinen et al., Submitted).

Applicability of Novel Monitoring Methods

Twelve methods are rated with very high and five with high applicability, while four methods are rated as moderate and one as low. The applicability rating showed no patterns among monitoring method categories. The methods with very high and high ratings can be recommended for Baltic routine monitoring. Here, single disadvantages in monitoring methods (e.g., a moderate environmental impact or a high expertise required) are overruled by their specific advantages. The Glider, Active Biomonitoring using Blue Mussels, IFC platforms and computer-based identification of organisms gained an overall "moderate" rating, while UAVs gained an overall "low" rating. These methods can be recommended for specific monitoring tasks and/or need further technical development to achieve a higher applicability.

Most of the methods are rated with respect to a specific monitoring objective or application and therefore, the rating is dependent on specific assumptions. Regarding DNA metabarcoding, the rating refers to the analysis of the species composition in bulk samples. The approach is limited as it does not allow storage of samples and does not reveal absolute abundances of the organisms (Leese et al., 2018). However, some studies have demonstrated relationships between the number of reads and species abundance when calculating DNA-based indices (Aylagas et al., 2018; Ushio et al., 2018; Schenk et al., 2019). In general, molecular methods have the potential to enhance the monitoring of several MSFD descriptors and thus are a promising approach for future marine monitoring (Danovaro et al., 2016; Valentini et al., 2016; Weigand et al., 2019; Filipe et al., 2019).

In case of Gliders, the technology seems not advanced enough for a cost-efficient monitoring so far, but due to the high potential of this method, research is conducted to further enhance its applicability (e.g., Meyer, 2016; Alenius et al., 2017). The method needs further improvement, since about 41% of the missions in shallow water currently fail due to platform loss or technical defects (like leakages or failures in the power supply or buoyancy; Brito et al., 2014). But due to their high spatio-temporal resolution and coverage in data acquisition, the Gliders offer a high potential to improve the marine monitoring, which cannot be achieved by conventional underwater vehicles or research vessel-based methods (Brito et al., 2014). Furthermore, Gliders can be used to detect warfare relicts dumped in the sea, increasing the importance of further technical development.

In case of the UAVs, limitations such as relatively short operating times and civil aviation restrictions cause the low applicability rating. But UAVs have a high potential to sample small areas with high spatio-temporal resolution, also in remote areas. The sampling is less time consuming and less infrastructure is needed compared to research vessel-based sampling. Currently, there is a lot of research to improve the technology of the platforms and available sensors and in turn improve the cost-efficiency and applicability (e.g., Colefax et al., 2017). In conclusion, all the methods included in this analysis were identified as promising novel monitoring methods by stakeholders and therefore each method may have specific advantages for use in a novel monitoring system.

Coverage of Gaps by the Novel Methods

The novel methods can be used to fill gaps of type (i)–(iii) regarding all MSFD descriptors except seafood contamination

(**Table 3**). The main gaps of type (i) can be compensated using several of the reviewed methods, which partly allow for a higher spatial and/or temporal resolution of monitoring data due to their autonomous measurement (**Table 3**). We want to emphasize the use of Earth Observation to facilitate the observation of the entire assessment area in the open sea, which is a highly relevant topic in the MSFD.

The lack of indicators, and therefore gaps of type (ii), can be addressed for all descriptors but underwater noise/energy. Using (e)DNA metabarcoding, the monitoring of several descriptors can be enhanced, since new indicator species are made accessible. A promising method for an improved monitoring of food webs is SIA, using the novel indicator "food web length and stability." Regarding sea-floor integrity, the Artificial Substrates ARMS and ASU can be used to generate a more comprehensive data basis by monitoring the presence of particularly sensitive and/or tolerant species, but still, indicators for a better reflection of the descriptor remain to be developed. The monitoring of dumped munitions was addressed by several recently finished and ongoing research projects (e.g., MODUM—Towards the Monitoring of Dumped Munitions Threat, 2013–2016; UDEMM, 2016—Environmental monitoring for the delaboration of munitions on the seabed, 2016–2019; DAIMON—Decision Aid for Marine Munition, 2019–2021). For the detection and identification of dumped warfare relicts, ROTV and Gliders can be deployed, while the concentrations of leaking contaminants in the water can be monitored employing Active Biomonitoring using Blue Mussels or Passive Samplers. Regarding microplastics, the constant fragmentation and the large diversity within types of particles cannot be adequately addressed by a single method (Potthoff et al., 2017). Therefore, novel methods can be combined, e.g., by sampling larger particles using the Manta Trawl and complement these data by Rocket filtration samples and Sediment Corers. The applicability of the Earth Observation techniques to measure marine litter have been under study in recent years and methodologies are evolving (Martinez-Vicente et al., 2019).

Ecosystem services and climate change were also identified as missing descriptors and are addressed in recent research (HELCOM, 2013). The monitoring of these descriptors is a wide and complex field and therefore, was not addressed in this work. However, in the course of the BONUS FUMARI project, indicators for the monitoring of ecosystem services and novel methods to measure these were collected on the novel methods website http://freshwaterplatform.eu/fumari/.

The Need for Adaptable Monitoring Practices

With this overview and evaluation of monitoring methods, we strive to support the decision making and implementation of environmental monitoring. Even though the focus of this study is on filling the gaps in the Baltic monitoring, the addressed methods can also be applied for specific research questions and in other marine regions worldwide. An in-depth comparative analysis of the methods for the environmental status assessment was not envisaged by this study and is not necessarily feasible, due to their heterogeneous nature and the wide range of applications possible. Furthermore, the cost-efficiency of the addressed novel methods was not compared to the traditional methods they might replace or supplement. This is due to the wide applicability of the novel methods that can address several ecosystem elements and indicators, the high number of factors influencing the costs, and the lack of cost analyses regarding the specific methods. An alternative option for the cost evaluation, which is not addressed here, would be using depreciation costs rather than *investment costs*. We defined *investment costs* as the costs for the monitoring device or deployment system, including the necessary equipment, and personnel training; this limits the application of depreciation costs.

New game-changing or more effective novel methods may produce high value data that are not fully comparable to these produced by traditional methods and, thus, may fail to meet current legislative demands. Very often the suggested implementation of such novel methods may be dismissed due to a lack of full comparability, but it seems unreasonable to assume a full comparability of novel methods with old ones. The current legislation driving routine monitoring of the Baltic Sea was drafted against the backdrop of the scientific knowledge and the methods available at the time of drafting. In fact, such a tacit prerequisite may hinder both scientific progress as well as effective future management of the Baltic Sea.

While we do not advocate abrupt changes in monitoring or the replacement of old by novel methods in Baltic monitoring *per se*, we stress the need to review whether there is a need to re-examine and adapt our current monitoring. With this contribution, we want to highlight the need for adaptable monitoring practices. For this, parallel and standardised comparisons are of central importance (Blackman et al., 2019). However, such novel methods need to be mature enough to have gained considerable consensus within the scientific community as well as HELCOM and also to have resulted in standardised and replicable devices and process chains. In order to implement novel methods as parts of monitoring programmes, their applicability and cost-efficiency needs to be demonstrated in the considered ecosystem, the operational practices and data flows need to be managed, and guidance for the interpretation of the acquired data needs to be given (preferably including indicators that can use the data to assess the ecosystem status). The use of the novel method should be calibrated and standardised internationally to allow for comparison between different areas or deployments.

DATA AVAILABILITY STATEMENT

All datasets presented in this study are included in the article/**Supplementary Material**.

ETHICS STATEMENT

Written informed consent was obtained from the individuals for the publication of any potentially identifiable images or data included in this article.

AUTHOR CONTRIBUTIONS

LM designed the approach to conduct this study, coordinated the data acquisition, carried out the rating of methods, and wrote the manuscript. SB supervised the approach and data acquisition, and contributed to the rating of methods and the writing of the manuscript. KM and DH contributed to the design of the study, the coordination of data acquisition, and revised the manuscript. JA, EA, ABe, ABo, MK, FL, RL, ML, AL, UL, O-PM, TP, OS, JS, LU, and AW provided data and knowledge about specific methods and revised the manuscript. All authors contributed to the article and approved the submitted version.

FUNDING

This work resulted from the BONUS FUMARI project in collaboration with BONUS SEAM project, funded by BONUS (Art. 185), which is jointly funded by the EU, the Academy of Finland and the Swedish Research Council Formas. Furthermore, funding was received from the BmBF project MicroCatch_Balt, grant number 03F0788A. EA was supported by the Red Sea Research Center at KAUST. The data on ARMS and ASUs were obtained by DEVOTES (DEVelopment Of innovative Tools for understanding marine biodiversity and assessing good Environmental Status) project, funded by the European Union under the 7th Framework Programme, "The Ocean of Tomorrow" Theme (grant agreement no. 308392), www.devotes-project.eu.

ACKNOWLEDGMENTS

We thank Heidi Ahkola (SYKE), Matthias Labrenz (IOW), Jari Hänninen (UTU), Helena Filipsson (LU), Joanna Norkko (UH), Bengt Karlson (SMHI), and Eoin O'Gorman (Essex) for their help to collate information on the addressed methods. We are also grateful for the providers of the images to display the methods. We thank the stakeholders, which took part in the survey and shared their experiences and suggestions for an improved monitoring. We thank Jörg Strackbein (UDE) for establishing the online database of novel monitoring methods.

SUPPLEMENTARY MATERIAL

The Supplementary Material for this article can be found online at: https://www.frontiersin.org/articles/10.3389/fmars.2020.552047/full#supplementary-material

REFERENCES

Abramic, A., Martínez-Alzamora, N., González, del Rio, Rams, J., Barrachina, T., et al. (2014). New methodology for analysing and increasing the cost-efficiency of environmental monitoring networks. *Mar. Pollut. Bull.* 86, 161–173. doi: 10.1016/j.marpolbul.2014.07.029

Alenius, P., Tikka, K., Lips, U., Tuomi, L., Purokoski, T., Roiha, P., et al. (2017). "Euro-Argo in work and new potential of gliders in the Baltic Sea BOOS," in *Operational Oceanography Serving Sustainable Marine Development.* eds E, V. Fernández, D. Eparkhina, P. Gorringe, and G. Nolan (Bergen: Proceedings of the Eigth EuroGOOS International Conference), 143–148.

Andersen, J. H., Halpern, B. S., Korpinen, S., Murray, C., and Reker, J. (2015). Baltic Sea biodiversity status vs. cumulative human pressures. *Estuar. Coast. Shelf Sci.* 161, 88–92. doi: 10.1016/j.ecss.2015.05.002

Anderson, C. R., Berdalet, E., Kudela, R. M., Cusack, C. K., Silke, J., O'Rourke, E., et al. (2019). Scaling up from regional case studies to a global harmful algal bloom observing system. *Front. Mar. Sci.* 6:250. doi: 10.3389/fmars.2019.00250

Anttila, S., Fleming-Lehtinen, V., Attila, J., Junttila, S., Alasalmi, H., Hällfors, H., et al. (2018). A novel cyanobacterial surface accumulation indicator for the Baltic Sea. A novel earth observation based ecological indicator for cyanobacterial blooms. *Int. J. Appl. Earth Observ. Geoinform.* 64, 145–155. doi: 10.1016/j.jag.2017.09.007

Appel, D., Strehse, J. S., Martin, H. J., and Maser, E. (2018). Bioaccumulation of 2,4,6-trinitrotoluene (TNT) and its metabolites leaking from corroded munition in transplanted blue mussels (M. *edulis*). *Mar. Pollut. Bull.* 135, 1072–1078. doi: 10.1016/j.marpolbul.2018.08.028

Attila, J., Kauppila, P., Alasalmi, H., Kallio, K., Keto, V., and Bruun, E. (2018). Applicability of Earth Observation chlorophyll-a data in assessment of water status via MERIS – with implications for the use of OLCI sensors. *Rem. Sens. Environ.* 212, 273–287. doi: 10.1016/j.rse.2018.02.043

Aylagas, E., Borja, A., Muxika, I., and Rodríguez-Ezpeleta, N. (2018). Adapting metabarcoding-based benthic biomonitoring into routine marine ecological status assessment networks. *Ecol. Indic.* 95, 194–202. doi: 10.1016/j.ecolind.2018.07.044

Aßmann, S., Frank, C., and Körtzinger, A. (2011). Spectrophotometric high-precision seawater pH determination for use in underway measuring systems. *Ocean Sci.* 7, 597–607. doi: 10.5194/os-7-597-2011

Backer, H., Leppänen, J.-M., Brusendorff, A. C., Forsius, K., Stankiewicz, M., Mehtonen, J., et al. (2010). HELCOM baltic sea action plan - A regional programme of measures for the marine environment based on the ecosystem approach. *Mar. Pollut. Bull.* 60, 642–649. doi: 10.1016/j.marpolbul.2009.11.016

Belden, J., Lotufo, G., Biedenbach, J., Sieve, K., and Rosen, G. (2015). Application of POCIS for exposure assessment of munitions constituents during constant and fluctuation exposure. *Environ. Toxicol. Chem.* 34, 959–967. doi: 10.1002/etc.2836

Beldowski, J., Jakacki, J., Grabowski, M., Lang, T., Weber, K., Kotwicki, L., et al. (2018). "Chapter 9: Best Practices in Monitoring," in *Towards the Monitoring of Dumped Munitions Threat (MODUM)*, eds J. Beldowski, R. Been, and E. K. Turmus (Berlin: Springer Science and Business Media), 213–240. doi: 10.1007/978-94-024-1153-9

Bellanger, M., and Levrel, H. (2017). A cost-effectiveness analysis of alternative survey methods used for the monitoring of marine recreational fishing in France. *Ocean Coast. Manag.* 138, 19–28. doi: 10.1016/j.ocecoaman.2017.01.007

Birk, S., Bonne, W., Borja, A., Brucet, S., Courrat, S., Poikane, S., et al. (2012). Three hundred ways to assess Europe's surface waters: an almost complete overview of biological methods to implement the water framework directive. *Ecol. Indic.* 18, 31–41. doi: 10.1016/j.ecolind.2011.10.009

Blackman, R. C., Mächler, E., Altermatt, F., Arnold, A., Beja, P., Boets, P., et al. (2019). Advancing the use of molecular methods for routine freshwater macroinvertebrate biomonitoring – the need for calibration experiments. *Metabarcod. Metagenom.* 3, 49–57. doi: 10.3897/mbmg.3.34735

Briant, N., Savoye, N., Chouvelon, T., David, V. R., Rodriguez, S., Charlier, K., et al. (2018). Carbon and nitrogen elemental and isotopic ratios of filter-feeding bivalves along the French coasts: an assessment of specific, geographic, seasonal and multi-decadal variations. *Sci. Total Environ.* 61, 196–207. doi: 10.1016/j.scitotenv.2017.08.281

Brito, M., Smeed, D., and Griffiths, G. (2014). Underwater glider reliability and implications for survey design. *J. Atmosph. Ocean. Technol.* 31, 2858–2870. doi: 10.1175/JTECH-D-13-00138.1

Cahill, A. E., Pearman, J. K., Borja, A., Carugati, L., Carvalho, S., Danovaro, R., et al. (2018). A comparative analysis of metabarcoding and morphology-based identification of benthic communities across different regional seas. *Ecol. Evol.* 8, 8908–8920. doi: 10.1002/ece3.4283

Carstensen, J., Andersen, J. H., Gustafsson, B. G., and Conley, D. J. (2014). Deoxygenation of the Baltic Sea during the last century. *Proc. Natl. Acad. Sci. U.S.A.* 111, 5628–5633. doi: 10.1073/pnas.1323156111

Charriau, A., Lissalde, S., Poulier, G., Mazzella, N., and Buzier, N. (2016). Overview of the Chemcatcher® for the passive sampling of various pollutants in aquatic environments Part A: principles, calibration, preparation and analysis of the sampler. *Talanta* 148, 556–571. doi: 10.1016/j.talanta.2015.06.064

Charrieau, L. M., Filipsson, H. L., Ljung, K., Chierici, M., Knudsen, K. L., and Kritzberg, E. (2018). The effects of multiple stressors on the distribution of coastal benthic foraminifera: a case study from the Skagerrak-Baltic Sea region. *Mar. Micropaleontol.* 139, 42–56. doi: 10.1016/j.marmicro.2017.11.004

Colefax, A. P., Butcher, P. A., and Kelaher, B. P. (2017). The potential for unmanned aerial vehicles (UAVs) to conduct marine fauna surveys in place of manned aircraft. *ICES J. Mar. Sci.* 75, 1–8. doi: 10.1093/icesjms/fsx100

Danovaro, R., Carugati, L., Berzano, M., Cahill, A. E., Carvalho, S., Chenuil, A., et al. (2016). Implementing and innovating marine monitoring approaches for assessing marine environmental status. *Front. Mar. Sci.* 3:213. doi: 10.3389/fmars.2016.00213

DEVOTES (2013). *Deliverable 5.1. Innovative Monitoring Techniques. Report on the Set up of the Field and Experimental Activities*. Research Report of the EU Research Project DEVOTES. Rome: CONISMA.

Emmerson, R., Nygård, H., Grimvall, A., Storr-Paulsen, M., Dinesen, G., Ritzau Eigaard, O., et al. (2019). *Deliverable 2.1: Holistic Synthesis of Reviews and Analysis of Current Baltic Sea Monitoring and Assessment*. Technical report of the EU Research Project BONUS SEAM. Gothenburg: University of Gothenburg.

EuroGOOS (2017). *Ferrybox Whitebook*. Technical and Scientific Report of the European Global Ocean Observing System (EuroGOOS). Brussels: EuroGOOS AISBL.

European Commission (2000). Directive 2000/60/EC of the European Parliament and of the Council of 23 October 2000 establishing a framework for community action in the field of water policy. *Off. J. Eur. Commun.* 327, 1–72.

European Commission (2008). Directive 2008/56/EC of the European Parliament and of the Council of 17 June 2008 establishing a framework for community action in the field of marine environmental policy (Marine Strategy Framework Directive). *Off. J. Eur. Commun.* 164, 19–49.

European Commission (2014). Technology Readiness Levels (TRL); Extract From Part 19 - Commission Decision C (2014) 4995. https://ec.europa.eu/research/participants/data/ref/h2020/wp/2014_2015/annexes/h2020-wp1415-annex-g-trl_en.pdf. (accessed March 26, 2019).

Filipe, A. F., Feio, M. J., Garcia-Raventós, A., Ramião, J. P., Pace, G., Martins, F. M. S., et al. (2019). The European Water Framework Directive facing current challenges: recommendations for a more efficient biological assessment of inland surface waters. *Inland Waters* 9:10. doi: 10.1080/20442041.2018.1494973

Floeter, J., van Beusekomb, J. E. E., Auch, D., Callies, U., Carpenter, J., Dudeck, T., et al. (2017). Pelagic effects of offshore wind farm foundations in the stratified North Sea. *Prog. Oceanogr.* 156, 154–173. doi: 10.1016/j.pocean.2017.07.003

Furlong, A., Osler, J., Christian, H., Cunningham, D., and Pecknold, S. (2006). *The Moving Vessel Profiler (MVP) - a Rapid Environmental Assessment Tool for the Collection of Water Column Profiles and Sediment Classification*. Technical Report AD1005165. Fairfax: Defense Technical Information Center.

González, P., Castaño, A., Peacock, E. E., Díez, J., Del Coz, J. J., and Sosik, H. M. (2019). Automatic plankton quantification using deep features. *J. Plankton Res.* 41, 449–463. doi: 10.1093/plankt/fbz023

Gustafsson, B. G., Schenk, F., Blenckner, T., Eilola, K., Meier, H. E. M., Müller-Karulis, B., et al. (2012). Reconstructing the development of baltic sea eutrophication 1850-2006. *Ambio* 41, 534–548. doi: 10.1007/s13280-012-0318-x

Harman, C., Allan, I. J., and Vermeirssen, E. L. M. (2012). Calibration and use of polar organic chemical integrative sampler – a critical review. *Environ. Toxicol. Chem.* 31, 2724–2739. doi: 10.1002/etc.2011

Harvey, E. T., Kratzer, S., and Philipson, P. (2015). Satellite-based water quality monitoring for improved spatial and temporal retrieval of chlorophyll-a in coastal waters. *Remote Sens. Environ.* 158, 417–430. doi: 10.1016/j.rse.2014.11.017

HELCOM (2007). *Baltic Sea Action Plan. Adopted at HELCOM Ministerial Meeting in Krakow, Poland*. Helsinki: HELCOM.

HELCOM (2013). *Climate change in the Baltic Sea Area: HELCOM thematic assessment in 2013. Baltic Sea Environment Proceedings 137*. Helsinki: HELCOM.

HELCOM (2016). *Hydrography and Oxygen in the Deep Sea Basins. HELCOM Baltic Sea Environment Fact Sheets*. Helsinki: HELCOM.

HELCOM (2017). *HELCOM Monitoring and Assessment Strategy, Attachment 4. HELCOM Ministerial Declaration from the 2013 Ministerial Meeting, updated in 2017 following the STATE & CONSERVATION meeting*. Copenhagen: HELCOM.

HELCOM (2018a). *State of the Baltic Sea – Second HELCOM holistic assessment 2011-2016. Baltic Sea Environmental Proceedings 155*. Helsinki: HELCOM.

HELCOM (2018b). *HELCOM Core Indicator Report. Chlorophyll-a*. Helsinki: HELCOM.

HELCOM (2018c). *HELCOM Thematic Assessment of Eutrophication 2011-2016. Baltic Sea Environment Proceedings No. 156*. Helsinki: HELCOM.

Hering, D., Borja, A., Jones, J. I., Pont, D., Boets, P., Bouchez, A., et al. (2018). Implementation options for DNA-based identification into ecological status assessment under the European Water Framework Directive. *Water Res.* 138, 192–205. doi: 10.1016/j.watres.2018.03.003

ICES (2018). *4.2 Baltic Sea Ecoregion - Fisheries Overview. Report of the International Council for the Exploration of the Sea (ICES)*. Copenhagen: ICES, 23. doi: 10.17895/ices.pub.4648

Jardine, T. D., Hobson, K. A., and Soto, D. X. (2017). "Introduction to Stable Isotopes in Food Webs," in *Food Forensics – Stable Isotopes as a Guide to Authenticity and Origin*, eds J. F. Carter and L. A. Chesson (Boca Raton, FL: CRC Press), 63–94. doi: 10.1201/9781315151649

Jeunen, G.-J., Knapp, M., Spencer, H. G., Lamare, M. D., Taylor, H. R., Stat, M., et al. (2019). Environmental DNA (eDNA) metabarcoding reveals strong discrimination among diverse marine habitats connected by water movement. *Mol. Ecol. Res.* 19, 426–438. doi: 10.1111/1755-0998.12982

JRC (2013). *Guidance on Monitoring of Marine Litter in European Seas. A guidance document within the Common Implementation Strategy for the Marine Strategy Framework Directive*. Scientific and Policy Report EUR 26113 of the MSFD Technical Subgroup on Marine Litter. Ispra: Joint Research Centre, 128.

JRC (2014). *Technical Guidance on Monitoring for the Marine Strategy Framework Directive*. Scientific and Policy Report EUR 26499 EN. Ispra: Joint Research Centre, 175.

Kahlert, M., Eilola, K., Mack, L., Meissner, K., Sandin, L., Strömberg, H., et al. (2020). Gaps in current Baltic Sea environmental monitoring Ű Science versus management perspectives. *Mar. Pollut.* 160:111669. doi: 10.1016/j.marpolbul.2020.111669

Karlson, B., Andersson, L. S., Kaitala, S., Kronsell, J., Mohlin, M., Seppälä, J., et al. (2016). A comparison of FerryBox data vs. Monitoring data from research vessels for near surface waters of the Baltic Sea and the Kattegat. *J. Mar. Syst.* 162, 98–111. doi: 10.1016/j.jmarsys.2016.05.002

Kelleher, J. D., Mac Namee, B., and D'Arcy, A. (2015). *Fundamentals of Machine Learning for Predictive Data Analytics*. Cambridge: The MIT Press, 624.

Kindt-Larsen, L., Dalskov, J., Stage, B., and Larsen, F. (2012). Observing incidental harbour porpoise Phocoena bycatch by remote electronic monitoring. *End. Species Res.* 19, 75–83. doi: 10.3354/esr00455

Leese, F., Bouchez, A., Abarenkov, K., Altermatt, F., Borja, A., Bruce, K., et al. (2018). Why we need sustainable networks bridging countries, disciplines, cultures and generations for aquatic biomonitoring 2.0: A perspective derived from the DNAqua-Net COST Action. *Adv. Ecol. Res.* 58, 63–99. doi: 10.1016/bs.aecr.2018.01.001

Lehikoinen, A., Olsson, J., Bergström, L., Bergström, U., Bryhn, A., Fredriksson, R., et al. (2019). Evaluating complex relationships between ecological indicators and environmental factors in the Baltic Sea: a machine learning approach. *Ecol. Indic.* 101, 117–125. doi: 10.1016/j.ecolind.2018.12.053

Lenz, R., and Labrenz, M. (2018). Small microplastic sampling in water: development of an encapsulated filtration device. *Water* 10:1055. doi: 10.3390/w10081055

Liblik, T., Karstensen, J., Testor, P., Alenius, P., Hayes, D., Ruiz, S., et al. (2016). Potential for an underwater glider component as part of the global

ocean observing system. *Methods Oceanogr.* 17, 50–82. doi: 10.1016/j.mio.2016.05.001

Lips, I., and Lips, U. (2017). The importance of Mesodinium rubrum at post-spring bloom nutrient and phytoplankton dynamics in the vertically stratified Baltic Sea. *Front. Mar. Sci.* 4:1–16. doi: 10.3389/fmars.2017.00407

Lips, I., Lips, U., Liblik, T., Kikas, V., Altoja, K., Buhhalko, N., et al. (2011). Vertical dynamics of summer phytoplankton in a stratified estuary (Gulf of Finland. Baltic Sea). *Ocean Dyn.* 61, 903–915. doi: 10.1007/s10236-011-0421-8

Liu, M., Zhang, Y., Shi, K., Zhu, G., Wu, Z., Liu, M., et al. (2019). Thermal stratification dynamics in a large and deep subtropical reservoir revealed by high-frequency buoy data. *Sci. Total Environ.* 651, 614–624. doi: 10.1016/j.scitotenv.2018.09.215

Lotufo, G. R., George, R. D., Belden, J. B., Woodley, C., Smith, D. L., and Rosen, G. (2019). Release of munitions constituents in aquatic environments under realistic scenarios and validation of polar organic chemical integrative samplers for monitoring. *Environ. Toxicol. Chem.* 38, 2383–2391. doi: 10.1002/etc.4553

Mack, L., Birk, S., and Hering, D. (2019). *Deliverable 2.1: Structure of the Review on Novel Monitoring Methods*. Research Report of the EU Research Project BONUS FUMARI. Essen: University of Duisburg-Essen.

Martinez-Vicente, V., Clark, J. R., Corradi, P., Aliani, S., Arias, M., Bochow, M., et al. (2019). Measuring marine plastic debris from space: initial assessment of observation requirements. *Rem. Sens.* 11:2443. doi: 10.3390/rs11202443

Meyer, D. (2016). Glider technology for ocean observations: a review. *Ocean Sci. Discuss.* 2016, 1–26. doi: 10.5194/os-2016-40

Meyer, D., Lips, U., Prien, R. D., Naumann, M., Liblik, T., Schuffenhauer, I., et al. (2018). Quantification of dissolved oxygen dynamics in a semi-enclosed sea - a comparison of observational platforms. *Cont. Shelf Res.* 169, 34–45. doi: 10.1016/j.csr.2018.09.011

Michener, R. H., and Kaufman, L. (2007). "Stable Isotope Ratios in Marine Food Webs: An Update," in *Stable Isotopes in Ecology and Environmental Science*, eds R. H. Michener and K. Lajtha (Malden: Blackwell Publishing), 202–230. doi: 10.1002/9780470691854

Müller, J. D., Schneider, B., Aßmann, S., and Rehder, G. (2018). Spectrophotometric pH measurements in the presence of dissolved organic matter and hydrogen sulfide. *Limnol. Oceanogr.* 16, 68–82. doi: 10.1002/lom3.10227

Nygård, H., Oinonen, S., Hällfors, H. A., Lehtiniemi, M., Rantajärvi, E., and Uusitalo, L. (2016). Price vs. value of marine monitoring. *Front. Mar. Sci.* 3:205. doi: 10.3389/fmars.2016.00205

Osterloff, J., Nilssen, I., Järnegren, J., van Engeland, T., Buhl-Mortensen, P., and Nattkemper, T. W. (2019). Computer vision enables short- and long-term analysis of Lophelia pertusa polyp behaviour and colour from an underwater observatory. *Sci. Rep.* 9:6578. doi: 10.1038/s41598-019-41275-1

Palacin-Silva, M., Seffah, A., Heikkinen, K., Porras, J., Pyhälahti, T., Sucksdorff, Y., et al. (2016). State-of-the art study in citizen observatories: technological trends, development challenges and research avenues. *Rep. Finn. Environ. Instit.* 28:100.

Papathanaopoulou, E., Simis, S., Alikas, K., Ansper, A., Anttila, S., Attila, J., et al. (2019). Satellite-assisted monitoring of water quality to support the implementation of the Water Framework Directive. *EOMORES white paper* 28. doi: 10.5281/zenodo.3463051

Pawlowski, J., Kelly-Quinn, M., Altermatt, F., Apothéloz-Perret-Gentil, L., Beja, P., Boggero, A., et al. (2018). The future of biotic indices in the ecogenomic era: Integrating (e)DNA metabarcoding in biological assessment of aquatic ecosystems. *Sci. Total Environ.* 63, 1295–1310. doi: 10.1016/j.scitotenv.2018.05.002

Petersen, W. (2014). FerryBox systems: state-of-the-art in europe and future development. *J. Mar. Syst.* 140, 4–12. doi: 10.1016/j.jmarsys.2014.07.003

Potthoff, A., Oelschlägel, K., Schmitt-Jansen, M., Rummel, C. D., and Kühnel, D. (2017). From the sea to the laboratory: characterization of microplastic as prerequisite for the assessment of ecotoxicological impact. *Integr. Environ. Assess. Manag.* 13, 500–504. doi: 10.1002/ieam.1902

Prien, R. D., and Schulz-Bull, D. E. (2016). Technical note: GODESS: a profiling mooring in the Gotland Basin. *Ocean Sci.* 12, 899–907. doi: 10.5194/os-12-899-2016

Roiha, P., Siiriä, S.-M., Haavisto, N., Alenius, P., Westerlund, A., and Purokoski, T. (2018). Estimating currents from argo trajectories in the Bothnian Sea, Baltic Sea. *Front. Mar. Sci.* 5:308. doi: 10.3389/fmars.2018.00308

Rombouts, I., Beaugrand, G., Fizzala, X., Gaill, F., Greenstreet, S. P. R., Lamare, S., et al. (2013). Food web indicators under the Marine Strategy Framework Directive: From complexity to simplicity? *Ecological Indicators* 29, 426–254. doi: 10.1016/j.ecolind.2012.12.021

Schenk, J., Geisen, S., Kleinboelting, N., and Traunspurger, W. (2019). Metabarcoding data allow for reliable biomass estimates in the most abundant animals on earth. *MBMG* 3:e46704. doi: 10.3897/mbmg.3.46704

Schneider, B., and Müller, J. D. (2018). *Biogeochemical Transformations in the Baltic Sea. Observations Through Carbon Dioxide Glasses*. London: Springer International Publishing, 110. doi: 10.1007/978-3-319-61699-5

Schöne, B. R., and Krause, R. A. Jr. (2016). Retrospective environmental biomonitoring – MusselWatch expanded. *Global and Planetary Change* 144, 228–251. doi: 10.1016/j.gloplacha.2016.08.002

Setälä, O., Magnusson, K., Lehtiniemi, M., and Norén, F. (2016). Distribution and abundance of surface water microlitter in the Baltic Sea: A comparison of two sampling methods. *Mar. Pollut. Bull.* 110, 177–183. doi: 10.1016/j.marpolbul.2016.06.065

Setlak, L., and Kowalik, R. (2019). Examination of the Unmanned Aerial Vehicle. *ITM Web of Conferences* 24, 01006. doi: 10.1051/itmconf/20192401006

Siiriä, S., Roiha, P., Tuomi, L., Purokoski, T., Haavisto, N., and Alenius, P. (2019). Applying area-locked, shallow water Argo floats in Baltic Sea monitoring. *J. Operat. Oceanogr.* 12, 58–72. doi: 10.1080/1755876X.2018.1544783

Söderström, S., and Kern, K. (2017). The ecosystem approach to management in marine Environmental governance: institutional interplay in the Baltic Sea Region. *Environ. Pol. Govern.* 27, 619–631. doi: 10.1002/eet.1775

Stoicescu, S.-T., Lips, U., and Liblik, T. (2019). Assessment of eutrophication status based on Sub-surface oxygen conditions in the gulf of Finland (Baltic Sea). *Front. Mar. Sci.* 19:54. doi: 10.3389/fmars.2019.00054

Strehse, J. S., Appel, D., Geist, C., Martin, H.-J., and Maser, E. (2017). Biomonitoring of 2,4,6-trinitrotoluene and degradation products in the marine environment with transplanted blue mussels (M. *edulis*). *Toxicology* 390, 117–123. doi: 10.1016/j.tox.2017.09.004

Szymczychta, B., Zaborska, A., Bełdowski, J., Kuliński, K., Beszczyńska-Möller, A., Kêdra, M., et al. (2019). "Chapter 4: The Baltic Sea," in *World Seas: An Environmental Evaluation, Volume One: Europe, The Americas and West Africa*, ed. C. Sheppard (Oxford: Academic Press), 85–111. doi: 10.1016/B978-0-12-805068-2.00005-X

Tamminga, M., Hengstmann, E., and Fischer, E. K. (2018). Microplastic analysis in the South Funen Archipelago. Baltic Sea, implementing manta trawling and bulk sampling. *Mar. Pollut. Bull.* 128, 601–608. doi: 10.1016/j.marpolbul.2018.01.066

UDEMM (2016). *Environmental Monitoring for the Delaboration of Munitions on the Seabed, 2016-2019*.

Ushio, M., Murakami, H., Masuda, R., Sado, T., Miya, M., Sakurai, S., et al. (2018). Quantitative monitoring of multispecies fish environmental DNA using high-throughput sequencing. *MBMG* 2:e23297. doi: 10.1101/113472

Uusitalo, L., Fernandes, J. A., Bachiller, E., Tasala, S., and Lehtiniemi, M. (2016). Semi-automated classification method addressing marine strategy framework directive (MSFD) zooplankton indicators. *Ecol. Indic.* 71, 398–405. doi: 10.1016/j.ecolind.2016.05.036

Valentini, A., Taberlet, P., Miaud, C., Civade, R., Herder, J., Thomsen, P. F., et al. (2016). Next-generation monitoring of aquatic biodiversity using environmental DNA metabarcoding. *Mol. Ecol.* 25, 929–942. doi: 10.1111/mec.13428

Venkatesan, R., Ramesh, K., Muthiah, M. A., Thirumurugan, K., and Atmanand, M. A. (2019). Analysis of drift characteristic in conductivity and temperature sensors used in Moored buoy system. *Ocean Eng.* 171, 151–156. doi: 10.1016/j.oceaneng.2018.10.033

Vrana, B., Mills, G. A., Allan, I. J., Dominiak, E., Svensson, K., Knutsson, J., et al. (2005). Passive sampling techniques for monitoring pollutants in water. *Trends Anal. Chem.* 24, 845–868. doi: 10.1016/j.trac.2005.06.006

Weigand, H., Beermann, A. J., Čiampor, F., Costa, F. O., Csabai, Z., Duarte, S., et al. (2019). DNA barcode reference libraries for the monitoring of aquatic biota in Europe: Gap-analysis and recommendations for future work. *Sci. Total Environ.* 678, 499–524. doi: 10.1016/j.scitotenv.2019.04.247

Williams, K., Rooper, C., and Harms, J. (2012). *Report of the National Marine Fisheries Service Automated Image Processing Workshop.* NOAA Technical Memorandum NMFS-F/SPO-121, U.S. Seattle: Department of Commerce, NOAA, 48.

WWF (2015). *Electronic Monitoring in Fisheries Management. Report Commissioned and Published by Worldwide Fund for Nature (WWF).* Gland: WWF.

WWF (2017). *Remote Electronic Monitoring – Why camera technology is a cost-effective and robust solution to improving UK fisheries management. Report Commissioned and Published by Worldwide Fund for Nature (WWF).* Gland: WWF.

Zampoukas, N., Piha, H., Bigagli, E., Hoepffner, N., Hanke, G., and Cardoso, A. C. (2012). *Monitoring for the Marine Strategy Framework Directive: Requirements and Options. Technical report EUR* 25187 EN. Luxembourg: JRC Scientific and Policy Reports, 42.

Zhang, Y., Pavlovska, M., Stoica, E., Prekrasna, I., Yang, J., Slobodnik, J., et al. (2020). Holistic pelagic biodiversity monitoring of the Black Sea via eDNA metabarcoding approach: From bacteria to marine mammals. *Environ. Int.* 135:105307. doi: 10.1016/j.envint.2019.105307

Conflict of Interest: The authors declare that the research was conducted in the absence of any commercial or financial relationships that could be construed as a potential conflict of interest.

Copyright © 2020 Mack, Attila, Aylagas, Beermann, Borja, Hering, Kahlert, Leese, Lenz, Lehtiniemi, Liess, Lips, Mattila, Meissner, Pyhälahti, Setälä, Strehse, Uusitalo, Willstrand Wranne and Birk. This is an open-access article distributed under the terms of the Creative Commons Attribution License (CC BY). The use, distribution or reproduction in other forums is permitted, provided the original author(s) and the copyright owner(s) are credited and that the original publication in this journal is cited, in accordance with accepted academic practice. No use, distribution or reproduction is permitted which does not comply with these terms.

This is the end of the publication

A Synthesis of Marine Monitoring Methods With the Potential to Enhance the Status Assessment of the Baltic Sea

by Leoni Mack, Jenni Attila, Eva Aylagas, Arne Beermann, Angel Borja, Daniel Hering, Maria Kahlert, Florian Leese, Robin Lenz, Maiju Lehtiniemi, Antonia Liess, Urmas Lips, Olli-Pekka Mattila, Kristian Meissner, Timo Pyhälahti, Outi Setälä, Jennifer S. Strehse, Laura Uusitalo, Anna Willstrand Wranne, Sebastian Birk

You might want to continue reading the synopsis at page 23, or jump back to the start of this publication at page 105.

Combined Approaches to Predict Microplastic Emissions Within an Urbanized Estuary (Warnow, Southwestern Baltic Sea)

by Sarah Piehl, Rahel Hauk, Esther Robbe, Boris Richter, Frauke Kachholz, Jannik Schilling, Robin Lenz, Dieter Fischer, Franziska Fischer, Matthias Labrenz, Gerald Schernewski

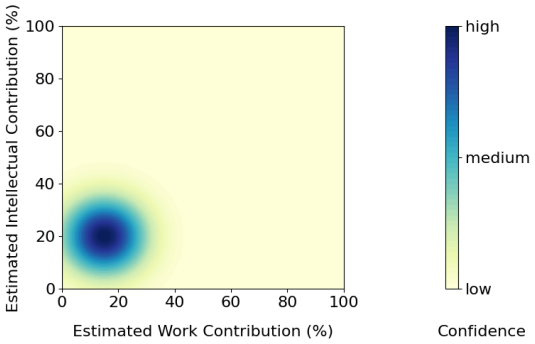
- **Date published**: March 29, 2021
- **Type**: Research Article
- **Published in**: Frontiers in Environmental Science, Frontiers
- **License**: CC-BY
- **DOI**: 10.3389/fenvs.2021.616765, **Reference**: [7]
- **Citations**: 40 (Crossref/DOI, 2025-11-18)

Contributions

SP and GS prepared the concept of the paper | All authors made substantial, direct, and intellectual contribution to the work and approved it for publication.

Quantitative own contributions based on self-assessment

In the dimensions of expended work effort and intellectual contribution, I consider my shares are likely to be between 10% and 20% and between 15% and 25% respectively. This is visualised below as an interpolated histogram of 500 samples from Gaussian distributions with the aforementioned estimates at plus/minus two standard deviations.



frontiers in Environmental Science

ORIGINAL RESEARCH
published: 29 March 2021
doi: 10.3389/fenvs.2021.616765

Combined Approaches to Predict Microplastic Emissions Within an Urbanized Estuary (Warnow, Southwestern Baltic Sea)

Sarah Piehl[1], Rahel Hauk[1], Esther Robbe[1,2], Boris Richter[3], Frauke Kachholz[3], Jannik Schilling[3], Robin Lenz[1], Dieter Fischer[4], Franziska Fischer[4], Matthias Labrenz[1] and Gerald Schernewski[1,2]*

[1]Leibniz Institute for Baltic Sea Research, Rostock, Germany, [2]Marine Research Institute, Klaipėda University, Klaipeda, Lithuania, [3]Department of Water Management, University of Rostock, Rostock, Germany, [4]Leibniz Institute of Polymer Research, Dresden, Germany

OPEN ACCESS

Edited by:
André Ricardo Araújo Lima, Center for Marine and Environmental Sciences (MARE), Portugal

Reviewed by:
Bruno Tassin, École des ponts ParisTech (ENPC), France
Lixin Zhu, East China Normal University, China

***Correspondence:**
Sarah Piehl
sarah.piehl@io-warnemuende.de

Specialty section:
This article was submitted to Toxicology, Pollution and the Environment, a section of the journal Frontiers in Environmental Science

Received: *13 October 2020*
Accepted: *01 February 2021*
Published: *29 March 2021*

Citation:
Piehl S, Hauk R, Robbe E, Richter B, Kachholz F, Schilling J, Lenz R, Fischer D, Fischer F, Labrenz M and Schernewski G (2021) Combined Approaches to Predict Microplastic Emissions Within an Urbanized Estuary (Warnow, Southwestern Baltic Sea). Front. Environ. Sci. 9:616765. doi: 10.3389/fenvs.2021.616765

Microplastic river emissions are known to be one of the major sources for marine microplastic pollution. Especially urbanized estuaries localized at the land-sea interface and subjected to microplastic emissions from various sources exhibit a high microplastic discharge potential to adjacent coasts. To adapt effective measures against microplastic emissions a more detailed knowledge on the importance of various microplastic sources is necessary. As field data is scarce we combined different approaches to assess microplastic emissions into the Warnow estuary, southwestern Baltic Sea. Resulting microplastic emission estimates are based on *in-situ* measurements for the catchment emissions, whereas for the remaining microplastic sources within the estuary literature data on microplastic abundances, and various parameters were used (e.g. demographical, hydrological, geographical). The evaluation of the different emission scenarios revealed that the majority of microplastic is likely discharged by the Warnow river catchment (49.4%) and the separated city stormwater system (43.1%) into the estuary, followed by combined sewer discharges (6.1%). Wastewater treatment plant emissions exhibit the lowest percentage (1.4%). Our approach to estimate anti-fouling paint particles emissions from leisure and commercial shipping activities was associated with highest uncertainties. However, our results indicate the importance of this source highlighting the necessity for future research on the topic. Based on our assumptions for microplastic retention within the estuary, we estimate a potential annual emission of 152–291 billion microplastics (majority within the size class 10–100 µm) to the Baltic Sea. Considering all uncertainties of the different applied approaches, we could assess the importance of various microplastic sources which can be used by authorities to prioritize and establish emission reduction measures. Additionally, the study provides parameters for microplastic emission estimates that can be transferred from our model system to other urbanized Baltic estuaries.

Keywords: microplastic, warnow estuary, baltic sea, sewer system, emission estimates, combined sewer overflow, anti-fouling paint particles

INTRODUCTION

Since the first description of small plastic particles in the marine environment (Colton et al., 1974; Morris and Hamilton, 1974), assessments of "microplastic" (MP) contamination revealed its ubiquitous distribution within aquatic ecosystems (Burns and Boxall, 2018; Geilfus et al., 2019). Concentrations of MPs span several orders of magnitude ranging from less than one to several hundreds of thousands of MPs per cubic meter in sea water (Wu et al., 2019). In sediments over ten thousand MPs per kilogram dry weight (DW) have been reported (Cunningham and Sigwart, 2019). Especially semi-enclosed seas with a large catchment area and limited water exchange through narrow straits, such as the Baltic Sea, are subjected to anthropogenic pressures deriving mainly from land-based activities like MP litter. Due to the omnipresence and longevity of MP litter and its potential adverse effects on organisms and human health (Sharma and Chatterjee, 2017; Wang et al., 2019) it has become an integral part of regulations for the protection of the marine environment (Directive of the European parliament, 2008; HELCOM, 2008; Resolution, 2020). The most relevant within the European Union, the Marine Strategy Framework Directive (MSDF, 2008/56/EC), requires its member states to achieve a good environmental status (GES) with marine litter representing one of the qualitative descriptors (D10) for the GES. For Baltic Sea member states, the directive is implemented within the Baltic Sea Action Plan (BSAP) of the Helsinki Convention (HELCOM). Its Regional Action Plan on Marine Litter (RAP ML) requires further "to establish an overview of the importance of the different sources of primary and secondary microplastics" (RL6, HELCOM, 2015) and calls for actions addressing sources of MPs, (i.e. RL4).

Rivers have already been recognized as a major input source of MP litter into the ocean (van Wijnen et al., 2019). Especially urbanized estuaries depict a potential hotspot for MP emissions to coastal waters with measured MP concentrations in urban surface waters reaching 100 items per liter (Leslie et al., 2017). Here a multitude of MP emission sources congregate within a confined space, such as recreational activities, shipping, wastewater emissions, tributaries, and leisure boat facilities. To implement targeted prevention measures against marine MP litter a detailed overview and assessment of the importance of various MP emission sources within urban estuaries is necessary. Concerning southwestern Baltic estuaries, the Warnow estuary, with a high degree of urbanization and industrialization, depicts a suitable model system.

Considering land-based MP emissions, major point sources are municipal and industrial wastewaters (Baresel and Olshammar, 2019; Bellasi et al., 2020). Due to high discharge volumes of wastewater treatment plants (WWTPs) they are considered as significant source even though most plants obtain a MP removal efficiency of >90% (with up to 99.9%) (Prata, 2018; Cristaldi et al., 2020; Uddin et al., 2020). An even higher share of MP emissions has been reported for combined sewer overflows (CSOs) in combined systems (Baresel and Olshammar, 2019) as well as stormwater in separated systems (Liu et al., 2019). Paint particles from buildings, structures, and shipping are thought to be another relevant source of MPs within urban estuaries (Sundt et al., 2014; Soroldoni et al., 2018). Here it must be differentiated between anticorrosive and antifouling paint particles (AFPPs) with the latter possibly possessing a higher relevance due to the self-polishing behavior of AFPPs (Watermann and Eklund, 2019). For example, in the Warnow estuary, a medium of 86.5 MP per kilogram DW and a maximum of 379 (±28) MPs per kilogram DW was measured within subtidal sediments with paint particles generally as common as other microplastics (Enders et al., 2019).

Nevertheless, data on MP inputs from diverse sources and abundances within any river mouth is still scarce (Li et al., 2018; Rezania et al., 2018). Besides challenges on collection of environmental MP samples, cost-effective and standardized operational monitoring methods are currently lacking. An alternative approach to estimate MP emissions is the development of emission scenarios based on available literature data, expert knowledge and via indirect parameters. For example near shore population density, gross domestic product, and mismanaged plastic waste were already utilized as predictors for plastic litter emissions on a global scale (Sherman and van Sebille, 2016; Schmidt et al., 2017; Isobe et al., 2019). Regarding MPs, Siegfried et al. (2017) estimated MP fluxes from European rivers to the sea by combining information on MP litter point sources, sewage management, and plastic retention during river transport. Discharge of MPs by urban waters to the Baltic Sea was further assessed utilizing exemplary sewer systems and a model city (Bollmann et al., 2019). Nevertheless, a spatially resolved differentiation of MP emission sources within an urbanized Baltic estuary is currently missing to the best of our knowledge. Due to its relatively small and well-defined area the Warnow estuary provides an ideal model system for which a comprehensive approach can be applied.

To support authorities in establishing an effective monitoring as well as in implementing mitigation measures, we assessed the importance of different MP sources exemplarily for the Warnow estuary. We first localized major MP point sources, here defined as sources within the estuary where a spatially explicit localization is possible. Secondly, a combination of different approaches was used to estimate MP emissions from the city sewer system and the river catchment as well as to assess AFPP emissions. The specific aims were 1) to establish an overview of the importance of different MP sources within the urbanized Warnow estuary as a model system, 2) to provide a first estimation on annual MP emissions from the estuary to the Baltic Sea, and 3) to assess the suitability of utilized parameters to support the development of simplified indicators for estuarine MP emissions into the Baltic Sea.

MATERIALS AND METHODS

Study System

The Warnow estuary (**Figure 1**), Mecklenburg-Western Pomerania, Germany, has a length of 13 km with a mean water depth of 5.6 m and a maximum depth of 15 m within the shipping channel up to the area of Breitling (Lange et al.,

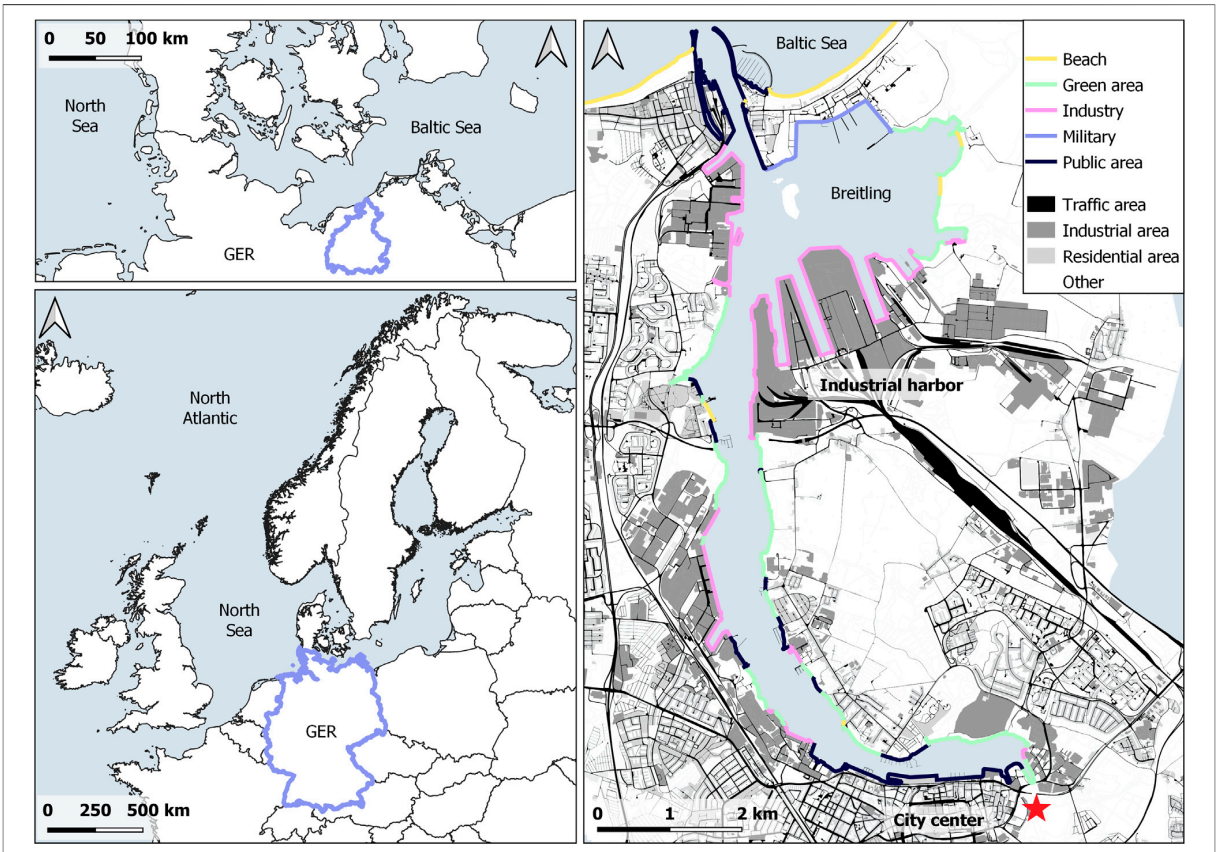


FIGURE 1 | Map of the Warnow catchment (blue line **upper left**) located in northwestern Germany **(lower left)** and the Warnow estuary **(right)** with land use sections around the estuary. The position of the weir where the Warnow river is discharging into the estuary is indicated by a red star. "Other" includes unsealed areas such as forests, agri- and horticulture. Source: Hanse-und Universitätsstadt Rostock (CC BY 4.0).

2020). The estuary holds a water volume of 49.6 million m^3 within an area of 12 km^2 (Bachor, 2005) and exhibits a water exchange time of around 30 days. The average water budget of the estuary is dominated by intruding Baltic Sea water with 1,180 km^3/a in comparison to 440 km^3/a freshwater inflow and a total outflow to the North Sea of 1,660 km^3/a (Szymczycha et al., 2019). The estuarine exchange flow of the tidal weak estuary is sensitive to wind stress and varying salinities of the adjacent coastal waters, which leads to frequent inversion of the classical estuarine circulation (Lange et al., 2020). The 56.5 km long riverbank of the estuary is mostly artificial (74%), and harbor and shipping lanes occupy 37% of the water surface area (Schernewski et al., 2019). In 2018 around 200 cruise ships arrived and around 19.6 million tons of freight and 3.3 million passengers were handled (Hansestadt Rostock, 2019). Besides, leisure boat facilities are common with a share of 6% of all moorings along the German Baltic Sea coast (Watermann et al., 2014). To maintain and safeguard shipping activities, parts of the estuary are regularly dredged. The maintenance interval of the inner and outer shipping lane (access to industrial harbor) is five to ten years whereby on average 60,000 m^3/a of dredged material is extracted (WSV, 2019). Other areas within the estuary are maintained on demand.

The city of Rostock surrounds the estuary and counts about 209,000 residents within an area of 181.4 km^2 yielding a population density of 1,151 residents per km^2 (Hansestadt Rostock, 2019).

The city area is shaped by a dense network of natural and artificial waterways. About 200 small streams with a total length of 196 km exist within the catchment of the city of Rostock. The city center is connected to a combined sewer system (**Figure 2**) but most of the catchment is connected to a separate system with a 430 km long canal network (KOGGE et al., 2018). The wastewater of Rostock is treated at the central wastewater treatment plant (WWTP). The treatment technology comprises mechanical treatment, an activated sludge followed by a two-step biofilter for post nitrification and denitrification. Taking industrial and commercial wastewater contributions into account the population equivalent (PE) of the WWTP is 400,000, corresponding to a wastewater production of 100 L per PE per day.

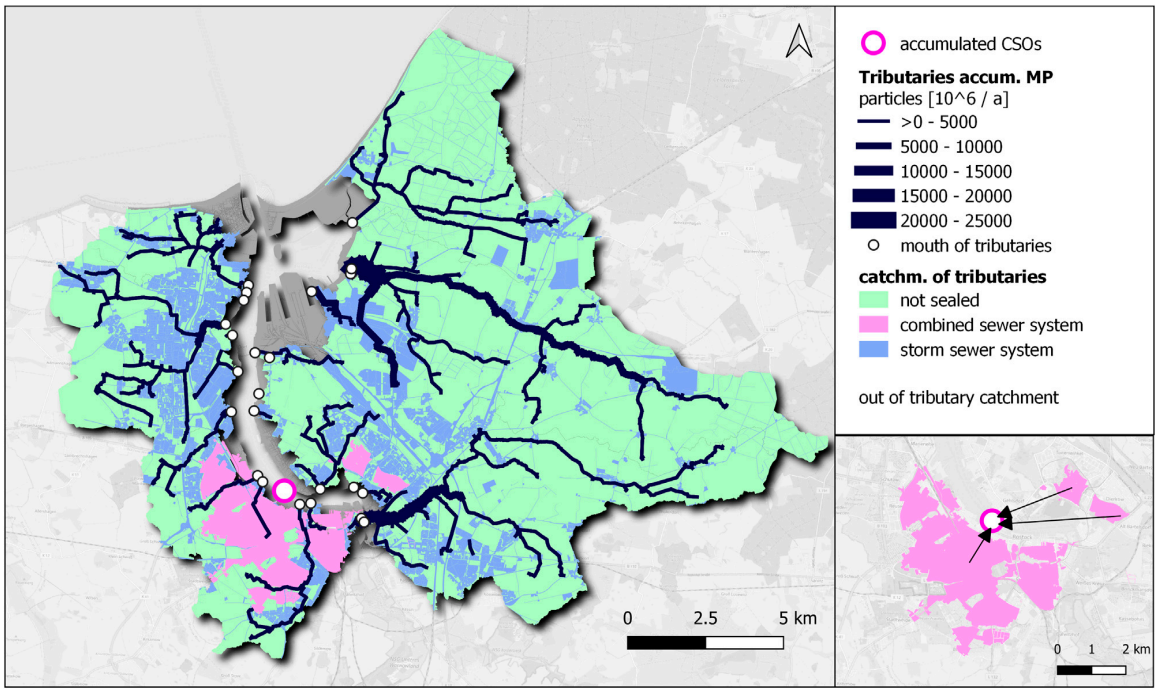


FIGURE 2 | Accumulation of microplastic (MP) emissions from stormwater (blue areas) along tributaries (dark blue lines) within the catchment of the estuary and input of MP emissions from the combined sewer system (magenta areas). Green areas are assumed not to be sealed and include e.g., agriculture, grassland, and parks.

The mean annual rainfall amounts to 621 mm (DWD, 2020) and annually a mean of 16.5 m^3/s of water is discharged from the Warnow river into the estuary. The discharge is regulated by a weir located at the southern part of the city of Rostock (**Figure 1**). The 149 km long Warnow river exhibits a catchment area of 3,280 km^2 with a population density of 60 persons per km^2.

The following described MP sources within the Warnow estuary were located through GIS data (KOGGE et al., 2018; OpenDataHRO, 2019; Wasserbuch, 2019). Despite additional diffuse emissions, e.g., through fragmentation of macroplastics or diffuse aerial inputs, the majority of land-based MP emissions is assumed to be covered according to current knowledge (Galafassi et al., 2019).

In total around 232 point sources for MPs and AFPPs are located within the estuary. Besides the input of the catchment, 24 tributaries discharge into the estuary (**Figure 2**). Among the 167 identified wastewater outlets are the WWTP outlet, 11 combined sewer outlets and 155 stormwater (STW) outlets. Regularly used moorings and leisure boat facilities depict potential emission points for AFPP. The industrial harbor maintains five docks with around 41 moorings. Additionally, five local ferry moorings, four cruise ship moorings as well as fifteen leisure boat facilities are located within the estuary. Due to insufficient data three operating shipyards were neglected for AFPP emission estimates in the current study.

The complex characteristics of MP particles (size, forms, types), the high number of potential sources and spatio-temporal variability of emissions as well as laborious and time-consuming analytical methods currently prevent comprehensive *in-situ* data collections. To provide a comprehensive picture for the Warnow Estuary the additional use of statistical data, literature, and the transfer of knowledge from similar systems was utilized. The different approaches to assess the importance of MP sources and emissions within the estuary are described in the following.

Rostock Sewer System Microplastic Emissions

Wastewater treatment plant

A concentration of 245 (IQR = 913–78) MPs/m^3 (including MPs <100 µm) was applied corresponding to the median of values from WWTPs of various countries with tertiary treatment providing MP analysis for particles <100 µm (**Supplementary Information SI1**). Microplastic emissions were multiplied with monthly discharge data of the WWTP effluent from 2016 to 2018 which was provided by the local WWTP (Nordwasser GmbH).

Combined sewer overflow emissions

Currently, the CSOs are not measured since the discharges and concentrations have to be determined on a high temporal resolution or flow equivalent. Within the scope of this study, the discharge volume was therefore conceptually determined. Assuming that the spillway structures were dimensioned according to the chemical oxygen demand (COD) approach of the ATV-A 128 regulations (DWA, 1992) at the time, the annual

TABLE 1 | Runoff of the annual precipitation of the combined sewerage catchment area. Runoff coefficients (ψ_m), annual rainfall (r), and rainfall runoff ($Q_{R_{CS}}$).

Catchment class	Area [ha]	ψ_m	r [l/m²]	$Q_{R_{CS}}$ [m³*10³/a]
Residential areas	368	0.79	621	1,805
Traffic areas	264	0.86	621	1,410
Industrial areas	95	0.68	621	401
Unsealed areas	433	0.14	621	377
				Σ 3,993

discharge volumes can be calculated. The annual MP emission is in turn the product of the annual discharge volume and the MP concentration. For the calculation of the CSO discharge quantity (**Eq. 1**), the permissible overflow rate corresponding to the DWA 128 regulations (DWA, 1992) is assumed (**Eq. 2**).

$$Q_{\mathrm{CSO}} = e_0 \times Q_{R_{\mathrm{CS}}}, \quad (1)$$

where Q_{CSO} corresponds to the discharge of CSOs (m³/a), e_0 to the permissible overflow rate, and $Q_{R_{\mathrm{CS}}}$ to the rainfall runoff of the combined sewer (m³/a).

The permissible overflow rate in relation to the COD was calculated using **Eq. 2** (DWA, 2006). Since the city sewer system is in transition from a combined sewer system to a separated sewer system, the COD concentration of dry weather flow is high. To ensure that a critical COD of 178 mg/L is not exceeded a larger proportion of stormwater is mixed with the wastewater. Hence, the resulting average mixing ratio (m = 11.68:1) between rainwater and wastewater is quite high. Accordingly, the calculated overflow concentration of COD is 178 mg/L (**Supplementary Information SI2**). This results in a permissible overflow rate of 34%.

$$e_0 = \frac{c_R - c_{\mathrm{WWTP}}}{c_e - c_{\mathrm{WWTP}}} = \frac{107\mathrm{mg/L} - 70\mathrm{mg/L}}{178\mathrm{mg/L} - 70\mathrm{mg/L}} \times 100 = 34\%, \quad (2)$$

where c_R is the COD concentration in the storm runoff of the combined sewer (mg/l), c_{WWTP} the COD concentration of the wastewater treatment plant (WWTP) effluent (mg/l), and c_e the COD concentration of the CSOs effluent (mg/l).

The rainfall runoff $Q_{R_{\mathrm{CS}}}$ was calculated as a function of specific runoff coefficients (ψ_{m}), and area sizes. Runoff coefficients were taken from a long-term simulation study with the Environmental Protection Agency (EPA) Storm Water Management Model (Rossman, 2015) by the Department of Water Management, University of Rostock, Germany. Catchment classes were differentiated for residential areas, traffic areas, industrial areas, and unsealed areas (**Table 1**). The latter including green spaces as well as forests and agricultural and horticultural areas. Based on the total runoff volume of around four million cubic meters per year (**Table 1**), the annual discharge volume of the CSOs was derived using **Eq. 1**.

$$Q_{CSO} = 34\% \times 3,992,905\mathrm{m}^3/a = 1,357,588\mathrm{m}^3/a, \quad (3)$$

According to the average mixing ratio (m = 11.68:1), the annual rainfall discharge of the CSOs is 1,269,794 m³ and the annual discharge wastewater of the CSO is 107,065 m³. The MP quantity (c_{MP}) in **Table 2** was derived from the use-specific concentration (Liu et al., 2019) and outflow fraction which corresponds to the percentage share of the rainfall runoff (**Table 1**). For untreated wastewater the median value of 143 (IQR = 910–68) MPs/l was calculated from data of nine studies (**Supplementary Information SI1**). All considered studies included the analysis of particles <100 µm.

Stormwater emissions

Mean annual MP emissions by stormwater along 24 tributaries were estimated for the riverine inflows below the Mühlendamm weir (**Figure 2**). Sealed and drained areas $A_{E,k}$ within the catchments of tributaries were identified and classified into three land use types in GIS by a spatial intersection with a high-precision land use map. The annual stormwater runoff Q_R of each drained area was represented by the effective rainfall, which is the part of the precipitation that flows superficially to the storm sewer network or stream section. It was calculated based on runoff coefficients shown in **Table 1** (c.f. rational method, DWA, 2006) for each subarea and the long-term average annual rainfall r_a of 621 L/m² (DWD, 2020):

$$Q_R = A_{E,k} \times r_a \times \psi_m, \quad (4)$$

where $A_{E,k}$ corresponds to the drained area (m²), r_a to the mean annual rainfall (l/m²/a), and ψ_m to the mean annual runoff coefficient. Microplastic emissions B_{MP} were calculated for each drained area using **Eq. 5**:

$$B_{\mathrm{MP}} = c_{\mathrm{MP}} \times Q_R, \quad (5)$$

where Q_R is the stormwater runoff corresponding to the effective precipitation (l/a). Microplastic concentrations c_{MP} of stormwater runoff were derived as mean values from Liu et al. (2019) for each land use type: residential (0.90 MP/l), traffic (0.49 MP/l), and industrial areas (13.16 MP/l).

Estimated MP emissions were allocated to the nearest watercourse section by a spatial join in GIS (**Supplementary Information SI3**). River geometries were available as line sections of 50 m length from the project KOGGE (KOGGE et al., 2018). Each river section is labeled by a unique identification number, which is composed of the classification number and a station number according to the German "LAWA guideline for the labeling of rivers" (WASSER, 2005). The hierarchical structure of the classification number and station number from the estuary to the river head makes it possible to identify river sections located below or above each section. The accumulation of these emissions along the flow path is performed by *Python* scripts in GIS.

Spatial resolved MP emissions of stormwater outlets directly discharging into the estuary are currently not possible due to lacking information regarding the wastewater system (grey area **Figure 2**). Nevertheless, similar calculations of MP runoff, based on available information on the share of industrial (5.3 km²), residential (3.7 km²), and traffic (2.4 km²) areas can be made based on **Eqs. 4, 5**.

River Catchment Microplastic Emissions

The number of MP particles released from the catchment into the estuary was taken from eight *in-situ* collected water surface samples from the Warnow river close to Kessin (N54°03′51.13,

TABLE 2 | Microplastic (MP) emission (B_{MP}) due to combined sewer overflows separated according to the proportion of waste- and rainwater. The outflow fraction corresponds to the percentage share of the rainfall runoff ($Q_{R_{CS}}$) of a catchment class from the total rainfall runoff ($Q_{R_{CS}}$) from **Table 1**. Microplastic concentrations (c_{MP}) for storm- (STW) and wastewater were obtained from the literature (**Supplementary Information SI1**).

Type	Catchment class	Outflow fraction (%)	Overflow [m³/a]	c_{MP} [MPs/l]	B_{MP} [MPs*10⁶/a]
STW	Residential areas	45	574,131	0.9	517
	Traffic areas	35	448,372	0.49	220
	Industrial areas	10	127,576	13.16	1,679
	Unsealed areas	9	119,716	—	—
Sum STW			1,269,794		2,415
Wastewater			107,065	143	15,310
					Σ 17,725

E12°10′15.60), about 3 km upstream the weir, during September and October 2018 and May to March 2019. Sampling was conducted using an encapsulated flow through filtration system as described by Lenz and Labrenz, (2018) with sample volumes between 150 and 600 L. The device was equipped with stainless steel filter cartridges (nominal 10 µm mesh size) in an enclosed setup. The sampling inlet was placed to sample the upper 10 cm of the water column facing the incoming flow. The individual sample volumes and dates can be found in the **Supplementary Table SI4**.

The sample material was further processed in a MP-work adapted laboratory according to Enders et al. (2020). All steps involving exposed sample material were conducted inside a laminar flow bench (S2020 1.8, Thermo Scientific). All chemicals and rinsing water used were filtered through muffled 1.5 µm glass fiber filters (Whatman 934-AH) in a MP-free environment. First, the sample material was recovered from the filter cartridges by soaking in a 15% H_2O_2 solution for 48 h with subsequent rinsing off the particulate matter into ceramic bowls. From there the decision tree proposed by Enders et al. (2020) was followed applying protocol module m1 (freeze drying), m4 (30% H_2O_2 digestion over 24 h), and m5 (simple density separation). In a final vacuum filtration on 10 µm stainless steel meshes the samples were thoroughly rinsed using MP-free ultrapurified water to wash out remaining solutes.

The samples were transferred from the 10 µm stainless steel meshes to 50 ml Erlenmeyer flasks and sent to the IPF Dresden for microspectroscopic analysis. For that purpose, the particle suspensions were filtrated onto 10 × 10 mm silicon filters (Käppler et al., 2015) for the following Raman analysis. The filtration took place in a particle-depleted laboratory under a laminar flow bench using a custom-made glass filtration device with PTFE adapters to host the silicon filters (Brandt et al., 2020). The silicon filters had a pore size of 50 µm with a pitch of 100 µm. The number, type, and color of the MP particles >50 µm of a filtrated sample were determined with a combination of optical particle detection and Raman microspectroscopy using the software GEPARD as described in Brandt et al., 2020.

Microplastic abundances in samples were corrected by MP abundances detected in laboratory and process blanks. Therefore, the mean MP number for each size and polymer type class was calculated and subtracted according to the size and polymer type class from each sample (**Supplementary Information SI4**). The MP data from the two different seasons (spring/autumn) were pooled for calculation of mean annual MP emissions from the catchment. Therefore, measured MP concentrations (C) were plotted against the river discharge (Q) measurements from the sampling day and a linear regression model was fitted to the data (in the following C-Q model; **Supplementary Information SI5**). Subsequently, the C-Q relationship was used to calculate annual MP emissions based on daily discharge data (m^3 per second) from the closest gauging station Rostock/Geinitzbrücke (N54°04′41.17, E12°09′15.16) for the years 2016–2018 (data provided by Staatliches Amt für Landwirtschaft und Umwelt Mittleres Mecklenburg 2019) based on **Eq. 6** (**Supplementary Information SI5**):

$$C = 132.41 + 18.62 \times Q, \quad (6)$$

where C corresponds to the MP concentration (MPs/day) and Q corresponds to the river discharge (m^3/s).

Anti-fouling Paint Particle Emissions

As another potentially significant MP source within urbanized estuaries we assessed anti-fouling paint particle (AFPP) emissions from leisure and commercial shipping activities (**Supplementary Information SI6**). For the leisure boat facility scenario AFPP release from the underwater ship hull of leisure boats were considered. Thereby, 65% of permanent leisure boats (PLANCO, 2004), which are assumed to be at berth for 50% of the time during the whole season (April-October), were considered. Number of berths within leisure boat facilities were obtained from the city of Rostock (OpenDataHRO). Utilizing emission scenarios for active ingredients from AFPPs it is assumed that 2.5 L of anti-fouling paint is applied per leisure boat and year by do-it-yourself maintenance work (OECD, 2005).

To convert paint volume applications to particle numbers a polymer content of 30% was assumed (Watermann and Eklund, 2019). As size distributions of AFPP particles detected in environmental samples are lacking, a basic emission scenario with an idealized AFP particle was applied to get a first impression on spatio-temporal emission patterns within the estuary. Therefore, MP spheres with a density of 1.6 g/cm³ (Daehne et al., 2017; Enders et al., 2019) and a diameter of 0.5 mm were used for conversion.

Generally, three AFPP emission scenarios were differentiated: emissions during in-service use (ISU), from high-pressure

washing (HPW), and from maintenance and repair work (MR). Emissions during ISU were set to 1% of paint applied (OECD, 2009) of which 50% were assumed to be released while the boats are moored at berth. For the HPW and MR scenario particle emissions were assumed to be equally distributed to soil and water, resulting in a fraction of 0.5 being discharged to the water. At the end of the season in November boats are taken out of the water and often cleaned by HPW where a removal factor of 0.2 of AFPPs was set (OECD, 2005). Only leisure sport facilities offering a slipway were considered for AFPP release through HPW. For MR work during December till March a removal factor of 0.3 and an emission factor of paint application of 0.0125 was adapted (OECD, 2005). Only facilities that store boats in proximity to the water (identified through satellite images) were considered for MR particle emissions.

Oversea ferries, cruise ships, RoRo (Roll-on Roll-off), tanker, and cargo ships were considered for the AFPP emissions during ISU from commercial shipping. A conservative theoretical coverage of 13 m^2/L of AFP was applied. To transfer the AFPP emissions of 1% during ISU to emissions within the estuary, average wetted surface area of different ship types (Miller et al., 2018), data on yearly inruns, and average time at berth for different ship categories (Lorentz and Moldsenhauer, 2014) were utilized (see **Supplementary Information SI6** for calculation).

Comparison of Emission Estimates and Potential Microplastic Discharge to the Baltic Sea

For MP emission estimates of the city sewer system (WWTP, CSO, and STW), particle size was considered as important parameter. We only considered data from studies including the analysis of MPs <100 µm, as MP particle number increases rapidly with decreasing particle size. The MP concentration for raw wastewater and WWTP effluent was obtained as median from several studies, whereas for STW emissions only one study transferable to our system was available to the best of our knowledge (Liu et al., 2019).

The analysis of *in-situ* obtained MP data for the Warnow river did not include MPs between 10 and 50 µm. As fragmentation of MP particles causes the generation of continually smaller MPs, they are expected to follow a power law particle distribution (Kooi et al., 2019). Thus, MP counts from *in-situ* river samples were grouped into size bins of 10 µm and a power law model fitted to the data (**Supplementary Information SI7**). The obtained coefficients (a = 9.231, b = −1.293) were used to predict MP abundance down to 10 µm. Our calculated annual MP emissions by the C-Q model was concurrently corrected by the relative share of 91% of the size class 10–50 µm.

A comparison with AFPP emissions was not considered due to the different data basis, utilizing sales volume of AFP, expert knowledge, and an idealized AFP particle for emission estimates.

To further estimate MP discharge to the Baltic Sea the following considerations and assumptions on MP density, and thus sinking behavior, were made. Microplastic data from *in-situ* measurements and the literature were grouped into two density classes. Low density (LD) MPs with a density <1.0 g/cm^3 included polymers such as polyethylene (PE) and polypropylene (PP). The high density (HD) class, with a density >1.0 g/cm^3, contained polymers such as polyethylene terephthalate (PET), polyvinylchloride (PVC), polyamide etc (**Supplementary Information SI4**).

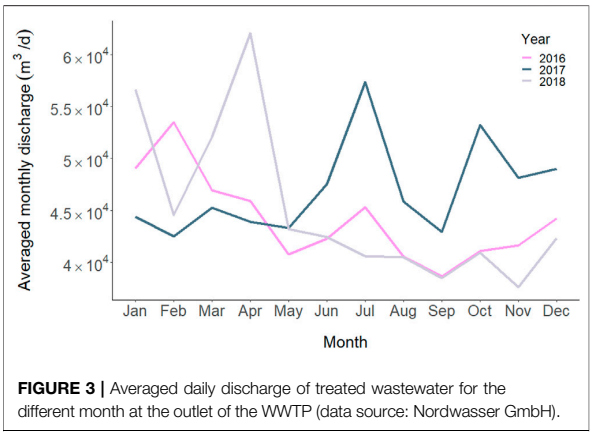


FIGURE 3 | Averaged daily discharge of treated wastewater for the different month at the outlet of the WWTP (data source: Nordwasser GmbH).

For high density AFPPs an accumulation close to their source could be shown for the Warnow estuary (Enders et al., 2019) and hence their retention within the estuary is very likely. In addition, HD-MPs with a higher density than seawater (1.025 g/cm^3) were assumed to sink as processes, such as biofouling or agglomeration (Rummel et al., 2017; Michels et al., 2018), increase MP density and thus the probability of MPs sinking to the riverbed. Besides, for MPs between 1–200 µm retention is reported to strongly increase with density (Besseling et al., 2017).

To provide a conservative estimate on annual MP emissions to the Baltic Sea retention of buoyant LD-MPs was additionally considered. Due to the complex hydrodynamic behavior of the weakly tidal Warnow estuary, measuring discharge and assessing water retention time is difficult. For the saltwater influenced Warnow estuary Rönspieß et al. (2020) reported a retention capacity for particulate phosphorus. Similar calculations for suspended particulate matter (SPM) from the supplementary information of this study (see Suppl. 9_Balance calculations of Rönspieß et al., 2020) results in a retention capacity of 31% for SPM respectively. This retention capacity was further assumed for LD-MPs.

RESULTS

Rostock City Sewer System Microplastic Emissions

On average an annual emission of about 4.1 billion MPs was calculated for the WWTP outlet based on the monthly discharge data of the years 2016–2018 (monthly mean emission of about 11 million MPs).

Similar to the discharge of the catchment, at the WWTP lowest and highest average daily discharge of treated wastewater,

TABLE 3 | Microplastic (MP) emission (B_{MP}) due to stormwater runoff separated according to the catchment class. Accumulated results for the catchment area of the tributaries as well as areas connected to stormwater outlets (grey area **Figure 2**) are shown. Microplastic concentrations (c_{MP}) were obtained from Liu et al. (2019). Runoff coefficients (ψm), annual rainfall (r), and rainfall runoff (Q_R).

Catchment class	Area [ha]	ψ_m	r [l/m^2]	Q_R [m^3*10^3/a]	c_{MP} [MPs/l]	B_{MP} [MPs*10^6/a]
Residential areas	2,510	0.79	621	12,314	0.9	11,082
Traffic areas	2,090	0.86	621	11,162	0.49	5,469
Industrial areas	1,960	0.68	621	8,277	13.16	108,921
Unsealed areas	10,420	0.14	621	9,059	—	—
						Σ 125,477

and thus MP emissions, were calculated for 2018 in November and April respectively (**Figure 3**).

Besides emissions from the WWTP, the rainwater from the combined sewer system pollutes the receiving water with around 2.4 billion particles per year, while around 15.3 billion particles per year are carried into the watercourse by the wastewater (**Table 2**). The total input of the combined sewer system is thus 17.7 billion particles per year.

Based on **Eq. 4** an annual total stormwater runoff of about 41 million m^3/a was calculated (**Table 3**). The 24 tributaries contribute to an additional 91 billion MP particles per year due to runoff from industrial (14.3 km^2), residential (21.4 km^2), and traffic areas (18.5 km^2). The individual contributions of the tributaries range from 1.6 million to 23 billion MPs per year at their mouth into the estuary (white points in **Figure 2**). Around 15% are released close to the weir, 32% at the western and 53% at the eastern sides of the estuary. As industrial areas are supposed to deliver high MP inputs per area according to Liu et al. (2019), especially the eastern tributaries account for high MP emissions in the estimation.

In addition, 34.5 billion MP particles are potentially being directly discharged (grey area **Figure 2**) into the estuary through several stormwater outlets. From the resulting total annual emissions of 125.5 billion MPs, 73% are thus released by the tributaries and 27% through stormwater outlets distributed along the estuary.

River Catchment Microplastic Emissions

For the Warnow river, MP concentrations from 57 to 388 particles/m^3 with a mean of 226.79 ± 119.39 and a median of 281 (IQR: 297–113) particles/m^3 (size range 0.05–5 mm) were measured. Considering the size classes in MP river samples, more than 90% of MPs were <300 µm within the first sampling campaign in autumn 2018. In the second sampling campaign 63% of detected MPs exhibited sizes <300 µm and 30% were between 300–1,000 µm (**Supplementary Information SI4**). Polyolefins (PE and PP) dominated among detected polymer types (72%), followed by polystyrene (13%). Polyethylene terephthalate (8%), polyoxymethylene (4%) and silicone (2%) had a minor share and polymethyl methacrylate and PVC contributed with less than 1% among detected polymer types (**Supplementary Information SI4**).

Applying the C-Q model to daily discharge data for the years 2016–2018, average annual MP emission account for about 13 billion MPs with a daily average of about 36 million MPs being released into the estuary (**Supplementary Information SI5**). Highest average river discharge, and thus calculated MP emissions, was observed in 2017 (18.3 ± 8.4 m^3/s), with high amounts of MPs being released during summer and October till December (**Figure 4**). In the years 2016 and 2018 monthly river discharge follows the generally observed pattern for the Warnow river (Pegelportal, 2020) with accordingly highest MP emissions calculated for January and February, thereafter decreasing until summer and starting to increase in autumn (**Figure 4**).

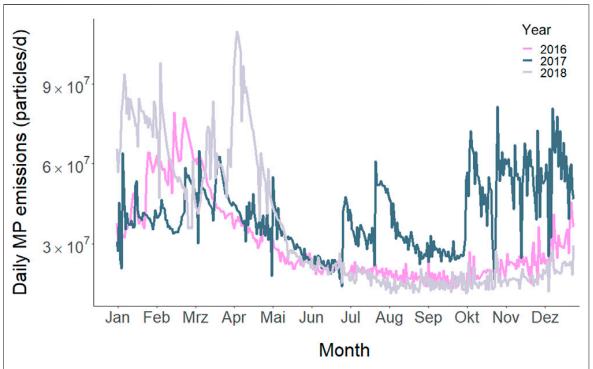


FIGURE 4 | Daily microplastic (MP) emissions by the Warnow river into the estuary calculated based on a linear relationship (F = 11.04, adj. R^2 = 0.6, p = 0.016; y = 132.41 + 18.62*x) of measured MP abundances in water surface (n = 8) and river discharge (data provided by Staatliches Amt für Landwirtschaft und Umwelt Mittleres Mecklenburg 2019).

Anti-fouling Paint Particle Emissions

For the considered 15 leisure boat facilities we estimated an annual emission of about 370 million AFPPs due to ISU, HPW, and MR. Thereof, 3% were released by presumably 1,625 permanent boats due to ISU during April and September. The majority was released by HPW after the season in November (1,274 boats) and due to MR work from November to March (50 and 47% respectively). Thus, areas where HPW is conducted depict potential spatio-temporal hotspots of AFPP release. Based on our assumptions there were no large differences between western and eastern sites of the estuary considering total AFPP emissions (42 and 58% of AFPP emissions; **Supplementary Information SI6**).

Applying the basic emission scenario for AFPP release during ISU from commercial shipping an annual emission of 4.4 billion AFPPs was estimated. Thereof, around 43 and 40% were released

TABLE 4 | Annual microplastic (MP) emissions and percentage share of different sources and density classes. STW: stormwater, CSO: combined sewer overflows, WWTP: wastewater treatment plant, LD: low density MPs (<1.0 g/cm^3), HD: high density MPs (>1 g/cm^3).

Source	Mean		LD		HD	
	[MPs*10^6/a]	[%]	[MPs*10^6/a]	[%]	[MPs*10^6/a]	[%]
Catchment (corrected)	143,965	49.4	103,655	47.2	40,310	56.3
STW	125,500	43.1	101,655	46.3	23,845	33.3
CSO	17,725	6.1	13,471	6.1	4,254	5.9
WWTP	4,064	1.4	935	0.4	3,130	4.4
Σ	291,254	100	219,716	100	71,539	100

TABLE 5 | Descriptive statistics for microplastic concentrations utilized for emission estimates. Data was obtained from the literature for wastewater treatment plant (WWTP) influents, effluents, and stormwater (STW). Microplastic concentration per m^3. IQR: interquartile range, MAD: median absolute deviation, CV_M: coefficient of variability for median. n: number of microplastic measurements.

	WWTP influent (n = 41)	WWTP effluent (n = 10)	STW (n = 7)	Warnow river (n = 8)
Min	1,440	6	490	57
Max	18,285,000	19,000	22,894	388
Median	143,330	245	1,409	281
MAD	192,204	228	1,363	92
CV_M	134	93	97	33

by tanker and cargo ships, 8% by ferries, and 6% by RoRo ships at the industrial port within the area of Breitling. Another 3% of AFPP emissions were released by cruise ships close to Warnemünde. Besides cruise ships, where the peak season is between May and September, a constant release of AFPPs can be assumed during the whole year for all other commercial ship types. For all scenarios it should be kept in mind that results are based on our assumptions and that the applied emission scenarios were calculated for idealized spherical AFPPs of 0.5 mm diameter (density 1.6 g/cm^3).

Comparison of Emission Estimates and Potential Discharge to the Baltic Sea

A total discharge of about 291 billion MPs were estimated to enter the Warnow estuary annually. Thereof about 1.4% are emitted by the WWTP, 6.1% due to CSO emissions, 49.4% by the catchment of the Warnow river, and 43.1% due to stormwater discharges within the city area (**Table 4**).

Microplastic concentrations of WWTP influents (influencing CSO emission estimates), effluents and within STW, obtained as median value considering several studies, show highest variability from 93 to 134% respectively. Microplastic concentrations for the Warnow river catchment, exhibit considerably lower variability (CV_M: 33%; **Table 5**).

Microplastics detected in the Warnow river samples were comprised of 72% LD and 28% HD polymers, with only small differences between sampling campaigns (**Supplementary Information SI4**). Low density polymers are also dominating in MP reports of stormwater runoff and combined sewer overflows. For stormwater runoff LD and HD polymers contribute to 81 and 19% respectively (Liu et al., 2019). Considering the mixing ratio of 11.68:1 for storm- and raw wastewater of the combined sewer system, a share of 76% for LD and 24% for HD polymers was calculated for CSO emissions (**Supplementary Information SI1**). For the MP composition within the effluent at the WWTP a detailed report on a plant with a tertiary treatment in Germany was utilized (Mintenig et al., 2014). Here a higher share of HD polymers (about 77%) was reported, which is in concordance with other reports (Sun et al., 2019).

In total, 75% of MPs released to the estuary belong to the class of LD-MPs and 25% to the class of HD-MPs (**Table 4**). Under the assumption that HD-MPs and 31% of LD-MPs are retained within the estuary (see *Materials and Methods* 2.5), about 152 billion MPs would be released into the Baltic Sea annually.

DISCUSSION

Microplastic Emission Estimates Into the Estuary

Considering all limitations of our emission scenarios, about 291 billion MPs potentially enter the estuary annually. Thereby, the outlet of the WWTP has the lowest percentage of MP emissions (1.4%, **Table 4**), which is in line with previous studies (Simon et al., 2018; Conley et al., 2019). Calculated MP emissions due to CSOs (6.1%) are about five times higher and stormwater runoff from the city area of Rostock exhibits the highest percentage (43.1%) among sewer system emissions. The higher the retention of a compound within a WWTP, the more relevant are discharges due to CSOs and stormwater (Bollmann et al., 2019), which is in line for MPs with a retention by up to 99.9% for plants with tertiary treatment (Prata, 2018). A general seasonal pattern of MP emissions by WWTP outlets could not be detected by a comprehensive study of Conley et al. (2019). Instead, MP concentrations in effluents were found to vary by a factor of 4.8 over the course of the year. In our scenarios MP discharge by stormwater runoff and CSOs is related to precipitation and as a result MP emission for the Warnow estuary would be highest during summer month (**Supplementary Information SI8**). For stormwater runoff and CSOs other factors than precipitation could likewise influence temporal MP emissions. For example, precipitation pattern as well as deposition time before runoff will influence MP runoff from a surface to discharging natural and culture-technical waterways. Besides, particle retention within waterways will differ, which was not accounted for. In our scenarios data from one study reporting MP emissions separated by different land use categories (Liu et al., 2019) was used for MP emissions by stormwater runoff. Here MP emissions per area within the land use categories can vary over time and region. Our utilized MP values are rather conservative, considering reports of on average 7,713 to 111,000 MP/m^3 (>20 µm) in stormwater (Bondelind et al., 2020). Further, tire and road wear particles which can exhibit a significant share were

TABLE 6 | Parameters for microplastic (MP) emission scenarios for the sewer system. WWTP: wastewater treatment plant, CSO: combined sewer overflow, STW: stormwater, WW: wastewater, TRWP: tire and road wear particles. Data sources for utilized MP concentrations are provided within **Supplementary Table SI1**).

Microplastic emission scenario Parameter	Variable	Value Warnow estuary	Unit
Area city		181.4	km^2
Population density city		1,151	Person/km^2
WWTP emissions [MPs/a]			
= annual processed WW [m^3/a] * MPs [MPs/m^3]			
Annual processed WW		16,588,932	m^3/a
MP concentration effluent		245	MPs/m^3
STW emissions [MPs/a]			
= rainfall runoff [l/a] * MPs [MPs/l]			
rainfall runoff [l/a] = drained area [m^2] * mean annual precipitation [l/m^2/a] * runoff coefficient			
Drained area	Traffic area	20.9	km^2
	Industrial area	19.6	km^2
	Residential area	25.1	km^2
	Unsealed area	104.2	km^2
Mean annual precipitation		621	l/m^2
Runoff coefficient	Traffic area	0.86	
	Industrial area	0.68	
	Residential area	0.79	
	Unsealed area	0.14	
MP concentration (*TRWPs not included*)	Traffic area	494	MPs/m^3
	Industrial area	13,164	MPs/m^3
	Residential area	898	MPs/m^3
CSO Emissions [MPs/a]			
= discharge raw WW [m^3/a] * MPs in raw WW [MPs/m^3]			
+ ∑(area specific overflow [m^3/a] * area specific MPs [MPs/m^3])			
discharge raw WW = discharge CSO [m^3/a] * 1/12			
discharge STW = discharge CSO [m^3/a] * 11/12			
discharge CSO [m^3/a] = permissible overflow rate [%] * rainfall runoff [m^3/a]			
area specific overflow [m^3/a] = % share of discharge STW			
Permissiable overflow rate		34	%
Drained area	Traffic area	2.6	km^2
	Industrial area	1.0	km^2
	Residential area	3.7	km^2
	Unsealed area	4.3	km^2
Mixing ratio STW: Raw WW		11.68:1	
MP concentration raw WW		143,000	MPs/m^3

not included in the study by Liu et al. (2019) and are accordingly not represented by our results. When comparing MP emissions among sources the general high variability of MP concentrations has to be taken into account. In our scenarios utilized MP concentrations for raw wastewater (influencing CSO emission estimates) and WWTP effluent were highly variable ($CV_{M:}$ 134 and 93%) (**Table 5**). But even an increase of 93% of MP emissions for WWTP effluents and 134% for raw wastewater would not notably change the high share of stormwater and river catchment emissions which would still contribute with about 40 and 45% respectively.

Another relevant share of MP is very likely emitted by the catchment of the Warnow river (49.4%; **Table 4**) which discharges about 95% of river water into the estuary (Bachor 2005). The Warnow river discharge varied about 78% within the considered three years with a recorded minimum and maximum values of 0.03 and 60.97 m^3/s respectively. Our *in-situ* measurements only covered river discharge values up to about 15 m^3/s (**Supplementary Information SI5**). Due to high variability of MP concentrations for low flow conditions and a small number of measurements the C-Q relationship is not very robust and needs further validation. But in contrast to precipitation patterns in the city and thus MP discharge through stormwater runoff, highest mean annual discharge of the Warnow river is occurring during winter month (Pegelportal, 2020). An accordingly assumed higher probability of MP emissions agrees with predicted peak MP emissions for the northern hemisphere between January and April (Lebreton et al., 2017).

While our AFPP emission estimates are associated with highest uncertainty and provide qualitative rather than comparable quantitative information, they indicate the importance of this source for the estuary. In-service use (ISU) emissions by commercial shipping for example would result in an annual release of about 4.4 billion AFPPs. Total emissions of AFPP by leisure boats add to another 370 million AFPP according to our scenarios, which represent conservative estimates. Here it needs to be considered that the applied removal and emission factors for AFPPs were provided by experts over a decade ago and that their present-day validity needs further investigation. For comparison, an additional scenario was calculated based on the annual sales

volume of AFP of 794 tons for leisure boats in Germany (and an emission factor of 50% during ISU (Daehne et al., 2017)). Considering the share of berth in the Warnow estuary of 0.79% and transferring this number to our scenario this would amount to about 3.7 billion AFPPs per year (**Supplementary Information SI6**). The example shows the high uncertainties associated with different assumptions. It should further be noted that a single estimate on plastic polymer content of a typical AFPP was used. Common commercial and leisure boat antifouling paint systems span a wide range of compositions, including several polymers in varying amounts as well as non-polymer-based matrices. Nevertheless, our estimates are again conservative considering the applied relatively large particle diameter of 0.5 mm. For example, if adjusting particle diameter to 0.1 mm the total release of AFPPs drastically increases to about 594 billion AFPPs per year. Although our AFPP emission scenarios only provide a very rough first estimation of this source, they are likewise able to provide spatial information on AFPP emissions (**Supplementary Figure SI6**).

Retention of Microplastics and Emission Potential to the Baltic Sea

According to our assumptions an estimated 152 to 291 billion MPs larger than 10 µm (majority <100 µm) are annually discharged from the Warnow estuary to the Baltic Sea.

Currently there is only limited information on MP retention within rivers and no comparable data for estuarine systems to the best of our knowledge. Besides particle characteristics (density, shape, size) and processes altering particle density (Rummel et al., 2017; Michels et al., 2018), the hydrology, morphology, and management of the estuary are important factors for MP retention.

For our study system there are several factors promoting the retention of MPs within the estuary. Deposited and/or sinking polymers are subjected to a predominating upward transport with higher saline bottom water under the general estuarine circulation pattern (Lange et al., 2020). Further river transport inland is prevented by a weir and in the city area close to the weir deposition of particles is promoted by decreased flow velocities (Rönspieß et al., 2020). In addition, floating MPs can be trapped within reed belts or retained due to deposition at riverbanks within the estuary. On the other hand, it has been reported that high amounts of MPs can be mobilized during storm events (Hurley et al., 2018; Hitchcock, 2020). Nevertheless, frequent dredging activities within the estuary to sustain the depth of shipping channels further indicate a net accumulation of particulate matter within the estuary.

Although there is a high probability that the HD-MPs and part of the LD-MPs are retained within the estuary, MPs <10 µm are currently not considered which would additionally contribute to MP emission numbers. Moreover, diffuse emission through for example aerial inputs or fragmentation of macroplastic were not accounted for within the current MP emission scenarios. Thus, the calculated 152 to 291 billion MPs entering the Baltic Sea annually provide a first reasonable estimate.

Besides, comparing our predicted MP emission estimates to the Baltic Sea with literature data yields a rather conservative estimate. For example, Zhao et al. (2019) estimated an annual discharge of 16–20 trillion MPs (>60 µm) from the Changjiang estuary to the ocean. Another study measuring a comparable size class of MPs (>20 µm) in the Nakdong River in South Korea report an annual discharge of 5.4–11 trillion MPs to the ocean (Eo et al., 2019). Dividing the values by the population of the Nakdong catchment results in an emission of 0.5–1.1 million MPs per capita per year which is in a comparable order of magnitude as compared to our calculation (388–746 thousand MPs per capita per year).

Practical Implications of Applied Emission Scenarios

To estimate and compare sewer system related MP emissions from the city area information on land use categories of the drained area in combination with corresponding runoff coefficients, MP concentrations, and amount of precipitation were combined (**Table 6**). With the applied routing-method (**Supplementary Information SI3**) spatially differentiated MP emission estimates by stormwater could be provided. The approach is transferable to other areas, provided that a coherent, hierarchical network of watercourses with associated subcatchments is available.

Generally, precipitation seems to be a suitable proxy for temporal emissions of MPs from impervious surfaces. This is supported by a recent study, reporting a positive relationship between MP concentrations in an estuary and the average rainfall across previous five days (Hitchcock, 2020). For MP emission estimates through CSOs a permissible overflow rate was calculated based on German water management guidelines. In combination with the mixing ratio of discharged stormwater and raw wastewater (mixing ratio 11.68:1) comparable MP emissions could be calculated. Baresel and Olshammar (2019) calculated annual CSO by assuming a fraction of 1.5% of total WWTP inflows and assessed MP emissions by WWTPs and different CSO types. Results showed that weather induced CSO contributed to at least 18% to >50% of MP emissions to the Baltic Sea. Transferring this approach to the sewer system in Rostock would result in about two times higher annual inputs (37 billion MPs per year). In a study additionally considering stormwater MP emissions into the Baltic Sea, CSO emissions had the lowest contribution of MP discharge (Bollmann et al., 2019). And in contrast to our results, high amounts of MP were emitted by treated wastewater (WWTPs). The assumed high amount of treated wastewater discharge (about four times higher than untreated stormwater discharge) and a lower runoff coefficient for impervious surfaces by Bollmann et al. (2019) can explain the discrepancy. Stormwater discharge was about 2.5 times higher than processed wastewater discharge in our study. Moreover, area-specific runoff coefficients were utilized (**Table 6**) which is, considering potential local adaptions, recommended for future studies. Microplastic emissions are

generally controlled by anthropogenic activities (Zhao et al., 2020). As those activities differ among land use, MP emissions should further be differentiated according to specific land use categories. The relevance of unsealed areas is still uncertain and despite the low runoff coefficient, meaning lower MP discharge, those areas contribute to the highest share, (e.g. ~60% in the city area). However, for forst and agricultural soil a higher storage capacity as compared to urban soils has been postulated (Nizzetto et al., 2016) which needs further validation.

For the city area the calculated load of MPs per area would amount to about two billion MPs/km^2/a accounting for traffic, industrial, and residential areas. For the Warnow catchment 3% (98 km^2) of land use is urban area (Bauwe et al., 2019). Assuming a comparable share of catchment classes and population density this would amount to a calculated MP emission of about 200 billion MPs/a. At the weir MP concentration of about 144 billion MPs/a were estimated which is 28% less. This approximation is indeed very rough. But with knowledge on the share of catchment classes of urban areas and more robust data on MP concentration within the according runoff one could approximate retention within rivers.

To estimate river (micro) plastic emissions often mean or median (micro)plastic concentrations in conjunction with mean river discharge have been used (Lebreton et al., 2017; Atwood et al., 2019; Schöneich-Argent et al., 2020). Increased emissions of MPs with increased river discharge has been reported (Wagner et al., 2019) and for the rural Warnow river catchment we observed a significant linear C-Q relationship ($p < 0.05$). Opposed to our results, a C-Q relationship for the rural subcatchment in the study of Wagner et al. (2019) was not detected. The different results can be explained by different MP sampling and analysis techniques which were confined to three polymer types and a lower size limit of 0.5 mm (Wagner et al., 2019). Besides, varying characteristics of rivers and their catchment areas could lead to different results and thus, it needs further investigations on the transferability of C-Q relationships to other systems. A semi-log regression model exhibited a similar model fit (**Supplementary Information SI5**) but additional data covering a wider range of river discharge values would be needed to precisely describe the relationship between MP concentration and river discharge. An exponential or logarithmic increase of MP concentrations with river discharge seems likewise plausible. Higher flow velocities caused by higher discharge or floods can lead to a remobilization of MP within riverbed sediments (Hurley et al., 2018). In addition, increased flow velocities and water levels within a river course can result in remobilization of plastic litter from riverbanks (van Emmerik et al., 2019). High precipitation and following increased runoff from impervious surfaces of urban areas as well as additional wastewater discharges contribute to an increased MP emission into river systems. Yet, our approach accounts for the uncertainty of the Warnow river discharge which was highly variable among month (highest variability in 2018 from 82% in October to 12% in January). Nevertheless, to obtain information on temporal MP emission patterns we support previous suggestions by Wagner et al. (2019) to establish C-Q relationships as proxy to estimate river catchment plastic emissions. Thereby the whole size fraction of MPs as well as a broad range of discharge conditions should be covered.

Finally, combining information from our emission scenarios three potentially high influenced areas by MP emissions could be identified within the estuary (I) the area behind the weir due to emissions from the catchment and loadings of stormwater runoff from large industrial areas (~18% of emissions from all tributaries) (II) the recreational city harbor receiving MPs from the CSO outlets and potential high inputs of AFPPs through several large leisure boat facilities, and (III) the area of Breitling within the northeastern part of the estuary due to high inputs of stormwater (~51% of emissions from all tributaries) and potential MP emissions from the area of the industrial harbor as well as AFPP emissions from the high share of commercial shipping activities in this area (**Figure 1**).

CONCLUSION

Based on our combined approach major MP emissions into the Warnow estuary occur in the following order: stormwater and river catchment > CSO > WWTP. Keeping in mind differences among emission scenarios it still can be assumed that MP emissions by the city sewer system are likely as important as accumulated MP emissions by the catchment of the Warnow river. Furthermore, increased MP emissions from the river catchment probably occur during winter driven by higher water discharge, whereas higher MP emissions from the city sewer system are expected through higher precipitation during summer. Calculated annual MP discharges to the Baltic Sea ranged between 152 and 291 billion MPs whereas most uncertainty results from catchment emission scenarios as well as retention of MP particles within the estuary. A comparison of our MP emission estimates from the city sewer system with existing studies highlights the necessity to consider all components of a sewer system to gain a comprehensive knowledge on the importance of various MP sources and pathways.

DATA AVAILABILITY STATEMENT

The original contributions presented in the study are included in the article/**Supplementary Material**, further inquiries can be directed to the corresponding author.

AUTHOR CONTRIBUTIONS

SP and GS prepared the concept of the paper. All authors made substantial, direct, and intellectual contribution to the work and approved it for publication.

FUNDING

This research was funded by the German Federal Ministry of Education and Research (BMBF) project MicroCatch_Balt (03F0788A), and the BONUS MICROPOLL project supported by BONUS (Art 185), funded jointly by the European Union and BMBF (03F0775A).

ACKNOWLEDGMENTS

We like to thank Jens Tränckner and Kristina Enders for constructive discussions and comments on the manuscript as well as Anne Oelschner (Stalu-MM), Henri Hoche and Holger Stählke (Nordwasser GmbH), Ulrike Leppin, Ricarda Neumann, and Michael Jeschke (port authority) for providing data and information. Further we would like to thank the reviewers, helping to improve the quality of the manuscript through constructive comments and criticism.

SUPPLEMENTARY MATERIAL

The Supplementary Material for this article can be found online at: https://www.frontiersin.org/articles/10.3389/fenvs.2021.616765/full#supplementary-material.

REFERENCES

Atwood, E. C., Falcieri, F. M., Piehl, S., Bochow, M., Matthies, M., Franke, J., et al. (2019). Coastal accumulation of microplastic particles emitted from the Po River, Northern Italy: comparing remote sensing and hydrodynamic modelling with *in situ* sample collections. *Mar. Pollut. Bull.* 138, 561–574. doi:10.1016/j.marpolbul.2018.11.045

Bachor, A. (2005). *Nährstoff- und Schwermetallbilanzen der Küstengewässer Mecklenburg-Vorpommerns unter besonderer Berücksichtigung ihrer Sedimente*. Greifswald: Landesamtes fur Umwelt Naturschutz und Geologie Mecklenburg-Vorpommern, 235.

Baresel, C., and Olshammar, M. (2019). On the importance of sanitary sewer overflow on the total discharge of microplastics from sewage water. *J. Environ. Prot.* 10, 1105–1118. doi:10.4236/jep.2019.109065

Bauwe, A., Eckhardt, K.-U., and Lennartz, B. (2019). Predicting dissolved reactive phosphorus in tile-drained catchments using a modified SWAT model. *Ecohydrology and Hydrobiology* 19, 198–209. doi:10.1016/j.ecohyd.2019.03.003

Bellasi, A., Binda, G., Pozzi, A., Galafassi, S., Volta, P., and Bettinetti, R. (2020). Microplastic contamination in freshwater environments: a review, focusing on interactions with sediments and benthic organisms. *Environments* 7, 30. doi:10.3390/environments7040030

Besseling, E., Quik, J. T., Sun, M., and Koelmans, A. A. (2017). Fate of nano- and microplastic in freshwater systems: a modeling study. *Environ. Pollut.* 220, 540–548. doi:10.1016/j.envpol.2016.10.001

Bollmann, U. E., Simon, M., Vollertsen, J., and Bester, K. (2019). Assessment of input of organic micropollutants and microplastics into the Baltic Sea by urban waters. *Mar. Pollut. Bull.* 148, 149–155. doi:10.1016/j.marpolbul.2019.07.014

Bondelind, M., Sokolova, E., Nguyen, A., Karlsson, D., Karlsson, A., and Björklund, K. (2020). Hydrodynamic modelling of traffic-related microplastics discharged with stormwater into the Göta River in Sweden. *Environ. Sci. Pollut. Res. Int.* 27, 24218–24230. doi:10.1007/s11356-020-08637-z

Brandt, J., Bittrich, L., Fischer, F., Kanaki, E., Tagg, A., Lenz, R., et al. (2020). High-throughput analyses of microplastic samples using fourier transform infrared and Raman spectrometry. *Appl. Spectrosc.* 74, 1185–1197. doi:10.1177/0003702820932926

Burns, E. E., and Boxall, A. B. A. (2018). Microplastics in the aquatic environment: evidence for or against adverse impacts and major knowledge gaps. *Environ. Toxicol. Chem.* 37, 2776–2796. doi:10.1002/etc.4268

Colton, J. B., Burns, B. R., and Knapp, F. D. (1974). Plastic particles in surface waters of the northwestern atlantic. *Science* 185, 491–497. doi:10.1126/science.185.4150.491

Conley, K., Clum, A., Deepe, J., Lane, H., and Beckingham, B. (2019). Wastewater treatment plants as a source of microplastics to an urban estuary: removal efficiencies and loading per capita over one year. *Water Res. X* 3, 100030. doi:10.1016/j.wroa.2019.100030

Cristaldi, A., Fiore, M., Zuccarello, P., Conti, G. O., and Grasso, A. (2020). Efficiency of wastewater treatment plants (WWTPs) for microplastic Removal : a systematic review. *Int J Environ Res Public Health* 17 (21), 8014. doi:10.3390/ijerph17218014

Cunningham, E. M., and Sigwart, J. D. (2019). Environmentally accurate microplastic levels and their absence from exposure studies. *Integr. Comp. Biol.* 59, 1485–1496. doi:10.1093/icb/icz068

Daehne, D., Fürle, C., Thomsen, A., Watermann, B., and Feibicke, M. (2017). Antifouling biocides in German marinas: exposure assessment and calculation of national consumption and emission. *Integr. Environ. Assess. Manag.* 13, 892–905. doi:10.1002/ieam.1896

Directive of the European Parliament (2008). Establishing a framework for Community action in the field of marine environmental policy (Marine Strategy Framework Directive). *Official J. Eur. Union* L164, 19–40.

DWA (1992). Arbeitsblatt ATV-A 128: richtlinien für die Bemessung und Gestaltung von Regenentlastungsanlagen in Mischwasserkanälen. *Deutsche Vereinigung für Wasserwirtschaft, Abwasser und Abfall e. V.*(London, United Kingdom: DWA).

DWA (2006). *Arbeitsblatt 118: hydraulische Bemessung und Nachweis von Entwässerungssystemen. Deutsche Vereinigung für Wasserwirtschaft, Abwasser und Abfall e. V*. (London, United Kingdom: DWA).

DWD (2020). *Warnemünde. DWD – deutscher wetterdienst* https://rcccm.dwd.de/DE/wetter/wetterundklima_vorort/mecklenburg-vorpommern/warnemuende/_node.html (German Weather Service) accessed on 07 23, 2020).

Enders, K., Käppler, A., Biniasch, O., Feldens, P., Stollberg, N., Lange, X., et al. (2019). Tracing microplastics in aquatic environments based on sediment analogies. *Sci. Rep.* 9, 15207. doi:10.1038/s41598-019-50508-2

Enders, K., Lenz, R., Ivar do Sul, J. A., Tagg, A. S., and Labrenz, M. (2020). When every particle matters: a QuEChERS approach to extract microplastics from environmental samples. *MethodsX* 7, 100784. doi:10.1016/j.mex.2020.100784

Eo, S., Hong, S. H., Song, Y. K., Han, G. M., and Shim, W. J. (2019). Spatiotemporal distribution and annual load of microplastics in the Nakdong River, South Korea. *Water Res.* 160, 228–237. doi:10.1016/j.watres.2019.05.053

Galafassi, S., Nizzetto, L., and Volta, P. (2019). Plastic sources: a survey across scientific and grey literature for their inventory and relative contribution to microplastics pollution in natural environments, with an emphasis on surface water. *Sci. Total Environ.* 693, 133499. doi:10.1016/j.scitotenv.2019.07.305

Geilfus, N. X., Munson, K. M., Sousa, J., Germanov, Y., Bhugaloo, S., Babb, D., et al. (2019). Distribution and impacts of microplastic incorporation within sea ice. *Mar. Pollut. Bull.* 145, 463–473. doi:10.1016/j.marpolbul.2019.06.029

Hansestadt Rostock (2019). *Statistisches jahrbuch hansestadt Rostock 2019* https://rathaus.rostock.de/sixcms/media.php/rostock_01.a.4984.de/datei/_Statistisches%20Jahrbuch%202019.pdf (Accessed on 10 06, 2020)

HELCOM (2008). Marine litter within the baltic region convention, 1–6.

HELCOM (2015). Regional action plan on marine litter (RAP ML), 1–15.

Hitchcock, J. N. (2020). Storm events as key moments of microplastic contamination in aquatic ecosystems. *Sci. Total Environ.* 734, 139436. doi:10.1016/j.scitotenv.2020.139436

Hurley, R., Woodward, J., and Rothwell, J. J. (2018). Microplastic contamination of river beds significantly reduced by catchment-wide flooding. *Nat. Geosci* 11, 251–257. doi:10.1038/s41561-018-0080-1

Isobe, A., Iwasaki, S., Uchida, K., and Tokai, T. (2019). Abundance of non-conservative microplastics in the upper ocean from 1957 to 2066. *Nat. Commun.* 10, 13. doi:10.-019-0831610.1038/s41467-019-08316-9

KOGGE (2018). *Kommunale Gewässer gemeinschaftlich Entwickeln. Ein Handlungskonzept für kleine urbane Gewässer am Beispiel der Hanse- und Universitätsstadt Rostock. Abschlussbericht des BMBF-Forschungsverbundprojektes KOGGE*. Editors J. Tränckner and A. Walter (Rostock, Germany: Universität Rostock. doi:10.18453/rosdok_id00002435

Kooi, M., and Koelmans, A. A. (2019). Simplifying microplastic via continuous probability distributions for size, shape, and density. *Environ. Sci. Technol. Lett.* 6, 551–557. doi:10.1021/acs.estlett.9b00379

Käppler, A., Windrich, F., Löder, M. G. J., Malanin, M., Fischer, D., Labrenz, M., et al. (2015). Identification of microplastics by FTIR and Raman microscopy: a novel silicon filter substrate opens the important spectral range below 1300 cm−1 for FTIR transmission measurements. *Anal. Bioanal. Chem.* 407, 6791–6801. doi:10.1007/s00216-015-8850-8

Lange, X., Klingbeil, K., and Burchard, H. (2020). Inversions of estuarine circulation are frequent in a weakly tidal estuary with variable wind forcing and seaward salinity fluctuations. *J. Geophys. Res. Oceans* 125. doi:10.1029/2019JC015789

Lebreton, L. C. M., van der Zwet, J., Damsteeg, J., Slat, B., Andrady, A., and Reisser, J. (2017). River plastic emissions to the world's oceans. *Nat. Commun.* 8, 15611. doi:10.1038/ncomms15611

Lenz, R., and Labrenz, M. (2018). Small microplastic sampling in water: development of an encapsulated filtration device. *Water* 10, 1055. doi:10.3390/w10081055

Leslie, H. A., Brandsma, S. H., van Velzen, M. J., and Vethaak, A. D. (2017). Microplastics en route: field measurements in the Dutch river delta and Amsterdam canals, wastewater treatment plants, North Sea sediments and biota. *Environ. Int.* 101, 133–142. doi:10.1016/j.envint.2017.01.018

Li, J., Liu, H., and Paul Chen, J. (2018). Microplastics in freshwater systems: a review on occurrence, environmental effects, and methods for microplastics detection. *Water Res.* 137, 362–374. doi:10.1016/j.watres.2017.12.056

Liu, F., Olesen, K. B., Borregaard, A. R., and Vollertsen, J. (2019). Microplastics in urban and highway stormwater retention ponds. *Sci. Total Environ.* 671, 992–1000. doi:10.1016/j.scitotenv.2019.03.416

Lorentz, A., Düring, I., and Moldenhauer, H. (2014). Immissionssituation Hafen Rostock 2012. Luftschadstoffgutachten. Report of the engineering office Lohmeyer GmbH & Co. KG on behalf of the Landesamt fur Umwelt, Naturschutz und Geologie Mecklenburg-Vorpommern (LUNG). 48.

Michels, J., Stippkugel, A., Lenz, M., Wirtz, K., and Engel, A. (2018). Rapid aggregation of biofilm-covered microplastics with marine biogenic particles. *Proc. Biol. Sci.* 285, 20181203. doi:10.1098/rspb.2018.1203

Miller, A. W., Davidson, I. C., Minton, M. S., Steves, B., Moser, C. S., Drake, L. A., et al. (2018). Evaluation of wetted surface area of commercial ships as biofouling habitat flux to the United States. *Biol. Invasions* 20, 1977–1990. doi:10.1007/s10530-018-1672-9

Mintenig, S., Löder, M., and Gerdts, G. (2014). "(OOWV) in niedersachsen. Alfred-Wegener-Instituts (AWI)," in *Mikroplastik in ausgewählten Kläranlagen des Oldenburgisch- Ostfriesischen Wasserverbandes. Int-Veen IFinal report for the Oldenburgisch- Ostfriesischer Wasserverband (OOWV) Niedersächsischer und des Niedersächsischer Landesbetrieb für Wasserwirtschaft, Küsten- und Naturschutz (NLWKN)*, 18.

Morris, A. W., and Hamilton, E. I. (1974). Polystyrene spherules in the bristol channel. *Mar. Pollut. Bull.* 5, 26–27. doi:10.1016/0025-326X(74)90311-7

Nizzetto, L., Bussi, G., Futter, M. N., Butterfield, D., and Whitehead, P. G. (2016). A theoretical assessment of microplastic transport in river catchments and their retention by soils and river sediments. *Environ. Sci. Process. Impacts* 18, 1050–1059. doi:10.1039/C6EM00206D

OECD (2005). *Emission scenario document on antifouling productsSeries on emission scenario documents.* Paris, France: OECD Environment Directorate, Environment, Health and Safety Division *No. 13* www.oecd.org/ehs/, ENV/JM/MONO(2005)8.

OECD (2009). *Emission scenario documents on coating industry (Paints, Laquers and Varnishes). Series on emission scenario documents, Paris, France: OECD Environment Directorate, Environment, Health and Safety Division No. 22.* ENV/JM/MONO, 24 www.oecd.org/ehs/.

OpenDataHRO (2019). *Hanse- und Universitätsstadt Rostock* https://www.opendata-hro.de/ (Accessed on 01 23, 2019).

Pegelportal, M-V. (2020). *Landesamt für Umwelt, Naturschutz und Geologie Mecklenburg-Vorpommern* https://pegelportal-mv.de/pdf/pegelsteckbrief_04402.2.pdf (Accessed on 10 06, 2020).

PLANCO (2004). *Standortkonzepte für Sportboothäfen an der Ostseeküste. Planco-Consultig GmbH Schwerin. Ministerium für Arbeit, Bau und Landesentwicklung Mecklenburg-Vorpommern (Hrsg)*. Schwerin, Germany, 238pp.

Prata, J. C. (2018). Microplastics in wastewater: state of the knowledge on sources, fate and solutions. *Mar. Pollut. Bull.* 129, 262–265. doi:10.1016/j.marpolbul.2018.02.046

Resolution, U. N. (2020). *Transforming our world: the 2030 agenda for sustainable development*. New York, NY, United States: United Nations.

Rezania, S., Park, J., Md Din, M. F., Mat Taib, S., Talaiekhozani, A., Kumar Yadav, K., et al. (2018). Microplastics pollution in different aquatic environments and biota: a review of recent studies. *Mar. Pollut. Bull.* 133, 191–208. doi:10.1016/j.marpolbul.2018.05.022

Rönspieß, L., Dellwig, O., Lange, X., Nausch, G., and Schulz-Bull, D. (2020). Spatial and seasonal phosphorus dynamics in a eutrophic estuary of the southern Baltic Sea. *Estuarine, Coastal Shelf Sci.* 233, 106532. doi:10.1016/j.ecss.2019.106532

Rossman, L. A. (2015). *Storm water management model user's manual*. Cincinnati, OH, United States: U.S. Environmental Protection Agency.Version 5.1.

Rummel, C. D., Jahnke, A., Gorokhova, E., Kühnel, D., and Schmitt-Jansen, M. (2017). Impacts of biofilm formation on the fate and potential effects of microplastic in the aquatic environment. *Environ. Sci. Technol. Lett.* 4, 258–267. doi:10.1021/acs.estlett.7b00164

Schernewski, G., Paysen, P., Robbe, E., Inácio, M., Schumacher, J., and Lillebø, A. I. (2019). Ecosystem service assessments in water policy Implementation : an analysis in urban and rural estuaries. *Front. Mar. Sci.* 6, 1–17. doi:10.3389/fmars.2019.00183

Schmidt, C., Krauth, T., and Wagner, S. (2017). Export of plastic debris by rivers into the sea. *Environ. Sci. Technol.* 51, 12246–12253. doi:10.1021/acs.est.7b02368

Schöneich-Argent, R. I., Dau, K., and Freund, H. (2020). Wasting the North Sea?—a field-based assessment of anthropogenic macrolitter loads and emission rates of three German tributaries. *Environ. Pollut.* 263, 114367. doi:10.1016/j.envpol.2020.114367

Sharma, S., and Chatterjee, S. (2017). Microplastic pollution, a threat to marine ecosystem and human health: a short review. *Environ. Sci. Pollut. Res. Int.* 24, 21530–21547. doi:10.1007/s11356-017-9910-8

Sherman, P., and van Sebille, E. (2016). Modeling marine surface microplastic transport to assess optimal removal locations. *Environ. Res. Lett.* 11, 014006. doi:10.1088/1748-9326/11/1/014006

Siegfried, M., Koelmans, A. A., Besseling, E., and Kroeze, C. (2017). Export of microplastics from land to sea. A modelling approach. *Water Res.* 127, 249–257. doi:10.1016/j.watres.2017.10.011

Simon, M., van Alst, N., and Vollertsen, J. (2018). Quantification of microplastic mass and removal rates at wastewater treatment plants applying Focal Plane Array (FPA)-based Fourier Transform Infrared (FT-IR) imaging. *Water Res.* 142, 1–9. doi:10.1016/j.watres.2018.05.019

Soroldoni, S., Castro, Í. B., Abreu, F., Duarte, F. A., Choueri, R. B., Möller, O. O., et al. (2018). Antifouling paint particles: sources, occurrence, composition and dynamics. *Water Res.* 137, 47–56. doi:10.1016/j.watres.2018.02.064

Sun, J., Dai, X., Wang, Q., van Loosdrecht, M. C. M., and Ni, B. J. (2019). Microplastics in wastewater treatment plants: detection, occurrence and removal. *Water Res.* 152, 21–37. doi:10.1016/j.watres.2018.12.050

Sundt, P., Schulze, P. E., and Syversen, F. (2014). *Sources of microplastics-pollution to the marine environment*. Asker, Norway: Norwegian Environment AgencyMepex Consult. 86.

Szymczycha, B., Zaborska, A., Bełdowski, J., Kuliński, K., Beszczyńska-Möller, A., Kędra, M., et al. (2019). *Chapter 4—the Baltic Sea. World seas: an environmental evaluation*. Editor C. Sheppard. 2nd ed. (Cambridge, MA, United States: Academic Press), 85–111.

Uddin, S., Fowler, S. W., and Behbehani, M. (2020). An assessment of microplastic inputs into the aquatic environment from wastewater streams. *Mar. Pollut. Bull.* 160, 111538. doi:10.1016/j.marpolbul.2020.111538

van Emmerik, T., Tramoy, R., van Calcar, C., Alligant, S., Treilles, R., Tassin, B., et al. (2019). Seine plastic debris transport tenfolded during increased river discharge. *Front. Mar. Sci.* 6, 1–7. doi:10.3389/fmars.2019.00642

van Wijnen, J., Ragas, A. M. J., and Kroeze, C. (2019). Modelling global river export of microplastics to the marine environment: sources and future trends. *Sci. Total Environ.* 673, 392–401. doi:10.1016/j.scitotenv.2019.04.078

Wagner, S., Klöckner, P., Stier, B., Römer, M., Seiwert, B., Reemtsma, T., et al. (2019). Relationship between discharge and river plastic concentrations in a

rural and an urban catchment. *Environ. Sci. Technol.* 53, 10082–10091. doi:10.1021/acs.est.9b03048

Wang, W., Gao, H., Jin, S., Li, R., and Na, G. (2019). The ecotoxicological effects of microplastics on aquatic food web, from primary producer to human: a review. *Ecotoxicol. Environ. Saf.* 173, 110–117. doi:10.1016/j.ecoenv.2019.01.113

WASSER (2005). *Länderarbeitsgemeinschaft Wasser. Richtlinie für die Gebiets- und Gewässerverschlüsselung*. Berlin, Germany: Kulturbuch-Verl.

Wasserbuch, M-V. (2019). *Landesamt für Umwelt, Naturschutz und Geologie Mecklenburg-Vorpommern (LUNG)* https://www.geoportal-mv.de/portal/Geowebdienste/Fachthemen/Wasser (Accessed via GeoPortal.MV on 03 18, 2019).

Watermann, B., Daehne, D., Fürle, C., and Thomsen, A. (2014). *Sicherung der Verlässlichkeit der Antifouling-Expositionsschätzung im Rahmen des EUBiozid-Zulassungsverfahrens auf Basis der aktuellen Situation in deutschen Binnengewässern für die Verwendungsphase im Bereich Sportboothäfen*, Dessau-Roßlau, Germany: Umwelt Bundesamt, 160.

Watermann, B., and Eklund, B. (2019). Can the input of biocides and polymeric substances from antifouling paints into the sea be reduced by the use of non-toxic hard coatings?. *Mar. Pollut. Bull.* 144, 146–151. doi:10.1016/j.marpolbul.2019.04.059

WSV (2019). *Planunterlagen—anpassung der seewärtigen Zufahrt zum Seehafen Rostock—baggergutverbringungskonzept.*Stralsund, Germany: Waterways and Shipping Administration (WSV).

Wu, P., Huang, J., Zheng, Y., Yang, Y., Zhang, Y., He, F., et al. (2019). Environmental occurrences, fate, and impacts of microplastics. *Ecotoxicol. Environ. Saf.* 184, 109612. doi:10.1016/j.ecoenv.2019.109612

Zhao, S., Wang, T., Zhu, L., Xu, P., Wang, X., Gao, L., et al. (2019). Analysis of suspended microplastics in the Changjiang Estuary: implications for riverine plastic load to the ocean. *Water Res.* 161, 560–569. doi:10.1016/j.watres.2019.06.019

Zhao, W., Huang, W., Yin, M., Huang, P., Ding, Y., Ni, X., et al. (2020). Tributary inflows enhance the microplastic load in the estuary: a case from the Qiantang River. *Mar. Pollut. Bull.* 156, 111152. doi:10.1016/j.marpolbul.2020.111152

Conflict of Interest: The authors declare that the research was conducted in the absence of any commercial or financial relationships that could be construed as a potential conflict of interest.

Copyright © 2021 Piehl, Hauk, Robbe, Richter, Kachholz, Schilling, Lenz, Fischer, Fischer, Labrenz and Schernewski. This is an open-access article distributed under the terms of the Creative Commons Attribution License (CC BY). The use, distribution or reproduction in other forums is permitted, provided the original author(s) and the copyright owner(s) are credited and that the original publication in this journal is cited, in accordance with accepted academic practice. No use, distribution or reproduction is permitted which does not comply with these terms.

This is the end of the publication

Combined Approaches to Predict Microplastic Emissions Within an Urbanized Estuary (Warnow, Southwestern Baltic Sea)

by Sarah Piehl, Rahel Hauk, Esther Robbe, Boris Richter, Frauke Kachholz, Jannik Schilling, Robin Lenz, Dieter Fischer, Franziska Fischer, Matthias Labrenz, Gerald Schernewski

You might want to continue reading the synopsis at page 24, or jump back to the start of this publication at page 123.

Identification and quantification of microplastic particles in drinking water treatment sludge as an integrative approach to determine microplastic abundance in a freshwater river

by Henrik Siegel, Franziska Fischer, Robin Lenz, Dieter Fischer, Martin Jekel, Matthias Labrenz

- **Date published**: July 04, 2021
- **Type**: Research Article
- **Published in**: Environmental Pollution, Elsevier

- **License**: © Elsevier

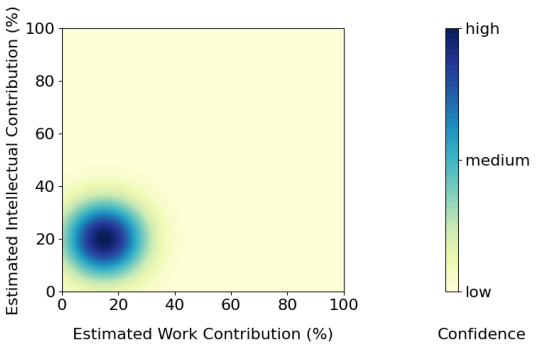
- **DOI**: 10.1016/j.envpol.2021.117524, **Reference**: [8]
- **Citations**: 19 (Crossref/DOI, 2025-11-18)

Contributions

HS: Methodology, Investigation, Formal analysis, Writing - original draft | FF: Investigation, Formal analysis, Writing - Review & editing | RL: Investigation, Formal analysis, Writing - Review & editing | DF: Formal analysis, Writing Review & editing | MJ: Methodology, Writing - Review & editing | ML: Resources, Methodology, Writing - Review & editing.

Quantitative own contributions based on self-assessment

In the dimensions of expended work effort and intellectual contribution, I consider my shares are likely to be between 10% and 20% and between 15% and 25% respectively. This is visualised below as an interpolated histogram of 500 samples from Gaussian distributions with the aforementioned estimates at plus/minus two standard deviations.



Environmental Pollution 286 (2021) 117524

Contents lists available at ScienceDirect

Environmental Pollution

journal homepage: www.elsevier.com/locate/envpol

Identification and quantification of microplastic particles in drinking water treatment sludge as an integrative approach to determine microplastic abundance in a freshwater river☆

Henrik Siegel [a], Franziska Fischer [b], Robin Lenz [a], Dieter Fischer [b], Martin Jekel [c], Matthias Labrenz [a,*]

[a] Leibniz-Institut für Ostseeforschung Warnemünde (IOW), D-18119, Rostock, Germany
[b] Leibniz-Institut für Polymerforschung Dresden (IPF), D-01069, Dresden, Germany
[c] Technische Universität Berlin (TU Berlin), 10623, Berlin, Germany

ARTICLE INFO

Keywords:
Microplastic
Freshwater
Integrative
Sampling
Coagulation/flocculation
Water treatment

ABSTRACT

Microplastic (MP) has been detected ubiquitously in freshwater systems. Until now MP sampling, however, is predominantly based on short-term net or pumping and filtration systems which can only provide snapshots of MP abundance; especially in flowing water bodies. To improve representativeness in the determination of MP occurrences in these aquatic compartments, an integrative approach that covers larger water volumes for a longer period of time is required. In this regard, surface water supplied drinking water treatment plants (DWTPs) represent an opportunity. In DWTPs, suspended solids from thousands of cubic metres of raw water are continuously removed over several hours and enriched in coagulation/flocculation and filtration processes. Our hypothesis was that MP is also removed to a full extent, like suspended solids, and that an integrative approach for identification and quantification in raw water can be derived from the analysis of MP in the treatment sludge. To prove this hypothesis, treatment sludge from a riverside DWTP (Warnow river, North-Eastern Germany) was analysed for MP > 50 μm. A sample purification protocol overcoming potential matrix effects caused by co-agulants and flocculants was developed and validated. MP was analysed using micro-Raman spectroscopy. MP occurrence determined for the Warnow river was compared with *in situ* reference sampling using an established pumping and filtration system at relatively stable flow conditions. As result, the number of MP particles derived from treatment sludge was extrapolated to 196 ± 42 m^{-3} for the Warnow river and is statistically insignificantly different from 233 ± 36 m^{-3} identified by conventional water sampling. In addition, the polymer distribution and particles shape indicated the validity of the integrative concept. Consequently, the determination of MP abundance for freshwater systems based on DWTP treatment sludge represents an adequate method to estimate MP concentrations in flowing waters in an integrative way.

1. Introduction

The pervasive presence of plastic contamination in the environment is considered to be a challenging global problem. Plastic debris covers a wide range of sizes, with synthetic polymer particles with a longest dimension of < 5 mm defined as microplastics (MPs) (GESAMP Joint group of experts on the scientific aspects of marine environmental protection, 2015).

As MP is suspected of ecotoxicological effects, a vast number of studies aimed to assess the abundance of MP in the environment in sediments, biota or aquatic waterbodies (Browne et al., 2008; Browne et al., 2011; Claessens et al., 2011; Cole et al., 2013; Doyle et al., 2011; Dubaish and Liebezeit, 2013; Eriksen et al., 2013a; Eriksen et al., 2013b; Murray and Cowie, 2011; Ng and Obbard, 2006; Ugolini et al., 2013). Regarding the latter studies, sampling was initially based on trawling with mesh sizes > 300 μm (Hidalgo-Ruz et al., 2012). As evidence mounted that MP numbers significantly increase at decreasing particle size in environmental samples, the requirement for sampling strategies

☆ This paper has been recommended for acceptance by Eddy Y. Zeng.
* Corresponding author.
E-mail address: matthias.labrenz@io-warnemuende.de (M. Labrenz).

https://doi.org/10.1016/j.envpol.2021.117524
Received 25 February 2021; Received in revised form 26 April 2021; Accepted 17 May 2021
Available online 4 June 2021
0269-7491/© 2021 Elsevier Ltd. All rights reserved.

also capturing particles down to 1 μm emerged. From there, sampling was also conducted by pumping and filtration instrumentations or filling bottles (Koelmans et al., 2019; Li et al., 2018; Triebskorn et al., 2019). Using these approaches, sampling procedures lasted for a few minutes up to several hours and the sampled volume varied between some hundred litres to several cubic meters (Li et al., 2018). In consequence, MP abundances determined for the observed waterbody were principally based on a snapshot in terms of time and space and, especially in the case of strongly fluctuating MP loads, potentially biased. To overcome this problem an integrative sampling strategy is required which allows time and volume-related sources of inaccuracy in the MP determination to be minimised.

One integrative approach would be to benefit from the particle removal processes in drinking water treatment plants (DWTPs) for river water. During particle removal by coagulation/flocculation processes, particles are separated from the water phase, largely by the use of metallic salts (iron and aluminium) and polymeric flocculant aids like polyacrylamide (PAM) (Bratby, 2016). With regard to DWTPs, coagulation and flocculation plus filtration are considered to be promising removal technologies for MP (Lapointe et al., 2020; Novotna et al., 2019; WHO, 2019). MPs captured in both coagulation/flocculation and filtration treatment are continuously removed and enriched in the treatment sludge. Hence, by analysing treatment sludge from DWTPs, the abundance of MP in the directly affiliated water reservoir can be extrapolated. DWTPs fed by freshwater bodies are common elements of the drinking water supply chain worldwide and have a defined relationship between the treated raw water volume of thousands of cubic metres and the capture time of several hours. The treatment sludge, which is composed of the suspended solids of the raw water, thus represents an integrative approach to investigate the occurrence of MP in the adjacent aquatic environmental compartment, as DWTP-systems are designed for a near-to complete removal of particles, including all pathogenic viruses and bacteria. Viewing the likely large diurnal fluctuations in freshwater systems, an integrative approach may provide useful, reproducible and cost-effective information for MP emission assessments.

In the presented study, abundance of MP $>$ 50 μm in the German freshwater Warnow river was investigated by analysing treatment sludge samples from an affiliated DWTP using micro-Raman spectroscopy. The Warnow river was chosen because it seems to be characterised by a rather stable MP load over the course of the year (Piehl et al., 2021), which facilitates comparability with our integrative approach. Piehl et al. (2021) compiled source-specific MP emission data from literature and samplings for the Warnow river estuary, indicating low-variable estuary discharges of $152*10^9$ to $291*10^9$ MPs per year. The Warnow river catchment itself served as transport pathway for 49.1 % of the total MP emissions (Piehl et al., 2021).

For the integrative determination of MP abundance for the Warnow river, a purification protocol for the extraction of MP from sludge matrix was developed. Method validation included (i) recovery experiments, (ii) instrumental examinations of the impact of polymeric flocculants in spectroscopic particle detection and (iii) a comparison of the calculated MP load with the results from conventional sampling at the investigated river.

2. Materials and methods

2.1. Study site and sampling

Treatment sludge sampling was performed at the DWTP Rostock located at the end of the upper flow of the Warnow river, north-eastern Germany. The Warnow river traverses along 155 km with a catchment area of 3,324 km^2. At the DWTP Rostock, raw water is collected near the surface to an average water depth of 1.5 m and its purification is achieved by pre-ozonation, coagulation/flocculation with sedimentation, sand filtration and ozonation plus granular activated carbon filtration (Fig. 1). For coagulation/flocculation, polyaluminium chloride (PAC) and PAM are applied. On average, 35,000 m^3 raw water is purified to drinking water per day. The solids and particles from raw water are separated into treatment sludge, which originates from both coagulation/flocculation/sedimentation and sand filter backwashing, leading to a daily amount of 500 m^3 non-thickened sludge at the DWTP Rostock.

In April and May 2020 four 500 mL treatment sludge samples with a dry matter content of 1.0–1.5 % were collected at the DWTP: two samples were taken on one day per month under dry weather conditions, respectively. Treatment sludge samples were taken at a sludge drainage tank using a metal scoop, and subsequently transferred into Erlenmeyer flasks closed with glass stoppers. Sampling flasks were pre-cleaned by rinsing with MP-free (MPF) filtered MilliQ water and baking for 5 h at 500 °C in a muffle oven (L15/11/B170, Nabatherm GmbH). Samples were stored at 4 °C in the dark prior to analysis. Two blanks of 500 mL MPF-MilliQ water served as negative control for analysis, being conveyed into Erlenmeyer flasks identically to the samples at the sampling location.

2.2. Sample preparation

2.2.1. Contamination mitigation

To diminish the risk of contamination, clothes only made of natural fibres and a cotton lab coat were worn during sample preparation. Nitrile hand gloves rinsed with MPF-water, filtered through a filter cartridge at mesh size of 10 μm (01WTGD05; Wolftechnik Filtersysteme GmbH & Co), were used throughout sample treatment. Samples were processed in a laminar flow box and room air was additionally filtered by a HEPA filter (Vita Shield IPS, Philips). Before usage, all solutions were filtered to 2.7 μm with a glass fibre filter (Whatman 934-AH) and all materials were thoroughly cleaned with MPF-water. Prior to sample contact, beakers and aluminium foil were rinsed with MPF-water and baked for 5 h at 500 °C. Solutions and glass equipment were covered at all times with aluminium foil. Application of plastic materials was avoided except for vacuum filtration seals made of polytetrafluorethylene (PTFE). In consequence, PTFE was excluded from MP analysis. Given the relatively low production volume of PTFE (PlasticsEurope, 2019), this polymer is expected to occur very rarely in environmental

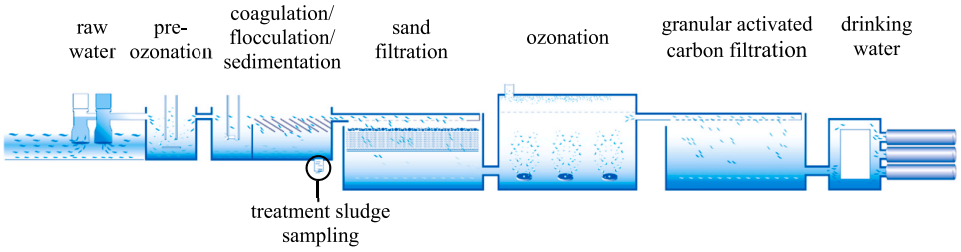


Fig. 1. Process flow diagram of the DWTP Rostock (abstracted from Nordwasser GmbH; https://www.nordwasser.de/trinkwasser/versorgung/wasserwerk-rostock). The treatment sludge is a combined sludge from both coagulation/flocculation/sedimentation and sand filter backwashing.

samples. Similarly, the carbazole dioxazine compound Pigment Violet 23 that was used in the nitrile gloves was excluded from analysis.

2.2.2. Purification protocol

Treatment sludge samples were stored for 24 h at 4 °C in the dark. After this settling time, a sediment layer was formed and the sample supernatant was 10 μm-filtered using a stainless steel filter (Spörl KG). The transfer of sample particles was ensured by consistently rinsing the glassware several times throughout the purification process. To efficiently purify and completely analyse a treatment sludge sample of 500 mL, the sediment layer was split into four aliquots of 50 mL (termed as subsamples) and then the 10 μm filter comprising particles from the supernatant was added to one of the four subsamples. The subsamples were frozen for 8 h at −20 °C, followed by freeze-drying for 60 h at 30 °C and 0.37 mbar (Delta 1–24 LSCplus, Christ). Blanks as negative controls were used to detect potential sample contamination. They were processed according to this protocol, starting with the sampling and covering all following processing steps.

The subsamples were resuspended in 50 mL of MPF-water. Dissolving the floc structure of the hydrolysed Al-coagulant was achieved by dropwise adding 925 μL 10 % (w/w) HCl (Carl Roth, Germany) to generate pH 3.0. Subsamples were incubated for 48 h at 40 °C with a consistent stirring speed of 50 rpm. The acidified subsamples were then vacuum filtered at 10 μm. Filter cake was washed five times with 20 mL of a pH 3.0-solution, composed of 2.4 mL 10 % (w/w) HCl in 1 L MPF-water. The solid residue was resuspended in 20 mL MPF-water and exposed for 30 s to an ultrasonic bath at 35 kHz (Sonorex Super, Bandelin).

To digest organic matter, 200 mL 30 % (v/v) H_2O_2 (Carl Roth, Germany) were added. After a seven-day incubation at 40 °C, all four subsamples of one original treatment sludge sample were merged and vacuum filtered on a 10 μm filter. Extraction of MP was accomplished with sodium polytungstate solution (SPT; TC-Tungsten Compounds) comprising a density of 1.8 g*mL^{-1}, which exceeds the density of most polymer types (Enders et al., 2020). The sample was suspended in 50 mL SPT solution, promoted by 30 s in ultrasonic bath at 35 kHz, and transferred into a separation funnel filled with 100 mL SPT. The separation funnel rested for 5 days before the sediment fraction was discarded. The supernatant containing floating particles was vacuum filtrated onto a 10 μm filter followed by five cycles of rinsing with 10 mL MPF-MilliQ water.

For Raman microscopy, the sample was finally filtered using a tailor-made glass apparatus onto a 10 × 10 mm-silicon filter substrate (Käppler et al., 2015) with 50 μm pores, cleaned with 3 % (v/v) H_2O_2 and sonication in MPF-MilliQ water (Brandt et al., 2020). Each prepared treatment sludge sample was filtered on one silicon filter without prior homogenization, so that a monolayer of single particles was kept as the maximum filter load. For this final step, a blind of 150 mL MPF-MilliQ water per sample was prepared on a silicon filter with 10 μm pore size.

The number of MP in treatment sludge was converted to riverside concentrations by multiplying the MP concentration in the treatment sludge samples (c(MP, treatment sludge)) by the volume of treatment sludge accumulated at the DTWP Rostock (V(treatment sludge)), divided by the corresponding volume of raw water treated by the DTWP (V(treated raw water)):

c(MP, riverside) = (c(MP, treatment sludge) * V(treatment sludge))/ V(treated raw water).

2.3. Method validation

2.3.1. MP recovery

For quantitative validation of the sample preparation protocol, MP recovery rates were determined. Therefore, triplicates of 150 mL treatment sludge were spiked with 20–40 particles of model MP, and treated in accordance to the descriptions in 2.2.2. As model MP, two types of fluorescent PE microspheres representing low-density plastics (63–75 μm, 1.013 g*mL^{-1} and 125–150 μm, 1.025 g*mL^{-1}, both Cospheric, USA), and cylindrical polyamide 6 (PA 6) particles representing high-density plastic (450 μm, 1.14 g*mL^{-1}, Lanxess, Germany) were used (details listed in Table S1).

The MP added were visually identified using a binocular at 4× magnification (Stema 2000; Carl Zeiss).

2.3.2. Impact of flocculant chemicals

To investigate elimination of PAC during acid treatment, Al-content in treatment sludge sample was determined by EDX spectroscopy before and after acidification (Merlin-Compact VP microscope, Carl Zeiss, coupled with EDX, Oxford-Instruments). 1 μL of a sample was placed on a polycarbonate filter (Whatman Cyclopore PC Polycarbonate Membrane Filters, 8 μm) and dried for 5 h at 50 °C. X-ray emission was stimulated by an incident electron beam of 15 kV applied in area scan mode. Element identification was based on sum spectra evaluation using the software Inca and Aztec.

Inductively coupled plasma optical emission spectrometry (ICP-OES) was used to determine Al-concentration in the filtrate originating from the acidic wash. 5 mL of the filtrate were collected from every washing step, mixed with 100 μL 1 M HNO_3 (Carl Roth, Germany) and filtered to 0.2 μm. ICP-OES measurement was performed at a wavelength of 310 nm (iCAP 7400 Duo, Thermo Fisher Scientific).

By adsorption on particle surfaces, PAM could possibly trigger Raman signals that impede the identification of MP. Potential spectroscopic interference of PAM was studied by flocculation tests reflecting the working conditions at the DTWP Rostock. Experiments were conducted in a jar apparatus with an axial paddle stirrer (MiniStar20 digita IKA, Omnilab). As reference solids aluminium oxide (63–200 μm; Al_2O_3 90 active neutral, Merck, Germany) and PA 6 (as model MP < 250 μm; Lanxess, Germany) were used. These particle sizes reflect MP size classes expected to be frequently found in freshwater systems (Triebskorn et al., 2019). Despite the prominent levels of polyolefin plastics in environmental samples, the flotation of polyolefins in water might complicate lab-scale flocculation and consequently, application as reference material was avoided. Tap water served as matrix providing a mostly identical mineral composition without any disturbing solids compared to raw water from the DWTP. PAC (9 % (w/w) Al, 21 % (w/w) Cl, Sachtoklar® 39, Venator, Germany) and PAM (0.1 % (w/w) stock solution; Synthofloc™ 8022 TW, Venator, Germany) from the DWTP Rostock were applied.

180 mg aluminium oxide and PA 6 were separately suspended in 1.8 L tap water. To best reflect conditions at the DWTP, pH was adjusted to 7.1 by adding 2.25 mL 1 M NaOH (Carl Roth, Germany). Particles were coagulated with 74 μL PAC (corresponding to 5 mg*L^{-1} Al) at a stirring frequency of 250 rpm for 90 s. Flocculation was achieved adding 0.9 mL and 3.6 mL PAM-stock solution respectively, at a mixing speed of 150 rpm maintained for 30 s. As a result, ratios of 0.5 % (w/w) and 2 % (w/w) PAM to the solids content were generated, covering the expected amount of about 1 % (w/w) PAM in treatment sludge from the DWTP. The suspension was stirred for 20 min at 50 rpm and formed flocs were then allowed to sediment for 30 min.

Flocculation test samples were analysed using micro-Raman spectroscopy by directly pipetting a few millilitres onto a silicon wafer and drying for 10 min on a heating plate at < 100 °C. Rinsing was avoided to not loose particle flocs. Flocculated particles were automatically analysed in subareas of 1 mm^2 on each wafer. For selected particles, further Raman spectra were acquired at the top, centre and close to the wafer surface to test for material homogeneity.

2.4. Reference in situ sampling

For conventional sampling up to 10 cm below the water surface the mobile instrumentation “Rocket” was used (Lenz & Labrenz, 2018). Shore-side sampling (termed as *in situ*) was performed eight times in total at the Warnow river, in autumn 2018 and spring 2019, at a distance

of 4 m to the bank and 2 km away from the DWTP. Sampling lasted for about 1 h and sampled volume accounted for 0.2–0.6 m^3 until the filters of 10 μm pore size were clogged. Filters were stored in closed jars at 4 °C in the dark. The following sample preparation consisted of oxidation and density separation according to Enders et al. (2020). A negative control for every sampling campaign was taken by installing and then removing four filter cartridges from the "Rocket" before being further processed as laboratory blanks.

2.5. Micro-Raman spectroscopy

Spectroscopic detection of MP targeted the identification of polymer type, number and shape. This was performed using the GEPARD software as described by Brandt et al. (2020) with the Raman imaging microscope WITec® alpha 300 R (532 nm laser, 5 and 10 mW laser intensity, 0.5 s integration time, 5 accumulations, 20× objective, 50-3600 cm^{-1} spectral range). Spectra were identified by comparison to in-house databases containing 105 spectra of polymers, pigments/dyes and organic and inorganic reference material using the TrueMatch® software (WITec®). The quality of a database match was quantified with the Pearson correlation coefficient as hit quality index (HQI). The HQI indicates the accuracy of fit between the unknown spectrum and the reference spectrum and ranges from 0 to 100. Database matches were manually checked down to HQI 5.0 and matches with a lower HQI were discarded, as below this threshold the database search parameter (Brandt et al., 2020) did not allow reliable material identification. In contrast to the flocculation test samples, for analysis of the environmental samples the entire 10 × 10 mm silicon wafer was measured.

MP particle size was determined by fitting an ellipse geometry on the particle contour resulting in a long and a short particle dimension (Brandt et al., 2020). The length of fibres corresponded to half the circumference of the fibre edge line. The short fibre dimension resulted from doubling the maximum distance of a fibre edge point to the virtual fibre centreline (Brandt et al., 2020). MP size classification was based on the long particle and fibre dimensions, respectively.

The blanks were used to identify and quantify MP particles that could come from a contamination during the experiments rather than the sample itself. For this purpose, the MP particles in blank samples were grouped into phenotypes according to polymer type, shape and colour. Phenotypes matching in the filtration blind and the corresponding sample preparation blank were discarded from the latter. The phenotypes remaining for the sample preparation blanks were compared and subtracted from the counts in the associated set of environmental samples.

2.6. Statistical analysis

Treatment sludge-based determination of MP abundance for the Warnow river was compared with the *in situ* results by two-sample *t*-test assuming unequal variances. A 95 % confidence interval was set, so that p-value < 0.05 indicates probable significant differences of MP occurrence.

3. Results

3.1. Method validation

3.1.1. Recovery

Following the sample preparation procedure 100 ± 0.0 % of the 450 μm PA 6 particles were recovered. With decreasing particle size the recovery decreased to 93.6 ± 1.0 % for PE 125–150 μm and 88.0 ± 3.0 % for PE 63–75 μm (Table S1, results reported as average ± standard deviation).

3.1.2. Impact of flocculant chemicals

According to EDX analysis, Al-content decreased from originally 33.9 ± 1.5 (w/w) % to 2.2 ± 1.0 (w/w) % after acidification of treatment sludge sample (Fig. S1, results reported as average ± standard deviation). ICP-OES confirmed the elimination of the coagulant as the Al-concentration shifted from 96.4 $mg*L^{-1}$ after the first washing step to 0.12 $mg*L^{-1}$ at the fifth washing step (Fig. S2).

To check whether the Raman signals of PAM impede the MP identification, the spectrum of the pure PAM was compared to the spectra of aluminium oxide and PA 6 (Fig. S3). As distinguishing criterion to PA 6, the PAM spectrum exhibits two overlapping carbonyl bands at wavenumbers 1500-1750 cm^{-1}, representing stretching vibrations of carboxy and amide functions. Further, the PAM spectrum displays a double band in wavenumber range 3000–3500 cm^{-1}, associated with stretching vibrations of its primary amide. However, no signals of PAM were ever detected: (i) neither in automated scan of particle flocs prepared by filtration or heating, (ii) nor in different particle layers, (iii) nor for different PAM dosages (Fig. S4, S5). In conclusion, the designed workflow resulted in purified treatment sludge samples directly analysable in micro-Raman spectroscopy (Fig. 2).

3.2. Contamination rates

Negative controls for sample preparation and wafer filtration revealed contaminations with MP particles and fibres composed of PE, PP, polystyrene (PS), polyethylene terephthalate (PET), acrylonitrile butadiene styrene (ABS), polyphenylene sulfide (PPS) and silicon rubber (Table S2). White PET fibres were the primary contaminant with an average number of 4 fibres per blank. As PPS particles were found to be introduced by the final sample filtration step, this polymer was excluded from analysis. However, with a ratio of less than 5 %, the contamination level was well below the MP concentration range in all environmental samples.

Thus, the validation outcomes showed that our approach was suitable for MP analysis in treatment sludge enabling MP analyses for the Warnow river:

3.3. Determination of MP abundance for the Warnow river

For the Warnow river, MP concentration derived from treatment sludge of the DWTP was extrapolated to 196 ± 42 m^{-3}, reported as average MP concentration ± standard deviation. Each pair of two treatment sludge samples analysed correlated with a total sludge amount of 20 m^3 accrued from 1000 m^3 raw water from the Warnow river abstracted inside of 3 h per sampling day. By *in situ* sampling campaigns, MP abundance was determined to be 233 ± 36 m^{-3}, whereby the *t*-test did not show any significant differences between *in situ* and DWTP, with exception for the polymer category "others" (Table 1).

The MP detected consisted of 12 different polymer types: PE, PP, PS, PET, polyvinyl chloride (PVC), polyoxymethylene, polymethylmethacrylate, polysiloxane, ABS, acrylic resin, epoxy resin and silicone rubber. PE dominated in all samples with an average proportion of 37.8 %, followed by PP (31.0 %) and PS (24.4 %, Fig. S6).

MP sizes investigated ranged from 50 to 5000 μm, and size fraction 101–300 μm prevailed in DWTP as well as *in situ* (Fig. S7). While no MP > 500 μm was detected in DWTP, such larger fragments and fibres were captured *in situ* (Fig. 3). However, regarding MP morphology being classified into irregular shaped fragments, spherules and fibres, MP characteristics were very similar: fragments were the most abundant MP shape accounting for 83.3 % for DWTP and 79.9 % *in situ* (Fig. S8). Fibres constituted 16.7 % for DWTP and 19.9 % *in situ*. Spherules were the least abundant and did not occur in the DWTP and amounted to 0.2 % *in situ*.

4. Discussion

In this study, the abundance of MP > 50 μm was integratively

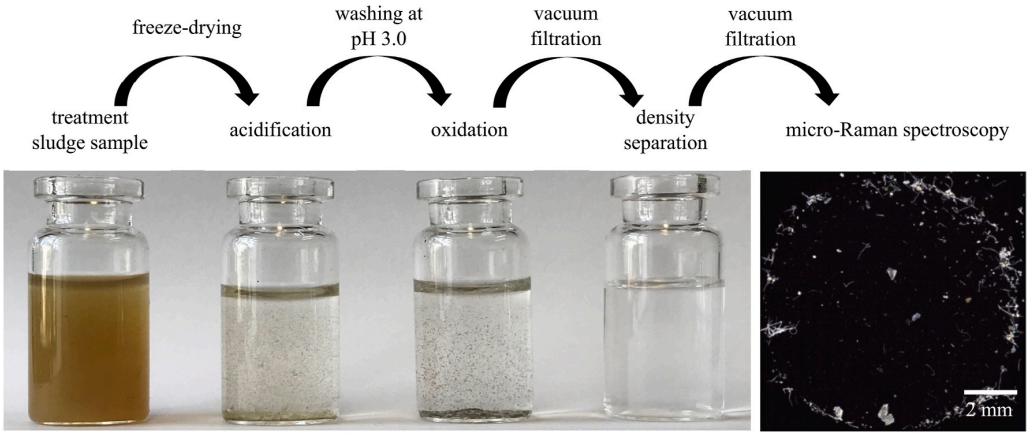


Fig. 2. Workflow for sample preparation. The depicted 10 mL treatment sludge aliquot elucidates the purification progress during sample treatment. The right image shows a silicon wafer ready for micro-Raman spectroscopy, loaded with the residual particles from 500 mL purified treatment sludge.

Table 1
Abundance of MP for the Warnow river determined by treatment sludge analysis (DWTP) and conventional samplings (*in situ*). MP abundance is reported as average ± standard deviation. P-value below 0.05 indicate statistical significance marked by asterisk.

Polymer	# MP m^{-3}		p
	DWTP[a]	*in situ*[b]	
PE	117 ± 90	63 ± 73	0.40
PP	34 ± 28	107 ± 94	0.09
PS	45 ± 20	33 ± 14	0.39
PET	0 ± 0	12 ± 21	0.17
PVC	0 ± 0	2 ± 4	0.20
Others	0 ± 0	17 ± 14	0.02*
Total	**196 ± 42**	**233 ± 36**	**0.70**

[a] based on 4 independent replicates.

[b] based on 8 independent replicates.

determined for the German Warnow river by analysing treatment sludge from an affiliated DWTP. The MP concentration and polymer distribution derived for riverside coincided with the results from conventional *in situ* samplings, thereby validating the integrative approach.

4.1. Evaluation of the integrative approach

Despite the similarities in the results, there was nevertheless a discrepancy in the occurrence of MP > 500 µm between DWTP and *in situ*, as no MP of this size range was detected in DWTP, but an average MP abundance of 29 m^{-3} was found *in situ*. For every MP size fraction investigated in this study, the *in situ* number of MP was about 20 times higher than that for DWTP (Fig. S7). Transferring this trend to MP size fraction > 500 µm indicates that only 1–3 MPs would have been detected in 500 mL treatment sludge which falls within the error range of the MP analysis. To overcome the potential bias in MP size distribution for future investigations, increasing the sample volume of treatment sludge by 2–3 times is recommended.

MP size distribution can also be affected by MP transportation in freshwater systems as this mainly depends on particle size, density and flow velocity (Horton et al., 2017). For the Warnow river, a dry weather flow rate of about 0.07 m/s (10 m^3/s) during sampling can favour sedimentation of larger and higher density plastic particles, limiting their drift compared to smaller and lower density MPs (Besseling et al., 2017; Nizzetto et al., 2016; Pivokonsky et al., 2020). The proximity of DWTP and the *in situ* sampling site was chosen to ensure comparable MP transport behaviour so that the *in situ* samples can be considered as representative for the raw water sucked by the DWTP. In this regard, the "Rocket" sampling device as well as the DWTP both collected raw water from the Warnow river surface. However, complementary sediment studies can contribute to explore the role of the river sediment as a MP

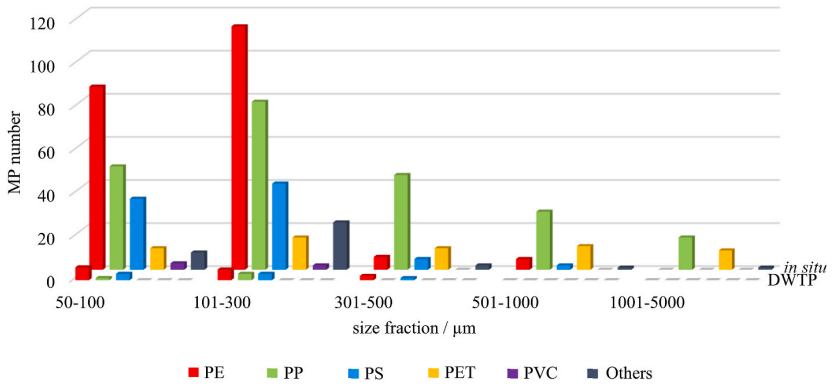


Fig. 3. Distribution of MP polymer type and MP size fraction. MP size classification was based on the longest dimension of the particles and the fibres, respectively. The size fraction 101–300 µm formed the modal value for both DWTP and *in situ*.

sink (Osinski et al., 2020). In any case, the MPs in DWTP consisted of PE, PP and PS, while selected *in situ* samples additionally comprised PET, PVC and other thermoplastics and elastomers. This discrepancy is attributed to a temporal source dynamics for MP in the aquatic environment as not every *in situ* sample contained the aforementioned MP polymer types (Campanale et al., 2020; Cohen et al., 2019; Piehl et al., 2021; Rodrigues et al., 2018; Stanton et al., 2020).

For the average MP abundance, a disparity of 19 % is stated between DWTP and *in situ*. However, no significant differences either for the average MP concentration or for the frequency of the prevailing polymers PE, PP, PS, PET and PVC were discerned. Moreover, the MPs in DWTP and *in situ* displayed similar proportions of fragments and fibres. The integrative approach is based on the entire MP elimination from raw water in particle removal processes. In respect to coagulation/flocculation/sedimentation, previous studies have investigated MP removal either in lab-scale experiments or also at operating DWTPs, resulting in very different removal efficiencies.

For ordinary coagulant dosages of < 20 mg*L^{-1}, Ma et al. (2019a, 2019b) attained a removal of 8 % for PE fragments (< 500 μm) after respective treatment with ferric chloride and aluminium chloride in a synthetic drinking water matrix. Zhang et al. (2020) captured 14 % of PE beads (45–53 μm) in coagulation/flocculation/sedimentation with alum and polydiallyldimethylammonium chloride, and biofilm formation on PE enhanced separation efficiency up to 16 %. In contrast, Lapointe et al. (2020) removed 97 % of polyester fibres (581 μm average length), 84 % of PS microspheres (140 μm) and 82 % of pristine PE microspheres (140 μm) using aluminium coagulant and PAM. After exposure to ultraviolet radiation and natural organic matter, removal of weathered PE (140 μm) increased to 99 % (Lapointe et al., 2020). Rajala et al. (2020) removed 99 % of spherical PS beads (<10 μm) using ferric chloride and after application of PAC removal reached 98 %.

Surveying MP coagulation/flocculation/sedimentation at surface water supplied DWTPs, Pivokonsky et al. (2020) determined a MP removal rate of 62 % (> 1 μm) being composed of 13 different polymer types. Wang et al. (2020) reported a maximum removal of 55 % for MP of the same size range comprised of 6 different plastic types. While Lapointe et al. (2020) and Rajala et al. (2020) observed a decreasing MP removal with increasing particle size, this trend was opposing for both field studies: MP removal enhanced at larger particle sizes, whereby fibres were most effectively captured in coagulation/flocculation in view of their settling and aggregation ability (Katrivesis et al., 2019). Regarding the DWTP Rostock, pre-ozonation links raw water abstraction and coagulation/flocculation/sedimentation. For post-ozonation, Wang et al. (2020) reported an increase in the number of MP < 5 μm by 16 % ascribed to shearing forces that led to MP fragmentation. However, this is below MP size range being investigated in this study. As the pre-ozonation aims for the oxidation of iron and manganese, more research is required to study the fate of MP especially for small size categories (< 50 μm) at this DWTP process stage.

Hitherto, Lapointe et al. (2020) and Rajala et al. (2020) provide the most comprehensive laboratory studies on MP coagulation/flocculation with an experimental setup meeting typical working conditions at DWTPs, and pointing towards extensive MP removal. The low MP separation reported by Ma et al. (2019a, 2019b) could result from the high mixing speed and the short settling time applied in combination with possible flotation of PE flocs. At the DWTP Rostock, particle aggregates passing through coagulation/flocculation/sedimentation are likely to be retained by subsequent sand filtration as these filters hold back particles and aggregates in the micrometre range (Talvitie et al., 2017). As the sand filter is backwashed daily and the backflushing water is returned to coagulation/flocculation to promote particle removal, MPs from raw water are recovered in the treatment sludge. Therefore, backwashing of sand filters increases representativeness in the determination of riverside MP abundance by analysing treatment sludge. To substantiate MP removal rates at operating DWTPs, a higher number of field studies are vital. For the DWTP Rostock, however, the drinking water itself did not contain any MP > 50 μm as confirmed by micro-Raman analysis (Siegel, unpublished data).

MPs in freshwater systems are exposed to environmental degradation forces impairing particle structure by photooxidation and shearing stress, the level of which is dependent on residential time (Cai et al., 2018; Da Costa et al., 2018; Niu et al., 2021). Lapointe et al. (2020) deduced strong interactions between coagulants, flocculants and weathered MP due to modified particle surface properties by natural organic matter coating or roughness, resulting in higher removal efficiencies compared to unscathed MP. In this regard, further investigations are necessary to address the effect of biofilms in the coagulation/flocculation of weathered MP.

The integrative approach in this study is determined by period and volume of raw water abstraction leading to treatment sludge accumulation at the DWTP. To ensure both sludge sample homogeneity and sample representativeness for the entire 20 m^3 of treatment sludge, sampling was conducted simultaneously to treatment sludge removal from the coagulation/flocculation/sedimentation plant. For the DWTP Rostock, sludge removal occurred at regular intervals of 3 h, but depending on the process control at other DWTPs, this timing, as well as the corresponding period of raw water intake, can differ. In contrast, conventional sampling methods commonly are based on shorter timeframes.

Moreover, treatment sludge investigations at DWTPs generally have higher reproducibility compared to spot-selective sampling with nets or pumping systems: DWTPs are stationary, continuously operating facilities with high process stability and consistency. For non-stationary sampling devices, ensuring reproducible results requires the correct alignment of the sampling system according to sampling purpose as well as comparable additional equipment like flowmeters (Hidalgo-Ruz et al., 2012; Löder and Gerdts, 2015; Stock et al., 2019). Thus, integrative sampling is a more reliable approach for long term monitoring of MP loads in rivers.

4.2. Sample preparation method

To validate sample preparation, recovery experiments with PE and PA 6 were conducted. MP recovery appeared to be more dependent on particle size than on density, as MP adhesion to surfaces increases at decreasing particle sizes (Stock et al., 2020). Vacuum filtration and density separation were the purification steps with highest MP loss when the samples were transferred to other glass equipment. Recovery could also be affected by the fluorescent coating of the PE spheres which facilitated surface adhesion compared to untreated or weathered PE (Waldman and Rillig, 2020). Nevertheless, the obtained recovery rate of 85–100 % is comparable to previous MP purification methods (Claessens et al., 2013; Miller et al., 2017; Quinn et al., 2017).

Preservation of MP structure and morphology was ensured by the consideration of the following sample preparation conditions: (i) MP is considered to be resistant against minimum pH 3.0 and maximum temperature 40 °C (Stock et al., 2019); (ii) hydrogen peroxide is a common oxidant which does not degrade MP (Tagg et al., 2015); (iii) HCl was used for acidification to avoid oxidative MP impairment (Enders et al., 2017). For sample homogenization, ultrasonication was used for a total of 1 min. While brittle and aged MP can fragment under several minutes of sonication (Löder and Gerdts, 2015), no alternative method for particle disaggregation with a comparable effectiveness was available. It is worth noting that the model MP from recovery experiments did not exhibit any obvious damages after sample preparation in microscopic appraisal.

Regarding spectroscopic particle detection, PAM neither led to misidentification of inorganic particles as MP nor inhibited the interpretation of other polymer spectra. PAM interference on particle surfaces is expected to depend on the degree of PAM coverage and layer thickness. Flocculation tests indicate that PAM chains sorb to flocculated particles, but as a result of the low dosage in water treatment, coating is

insufficient to provoke interfering signals. Furthermore, the absence of PAM signals in flocculation test samples being filtered and heated indicate that the polymer was not thermically impaired. Likewise, no thermal damage was observed for PA 6 based on the Raman spectra congruence after both preparation procedures. Thus, PAM did not interfere or hamper the spectroscopic identification of flocculated particles.

5. Conclusions

MPs in surface water from the Warnow river were representatively recovered in treatment sludge from an affiliated DWTP. Treatment sludge correlated with a total of 1000 m^3 raw water intake over a period of 3 h, framing the integrative approach to determine riverside MP abundance. The validation of the integrative approach was derived from the conformity of concentration and polymer distribution from reference *in situ* sampling based on the assumption of a consistent MP load for the Warnow river.

To further evaluate the integrative approach, future research activities should emphasize MP removal at individual process stages at operating DWTPs to complement current laboratory studies. Additional sampling of treatment sludge and *in situ* for different hydrological situations and seasons would strengthen the method validation to predict MP concentrations by analysing DWTP sludge. The widespread exploitation of surface waters as drinking and process water reservoirs, and common coagulation/flocculation treatment highlights the transferability of the integrative concept. The concentration of suspended solids from raw water into treatment sludge opens up the potential to conclude local MP freshwater abundance by analysing a manageable sample set which thus exceeds time and volume capacity of current sampling instrumentations. In consequence, integrative determination of MP abundance can be transferred to flowing waters with fluctuating MP load to derive more reliable conclusions on MP abundance compared to short-term sampling strategies.

CRediT author statement

Henrik Siegel: Methodology, Investigation, Formal analysis, Writing - original draft. **Franziska Fischer**: Investigation, Formal analysis, Writing - Review & editing. **Robin Lenz**: Investigation, Formal analysis, Writing - Review & editing. **Dieter Fischer**: Formal analysis, Writing - Review & editing. **Martin Jekel**: Methodology, Writing - Review & editing. **Matthias Labrenz**: Resources, Methodology, Writing - Review & editing.

Declaration of competing interest

The authors declare that they have no known competing financial interests or personal relationships that could have appeared to influence the work reported in this paper.

Acknowledgement

This research was funded by the project MicroCatch_Balt (03F0788A) supported by the Federal Ministry of Education and Research (BmBF). The authors thank the Nordwasser GmbH for kind assistance in sampling and also Kristina Enders, Juliana Ivar do Sul and Alexander Tagg for helpful discussions or English proofreading, respectively.

Appendix A. Supplementary data

Supplementary data to this article can be found online at https://doi.org/10.1016/j.envpol.2021.117524.

References

Besseling, E., Quik, J.T.K., Sun, M., Koelmans, A.A., 2017. Fate of nano- and microplastic in freshwater systems: a modeling study. Environ. Pollut. 220, 540–548. https://doi.org/10.1016/j.envpol.2016.10.001.

Brandt, J., Bittrich, L., Fischer, F., Kanaki, E., Tagg, A., Lenz, R., Labrenz, M., Brandes, E., Fischer, D., Eichhorn, K.J., 2020. High-throughput analyses of microplastic samples using fourier transform infrared and Raman spectrometry. Appl. Spectrosc. 74 (9), 1185–1197. https://doi.org/10.1177/0003702820932926.

Bratby, J., 2016. Coagulation and Flocculation in Water and Wastewater Treatment, third ed. IWA Publishing https://www.iwapublishing.com/books/9781780407494/coagulation-and-flocculation-water-and-wastewater-treatment-third-edition.

Browne, M.A., Dissanayake, A., Galloway, T.S., Lowe, D.M., Thompson, R.C., 2008. Ingested microscopic plastic translocates to the circulatory system of the mussel, *Mytilus edulis* (L.). Environ. Sci. Technol. 42 (13), 5026–5031. https://doi.org/10.1021/es800249a.

Browne, M.A., Crump, P., Niven, S.J., Teuten, E., Tonkin, A., Galloway, T., Thompson, R., 2011. Accumulation of microplastic on shorelines woldwide: sources and sinks. Environ. Sci. Technol. 45 (21), 9175–9179. https://doi.org/10.1021/es201811s.

Cai, L., Wang, J., Peng, J., Wu, Z., Tan, X., 2018. Observation of the degradation of three types of plastic pellets exposed to UV irradiation in three different environments. Sci. Total Environ. 628–629, 740–747. https://doi.org/10.1016/j.scitotenv.2018.02.079.

Campanale, C., Stock, F., Massarelli, C., Kochleus, C., Bagnuolo, G., Reifferscheid, G., Uricchio, V.F., 2020. Microplastics and their possible sources: the example of Ofanto river in southeast Italy. Environ. Pollut. 258 https://doi.org/10.1016/j.envpol.2019.113284.

Claessens, M., Meester, S. De, Landuyt, L., Van, Clerck, K. De, Janssen, C.R., 2011. Occurrence and distribution of microplastics in marine sediments along the Belgian coast. Mar. Pollut. Bull. 62 (10), 2199–2204. https://doi.org/10.1016/j.marpolbul.2011.06.030.

Claessens, M., Van Cauwenberghe, L., Vandegehuchte, M.B., Janssen, C.R., 2013. New techniques for the detection of microplastics in sediments and field collected organisms. Mar. Pollut. Bull. 70 (1–2), 227–233. https://doi.org/10.1016/j.marpolbul.2013.03.009.

Cohen, J.H., Internicola, A.M., Mason, R.A., Kukulka, T., 2019. Observations and simulations of microplastic debris in a tide, wind, and freshwater-driven estuarine environment: the Delaware Bay. Environ. Sci. Technol. 53 (24), 14204–14211. https://doi.org/10.1021/acs.est.9b04814.

Cole, M., Lindeque, P., Fileman, E., Halsband, C., Goodhead, R., Moger, J., Galloway, T. S., 2013. Microplastic ingestion by zooplankton. Environ. Sci. Technol. 47 (12), 6646–6655. https://doi.org/10.1021/es400663f.

Da Costa, J.P., Nunes, A.R., Santos, P.S.M., Girão, A.V., Duarte, A.C., Rocha-Santos, T., 2018. Degradation of polyethylene microplastics in seawater: insights into the environmental degradation of polymers. J. Environ. Sci. Health A 53 (9), 866–875. https://doi.org/10.1080/10934529.2018.1455381.

Doyle, M.J., Watson, W., Bowlin, N.M., Sheavly, S.B., 2011. Plastic particles in coastal pelagic ecosystems of the Northeast Pacific ocean. Mar. Environ. Res. 71 (1), 41–52. https://doi.org/10.1016/j.marenvres.2010.10.001.

Dubaish, F., Liebezeit, G., 2013. Suspended microplastics and black carbon particles in the Jade system, southern North Sea. Water Air Soil Pollut. 224 (2), 1–8. https://doi.org/10.1007/s11270-012-1352-9.

Enders, K., Lenz, R., Beer, S., Stedmon, C.A., 2017. Extraction of microplastic from biota: recommended acidic digestion destroys common plastic polymers. ICES J. Mar. Sci. 74 (1), 326–331. https://doi.org/10.1093/icesjms/fsw173.

Enders, K., Lenz, R., Ivar do Sul, J.A., Tagg, A.S., Labrenz, M., 2020. When every particle matters: a QuEChERS approach to extract microplastics from environmental samples. Methods (Duluth) 7, 100784. https://doi.org/10.1016/j.mex.2020.100784.

Eriksen, M., Mason, S., Wilson, S., Box, C., Zellers, A., Edwards, W., Farley, H., Amato, S., 2013a. Microplastic pollution in the surface waters of the laurentian great lakes. Mar. Pollut. Bull. 77 (1–2), 177–182. https://doi.org/10.1016/j.marpolbul.2013.10.007.

Eriksen, M., Maximenko, N., Thiel, M., Cummins, A., Lattin, G., Wilson, S., Hafner, J., Zellers, A., Rifman, S., 2013b. Plastic pollution in the South Pacific subtropical gyre. Mar. Pollut. Bull. 68 (1–2), 71–76. https://doi.org/10.1016/j.marpolbul.2012.12.021.

GESAMP Joint group of experts on the scientific aspects of marine environmental protection, 2015. Sources, fate and effects of microplastics in the marine environment: a global assessment. Rep. Stud. GESAMP 90, 96. https://doi.org/10.13140/RG.2.1.3803.7925.

Hidalgo-Ruz, V., Gutow, L., Thompson, R.C., Thiel, M., 2012. Microplastics in the marine environment: a review of the methods used for identification and quantification. Environ. Sci. Technol. 46 (6), 3060–3075. https://doi.org/10.1021/es2031505.

Horton, A.A., Walton, A., Spurgeon, D.J., Lahive, E., Svendsen, C., 2017. Microplastics in freshwater and terrestrial environments: evaluating the current understanding to identify the knowledge gaps and future research priorities. Sci. Total Environ. 586, 127–141. https://doi.org/10.1016/j.scitotenv.2017.01.190.

Käppler, A., Windrich, F., Löder, M.G.J., Malanin, M., Fischer, D., Labrenz, M., Eichhorn, K.J., Voit, B., 2015. Identification of microplastics by FTIR and Raman microscopy: a novel silicon filter substrate opens the important spectral range below 1300 cm^{-1} for FTIR transmission measurements. Anal. Bioanal. Chem. 407 (22) https://doi.org/10.1007/s00216-015-8850-8.

Katrivesis, F.K., Karela, A.D., Papadakis, V.G., Paraskeva, C.A., 2019. Revisiting of coagulation-flocculation processes in the production of potable water. J. Water Process Eng. 27, 193–204. https://doi.org/10.1016/j.jwpe.2018.12.007.

Koelmans, A.A., Mohamed Nor, N.H., Hermsen, E., Kooi, M., Mintenig, S.M., De France, J., 2019. Microplastics in freshwaters and drinking water: critical review and assessment of data quality. Water Res. 155, 410–422. https://doi.org/10.1016/j.watres.2019.02.054.

Lapointe, M., Farner, J.M., Hernandez, L.M., Tufenkji, N., 2020. Understanding and improving microplastic removal during water treatment: impact of coagulation and flocculation. Environ. Sci. Technol. 54 (14), 8719–8727. https://doi.org/10.1021/acs.est.0c00712.

Lenz, R., Labrenz, M., 2018. Small microplastic sampling in water: development of an encapsulated filtration device. Water 10 (8), 1055. https://doi.org/10.3390/w10081055.

Li, J., Liu, H., Paul Chen, J., 2018. Microplastics in freshwater systems: a review on occurrence, environmental effects, and methods for microplastics detection. Water Res. 137, 362–374. https://doi.org/10.1016/j.watres.2017.12.056.

Löder, M.G.J., Gerdts, G., 2015. Methodology used for the detection and identification of microplastics - a critical appraisal. Marine Anthropogenic Litter 201–227. https://doi.org/10.1007/978-3-319-16510-3_8.

Ma, B., Xue, W., Ding, Y., Hu, C., Liu, H., Qu, J., 2019a. Removal characteristics of microplastics by Fe-based coagulants during drinking water treatment. J. Environ. Sci. (China) 78, 267–275. https://doi.org/10.1016/j.jes.2018.10.006.

Ma, B., Xue, W., Hu, C., Liu, H., Qu, J., Li, L., 2019b. Characteristics of microplastic removal via coagulation and ultrafiltration during drinking water treatment. Chem. Eng. J. 359, 159–167. https://doi.org/10.1016/j.cej.2018.11.155.

Miller, M.E., Kroon, F.J., Motti, C.A., 2017. Recovering microplastics from marine samples: a review of current practices. Mar. Pollut. Bull. 123 (1–2), 6–18. https://doi.org/10.1016/j.marpolbul.2017.08.058.

Murray, F., Cowie, P.R., 2011. Plastic contamination in the decapod crustacean *Nephrops norvegicus* (L.). Mar. Pollut. Bull. 62 (6), 1207–1217. https://doi.org/10.1016/j.marpolbul.2011.03.032.

Ng, K.L., Obbard, J.P., 2006. Prevalence of microplastics in Singapore's coastal marine environment. Mar. Pollut. Bull. 52 (7), 761–767. https://doi.org/10.1016/j.marpolbul.2005.11.017.

Niu, L., Li, Y., Li, Y., Hu, Q., Wang, C., Hu, J., Zhang, W., Wang, L., Zhang, C., Zhang, H., 2021. New insights into the vertical distribution and microbial degradation of microplastics in urban river sediments. Water Res. 188, 116449. https://doi.org/10.1016/j.watres.2020.116449.

Nizzetto, L., Bussi, G., Futter, M.N., Butterfield, D., Whitehead, P.G., 2016. A theoretical assessment of microplastic transport in river catchments and their retention by soils and river sediments. Environ. Sci. Process. Impact. 18 (8), 1050–1059. https://doi.org/10.1039/c6em00206d.

Novotna, K., Cermakova, L., Pivokonska, L., Cajthaml, T., Pivokonsky, M., 2019. Microplastics in drinking water treatment - current knowledge and research needs. Sci. Total Environ. 667, 730–740. https://doi.org/10.1016/j.scitotenv.2019.02.431.

Osinski, R.D., Enders, K., Gräwe, U., Klingbeil, K., Radtke, H., 2020. Model uncertainties of a storm and their influence on microplastics and sediment transport in the Baltic Sea. Ocean Sci. 16 (6), 1491–1507. https://doi.org/10.5194/os-16-1491-2020.

Piehl, S., Hauk, R., Robbe, E., Richter, B., Kachholz, F., Schilling, J., Lenz, R., Fischer, D., Fischer, F., Labrenz, M., Schernewski, G., 2021. Combined approaches to predict microplastic emissions within an urbanized estuary (Warnow, southwestern Baltic Sea). Front. Environ. Sci. 9, 41. https://doi.org/10.3389/FENVS.2021.616765.

Pivokonsky, M., Pivokonská, L., Novotná, K., Čermáková, L., Klimtová, M., 2020. Occurrence and fate of microplastics at two different drinking water treatment plants within a river catchment. Sci. Total Environ. 741, 140236. https://doi.org/10.1016/j.scitotenv.2020.140236.

PlasticsEurope, 2019. Plastics - the Facts 2019. An Analysis of European Plastics Production, Demand and Waste Data. https://www.plasticseurope.org/de/resources/publications/1804-plastics-facts-2019.

Quinn, B., Murphy, F., Ewins, C., 2017. Validation of density separation for the rapid recovery of microplastics from sediment. Anal. Methods 9 (9), 1491–1498. https://doi.org/10.1039/c6ay02542k.

Rajala, K., Grönfors, O., Hesampour, M., Mikola, A., 2020. Removal of microplastics from secondary wastewater treatment plant effluent by coagulation/flocculation with iron, aluminum and polyamine-based chemicals. Water Res. 183, 116045. https://doi.org/10.1016/j.watres.2020.116045.

Rodrigues, M.O., Abrantes, N., Gonçalves, F.J.M., Nogueira, H., Marques, J.C., Gonçalves, A.M.M., 2018. Spatial and temporal distribution of microplastics in water and sediments of a freshwater system (Antuã River, Portugal). Sci. Total Environ. 633, 1549–1559. https://doi.org/10.1016/j.scitotenv.2018.03.233.

Stanton, T., Johnson, M., Nathanail, P., MacNaughtan, W., Gomes, R.L., 2020. Freshwater microplastic concentrations vary through both space and time. Environ. Pollut. 263, 114481. https://doi.org/10.1016/j.envpol.2020.114481.

Stock, F., Narayana, B., K, V., Scherer, C., Löder, M.G.J., Brennholt, N., Laforsch, C., Reifferscheid, G., 2020. Pitfalls and Limitations in Microplastic Analyses, vols. 1–30. Springer, Berlin, Heidelberg. https://doi.org/10.1007/698_2020_654.

Stock, F., Kochleus, C., Bänsch-Baltruschat, B., Brennholt, N., Reifferscheid, G., 2019. Sampling techniques and preparation methods for microplastic analyses in the aquatic environment – a review. Trends Anal. Chem. 113, 84–92. https://doi.org/10.1016/j.trac.2019.01.014.

Tagg, A.S., Sapp, M., Harrison, J.P., Ojeda, J.J., 2015. Identification and quantification of microplastics in wastewater using focal plane array-based reflectance micro-FT-IR imaging. Anal. Chem. 87 (12), 6032–6040. https://doi.org/10.1021/acs.analchem.5b00495.

Talvitie, J., Mikola, A., Koistinen, A., Setälä, O., 2017. Solutions to microplastic pollution – removal of microplastics from wastewater effluent with advanced wastewater treatment technologies. Water Res. 123, 401–407. https://doi.org/10.1016/j.watres.2017.07.005.

Triebskorn, R., Braunbeck, T., Grummt, T., Hanslik, L., Huppertsberg, S., Jekel, M., Knepper, T.P., Krais, S., Müller, Y.K., Pittroff, M., Ruhl, A.S., Schmieg, H., Schür, C., Strobel, C., Wagner, M., Zumbülte, N., Köhler, H.R., 2019. Relevance of nano- and microplastics for freshwater ecosystems: a critical review. Trends Anal. Chem. 110, 375–392. https://doi.org/10.1016/j.trac.2018.11.023.

Ugolini, A., Ungherese, G., Ciofini, M., Lapucci, A., Camaiti, M., 2013. Microplastic debris in sandhoppers. Estuar. Coast Shelf Sci. 129, 19–22. https://doi.org/10.1016/j.ecss.2013.05.026.

Waldman, W.R., Rillig, M.C., 2020. Microplastic research should embrace the complexity of secondary particles. Environ. Sci. Technol. 54 (13), 7751–7753. https://doi.org/10.1021/acs.est.0c02194.

Wang, Z., Lin, T., Chen, W., 2020. Occurrence and removal of microplastics in an advanced drinking water treatment plant (ADWTP). Sci. Total Environ. 700 https://doi.org/10.1016/j.scitotenv.2019.134520.

Who, 2019. Microplastics in Drinking-Water. http://www.who.int/water_sanitation_health/publications/microplastics-in-drinking-water/en/.

Zhang, Y., Diehl, A., Lewandowski, A., Gopalakrishnan, K., Baker, T., 2020. Removal efficiency of micro- and nanoplastics (180 nm–125 μm) during drinking water treatment. Sci. Total Environ. 720 https://doi.org/10.1016/j.scitotenv.2020.137383.

This is the end of the publication

Identification and quantification of microplastic particles in drinking water treatment sludge as an integrative approach to determine microplastic abundance in a freshwater river

by Henrik Siegel, Franziska Fischer, Robin Lenz, Dieter Fischer, Martin Jekel, Matthias Labrenz

You might want to continue reading the synopsis at page 24, or jump back to the start of this publication at page 140.

Measuring impacts of microplastic treatments via image recognition on immobilised particles below 100 µm

by Robin Lenz, Kristina Enders, Franziska Fischer, Josef Brandt, Dieter Fischer, Matthias Labrenz

- **Date published**: July 18, 2021
- **Type**: Research Article
- **Published in**: Microplastics and Nanoplastics

- **License**: CC-BY

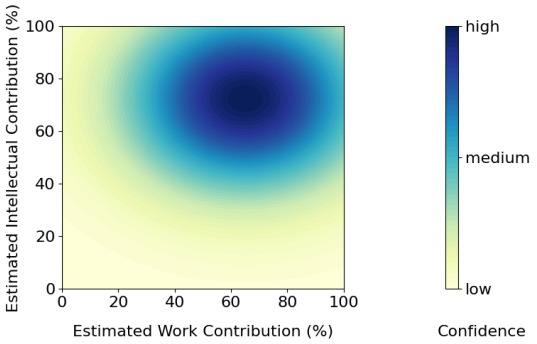
- **DOI**: 10.1186/s43591-021-00012-0, **Reference**: [9]
- **Citations**: 13 (Crossref/DOI, 2025-11-18)

Contributions

RL, KE, DF and ML developed the idea for this research | RL, KE, and FF contributed the conception and design of the work | RL, KE and FF conducted the acquisition, analysis and interpretation of data | RL and JB created new software used in the work | JB provided code revision | RL, KE and FF have drafted the manuscript | JB, DF and ML substantively revised it. The authors read and approved the final manuscript.

Quantitative own contributions based on self-assessment

In the dimensions of expended work effort and intellectual contribution, I consider my shares are likely to be between 50% and 80% and between 60% and 85% respectively. This is visualised below as an interpolated histogram of 500 samples from Gaussian distributions with the aforementioned estimates at plus/minus two standard deviations.



Lenz *et al. Microplastics and Nanoplastics* (2021) 1:12
https://doi.org/10.1186/s43591-021-00012-0

Microplastics and Nanoplastics

RESEARCH ARTICLE Open Access

Measuring impacts of microplastic treatments via image recognition on immobilised particles below 100 µm

Robin Lenz[1*], Kristina Enders[1], Franziska Fischer[2], Josef Brandt[3], Dieter Fischer[2] and Matthias Labrenz[1*]

Abstract

The treatment of samples for microplastic (MP) analysis requires purification steps that sufficiently reduce the non-MP content while preserving the targeted particles integrity. Besides their macromolecular structure this also encompasses their in situ numbers and sizes. However, any step of sample manipulation will come at a cost: particle loss, fragmentation, coagulation or degradation may lead to distorted results, predominantly in the smaller fraction of the MP size range. Therefore, the evaluation of MP resistivity against applied methods such as chemical digestions is a vital criterion for obtaining meaningful results on MP content of a sample. We developed a framework to test the applicability of MP purification methods and apply it to four protocols commonly used to prepare environmental samples for MP particle identification. The approach was designed for MP particles being too small to be handled manually (i.e. 10–70 µm). The evaluation consists of a two-tiered assay: a simple particle suspension approach is used to confirm a post-treatment qualitative recognisability of the target polymers by the analysis method of choice (here Raman and FTIR). In a following quantitative part, immobilised particles are used to evaluate the preservation of particle numbers and areas after the treatment on an individual particle level. A Python image analysis package was written that identifies, matches and measures particles on pairs of pre- and post-treatment images, and is available as open source software. Our results show that the chemical digestions using hydrogen peroxide, cooled Fenton's and a combined alkaline / oxidative treatment using potassium hydroxide and sodium hypochlorite are suitable methods for preparing MP samples for a microspectroscopic analyses. Also acidic sodium polytungstate solution used for MP density separations and a pentane based protocol for lipid removal were found applicable for small sized MP. Certain degradative effects were found when acrylonitrile butadiene styrene is exposed to acidic treatments, as well as for MP from acrylate and epoxy based paint resins in strong oxidative regimes. Several paint resins tested here were spectroscopically not identifiable by polymer attributed bands even before treatment, indicating that these materials might slip through analyses of environmental samples and consequently being underreported. We conclude that evaluating chemical treatment procedures on MP < 100 µm is feasible, despite limitations of the current methodology which we discuss. Our results provide more certainty on the tested methods for MP studies specifically targeting small sizes and should be extended for more protocols used in MP laboratory practises.

Keywords: Microplastics, Purification, Digestion, Qualitative, Quantitative, Resistivity, Method evaluation, Validation, Image recognition

* Correspondence: robin.lenz@io-warnemuende.de; matthias.labrenz@io-warnemuende.de
[1]Leibniz Institute for Baltic Sea Research Warnemünde, Seestraße 15, 18119 Rostock, Germany
Full list of author information is available at the end of the article

Springer Open

© The Author(s). 2021 **Open Access** This article is licensed under a Creative Commons Attribution 4.0 International License, which permits use, sharing, adaptation, distribution and reproduction in any medium or format, as long as you give appropriate credit to the original author(s) and the source, provide a link to the Creative Commons licence, and indicate if changes were made. The images or other third party material in this article are included in the article's Creative Commons licence, unless indicated otherwise in a credit line to the material. If material is not included in the article's Creative Commons licence and your intended use is not permitted by statutory regulation or exceeds the permitted use, you will need to obtain permission directly from the copyright holder. To view a copy of this licence, visit http://creativecommons.org/licenses/by/4.0/.

Introduction

Microplastic (MP) purification techniques were developed by a number of studies in order to facilitate measurements of abundance of this inhomogeneous group of environmental contaminants [1–12] and reviews of recent developments are available [13–18]. Within MP, practically any synthetic polymeric material can be of interest, among others classical thermoplastics, varieties of elastomers as well as paint resins. The challenge has been to extract all relevant particles from the large diversity of sample matrices.

Depending on the system studied these matrices typically consist to large degrees of inorganic fractions like minerals from sediments and soils [19], and organic content such as detritus, tissue or microbial films, particularly confounding spectroscopic analysis [20]. The contained MP loads often range in the ppm to ppt (w/w, [21]). Physical density and chemical inertness to certain degradative agents are the two most harnessed properties of MP to facilitate a separation from the respective sample matrix. However, both of these principles involve deficiencies contributing to uncertainties in the resulting numbers or masses of MP obtained through the subsequent analysis of the treated samples.

For density separation, hydrodynamic problems occur that can hinder the intended particle advection. These include flocculation or coagulation of targeted and non-targeted particles altering the apparent density [22] as well as forces such as turbulence and adhesion [23] counteracting the — with decreasing particle size diminishing — impact of buoyancy. Also mechanical action involved in any extraction technique can contribute to errors for instance if samples are incompletely transferred between vessels or particles are altered through activities such as shaking, grinding, stirring or ultrasonication [24]. In chemical digestion processes loss of relevant particles can occur through unwanted chemical interactions of certain MP species with the applied digestant such as oxidation, hydrolytic polymer chain cleavage, or bleaching.

Purification steps aiming at the removal of non-targeted material through dissolution involve chemicals that exhibit degradative effects on these materials while — in the optimal case — leaving the present MP unimpacted. Based on the high chemical diversity of both, the material group of plastics and the unwanted constituents, the selection of suitable protocols for purification are a critical and difficult task. This includes the rigorous testing of the MP particles resistivity to a method in question. A broad range of plastic polymer types needs to be examined, as their large chemical diversity provides a variety of possibilities for chemical degradation. The size range of particles being tested needs to match the lower sizes of MP targeted by the planned environmental studies aiming to apply the respective protocol. Existing method development and validation studies often tested against larger MP or macroplastic items [1, 25, 26], which allows relatively simple experimental designs. The resistance of larger plastic objects (e.g. millimetre sized pellets) against a digestive reagent is, however, no sufficient cause to assume that this would be equally the case for MP orders of magnitude smaller. Hence, MP particles in the lower μm size are of paramount importance in method validation tests, which was also emphasised by another recent study [12]. There are reasons to attest them a higher vulnerability to chemical degradation than larger particles, due to their increased surface to volume ratio, resulting in a higher number of exposed polymer backbones, functional groups and chain ends. Furthermore, the polymer matrices of MP particles in the lower micrometre scale are not necessarily homogenous, even when coming from the same origin. In the environment, weathering may reach individual particles differently and therefore produce varieties of particles differing in mean molecular weight and prevalent functional groups as well as end groups. The shares of crystalline and amorphous domains (i.e. regions of different chain folding and conformation) are related to vulnerability to degradation [27] and the typical domain size depends on the molecular weight of the chain fragment [28]. In semi-crystalline polymers the sizes, numbers and shapes of MP formed in fragmentation of degrading macroplastics depend on their crystalline morphology [29]. Varying additive content also influences certain polymer properties like mechanical strength or oxidative resistance [30].

Aim and scope

The scope of the present study is to evaluate the resistance of MP against chosen chemical agents on the example of treatment protocols previously recommended for purification of MP samples (as summarised by Enders et al. [31]). As stated above, there is already an extensive knowledge base in the literature on a variety of treatment methods, although rather heterogeneous. There is a knowledge gap, however, for resistivity of particles in the lower μm sizes, including a lack of methods for manipulations and measurements on an individual particle basis and simultaneously in large numbers. The endpoint of evaluation hereby should be the qualitative and quantitative detectability of the treated MP by microspectroscopic analyses and microscopic imaging. Our contribution is to study the impact of protocols including oxidative, alkaline, acidic and organic solvent based chemicals. They are tested on 19 polymer types (including 5 synthetic paint resins) in the size range of 10 to 70 μm (Table 1). Our primary objective is to enable method testing for particles below 100 μm, which

Table 1 Specifications of test MP particles, [a] rosin may not be regarded as a polymeric resin matrix, but was included as it is a common ingredient in self-eroding antifouling coatings of ships, and may therefore be a relevant type of environmental paint flakes

Group	Sample Name	Long Name	Origin (product name and manufacturer)	Colour	Density
Commodity Plastics	ABS	acrylonitrile butadiene styrene	Terluran GP-22, Ineos Styrolution	white	1.04
	EVA	ethylene vinyl acetate	Escorene Ultra FL 00328, Exxon Mobil	white	0.951
	HDPE	high density polyethylene	HDPE HTA 108, Exxon Mobil	white	0.961
	LDPE	low density polyethylene	LDPE LD 100.BW, Exxon Mobil	white	0.923
	PA6	polyamide 6	Ultramid B40, BASF	white	1.14
	PA6.6	polyamide 6.6	Ultramid A34 01, BASF	white	1.13
	PA12	polyamide 12	Vestamid L1600, Evonik	white	1.01
	PC	polycarbonate	Lexan 121R, Sabic	white	1.2
	PET	polyethylene terephthalate	ES306030/1 powder, Goodfellow	white	1.3–1.4
	PMMA	polymethyl methacrylate	Plexiglas 8N, Evonik	white	1.19
	PP	polypropylene	Moplen HP400R, LyondellBasell	white	0.9
	PS	polystyrene	Polystyrol 143 E, BASF	white	1.043
	PVC	polyvinylchloride	EVIPOL SH6830, Globichem	white	~ 1.4
	TPU	thermoplastic polyurethane	Elastollan C85A10, BASF	white	1.19
Paint resins	rosin [a]	maritime antifouling rosin resin	Hempel's Classic 76110, Hempel	red	n/a
	acrylate	general purpose primer acrylic resin	b1, J.W. Ostendorf	white	n/a
	PU	anticorrosive polyurethane resin	Temadur SC 533, Tikkurila Oyj	black	n/a
	epoxy	maritime anticorrosive epoxy resin	Hempadur 45148, Hempel	red	n/a
	alkyd	maritime primer alkyd resin	Hempel's Underwater Primer 26030, Hempel	grey	n/a

cannot easily be handled or manipulated due to their small size. A description of where the scope of this study has its boundaries is detailed further in the SI (S1).

We evaluate polymer resistivity to each protocol based on the following two questions:

- Qualitative: Are there diminishing effects on the spectroscopic recognisability of the polymer?
- Quantitative: Are sizes or particle numbers significantly altered?

Besides the reporting of the tested resistivities, this study commits to the principles of the open science approach, wherefore underlying data and procedures, including all implementations of algorithms that were developed in this study, are made publicly available.

Comparison of our concept to other approaches in current literature

Several studies reported polymer resistivity based on particle recoveries in spiked real matter matrices (e.g. sediments [10], soil and sludge [32, 33], or biota [10, 11]). This allows combining the evaluation of the efficacy of a digestion (matrix reduction) and the possible effect on the MP particles. However, also interactions between the matrix and MP particles may occur and can obfuscate the effects of the treatment itself on the polymers. While this may be regarded as being more realistic with respect to an actual environmental MP purification, it is less comparable and generalisable. The influence of matrix parameters (e.g. grain size, material composition) and the interaction with the spiked MP particles (coagulation, grinding, etc.) during purification treatments are not yet well understood [31]. When the focus is primarily on effects of the treatment on the polymer, the combination of digestion efficiency and polymer resistivity tests is not compulsory to yield insight into effects individual treatments may have on certain polymer particles. We chose to operate in a matrix-free environment, as to gain primary insight into the genuine reagents-particles-interactions, but acknowledge that these treatments would only practically be used in the presence of a matrix, that must be reduced, as this is the primary goal of these treatments. Hence, our assessments can be valuable basis for future matrix-specific treatment validations, which are an important and logical next step.

Evaluation tests could be done without a matrix solely by applying the treatment to a particle suspension. The post-treatment state may then be measured by solid state technique, e.g. microscopic imaging after an additional filtration step, or by liquid phase techniques such as Beckman-Coulter-Counters, flow-cytometry, laser diffraction or dynamic image analysis. Each of these techniques will have their own advantages and limitations,

but commonly, it can be said that the experimental setup and conduction would be comparably simple, as the techniques are well established, and large particle amounts could be measured (for microscopic imaging with the constraint of required filter area and measuring time). It is however not possible to relate the post-treatment measurements directly to the pre-treatment state of the same particle. When measuring effects on median particle sizes or similar properties, this is of little relevance when the particle number is large enough to yield meaningful statistical aggregates. Particle counts and their treatment-induced changes, are, however, not readily inferred from suspended bulk measurements. Furthermore, approaches working with mobile particles are prone to errors owed to the manual handling of the particles (e.g. filtration, rinsing), which are difficult to account for when working with small MP. Here lies the prospect of the technique used in the present study, where MP particles are immobilised on a plane surface, and microscopic measurements of individual particles can be linked between pre- and post-treatment conditions.

General background on the experimental model design

To evaluate the applicability of MP treatment protocols, we expose the test material of irregularly shaped MP particles to the chemicals and physical conditions of the respective protocol (Fig. 1). Before and after exposure we take the measurements on those particles as detailed below.

In a typical MP particle-based analysis the particle material is first qualitatively determined (e.g. spectroscopically, to decide acceptance or rejection as MP) and, second, for confirmed MP further properties are obtained optically (e.g. size, colour, shape). For our method validation concept, we formalised those distinct categories of measurements as two separate experimental approaches that are each optimised for their respective requirements.

Using qualitative measurements, i.e. Raman and Fourier transform infrared (FTIR) spectra, we need to determine whether a reagent has reacted with a polymer to a degree that it would no longer be recognised as what it is by means of its spectroscopic signal. To obtain this information it is not necessary to handle individual particles, which is difficult and time demanding in the targeted size range. Instead, here it is sufficient to work with bulk particle suspensions. An approximate amount of test particles is added to the liquid reagent and removed after the treatment period is over. A complete recovery of particles is not necessary. Spectra can then be acquired on any of the recovered particles. However, qualitative measurements alone are insufficient to evaluate a protocol's applicability. We need to assume that fractions of particles could be destroyed by the treatment, while others persisted and could be measured.

Quantitative measurements allow us to make a statement on whether and to which degree particles have been lost or deformed during the treatment. Due to the chosen size range individual handling of particles (e.g. by

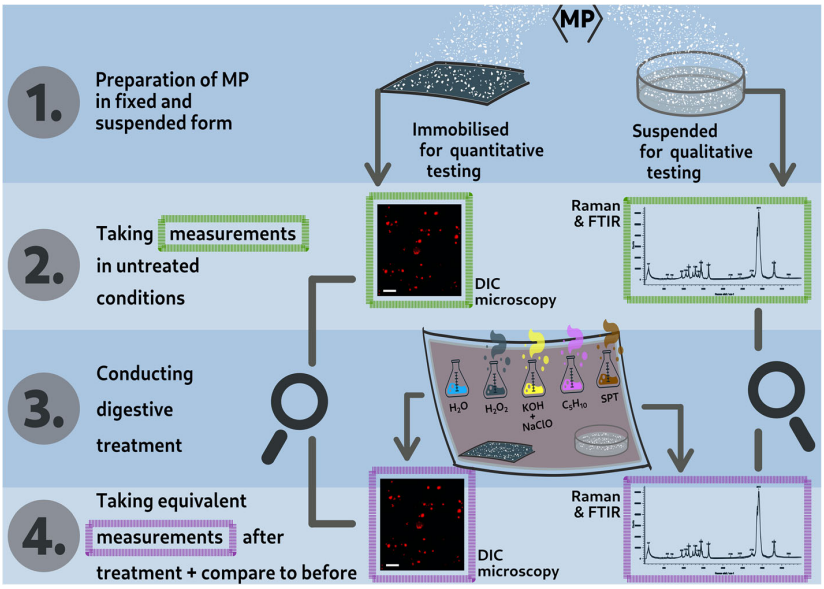


Fig. 1 Schematic visualisation of the method validation concept in a qualitative and a quantitative workflow

tweezers) for transfer or counting, is no suitable approach here. At the same time, large numbers of particles should be processed to allow for a robust statistical analysis of the measurements. The here presented approach is based on immobilising the MP particles on a silicon wafer coated with a thin film of epoxy resin. This method allows us to compare pre- and post-measurements on an individual particle basis which enables a more granular analysis, e.g. with respect to differences across the particle size spectrum. A microscopic image of a defined region of the wafer serves as the pre-treatment data point and is compared to an image of the exact same region after the treatment has been conducted.

It should be noted here that this combination of a qualitative and quantitative approach will not be able to pick up qualitative-only effects (i.e. chemical alterations not leading to effects on the quantitative particle properties), that do not occur in all particles of a polymer in a specific treatment, but rather only a hypothetical minority with certain characteristics. By the nature of the particles used herein - all being produced in the same manner from pristine raw materials - such deviant behaviours are not assumed to be occurring relevant numbers. It would be, however, a question worth investigating for future studies aiming at particle stability during treatments with a more detailed focus on exact particle properties, such as very narrow size and shape ranges, or specific surface properties.

Methods

Preparation of polymer test materials

For the group of commodity plastics pre-production polymer pellets were cryo-milled and sieved to yield particles of the targeted size range. The raw materials of each polymer type (see Table 1), were individually submitted to cryogenic ball milling (Retsch CryoMill, 50 ml grinding jar, 25 mm ball, 5–6 g raw material, pre-cooling: 10 min at 5 Hz, 6 grinding cycles consisting of 2 min milling at 35 Hz and 2 min cooling at 5 Hz). The fraction that was used in the following procedures consisted of particles that passed a 71 μm, but were retained on a 10 μm stainless steel analytical sieve (Topas GmbH). The group of paint resin polymers was obtained from commercial consumer or industrial products of common outdoor appliances or maritime paints, which were tempered as recommended by the manufacturers and squeegeed in customary manner. Films were left to cure and later ground and sieved as described above by cryo-milling.

Treatment specifications

The specifications were adapted from the original protocol references and are detailed in Table 2. All treatment solutions were filtrated at 1.5 μm prior to application (vacuum filtration in glass bottles, Whatman 943-AH glass filter membranes) and 3–5 ml of the respective reagent were added to ensure that all MP particles were wetted.

In contrast to all other treatments, the H_2O_2 treatments were not consistent between the qualitative and the quantitative analyses. Qualitatively we tested Fenton's catalysed H_2O_2 digestions (cooled and uncooled), as well as a non-catalysed 2 weeks long exposure. The quantitative approach did not include Fenton's catalysed reactions. The strongly exothermic progression of Fenton's reactions were regarded as a practically not feasible application for the particle immobilisations: strong heat and foam formation would hinder an equal exposure of all particles on a wafer. Also the 2 weeks long exposure

Table 2 Short specifications and protocol references to the tested treatments

Treatment name	Specifications	Protocol Reference
Water (negative control)	ultra-purified water, 24 h, RT	–
H_2O_2 Fenton's (Fe) uncooled [a]	30% H_2O_2 + catalyst (6.67 mg ml^{-1} of Fe(II)SO_4, pH 4), ca. 10 min, max. 85 °C (measured after 5 min)	[2]
H_2O_2 Fenton's (Fe) cooled [a]	30% H_2O_2 + catalyst (6.67 mg ml^{-1} of Fe(II)SO_4, pH 4), 24 h, 20–30 °C (on ice, measured after 5 min)	[2]
H_2O_2 LT [a]	30% H_2O_2, non-catalysed, 14 days, RT	[31]
H_2O_2 [b]	30% H_2O_2, non-catalysed, 24 h, RT	[31]
KOH + NaClO	per 1 L: 700 ml H_2O, 150 ml NaClO 14% active chlorine and 150 ml saturated KOH (1120 g L^{-1}), 5 h, RT	[1]
Pentane (C_5H_{10})	15 min in an immiscible water - ethanol (pH 3) - pentane mixture (5:1:1), shaken 3 times, 30–35 °C	[31]
SPT	Sodium polytungstate solution 1800 kg m^{-3}, acidified with HCl (pH 3), 24 h, RT	[31]
HCl (positive control) [b]	one wafer with PA6, only for image processing algorithm calibration: 10% HCl, 20 min, RT, to fully dissolve MP	–

RT room temperature, *LT* Long term
[a] only in qualitative part, [b] only in quantitative part

to non-catalysed H_2O_2 was replaced by a 24 h period, as it was uncertain whether the epoxy adhesive layer would withstand the 2 weeks exposure to a degree necessary to uphold its function of immobilising the particles. For many MP sample purifications scenarios this still resembles a typical application duration, i.e. for water samples [31]. The longer treatment in the qualitative part could be regarded to cover any effects that would also occur in the 24 h quantitative measurements, but not necessarily vice versa. This should be kept in mind when drawing detailed conclusions from the here presented data on the specific treatment protocols.

Qualitative analysis

Preparation and spectra acquisition

Prior to treatment, FTIR and Raman spectra were obtained on the milled test-MP particles as a spectroscopic reference. Approximately 5 mg of each of these particles were submitted to the respective treatments (Table 2). After the treatment procedure was completed, the particles were retained in a wet filtration on a vacuum filtration device with a stainless steel sieve of 10 μm nominal pore size (Spörl KG). On the filter, the particles were thoroughly rinsed with MP-free H_2O (prepared according to Enders et al. [31]) before few particles were manually transferred to a Si wafer as a plane spectroscopic substrate. Post-treatment spectroscopy was conducted using ATR-FTIR (PerkinElmer Spotlight 400, spectral resolution: 4 cm^{-1}, 32 scans, or Bruker ATR microscope Hyperion 2000 with 20x ATR objective, coupled to Bruker FTIR spectrometer Vertex 70, spectral resolution: 4 cm^{-1}, 100 scans) and Raman microscopy (Renishaw, inVia Qontor, laser: 532 nm, 100 accumulations, 0.5 s per scan, magnification: 50x, laser power: 60 μW - 4 mW). The settings used for each instrument were manually chosen to provide a sufficient spectroscopic data quality that allowed for the intended analyses and conclusions to be drawn. Which spectra were measured on which instrument and settings may be inferred from the deposited spectra data set [34], where the name of the spectrometer is given for each spectrum measured. For each treatment and polymer, three different MP particles were spectroscopically analysed as replicates as a minimum.

Data analysis

To compare and evaluate the Raman spectra, all replicates of one treatment and a representative spectrum of the untreated material (reference) were plotted together using the Renishaw WiRE 5.2 software. Changes, such as baseline shifts or the occurrence of new peaks were noted. For spectra with newly emerged peaks, a library search was conducted using the WITec TrueMatch 5.2 software. We searched the range of 200 to 4000 cm^{-1} after a shape background subtraction was applied (subtract shape size: 200). The hit quality index (HQI) was then calculated as the Pearson Correlation Coefficient of the non-derivative spectra. The commercially available ST Japan Raman libraries for pristine polymer references were used. For the FTIR spectra, reference and treatment-specific spectra were plotted in the same way using either the Perkin Elmer Spectrum software or the Bruker OPUS (v7.5) software and changes were noted. Manual spectra evaluation was used to detect any changes in molecular vibration frequencies and to suggest their origin. For example, the emergence of new IR bands in the range of 1580–1600 cm^{-1} and 1350–1380 cm^{-1} indicates generation of a carboxylic acid salt as a result of polymer oxidation. The FTIR spectroscopic evaluations included also the calculation of HQIs, which were performed to assist in the manual spectra evaluation, but were deliberately not used as the sole decision criterion. Their calculation was conducted in the Bruker OPUS software using the proprietary Euclidean-distance-based HQI algorithm and the following list of libraries: ATR-LIB-COMPLETE Vol 1–3 (ST Japan), Hummel Industrial Polymers (Chemical Concepts), Hummel (Bruker), MERCK (Bruker), Polymer library (Bruker), General library IR (Bruker) and a custom library of self-measured common polymer types.

To classify changes in the spectroscopic signals, we assigned each treated polymer to one of four categories (Table 3). The decision on a category was derived as the result of the manual spectra evaluation as described above. Where replicates exhibited different changes in spectra, the decision was based on what the majority of replicates indicated. We defined the categories with the goal to differentiate the spectra into groups of similar chances for successful spectroscopic polymer recognition. Similar categorisation approaches have been taken by other MP treatment validation studies [1, 14]. Category "x" was assigned when an evaluation could not be conducted, because, independent of treatment, no exploitable spectral bands spawned from the respective polymer with the respective spectroscopic technique.

When identifying environmental MP spectroscopically, usually semi-automated library searches are used instead of manual spectra evaluations. For a subset of the polymer types, we reported Raman HQI values of the highest correct polymer type match and compared deviations between the reference HQI (untreated polymer) and HQI of treated replicates with our manual category assignments.

Quantitative analysis

Based on the qualitative test and previously published resistance studies, a set of polymers and treatments was selected for further quantitative analysis. The decision to

Table 3 Categories used to evaluate the impact of a treatment on the spectroscopic recognisability of the treated polymers. Exemplary spectra for each category can be found at the given page numbers in the respective data deposits: [a] Raman+FTIR_commodityPolymers.pdf, [b] Raman+FTIR_paintResins.pdf

Category	Definition	Consequences	Example Spectra Raman	Example Spectra FTIR
0	no relevant changes, spectra identical within natural background noise levels	polymer recognition unhindered	p. 77 in [34][a]	p. 156 in [34][a]
1	changes in non-band spectral properties, i.e. baseline slope or elevation, fluorescence	polymer recognition unhindered, changes do not mask polymer bands	p. 44 in [34][a]	n/a
2	emergence of new bands or individual band intensities increased due to polymer degradation processes (e.g. oxidation)	polymer recognition largely unhindered, changes do not mask polymer bands	p. 23 in [34][b]	p. 11 in [34][a]
3	removal or strong alteration of polymer specific bands	polymer recognition is hindered	p. 20 in [34][b]	n/a
x	no polymer specific spectrum measurable independent of treatment	no evaluation possible	p. 31 in [34][b]	p. 41 in [34][b]

not analyse all polymers that were included in the qualitative part was due to the limited analytical capacities. Of chemically similar polymer types only one representative was used (polyethylenes and polyamides). In the group of paint resins, we limited the selection to the acrylate and epoxy based products, of which we got usable results in the qualitative part of the study.

Preparation of particle immobilisations

For the quantitative analysis particles were immobilised on silicon wafers with a thin epoxy resin layer as an adhesive (see Fig. 2). Rectangular pieces, ca. 1–2 cm^2, 700 µm thick, were cut from the silicon wafer material and initially cleaned by being immersed and rotated for at least 10 min in piranha solution (H_2SO_4 60% and H_2O_2 30% mixed in a 1:1 ratio just before the wafers were added). The cleaned wafers were coated with a layer of epoxy resin (L20 + EPH 161 thinned with acetone, 100:25:25 weighed ratio, Hexion). The resin has a drip time of 90 min. A single wafer piece was mounted on a spin coater chuck and spun at 7500 rpm for approximately 20 s (Polos BL MCD, APT GmbH, Germany). The film thickness was determined via z-axis differences for focus on the wafer surface versus focus on the film surface using the same instrument and settings as described below (Image acquisition and reagent application). On eight random locations the mean thickness was 4.25 µm with a standard deviation of 1.98. After a short curing interval of approximately 2 min, the test-MP of one polymer type were applied to the glue surface by trickling them through a stainless steel mesh (100 µm pore size, held approximately 5 cm above the wafer) with help of a metal spatula. The particles came to rest on the still adhesive resin layer and the wafer was left at 40 °C to fully cure overnight. For each treatment, one wafer per polymer was prepared in this way. During spin coating and particle application the wafers were only handled inside a ventilated cabinet and were placed in closed-lid transparent polystyrene boxes for transport and curing, as to prevent unintended dust particle settling.

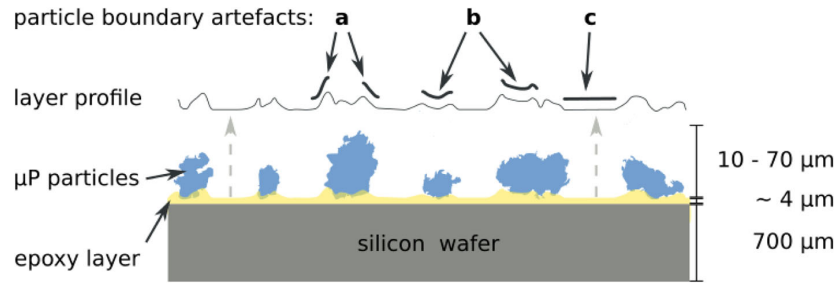


Fig. 2 Composition of the microscopic substrate. MP particles imaged in reflected DIC mode appeared bright on dark background, however the contrast depended on the presence and direction of topographical features in the range of the polarised beam shear. Boundary creeping effects can lead to deviations or defects in the epoxy layer around particles, which may scatter light and become visual obstacles for image analysis: (a) sloping due to attraction to particle, (b) pit formation (depressions which become visible when particles would be destroyed). Normal smooth layer surface (c) typically found in inter-particle space shows no optical interference and provides an evenly dark background. Drawing not to scale

Image acquisition and reagent application

Optical microscopic images were acquired with a Zeiss Axio Imager.Z2m digital microscope on a defined region of each coated wafer (prior to treatment) after they had been rinsed with ultra-purified H_2O and dried with nitrogen purge gas to remove any loose particles or dust. Each wafer was then exposed to one of the treatment reagents (see Table 2) and rinsed again with ultra-purified H_2O to remove any residual chemical reagents. A post-treatment image was then obtained from the same area on the wafer as for the pre-treatment image. All images were taken using the Zeiss Zen software v2.7, a 20 x objective in reflected light differential interference contrast (DIC) mode. DIC was chosen as it gave the largest contrast difference between particles and background, when compared with other techniques (bright field and dark field). The resulting image signal-to-noise ratio depended however strongly on the polymer type, limiting the applicability of this technique for some polymers (i.e. PVC and PMMA, see also section Methodological caveats for an evaluation of diagnostic limitations). Images were acquired as tiling mosaics with a fixed zero overlap stitching. It was necessary to postprocess the images manually. For pairs of corresponding pre- and post-treatment images areas of visual artefacts (e.g. air entrainment on wafer borders) were cropped simultaneously (Fig. 3 shows the differences between original and processed images). Differing light conditions in the original images were accounted for by histogram adaptation (conducted equally for pre- and post-image pairs). The images used for analysis were in 8-bit tiff format with a pixel resolution of 0.72 μm px^{-1}.

Image analysis

Particle identification algorithm The analysis routine for the DIC images was written in python and is available for use and contribution under GNU GPL v3.0 at: https://github.com/robna/ImmobileParticles_MatchAndAnalyse, and as a static citable version [35]. A number of open source python libraries were used, most notably: Altair [36] which builds on the declarative visualisation grammar Vega-Lite [37], pandas [38, 39], statsmodels [40], OpenCV [41] and SKimage [42]. The routine consists of a three-step procedure (Table 4).

First, a particle recognition routine identifies particles on both the pre- and the post-treatment image. Their coordinates are used to align the images, i.e., to remove any image tilt and offset. From the aligned images, for each particle in the pre-treatment image the corresponding particle in the post-treatment image is identified (if present). This particle matching allows determining and comparing particle statistics, such as size or brightness, before and after the treatment on a per-particle basis.

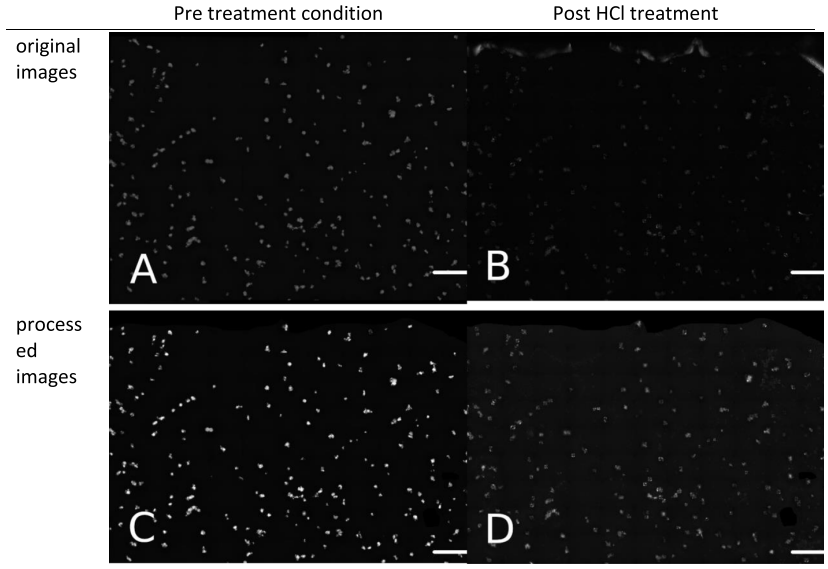
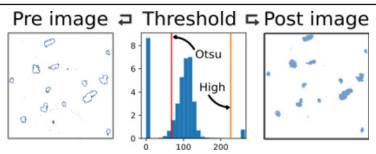
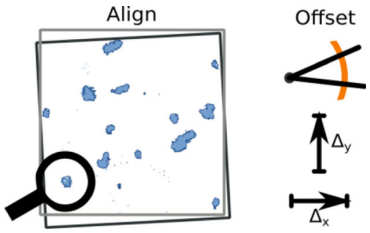
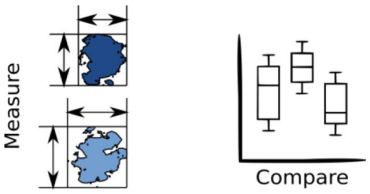


Fig. 3 DIC images were used to document the state of particles. The here shown examples were used as the calibration pair for particle recognition, where PA6 particles were exposed to HCl, leading to their complete destruction by polymer hydrolysation. What is left after the treatment are visual marks on the epoxy layer (depressions), where particles sat. For a successful automated image analysis, particles need to be identified in pre- and post-images, while depressions need to be excluded. **a**: pre-treatment image with high contrast between bright particles and dark background. **b**: post-treatment image with depressions still recognisable as visual marks of weaker brightness. **c, d**: equivalent to A and B but after the manual postprocessing step

Table 4 Steps of the image analysis. More detailed documentation of the applied algorithms is provided along with the source code https://github.com/robna/ImmobileParticles_MatchAndAnalyse

Initial particle detection		• particles get separated from background by thresholding with hysteresis [43] – a lower threshold is calculated using Otsu's method [44], which selects full particle areas – areas are accepted as particles if > 10% of their pixels also exceed a higher threshold fixed at 75% maximum brightness
Finding corresponding particles		• image registration: pre- and post-images get aligned – particles found in pre- image are matched to equivalent particles in post-image if present
Obtaining particle properties		• matched particles get measured on pre- / post-images • measurements are used to compute change rates of properties

Using a positive control for calibration of particle detection The task of the automated image analysis is to discriminate particles from background and match corresponding particles in pre- and post-treatment images. In case a treatment would have destroyed particles, marks in the resin layer are expected to remain visible in the post-treatment image (e.g. a depression where the particle was sitting) and could potentially be falsely classified as a particle. Hence, the detection method has to be capable of distinguishing depressions from actual particles as well. For this purpose, as a positive control, we used one additional wafer with PA6 particles. This wafer was submerged in hydrochloric acid (37%) for 20 min at room temperature (which was shown to completely dissolve PA6, [14]). Pre- and post-imaging, as well as any rinsing steps were conducted as described above. The images that were obtained of this wafer are shown below (Fig. 3). They also serve as a general example of the type of image material that the quantitative part of this study is based on.

The destruction of the particles was confirmed by Raman microscopy (Renishaw, inVia Qontor, laser: 532 nm). Twenty randomly selected depressions in the epoxy layer were analysed, where no distinct PA6 spectrum was present in 17 out of 20 cases (85.0%). In places where PA6 attributed bands could still be detected, a visual microscopic inspection revealed that particle structures were no longer clearly recognisable, indicating that only residues of the PA material were left. This shows that the HCl treated PA6 wafer can be regarded as a suitable positive control where ≥ 85% of particles were effectively removed and can be used for calibration of the particle detection algorithm. Translated to a non-embedded particle system (e.g. suspensions) where particles would be exposed to the digestant from all sides, this is likely to be a complete particle loss.

The calibration of the particle detection algorithm was conducted on several parameters, most notably the upper brightness threshold, the tolerated displacement and particle size limits. For various combinations of values of these parameters, the resulting particle numbers detected in the pre- and post-treatment images of the positive control wafer were compared with the goal of identifying the parameter set that produced the lowest false positive and false negative errors. Because particles were intentionally destroyed on this wafer, false positives are equivalent to features being recognised on the post-treatment image, while false negatives correspond to particles remaining undetected on the pre-treatment image, despite being obviously present to a human observer. This optimised parameter set was then used for the particle detection in all other images and can be viewed in the source code.

The calibrated image analysis resulted in a particle count reduction of 85.2% ($n_{matched}/n_{pre} = 30/203$), which corresponds to the visually and Raman spectroscopically determined particle loss of 85%. In the 30 remaining particles the average area was reduced by 86.3% ($A_{post,\ matched}/A_{pre,\ matched} = 320/2332\ \mu m^2$, compare Fig. 6). For this fraction it remains unclear whether the particles had

been destroyed incompletely (thus, identified correctly), or misidentified as false positives, despite having been removed. This can occur due to the misidentification of depressions with bright embedded air bubbles or optical artefacts (e.g. bright halos appearing around depressions, see also Fig. 3 bottom images), which could not be avoided. This sets a measurement uncertainty, and if any of the tested treatments would have caused an equivalent reduction in particles, it should ultimately be interpreted as a complete destruction.

Data analysis

As the number of particles per imaged wafer was not constant, measured values of counts and particle area are reported as relative changes. In counts (n) they are calculated from the number of particles in a pre-treatment image which could be matched to a particle present in the corresponding post-treatment image in relation to the total pre-treatment particle count. A relative particle loss $L_{rel.}$ is calculated according to Eq. 1, ranging from 0.0 (all particles were matched) to 1.0 (all lost). Particle areas were aggregated as the mean area per matched particle $\bar{a}$ in both, pre- and post-treatment images, whereof relative changes $C_{rel.}$ were calculated (Eq. 2).

$$L_{rel.}(n) = 1 - \frac{n_m}{n_{pre}} \tag{1}$$

$$C_{rel.}(\bar{a}) = \frac{\bar{a}_{post}}{\bar{a}_{pre}} - 1 \tag{2}$$

Where

n_{pre}= number of particles in pre-treatment images.

n_m= number of particles that could be matched between pre- and post-treatment images. Indices for a alike.

Statistics Influences of non-treatment factors, such as varying contrast and image quality as well as available particle number on a wafer, appeared to have confounding effects on the successful particle recognition and matching. These factors were formalised as n_{pre} being the total particle count that could be identified on a particular wafer before treatment exposure on the one hand, and a range of image histogram obtained variables (Table 5), on the other.

Generalised linear model (GLM) residual analyses were used to estimate and remove these impact of the confounding factors. For an application-oriented introduction and references for further reading on GLMs, we recommend the website of the statistical package statsmodels [45], which was used here for the model calculations. The models followed the form of Eq. 3, with X being an $i \times j$ matrix of the linearly combined independent explanatory variables (predictor terms), y being the dependent response variable and $g(.)$ some function of the conditional expectation of the response, that links it to the linear term of p predictors multiplied with individual coefficients β_j.

$$g(E(y = y_i | X = x_i)) = \sum_{j=0}^{p} \beta_j \cdot x_{ij} \tag{3}$$

For particle count losses, the binomial distributions for particles matched (successes) and lost (failure) were used as the dependent variable. The model was fitted to the predictor terms using a logistic link function (as given in

Table 5 Image quality related attributes tested as explanatory confounding factors in the statistical modelling applied to the quantitative particle data. Lo = lower threshold as calculated by the particle hysteresis detection algorithm. [a] chosen as suitable for modelling of influences on particle count loss, [b] chosen as suitable for modelling of influences on particle area change, [c] used for calculation of the background distortion index (BDI)

Name	Description	Mathematical Expression
pre_histBGpeak	pre-treatment image background brightness	grey value at the local histogram maximum between but not including 0 and Lo
pre_histFGpeak	pre-treatment image foreground brightness	grey value at the local histogram maximum between but not including Lo and 255
post_histBGpeak	post-treatment image background brightness	grey value at the local histogram maximum between but not including 0 and Lo
post_histFGpeak	post-treatment image foreground brightness	grey value at the local histogram maximum between but not including Lo and 255
pre_histDelta [a]	contrast spreading between the image background and foreground prior to treatment	pre_histFGpeak−pre_histBGpeak
histBGpeakSum [c]	combined background brightnesses	pre_histBGpeak + post_histBGpeak
histBGpeakDist [b, c]	mismatch between pre- and post-treatment background brightness	| pre_histBGpeak−post_histBGpeak |

Eq. 4, with π_i being the probability of a single success, which is equivalent to the predicted response $\hat{y}$). For particle areas the absolute mean of area changes of each wafer was modelled using an identity link of the mean μ (Eq. 5) assuming a *Gamma* distribution.

$$g(\pi_i) = \ln\left(\frac{\pi_i}{1-\pi_i}\right) = \ln\left(\frac{\hat{y}_{i,n_{matched}}}{\hat{y}_{i,n_{lost}}}\right) \quad (4)$$

$$g(\mu) = \mu \quad (5)$$

The model was optimised by systematically varying the type and number of employed predictors, whereby the final set was chosen according to the significance of the obtained coefficients, the models deviance and general logic explainability of the ensemble. For both models (count loss and area change) n_{pre} was chosen as one predictor. A second predictor was chosen from the set of image quality related attributes and is indicated with asterisks in Table 5.

The resulting model setups are shown in pseudo-formula notation in Eq. 6 and Eq. 7 for the count loss and area change GLM respectively.

$$particle_counts[successes, failures] \sim \beta_0 + \beta_1\, n_{pre} + \beta_2\, \text{pre_histDelta} \quad (6)$$

$$area_change \sim \beta_0 + \beta_1\, n_{pre} + \beta_2\, \text{histBGpeakDist} \quad (7)$$

The predicted response was then taken as the portion of particle loss caused by the confounders, whereas the responses standard residuals were regarded as the remaining unexplained, hence treatment-attributed portion of the effect. Only where the residuals exceeded the 95% prediction interval of the water fitted response, effects were interpreted as significant.

Besides for the GLM models the image quality predictors (Table 5) were also used to calculate a generic index (background distortion index, BDI, see Eq. 8) providing a rough estimation of contrast problems due to the image background brightness level. The index number is higher for image pairs of worse quality. It was used for illustration purposes and to determine a limit of which images are not of acceptable quality and need to be excluded from analysis. The two coefficients α and γ were empirically found by optimising an ordinary least squares regression of relative particle losses against BDI. The calculated BDIs were normalised to range from 0 to 100, in order to be independent of the average image brightness. A BDI of 0 corresponds to the best and 100 to the worst image quality present.

$$BDI = \alpha\, \text{histBGpeakSum} + \gamma\, \text{histBGpeakDist} \quad (8)$$

with $\alpha = 2$, and $\gamma = 9$.

Using negative controls for method uncertainty estimations As a negative control, one wafer per polymer type was exposed to ultra-purified water (see Table 2). The GLMs were trained using an iteratively reweighted least squares algorithm [46] on the set of the negative control samples (see SI (S2) for details).

Results and discussion

Qualitative analysis

Commodity polymers

Overall, none of the post-treatment polymer spectra, both in FTIR and Raman, showed substantial spectral band changes that would hinder recognition (Fig. 4, Commodity polymers). However, minor alterations were detected in several cases, which are further detailed below.

Using Raman, increased fluorescence or baseline shifting (category 1 changes) were the most frequently seen effects, but did not hinder a successful recognition of the MP's polymer type. Only for PVC in the H_2O_2 Fe uncooled treatment clear degradation effects on the polymer basis became visible in multiple measured replicate spectra. Two peaks around 1124 and 1511 cm^{-1} ($C = C$ double bonds) strongly increased, which are a direct result of the dehydrochlorination reaction due to thermo-oxidative processes [47]. It is noteworthy that these degradation processes appear to affect individual PVC particles differently, as we see from the varying spectral characteristics between the replicate measurements (see also deposited spectroscopic data at https://doi.org/10.5281/zenodo.4568683 [34]) and also from varying degrees of visual yellowing from white over beige to yellowish brown across particles.

In 10 out of the 125 Raman measurements multiple new peaks appeared which could not be attributed to specific functional group frequencies and were therefore not regarded as a polymer related change (these cases are indicated by * in Fig. 4, compare annotated deposited spectra [34]). These peaks were treatment and polymer unspecific and most frequently appeared in the water control. This lead to the suspicion that the water, used to rinse after the treatment, introduced the impurities. Switching to ultra-purified water for the remaining tests (i.e. H_2O_2 LT, Pentane, SPT) completely prevented these unknown peaks. They do not carry exploitable information for the question of polymer recognisability and their emphasis in Fig. 4 merely serves the purpose of clarity when comparing the here presented results to the original spectra provided in the deposited spectra [34].

In FTIR, the polymer basis was always clearly identifiable. We detected, however, minor polymer degradation processes in the H_2O_2 LT treatment. This concerned ABS, PC, PMMA, PP, PVC, TPU where new bands could be assigned to carboxylic acids which may have

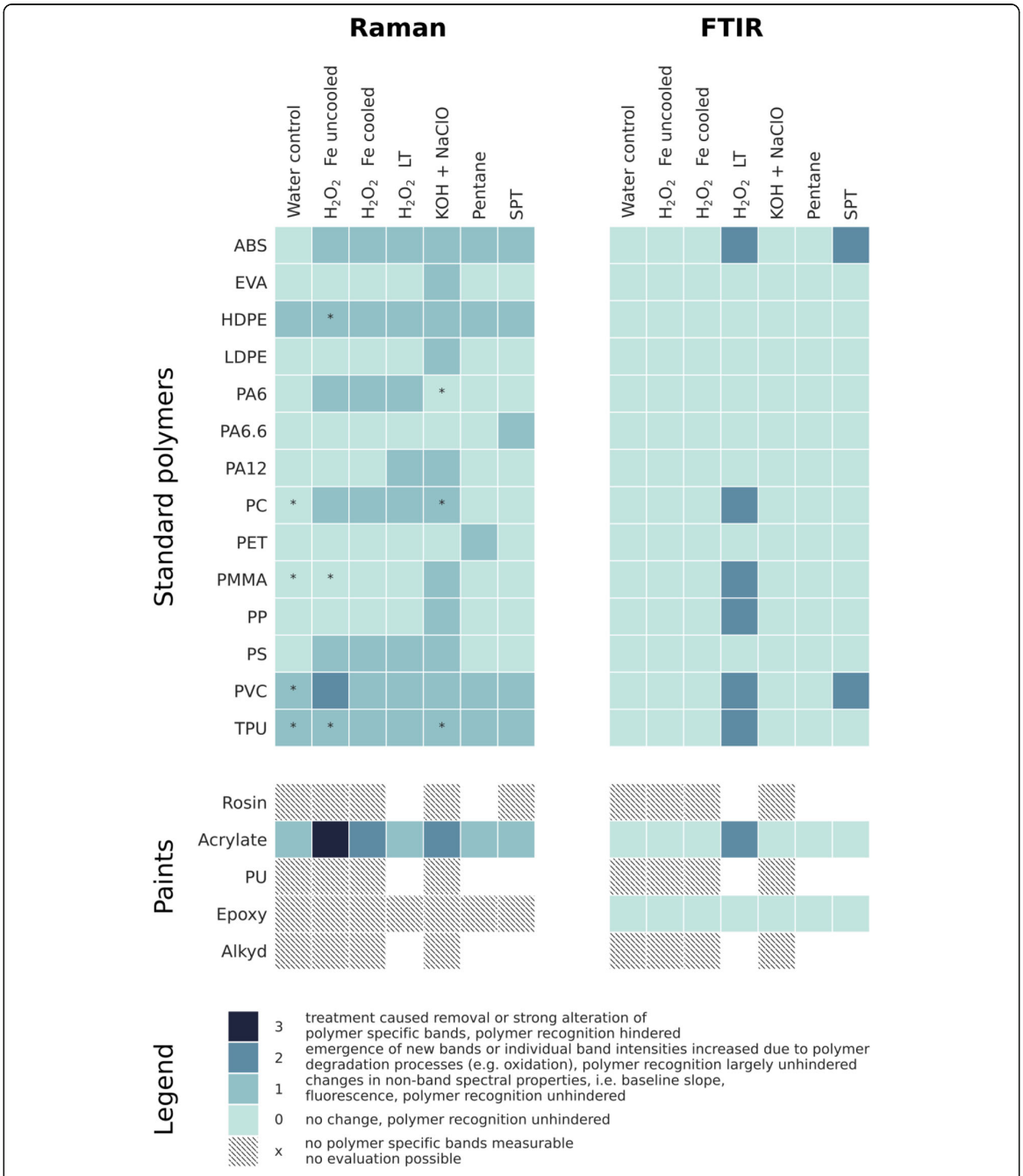


Fig. 4 Spectral changes expressed as categories as they were assigned by manually comparing the post-treatment spectra to the pre-treatment references. Asterisks (*) indicate spectra with newly evolved bands which, however, could be traced back to inorganic impurities originating from the rising water (not used in category assignment). White tiles indicate data not available (measurements were not taken due to expected unexploitable spectra, as other measurements of the same polymers indicated)

resulted from oxidising polymer chain ends. In the SPT treatment, similar oxidations were observed for ABS and PVC. The corresponding Raman spectra, however, did not systematically indicate these changes. This is plausible as FTIR is sensitive to polar organic groups, such as $C=O$ and its variations (e.g. esters, anhydrides, amides, imides), while Raman is less sensitive to these.

It appears that for FTIR category 2 changes occur rather treatment-specific, whereas for Raman spectra no treatment-specific impacts were seen. Instead, several cases of category 1 effects appeared in a rather polymer-specific manner. Although category 1 effects were also found in the water control of HDPE and TPU, it is noticeably the actual treatments that got assigned to this category.

As Fig. 5 shows, the HQI of the treated samples lie in the range of the untreated reference for most tested polymer types. For some treatments, the HQI range of the replicates varied more than for others. In the case of LDPE, the HQI distribution reflects the assignment of the categories (compare Fig. 4). That is, the KOH + NaClO treatment introduced category 1 changes, while no significant changes occurred in the other treatments. Only for KOH + NaClO, the HQI drops to around 90–59 for the different replicate spectra. Similarly, the correct material type was found amongst the first ten hits in the library search, except two single replicates of a polymer-treatment-combination. One pentane-treated HDPE was identified as aliphatic fatty acid or alcohol. This is, from our experience, a frequently occurring problem in Raman spectroscopy. This and the fact that it only happened for one in three replicates should not lead to classifying the pentane treatment as harmful for this polymer type. The second not correctly identified spectrum resulted from a KOH + NaClO-treated PET replicate. Here, the occurrence of the inorganic contaminant calcium carbonate led to extra bands that prevented a semi-automated polymer identification. Overall, this confirms the assumption that none of the treatments induced changes that prevented the identification by a manually supervised spectral library search, as it is common in microplastics research. The result of a HQI based polymer attribution depends, however, on the available references, the applied algorithm and search parameters. It is not generalisable between studies and laboratories and therefore not used as a systematic evaluation criterion here.

In summary, our qualitative results indicate that, regarding the spectroscopic recognisability of MP

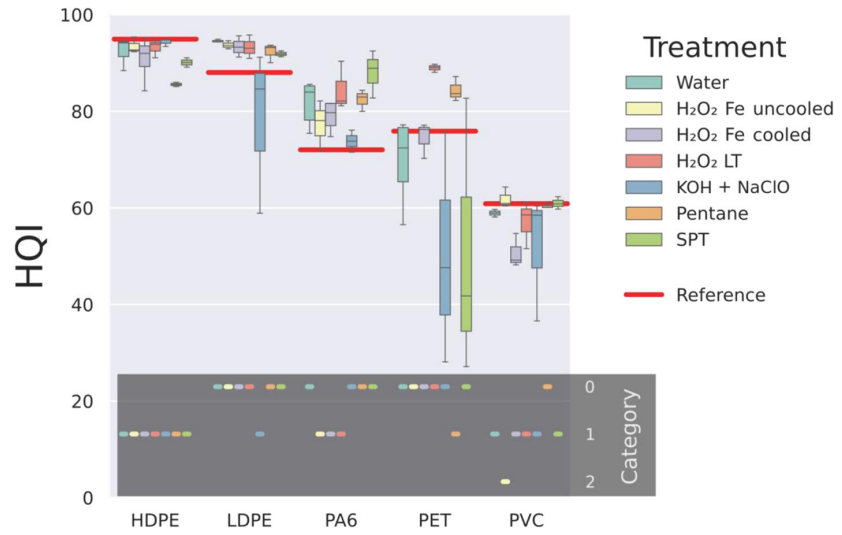


Fig. 5 Raman Hit quality indices (HQI) were measured on a subset of polymers for all treatments against a commercial library (ST Japan). Red lines (Reference) indicate which HQI level was reached using a spectrum of the untreated material of the respective polymer. Boxes show median HQI and .25 / .75 percentiles of a set of replicate spectra, $n \geq 3$. The grey box at the bottom provides the assigned qualitative categories for comparison. Note that categories were assigned in a manual spectral evaluation process and deliberately not based on the HQI values. Apparent discrepancies are discussed in the text. Both, manual categorisation and achieved HQI values, are resulting in the same predicate regarding polymer recognisability: the tested treatments do not alter spectra in a way that a successful polymer identification would be hindered

particles of any of the tested commodity polymers, all of the tested treatments are safe to apply, when the chosen analysis technique is either FTIR or Raman spectroscopy. However, effects on the treated polymers spectra, that were less critical to polymer recognition (i.e. category 1, Table 3), occurred frequently. Raman baseline shifts can be caused by heating of the sample during measurement [48]. Fluorescence mainly originates from sample characteristics, but background conditions such as ambient lighting, can play a role as well [49]. Both effects are too unspecific to be assigned to a polymer degradation process. Changes in the ATR-FTIR baseline can occur due to multiple changes in the optical path, e.g. the contact between the sample and the ATR crystal. They reflect physical rather than chemical changes, and again, are not fit to indicate a change in the polymer composition.

Paint resins

Out of the five paints, in all but one (acrylate) the polymer resin was not identifiable, already in the pre-treatment Raman spectra. In the KOH + NaClO as well as in the H_2O_2 Fe cooled treatment acrylate showed effects of degradation, however, was still recognisable. After the uncooled H_2O_2 Fe treatment, however, the polymer related bands were not found any longer, making an identification impossible. All other four paint spectra were substantially masked by fluorescence in both pre- and post-treatment spectra. In some cases, pigments (inorganic bands) dominated the spectra. One black (PU) and one grey paint (alkyd) showed an additional band which is indicative for black carbon (1343 cm^{-1} and 1581 cm^{-1}, [47]). But as black carbon can stem from various sources in environmental samples, without any signal of the polymer bases the Raman spectra of these paint resins are unspecific and an identification by an automated detection procedure is not possible. As a result, no conclusions can be drawn concerning effects of the tested treatments on the polymer bases and associated processes of polymer degradation based on Raman spectroscopy.

The polymeric binders were clearly detectable for acrylate and epoxy based paints using FTIR spectroscopy. In these paints none of the treatments lead to a change in spectral quality, except the H_2O_2 LT treatment, which introduced carboxylic acid salt signatures around 1600, 1350 and 789 cm^{-1} in acrylic paint, indicating polymer oxidation processes. While for PU based paint no exploitable spectral properties could be found in neither pre- nor post-treatment spectra, the paints based on rosin and alkyd exhibited some weaker bands that could be attributed to the organic binder matrix by an experienced spectroscopist, however not with sufficient confidence. Hence, we note that only the epoxy and the acrylic paint can be regarded as reliably identifiable by their polymer FTIR bands and are thus useful for evaluating the treatments effects on polymer recognisability. Chemical treatment-caused spectral changes i.e. bands weakening or disappearing were found in acrylic paint for H_2O_2 (Fe + LT) and SPT treatments. This did, however, not hinder the recognition of the polymeric binder as only inorganic components were affected indicating mineral depletion ($CaCO_3$). Thus, no restricting categories were assigned based on this observation (Fig. 4).

Comparing Raman and FTIR spectra of paints, overall masking was weaker in the FTIR spectra. Where peak changes were present, they were dominatingly caused by pigments or other fillers, for both techniques. Only for acrylic paint the strong thermo-oxidative regime of high temperature Fenton's catalysed H_2O_2 treatment made an unambiguous spectral recognition impossible in Raman, however not in FTIR.

In paints based on rosin, polyurethane and alkyd the detection of binder matrix bands was not possible already on the untreated material (at least not to a degree of certainty that would allow the identification if the material was unknown). Thus, degradative effects of the treatments cannot be studied with the here applied techniques. Our conclusions are limited to the observation that in general a reliable detection of paint flakes of these resins using spectroscopic identification is not guaranteed. In contrast to commodity plastics, paint resins are typically composed of high amounts of non-polymeric constituents and only a smaller portion of the polymer itself. Accordingly, it is questionable whether paint resins can be exhaustively and reliably identified in environmental systems using spectroscopic methods [20, 50]. The chemical bonds of many inorganic and organic pigments and other paint constituents are strong Raman scatterers, which renders them well detectable in Raman spectra (also better than with FTIR). On the downside they frequently mask the weaker bands of the polymeric binder due to their strong intensities or additional fluorescence. Large reference libraries containing spectra of large varieties of paint composites preferably from different manufacturers might be able to detect paint flake MP based on their (pigment dominated) fingerprint. This approach has also been taken by other studies [13, 51]. Most pigments are, however, not solely applied in synthetic polymers but in a large diversity of technical applications, which is why an indirect identification of MP via those pigments cannot be done in a systematic way. Furthermore, due to the large variety in different paint compositions, an automatic detection is limited unless the particular paint product is available in the spectral library.

Quantitative analysis

Particle property comparisons

As for the qualitative data, a high level overview on the quantitative data can be gained from the heat maps that summarise the relative changes that we could attribute to the treatments (Fig. 6). Noticeable are elevated values present in various polymers exposed to the H_2O_2 treatment. Further, for ABS, PC and epoxy based paint there are higher values found across treatments.

To enable a deeper insight into the quantitative dataset, we provide an interactive version of the heat map figures (Fig. 6), augmented with plots of individual particle data showing detailed and aggregated differences between pre- and post-treatment images. It may also be used to understand the necessity and effect of the GLM corrections that were applied to the data. The interactive figure may be downloaded from: https://doi.org/10.5281/zenodo.4568524 [52].

Particle counts From the GLM corrected data, it can be seen that the majority of polymer treatment combinations did not show any loss significantly different from the negative control. Exceptions are the SPT treated ABS (30%) and the H_2O_2 treatments of epoxy based paint and PC (46% and 25%, respectively). For these three polymers also the corresponding water treatments show particle losses higher than any of the other polymers. This indicates that for images of these polymers not all of the confounding effects could be removed by the GLM correction, and the actual treatment caused changes must be lower.

For the H_2O_2 treated epoxy paint particles we conclude that the relative loss in the GLM corrected data is indeed indicative of an actual treatment caused effect. Influences of confounding factors were comparably low for this image pair (n_{pre} = 212, BDI = 0). The modal value of particle brightness is reduced in the post-treatment image (pre_histFGpeak = 183 and post_histFGpeak = 103 out of maximum of 255, respectively, see Table 5 for explanations), indicating a possible material erosion, which could not be explained by other factors. This is further substantiated by looking at individual particles in a pre-post-comparison, where dark indentations or holes become visible, in places where the particle surface or boundary were priorly intact (Fig. 7).

It is known that certain polyepoxides are susceptible towards peroxides, in fact, this is utilised in certain technical applications. One study used 24% and 50% H_2O_2 to superficially degrade epoxy resins and expose embedded fibres in a fibre reinforced polymer (FRP) [53]. For the recycling of carbon fibres from FRPs, acetified H_2O_2 (30%) was

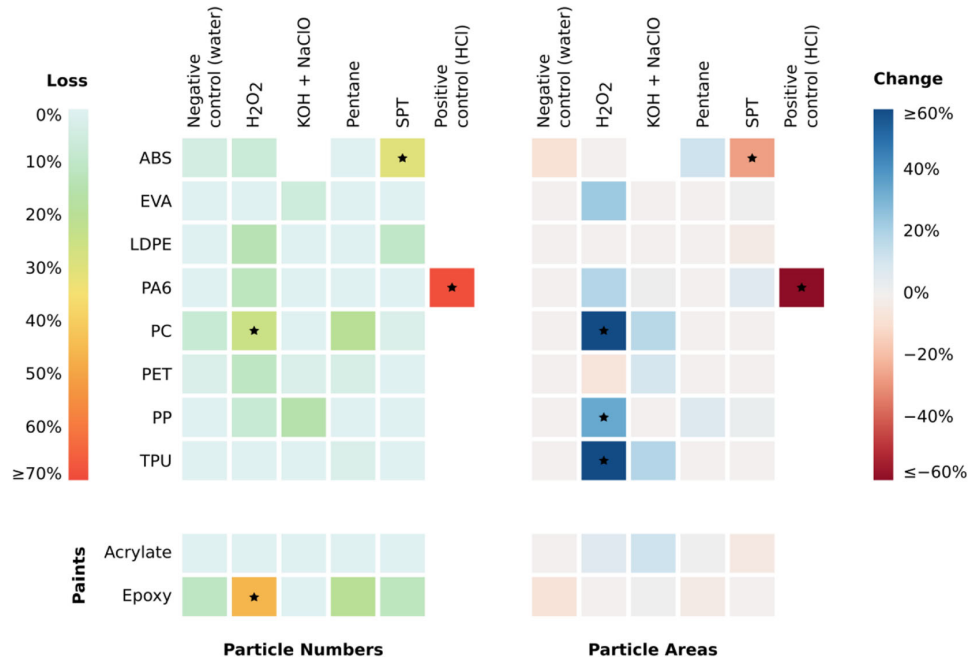


Fig. 6 Relative changes on particle numbers and mean particle area as obtained from the image analysis and subsequent GLM correction. Changes are shown in percent of the matched values to pre-treatment values. Significant changes that exceed the 95% prediction interval of the negative controls are marked by an asterisk. White tiles indicate data not being available for different reasons (for details see Methodological caveats. Uncorrected values and underlying per-particle data can be viewed in the interactive version of this fig [52].

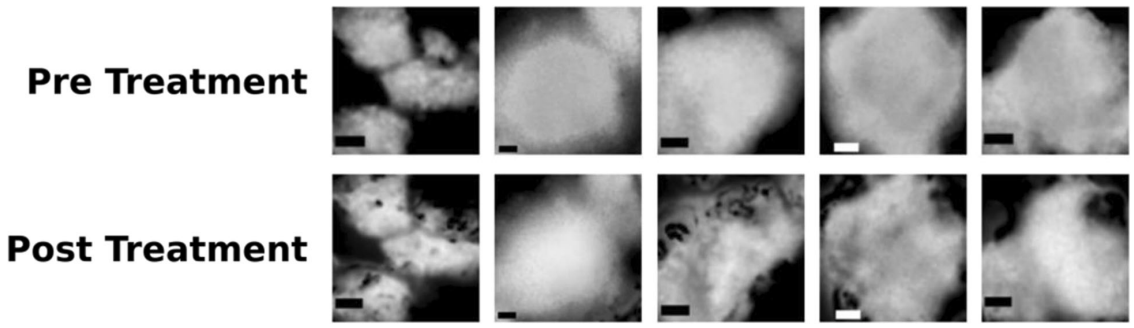


Fig. 7 Particles of epoxy based paint resin treated with H_2O_2. Images show the same particles before and after the treatment. The post-treatment images (bottom row) show dark spots where the particles have allegedly been damaged by the treatment. Scale bar equals 10 μm

deemed effective for an epoxide matrix decomposition in an overnight treatment [54]. When epoxy resin particles are targeted within environmental MP studies and peroxide digestion protocols are applied, we recommend for future studies to note that numbers are likely underrepresenting the actual environmental load for these polymers. In our data the corrected particle loss exceeded that of the epoxy water digestion by 35 percentage points. Hence, it can be assumed, that a reported concentration of epoxy MP particles in a certain environment are only covering approximately 65% of the total load present, at least for particles in the here studied size range.

The effect of H_2O_2 could also be seen on the epoxy layer that we used to immobilise the particle on the Si wafers. Increased brightness and haziness of the image background was apparent especially around the wafer edges, which made more encroachments by manual image postprocessing necessary in those wafers. Small defects in the layer were promoted to brighter visual appearances after the treatment that could lead to false positive detections, while increased brightness in the near field surrounding of particles, is likely a contributor to the observed particle area growth that was observed in several H_2O_2 treated polymers. These effects on the layer show that with the epoxy resin used here, we have not yet found the optimal immobilisation adhesive for the purpose of the study. We argue though, that the effects do not constitute a failure of the immobilisation technique, as we know from the positive control wafer (PA6 treated with HCl) the detailed visual characteristics of spots where particles got removed from the layer. Such appearances were not what we could typically observe in the images of H_2O_2 treated wafers, instead, the image objects at places where particles were expected generally resembled what particles looked like in the other treatments (including the negative control water treatment). This is yet not sufficient evidence to fully exclude that a loosening of particles may have occurred in some places due to the layer being affected, but it shows the this was not predominant process. Hence we conclude: the spin-coated epoxy layer did resist our H_2O_2 treatment at least to a degree that particles could be held in place and measured after the treatment. It could be further improved by finding an adhesive composition that does not show any visual nor integrity-related impacts from any of the tested treatments. Experiences and advice from our adhesive layer development phase are detailed in the SI (S3).

The wafer of H_2O_2 treated PC suffered the problem of having a low total particle number (n_{pre} = 26), which could not be entirely alleviated by the applied GLM correction. The particle brightness was not reduced on this wafer after the treatment (pre_ and post_histFGpeak were at 88 and 89, respectively), suggesting that there was no treatment caused effect acting on all particles collectively. Instead the loss was driven by only six particles that could not be matched between the images. The low n_{pre} is thus regarded here as the main reason for the resulting significant loss.

The loss of particles from the SPT treated ABS wafer should only with certain reservations be seen as an indicator of particle degradation, as the image quality was on the brink of our exclusion level (BDI = 26). We interpret the observed losses as partly treatment caused and discuss this interpretation below (Comparison of qualitative and quantitative results).

Most prominent, but also expected, is the loss of nearly all particles in the positive control wafer (HCl on PA6), where 69% of pre-treatment particles could no longer be confirmed to be present post treatment (85%, without GLM correction, see also Using a positive control for calibration of particle detection).

Particle areas In contrast to particle counts, changes of particle area were recorded to differ in negative (area decrease) as well as positive (area increase) direction. The largest decrease of particle area can be seen in the positive control, however, also the SPT treated ABS was recorded with a significant area reduction of 30%. But as noted above, one should take this result with caution,

due to the low image quality of this wafer. Several polymers treated with H_2O_2 revealed significant area increases post treatment (PP, TPU and PC with a 34%, 60% and 220% average increase, respectively). The extreme increase in particle area of PC was mostly caused by two outliers where in the pre-treatment image the particle was only partly detected by the thresholding algorithm. An increase in area or particle volume would not hinder a MP detection, however, it may lead to a distorted representation of particle sizes.

For the H_2O_2 treated epoxy paint particles, where we described a significant particle loss above, we do not see a change in area for the remaining matched particles. The formation of dark holes in particles (Fig. 7) is not represented in the post-treatment area measurements, because particles are identified as closed shapes by the detection algorithm.

Methodological caveats

The here presented technique for quantitative MP treatment evaluation was limited in two ways. Limitations were caused either by effects of a specific treatment on the adhering epoxy layer, or, by polymer specific characteristics which impeded a contrast rich DIC imaging.

The KOH + NaClO treatment disrupted the adhesion between the spin coated layer and the underlying Si wafer, which lead to a partial or complete detachment of the epoxy film and wrinkling artefacts on the images in several cases. The film itself did not seem to be degraded or otherwise affected as microscopic imaging could confirm that the epoxy matrix and attached MP particles were visually intact. However, the correct placement for a post-treatment imaging was disturbed and the layers were partially outside of the microscope's focal plane, which resulted in darker areas that could no longer be recognised by the particle detection. This affected especially the KOH + NaClO treated wafers of PP and PET, where such areas needed be mutually excluded from the pre- and post-treatment images in the manual image postprocessing. The H_2O_2 treatment had a different effect on the epoxy layer, however without affecting the image quality to an extent where the image analysis would be impeded. The wafers treated with H_2O_2 were showing varying degrees of obliqueness in the otherwise clear epoxy layer, indicating a surface affect or softening of the layer. The resulting implications are discussed in the above section.

For PVC, PMMA, PS and, to a lesser degree, ABS the chosen microscopy mode (reflected DIC) was not able to generate images that have a good particle to background contrast. The image postprocessing did increase the particle brightness for the particle detection algorithm but at the cost of a proportionally gained brightness of the image background. For reasons unbeknown to us, the surface topography of MP particles of these polymers did not create an optical path length difference that would allow for contrast rich DIC images. The size range of the particles of these polymers was not different than for the other polymers and further investigations beyond the scope of the study would be necessary to clarify whether this is indeed due to polymer specific optical characteristics or rather special interactions between the particles and the uncured epoxy layer at the time of application. Unless a solution is found to create particles and immobilisations of these four polymers that yield a sufficient contrast, the more suitable approach would be applying a different microscopic technique. Possible candidates are discussed in the SI (S3).

With the current state of the experimental approach, the polymers of PVC, PS and PMMA, could not be included in the analysis, due to the above-mentioned reasons. PMMA and PVC were excluded due to low image qualities. Of the ABS wafers only the KOH + NaClO treated sample had image qualities that resulted in a BDI exceeding the set cut-off of 27. For PS, however, the BDI was not able to ascertain that the image quality was unsuitable for an analysis, because the image defects in PS were slightly different than in PVC and PMMA. While the latter showed a general and evenly low contrast between particles and background, PS had mostly a stronger contrast but included many optical artefacts (i.e. bright ring-like halos around particles). It was attempted in image postprocessing to remove the artefacts manually, however, the PS images could not be improved sufficiently. Images of PVC and PS can be viewed in the deposited imaging dataset at https://doi.org/10.5281/zenodo.4568488 [55] as an example of the contrast problems.

The above discussed caveats currently pose certain limitations in terms of applicability, explanatory power and required work effort. The true value, however, is present here as the possibility of the immobilisation approach to study effects on individual particles simultaneously on large particle numbers in the smaller MP size ranges. How this compares to other concepts is discussed below in the section Comparison of experimental concepts. Additionally, in the SI we describe more detailed the lessons learned and attempts to further methodological improvements for interested readers (S3).

Comparison of qualitative and quantitative results

While the quantitative particle data provides insights in the particle-based alterations of a treatment, it does not convey whether these can be recorded by the chosen analysis technique (here Raman and FTIR spectroscopy). As an example, particles might still be present after a treatment, but changes on the surface of the particles or the polymer matrix might render them undetectable.

The other way round - a polymer type is recognised post treatment but the quantitative measurements reveal particle losses or area changes - is also a possible scenario. In fact, the epoxy based paint resin in our data is an example, where we observed a significant particle loss after a 24 h H_2O_2 exposure, while FTIR recorded no changes to the polymer spectrum even after a prolonged 2 weeks' exposure or the uncooled Fenton's with its 80 + °C temperatures. The two-tiered approach, providing qualitative and quantitative data on the same polymer treatment model systems, therefore allows for a higher certainty on the applicability of the tested treatments. For a comprehensive evaluation both aspects are of importance.

A related study also reported qualitative (spectroscopic) and quantitative (recovery of spiked particles) data [11]. They noted a qualitative change on H_2O_2 treated PVC (see also below section for further details: Comparison of our results to current literature), however could not confirm that the described polymer degradation would manifest in the quantitative measurements.

In our data, SPT treated ABS that was indicating negative changes in particle numbers in the quantitative result, also showed alterations in the spectra of FTIR (assigned category 2, emergence of new bands or band intensities altered), and Raman (category 1, baseline drift). The treatment with SPT resembles a density separation where HCl is used to acidify the solution to pH 3, in order to prevent sodium poly tungstate precipitation [31]. We know that ABS is attacked by acidic digestions [1], however, this was only shown for highly concentrated and strongly oxidative acids (HNO_3 69% and $HClO_4$ 70%), neither of which applies to the here deployed solution. As it was demonstrated there, the acidic treatment lead to a bloating and bubbling dissolution of the macroplastic piece that was tested [1]. The present results indicate an area reduction of those particles that were found again after the treatment. A testable conjecture beyond the scope of this study, is that a count and area decrease was detectable – despite working under a much weaker acidic environment – because of the small size range of particles that were used here, and which potentially are more easily damaged by acids.

Comparison of our results to current literature

To our knowledge, polymer chemical resistance tests in qualitative and quantitative manner have not yet been performed on such small MP particles. Partly related studies reported recovery rates of > 90% of spiked particles using fluorescence-labelled microspheres ≤ 30 μm as representatives of small MP for a novel magnetic separation [12] and in a density separation and digestions [10]. Working with aliquoted pipetting of bulk particle suspensions, they noted that direct comparisons of the same particles' pre- and post-treatment counts was infeasible in this size range [12]. Generally, our overall finding, that, with respect to spectroscopic recognisability, no considerable changes to the polymeric bands were caused by the tested treatments on MP < 70 μm, is in agreement with other studies which used larger MP particles. One study tested the same KOH + NaClO protocol on a similar set of 12 commodity polymers (≥ 5 mm) and performed Raman spectroscopy on pre- and post-treatment particles, finding no relevant changes on the polymer matrix [1]. Dehaut et al. [5] applied a KOH protocol without an additional oxidiser, also reporting no effect on Raman spectra even at 60 °C in all 11 polymers that were comparable between their and our study. Similarly, Hurley et al. [25] found no significant spectral changes applying a Fenton's protocol (cooled, < 40 °C) to a set of 8 different commodity polymers (~ 3 mm) using FTIR.

In our Raman measurements, the only polymer degradative effect was observed in PVC, where the formation of $C=C$ double bonds (caused by dehydrochlorination) occurred only in the uncooled H_2O_2 Fe treatment (> 80 °C, 10 min) as a direct consequence of thermo-oxidative processes on the polymer matrix (as we also observed in an early study [47]). Likewise, Raman spectra measured by Karami et al. [11] on PVC particles treated with 50 °C H_2O_2 were described as being diminished in the $C-Cl$ stretching band, which would be indicative of the same dehydrochlorination process that we observed. But, as mentioned above, PVC exposed to 60 °C in a KOH based treatment (10%, 24 h) exhibited no effect on Raman spectra [5], albeit the presence of a hydrolytic and thermo-oxidative pressure. The difference lies apparently in the stronger oxidising potential of the H_2O_2, that induces detectable – but non-critical – polymer degradation of PVC. It should be noted though, that the occurrence of PVC thermo-oxidative degradation depends on the specific PVC material and its added stabilisers. It is plausible that for other PVC compositions this effect may be induced alone by temperature rises above 60 °C.

In general, negative impacts of elevated temperatures during treatments have also been demonstrated by various studies. For instance, increased mass loss for PA in H_2O_2 (among other treatments), was reported for temperatures between 60 and 70 °C [14] and for > 70 °C [25]. In our qualitative analysis PA did not show signs of degradation, however, we cannot infer whether particle losses or area changes may have resulted from these treatments, as no treatments involving elevated temperatures were part of our quantitative analysis. Yet, the non-catalysed H_2O_2 treatment (room temperature) resulted in no change of PA6 particle numbers or areas.

For the pentane treatment [31] we could now demonstrate polymer resistivity among our test series. The protocol, which involves a weakly acidic digestant (ethanol acidified to pH 3 using acetic acid is added to the sample before pentane), had no impact on the spectra of any of the tested polymers, hence also not on the polyamides, known to be susceptible to acidic degradation. PA6 particles, which we tested quantitatively, suffered no detectable impact by the pentane treatment in particle numbers or areas. Similarly, the acidic SPT was not affecting particle numbers or sizes, except for ABS, where a minor degradative effect could not be excluded, based on our data.

It was reported that PA6.6 melted when applying H_2O_2 at 70 °C and a significant weight and size loss was measured [25]. In our uncooled catalysed H_2O_2 treatment (reaching up to 85 °C for the 10 min treatment duration) PA 6 showed a yellowing effect despite not showing significant quantifiable losses in size or area. Potentially, the temperature exposure in our treatment was not long enough to melt the polymer compared to their exposure time (12 h).

Studies exist that found degradative effects of alkaline protocols on PET [5, 14, 25], however also other factors such as elevated temperatures were involved in some of these cases. Our qualitative results of the protocol using KOH + NaClO do not show signs of degradation of PET in FTIR or Raman spectra; neither do we see a significant particle loss or area change in the quantitative data. The quantitative are, however, of lower confidence, as these samples were affected by the KOH + NaClO induced displacement of the epoxy layer, complicating image analyses.

Comparison of experimental concepts

To our knowledge, working with particles immobilised by adhesives to obtain quantitative measurements has not been performed so far. A related approach was developed recently for measuring PS nanoplastic spheres, where etched cavities in Si wafers were serving as a nanofabricated grid [56]. Particles placed in suspension on the cavity array were assembling by capillary forces and thus temporarily arrested for subsequent material and size determination using Raman spectroscopy. Alternative approaches to microscopy have been applied to determine size changes, such as laser sizing [57]. However, when measuring in wet dispersion problems can arise for polymers with a lower density than water as a sufficient particle dispersion can be challenging to achieve. Absolute particle counts cannot be determined using this technology and problems can arise if post-treatment particle numbers fall below the measurement limit of the specific laser sizer [57]. Also Coulter counters or flow cytometry, might be suitable techniques for these kind of measurements. Usually applied for counting plankton or cells, they allow simultaneous count and size measurements. A disadvantage, however, is the necessity for a filtration step to purify the particles for a post-treatment measurement. Finally, direct microscopic imaging of filtered bulk particle suspensions before and after a treatment could be a viable approach as well. However, like all methods using mobile particles entails the problem, that count data is difficult to obtain for small-sized MP. Particles can get lost in transfer steps and effects like breaking apart, aggregation, handling loss or real treatment-caused degradation are difficult to disentangle. This has been observed by others as well. Thiele et al. [13] used MP particles < 600 µm (that could still be manually handled) for spiking and recovery tests in a treatment evaluation and reported issues with particle loss in transfer steps that needed to be mathematically accounted for. With an immobile particle approach these problems do not arise.

Conclusion

We identified the need in the scientific community for a method to evaluate the impact of treatment procedures on MP particles that are smaller than what can be easily be handled manually, e.g. using fine-tipped tweezers. Studies which aim at identifying MP in the lower µm sizes rely on the certainty that the investigated MP particles are not destroyed by the chosen sample purification protocol.

In summary, we could show that conducting treatment evaluations with immobilised MP particles in the lower micrometre sizes is possible and has a range of advantages. From a theoretical perspective this could be readily adapted for even smaller MP and nanoplastics. In contrast to mobile particle approaches, particle properties changing due to a treatment can be studied here on individual particle level.

For the first time it was possible to demonstrate for MP as small as 10 µm, that purification methods, which are already routinely used, do not substantially alter the spectroscopic detectability, nor quantitative properties for many of the most common polymer types. Our results substantiate the validity of applications that extract particles in this size range by those methods. It turned out that polymer resins used as binders in synthetic paints are distinct from MP derived from commodity plastics. In chemical treatments they were more easily taking damage and their spectroscopic recognisability was severely limited independent of treatment. A tentative conclusion hereof is that numbers of paint flakes, found in environmental samples, are likely to be underestimated compared to other MP species.

We recommend that future studies take up the approach – and lessons learned – for qualitative and quantitative evaluations on immobilised MP, to yield further certainty of applicability of their respective methodological setups.

Abbreviations
MP: Microplastic(s); BDI: Background distortion index; DIC: Differential interference contrast microscopy; FRP: Fibre reinforced polymer(s); FTIR: Fourier transform infrared spectroscopy; GLM: Generalised linear model(s); HQI: Hit quality index; Lo: Lower threshold; LT: Long term; RT: Room temperature; SI: Supplementary information; SPT: Sodium polytungstate

Supplementary Information
The online version contains supplementary material available at https://doi.org/10.1186/s43591-021-00012-0.

Additional file 1.

Acknowledgements
For helpful comments and expertise, we thank Klaus-Jochen Eichhorn, Mikhail Malanin and Lars Bittrich. Support in laboratory work was kindly provided by Elisavet Kanaki, Pia Ulischberger, Anne Rödiger, Piotr Jachimowicz, Julia Muche and Juliana Ivar do Sul.

Authors' contributions
RL, KE, DF and ML developed the idea for this research; RL, KE, and FF contributed the conception and design of the work; RL, KE and FF conducted the acquisition, analysis and interpretation of data; RL and JB created new software used in the work; JB provided code revision; RL, KE and FF have drafted the manuscript; JB, DF and ML substantively revised it. The authors read and approved the final manuscript.

Funding
Funding of this study was received from the project MicroCatch_Balt (German Federal Ministry of Education and Research (BMBF), grant number 03F0788A) and the BONUS project Micropoll (funded jointly by the European Union and the BMBF, grant number 03F0775A). Open Access funding enabled and organized by Projekt DEAL.

Availability of data and materials
- The source code of the image and statistical analysis and visualisation is available as a static archive on Zenodo [35] with the identifier https://doi.org/10.5281/zenodo.4592319 and as a repository on Github at https://github.com/robna/ImmobileParticles_MatchAndAnalyse
- The interactive figure that was used for the exploration and analysis of the quantitative dataset of this study is available on Zenodo [52] with the identifier https://doi.org/10.5281/zenodo.4568524
- DIC microscopy data that support the quantitative findings of this study are available on Zenodo [55] with the identifier https://doi.org/10.5281/zenodo.4568488. This includes all pre- and post-treatment images after manual processing and downscaling (as used in the analysis). Original raw imaging data is not provided there due to large file size (> 1 TB), but are available upon reasonable request from the authors.
- The Raman and FTIR spectroscopy data that support the qualitative findings of this study are available on Zenodo [34] with the identifier https://doi.org/10.5281/zenodo.4568683.

Declaration

Competing interests
The authors declare that they have no competing interests.

Author details
[1]Leibniz Institute for Baltic Sea Research Warnemünde, Seestraße 15, 18119 Rostock, Germany. [2]Leibniz Institute of Polymer Research Dresden, Hohe Straße 6, 01069 Dresden, Germany. [3]University of Gothenburg, Department of Marine Sciences, Kristineberg 566, S-45178 Fiskebäckskil, Sweden.

Received: 15 March 2021 Accepted: 17 June 2021
Published online: 18 July 2021

References
1. Enders K, Lenz R, Beer S, Stedmon CA. Extraction of microplastic from biota: recommended acidic digestion destroys common plastic polymers. ICES J Mar Sci. 2017;74(1):326–31. https://doi.org/10.1093/icesjms/fsw173.
2. Tagg AS, Harrison JP, Ju-Nam Y, Sapp M, Bradley EL, Sinclair CJ, et al. Fentons reagent for the rapid and efficient isolation of microplastics from wastewater. Chem Commun. 2017;53(2):372–5. https://doi.org/10.1039/c6cc08798a.
3. Löder MGJ, Imhof HK, Ladehoff M, Löschel LA, Lorenz C, Mintenig S, et al. Enzymatic purification of microplastics in environmental samples. Environ Sci Technol. 2017;51(24):14283–92. https://doi.org/10.1021/acs.est.7b03055.
4. Kühn S, van Werven B, van Oyen A, Meijboom A, Rebolledo ELB, van Franeker JA. The use of potassium hydroxide (KOH) solution as a suitable approach to isolate plastics ingested by marine organisms. Mar Pollut Bull. 2017;115(1-2):86–90. https://doi.org/10.1016/j.marpolbul.2016.11.034.
5. Dehaut A, Cassone A-L, Frère L, Hermabessiere L, Himber C, Rinnert E, et al. Microplastics in seafood: benchmark protocol for their extraction and characterization. Environ Pollut. 2016;215:223–33. https://doi.org/10.1016/j.envpol.2016.05.018.
6. Avio CG, Gorbi S, Regoli F. Experimental development of a new protocol for extraction and characterization of microplastics in fish tissues: first observations in commercial species from Adriatic Sea. Mar Environ Res. 2015;111:18–26. https://doi.org/10.1016/j.marenvres.2015.06.014.
7. Nuelle M-T, Dekiff JH, Remy D, Fries E. A new analytical approach for monitoring microplastics in marine sediments. Environ Pollut. 2014;184:161–9. https://doi.org/10.1016/j.envpol.2013.07.027.
8. Mathalon A, Hill P. Microplastic fibers in the intertidal ecosystem surrounding Halifax Harbor, Nova Scotia. Mar Pollut Bull. 2014;81(1):69–79. https://doi.org/10.1016/j.marpolbul.2014.02.018.
9. Cole M, Webb H, Lindeque PK, Fileman ES, Halsband C, Galloway TS. Isolation of microplastics in biota-rich seawater samples and marine organisms. Sci Rep. 2014;4(1). https://doi.org/10.1038/srep04528.
10. Claessens M, Cauwenberghe LV, Vandegehuchte MB, Janssen CR. New techniques for the detection of microplastics in sediments and field collected organisms. Mar Pollut Bull. 2013;70(1-2):227–33. https://doi.org/10.1016/j.marpolbul.2013.03.009.
11. Karami A, Golieskardi A, Choo CK, Romano N, Ho YB, Salamatinia B. A high-performance protocol for extraction of microplastics in fish. Sci Total Environ. 2017;578:485–94. https://doi.org/10.1016/j.scitotenv.2016.10.213.
12. Grbic J, Nguyen B, Guo E, You JB, Sinton D, Rochman CM. Magnetic extraction of microplastics from environmental samples. Environ Sci Technol Lett. 2019;6(2):68–72. https://doi.org/10.1021/acs.estlett.8b00671.
13. Thiele CJ, Hudson MD, Russell AE. Evaluation of existing methods to extract microplastics from bivalve tissue: adapted KOH digestion protocol improves filtration at single-digit pore size. Mar Pollut Bull. 2019;142:384–93. https://doi.org/10.1016/j.marpolbul.2019.03.003.
14. Pfeiffer F, Fischer EK. Various digestion protocols within microplastic sample processing evaluating the resistance of different synthetic polymers and the efficiency of biogenic organic matter destruction. Front Environ Sci. 2020;8. https://doi.org/10.3389/fenvs.2020.572424.
15. Lusher AL, Welden NA, Sobral P, Cole M. Sampling, isolating and identifying microplastics ingested by fish and invertebrates. Anal Methods. 2017;9(9):1346–60. https://doi.org/10.1039/c6ay02415g.
16. Vandermeersch G, Cauwenberghe LV, Janssen CR, Marques A, Granby K, Fait G, et al. A critical view on microplastic quantification in aquatic organisms. Environ Res. 2015;143(Pt B):46–55. https://doi.org/10.1016/j.envres.2015.07.016.
17. Bläsing M, Amelung W. Plastics in soil: analytical methods and possible sources. Sci Total Environ. 2018;612:422–35. https://doi.org/10.1016/j.scitotenv.2017.08.086.
18. Quinn B, Murphy F, Ewins C. Validation of density separation for the rapid recovery of microplastics from sediment. Anal Methods. 2017;9(9):1491–8. https://doi.org/10.1039/c6ay02542k.
19. Elert AM, Becker R, Duemichen E, Eisentraut P, Falkenhagen J, Sturm H, et al. Comparison of different methods for MP detection: what can we learn from them, and why asking the right question before measurements matters? Environ Pollut. 2017;231(Pt 2):1256–64. https://doi.org/10.1016/j.envpol.2017.08.074.

20. Käppler A, Fischer D, Oberbeckmann S, Schernewski G, Labrenz M, Eichhorn K-J, et al. Analysis of environmental microplastics by vibrational microspectroscopy: FTIR, Raman or both? Anal Bioanal Chem. 2016;408(29):8377–91. https://doi.org/10.1007/s00216-016-9956-3.
21. Fischer M, Scholz-Böttcher BM. Microplastics analysis in environmental samples recent pyrolysis-gas chromatography-mass spectrometry method improvements to increase the reliability of mass-related data. Anal Methods. 2019;11(18):2489–97. https://doi.org/10.1039/c9ay00600a.
22. Zobkov MB, Esiukova EE. Evaluation of the Munich plastic sediment separator efficiency in extraction of microplastics from natural marine bottom sediments. Limnol Oceanogr Methods. 2017;15(11):967–78. https://doi.org/10.1002/lom3.10217.
23. Enders K, Lenz R, Stedmon CA, Nielsen TG. Abundance, size and polymer composition of marine microplastics ≥ 10 μm in the Atlantic Ocean and their modelled vertical distribution. Mar Pollut Bull. 2015;100:70–81. https://doi.org/10.1016/j.marpolbul.2015.09.027.
24. Löder MGJ, Gerdts G. Methodology Used for the Detection and Identification of Microplastics—A Critical Appraisal. In: Bergmann M, Gutow L, Klages M. (eds) Marine Anthropogenic Litter. Cham: Springer; 2015. https://doi.org/10.1007/978-3-319-16510-3_8.
25. Hurley RR, Lusher AL, Olsen M, Nizzetto L. Validation of a method for extracting microplastics from complex, organic-rich, environmental matrices. Environ Sci Technol. 2018;52(13):7409–17. https://doi.org/10.1021/acs.est.8b01517.
26. Budimir S, Setälä O, Lehtiniemi M. Effective and easy to use extraction method shows low numbers of microplastics in offshore planktivorous fish from the northern Baltic Sea. Mar Pollut Bull. 2018;127:586–92. https://doi.org/10.1016/j.marpolbul.2017.12.054.
27. Julienne F, Delorme N, Lagarde F. From macroplastics to microplastics: role of water in the fragmentation of polyethylene. Chemosphere. 2019;236:124409. https://doi.org/10.1016/j.chemosphere.2019.124409.
28. Allegra G, Famulari A. Chain statistics in polyethylene crystallization. Polymer. 2009;50(8):1819–29. https://doi.org/10.1016/j.polymer.2009.01.063.
29. Julienne F, Lagarde F, Delorme N. Influence of the crystalline structure on the fragmentation of weathered polyolefines. Polym Degrad Stabil. 2019;170:109012. https://doi.org/10.1016/j.polymdegradstab.2019.109012.
30. Ober CK, Müllen K. Introduction applications of polymers. In: Matyjaszewski K, Möller M. (eds) Polymer science: a comprehensive reference: Elsevier; 2012. p. 1–8. https://doi.org/10.1016/B978-0-444-53349-4.00199-0.
31. Enders K, Lenz R, do Sul JAI, Tagg AS, Labrenz M. When every particle matters: a QuEChERS approach to extract microplastics from environmental samples. MethodsX. 2020;7:100784. https://doi.org/10.1016/j.mex.2020.100784.
32. Wang Z, Taylor SE, Sharma P, Flury M. Poor extraction efficiencies of polystyrene nano- and microplastics from biosolids and soil. PLoS One. 2018;13(11):e0208009. https://doi.org/10.1371/journal.pone.0208009.
33. Lares M, Ncibi MC, Sillanpää M, Sillanpää M. Intercomparison study on commonly used methods to determine microplastics in wastewater and sludge samples. Environ Sci Pollut R. 2019;26(12):12109–22. https://doi.org/10.1007/s11356-019-04584-6.
34. Lenz R, Enders K, Fischer F, Brandt J, Fischer D, Labrenz M. Raman and FTIR spectra used in: Lenz et al. 2021, "Measuring impacts of microplastic treatments via image recognition on immobilised particles below 100 μm"; 2021. https://doi.org/10.5281/zenodo.4568683.
35. Lenz R, Enders K, Fischer F, Brandt J, Fischer D, Labrenz M. ImmobileParticles_MatchAndAnalyse: Python code used for analysis of image data in Lenz et al. 2021, "Measuring impacts of microplastic treatments via image recognition on immobilised particles below 100 μm"; 2021. https://doi.org/10.5281/zenodo.4592319.
36. VanderPlas J, Granger B, Heer J, Moritz D, Wongsuphasawat K, Satyanarayan A, et al. Altair: interactive statistical visualizations for Python. J OSS. 2018;3(32):1057. https://doi.org/10.21105/joss.01057.
37. Satyanarayan A, Moritz D, Wongsuphasawat K, Heer J. Vega-lite: a grammar of interactive graphics. IEEE Trans Visual Comp Graphics (Proc InfoVis). 2017;23(1):341–50. https://doi.org/10.1109/tvcg.2016.2599030.
38. The pandas development team. Pandas-dev/pandas: pandas; 2020. https://doi.org/10.5281/zenodo.3509134.
39. McKinney W. Data structures for statistical computing in Python. In: van der WS, Jarrod M, editors. Proceedings of the 9th Python in Science Conference; 2010. p. 56–61.
40. Seabold S, Perktold J. Statsmodels: econometric and statistical modeling with Python. In: 9th python in science conference; 2010.
41. Bradski G. The OpenCV library. Dr Dobb's J Software Tools. 2000;25:120–5.
42. Van Der WS, Schönberger JL, Nunez-Iglesias J, Boulogne F, Warner JD, Yager N, et al. scikit-image: Image processing in Python. PeerJ. 2014;2:e453. https://doi.org/10.7717/peerj.453.
43. Canny J. A computational approach to edge detection. IEEE T Pattern Anal. 1986;PAMI-8(6):679–98. https://doi.org/10.1109/tpami.1986.4767851.
44. Otsu N. A threshold selection method from gray-level histograms. IEEE Trans Syst Man Cybern. 1979;9(1):62–6. https://doi.org/10.1109/tsmc.1979.4310076.
45. Statsmodels Contributors. 2021. Statsmodels.org. https://www.statsmodels.org/stable/glm.html. Accessed 29 Jan 2021.
46. Green PJ. Iteratively reweighted least squares for maximum likelihood estimation, and some robust and resistant alternatives. J R Stat Soc Ser B Methodol. 1984;46(2):149–70. https://doi.org/10.1111/j.2517-6161.1984.tb01288.x.
47. Lenz R, Enders K, Stedmon CA, Mackenzie DMA, Nielsen TG. A critical assessment of visual identification of marine microplastic using Raman spectroscopy for analysis improvement. Mar Pollut Bull. 2015;100(1):82–91. https://doi.org/10.1016/j.marpolbul.2015.09.026.
48. Zouboulis E, Renusch D, Grimsditch M. Advantages of ultraviolet Raman scattering for high temperature investigations. Appl Phys Lett. 1998;72(1):1–3. https://doi.org/10.1063/1.121437.
49. Butler HJ, Ashton L, Bird B, Cinque G, Curtis K, Dorney J, et al. Using Raman spectroscopy to characterize biological materials. Nat Protoc. 2016;11(4):664–87. https://doi.org/10.1038/nprot.2016.036.
50. Imhof HK, Laforsch C, Wiesheu AC, Schmid J, Anger PM, Niessner R, et al. Pigments and plastic in limnetic ecosystems: a qualitative and quantitative study on microparticles of different size classes. Water Res. 2016;98:64–74. https://doi.org/10.1016/j.watres.2016.03.015.
51. Piehl S, Hauk R, Robbe E, Richter B, Kachholz F, Schilling J, et al. Combined approaches to predict microplastic emissions within an urbanized estuary (Warnow, southwestern Baltic Sea). Front Environ Sci. 2021;9. https://doi.org/10.3389/fenvs.2021.616765.
52. Lenz R, Enders K, Fischer F, Brandt J, Fischer D, Labrenz M. Interactive figure for exploration and analysis of the quantitative image data set in Lenz et al. 2021, "Measuring impacts of microplastic treatments via image recognition on immobilised particles below 100 μm"; 2021. https://doi.org/10.5281/zenodo.4568524.
53. de Sousa Menezes M, Queiroz EC, Soares PV, Faria-e-Silva AL, Soares CJ, Martins LRM. Fiber post etching with hydrogen peroxide: effect of concentration and application time. J Endod. 2011;37(3):398–402. https://doi.org/10.1016/j.joen.2010.11.037.
54. Navarro CA, Kedzie EA, Ma Y, Michael KH, Nutt SR, Williams TJ. Mechanism and catalysis of oxidative degradation of fiber-reinforced epoxy composites. Top Catal. 2018;61(7-8):704–9. https://doi.org/10.1007/s11244-018-0917-2.
55. Lenz R, Enders K, Fischer F, Brandt J, Fischer D, Labrenz M. DIC microscopy images used in: Lenz et al. 2021, "Measuring impacts of microplastic treatments via image recognition on immobilised particles below 100 μm"; 2021. https://doi.org/10.5281/zenodo.4568488.
56. Valsesia A, Quarato M, Ponti J, Fumagalli F, Gilliland D, Colpo P. Combining microcavity size selection with Raman microscopy for the characterization of nanoplastics in complex matrices. Sci Rep. 2021;11(1):362. https://doi.org/10.1038/s41598-020-79714-z.
57. Al-Azzawi MSM, Kefer S, Weißer J, Reichel J, Schwaller C, Glas K, et al. Validation of sample preparation methods for microplastic analysis in wastewater matrices reproducibility and standardization. Water. 2020;12(9):2445. https://doi.org/10.3390/w12092445.

Publisher's Note

Springer Nature remains neutral with regard to jurisdictional claims in published maps and institutional affiliations.

This is the end of the publication

Measuring impacts of microplastic treatments via image recognition on immobilised particles below 100 µm

by Robin Lenz, Kristina Enders, Franziska Fischer, Josef Brandt, Dieter Fischer, Matthias Labrenz

You might want to continue reading the synopsis at page 20, or jump back to the start of this publication at page 150.

A Public Database for Microplastics in the Environment

by Natalja Čerkasova, Kristina Enders, Robin Lenz, Sonja Oberbeckmann, Josef Brandt, Dieter Fischer, Franziska Fischer, Matthias Labrenz, Gerald Schernewski

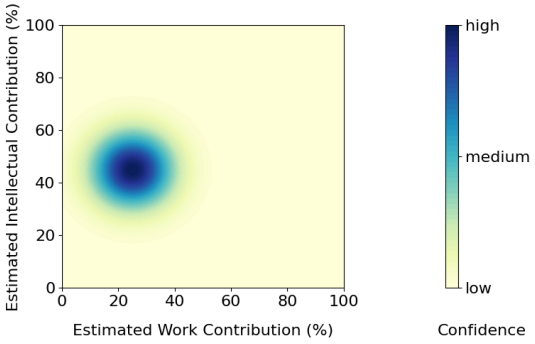
- **Date published**: February 15, 2023
- **Type**: Research Article
- **Published in**: Microplastics, MDPI
- **License**: CC-BY
- **DOI**: 10.3390/microplastics2010010, **Reference**: [10]
- **Citations**: 15 (Crossref/DOI, 2025-11-18)

Contributions

Conceptualisation, database development and writing: N.Č. | DB structure conceptualisation, support of database development, writing, visualisations and editing: K.E., R.L., J.B., D.F., F.F. | Writing and complementary visualisation: G.S. | Editing, project administration and funding acquisition: S.O., M.L. | All authors have read and agreed to the published version of the manuscript.

Quantitative own contributions based on self-assessment

In the dimensions of expended work effort and intellectual contribution, I consider my shares are likely to be between 20% and 30% and between 40% and 50% respectively. This is visualised below as an interpolated histogram of 500 samples from Gaussian distributions with the aforementioned estimates at plus/minus two standard deviations.



microplastics

MDPI

Article

A Public Database for Microplastics in the Environment

Natalja Čerkasova [1,2,*], Kristina Enders [3,4], Robin Lenz [3,4], Sonja Oberbeckmann [4], Josef Brandt [5], Dieter Fischer [3], Franziska Fischer [3], Matthias Labrenz [4] and Gerald Schernewski [1,4,*]

1 Marine Research Institute, Klaipeda University, Universiteto ave. 17, LT-92294 Klaipėda, Lithuania
2 Texas A&M AgriLife Research, 720 E Blackland Rd, Temple, TX 76502, USA
3 Leibniz Institute of Polymer Research Dresden; Hohe Straße 6, D-01069 Dresden, Germany
4 Leibniz-Institute for Baltic Sea Research, Seestrasse 15, D-18119 Rostock, Germany
5 Department of Marine Sciences, University of Gothenburg, Box 461, SE-405 30 Göteborg, Sweden
* Correspondence: natalja.cerkasova@ku.lt (N.Č.); gerald.schernewski@io-warnemuende.de (G.S.)

Abstract: During recent years plastics became one of the focuses of EU policy. A harmonisation and comparability of microplastics monitoring results across Europe is needed. The complexity of microplastic data makes it necessary to develop a specific, tailor-made database rather than adapting and modifying one of the existing databases. To meet this demand, we present a publicly accessible, flexible, and extendable structured relational database for particle-based microplastic data. The developed relational database is adaptive and meets the specific demands of microplastics, e.g., a large variety of sampling, processing and analytical methods, many types of plastics, and a very wide size spectrum ranging from micrometres to millimetres. In this paper we discuss the development of the database, data entry specifics, sample analysis methods, microplastics data manipulation and quality assurance, and database integration and accessibility.

Keywords: microplastic data; database; marine; particles; EU policies; Marine Strategy Framework Directive

check for updates

Citation: Čerkasova, N.; Enders, K.; Lenz, R.; Oberbeckmann, S.; Brandt, J.; Fischer, D.; Fischer, F.; Labrenz, M.; Schernewski, G. A Public Database for Microplastics in the Environment. *Microplastics* **2023**, 2, 132–146. https://doi.org/10.3390/microplastics2010010

Academic Editors: Nicolas Kalogerakis and Tony Robert Walker

Received: 30 December 2022
Revised: 15 January 2023
Accepted: 7 February 2023
Published: 15 February 2023

Copyright: © 2023 by the authors. Licensee MDPI, Basel, Switzerland. This article is an open access article distributed under the terms and conditions of the Creative Commons Attribution (CC BY) license (https://creativecommons.org/licenses/by/4.0/).

1. Introduction

Environmental policy in European countries is driven by ambitious European Union (EU) legislation, which has affects beyond the EU member states. Some major EU policy fields are the marine and coastal environment, nature and biodiversity, and water. The water policy aims at protecting the European Union's water resources and ecosystems and ensuring access to clean drinking and bathing water. This includes specific policies, e.g., on marine, surface, bathing and drinking water, floods, nitrate pollution, groundwater, urban wastewater, water reuse, water scarcity, and droughts. Most environmental policies are implemented though legally binding directives. These directives are accompanied by implementation guidelines that regulate, for example, monitoring, methodological standards, quality thresholds, and environmental quality assessment. A consequence of EU environmental policy implementation is the collection of enormous amounts of heterogeneous environmental data.

The need to deal with this data initiated the development of the EU Shared Environmental Information System (SEIS). It was established to improve the collection, exchange, and use of environmental data and information across Europe [1]. The SEIS serves as an umbrella for specific data platforms such as the Marine Information System for Europe (WISE-Marine) and regional sea platforms, e.g., for the North Sea (OSPAR), or the Baltic Sea (HELCOM). WISE-Marine and the regional platforms directly support European environmental policies' implementation. These international approaches are complemented by national environmental data platforms, for example, in Germany the Marine Data Infrastructure Germany (MDI:DE).

The general marine data management in Europe consists of three major elements: SeaDataNet, EMODnet, and Copernicus CMEMS. SeaDataNet is a distributed marine data

infrastructure for diverse in situ data sets. EMODnet is using available data for preparing multi-resolution maps of all European seas, and Copernicus is the earth observation program and offers information services mainly based on satellite data.

It is obvious that the large amount of heterogeneous data, multiple platforms that depend on data-exchange, and a wide range of potential data uses require rules that ensure data quality and accessibility. These rules are provided by the EU INSPIRE Directive. An important aspect is that INSPIRE contains guidelines on metadata documentation based on EN ISO 19115 and EN ISO 19119. Metadata provide the required background information about data. Metadata descriptions are a prerequisite so that data, physically stored in a database, can be found and used by others.

During recent years, plastics became one focus of EU policy. In 2018, the EU adopted the plastics strategy (EC COM/2018/028, 2018) with the aim to protect the environment and reduce marine litter. It is part of the circular economy action plan, revised in 2020, and builds on existing measures to reduce plastic waste. In the marine environment this is complemented by the EU Marine Strategy Framework Directive (MSFD 2008/56/EC). The MSFD has the aim to protect and achieve a good environmental status (GES) in marine ecosystems. The GES is assessed on the basis of eleven descriptors and marine litter is one of them, which aims to ensure that properties and quantities of marine litter do not cause harm to the coastal and marine environment. As a consequence, the state-of-pollution of the marine environment has to be assessed, environmental targets and associated indicators have to be developed, major emission sources have to be identified and quantified, and effective measures leading to reductions in marine litter pollution have to be tested. One focus is on trends in the amount, distribution, and composition of microplastics. This has caused a wide range of scientific and monitoring activities during the last decade and the need to establish joint databases that follow FAIR (Findable, Accessible, Interoperable, and Reusable) data principles [2].

A first European litter database, linked to EMODnet, exists [3]. It focuses on macro-litter, the size fraction above 25 mm, found at beaches using the 100 m monitoring method [4]. A recent review shows that the database suffers from many data weaknesses, for example, spatiotemporal heterogeneity, inconsistencies in the different litter identification lists, and variability in the survey protocols and data sources. The conclusion is that a harmonisation and comparability of results across Europe are still needed. For microplastics, a comparable database does not exist yet, but there are several lessons learned from the macro-litter beach database. A public microplastic database should be available at an early stage of monitoring. It needs to be flexible and adaptive and must meet the specific demands of microplastics, e.g., a large variety of sampling, processing and analytical methods, many types of plastics or a very wide size spectrum ranging from micrometres to five millimetres. The complexity of microplastic data makes it necessary to develop a specific, tailor-made database rather than adapting and modifying one of the existing marine databases. This means that the new database needs to be visible for and integrated into existing database structures.

To meet this demand, we present a publicly accessible, flexible, and extendable structured database (DB) for particle-based microplastic data, that meets the FAIR data principles, takes into account the INSPIRE metadata requirements, and is linked to and harvested by other databases.

2. Materials and Methods

2.1. Basic Requirements and Background

The database was developed to meet the data storage and reporting requirements of two international projects with focus on coastal and marine microplastics in the Baltic Sea region, namely Bonus MicroPoll (https://www.io-warnemuende.de/project/192/micropoll.html, accessed on 12 December 2022) and MicroCatch (https://www.io-warnemuende.de/microcatch-home.html, accessed on 12 December 2022). Database requirements were that relevant sample parameters had to be efficiently (i.e., no data loss, consistency, simplicity)

communicated between the entities. It had to be possible to reconstruct each individual microplastic particle's history from sampling to final analysis. This was the key for asserting data quality in terms of good scientific practice. It had to be possible for sample recruiters to share sample locations, sample type, sampling method, and time. Contact details of the responsible persons of each sub-task had to be taken into account. Important information concerning the sample purification, such as treated sample amount, blanks (contamination control), purification methods, and date had to be represented. Among relevant parameters of microplastic analysis were, e.g., polymer type, size, particle shape, colour, analysis method, the fraction analysed (if a purified sample was split), and blanks.

All the above information and additional required details were implemented into the Marine Plastic Database (MPDB) design and optimised over several years with respect to scientific accuracy, relevance, clarity, and consistency of terms and information within and across database tables. In particular, the two latter requirements were driven by the goal to make the MPDB publicly available. Therefore, we aimed at reducing the information to a minimum that is mandatory for marine plastic-monitoring in the environment. At the same time, it was important to keep flexibility with respect to the large variability of different sample requirements (e.g., concerning purification or analysis methods). The database had to take into consideration that microplastic monitoring involves different actors across various stages with different tasks, such as sample collection, sample purification, and spectroscopic analysis.

2.2. Types of Data

Quantitative microplastic (MP) data is typically either mass- or particle-based, both methods having their own advantages and limitations. Eventually, the targeted polymer types and size ranges, and the foremost research question determines the analytical method of choice.

Mass-based data, as for example from pyrolysis gas chromatography mass spectrometry (Py-GC-MS), usually necessitates less sample purification and hence accelerates data generation. Losses caused during pre-treatment, which particularly affect the small size classes, become obsolete and make this analysis especially advantageous for target particles in the sub-micrometre range. Limitations arise on the detection of multiple polymer types, as interferences can occur [5] that involve increasing resources and efforts when aiming at a large coverage of materials addressed by the umbrella term "microplastics". Microplastic particles' polymer types that appear in low amounts are prone to fall below the limit of detection if they belong to a rarely occurring type, or if the particles are so small that they, although being numerous, do not provide enough mass [6,7]. In any case, the main disadvantage is that only the mass of the MP polymer type is obtained and there is no information on particle sizes and their distribution.

Any research question that requires a higher resolution of particle size, examples are the determination of transport patterns, normalisation of biofilm coverage, or the encounter rates of potentially affected organisms necessary for a respective risk assessment, will demand or consider particle-based data acquisition. Particle-based analysis is usually performed using μ-Raman- or Fourier-Transform-Infrared-Microspectroscopy (FTIR) with the ability to detect very low numbers of polymer particles. The methods are either done in imaging or particle measurement mode. Imaging entails scanning the entire filter area and acquiring spectra at every pixel. After spectra evaluation, adjacent pixels with the same chemical classification are grouped as particles [8,9]. In particle measurement, at first an optical image of the filter is acquired, from which the location of the individual particles is determined, together with information about size, shape, and colour or texture. Only then are the spectra acquired at the locations where particles were found [10,11].

2.3. Morphological Properties of Microplastic Particles

The minimum size of particles to be detected depends on the spectroscopy technique used (FTIR: approx. 10–15 μm, Raman: approx. 1 μm). Which technique is used also de-

pends on the sensitivity of the analysis towards certain substances [12]. Spectra quality, and thus, method reliability can be impacted by fouling of particles or fluorescent components (in case of Raman).

Using the particle-based approach, concentrations are typically reported as MP counts per unit environmental matrix (e.g., kg^{-1}, or m^{-3}). In addition, other particle characteristics, such as shape properties or colour can be determined on a per-particle basis.

The particle count concentrations themselves are, however, of limited usefulness when being reported without substantial context. As an example, estimates of how many trillion "pieces" of MP are polluting the ocean, are readily incorporated and circulated by various media [13,14]. It is questionable if actual informative content about the pollution's extent can be conveyed in this manner, or rather, if a broader public attraction is intended simply by the magnitude of an unimaginable high number. Representations of particle sizes (e.g., as individual particle properties or continuous distributions [15]) and study design details (e.g., applied mesh sizes) are examples of such augmenting data that should preferably be communicated alongside MP concentrations. The same is true for comparative data on natural particles where applicable (e.g., as proxy for the hydrodynamic regime in sediment MP studies [16]). An appropriate database structure for particle-based MP pollution data should therefore provide the possibility to map all relevant morphological data which is then available for any future assessment. From simple to sophisticated, such morphological properties ("morphologicals" hereafter) may include size class [16,17], longest size dimension, [18] or multiple size dimensions, area [19,20], circumference, or shape related aspects, such as sphericity, convexity, eccentricity, right up to fully 2D or 3D descriptions of the irregular particles (e.g., as point meshes). Referenced studies in the above list give examples from the scientific literature that utilised the respective morphological features to describe their identified particles. The more sophisticated morphological features may have higher demands for the analytical process, but they give the resulting data set a higher diagnostic quality for describing the interactions the identified particles may invoke in the environment. Although not trivial, particle mass estimates may be inferred if the reported particle morphological data are of sufficient detail, i.e., at least a proper shape classification and maximum extents in 3 dimensions. This allows to link the realms of particle- and mass-based analyses, which would be highly beneficial to the field of MP research. In contrast, inferring morphological data from destructive mass-based analytics is unfeasible.

Fortunately, for the choice of appropriate morphological features, it is not necessary to start ab initio, as much knowledge can be transferred from other particle-based research fields, such as from sedimentology, with a great repertoire on various size characteristics of sediment grains [16,20,21].

2.4. Software and Tools

Prerequisite for a database is that it contains a structured set of data, meaning that data should be organised using formal design and modelling techniques. Structured data, which usually reside in relational databases, provide benefits, including but not limited to data integrity and independence from applications or programs, increased consistency, decreased updating errors, improved data access to users, and data security. This ensures that the research data meet the FAIR principles—findable, accessible, interoperable, and reusable. It is worth noting that the mentioned advantages entail additional expenses such as the time and intellectual requirements to design a complex database, possible software and hardware costs, and costs for training the personnel to use and administrate, as well as maintain the database.

An SQL (structured query language) database can be effectively set up to represent multiple levels of abstractions. It is a collection of highly structured tables, wherein each row reflects a data entity, and every column defines a specific information field. Relational databases are built using the structured query language to create, store, update, and retrieve data.

The MySQL™ software delivers a very fast, multithreaded, multi-user, and robust SQL database server [22], hence was considered to be a perfect tool for the development of the MP database. The MySQL software is Dual Licensed; in this study the MySQL as an Open-Source product under the terms of the GNU General Public License (https://www.fsf.org/licenses/, accessed on 10 December 2022) was used. Depending on user preferences and requirements, other tools were in use as well, such as the HeidiSQL, [23] MySQL Workbench (https://www.mysql.com/products/workbench/, accessed on 10 December 2022), and certain Python libraries (mysql.connector [24]) for automated access to the DB. Any relational database management system (RDBMS) can be used to access the database, as long as it uses SQL as its standard database language. The database server is hosted by the Leibniz Institute for Baltic Sea Research Warnemünde-IOW, which allows usage by registered users. As in any database management system (DBMS), users may perform tasks which correspond to their rights, granted by the administrator: view, edit, delete, etc. The possible database usage possibilities are explained in MySQL documentation (available at https://dev.mysql.com/doc/, accessed on 10 December 2022), and many tutorials and videos present online [25].

2.5. Database Development

The database development process was conducted following a classical waterfall model [26], with iterative process revision (Figure 1). Firstly, specific needs for data were identified, followed by determination of data types. The first step was carried out mainly by the environmental scientists, who oversaw collecting or analysing samples; judging from their experience, these users could immediately identify what data should be collected, whether it is possible to collect all the data (obligatory fields in the database), which data is optional or incidental (optional fields), and what could be further used in later research (quantification of entries). This step was followed by a conceptual model development, which established connections between possible tables and entities. The conceptualisation was completed with tight communication between the team members, who oversaw sampling and analysis, and those responsible for the MPDB technical implementation (database developer). Where one could identify the relationships between data, the other could comment on the possibility of implementing such a relationship and to assure database structure logic.

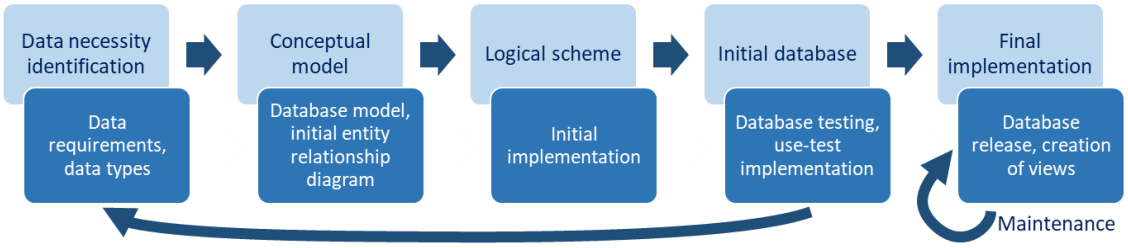


Figure 1. Marine Plastic Database development process stages.

Further steps (logical schema, initial and final implementation) were completed by the developer, based on the possible use-case scenarios, provided by the MPDB users. Currently the database is in its finalised stage, with maintenance and the support to create custom database views on demand. Database views are pre-established query commands, which are kept in the database dictionary to generate a certain preview of structured data, possibly combining entries from multiple tables or other views, performing certain calculations, or simplifying multiple tables to a single table, which can then be used for further data analysis. The use of such views greatly facilitates data extraction for specific repetitive evaluation tasks.

The MPDB development stages 1 to 4 (see Figure 1) were revisited several times, as some requirements and improvement suggestions were received after the initial test-

ing of the database, which in turn assured a reliable product that suits the users and stakeholder needs.

2.6. Data Entry

The most efficient method of data entry depends on the type of data, its amount, and the frequency with which it accrues. Some data entries are best entered manually, e.g., to populate the 'contributors' table (a contributor is a person who is working with the samples or analysis), or some categories, such as the 'colour' or the 'shape' (we use the term "auxiliary" tables, when describing such entity properties). Such tables are usually referred to as pre-populated categories. For bulk data entry, however, a manual approach would be counter-productive and undermine the development of the relational database in the first place. Instead, the database ought to be populated wherever possible with bulk entries using queries, spreadsheets (comma-separated values (CSV) sheets), any structured text document, as well as using fully- or semi-automated scripts.

Data entry for the 'samples' table were most useful in the form of SQL 'insert' queries which pulled a prepared CSV file into the table. The creation of data describing samples typically involves highly manual tasks, such as insertion of information from handwritten field work logbooks. Most researchers will prefer a simple spreadsheet application for this work. In such a case, a simple export of the DB table into a CSV file format may be utilised and further used as a template where the new data can be appended. This ensures that the later CSV upload to the DB can be completed by a standard SQL script without errors or data incompatibilities in a semi-automated way.

The tables containing actual analytical result data (such as 'particles' or 'analysis') receive the highest number of entries (as there may be hundreds or thousands of MP particles per sample) and are therefore impractical to be populated by manual data entry or individual CSV files. For this purpose, a Python software package was developed which performs an automated particle measurement and data evaluation and entry [27]. Using the mysql.connector Python library [24] allowed streamlining the necessary data compilation, conversion, and SQL insertion to reduce manual effort to a minimum. The custom-made graphical user interface (GUI) allowed reviewing summarised and categorised particle information and uploading the results of hundreds of particles in less than a minute.

3. Results

3.1. Database Structure

The final structure of the MPDB is presented in an enhanced entity-relationship (EER) database diagram which represents requirements and complexities of the developed database (Figure 2). There are 14 auxiliary tables, 3 main, and 2 junction tables. The data in the auxiliary tables have to be entered only once or updated very rarely, i.e., if new contributors (a person who is working with the samples or analysis) are engaged in the procedure, then their information should be entered once. Every contribution (sample or analysis) will be automatically assigned to that person with a unique ID. Hence, the information is stored once and is referenced via a foreign key attribute.

The three main tables of the database are: samples, analysis, and particles (see also Figure 3). Any sample may be analysed via various methods and yield many particles. For instance, a certain sample was treated with several different purification methods, all of which had to be registered in the database. Similarly, a certain particle could be measured with both methods, FTIR and Raman, yielding individual results that should all be included in the MPDB. Hence, the standard relational database rule of one-to-one or one-to-many relationship is not sufficient; a many-to-many connection had to be established. This is achieved via the two associative or junction tables: 'sample2methods' and 'particles2analysis'. The connections are stored in these junction tables via the copies of the primary keys of joining tables (Figure 2).

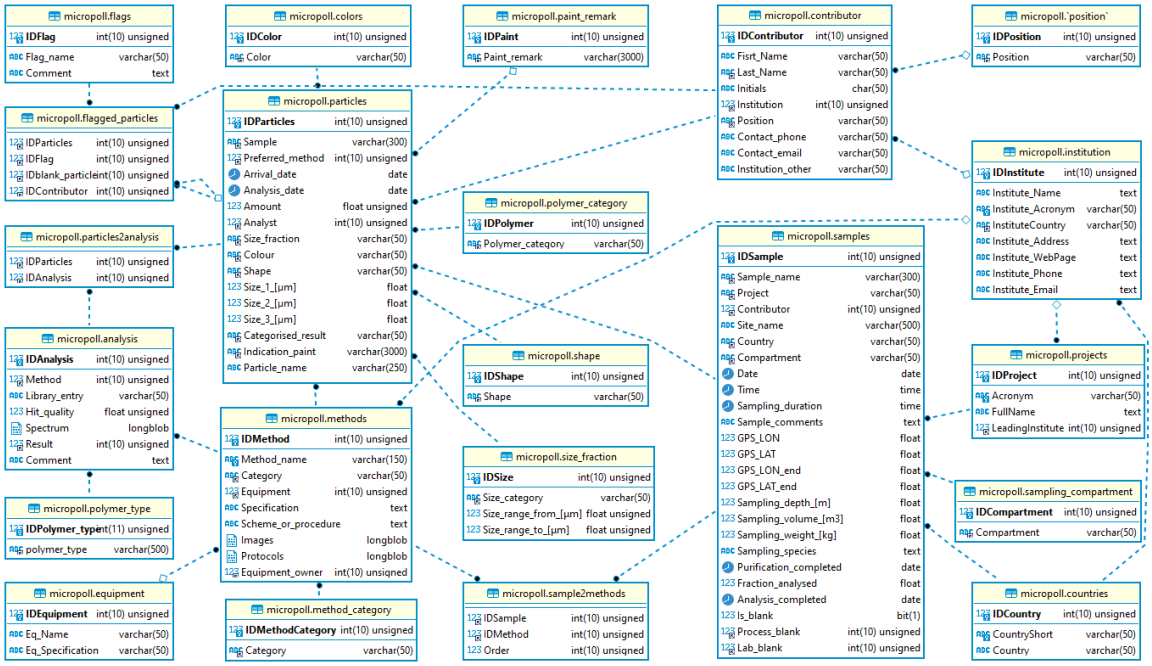


Figure 2. Enhanced entity-relationship diagram of the final version of the Marine Plastic Database.

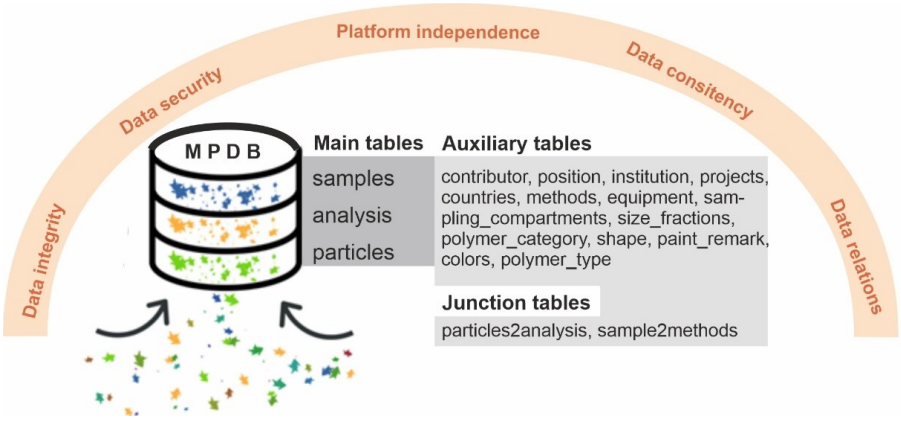


Figure 3. The Marine Plastic Database with main and auxiliary tables as well as requirements and advantages.

The database users usually work with the main tables and the junction tables. The unique ID keys are assigned automatically. The 'samples' table receives entries for actual environmental samples as well as blank samples for contamination control. The field 'Is_blank' requires a Boolean-type entry to unambiguously mark the type of each sample. We use two different kinds of blanks: one covering the particle analysis steps (called lab blanks) and others covering the sample purification (called process blanks).

Lab blanks represent potential contamination introduced during analysis preparation and spectroscopic measurement (FTIR or Raman microspectroscopy) of a sample, which is a critical step for introducing contaminations. There is one corresponding lab blank for each environmental sample. Process blanks cover the sample type-specific treatment pipeline [28], where a group of process blanks typically represent potential contamination

from the purification procedures of all environmental samples treated alike during a certain time period.

Based on the 'Is_blank' flag, and the entries for 'Process_blank' and 'Lab_blank' an extraction of either type of samples (environmental sample, process blank, lab blank) can be achieved easily by querying the wanted sequence. Particles found in a blank may be used to adjust the particle numbers of their corresponding environmental samples. A recommendation of how to implement a blank correction in the particle domain is given in Section 3.4. A recent review on blank procedures [29] evaluates several further options.

3.2. Data Extraction and Example Queries

Database data retrieval for further analysis is usually done via the data export of views. Database users may use the existing views or ask the administrator to create views based on their description.

3.2.1. Data Filtering Scenario

Some data may need only a simple filtering from one specific table. A simple data filter example may be as follows:

"every sample, from the MicroCatch project from compartment "water" from location between 12.17–12.2 and 53.95–55.0 (lat, long) in the year 2018".

The SQL query snipped for the example is:

*SELECT * FROM 'samples'*
WHERE
samples.Project = 'MicroCatch' AND
samples.Compartment = 'water' AND
year(samples.Date) = 2018 AND
samples.GPS_LON >= 12.17 AND samples.GPS_LON <= 12.2 AND
samples.GPS_LAT >= 53.95 AND samples.GPS_LAT <= 55.0;

3.2.2. Data Retrieval from Two Tables Scenario

When extraction of data from multiple tables is needed, the best solution is to create a new joint table, which is called a View, where all the related data entries are linked. After this, the new table can be filtered as in the data filtering scenario. An example for this scenario can be a modified query, as follows:

"every particle, from location between 12.17–12.2 and 53.95–55.0 (Lat, long) in 2018, with a size fraction of 11–100 µm".

Creation of view:

CREATE VIEW 'particles_v_samples' AS
SELECT p.'Sample',s.'Date', s.'GPS_LON', s.'GPS_LAT',p.'Size_fraction'
FROM 'particles' AS p
INNER JOIN 'samples' AS s
ON p.'Sample' = s.'Sample_name';

Filtering the view:

*SELECT * FROM micropoll.particles_v_samples*
WHERE
year(particles_v_samples.year) = 2018 AND
particles_v_samples.GPS_LON >= 12.17 AND particles_v_samples.GPS_LON <= 24.2 AND
particles_v_samples.GPS_LAT >= 53.95 AND particles_v_samples.GPS_LAT <= 59.0 AND
particles_v_samples.Size_fraction = '11–100';

3.2.3. Data Extraction to a Local File Scenario

The data may be extracted to a spreadsheet or other formats for further analysis. Extraction requires either the usage of DBMS tools (like the export tools available from MySQL workbench, or HeidiSQL), or the direct application of SQL commands:

INTO OUTFILE 'D:\full_path\samples_table.csv'

FIELDS TERMINATED BY ','
ENCLOSED BY '"'
LINES TERMINATED BY '\n';

The provided examples present only a fraction of the user possibilities and may be modified, i.e., to include only unique values of entries, or additional fields or filters. As the stored data has a spatial locator (X and Y coordinates), one can, for example, utilise the functionality of various GIS tools and plugins to plot and represent the data on maps.

3.3. Data Quality Assurance—Dealing with Different Particles

Microplastics—being particulate pollutants that are typically investigated individually for properties such as material, colour, shape, or size—generate data on a per particle basis (at least for quantitative particle-based studies). For statistical analysis, interpretation and dissemination to the general public and stakeholders, data are typically transferred to aggregated information, e.g., counts of particles or averages of sizes, which are reported per sample, or time, or region. This section aims to elucidate the importance of a transparent handling and dissemination of the raw particle data as a means for better data compatibility and re-usability among MP studies. The understanding of particle-based vs. aggregated data is crucial to be able to perform data operations, such as correcting for self-contamination (blank correction) or limit of detection (to be implemented for removal of singular erroneous or misfit results) as explained in the examples below.

Conceptually, we distinguish between data in the "sample domain" (sampling metadata such as sample quantity, location, dates) as opposed to the "particle domain" (individual properties of each particle). Particle domain data (PDD) can be used to generate sample domain data (SDD) by aggregation. Sums, means, or other descriptive statistics of PDD from a particular sample or sample group may be aggregated to yield the respective SDD. SDD, in turn, cannot be decomposed into the underlying PDD because the information on individual particles is lost in aggregation.

Figure 4 illustrates the distinct representations of data that are handled by the MPDB: in PDD the base of a single entry is an individual particle and it holds particle property data; whereas in SDD the base is a sample, which has sample metadata and aggregated particle data. The phenotyping procedure (PhT) is used to conduct operations on PDD and translate them into SDD.

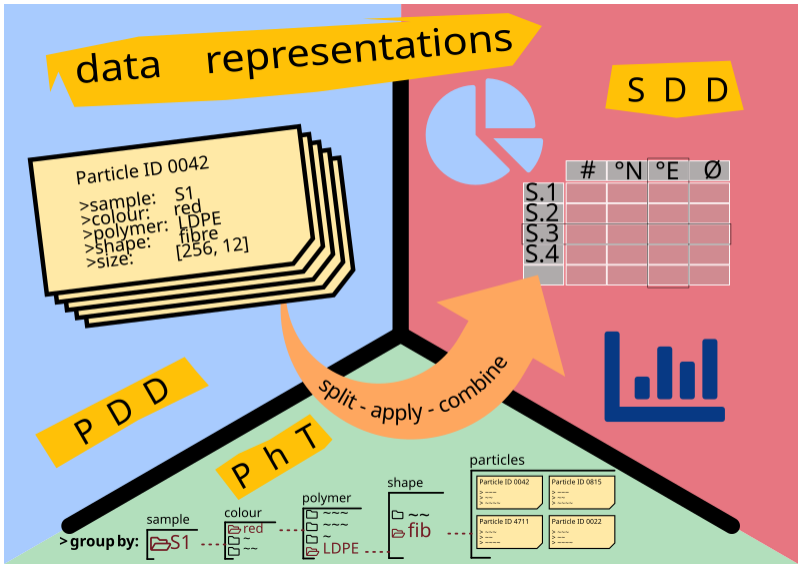


Figure 4. The distinct representations of data that are handled by the MPDB and the algorithms we use are illustrated in this info graphic.

To elaborate the implications of the distinction of SDD and PDD, let us consider the concentration of MP of a sample. In SDD this would be a number of MP per reference quantity of the environmental matrix (e.g., 100 m^{-3} or 23 kg^{-1}). Here, each MP within that number is considered equal, as there are no individual particles regarded by SDD, only their sum. If the underlying raw data (PDD) would only consist of identical particles, a value correction would seem intuitively feasible by a simple subtraction of the required amount. However, MP samples usually do not consist of a number of homogeneous MP particles, but for example, of a red PET fibre and a transparent PE fragment, which can only provide information on possible sample contamination of their kind and not of MP in general. The blank correction must, therefore, be done in PDD, where each particle is *not* equal. In PDD, a subtraction in a mathematical sense is, however, not possible, as each datum represents an individual, not an aggregation. Instead, an elimination of individuals can be an approach to facilitate the correction.

In case of negligible contamination, this theoretical excursion into particle identity should be of little relevance for reported MP data. However, experience shows that (1) contamination is an issue of concern, especially for studies working with small MP, and (2) not seldomly, MP data sets are on the brink of statistical exploitability due to low numbers of the costly to identify specimens, therefore data handling and sanitation procedures are to be chosen carefully.

The here described implications of working with particle data versus aggregated data does not only apply to MP research. Approaches of particle-based data conversion are, for example, discussed in polydisperse systems modelling [28].

3.4. Data Sanitation-Phenotyping and Blank Subtraction

As stated above, the omnipresence of MP easily leads to self-contamination of MP samples, which necessitates blank sample corrections. As the raw data of particle-based MP studies is represented in PDD, a number of individual particles needs to be selected for being regarded as introduced by the sampling and lab procedures, and therefore rejected from final results. The decision of which particle needs to be eliminated must be based on a set of rules. Naturally, there will be no perfect correspondent among the individuals, so the rules need to be designed to find the best matching pair of a blank and an environmental MP particle. Although we know what particles were present in the environmental and respective blank samples, the result will differ depending on the selected elimination rules and methods. To facilitate a matching procedure between 'non-equal' particles, we propose a phenotyping procedure that aggregates all relevant categorical particle properties and uses size as single continuous measure for discrimination. A phenotype is a group of particles that share the same values for 'sample', 'colour', 'shape', and 'polymer type'. It is recommended to unify the categories of colour and shape into few, unambiguous clusters, i.e., red, green, blue, other, or fibre, non-fibre. More detailed specifications of phenotypes come along with a higher uncertainty (e.g., due to differences in illumination or particle shape recognition), especially when working with small MP. Particle size may be converted into a single measure, if not already so, i.e., in some cases we receive a major and a minor length for each particle (first and second dimension), where we take the geometric mean of the two as it is more area-preserving than the arithmetic mean. Phenotyping provides groups of particles which are both SDD (number of particles of phenotype X per sample Y) as well as PDD (the actual particle data in each phenotype group including the single measure size attribute).

It now becomes possible to conduct a blank correction process in PDD by identifying the corresponding blank for the sample in question and consecutively matching the phenotypes present in both. Particle elimination may then be conducted by matching and removing the nearest sized sample particle for each blank particle one by one. In a case where multiple (process-) blanks were taken to cover the same work process they would be, together as a group, valid for all samples prepared by that process. Consequently, for a certain phenotype, the average number of particles per blank is equal to its expected value

of contamination from the work processes covered by the blanks. However, averaging is a SDD operation and cannot be easily performed in PDD. Therefore, we recommend the following procedure/algorithm:

- After phenotyping (as described above) the lists of particles are—for each phenotype separately—concatenated from all blanks;
- The combined list is sorted by size;
- It then needs to be shortlisted to only yield the number of particles required by the SDD average (hence, total number of particles of the respective phenotype in all blanks divided by the number of blanks and rounded to the next integer);
- To achieve minimal size distribution deformation, the particles would best be selected beginning from the median of the sorted combined list and selecting every *n-th* element towards smaller and larger sizes alternately until *k* particles are selected, with *n* being the number of blanks and *k* the respective phenotype's SDD average;
- The shortlisted group of particles may be used further for the actual blank subtraction procedure on the sample particles in the same way as if there was only one relevant blank available.

Rounding, stereotyping particles into phenotypes, and the use of a unified size measure are assimilations that unavoidably introduce distortions, leading to an apparent, systematic error in the results. After all, every particle is *not* equal.

3.5. Data Manipulation and Quality Assurance

Depending on the analysis setup, it may be adequate to eliminate rarely occurring outliers from the data set, such as unlikely polymer types, which may otherwise elicit wrong-headed conclusions. For example, it might be decided that for a particle phenotype that occurs only once in the entire data set or in a sample, there is not enough analytical support that this is a valid particle, and it should thus be excluded as an outlier. This concept is also known as limit of detection and limit of quantification and applied in many other analytical research branches [30–32] in order to increase the soundness of a particular dataset. In MP analysis, such rare occurrences may be caused by poor signal-to-noise spectra, cosmic ray artefacts in Raman spectra, or unsystematic human error, which may justify setting a limit of detection.

However, sample size, reference library size, number of blanks, and whether it is applied on sample or data set level, are just a few factors that influence the outcome of such limit determination. This is mainly due to the statistics of small numbers, which MP data scientists are faced with. Where total MP numbers are low, the ultimate probability for certain particle (pheno-)types to appear is accordingly low. In such cases, data become less robust by eliminating phenotypes below the limit of detection, hence one might conclude that 'every particle counts'. Nevertheless, an initial data quality check is recommended to identify instances of rarely occurring phenotypes, as they can lead to the detection of erroneous data entries.

3.6. Database Integration and Accessibility

An important aspect is the MPDB connection to existing international database structures. A prerequisite to comply with FAIR principles is a description of the data available in the database: the metadata. MPDB is hosted by the Leibniz Institute for Baltic Sea Research (IOW) and stored on a server under the micropoll.io-warnemuende.de domain, and the metadata are available at http://micropoll.io-warnemuende.de/iow-metadata.xml, accessed on 20 December 2022. The MPDB metadata are stored on a central meta-database at IOW, IOWMETA. IOWMETA transfers this meta-information to national German databases and major international databases. This ensures knowledge about the existence of MPDB and its content (Figure 5).

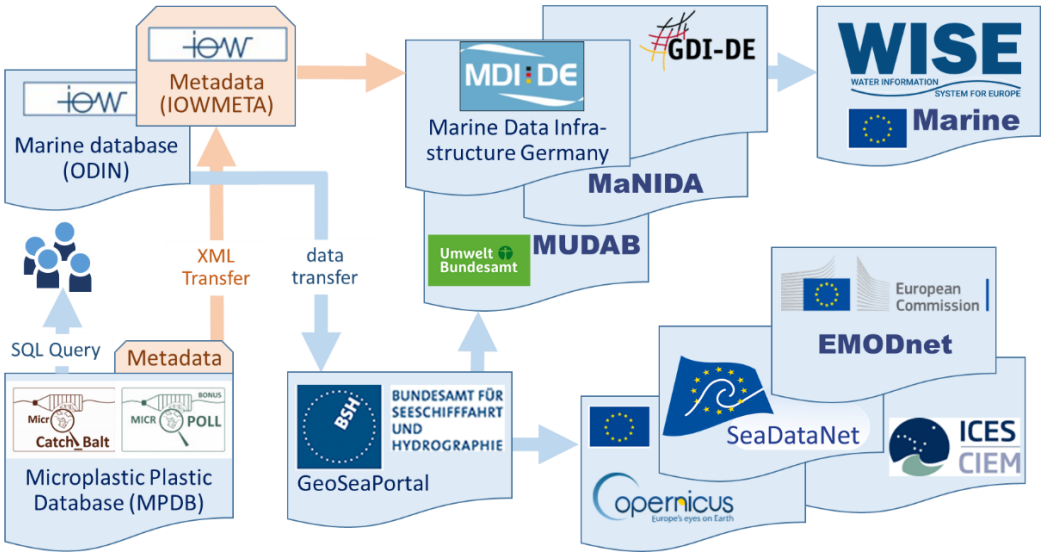


Figure 5. Integration of the microplastic database into national German and international database structures.

The second important aspect is access to the data. Presently, potential users may request MPDB access via e-mail to the main author. The potential database users are encouraged to familiarise themselves with the database documentation (Supplementary Materials).

4. Discussion

We provide the first elaborated MP-related database and aim at contributing towards a universal data repository. SQL-supporting DBMS tools provide flexible data entry and storage possibilities with many applications in various fields. The development and maintenance of such a database requires significant knowledge and resources that are hardly always available. One solution is the use of already established and tested database models. This can be achieved by replicating the DB structure from the EER diagrams (Figure 2) or directly via the provided SQL 'create...' statements (see Data availability statement below). The MPDB structure can be used for developing new, modified data repositories. The database re-installation and maintenance can be handled by IT departments of other research facilities or can be outsourced to such service providers. This has been done with respect to the Leibniz Institute of Polymer Research Dresden who uses and further develops an independent version of the database with a focus on microplastic in food. Alternatively, the presented MPDB version, which is hosted by the Leibniz Institute for Baltic Sea Research, can be used and further developed on request. This solution ensures that the database content is visible for other databases, through the metadata data information, and the content accessible on request.

Environmental sciences benefit from open-access data, developed and stored in structured relational databases. Taking into account that almost any sampling and analysis campaigns are costly, comparable data repositories with transparent metadata and structure are of importance for the scientific community and stakeholders.

Knowledge on emission, transport, and behaviour of microplastic in the environment presently largely results from calculations and modelling studies. Examples for the Baltic Sea are the approaches by Osinski [33], Piehl [34], or Schernewski [35,36]. A major shortcoming is the lacking result validation with microplastic field data. The MPDB and its content is a major step to overcome this weakness. The usage of structured databases ensures access to reliable data. Invalid, incomplete, or faulty data entries are detected, removed, or clarified either in the data entry phase (i.e., data with missing required fields

is not allowed in the database), or data usage (i.e., the retrieval of data, which is not related to a specific attribute will not appear in the generated view).

5. Conclusions and Outlook

The Marine Plastic Database meets all technical requirements with respect to data storage and documentation, but access to data requires expert knowledge. For end-users or stakeholders (non-researchers/scientists) the MPDB is presently not user-friendly. Several possible solutions might be examined to shape the data for easy interpretation. This process would involve two stages: (1) developing use-case scenarios for data entry/viewing/presentation, and (2) development of a front-end application or solution. Possible stakeholder use-case scenarios might be the preview of abundance of MP in their region or area of interest, prevailing MP types and their sources (media), etc. The front-end implementation solution examples would be to create an online platform for MPDB data filtering and preview, or a standalone tool (an application), developed solely for the user. To achieve this, one would require further development (web or application), extra tools and services (i.e., a server with management software). All these solutions can be explored in future uses of the MPDB. We welcome the usage of the database and are open for a collaboration aiming at an improved user-friendliness.

Supplementary Materials: The following supporting information can be downloaded at http://micropoll.io-warnemuende.de/Guideline_for_usage_of_Microplastic_Database.pdf: Guideline for Usage of Microplastic Database.

Author Contributions: Conceptualisation, database development, and writing, N.Č.; DB structure conceptualisation, support of database development, writing, visualisations, and editing, K.E., R.L., J.B., D.F., and F.F., writing and complementary visualisation, G.S.; editing, project administration and funding acquisition, S.O. and M.L. All authors have read and agreed to the published version of the manuscript.

Funding: This research was supported by project BONUS MICROPOLL project supported by BONUS (Article 185), funded jointly by the European Union and national funding agencies (the German Federal Ministry of Education and Research (BMBF, 03F0775A;) as well as project MicroCatch_Balt (BMBF, 03F0788A)).

Institutional Review Board Statement: Not applicable.

Informed Consent Statement: Not applicable.

Data Availability Statement: Data are available in a publicly accessible repository. The data presented in this study are openly available in a repository at Zenodo [37]. The data contain an SQL database export, which can be used to create the MPDB discussed in this article.

Conflicts of Interest: The authors declare no conflict of interest.

Abbreviations

DB—database; EER—enhanced entity-relationship; FAIR—findable, accessible, interoperable, and reusable; FTIR—Fourier-Transform-Infrared-Microspectroscopy, MP—microplastic; MPDB—Marine Plastic Database; PDD—particle domain data; SDD—sample domain data; SQL—structured query language.

References

1. European Comission. *Shared Environmental Information System (SEIS)*; European Comission: Brussels, Belgium, 2020; Available online: https://www.eea.europa.eu/ds_resolveuid/FWIZEG45MT (accessed on 29 December 2022).
2. Wilkinson, M.D.; Dumontier, M.; Aalbersberg, I.J.; Appleton, G.; Axton, M.; Baak, A.; Blomberg, N.; Boiten, J.-W.; da Silva Santos, L.B.; Bourne, P.E.; et al. The FAIR Guiding Principles for Scientific Data Management and Stewardship. *Sci. Data* **2016**, *3*, 160018. [CrossRef]

3. Addamo, A.M.; Brosich, A.; Chaves Montero, M.M.; Giorgetti, A.; Hanke, G.; Molina Jack, M.E.; Vinci, M. *Marine Litter Database Lessons Learned in Compiling the First Pan-European Beach Litter Database*; Publication Office of the European Union: Luxembourg, 2018; ISBN 9789279978661. [CrossRef]
4. European Commission. *MSDF Guidance on Monitoring Marine Litter*; Publications Office of the European Union: Luxembourg, 2013; ISBN 9789279978661. Available online: https://mcc.jrc.ec.europa.eu/documents/201702074014.pdf (accessed on 29 December 2022).
5. Rauert, C.; Pan, Y.; Okoffo, E.D.; O'brien, J.W.; Thomas, K.V. Extraction and Pyrolysis-GC-MS Analysis of Polyethylene in Samples with Medium to High Lipid Content. *J. Environ. Expo. Assess.* **2022**, *1*, 13. [CrossRef]
6. Fischer, M.; Scholz-Böttcher, B.M. Microplastics Analysis in Environmental Samples–Recent Pyrolysis-Gas Chromatography-Mass Spectrometry Method Improvements to Increase the Reliability of Mass-Related Data. *Anal. Methods* **2019**, *11*, 2489–2497. [CrossRef]
7. Hermabessiere, L.; Himber, C.; Boricaud, B.; Kazour, M.; Amara, R.; Cassone, A.-L.; Laurentie, M.; Paul-Pont, I.; Soudant, P.; Dehaut, A. Optimization, Performance, and Application of a Pyrolysis-GC/MS Method for the Identification of Microplastics. *Anal. Bioanal. Chem.* **2018**, *410*, 6663–6676. [CrossRef] [PubMed]
8. Primpke, S.; Lorenz, C.; Rascher-Friesenhausen, R.; Gerdts, G. An Automated Approach for Microplastics Analysis Using Focal Plane Array (FPA) FTIR Microscopy and Image Analysis. *Anal. Methods* **2017**, *9*, 1499–1511. [CrossRef]
9. Primpke, S.; Dias, P.A.; Gerdts, G. Automated Identification and Quantification of Microfibres and Microplastics. *Anal. Methods* **2019**, *11*, 2138–2147. [CrossRef]
10. Anger, P.M.; von der Esch, E.; Baumann, T.; Elsner, M.; Niessner, R.; Ivleva, N.P. Raman Microspectroscopy as a Tool for Microplastic Particle Analysis. *TrAC Trends Anal. Chem.* **2018**, *109*, 214–226. [CrossRef]
11. Brandt, J.; Bittrich, L.; Fischer, F.; Kanaki, E.; Tagg, A.; Lenz, R.; Labrenz, M.; Brandes, E.; Fischer, D.; Eichhorn, K.-J. High-Throughput Analyses of Microplastic Samples Using Fourier Transform Infrared and Raman Spectrometry. *Appl. Spectrosc.* **2020**, *74*, 1185–1197. [CrossRef]
12. Käppler, A.; Fischer, D.; Oberbeckmann, S.; Schernewski, G.; Labrenz, M.; Eichhorn, K.-J.; Voit, B. Analysis of Environmental Microplastics by Vibrational Microspectroscopy: FTIR, Raman or Both? *Anal. Bioanal. Chem.* **2016**, *408*, 8377–8391. [CrossRef] [PubMed]
13. Georgiou, A. Microplastics in the Ocean May Be Vastly Underestimated, with up to 125 Trillion Particles Floating Around, Study Says. Available online: https://www.newsweek.com/microplastics-ocean-vastly-underestimated-125-trillion-particles-floating-around-1505404 (accessed on 29 December 2022).
14. Simon Matt Who's to Blame for Plastic Microfiber Pollution? | WIRED. Available online: https://www.wired.com/story/whos-to-blame-for-plastic-microfiber-pollution/ (accessed on 29 December 2022).
15. Kooi, M.; Koelmans, A.A. Simplifying Microplastic via Continuous Probability Distributions for Size, Shape, and Density. *Environ. Sci. Technol. Lett.* **2019**, *6*, 551–557. [CrossRef]
16. Enders, K.; Käppler, A.; Biniasch, O.; Feldens, P.; Stollberg, N.; Lange, X.; Fischer, D.; Eichhorn, K.J.; Pollehne, F.; Oberbeckmann, S.; et al. Tracing Microplastics in Aquatic Environments Based on Sediment Analogies. *Sci. Rep.* **2019**, *9*, 1–15. [CrossRef] [PubMed]
17. Bergmann, M.; Wirzberger, V.; Krumpen, T.; Lorenz, C.; Primpke, S.; Tekman, M.B.; Gerdts, G. High Quantities of Microplastic in Arctic Deep-Sea Sediments from the HAUSGARTEN Observatory. *Environ. Sci. Technol.* **2017**, *51*, 11000–11010. [CrossRef] [PubMed]
18. Enders, K.; Lenz, R.; Stedmon, C.A.; Nielsen, T.G. Abundance, Size and Polymer Composition of Marine Microplastics $\geq$10μm in the Atlantic Ocean and Their Modelled Vertical Distribution. *Mar. Pollut. Bull.* **2015**, *100*, 70–81. [CrossRef] [PubMed]
19. Frère, L.; Paul-Pont, I.; Moreau, J.; Soudant, P.; Lambert, C.; Huvet, A.; Rinnert, E. A Semi-Automated Raman Micro-Spectroscopy Method for Morphological and Chemical Characterizations of Microplastic Litter. *Mar. Pollut. Bull.* **2016**, *113*, 461–468. [CrossRef]
20. Vianello, A.; Jensen, R.L.; Liu, L.; Vollertsen, J. Simulating Human Exposure to Indoor Airborne Microplastics Using a Breathing Thermal Manikin. *Sci. Rep.* **2019**, *9*, 8670. [CrossRef]
21. Altuhafi, F.; O'Sullivan, C.; Cavarretta, I. Analysis of an Image-Based Method to Quantify the Size and Shape of Sand Particles. *J. Geotech. Geoenvironmental Eng.* **2013**, *139*, 1290–1307. [CrossRef]
22. MySQL::MySQL Installer Release Notes. Available online: https://dev.mysql.com/doc/relnotes/mysql-installer/en/ (accessed on 29 December 2022).
23. Becker Ansgar HeidiSQL Technical Help Document. Available online: https://www.heidisql.com/help.php#credits (accessed on 29 December 2022).
24. Mysql-Connector-Python·PyPI. Available online: https://pypi.org/project/mysql-connector-python/ (accessed on 29 December 2022).
25. MySQL Team: MySQL Workbench Manual. Available online: https://dev.mysql.com/doc/workbench/en/ (accessed on 29 December 2022).
26. Wescon, I. Managing the Development of Large Software Systems. In Proceedings of the 9th International Conference on Software Engineering, Monterey, CA, USA, 30 March–2 April 1987; IEEE Computer Society Press: Washington, DC, USA, 1987; pp. 328–338.
27. Čerkasova, N.; Enders, K.; Lenz, R.; Brandt, J.; Fischer, F. Guideline for Usage of Microplastic Database. 2020. Available online: http://micropoll.io-warnemuende.de/Guideline_for_usage_of_Microplastic_Database.pdf (accessed on 29 December 2022).

28. Enders, K.; Lenz, R.; Ivar do Sul, J.A.; Tagg, A.S.; Labrenz, M. When Every Particle Matters: A QuEChERS Approach to Extract Microplastics from Environmental Samples. *MethodsX* **2020**, *7*, 100784. [CrossRef]
29. Dawson, A.L.; Santana, M.F.M.; Nelis, J.L.D.; Motti, C.A. Taking Control of Microplastics Data: A Comparison of Control and Blank Data Correction Methods. *J. Hazard. Mater.* **2023**, *443*, 130218. [CrossRef]
30. Lux, L.; Phal, Y.; Hsieh, P.-H.; Bhargava, R. On the Limit of Detection in Infrared Spectroscopic Imaging. *Appl. Spectrosc.* **2022**, *76*, 105–117. [CrossRef]
31. Klymus, K.E.; Merkes, C.M.; Allison, M.J.; Goldberg, C.S.; Helbing, C.C.; Hunter, M.E.; Jackson, C.A.; Lance, R.F.; Mangan, A.M.; Monroe, E.M.; et al. Reporting the Limits of Detection and Quantification for Environmental DNA Assays. *Environ. DNA* **2020**, *2*, 271–282. [CrossRef]
32. Saadati, N.; Abdullah, M.P.; Zakaria, Z.; Sany, S.B.T.; Rezayi, M.; Hassonizadeh, H. Limit of Detection and Limit of Quantification Development Procedures for Organochlorine Pesticides Analysis in Water and Sediment Matrices. *Chem. Cent. J.* **2013**, *7*, 63. [CrossRef] [PubMed]
33. Osinski, R.D.; Enders, K.; Gräwe, U.; Klingbeil, K.; Radtke, H. Model Uncertainties of a Storm and Their Influence on Microplastics and Sediment Transport in the Baltic Sea. *Ocean Sci.* **2020**, *16*, 1491–1507. [CrossRef]
34. Piehl, S.; Hauk, R.; Robbe, E.; Richter, B.; Kachholz, F.; Schilling, J.; Lenz, R.; Fischer, D.; Fischer, F.; Labrenz, M.; et al. Combined Approaches to Predict Microplastic Emissions Within an Urbanized Estuary (Warnow, Southwestern Baltic Sea). *Front. Environ. Sci.* **2021**, *9*, 616765. [CrossRef]
35. Schernewski, G.; Radtke, H.; Hauk, R.; Baresel, C.; Olshammar, M.; Osinski, R.; Oberbeckmann, S. Transport and Behavior of Microplastics Emissions from Urban Sources in the Baltic Sea. *Front. Environ. Sci.* **2020**, *8*, 579361. [CrossRef]
36. Schernewski, G.; Radtke, H.; Hauk, R.; Baresel, C.; Olshammar, M.; Oberbeckmann, S. Urban Microplastics Emissions: Effectiveness of Retention Measures and Consequences for the Baltic Sea. *Front. Mar. Sci.* **2021**, *8*, 594415. [CrossRef]
37. Čerkasova, N.; Enders, K.; Lenz, R.; Brandt, J.; Fischer, F. MPDB: Marine Plastics DataBase. Available online: https://zenodo.org/record/7495007 (accessed on 30 December 2022).

Disclaimer/Publisher's Note: The statements, opinions and data contained in all publications are solely those of the individual author(s) and contributor(s) and not of MDPI and/or the editor(s). MDPI and/or the editor(s) disclaim responsibility for any injury to people or property resulting from any ideas, methods, instructions or products referred to in the content.

This is the end of the publication

A Public Database for Microplastics in the Environment

by Natalja Čerkasova, Kristina Enders, Robin Lenz, Sonja Oberbeckmann, Josef Brandt, Dieter Fischer, Franziska Fischer, Matthias Labrenz, Gerald Schernewski

You might want to continue reading the synopsis at page 22, or jump back to the start of this publication at page 173.

MPX_specDB: MicroPlastiX Spectra Database

by Robin Lenz, Franziska Fischer, Melinda Arnold, Verónica Fernández-González, Carmen María Moscoso Pérez, José Manuel Andrade-Garda, Soledad Muniategui-Lorenzo, Dieter Fischer

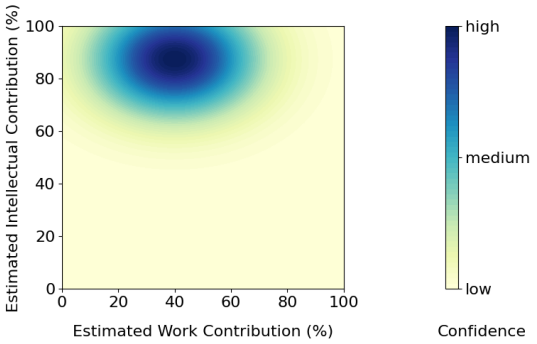
- **Date published**: July 07, 2023
- **Type**: Dataset
- **Published in**: Radar4Chem (chemical data), Zenodo (software)
- **License**: CC-BY-SA+GNUv3
- **DOI**: 10.5281/zenodo.12511025, **Reference**: [11]
- **Citations**: n/a

Contributions

[**Note**: *No author contribution statement is available for this publication. The following partial contribution statement is created for this thesis only to the best of my knowledge and belief.*] RL provided the conceptualisation of data management, harmonised the data, wrote analytical and user interface software and prepared the data and code publications hosted on Radar4Chem and Github, respectively.

Quantitative own contributions based on self-assessment

In the dimensions of expended work effort and intellectual contribution, I consider my shares are likely to be between 30% and 50% and between 80% and 95% respectively. This is visualised below as an interpolated histogram of 500 samples from Gaussian distributions with the aforementioned estimates at plus/minus two standard deviations.



DOI 10.5281/zenodo.12511025

Database of Raman and ATR-FTIR spectra of weathered and biofouled polymers

Brought to you by the JPI Oceans project MicroplastiX

Authors:

- Robin Lenz[1]
- Franziska Fischer[1]
- Melinda Arnold[1]
- Verónica Fernández-González[2]
- Carmen María Moscoso Pérez[2]
- José Manuel Andrade-Garda[2]
- Soledad Muniategui-Lorenzo[2]
- Dieter Fischer[1]

Affiliations:

- [1]Leibniz Institute of Polymer Research Dresden, Hohe Straße 6, 01069 Dresden, Germany
- [2]University of A Coruña, Campus da Zapateira s/n, 15071, A Coruña, Spain

Citation:

To cite the most recent release of the MPX_specDB code please refer to:

> Lenz R, Fischer F, Arnold M, Fernández-González V, Moscoso-Pérez CM, Andrade-Garda JM, Muniategui-Lorenzo S, Fischer D, Database of Raman and ATR-FTIR spectra of weathered and biofouled polymers, 2023, https://doi.org/10.5281/zenodo.8314801.

The raw spectra collection can be found on the chemical research data repository Radar4Chem and is citeable as:

> Lenz R, Fischer F, Arnold M, Fernández-González V, Moscoso-Pérez CM, Andrade-Garda JM, Muniategui-Lorenzo S, Fischer D, MicroPlastiX SpecDB, https://doi.org/10.22000/1820.

Contents

This dataset is a spectroscopic library strucutred as a document database. It contains Raman and ATR-FTIR spectra of weathered and biofouled polymers which can be viewed via an interactive app.

> Project MicroPlastiX's Task 4.1 (formerly Task 3.4) examines the biofouling and colonization dynamics of plastic fragments.

In *in situ* experiments, plastic sheets of **10 different polymers** were deployed in the marine environment across **five geographical locations**. Their immersion in stainless steel cages for different intervals, over four seasons, imitates real-world exposure.

View the app

A live version of the app can be found here: https://robna.github.io/MPX_specDB/.

Local use

Using the app

You can use the `Pipfile` to set up a virtual python environment using pipenv or, alternatively the `requirements.txt` with a virtual env and package manager of your choice.
When using pipenv, open a terminal in the project directory and run `pipenv install` to install all dependencies.
Then run `pipenv run streamlit run app.py` to start the app.

Assessing the data manually

Individual spectra can be found in the `data/spectra` folder, while all available information on the samples is stored in the `data/meta/metadata.json` file. Both will only be populated after the first run of the app or can be obtained from Radar4Chem.
The spectra filenames follow the pattern `[region]_[polymer]_[biofilm]_[analysis]_[hash].csv` where `hash` holds the first 8 characters of the sha256 hash of the spectrum data, in order to create unique filenames.
You can download or clone the repository to your local machine and use the `metadata.json` file to search for spectra of interest, e.g. by opening it in the Firefox browser which has some basic capabilities for navigating and searching in json files.

License

Software code in this repository is licensed as specified in the LICENSE.md file.
Spectroscopic data and meta data is licensed under CC BY SA 4.0.

This is the end of the publication

MPX_specDB: MicroPlastiX Spectra Database

by Robin Lenz, Franziska Fischer, Melinda Arnold, Verónica Fernández-González, Carmen María Moscoso Pérez, José Manuel Andrade-Garda, Soledad Muniategui-Lorenzo, Dieter Fischer

You might want to continue reading the synopsis at page 27, or jump back to the start of this publication at page 190.

What Goes Around Should Not Move Around: Immobilizing Microplastics as a New Approach for Analytical Ring Trials

by Robin Lenz, Kristina Enders, Eva Cseperke Vizsolyi, Mareike Schumacher, Julia Lötsch, Martin G. J. Löder, Gabriele Eder, Yuliya Voronko, José Manuel Andrade-Garda, Soledad Muniategui-Lorenzo, Christian Laforsch, Dieter Fischer, Matthias Labrenz

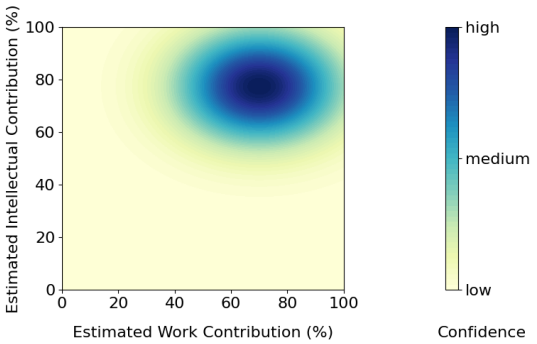
- **Date published**: December 03, 2024
- **Type**: Research Article
- **Published in**: Environmental Science & Technology
- **License**: CC-BY
- **DOI**: 10.1021/acs.est.4c09427, **Reference**: [12]
- **Citations**: 2 (Crossref/DOI, 2025-11-18)

Contributions

R.L. and K.E. invented the serial ILC concept and the silicon-based particle immobilizations, contributed to Raman and FTIR measurements, analyzed the data, and drafted the manuscript | E.C.V. and M. Löder contributed to FTIR measurements, created the samples for the parallel ILC and developed the alumina-based particle immobilizations | M.S. and J.L. contributed to Raman measurements | G.E. and Y.V. contributed to FTIR measurements | J.M.A.G. and S.M.L. contributed to LDIR measurements | D.F. and M. Labrenz supervised the work | All authors reviewed the manuscript draft.

Quantitative own contributions based on self-assessment

In the dimensions of expended work effort and intellectual contribution, I consider my shares are likely to be between 60% and 80% and between 70% and 85% respectively. This is visualised below as an interpolated histogram of 500 samples from Gaussian distributions with the aforementioned estimates at plus/minus two standard deviations.



Environmental Science & Technology

pubs.acs.org/est

Article

Open Access

This article is licensed under CC-BY 4.0

What Goes Around Should Not Move Around: Immobilizing Microplastics as a New Approach for Analytical Ring Trials

Robin Lenz,* Kristina Enders, Eva Cseperke Vizsolyi, Mareike Schumacher, Julia Lötsch, Martin G. J. Löder, Gabriele Eder, Yuliya Voronko, José Manuel Andrade-Garda, Soledad Muniategui-Lorenzo, Christian Laforsch, Dieter Fischer,* and Matthias Labrenz*

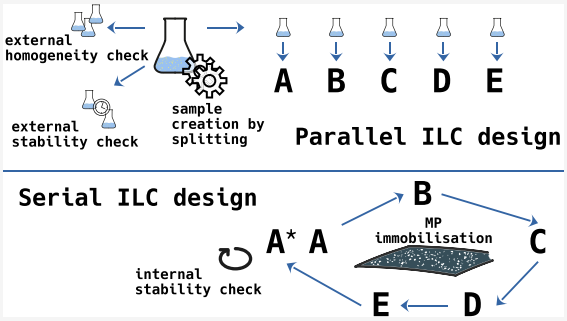
Cite This: https://doi.org/10.1021/acs.est.4c09427

Read Online

ACCESS | Metrics & More | Article Recommendations | Supporting Information

Downloaded via 193.175.232.79 on December 4, 2024 at 09:15:02 (UTC).
See https://pubs.acs.org/sharingguidelines for options on how to legitimately share published articles.

ABSTRACT: Microplastics have gained importance as pervasive environmental particulate pollutants. Their analysis demands precise quantification methods, with interlaboratory comparisons (ILCs) being crucial for performance assessment. Typically, ILCs follow a parallel design: participants each analyze their own sample specimen, often with significant variability due to challenges in producing identical subsamples of the particulate analyte, inseparably masking the relevant uncertainty sources the ILC intends to measure. We provide a filtration-immobilization approach for particles ≤100 μm, creating permanently immobilized microplastics samples. This enables serial ILC designs where participants sequentially measure the same sample. Demonstrating the concept using 5 polymers immobilized on 10 μm pore-sized silicon filters, we expose the specific measurement uncertainty being 77% lower than the total combined uncertainty observed in a parallel ILC (relative standard deviations: 5 and 23%, respectively). Particle immobilization opens further applications in sample archiving and creation of durable reference samples also for other fields of particulate matter research beyond microplastics.



KEYWORDS: *spectroscopy, microscopy, particles, colloid, proficiency, validation, round robin, fixation*

INTRODUCTION

The contamination of the environment with microplastics (MPs), i.e., synthetic polymer particles commonly accepted to be between 1 and 1000 μm,[1] has created a need for reliable data on the characteristics and quantities of MPs. This has led to a wide variety of methodological developments. The resulting significant differences in resolution and quality of analyses are impeding the comparability of data between studies[2−4] and more comprehensive environmental risk assessments.[5]

To solve this issue, interlaboratory comparisons (ILCs) play a crucial role in evaluating the reliability and accuracy of methods for the characterization and quantification of MP particles in various samples,[6] including environmental, food, and tissue matrices. Several ILC studies aimed at MP-analytical proficiency can be found in the recent literature[6−14] using different sample types such as environmental matrices spiked with specific MP types,[13] artificial samples such as suspensions,[12] or MP particles in solid media like tablets or ice cubes.[6,11] These studies typically follow a parallel design, where each participant receives and analyzes their own sample specimen, assuming equality in MP numbers and composition. This design, based on reporting guidelines like DIN 38402-45:2014-06, as cited by ref 12, ISO 13528,[15] or the IUPAC technical report,[16] resembles established procedures for soluble analytes, where homogeneity issues are less of a concern and accurate reference measurements are available. As particulate pollutants, MPs pose significant challenges to this equality assumption, especially for particle sizes in the lower micrometer range where individual handling of particles is impractical.[17]

The need for comparable and reliable MP quantification led to innovations in creating homogeneous sample specimens for ILCs and reference materials,[11,18−20] as well as assessment and correction methods[8,21] and reporting guidelines.[22,23] Their perpetual integration in new ILCs can improve precision and reduce the uncertainty of the true MP content, gradually making the determination of analytical proficiency more reliable. However, the fundamental problem remains: parallel ILC designs capture compounded effects caused by a range of

Received: September 5, 2024
Revised: October 25, 2024
Accepted: October 25, 2024

ACS Publications

© XXXX The Authors. Published by American Chemical Society

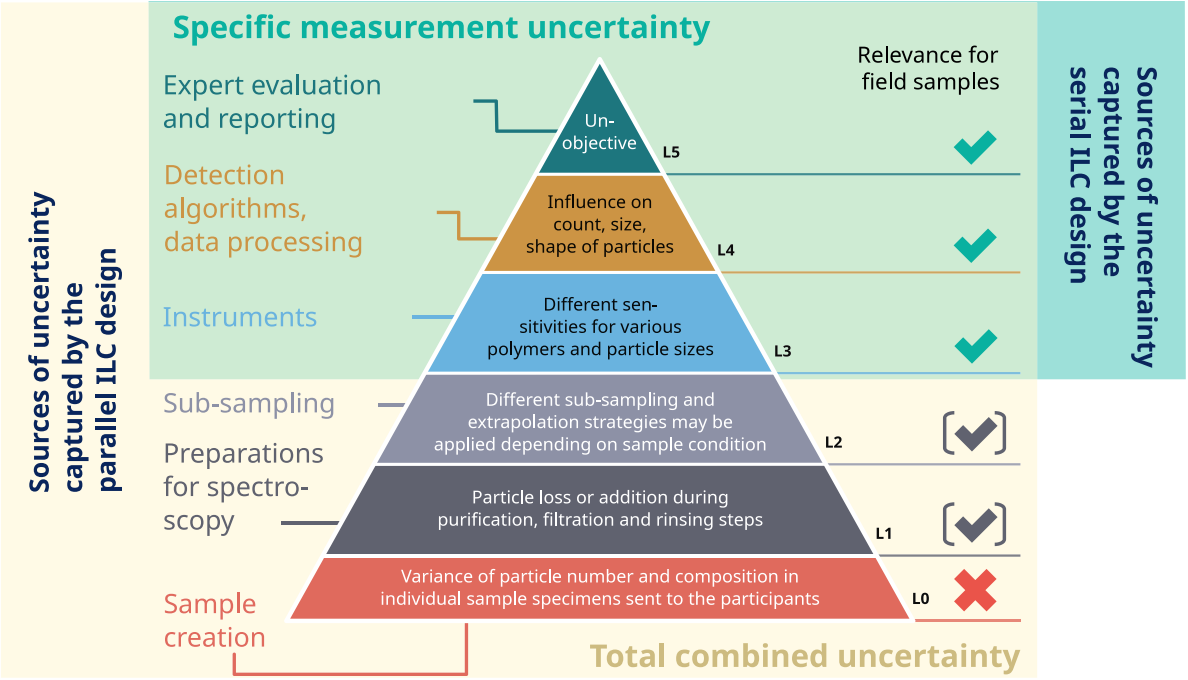


Figure 1. Uncertainties propagating through the pipeline of MP quantification. Colored areas enclose the shares captured by parallel (beige) and serial (mint) ILC design concepts. The relevance of the uncertainty contributors with regard to field samples is shown to the right of the pyramid. It is highlighted that uncertainties arising from the way in which the parallel ILC sample is produced (L0) are irrelevant to real samples and should therefore preferably be excluded by an ILC design. Other uncertainty sources (L1 and L2) can be relevant, but because they depend on the sample conditions, they should be addressed separately from an ILC estimating the specific measurement uncertainty.

uncertainty sources whose contributions cannot be further decomposed (Figure 1). At this point, it is important to emphasize the principles of metrology, such as uncertainty propagation according to the "Guide to the expression of uncertainty in measurement" (GUM)[24] by the Joint Committee for Guides in Metrology (JCGM) whose terminology we apply here to the field of MP analysis.

All steps from planning the sampling to evaluating and reporting the final data contribute to the combined uncertainty in the MP-analytical chain. Therefore, any uncertainties intrinsic to the production of the parallel sample specimens, e.g., from splitting or weighing, are included at the base of the final result (Figure 1). Here, we use the term "specific measurement uncertainty" to describe the combined uncertainty associated with the chemical measurement acquisitions (e.g., microspectroscopy), data evaluation, manual result control, and reporting (Figure 1, L3−L5). In parallel ILCs, the specific measurement uncertainty is inseparable from uncertainty contributions of production and distribution of sample specimens (Figure 1, L0), sample treatments like purification and measurement preparations (Figure 1, L1), and subsampling (Figure 1, L2). The first is specific to the ILC design itself and, as such, not informative about a participant's proficiency to quantify MP field samples (compare Figure 1, "Relevance for field samples"). The latter two are of potential relevance when considering field samples but may vary depending on the pretreatment requirements of the matrix such as sediments, biota, or food samples. They should, therefore, be addressed by separate QA/QC measures[25] or a posteriori data alignments.[5]

Currently there is no approach available to investigate the specific measurement uncertainty in ILCs to build the basis for a subsequent evaluation of the total combined uncertainty of the whole sample preparation and analysis process. To address this gap, we adapt the concept of MP particle immobilizations, first described for experiments in the ≤100 μm size fraction,[17,26] to the requirements of ILCs using an inorganic adhesive. For two common spectroscopic substrate types, porous Si wafers and alumina membranes, we describe an immobilization-by-filtration approach, leading to a permanent fixation of particles on the surface of the carrier. It can be measured sequentially by all ILC participants, with each laboratory measuring the same filter and passing it onto the next participant in the ILC consortium. This methodological paradigm shift renders the ILC literally a "ring trial", or "round-robin test" as it is also often called, relating to its historic meaning of an institution of coordinated collective activity.[27,28] We refer to this concept as the serial design to distinguish it from the parallel ILC design. It eliminates the unwanted uncertainty sources introduced by the repetitive sample specimen creation in the parallel design approach. Therefore, the observed variance of the results represents a more accurate magnitude of the specific measurement uncertainty.

METHODS

We conducted a comparison between a parallel design ILC where participants received independent sample specimens of samples P1−P3 and serial ILCs where participants received the same specimens of three different sample types subsequently: S1−S3 (Table 1).

https://doi.org/10.1021/acs.est.4c09427
Environ. Sci. Technol. XXXX, XXX, XXX−XXX

Table 1. Sample Names and Their Poolings (Pool) that Were Prepared for the Parallel and Serial ILC Designs Are Listed with Their Key Specifications

Pool	Sample names	Design concepts: parallel	Design concepts: serial	Immobilisation	Target area determined by	Substrate for transport	Particles
P	P1	✓		n/a		aqueous suspension, 0.005% surfactant (TritonX)	cryo-milled fragments of LDPE, PA12, PET, PP, PS retained in dry-sieving between 71 µm and 10 µm analytical stainless steel sieves
P	P2	✓					
P	P3	✓					
S2	S1		✓	potassium silicate solution 10%	coordinate definition	Si filter 10 µm	
S2	S2.1		✓		laser engraving area A1	Si filter 1 µm	
S2	S2.2		✓		laser engraving area A2		
S2	S2.3		✓		laser engraving area A3		
S2	S2.4		✓		laser engraving area A4		
S3	S3.1		✓		colour marking	alumina filter 0.2 µm (Anodisc)	
S3	S3.2		✓				

To encourage broader adoption, we emphasize that the proposed serial ILCs using immobilized particle samples can be conducted using standard laboratory equipment. Any special or custom-made devices, although detailed here for possible replication, can be replaced by commercially available alternatives without compromising the immobilization's success.

Sample Preparation. Sample preparation steps were conducted in specialized MP-analytical laboratories under laminar flow benches. As an exception, steps involving handling of dry MP powders such as grinding, mixing, or adding powders to suspension media were conducted outside the laminar flow bench to avoid workplace contamination. White cotton lab coats were used during all procedures.

We obtained the MP particles by sieving five previously cryo-milled (Cryomill, Retsch, Germany) environmentally relevant polymers. The resulting particle shapes were irregular (see also Figure SI5.2). Fibers were not included in this study. We used low-density polyethylene (LDPE), polyamide 12 (PA12), polyethylene terephthalate (PET), polypropylene (PP), and polystyrene (PS). The raw materials and grinding and sieving procedures were identical as reported by a previous study.[17]

The creation of the aqueous suspension samples P1−P3 and the adhesive particle suspension for the immobilized samples S1 and S2 is described in full detail in SI1. In the samples of the serial ILC design (S1−S3), the homogeneity of particle distribution on the filters was not assumed or required, as all participants measured the same defined area of each sample. The selected measurement areas were chosen based on their representativeness of the overall particle immobilization.

Immobilization on Si Wafers. Porous silicon wafers were inserted in the precleaned filtration apparatus,[29] connected to an adjustable vacuum pump (SC920, KNF Neuberger). The device contained red PTFE discs for sealing. For sample S1, a silicon wafer was used (11 mm length and width and 250 µm thickness) with conical pores (15/8 µm terminal diameters and 55 µm interpore distance) supplied by Fraunhofer Institute for Reliability and Microintegration, Moritzburg, Germany; for more details, see ref 30. We refer to it as a nominal 10 µm filter.

For S2, we used a nominal 1 µm pore size filter (Si wafer: 10 mm length and width, 200 µm thickness, cylindrical 1 µm pore diameter, 1.5 µm interpore distance, from SmartMembranes GmbH, Halle, Germany).

The prepared potassium silicate adhesive particle suspension (SI1) was placed on top of a high-frequency excentrical shaker for homogenization, while volumes were being extracted for filtration using 1 mL Pasteur glass pipettes. We applied 2 and 6 mL for S1 and S2, respectively, where particle coverage was found to be suitable on visual inspection. Filtration was conducted at approximately 100 mbar. After curing in a vacuum drying oven (40 °C, 100 mbar, 12 h), filters were flushed with running MP-free water and compressed air to remove any loose particles. This rinsing process was repeated three times. Dark field microscopic images were acquired after each iteration to evaluate the removal of loose material. It was considered complete as no substantial further changes in the particle amounts could be manually observed between the images taken after the second and third rinse.

Immobilization on Alumina Filters. The dry powder mixture of MP particles was suspended in MP-free water and filtered onto an Al_2O_3 membrane (Anodisc, Whatman, polypropylene outer ring support, 45 µm height, 25 mm diameter, 60 µm membrane thickness, 0.2 µm pore size). The filter was then placed inside a glass Petri dish on top of a droplet of the potassium silicate adhesion medium (SI1), which was allowed to soak through the filter material by capillary rising, wetting the particles from below. Two filters of this type were created and measured, S3.1 and S3.2, with different amounts of MP particles.

Target Area Definition. Measuring the entire filter area was not a viable approach for several participants in terms of measurement time and amount of data produced. Instead, rectangular areas of approximately 2 by 2 mm were defined for measurement by each participant. Three approaches to marking the specific target areas were investigated, coordinate definition, laser engraving, and color markings, for samples S1−S3, respectively (see also Table 1 and Figure 2 as well as details and dimensions provided in SI2).

Serial ILC Round Trip. The filters were sent to the participants in custom-made filter holders (Figure SI3) by standard mail. In the case of Si filter samples (S1 and S2), participants were advised to rinse the sample with MP-free water and dry it with compressed air prior to measurement to avoid contamination. For the Al_2O_3 membrane sample S3, this was not possible due to the fragile nature of the substrate. Al_2O_3 membranes provide a less smooth and less even surface than the samples prepared on Si filters. Hence, participants were advised to use adhesive tape on the outer ring support to improve surface flatness during measurement. Participants measured the samples using the method of their choice before repackaging them and sending them onto the next participant. Finally, the samples were received and remeasured by the host participant to assess potential particle losses from the repetitive handling and transport.

Sample Analysis. The samples from the parallel and serial ILCs were analyzed individually by each participant with no further requirements other than using their laboratory's state-of-the-art MP analysis techniques and parameters like they would use to analyze field samples. A total of eight participants were involved in the measurements; however, due to the

https://doi.org/10.1021/acs.est.4c09427
Environ. Sci. Technol. XXXX, XXX, XXX−XXX

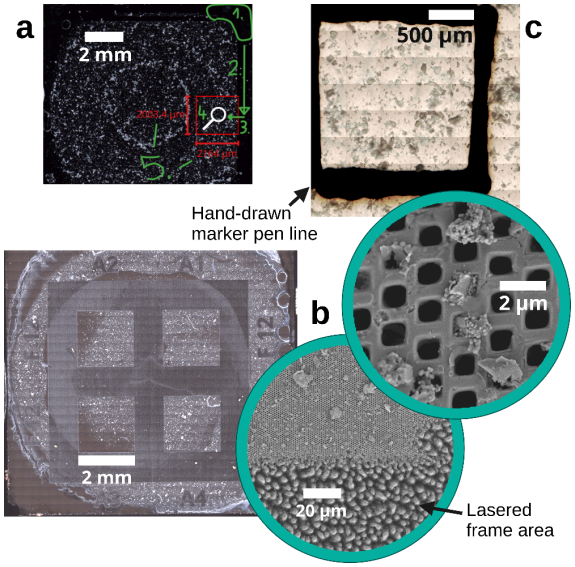


Figure 2. Approaches to defining the measurement area. (a) Dark field image of sample S1 with visual guidelines (green) provided to the participants for manual targeting. (b) Laser-engraved frame and resulting target areas A1−A4 of sample S2 shown as a dark field overview with insets showing SEM images of the area boundaries and the square 1 μm pores. (c) Bright field overview of the Al_2O_3 membrane sample S3 with the target area defined by a black marker.

developmental character of this study, not every participant measured every sample and the order of participants varied between samples. Table 2 details the chosen techniques and key parameters of the participants, as well as the samples they measured. A participant in the context of this study is a unique constellation of an institute, an analyst, a measurement instrument, and an analysis software. Participants A−D and G were located all at the same institute and differed only in the technical and analytical choices as described in Table 2.

Common Area Correction. The target area definition of samples S1 and S3 (compare Figure 2a and Figure 2c) resulted in slightly different areas measured by each participant. This was partly due to different rotation angles of the sample on the instrument stages, different image acquisition modes of the instruments, and/or manual inaccuracies. To evaluate results from the same area only, the largest common area was defined by superimposing the obtained particle distribution images in the GNU image manipulation software (https://gimp.org). All images were manually registered to a common coordinate system. A rectangle contained within each image was then defined graphically as the common measurement area. Particles completely outside this common area were counted for each image and polymer type, and their numbers were subsequently subtracted from the original particle counts reported by each participant. The definition of the target area by laser engraving for sample S2 made such a correction unnecessary. The areas were sharply defined and macroscopically visible. As particles in the interstices were burnt off by the laser, a simple measurement of a slightly larger area gave the same particle numbers as measuring an area to its exact extent.

Statistical Analysis. Results were reported by participants as numbers of particles per polymer type, size range, and sample. Total MPs (TMPs) were calculated as the sum of particles of the five added polymers. We use the terms P, S2, and S3 to refer to mean aggregated results from samples P1−P3, S2.1−S2.4, and S3.1−S3.2, respectively. For results derived from Raman spectroscopy, only size classes ≥10 μm were considered to increase comparability to FTIR results, which were left untruncated.

In the absence of an unbiased reference value for the MP particle numbers in the samples, we used the arithmetic mean and standard deviation between participants as measures of centrality and agreement. To evaluate the deviation of the ith participant's result (P_i) obtained for a sample from the overall mean of the results reported by all participants for that sample, we calculated a "relative deviation from the mean" (RMD, eq 1) where $\bar{P}$ denotes the overall sample mean.

$$\mathrm{RMD} = \left(\frac{P_i}{\bar{P}} - 1\right)\cdot 100\% \quad (1)$$

Using the relative standard deviation among participants (RSD, eq 2), we compare the dispersion of reported results between the different ILC design concepts.

Table 2. ILC Participants with Spectroscopic Techniques and Measured Samples

		technique	instrument	measurement parameters	software	analyzed samples
participant	A	Raman microscopy	WITec alpha300R	20× objective, 532 nm, 10 mW, 10 × 0.5 s acquisitions	Gepard[31]	all
	B				Witec ParticleScout + Gepard[31]	S1, S2, S3
	C				Gepard[31] + ML-prototype Raman[a]	S1
	D	micro-FTIR imaging	PerkinElmer Spotlight400	transmission, IR range of 4000−650, 8 cm^{-1} resolution, 4 scans/pixel (6.25 μm)	ML-prototype FTIR[a]	all
	E					
	F		Bruker Lumos II	transmission, IR range of 3600−1250, 8 cm^{-1} resolution, 2 scans/pixel (5.7 μm)	Bruker Opus v7.5 + BayreuthMicroplasticsFinder[32]	P1, P2, P3, S2, S3
	G	Raman microscopy	Renishaw inVia Qontor	20× objective, 633 nm, 50% power, 7 × 0.5 s acquisitions	Gepard[31]	S1, S2, S3
	H	LDIR imaging	Agilent 8700LDIR	quantum-cascade laser IR source, IR range of 1800−975, 8 cm^{-1} resolution, 1 scan/particle	Agilent Clarity software v1.5	S2

[a]Machine learning-based prototypes for MP quantification developed by Purency GmbH, Vienna, Austria.

https://doi.org/10.1021/acs.est.4c09427
Environ. Sci. Technol. XXXX, XXX, XXX−XXX

$$\mathrm{RSD} = \frac{\sqrt{\frac{\sum_{i=1}^{n}(P_i - \overline{P})^2}{n}}}{\overline{P}} \cdot 100\% \quad (2)$$

Due to the low number of participants using Raman ($N \leq 4$) and FTIR ($N \leq 3$) spectroscopy, mean differences between these groups were evaluated by one-sided, nonpaired, exact permutation tests[33] and accepted as statistically significant for $p \leq 0.05$, i.e., the proportion where the mean of values assigned to the lower group was greater than the mean of values assigned to the higher group in not more than 5% of all possible permutations.

Results were regarded as statistical outliers where experimental values were more than 1.5 times the interquartile range below the first or above the third quartile of all participants. They were excluded where technically justified, i.e., where a limited compatibility between the properties of a certain ILC sample and the applied measurement technique was identified.

The stability of a sample was evaluated by comparing the TMP measurements, conducted by the same participant, at the beginning x_{pre} and at the end x_{post} of the serial ILC. We used a stability criterion c (eq 4) in adaptation from ISO 13528.[15] Here, we used the ratio between the "two-sided" relative pre/postdeviation Δ_{rel} (eq 3) and the RSD among the participants as a stability criterion, accounting for the fact that samples with multiple measurement areas may not have comparable absolute MP particle numbers. "Two-sided" here indicates that we take the double of the difference from the mean as the expected deviation range would be centered around the mean going into positive and negative directions.

$$\Delta_{rel} = \frac{2 \cdot |\overline{x}_{pre,post} - x_{pre}|}{\overline{x}_{pre,post}}, \text{ with } \overline{x}_{pre,post} = \frac{x_{pre} + x_{post}}{2} \quad (3)$$

$$c = \frac{\Delta_{rel}}{\mathrm{RSD}} \quad (4)$$

Acceptable stability was expected when $c \leq 0.3$. When the calculated stability was only marginally above this threshold, c had to be corrected to include the measurement uncertainty (u) according to eq 6 as recommended for testing against the same threshold.[15] We determined u as the average relative distance of r replicate postmeasurements from their mean (eq 5).

$$u = \frac{\sum_{i=1}^{r} |\overline{x}_{post} - x_{post,i}|}{r \cdot \overline{x}_{post}}, \text{ with } \overline{x}_{post} = \frac{\sum_{i=1}^{r} x_{post,i}}{r} \quad (5)$$

$$c = \frac{\Delta_{rel}}{\mathrm{RSD} + 2\sqrt{u^2 \cdot \Delta_{rel}}} \quad (6)$$

A spreadsheet file that was used for the calculations and figure generations and a Jupyter notebook containing the calculations of the permutation tests are provided in the data deposit.[34]

RESULTS AND DISCUSSION

We report on a novel immobilization technique for MPs and its application in serial ILCs compared to parallel ILCs. As absolute numbers of particles varied significantly between samples, we show the numbers of MP particles reported by the participants here relative to their mean (Figure 3), but raw count data are presented as bar charts in the Supporting Information (Figure SI4.1).

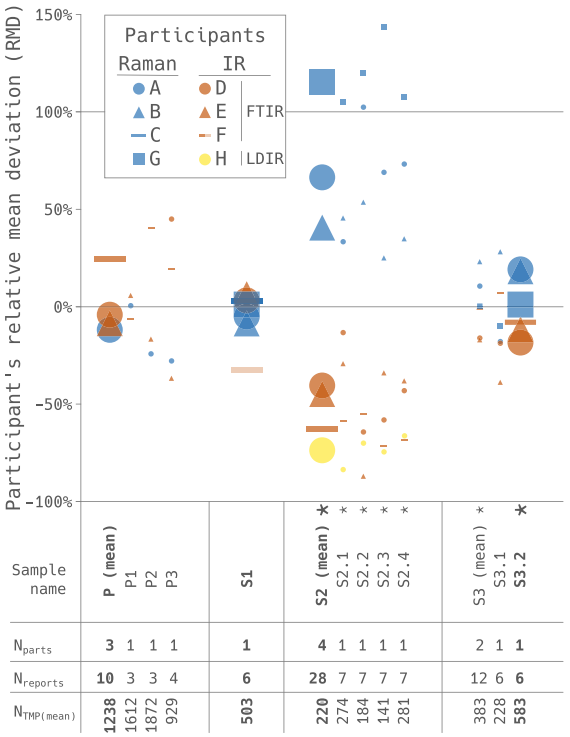


Figure 3. Particle numbers shown as percentage deviation from the participant mean per sample (RMD). Large symbols show the most important results per sample type. These are the pooled results for P and S2 where multiple sample parts were available and the single sample results S1 and S3.2. Sample S3.1 needed to be excluded for lack of stability. Small symbols indicate the RMDs for the constituting sample parts. Asterisks indicate significant differences between the subgroups' mean RMDs (Raman vs IR, see also Table 2 for references of the techniques used by each participant). Participant F's result for sample S1 was excluded as a statistically and technically justified outlier, and it is shown here semitransparently for reference only (not included in the mean calculation). Key data of the samples are provided below the horizontal axis. Sample name: terminology used according to Table 1 (P: samples used in parallel ILCs; S: samples used in serial ILCs). N_{parts}: number of parts that were pooled under this sample name. $N_{reports}$: number of reports returned by participants (for brevity showing the sum of reports in multipart samples). N_{TMP}: reported particle numbers of TMP as mean over participants (polymer and participant-specific results are provided in the data deposit[34]). Absolute particle numbers are shown in Figure SI4.1.

The serial ILC design, by isolating the specific measurement uncertainty, significantly reduces observed variation among participants compared to the parallel ILC, with a 77% lower RSD in the small-scale ILC comparison we conducted here (Figure 4).

Isolation of the Specific Measurement Uncertainty by MP Immobilization. The parallel ILCs resulted in an RSD of 23% as derived from the mean of the three suspended samples, following Table 1 (pooled as sample P in Figure 4). The RSD spreads from 5% (P1) to 34% (P3) and is shown as whiskers in Figure 4. The high RSD, along with the absence of a consistent

https://doi.org/10.1021/acs.est.4c09427
Environ. Sci. Technol. XXXX, XXX, XXX−XXX

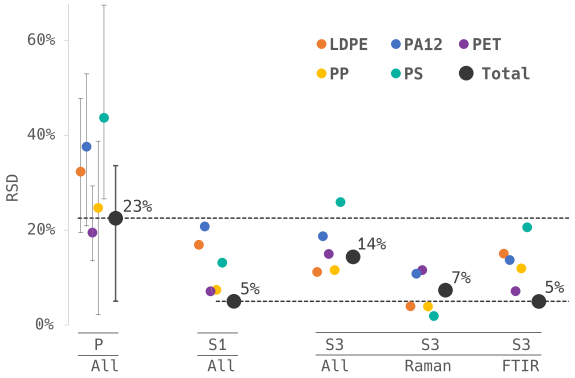


Figure 4. RSD among participants for the different ILC samples. Dashed lines indicate the RSD levels of TMP in the serial ILC of S1, which was 77% lower than in the parallel ILC design (results of samples P1, P2, and P3 were pooled as "P"). Whiskers show the extents to the minimum and maximum of the unpooled RSD values. RSD values of S2 can be seen in an extended version in the Supporting Information (Figure SI4.2). P, parallel samples; S, serial samples.

pattern among participants over the three samples (see Figure 4, P1−P3, for details), suggests that uncertainty sources like sample production, transport, and preparation for spectroscopy (see L0−L2 in Figure 1) may have contributed an important share of the overall variation of the results. Hence, the magnitude of the specific measurement uncertainty (L3−L5, Figure 1) cannot be estimated. The serial ILCs, with particles immobilized on the measurement substrates, exclude production- and preparation-derived uncertainties by design, as every participant measures the same sample. Thus, the specific measurement uncertainty can be investigated independently.

The S1 series on the 10 μm Si filter substrate resulted in an RSD of 5% (with participants A−E and G, Figure 4), giving an indication of the specific measurement uncertainty within the ILC consortium. It is observed that, generally, individual polymers have a larger RSD than TMP. The TMP individual values reported by the participants vary with RMDs between −9 and +6% around their mean (Figure 3). There was no significant difference between the RMD means of the ad hoc Raman and Fourier transform infrared (FTIR) subgroups for S1.

To test whether the serial ILC concept can be extended to other applications, a smaller pore size Si filter (S2) and aluminum oxide as another common filter substrate (S3) were explored in further ILCs. While the FTIR participants reported largely consistent results for the Al_2O_3-based sample S3, participant F reported difficulties in obtaining a reliable measurement result for the Si sample S1. Their analysis technique is based on a machine-learning polymer recognition model trained on Al_2O_3 substrates, which can be expected to have limited compatibility with the Si substrate. This underlines the importance of taking filter substrate preferences into account when designing an ILC. The use of different filter substrates can help to make an equitable assessment.

The overall RSD of S3 is 14% with regard to all participants (A, B, and D−G). However, when separated by the spectroscopic technique, the RSD is comparable to what has been described for S1: 7 and 5% for Raman and FTIR spectroscopy, respectively (Figure 4). Raman-based measurements of S3 have, on average, a significantly higher RMD of 25 percentage points (%pt) difference, significant at $p \leq 0.05$ (Figure 3) compared to FTIR-based techniques. The other filter S3.2 is excluded from analysis as a substantial particle loss of 21% has been recorded between pre- and postmeasurements of the host participant, indicating that the immobilization was not sufficient (see also Figure 6 and Stability of Filtration-Immobilization).

For the 1 μm Si filter (S2), an even stronger segregation can be observed with respect to the spectroscopic technique. On average, Raman participants are >120%pt higher in terms of RMD compared to FTIR and LDIR. Accordingly, the RSD is substantially higher: 71% for TMP and up to 91% for the individual polymers, exceeding the RSD of the parallel ILC. In order not to distort the scale of Figure 4, S2 was omitted there. An extended version including S2 is presented in the Supporting Information (Figure SI4.2). We assume that a reason for the observed systematically lower TMP estimates of the FTIR and LDIR participants for the 1 μm filter S2, and, although weaker, for the Al_2O_3 filters S3 (see also Figure SI4.1), is likely an excess of potassium silicate adhesive, which remains in the smaller pores due to capillary forces and thus adversely affects the FTIR signal intensity. Further, the properties of Si wafer filters like material thickness and pore diameter, pattern, and distance could cause interferences in the IR wavelengths.[30] In combination with the potassium silicate adhesive, this may have reduced polymer recognition for IR-based techniques. This was indeed the case when considering the LDIR transflectance measurements as the spectra of many particles appeared "blurred" or distorted due to the partial coverage by the adhesive. In transflectance, the IR light interacts twice with the surface of the particles plus with the reflecting substrate.

Radar charts in Figure 5 show the RMDs of the participants for the five polymer types. The closer the lines are to the most intense color region (RMD ± 10%), the higher the consensus within the consortium. The host or initial participant is located at the top of the polygon, and the other participants follow clockwise in the order the samples were sent around. The trials

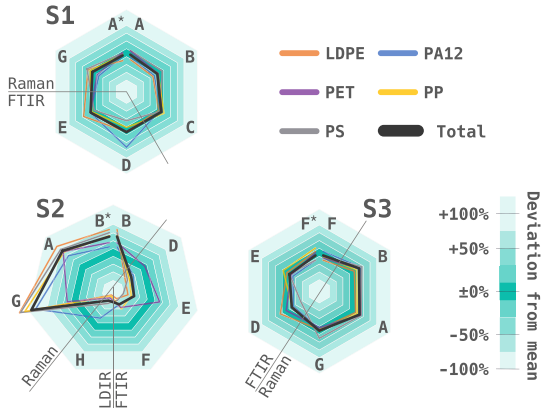


Figure 5. Reported results of the three serial ILC trials with samples S1−S3 as percentage deviation from the overall participant mean. Entries marked by asterisks indicate the post-transport control measurement of each ILC sample and do not constitute an own participant. Hairlines delineate the ad hoc subgroups of Raman, FTIR, and LDIR measurements.

https://doi.org/10.1021/acs.est.4c09427
Environ. Sci. Technol. XXXX, XXX, XXX−XXX

finish with remeasurement by the host (marked with an asterisk in Figure 5) to determine the immobilization stability. The remeasurement results were not included in the mean for the RMD calculations.

S1 showed high consensus among the participants (Figure 5). Overall, we conclude that the use of the 10 μm Si filter, in contrast to 1 μm pore-sized filter S2, allowed better comparability between Raman and FTIR results. We attribute this observation to the resulting size range of particles (excluding the sub-10 μm fraction), which is better suited to the typical limits for FTIR, and to a lower capillary retention of the potassium silicate adhesive in the larger pores of S1.

As to the polymer type, the largest singular positive deviation from the overall participants mean in S1 occurs for the polyamide PA12, which has been identified as a software-caused false-positive problem by participant D. The machine learning-based analysis was sensitive to even weak presence of bands in the natural amide region, leading to pixels being erroneously classified as polyamide. This illustrates that the isolation of the specific measurement uncertainty achieved herein enables certain analysis pipelines to be debugged.

Neither parallel nor serial ILC designs can determine the absolute truth of the particle number present. This is clearly so when particle sizes get close to the instrumental detection limits, as it was the case here, at least for FTIR and LDIR at around 10 μm. Nevertheless, when only larger sizes are considered, agreement might be possible and very relevant. At least for the immobilized design, a theoretically viable—but very time-consuming—way to obtain an accepted true reference value would be an analysis with individual optical microscopy and manual spectroscopic assessment of all immobilized particles in a target area of a sample. However, even then, it would be difficult to achieve absolute certainty about the number of MP particles present. In borderline cases, it may be impossible even for human assessors to make a final decision about the extent of a single particle, because MPs do not always exhibit unequivocally visually separable particle boundaries.

The serial ILC performed here serves as a demonstrative proof of concept for the idea of using immobilized samples in serial ILCs. We recommend for benchmarking or standardizing ILCs, prepared in this manner, to use replicated samples as well as repetitions of the pre- and postmeasurements ($n \geq 3$). They serve as a control of successful immobilization and allow to estimate the intra-analytical measurement uncertainty. Furthermore, the number of participants was low and the apparent particle numbers varied between the different ILC types (see also the table within Figure 3). Presenting more equal particle numbers to a larger group of participants will lead to increased stability of the uncertainty estimations that can be attributed to the applied analysis techniques.

Stability of Filtration-Immobilization. The development of the immobilization method in the present study was adapted from a previous approach where spin-coating was used to distribute an adhesive on a carrier.[17] The change to the filtration-immobilization principle proved advantageous as the amount of residual adhesive on the substrate surface is substantially reduced. We provide insights of spectroscopic effects of the remaining adhesive in SI5.

In the serial ILC concept, the host participant repeats their measurements after the ring trial completion to ascertain whether particle loss occurred (Figure 6). Negligible differences indicate the adequate stability and permanence of the immobilization.

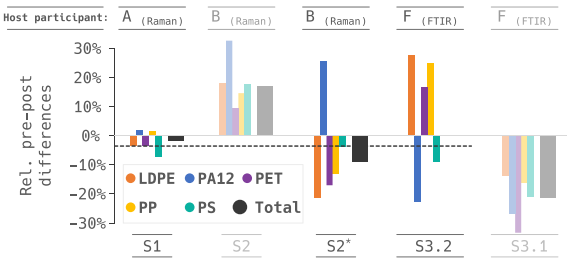


Figure 6. Relative differences of particle numbers per polymer identified by the host participant before and after the serial ILC. S2* was calculated only on the particle fraction ≥20 μm due to the reasons explained in the main text. The dashed line indicates the change in particle counts as the average "pre/postdifferences" of those samples with acceptable sample stability, i.e., only opaquely plotted bars. Note that the value for total MPs was very low in S3.2 (bar not visible).

Participant B, who made the pre/postcomparison of sample S2 using Raman spectroscopy, received a software upgrade from the manufacturer between the two measurements that improved the instrument's ability to detect smallest particles. The stability of the immobilization was therefore only evaluated on the ≥20 μm particle fraction of the pre- and postmeasurements. The comparison including particles between 10 and 20 μm is presented for reference (Figure 6) and shows a spurious increase in the abundance of particles in the postmeasurement.

In adaptation of the ISO 13528[15] stability criteria c (eqs 4 and 6) to the serial ILC, we observe that samples S1, S2, and S3.2 qualify for being included in the ILC results. Their relative pre/postdifferences are within the threshold for acceptable stability of $c \leq 30\%$, namely, at 25, 14, and 1% of the interparticipant RSDs, respectively. For sample S1, this result was obtained using eq 6 with an expected measurement uncertainty of 0.056 and would have been 32% when using eq 4.

In addition to actual changes in particle numbers due to sample transport, deviations between pre/postmeasurements are also influenced by the expected—and here unknown—intra-analytical variance of the host participants. However, the overall low pre/postdifference (Figure 6; dashed line: −4% on average of the samples accepted according to the "criterion c") implies that only relatively small intra-analytical variances are to be expected here.

There was an apparent difference of immobilization stability between the two Al_2O_3 filters (S3.1 and S3.2). In contrast to the Si filters, a rinsing procedure to remove insufficiently immobilized particles after curing was not applied due to the fragility of the material. Future studies aiming for immobilized samples on alumina membranes should explore other solutions for removing loose particles.

Pre/postdifferences in the individual polymer types appear to largely cancel out each other in TMP, which is especially obvious for samples S2 and S3.2. This indicates a differential polymer type misclassification problem, not only between participants (Figure 4) but also intra-analytically. This reveals an interesting research question on whether there is in general

https://doi.org/10.1021/acs.est.4c09427
Environ. Sci. Technol. XXXX, XXX, XXX−XXX

a significantly lower uncertainty on TMP counts than on quantifications of individual polymers.

Perspective of Environmental Particle Evaluation. Below, we summarize the lessons learned from the interlaboratory trials presented here and give recommendations to encourage much needed further methodological advancement in this area. The approach we present here is targeting the size range of about 10−100 μm. It would likely be suitable for MPs up to about 500 μm, but the effectiveness of the filtration immobilization is yet to be evaluated in this size range. As such, we only cover a part of the environmentally relevant MPs. For larger sizes, simpler methods like obtaining a true reference value by manual counting become viable and are therefore likely to be preferred.

With sample S1, we found a 10 μm filter well suited for comparative measurements with Raman, FTIR, and LDIR spectroscopy, while the 1 μm filter S2 posed several obstacles to FTIR and LDIR detection. This includes a higher presence of particles in size ranges where physical limitations restrict successful detection by these techniques. In Raman spectroscopy, potassium silicate shows distinct bands at 545 and 1029 cm^{-1} (Figure SI5.1), but they did not interfere with the polymer classification, primarily because Raman spectroscopy is acting on the up-facing surfaces of the particles, where little or no excess adhesive is expected. For FTIR and LDIR spectroscopy measured in transmission and transflectance modes, respectively, any adhesive between the particles and the filter surface or inside the filter pores will interact with the IR light. However, this will not result in conjugate spectra (i.e., polymer spectra clearly superimposed inorganic bands of the adhesive) because the FTIR measurements for polymer identification were made against a background of potassium silicate on the filter material. Instead, the IR adsorption of the silica compounds manifests itself as increased noise because it limits the IR energy that can reach the detector. Regarding the concentration of potassium silicate, we chose the lowest tested concentration as the best option. It seems reasonable thinking that further dilutions may be a promising endeavor to decrease potential impacts to certain techniques.

Many analytical protocols employ subsampling measurement approaches due to instrumental or computational limitations or to reduce measurement time. This entails extensive extrapolation of the actual measurement result to the whole sample, contributing to the uncertainty propagation. In fact, subsampling approaches (see also Figure 1) have been demonstrated to cause substantial errors in the determination of the total particle numbers.[25] A major advantage of the immobilized serial ILC design is that such a subsampling error is eliminated by the precise definition of a commonly measured area. Here, the laser engraving technique developed for Si filter S2 proved to be highly useful in that it expedites and unifies measurements and result evaluations. Due to the particles being removed from the interstice, minor unavoidable differences in the size and positioning of the measurement areas will not significantly affect the results when all participants select areas slightly larger than the visible target areas.

For a permanently immobilized serial ILC sample, we consider three properties to be most desirable:

- The substrate and immobilization achieve sufficient stability, i.e., they withstand the repetitive handling, transportation, and measurement.
- Its physical properties do not interfere with or discriminate against certain measurement techniques, e.g., sufficient IR transparency is warranted.
- The sample allows for some form of return to original state, e.g., by rinsing off any adherent contaminating particles prior to each participant's measurement.

Compared to the creation of numerous sample specimens for parallel ILCs, the immobilized approach requires less strict contamination control during production. Contamination during sample generation is excluded by design as everything that gets immobilized becomes part of the sample. It is still advisable to prepare samples under reasonable analytical laboratory conditions to avoid unintentionally introduced particles, producing spurious results.

Outlook and Future Perspectives. The immobilized filters in our serial ILC were prepared at small research laboratory scale. While offering significant advantages over traditional parallel designs, they are not intended as a permanent solution. They serve as an intermediate step in establishing robust analytical protocols and identifying sources of measurement uncertainty. However, the concept should be the taken up for the development and supply of certified reference materials (CRMs) that can be routinely used for method validation and quality control in laboratories worldwide. CRMs, produced and certified by accredited organizations such as the European Joint Research Centre (JRC), the German Federal Institute for Materials Research and Testing (BAM), the National Metrology Institute of Japan (NMIJ), the International Atomic Energy Agency (IAEA), or the United States National Institute of Standards and Technology (NIST), provide a standardized and traceable means of validating analytical methods and ensuring interlaboratory comparability. For MPs, however, the provision of CRMs presents unique challenges due to the particulate nature of the analyte. Collaboration between research institutions, regulatory bodies, and accredited reference material producers is essential to overcome these challenges and establish commercially available immobilized and suspended CRMs for MP analysis.

With immobilized MP CRMs available, automated reproducible measurements may be set up with minimal manual involvement. These procedures can run routinely on a periodic schedule or after any changes in measurement protocols, equipment, or personnel. Over time, the results can become highly valuable for the laboratory to monitor the relative analytical proficiency and spot any arising problems in MP detection.

Further questions should be addressed to establish a broader applicability of the immobilized samples. For instance, knowledge on immobilization stability of larger MP sizes (e.g., 100−1000 μm), fibers or natural particulates, may allow for an application also to field samples. This can reduce particle loss or disarrangement in the transition from sample preparation to spectroscopic measurement. Additionally, it may be used to build up persistent sample archives for repeatable measuring. At the current stage, however, we do not recommend the immobilization technique for quantitative sample preservation. We included here steps of sample flushing to remove incompletely immobilized particles, which would obviously not be an option in field samples intended for MP quantification. Provided that the objective is to conduct an ILC or similar experiment—where the total number of MPs present

https://doi.org/10.1021/acs.est.4c09427
Environ. Sci. Technol. XXXX, XXX, XXX−XXX

in the sample prior to immobilization is not of interest—we may reasonably assume that the technique would work just as effectively if MPs from the environment were used instead of the milled and sieved pristine particles employed in this study.

Our results suggest that other research on particulate pollutants beyond like fly ashes, cement dust, soot, or spores can benefit from adapting the immobilization technique to yield reproducibly measurable samples. In particular, further developments targeting immobilization of atmospheric particulate matter samples will help in comparability studies of microspectroscopic and mass spectroscopic analyses[35,36] (see also SI6). Likewise, other multianalysis studies, such as correlative microscopy or spectroscopy, could benefit from enhanced precision and accuracy when working with particle immobilizations.

■ ASSOCIATED CONTENT

Data Availability Statement

Data of measured MP particles per sample and participant with statistical analysis and raw version of the figures created thereof are provided as a Microsoft Office Excel spreadsheet in the data and code deposit[34] at 10.5281/zenodo.10791088.

Supporting Information

The Supporting Information is available free of charge at https://pubs.acs.org/doi/10.1021/acs.est.4c09427.

Material and methodological details, additional microscopic and spectroscopic information, and an extended version of Figure 4 (PDF)

■ AUTHOR INFORMATION

Corresponding Authors

Robin Lenz − *Leibniz Institute of Polymer Research Dresden, Dresden 01069, Germany; Leibniz Institute for Baltic Sea Research Warnemünde, Rostock 18119, Germany;* orcid.org/0000-0003-4156-7380; Email: robin.lenz@ipfdd.de

Dieter Fischer − *Leibniz Institute of Polymer Research Dresden, Dresden 01069, Germany*; Email: fisch@ipfdd.de

Matthias Labrenz − *Leibniz Institute for Baltic Sea Research Warnemünde, Rostock 18119, Germany;* orcid.org/0000-0003-3452-8631; Email: matthias.labrenz@io-warnemuende.de

Authors

Kristina Enders − *Leibniz Institute of Polymer Research Dresden, Dresden 01069, Germany; Leibniz Institute for Baltic Sea Research Warnemünde, Rostock 18119, Germany*

Eva Cseperke Vizsolyi − *University of Bayreuth, Bayreuth 95440, Germany*

Mareike Schumacher − *Leibniz Institute of Polymer Research Dresden, Dresden 01069, Germany*

Julia Lötsch − *Leibniz Institute of Polymer Research Dresden, Dresden 01069, Germany*

Martin G. J. Löder − *University of Bayreuth, Bayreuth 95440, Germany;* orcid.org/0000-0001-9056-8254

Gabriele Eder − *Österreichisches Forschungsinstitut für Chemie und Technik, Wien 1030, Austria*

Yuliya Voronko − *Österreichisches Forschungsinstitut für Chemie und Technik, Wien 1030, Austria*

José Manuel Andrade-Garda − *University of A Coruña, A Coruña 15071, Spain*

Soledad Muniategui-Lorenzo − *University of A Coruña, A Coruña 15071, Spain*

Christian Laforsch − *University of Bayreuth, Bayreuth 95440, Germany*

Complete contact information is available at: https://pubs.acs.org/10.1021/acs.est.4c09427

Author Contributions

R.L. and K.E. invented the serial ILC concept and the silicon-based particle immobilizations, contributed to Raman and FTIR measurements, analyzed the data, and drafted the manuscript. E.C.V. and M. Löder contributed to FTIR measurements, created the samples for the parallel ILC, and developed the alumina-based particle immobilizations. M.S. and J.L. contributed to Raman measurements. G.E. and Y.V. contributed to FTIR measurements. J.M.A.G. and S.M.L. contributed to LDIR measurements. D.F. and M. Labrenz supervised the work. All authors reviewed the manuscript draft.

Funding

Financial support was received from the following: the CORNET project microplastics@food funded by the German Federal Ministry of Economic Affairs and Climate Action, IGF project no. 298 EBG; the JPI OCEANS project microplastiX funded by the German Federal Ministry of Education and Research under grant number 03F0852A, the Spanish Agencia Española de Investigación (grant PCI2020-112145, MCIN/AEI/10.13039/501100011033, and EU "Next Generation EU/PRTR"), and Galician Government (Xunta de Galicia, "Consolidación e Estructuración de Unidades de Investigación Competitivas", ED431C 2021/56); the Deutsche Forschungsgemeinschaft (DFG, German Research Foundation), project number 391977956, SFB 1357; the German BMBF research program "Plastics in the environment": MicroCatch_Balt "Investigation of Sinks and Sources of Microplastics from a Typical Catchment Area to the Open Baltic Sea", grant number 03F0788A; the EU-BONUS Programme "Blue Baltic": MICROPOLL "Multilevel assessment of microplastics and associated pollutants in the Baltic Sea", grant number 03F0775A.

Notes

The authors declare no competing financial interest.

■ ACKNOWLEDGMENTS

We thank the following for their help: Melinda Arnold and Mikhail Malanin (IPF Dresden) for FTIR measurements; Christian Norkus (Werkstatt TU Dresden) for assistance with the laser engraving of the Si filters; Maria auf der Landwehr (IPF Dresden) for providing SEM images; Benedikt Hufnagl (Hufnagl Chemometrics GmbH) for providing access to ML-prototype Raman and FTIR spectroscopy; Elisavet Kanaki and Robert Ohmacht for continuous improvement of the Gepard measurement software; Alexander Tagg for helpful comments on the manuscript draft.

■ REFERENCES

(1) ISO/TR 21960. *Plastics—Environmental Aspects—State of Knowledge and Methodologies*, 2020.

(2) Hidalgo-Ruz, V.; Gutow, L.; Thompson, R. C.; Thiel, M. Microplastics in the Marine Environment: A Review of the Methods Used for Identification and Quantification. *Environ. Sci. Technol.* **2012**, *46* (6), 3060−3075.

(3) Löder, M. G. J.; Gerdts, G. Methodology Used for the Detection and Identification of Microplastics—A Critical Appraisal. In *Marine*

Anthropogenic Litter; Bergmann, M.; Gutow, L.; Klages, M., Eds.; Springer International Publishing: Cham, 2015; pp 201−227.
(4) Hermsen, E.; Mintenig, S. M.; Besseling, E.; Koelmans, A. A. Quality Criteria for the Analysis of Microplastic in Biota Samples: A Critical Review. *Environ. Sci. Technol.* **2018**, *52* (18), 10230−10240.
(5) Koelmans, A. A.; Redondo-Hasselerharm, P. E.; Mohamed Nor, N. H.; Kooi, M. Solving the Nonalignment of Methods and Approaches Used in Microplastic Research to Consistently Characterize Risk. *Environ. Sci. Technol.* **2020**, *54* (19), 12307−12315.
(6) van Mourik, L. M.; Crum, S. J. H.; Martinez-Frances, E.; Bavel, B. van; Leslie, H. A.; de Boer, J.; Cofino, W. P. Results of WEPAL-QUASIMEME/NORMANs First Global Interlaboratory Study on Microplastics Reveal Urgent Need for Harmonization. *Sci. Total Environ.* **2021**, *772*, No. 145071.
(7) Thornton Hampton, L. M.; De Frond, H.; Gesulga, K.; Kotar, S.; Lao, W.; Matuch, C.; Weisberg, S. B.; Wong, C. S.; Brander, S.; Christansen, S.; Cook, C. R.; Du, F.; Ghosal, S.; Gray, A. B.; Hankett, J.; Helm, P. A.; Ho, K. T.; Kefela, T.; Lattin, G.; Lusher, A.; Mai, L.; McNeish, R. E.; Mina, O.; Minor, E. C.; Primpke, S.; Rickabaugh, K.; Renick, V. C.; Singh, S.; Van Bavel, B.; Vollnhals, F.; Rochman, C. M. The Influence of Complex Matrices on Method Performance in Extracting and Monitoring for Microplastics. *Chemosphere* **2023**, *334*, No. 138875.
(8) Wagner, J.; Robberson, W.; Allen, H. Analytical Precision Assessment for Microplastic Analyses. *Chemosphere* **2022**, *304*, 135295−135295.
(9) Langknecht, T.; Lao, W.; Wong, C. S.; Kotar, S.; El Khatib, D.; Robinson, S.; Burgess, R. M.; Ho, K. T. Comparison of Two Procedures for Microplastics Analysis in Sediments Based on an Interlaboratory Exercise. *Chemosphere* **2023**, No. 137479.
(10) de Frond, H.; Hampton, L. T.; Kotar, S.; Gesulga, K.; Matuch, C.; Lao, W.; Weisberg, S. B.; Wong, C. S.; Rochman, C. M. Monitoring Microplastics in Drinking Water: An Interlaboratory Study to Inform Effective Methods for Quantifying and Characterizing Microplastics. *Chemosphere* **2022**, *298*, No. 134282.
(11) Deuke, A.-K.; Fischer, E. *Microplastics on the Rocks: Adaption of a Method for the Preparation and Storage of Reference Material*; Zenodo, 2022.
(12) Müller, Y. K.; Wernicke, T.; Pittroff, M.; Witzig, C. S.; Storck, F. R.; Klinger, J.; Zumbülte, N. Microplastic Analysis-Are We Measuring the Same? Results on the First Global Comparative Study for Microplastic Analysis in a Water Sample. *Anal. Bioanal. Chem.* **2020**, *412* (3), 555−560.
(13) Becker, R.; Altmann, K.; Sommerfeld, T.; Braun, U. Quantification of Microplastics in a Freshwater Suspended Organic Matter Using Different Thermoanalytical Methods − Outcome of an Interlaboratory Comparison. *J. Anal. Appl. Pyrolysis* **2020**, *148*, No. 104829.
(14) Isobe, A.; Buenaventura, N.; Chastain, S.; Chavanich, S.; Cózar, A.; DeLorenzo, M. E.; Hagmann, P.; Hinata, H.; Kozlovskii, N.; Lusher, A.; Martí, E.; Michida, Y.; Mu, J.; Ohno, M.; Potter, G.; Ross, P. S.; Sagawa, N.; Shim, W. J.; Song, Y. K.; Takada, H.; Tokai, T.; Torii, T.; Uchida, K.; Vassillenko, K.; Viyakarn, V.; Zhang, W. An Interlaboratory Comparison Exercise for the Determination of Microplastics in Standard Sample Bottles. *Mar. Pollut. Bull.* **2019**, *146*, 831−837.
(15) ISO 13528. *Statistical Methods for Use in Proficiency Testing by Interlaboratory Comparisons*, 2022.
(16) Thompson, M.; Ellison, S. L. R.; Wood, R. The International Harmonized Protocol for the Proficiency Testing of Analytical Chemistry Laboratories (IUPAC Technical Report). *Pure Appl. Chem.* **2006**, *78* (1), 145−196.
(17) Lenz, R.; Enders, K.; Fischer, F.; Brandt, J.; Fischer, D.; Labrenz, M. Measuring Impacts of Microplastic Treatments via Image Recognition on Immobilised Particles below 100 Mm. *Microplastics Nanoplastics* **2021**, *1* (1), 12.
(18) Seghers, J.; Stefaniak, E. A.; La Spina, R.; Cella, C.; Mehn, D.; Gilliland, D.; Held, A.; Jacobsson, U.; Emteborg, H. Preparation of a Reference Material for Microplastics in Water—Evaluation of Homogeneity. *Anal. Bioanal. Chem.* **2022**, *414* (1), 385−397.
(19) Martínez-Francés, E.; Marie-Louise, T. M.; Craig, M.; Johansen, J. E.; Nizzetto, L.; Hurley, R.; Buenaventura, N.; Van Bavel, B. *Production of Microplastic Reference Materials*; Zenodo, 2022.
(20) Dehaut, A.; Himber, C.; Colin, M.; Duflos, G. Think Positive: Proposal of a Simple Method to Create Reference Materials in the Frame of Microplastics Research. *MethodsX* **2023**, *10*, No. 102030.
(21) Dawson, A. L.; Santana, M. F. M.; Nelis, J. L. D.; Motti, C. A. Taking Control of Microplastics Data: A Comparison of Control and Blank Data Correction Methods. *J. Hazard. Mater.* **2023**, *443*, No. 130218.
(22) Brander, S. M.; Renick, V. C.; Foley, M. M.; Steele, C.; Woo, M.; Lusher, A.; Carr, S.; Helm, P. A.; Box, C.; Cherniak, S. L. C.; Andrews, R. C.; Rochman, C. M. Sampling and Quality Assurance and Quality Control: A Guide for Scientists Investigating the Occurrence of Microplastics Across Matrices. *Appl. Spectrosc.* **2020**, *74* (9), 1099−1125.
(23) Cowger, W.; Booth, A. M.; Hamilton, B. M.; Thaysen, C.; Primpke, S.; Munno, K.; Lusher, A. L.; Dehaut, A.; Vaz, V. P.; Liboiron, M.; Devriese, L. I.; Hermabessiere, L.; Rochman, C.; Athey, S. N.; Lynch, J. M.; De Frond, H.; Gray, A.; Jones, O. A. H.; Brander, S.; Steele, C.; Moore, S.; Sanchez, A.; Nel, H. Reporting Guidelines to Increase the Reproducibility and Comparability of Research on Microplastics. *Appl. Spectrosc.* **2020**, *74* (9), 1066−1077.
(24) Joint Committee for Guides in Metrology. *Guide to the Expression of Uncertainty in Measurement — Part 1: Introduction*; Bureau International des Poids et Mesures, 2023.
(25) Brandt, J.; Fischer, F.; Kanaki, E.; Enders, K.; Labrenz, M.; Fischer, D. Assessment of Subsampling Strategies in Microspectroscopy of Environmental Microplastic Samples. *Front. Environ. Sci.* **2021**, *8*, No. 579676.
(26) Thaysen, C.; Munno, K.; Hermabessiere, L.; Rochman, C. M. Towards Raman Automation for Microplastics: Developing Strategies for Particle Adhesion and Filter Subsampling. *Appl. Spectrosc.* **2020**, *74* (9), 976−988.
(27) Leeson, P. T. Rational Choice, Round Robin, and Rebellion: An Institutional Solution to the Problems of Revolution. *J. Econ. Behav. Organ.* **2010**, *73* (3), 297−307.
(28) Pierson, R. H.; Fay, E. A. Guidelines for Interlaboratory Testing Programs. *Anal. Chem.* **1959**, *31* (12), 25A−49A.
(29) Kanaki, E.; Fischer, F.; Brandt, J.; Fischer, D. *A Filtration Apparatus for the Analysis of Microplastics*, Zenodo 2024.
(30) Käppler, A.; Windrich, F.; Löder, M. G. J.; Malanin, M.; Fischer, D.; Labrenz, M.; Eichhorn, K. J.; Voit, B. Identification of Microplastics by FTIR and Raman Microscopy: A Novel Silicon Filter Substrate Opens the Important Spectral Range below 1300 Cm(−1) for FTIR Transmission Measurements. *Anal. Bioanal. Chem.* **2015**, *407* (22), 6791−6801.
(31) Brandt, J.; Bittrich, L.; Fischer, F.; Kanaki, E.; Tagg, A.; Lenz, R.; Labrenz, M.; Brandes, E.; Fischer, D.; Eichhorn, K.-J. High-Throughput Analyses of Microplastic Samples Using Fourier Transform Infrared and Raman Spectrometry. *Appl. Spectrosc.* **2020**, *74* (9), 1185−1197.
(32) Hufnagl, B.; Stibi, M.; Martirosyan, H.; Wilczek, U.; Möller, J. N.; Löder, M. G. J.; Laforsch, C.; Lohninger, H. Computer-Assisted Analysis of Microplastics in Environmental Samples Based on μFTIR Imaging in Combination with Machine Learning. *Environ. Sci. Technol. Lett.* **2022**, *9* (1), 90−95.
(33) Welch, W. J. Construction of Permutation Tests. *J. Am. Stat. Assoc.* **1990**, *85* (411), 693−698.
(34) Lenz, R.; Enders, K.; Vizsolyi, É. C.; Schumacher, M.; Lötsch, J.; Löder, M. G. J.; Eder, G.; Voronko, Y.; Andrade-Garda, J. M.; Muniategui-Lorenzo, S. N.; Laforsch, C.; Fischer, D.; Labrenz, M. *Data and Supplementary Files of the Publication: "What Goes Around Should Not Move Around: Immobilizing Microplastics as a New Approach for Analytical Ring Trials*, Zenodo 2024.
(35) Primpke, S.; Fischer, M.; Lorenz, C.; Gerdts, G.; Scholz-Böttcher, B. M. Comparison of Pyrolysis Gas Chromatography/Mass

https://doi.org/10.1021/acs.est.4c09427
Environ. Sci. Technol. XXXX, XXX, XXX−XXX

Spectrometry and Hyperspectral FTIR Imaging Spectroscopy for the Analysis of Microplastics. *Anal. Bioanal. Chem.* **2020**, *412*, 8283−8298.
(36) Primpke, S.; Fischer, M.; Lorenz, C.; Gerdts, G.; Scholz-Böttcher, B. Quantifying Microplastics in Complex Environmental Samples: Py-Gc/Ms vs. Hyperspectral Ftir − Potential and Limitations. In *30th International Meeting on Organic Geochemistry (IMOG 2021)*; European Association of Geoscientists & Engineers: Online, 2021; pp 1−2.

https://doi.org/10.1021/acs.est.4c09427
Environ. Sci. Technol. XXXX, XXX, XXX−XXX

This is the end of the publication

What Goes Around Should Not Move Around: Immobilizing Microplastics as a New Approach for Analytical Ring Trials

by Robin Lenz, Kristina Enders, Eva Cseperke Vizsolyi, Mareike Schumacher, Julia Lötsch, Martin G. J. Löder, Gabriele Eder, Yuliya Voronko, José Manuel Andrade-Garda, Soledad Muniategui-Lorenzo, Christian Laforsch, Dieter Fischer, Matthias Labrenz

You might want to continue reading the synopsis at page 21, or jump back to the start of this publication at page 195.

Mapping the plastic legacy: Machine-learning enabled microplastic inventory prediction in aquatic sedimentary systems

by Kristina Enders, Robin Lenz, Franziska Fischer, Klaus Schwarzer, Guntram Seiß, Matthias Labrenz

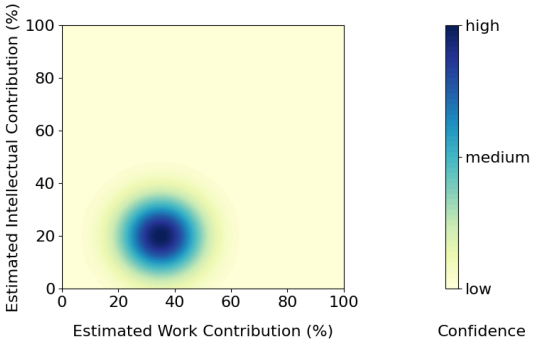
- **Date published**: 2025 (expected)
- **Type**: Unpublished
- **Published in**: n/a
- **License**: CC-BY (envisaged)
- **DOI**: n/a, **Reference**: [13]
- **Citations**: n/a

Contributions

Conceptualization: K.E., R.L., M.L. | Funding: D.F., M.L. | Method development: K.E., R.L. | Data acquisition and analysis: K.E., R.L., F.F., K.S. | Interpretation and modelling (NIXVEGS): R.L., K.E. | Modelling (PARTRACE, UnTRIM): G.S. | Writing: All authors contributed to writing the manuscript.

Quantitative own contributions based on self-assessment

In the dimensions of expended work effort and intellectual contribution, I consider my shares are likely to be between 30% and 40% and between 15% and 25% respectively. This is visualised below as an interpolated histogram of 500 samples from Gaussian distributions with the aforementioned estimates at plus/minus two standard deviations.



Mapping the plastic legacy with NIXVEGS: Machine-learning enabled microplastics prediction in sediments

Kristina Enders[1,2*], Robin Lenz[1,2], Franziska Fischer[2], Klaus Schwarzer[3], Guntram Seiß[4], Dieter Fischer[2], Matthias Labrenz[1*]

[1] Leibniz Institute for Baltic Sea Research Warnemünde (IOW), 18119 Rostock, Germany

[2] Leibniz Institute for Polymer Research (IPF), 01069 Dresden, Germany

[3] Christian-Albrechts-University of Kiel (CAU), 24118 Kiel, Germany

[4] The Federal Waterways Engineering and Research Institute (BAW), 22559 Hamburg, Germany

*Corresponding authors. Emails: enders-kristina@ipfdd.de, matthias.labrenz@io-warnemuende.de

Abstract: Aquatic sediments act as major sinks for microplastic (MP) pollution, yet accurately quantifying their MP distributions and inventories on a regional scale remains challenging, especially in hydrodynamically complex estuarine environments. Existing distribution models focus on ocean basins or simple hydrodynamic systems but lack sufficient adaptability to the spatial heterogeneity typical of estuaries. To address this limitation, we developed NIXVEGS, an open-source empirical spatial prediction pipeline adapting machine learning components like nested cross-validation and ensemble modeling specifically for the sparse data characteristic of environmental MP studies. It integrates granulometric proxies and spatio-temporal connectivity to predict MP distributions and provides data-driven decisions in model selection combined with performance validation on unseen data under the best possible utilization of the available observations. The model predictions increased spatial data coverage 7.6-fold from an original set of 26 analyzed MP sediment concentration in the Schlei estuary (Baltic Sea coast, Northern Germany). We demonstrate the application of NIXVEGS and use its predictions to estimate the region's sedimentary MP inventory at ~20 trillion particles (50-5000 µm) or ~14.3 tons. Estuarine sediments are key environments for monitoring MP pollution evolution, where NIXVEGS can assist regional plastic management and contribute to the understanding of a global MP budget.

Keywords: Grain size, Proxy, Geological analysis, Spectroscopy, FAIR data, Cross-validation, Predictive modeling, Environmental monitoring

Synopsis: We developed NIXVEGS, a predictive modeling tool leveraging readily obtainable sediment proxies, to significantly enhance the spatial coverage of microplastic concentrations from limited direct measurements.

Introduction

Sediments as the largest passive MP samplers

Global plastic cycling is influenced by a multitude of physical processes [1]. Similar to natural debris, the majority of the global plastic legacy ends up in sediments – places of continuous particle deposition [2,3]. Even initially buoyant MP are found to deposit in sediments as a result of particle agglomeration, biofouling and degradation [4], which manifests in their frequent presence in sedimentary environments [5,6]. The distribution dynamics of MP, like other suspended solids, are governed by the physics of particle motion. The hydrodynamic regime determines the sediment grain size distribution: while finer sediment particles dominate low-energy environments, coarser ones prevail in high-energy regimes due to their higher threshold for initiating motion [5,7,8]. The same principles apply to the transport of MP, as evident from observed correlations in MP concentrations and sediment grain size [5,9–11], yet, with an observable size shift due to the lower densities of plastics compared to natural sediment [5]. Unlike surface or intermediate water compartments, where MP levels fluctuate spatially and temporally, making unambiguous trend analyses difficult, sediments provide a more stable and integrated record of the temporal evolution and spatial extent of plastic pollution [12–16].

In systems of uninterrupted hydrodynamic connectivity and sufficient steady state with respect to distribution and sorting processes, granulometric normalization is an effective tool for studying sedimentary MP pollution levels [5]. It helps in evaluating the influence of the hydrodynamic regime or in performing source and sink analyses. If the hydrodynamic connectivity can be assumed to be sufficient, the MP distribution could readily be predicted based on a granulometric proxy [5]. However, for many environmental settings, this connectivity assumption does not hold. The local interplay between MP inputs, hydrodynamic forcing, geomorphological peculiarities, and spatial extent of the studied system may reveal spatio-temporal discontinuities in the granulometric normalized MP concentrations.

Reliably quantifying MP is crucial for assessing risk and changes in biogeochemical cycles [17–19]. While worldwide geological records show MP increasing in sediments since the 1950s [20–22], we still lack fundamental understanding of the mechanisms driving their distribution [23,24], and reliable quantification of MP inventories remains elusive. Indeed, sediments are among the least studied compartments for MP pollution [25,26] since quantifying this heterogeneous synthetic, polymeric material group [27] embedded within diverse sediment matrices is highly demanding. Despite MP-analytical methods improving in efficiency, their laborious nature restricts exhaustive measurement campaigns resulting in overall small datasets, especially if the full spectrum of MP sizes, shapes and polymers is covered [5]. Data scarcity spawns an incentive for MP distribution modeling, but it is challenged by the large material diversity and a lack of data analytical standards.

Given these challenges, hydrodynamic numerical models (HNMs) offer a promising approach to predicting sedimentary MP distributions and inventories by simulating particle transport dynamics directly. However, the accuracy of HNMs relies heavily on precise parameterization

of numerous complex processes, many of which remain incompletely understood [23,28,29]. Variables such as MP particle properties (e.g., shape, density, biofouling, degradation state) and environmental factors (such as sediment composition and biotic activity), require empirical data specific to MP for accurate representation. Additionally, directly transferring knowledge from sediment transport models to MP dynamics has notable limitations [23,24]. Sediment dynamics, despite extensively researched, continues to be acknowledged one of the least understood areas within Earth science [30], which pertains all the more to models where MP is added to the equation. Consequently, while HNMs exhibit strong theoretical foundations, their ability to reliably simulate MP distributions is often constrained by necessary assumptions and simplifications. Furthermore, model generalizability remains limited, as parameterizations and process equations usually cannot be directly applied from one environmental setting to another without significant adjustments [28].

For specific cases, state-of-the-art HNMs have helped to gain valuable first principle estimates of plastic pollution at ocean basin or global scales [18,31–33]. Others have provided detailed local insights based on hydro-numeric simulations of select key systems [34,35]. However, there is a lack of models for predicting MP distribution at regional scales, especially for systems of high geomorphological and hydrodynamic heterogeneity such as estuarine sediments. These ecosystems at the fluvial-marine interface, which typically represent bottlenecks for MP of terrestrial origin, and which are often affected by high anthropogenic activity, are ideal monitoring sites to study the evolution of (micro)plastic pollution. Hence, there is a clear need to model the regional-scale distribution pattern of MP and determine their inventories in these key indicator ecosystems. Empirical predictive modeling (EPM), relying on multivariate regression, can be harnessed in combination with selected techniques from modern machine learning (ML) methodology to provide a data-driven model and validation framework that can be applied to a wide range of systems. EPM facilitates a description of variable relations despite limited knowledge of the many underlying subprocesses involved by leveraging several easier-to-obtain covariates as predictors. EPM is often employed in water quality assessments [28].

Here we report the development of NIXVEGS (Nested Iterative (stratified) X-Validation-to-Ensemble-modeling through Grid Search): an open-source empirical spatial prediction tool using ML techniques to determine MP abundances in complex sedimentary ecosystems. NIXVEGS encompasses the complete ML pipeline for model selection, evaluation and prediction (SI, Fig. S4). The model founds on the hydrodynamic equivalence principle between MP and sediment grains. It is an integral part of a data analysis workflow starting with data preparation (querying MP data from the database MPDB [36], blind corrections and augmentation from external data sources) and concluding with geospatial interpolations and inventory estimation, all implemented as reproducibly executable Jupyter notebooks (see overview Fig. 1).

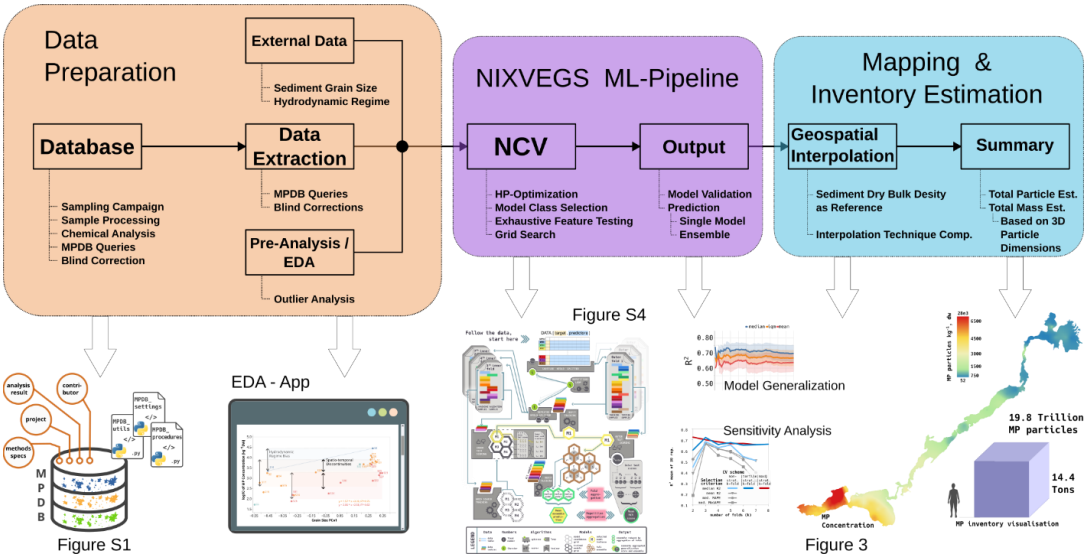


Figure 1. Overview of data analysis pipeline for prediction of the MP legacy in sedimentary systems. *Insight into all underlying MP and sediment data is provided in the accompanying web application for exploratory data analysis (EDA app).*

The model was established and validated on a MP dataset of 26 sediment samples in a field measurement campaign in spring 2018, taken along the 42 km long Schlei, and investigated using spectroscopic, geological and geo-chemical analyses (Fig. 2 A). The Schlei is influenced by the annual discharge of about 250 million m^3 of freshwater from several tributaries and by wind-driven inflow of brackish water through its open connection to the non-tidal Baltic Sea, resulting in a slight estuarine circulation. The Schlei combines several aspects of a complex geomorphological and hydrodynamic setup, and has a high societal and ecosystemic value. It has moreover been impacted by a major source of MP pollution, with meso- and microplastic snippets, leftovers from shredded, packaged food used in the biogas plant in the city of Schleswig, which entered the Schlei waterbody via the local waste water treatment plant (WWTP). Local newspapers published estimates of several tons supposedly being released over the course of 2-3 years [37]. A reliable model of MP pollution distribution could have supported knowledge-based decisions and effective regulatory interventions, but was lacking at the time of discovery of the pollution event.

NIXVEGS – a ML tool chain for empirical MP modeling

ML is now rapidly developing in the field of earth science [38] and has also been adopted in several areas of MP research, such as pollution level classification, spectral noise reduction, or polymer type and image classification [39–42]. Regarding MP concentration regression, however, there is no protocol available to yield local predictions or geospatial interpolations thereof [43].

NIXVEGS addresses this gap and accounts for the typical properties and requirements of regional MP prediction. Most ML use cases involve datasets with several orders more

observations than the typically small MP environmental datasets, making it challenging for ML to achieve high predictive power while performing stably under rigorous testing. NIXVEGS encompasses several key elements including model configuration grid search, nested cross-validation (NCV) with adjustable stratification, and ensembling for predictive stability. While each of these methods have individually been described previously, NIXVEGS combines and balances these elements in a novel manner to compensate difficulties arising from modeling with small datasets. With NCV being at the core of NIXVEGS, it safeguards against overfitting not only in the actual model training, but also in selection of predictor variables, model algorithms, and hyperparameters. For NIXVEGS' other core components (i.e., grid search, stratified k-fold cross-validation [CV], regression algorithms, predictions) we rely on functionalities implemented in the widely recognized ML libraries sci-kit-learn and xgboost [44,45]. How these components are linked together is described in the supplementary information (SI, Fig. S4).

NIXVEGS uses sediment grain size proxy variables as predictors describing the similarities in the hydrodynamic deposition behavior between MP and natural particles. Where areas are hydrodynamically well-connected, correlations of MP abundance with certain sediment grain size fractions are clearly evident [5]. However, if present, spatio-temporal discontinuities need to be accounted for by the EPM to effectively model the system's MP distribution, which is addressed by NIXVEGS. With this model framework we aim to provide the tools needed to generate realistic MP distribution maps, allowing us to estimate a sedimentary MP inventory for an entire geomorphological region.

Methods

We summarized the methodological steps crucial for the core of our analysis and model approach. Further details and reasoning for certain methodological choices are provided in a more comprehensive version of the methods section in the SI.

Sample collection

Sediment was collected at a total of 32 stations from May 14 – 16, 2018, using a Van Veen grab from aboard a ship (Klaashahn, IOW) in a transect from the Inner Schlei to the Baltic Sea opening [46]. The deliberate choice of the sampling locations aimed to balance grain size coverage (by consulting grain size maps of the Schlei [46]), spatial coverage (covering the entire extent and depths) and usage coverage (i.e., regions of more pristine and more anthropogenic character). After carefully opening the grab, the top 5 cm of sediment were transferred into a MP-free cleaned glass jars (one per sampling location and additionally also one sample of the 10-15 cm layer at S1, S2, S4, S10) and stored dark at 4°C. Of the 32 stations, 28 samples were later analyzed for MP, two only for sediment properties, and two were lost.

We used data on sediment properties from a second sample set, collected at 183 stations by an earlier sediment survey on courtesy of Kiel University. Information on sampling and analysis of this subset of data can be found in [46]. Principal procedural steps were comparable between the two studies. A van Veen grab was used to obtain 161 samples, whereas the 22

samples were taken using a gravity corer. For each core sample, sediment grain size measurements from the upper 5 cm were averaged for comparability to the grab samples.

MP sample preparation

The detailed MP extraction protocols, method validation and contamination prevention measures are documented in a separate method article [47]. We here report the essential procedural steps and refer to respective protocol modules (m1 – m6) as part of the modular decision tree (see Fig. 2 in [47]) as they are identical as described in these published protocols. Samples were freeze dried (m1), homogenized (m2) and defined dry masses (160 g on average) transferred into a density separation using sodium polytungstate (1.8 g cm^{-3}, m5). The application of the conical spiral conveyor (see Fig. 3 in [47]) in a customized glass separation funnel under addition of a few droplets of hydrogen peroxide allowed a gentle release and separation of lighter particles. Density and pH (3 – 3.4) were checked regularly and readjusted if necessary. Remaining organic constituents in the filtered supernatant were reduced by applying 30% hydrogen peroxide (m4.1). Samples were then filtered in the analytical laboratory (IPF Dresden) onto silicon filters with ~50 µm pore size using a custom-built glass filtration device [48] under a laminar flow cabinet (Telstar Aeolus V3) [49].

Larger MP suspects (> 1 mm) were individually picked and rinsed. In cases of particle overloading, stacked sieve filtration was applied (m6). Blanks covering the entire MP extraction (using an MP free sediment matrix, n = 8) and spectroscopic analysis pipeline (one per sample) were prepared to account for own MP contamination.

Spectroscopic analysis

MP particles on the Si-filters were identified and quantified via particle analysis combined with Raman µ-spectroscopy using the GEPARD software [48,50]. On a WITec alpha 300R microscope (Oxford Instruments Group), using a 20x objective with a 532 nm excitation, Raman spectra were acquired as 5 accumulated scans of 5 mW and 0.5 s integration. Larger particles were individually measured with Raman spectroscopy (WITec alpha 300R, Renishaw inVia Qontor) or ATR-FTIR spectroscopy (Bruker ATR microscope Hyperion 2000, coupled to a FTIR spectrometer Vertex 70) [51].

Geological and geochemical analysis

On homogenized and freeze-dried subsamples, deprived of organic matter by 30% H_2O_2, grain size distribution was analyzed in two replicates per sample using a Mastersizer 3000 (Malvern Panalytical) in wet dispersion mode with 10 s initial ultrasonication. Five consecutive measurements were performed and averaged for statistical analysis. Grain size data were exported in log scale in 116 histogram intervals.

TOC was calculated as averages of duplicates by subtraction of the total inorganic carbon (TIC) from the total carbon (TC). TIC and TC (TN, TS) determination was conducted on lyophilized, homogenized and ground sample material using the elemental analyzers multi-EA 4000 (Analytik Jena) and Euro-Vector EA (Hekatech).

The size distribution of organic matter was determined based on homogenized subsamples (5 – 40 g dry weight [dw]). The centrifuged supernatant of a density separation (sodium

polytungstate 1.8 g cm^{-3}) [52] was pipetted to a beaker. This process was repeated up to 10 times to ensure complete separation of the light fraction. Samples were filtered onto a 0.4 µm filter using MilliQ water [53], rinsed off and size analyzed using the laser-sizer Mastersizer 3000 in wet dispersion.

Data analysis and modeling summary

Reproducibly executable jupyter notebooks and python scripts (overview Fig. S1) were used to develop empirical and geospatial models and are available at https://github.com/robna/MPSchleiSediments under GNUv3 open-source license. This also includes a web app for exploratory data analysis (EDA app). More details and rationales on the development of the modeling pipeline are provided in the SI.

Response variable

We used the total particle- and mass-based MP abundances per kg sediment dw ($Concentration$ (Fig. S2), $MassConcentration$, see EDA app: sample domain data) as response variables for predictive modeling and spatial interpolation.

Database

MPDB, a MP-specific database [36] for FAIR-data compliant [54], particle-based analysis workflows (findable via the IOW-META database), was used to store MP related particle-, spectroscopic- and metadata (Fig. S1). The MPDB notebook contains the necessary functions to query the relevant entries from the MPDB. This includes the procedures of aggregating the particle-based raw data into sample-based data, according to the principles described in [36]. All relevant information that was extracted from the MPDB for the model development can also be seen in the EDA app.

Blank correction was done by matching MP phenotypes between environmental and blank samples (see also SI and [36] under 3.4. Data sanitation - Phenotyping and Blank Subtraction). In short, MP particle phenotypes were characterized by having the same sample, polymer type, shape and color properties.

Particle size, volume and mass and approximation

We advanced and validated (based on > 100 manual particle height measurements) the particle height determination algorithm in GEPARD to enable an accurate determination of all three spatial dimensions needed for more accurate conversion to volume, hence, mass-based data. The relevant changes can be comprehended in the GEPARD repository.

Volumes of irregular shaped particles V_{irr} were calculated as ellipsoids based on particle length l, width w and height h, according to Eq. 1. Fibers were approximated as cylindrical volumes V_{fib} (Eq. 2).

$$V_{irr} = \frac{\pi l w h}{6} \qquad (1)$$

$$V_{fib} = \frac{\pi l w^2}{4} \qquad (2)$$

Particle volumes were then multiplied by the density of the identified polymer type to yield particle masses (see "densities" in settings.py for used values).

Predictor variables

Predictors in the context of this study are vectors of non-MP related properties with values for each station (see SI for further details on their composition).

Geographic features

$Depth$, the water depth in meters at measured a sample's location. In lack of measured depths in the prediction dataset, depth values were sampled from a bathymetry map (digital elevation model [DEM], 5 m grid, provided on courtesy of the BAW, based on comprehensive bathymetric echosounder and multibeam echosounder measurements, for details on validation see SI, Fig. S3). $Dist_Land$ is measured as the shortest distance in meters between a sample's location and the shoreline.

Sediment grain size properties

Grain size variables were generated using GRADISTAT [55] on the log-scaled binned volume-based grain size distributions. Median grain size in µm (SED_D50) and the percentage below 63 µm ($perc_MUD$) was used. In addition, a 2D representation of grain size was calculated and used as predictor variables ($PCo1, PCo2$). They were created from a principal coordinate analysis (PCoA) using Bray-Curtis dissimilarity [56] as a distance measure.

Samples with missing data in either in TOC ($n = 26$) or the grain size variables SED_D50, $perc_MUD$, $PCo1$ and $PCo2$ ($n = 11$) were imputed by regressions as described in the SI (also including explanations for the choice of specific granulometric proxies).

Spatio-temporal discontinuity

A numeric model [57], based on the unstructured finite volume code UnTRIM (Unstructured Tidal Residual Mudflat model [58]), was used to simulate the hydrodynamic behavior of the Schlei. Simulated spherical drifters (300, 100, 50, 18 and 0 µm radius, 1.113 kg/m^3) were released for three different periods (2017-06-01 to 2017-08-01, 2017-10-15 to 2017-12-15, 2018-04-01 to 2018-06-01). They were traced forward [59] originating from 54°31'31.499"N, 9°36'11.582"E, a point at shore near the location of the highest granulometric normalized MP particle concentrations at S8 and S10 (see also Fig. 3 D). The resulting tracer paths were used to infer knowledge about how the tracers had moved through the system in respect to the sampling locations in four different implementations (see Table S1). Six variables (*Disco1* to *Disco6*) were generated using varying settings of these implementations (see Table S2). Tracks of location, depth and time step of each tracer are provided in the data sources.

ML pipeline

Through NIXVEGS (implemented in a jupyter notebook, Fig. 1, Fig. S4) we create a model which has predictive capabilities for estimating the response variable $Concentration$ for samples in the prediction set. Theoretically it is founded on the principles of cross-validation (CV) [60], or, more specifically, nested-cross-validation (NCV) [61], and grid-search (GS), i.e., the

exhaustive model optimization on a given parameter space. NIXVEGS is structurally similar to the NCV proposed by [62], but extends the concept by adaptations specifically addressing the problems and needs arising under small dataset conditions.

NIXVEGS' adjustable components are:

1. CV scheme:
   - number of *repetitions* for the outer and inner loop
   - number of *folds* for the outer and inner CV
2. scoring scheme:
   - *selection scorer*: evaluation metric used to select a "best" model in the grid-search procedure, see Table S3
     - *inner fold aggregator* of the selection scorer: median, interquartile mean (iqm), or mean
   - *generalization scorer*: evaluation metric used as the final generalization score, see Table S3
     - *outer fold aggregator*: median, iqm, or mean
     - *repetitions aggregator*: median, iqm, or mean
3. model candidate configurations:
   - *predictor variable sets*: selection from allowed variable combinations
   - *model class*: generalized linear models (GLM), gradient boosting for linear regressors (XGBlinear), gradient boosting for tree regressors (XGBtree), random forests (RF)
   - *model hyperparameter values*: depending on model class

Model algorithms

The tested model algorithms included two from the linear family. A GLM has previously been used to model MP concentrations, based on granulometric proxies [5]. In the present study the *GLM* was implemented for a gamma distribution with a log link using the TweedieRegressor class of the scikit-learn library with power=2 and a L2 regularization parameter alpha=0. A linear gradient boosting model, here referred to as *XGBlinear*, was implemented using the XGBRegressor class from the xgboost library [45]. It was set up with hyperparameters to resemble the settings of the GLM model, however, allowing ensembles of up to 300 base estimators with the fixed hyperparameter set: booster=gblinear, objective=reg:gamma, n_estimators=300, reg_alpha=0, reg_lambda=0. Two model classes of tree-based estimators were included for comparison to the linear models. *XGBtree* was also implemented from the XGBRegressor class of the xgboost library, sharing the same hyperparameters as *XGBlinear*, but using booster=gbtree. Additional decision-tree-related hyperparameters were varied and optimized within NIXVEGS based on the following allowed values: tree_method=exact, learning_rate=[0.1, 0.25], max_depth=[2, 3], min_child_weight=[5, 7]. A *RF* model [63], implemented using the RandomForrestRegressor class of the scikit-learn library, was allowed to vary in the following hyperparameters: n_estimators=[10, 100, 300], max_depth=[None, 2, 4], max_features=[None, 1/3]. All non-mentioned hyperparameters were left at their default values.

Model composition

After consolidation of the sample set, 26 samples were found usable for the modeling dataset, 187 for the prediction dataset.

A set of 12 predictor variables was available for the automated feature selection inside NIXVEGS:

- **granulometric proxies:** *in situ* measured SED_D50, $perc_MUD$ and the computed variable $PCo1$ as descriptors of the sediment grain size, and hence, the hydrodynamic regime. $PCo2$ was included for representing other, more oblique sediment characteristics.
- **discontinuity variables:** $Disco1$ to $Disco6$ generated from hydrodynamic tracer simulations (see SI). Parameter variations concerning passive or advective transport, seasonal coverage of the simulation time, sedimentation behavior and influence radius are described in SI
- **geographic properties:** water $Depth$ and $Dist_Land$ (distance to closest point at shore) were accepted as relevant geographical descriptors.

The choice of which combinations of predictor variables become part of the predictive model is left to the exhaustive feature selection of the CV optimization within NIXVEGS. Limitations on allowed predictor combinations (e.g., mutually exclusive features and model class dependent restrictions, see also SI) were applied to avoid collinearities and unnecessary expense of computation. This resulted in 130 and 18 distinct predictor variable sets for linear and tree-based model candidates, respectively.

Model validation

The CV and scoring schemes were chosen under consideration of the small dataset size and modeling goal. We used 100 and 10 randomized repeats, each with $k = 3$ folds splitting for the outer and inner CV loop, respectively. We used the coefficient of determination (R^2) as scorer for both, the selection and generalization scoring scheme. When the GS had trained and selected the best models, their outer test set scores were calculated and aggregated first across folds within repetitions (*outer fold aggregator*) as median, then across repetitions (*repetitions aggregator*) as mean, to obtain the final NCV generalization score.

While R^2 is the main scorer used here in model selection and to asses overall model performance, we also evaluated other statistical metrics including the Mean Squared Error (MSE), Mean Absolute Error (MAE), and Mean Absolute Percentage Error (MAPE) and, for the latter two also their median-version (MedAE and MedAPE). These metrics provide complementary perspectives on the uncertainties associated with the model predictions: R^2 normalizes the explained variance relative to the total variance, MSE, MAE and MedAE quantify the absolute deviations between observed and predicted values, whereas MAPE and MedAPE express these errors in relative terms. Table S3 details mathematical definitions and range meanings of these metrics.

Adaptation for small datasets

For validation of our model results, NIXVEGS provides the CV scores. A range of CV-related settings i.e., the number of folds *k*, the type of scorer and the use of a stratification scheme, were evaluated (Fig. 3 F). We tested different stratification schemes (i.e., tertile and $\frac{n}{k}$ quantile) to evaluate performance estimation more independent of the described sensitivities towards *k* arising from small datasets. Based on this sensitivity analysis, we use a repeated stratified k-fold CV scheme, with $k = n_{folds} = [3,3]$ drawn from $s = n_{strata} = [3,3]$, repeated $r = n_{repetitions} = [100 \ldots 500,10]$ times and scored using $scorer = [R^2, R^2]$, for the outer and inner CV of NIXVEGS, respectively (Fig. 3 F). This setup results in 300 to 1500 unique aggregable splits which is approximately on par with what a leave-two- or leave-three-out scheme would achieve (325 and 2600, respectively), but with the advantage that it allows for a more balanced response variable distribution. More details of the sensitivity analysis and reasoning for the chosen CV schemes are provided in the SI.

Prediction

$EPM_{ensemble}$

The ensemble of models is composed of $N_{\text{outer repetitions}} = 100$ members. Before predicting, every ensemble member was refit on the entire set of samples. Their individual predictions were then aggregated according to the *repetitions aggregator*, for each sample.

EPM_{single}

A single-model EPM was instantiated running a non-nested grid search CV with the same CV scheme and grid previously used in the inner NCV loop, selecting a 'best candidate' configuration. This configuration was then fitted to all data available before prediction.

MP mass calculations

The calculation of MP mass concentration was based on the summed observed MP particle masses per sample.

$MassConcentration$ at the prediction stations was then approximated from the predicted numeric $Concentration$ via an empirical regression ($R^2 = 0.910$, Eq. 3, Fig. S5)

$$MassConcentration = 0.1451 \cdot Concentration^{1.1894} \qquad (3)$$

Geospatial interpolation and inventory estimation

The predicted and observed values (together $n = 213$), were used to interpolate the response variables on a regular 10 m grid over the entire Schlei area. Three grids were independently interpolated: $Concentration$, $MassConcentration$ and $SedDBD$, i.e., sediment dry bulk density. For the final numeric- and mass inventory estimation, we used the interpolation method OK (Table S4), as it resulted in the lowest leave-one-out cross-validation (LOOCV) error in a comparison of several interpolation methods ($R^2 = 0.41$, for details see SI, Table S4). Sediment dry bulk density $SedDBD$ was interpolated likewise. The total MP inventory estimates $E_{\text{inventory}}$ were then calculated according to Eq. 4,

$$E_{\text{inventory}}(MP|\text{Schlei}) = \sum_{x,y} d^2 \cdot l \cdot \mathbf{SedDBD}_{xy} \cdot \mathbf{MPconc}_{xy} \qquad (4)$$

with (x, y) being the coordinate points of the MP concentration grid $MPconc$ and $SedDBD$, d the grid point distance and l the relevant sediment layer thickness.

Results

MP concentrations quantified in 28 Schlei surface sediment samples in sizes 50–5000 µm range from 52 to 27610 MP kg^{-1} dw, with a mean and median at 3967 and 1771, respectively. All MP data on sample and particle level can be viewed in the accompanying EDA app. Via NIXVEGS we achieve a 7.6-fold availability increase of MP data points in the Schlei (n = 213) and provide results of our model validation. Finally, we estimate MP concentrations on regular 10 m grid in the entire Schlei by geospatial interpolation and use the gridded data to obtain an approximate MP inventory within a sediment layer depth of 0–15 cm, relevant for the local time horizon of the plastic age.

Granulometric pre-analysis - proxy normalization reveals major discontinuities

Looking only within continuous subregions (e.g., Inner Schlei / Outer Schlei, Fig. 2 A), we see in the granulometric proxy-normalization of the MP concentrations that a significant fraction of the small-scale MP variability is explained by differences in hydrodynamic conditions (Fig. 2 B). This underscores the importance of taking local grain size distributions into consideration for planning MP sampling campaigns. If we sample only within a narrow part of the available grain size spectrum, we may inherit a substantial bias regarding the MP concentrations. This is referred to as the hydrodynamic regime bias. The following granulometric proxies, with their respective R^2 (average of Inner- and Outer Schlei) were found to be viable predictor candidates for an EPM: $PCo1$: 0.78 > $perc_MUD$: 0.76 > SED_D50: 0.63 > TOC: 0.61. This observation is in line with former study results of the well-connected Warnow estuary [5], where comparable R^2 were found ($perc_MUD$: 0.73, SED_D50: 0.8). Note that reported R^2 values refer to linear correlations between $\log_{10}$ of numeric MP concentration and the respective proxy. Discontinuities, however, result in an apparent segregation into different MP concentration levels (Fig. 2 B), that cannot be explained by the hydrodynamic regime effect. A comparison at hydrodynamic equivalence in fine-grained sediments, for instance, shows that stations S08, S03 and S22 span over two orders of magnitude.

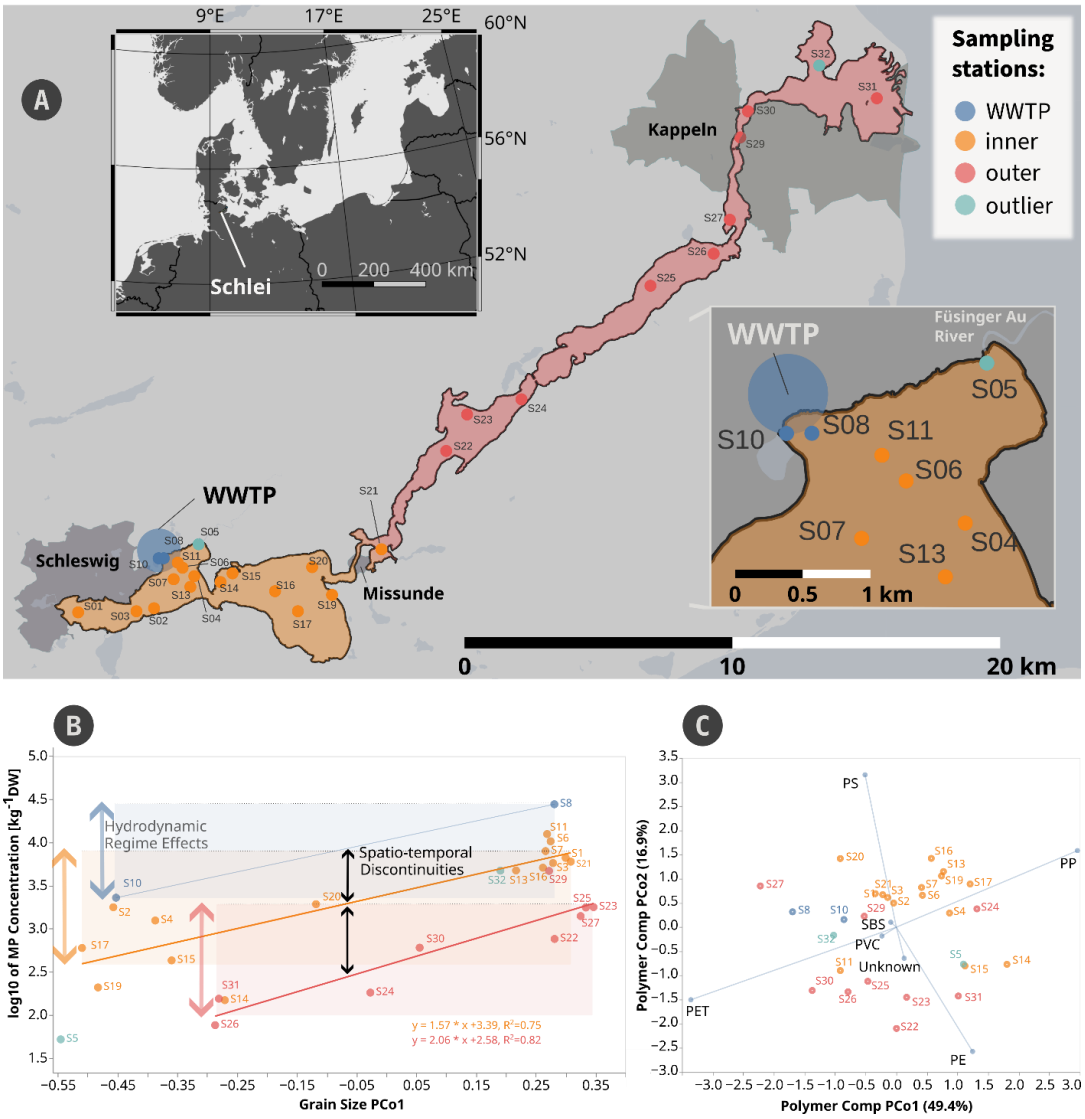


Figure 2. Granulometric normalization and spatio-temporal discontinuities in the MP dataset*. (A) Overview and regional map of the Schlei with sampling stations. (B) Granulometric proxy normalization of MP concentrations in Schlei sediments segregated by hydro-geomorphological subregions (inner and outer Schlei, orange and red). Small-scale outliers (green) are excluded from regression analysis. MP data are log transformed. The x-axis represents the first principal coordinate of sediment grain size where higher values correspond to finer sediments. To view plots of the other proxy variables we refer to the EDA app. (C) Principal coordinates of the polymer type composition. PE: polyethylene, PET: polyethylene terephthalate, PP: polypropylene, PS: polystyrene, PVC: polyvinylchloride, SBS: styrene-butadiene-styrene block-copolymer, Unknown: MP particles indirectly identified by contained pigments without knowledge of the specific polymeric matrix.*

When the MP dataset of the entire system is normalized with respect to the local hydrodynamic sorting conditions, spatio-temporal discontinuities become visible as deviations of the MP distribution pattern from the gradient of the granulometric proxy, demonstrated in Fig. 2 B. While spatial and temporal discontinuities are intimately linked, for comprehensibility we consider them separately below. The Schlei sediments provide favorable conditions to study these effects as both, spatial and temporal continuity as an assumption for granulometric proxy prediction is challenged by the geomorphological and hydrodynamic complexity of this system. Spatio-temporal discontinuities are herein defined as the deviation from the ideal state of a continuous hydrodynamic connectivity of all parts of the system.

Spatial discontinuity: A major discontinuity can be observed by the segregation of proxy-normalized samples into different MP pollution levels in inner and outer Schlei samples (Fig. 2 B). A narrowing, at the village of Missunde, constitutes a major geomorphological barrier, which represents an obstacle for MP to distribute beyond at equal rate.

Temporal discontinuity: The observable singling out of station S08 and S10 as the stations of the highest grain size normalized MP concentrations (Fig. 2 B), indicated the proximity of a significant MP point source with an input rate above the system's distribution efficiency. Indeed, the point source (WWTP) of the reported pollution incident is located there at the inner Schlei basin (Fig. 2 A). Other stations close by (S11, S06 and S07, zoomed-in inset Fig. 2 B) follow this trend. MP concentrations decreasing with distance from this region of highest MP contamination, despite the absence of geomorphological barriers, point towards a temporal discontinuity.

The findings from the granulometric and discontinuity analyses are twofold. Firstly, granulometric properties reveal information on the hydrodynamic influence that also drives parts of the MP distribution processes. Hence, they are important predictive variables for our proxy-based EPM. Secondly, to adequately represent MP concentrations and reach sufficient explanatory power, the proxy-based EPM must be extended by another key class of predictor variables describing locally present spatio-temporal discontinuities in the hydrodynamic distribution efficiency.

The variability in polymer composition also reflects this spatio-temporal segregation (Fig. 2 C). The faster sinking denser polymer types as PET, PS, or PVC are proportionally more abundant near the high MP concentration areas, supporting the identification of the major source region. Less dense polymers as PP or PE can propagate further outwards, where they are more abundantly found. Interestingly, S27, a station nearby a smaller WWTP, is most like the polymer composition found at the major source region, indicating a general WWTP polymer type fingerprint.

NIXVEGS results

The path of integrating granulometric, geographic and hydrodynamic spatio-temporal discontinuity predictors to produce an interpolated MP concentration prediction of the Schlei sediments is schematically shown in Fig. 3 A.

Model validation

The score of an NCV includes the evaluation of the selection process of model configurations, and is therefore an estimate of the performance (on unseen data) of the entire modeling pipeline. NCV ensures the evaluation is done on data that were not used during model training, providing a more realistic estimate of general performance. By contrast, with non-nested CV, there is no independent evaluation of the model selection, which entails the possibility of overfitting the model selection to the available data [64]. NIXVEGS achieved a generalization score of $R^2 = 0.70$ ($\sigma = 0.11$), aggregated as mean of 100 repetitions with 3 folds, aggregated as median (see Fig. 3 B). Aggregating up to 500 repetitions showed no significant difference in performance. Other metrics show the model's overall error in absolute terms (~1000 and ~1700 MP particles kg^{-1} dw for MedAE and MAE, respectively) or as relative numbers (~54%, ~110%). In NIXVEGS' jupyter notebook, an interactive version of Fig. 3 E allows exploring the local error on a per sample basis, while an additional histogram unravels the votes cast by members of the $EPM_{ensemble}$ in relation to the original observed MP concentration for a selected station.

Model selection

NIXVEGS generates a predictive model instance by performing a non-nested grid search CV with the same CV scheme previously used in the inner NCV loop. The resulting best-performing model configuration (here: GLM of family gamma with log link and the predictor set $perc_MUD$, $Disco1$, $Depth$) is then fitted to all available data before making predictions. We refer to this as the single empirical predictive model (EPM_{single}), which aligns with recommendations from the NCV methodology literature for deriving a predictive model instance after obtaining a robust NCV performance estimate.

However, through NIXVEGS we also obtain an empirical predictive model ensemble ($EPM_{ensemble}$) composed of the "best candidate" configurations, refitted to all data, of the various folds and repetitions. Its aggregation resembles the procedure previously used to aggregate the generalization score. There are justifications for each type of predictive models, EPM_{single} and $EPM_{ensemble}$ (details of justifications are provided in the SI). Notably, the EPM_{single} predictor set coincides with the most abundantly selected predictors in the $EPM_{ensemble}$ (Fig. 3 C), indicating a good model stability with respect to the predictor selection process. The predictor variables $perc_MUD$ and $PCo1$ (being similar to each other, $R^2_{PCo1,perc_MUD} = 0.98$) were the most abundantly selected granulometric predictors in the different ensemble members, however, never together in a single member due to the restrictions on mutually exclusive predictors (see SI).

There was a clear preference for discontinuity predictor variables computed from the mean time that tracers travelled until their first appearance in a station's vicinity. The predominant selection of $Disco1$ shows a preference for the longer time period 'allseasons'. A longer period is less sensitive to seasonal variations. The simulated drifter $Disco1$ indicates that a passive tracer (i.e., no advection) is a genuine measure of the distribution efficiency through the system. This is plausible because the depositional component is already covered in the model in form of the granulometric proxy. The importance of the proxy and discontinuity predictors can also be seen when the geographic variables are excluded (NIXVEGS generalization $R^2 = 0.66$, $\sigma = 0.12$).

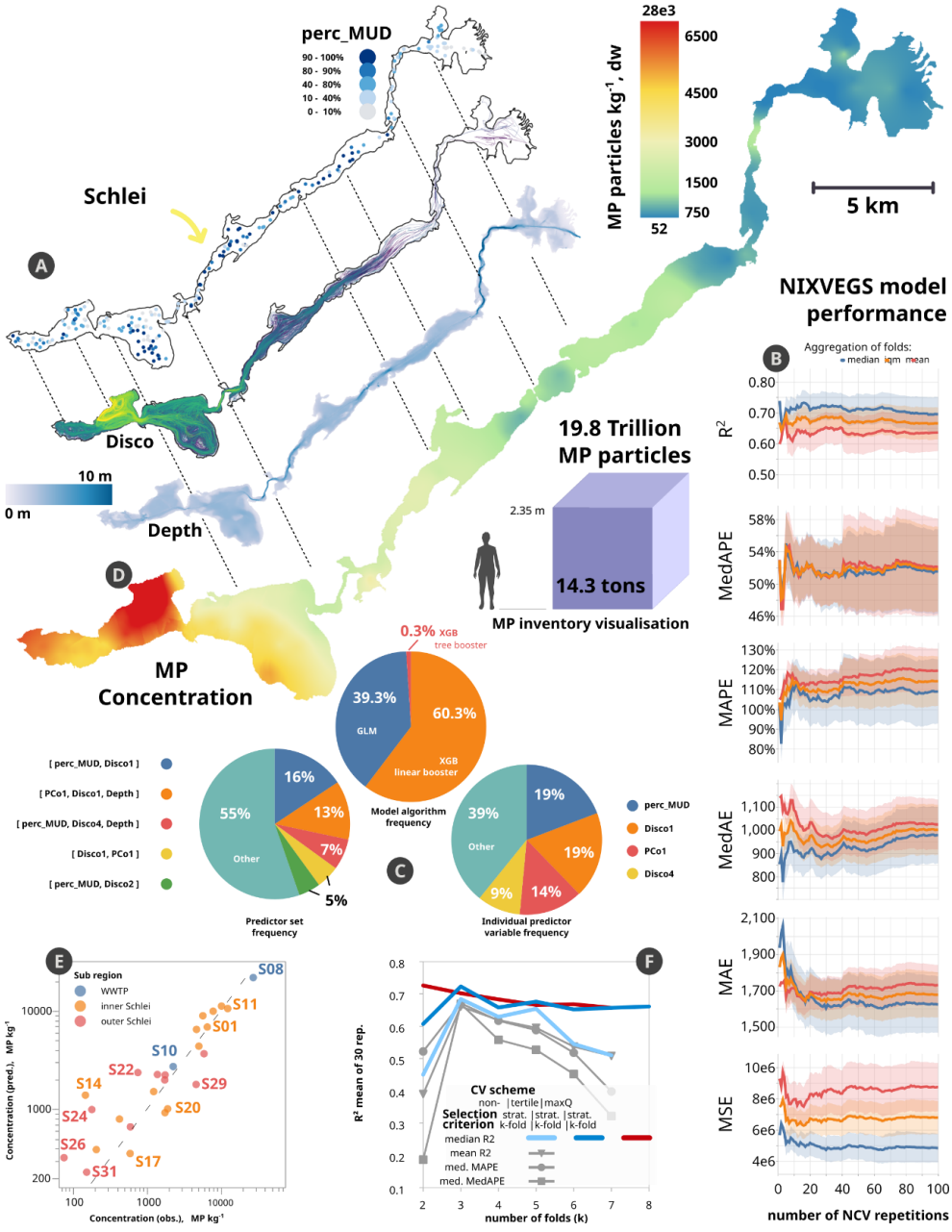


Figure 3. MP inventory estimation of the Schlei surface sediments (0-15cm). *(A) The map was created based on an empirical predictive model ensemble. A NCV modeling pipeline (NIXVEGS) performed model selection including predictor choice from a range of sedimentological, hydrodynamic, and geographical variables. (B) Metrics of model performance: evolution of means of accumulating randomized repeats of the NCV showed*

that a generalization performance of 0.70 (R^2, median of folds) can be expected for unseen data. Other metrics show the error evolution in the unit of the response variable (MAE, MedAE), its square (MSE) or as relative deviation (MAPE, MedAPE). (C) The composition of the ensemble revealed that primarily model classes based on linear regressors were selected in combination with the predictors perc_MUD (sediment fraction < 63 µm) and Disco1, a tracer simulation derived variable accounting for spatio-temporal discontinuities present in the system (C). (D) Geospatial interpolation of the predicted and observed MP concentrations (213 stations) on a 10 m grid by Ordinary Kriging. Highest concentrations can be found in the inner Schlei in the vicinity of a WWTP (at the location of the letter "D"). (E) shows the prediction residuals as deviation from the identity line (dashed). (F) shows the sensitivity analysis as mean of $N_{outer\ repetitions} = 30$ using different cross-validation schemes: 2 to 8 folds combined with strong stratification (maxQ: quantile stratification with $\frac{n}{k}$ quantiles), medium stratification (tertile) and no stratification (the latter also in different variations of the model selection criterion: median R^2, mean R^2, median MAPE and median MedAPE).

In a more streamlined and less complex waterway structure, with a major water input and output, discontinuity could be simplified by determination of the shortest distance through water from the main source. However, for our dataset, replacing predictors related to spatio-temporal discontinuities ($Disco1 - 6$) with a simple direct distance through water from the point of the trace release to each station, would result in a substantially lower R^2 score of 0.44. Indeed, for systems with a more complex hydrodynamic flow field such as the Schlei, major discontinuities occur that are better represented by the water's mean traveling time. The importance of the spatio-temporal discontinuity variables corroborates the conclusions of an earlier study reviewing the relevant literature in search for a MP-sediment relationship [5].

The two linear model algorithms (GLM, XGBlinear) vastly outperformed the tree models (XGBtree, RF) on the present regression problem (Fig. 3 C). In contrast to linear models, models using decision trees as base learners cannot predict outside the range of the response variable seen during training. The likelihood of the response extrema being excluded from the values seen during training of a particular split gets higher with decreasing size of the dataset. Tree-based models are especially strong in approximating highly-non-linear relationships and handling large predictor sets [63,65], neither of which apply here.

Model predictions

Given the size of the investigation area (51.2 km^2), with 213 predicted and observed stations, we reach a high-resolution picture of the inventory of ~4 MP stations per km^2. Interpolated on a regular 10 m grid, MP concentrations indicate accumulations mainly in the vicinity of city of Schleswig, the WWTP, as well as the southern part of the Inner Schlei's larger basin ("Große Breite"). The middle and outer stretches of the Schlei show 2 to 10-fold lower concentrations (Fig. 3 D).

Sensitivity analysis

The choice of the CV parameters, i.e., number of folds k, stratification scheme and model selection criterion, were based on theoretical considerations with respect to the small dataset size (see SI), aided by a sensitivity analysis of NIXVEGS' aggregated performance score towards changes in these CV parameters (Fig. 3 F). Both of the stratified schemes show a higher stability of the score for varying values of k, as compared to the non-stratified CV, signaling that a stratification is preferable to counteract the increased likelihood of drawing highly unrepresentative splits in small datasets. As the performance in stratified CV stays relatively stable for $k \geq 3$, the threefold tertile stratified CV emerges as a preferential choice allowing for robust performance evaluation while keeping computational demands low.

As the uncertainty associated with the model input is unknown (e.g., sampling, purification or measurement method uncertainties), we conducted sensitivity analyses, where we perturbed the target variable by adding 10% on all samples, or changing them ±5% (randomly repeated 5 times), or by excluding the most extreme value. The generalization score exhibited negligible changes, R^2 = 0.7, 0.63 – 0.7 and 0.72, respectively. The inventory estimate varied only around ±1.5% ($EPM_{ensemble}$) when introducing the random variance, showing the robustness of the model.

Estimated Schlei MP inventories

Based on the upper 15 cm sediment layer, the total inventory of the Schlei is thus estimated at 19.8 trillion MP particles, equating to approximately 14.3 tons of MP. These numbers are based on the combined observed and predicted MP concentrations using the $EPM_{ensemble}$ model. For EPM_{single}, the numbers are at 18.8 trillion MP particles and 14.3 tons, respectively. For reference and transparency, if we limit the inventory calculations strictly to the uppermost sediment layer (0–5 cm, from where most of our measured MP samples were taken), estimated MP numbers would be 6.6 and 6.3 trillion particles (~4.8 tons) for $EPM_{ensemble}$ and EPM_{single}, respectively. As we argue in the discussion, however, the 15 cm layer provides a more realistic inventory approximation of the accumulated MP legacy.

To put this unimaginable number of MP into perspective, all MP in the Schlei sediments tightly compressed would form a cube with a side length of 2.35 m (Fig. 3 D). When visualized as easily graspable everyday (macro)plastic objects, it would approximate 1 thin plastic knot bag (typically used for fruits, 9 µm thick, see details in SI) per interpolation cell (10 x 10 m), roughly 5 million bags in total.

Discussion

Evidence-based decision-making in environmental management relies on sufficiently spatially resolved data [66]. We demonstrate that robust EPMs of sedimentary MP distribution can be established using natural particulate and hydrodynamic proxies combined with rigorous validation techniques. Yet, a universal pre-trained model applicable to all sedimentary environments and MP compositions is neither realistic nor necessarily

desirable. Instead, EPMs offer the flexibility to adapt to regional MP levels, compositions, and the complex interactions of external factors (i.e., hydrodynamic forces, agglomeration, and biofouling) making them well-suited for targeted plastic management strategies. The developed modeling pipeline can be fed new data of other sedimentary systems, improving plastic monitoring and management in more regions at a significantly lower analytical expenditure. When planning sampling locations for modeling-ready datasets, it is important to consider both coverage of grain size variability and spatial extent. As a practical consideration, locations for labor-intensive MP-measured stations should prioritize granulometric diversity to improve normalization accuracy. Sediment-only stations, which are used as prediction points and from which more can be analyzed, should prioritize spatial coverage of the system and potential subsystems.

Mitigating systemic misestimations

Comparisons of MP pollution from several regions, as for example extensive meta-analyses [67], are often left with only average MP concentration values to establish pollution levels or inventories. In this study, sampling locations were deliberately chosen to broadly cover the available grain size spectrum. Yet, we see that simply projecting out the mean of our observed MP concentrations to estimate the system's MP inventory may yield results far from what we obtained through NIXVEGS. The average concentration of the 26 samples used to train the model lies at 3967 kg^{-1} dw, approximating an inventory of 31.4 trillion MP particles, which would be an > 50% overestimation compared to NIXVEGS' mean concentration of 2499 kg^{-1} or 19.8 trillion MP. Although the means in the above comparison vary considerably, they could have been very close by chance. However, without the model we would still only have knowledge of the local MP concentration at the few observed stations, whereas with NIXVEGS we could use the available sediment data to infer the spatial distribution of MP concentrations at 213 sites in total. Until MP analyses with significantly higher sample numbers are feasible, proxy models that account for the hydrodynamic regime allow efficient MP inventory estimation and detailed pollution mapping.

Controlling validation overoptimism

Under the acronym NIXVEGS we presented a model selection and validation pipeline whose outputs are twofold: an estimate of model performance on unseen data (generalization score) and a predictive model instance. If the same model selection would be conducted inside a non-nested (i.e., ordinary) CV - be it LOOCV or another scheme - the obtained score is expected to be higher, but includes the risk of the model selection criterion to be overfitted to the available data [64]. As such, NIXVEGS' nested CV score should be regarded as a conservative estimate on how good a model can be built to approximate the response variable, given a set of possible model configurations and the available data.

A non-nested CV is also run as part of NIXVEGS after the NCV score has been determined, but for a different purpose. Its score (being with R^2 = 0.88, as expected, higher than the NCV score) is neglected, knowing about its included bias. The resulting "best candidate" model configuration, however, is what gets utilized as the "EPM_{single}" predictive model instance.

The accompanying EDA app provides the possibility to approximate any of the available variables by a freely configurable GLM. The app's preset at loading shows the same model configuration found as NIXVEGS' "EPM_{single}". The LOOCV of this model can be seen further

down in the EDA app with an R^2 of 0.91, however, underlying the same caveat that such a score is less reliable due to the included bias.

Estuaries are key indicator environments

In a meta-analysis of various studies, we present a cross sedimentary compartment comparison normalized for the hydrodynamic regime which allows a reliable site-representative comparison of MP pollution levels (Fig. 4). We see that NIXVEGS' first principles of using granulometric proxies for spatial MP prediction may also find application in many other sedimentary environments. Yet, spatio-temporal discontinuities and multiple interfering major source inputs may be more difficult to track in the open sea, while beaches are additionally directly influenced by aerodynamic sorting processes and direct littering. Transitional systems [68] such as estuaries and fjords as well as riverine systems store some of the highest numeric MP concentrations, are closer to sources and may show changes faster in contrast to the open marine environment. While freshwater systems can reach exceptionally high pollution levels, it has been shown that they can be substantially diminished after flooding events [26,69], passing the MP load on to transitional systems that are usually more confined. This bottleneck effect positions estuaries as key indicator ecosystems for monitoring MP pollution, emphasizing the need for tools such as NIXVEGS to determine the MP inventory.

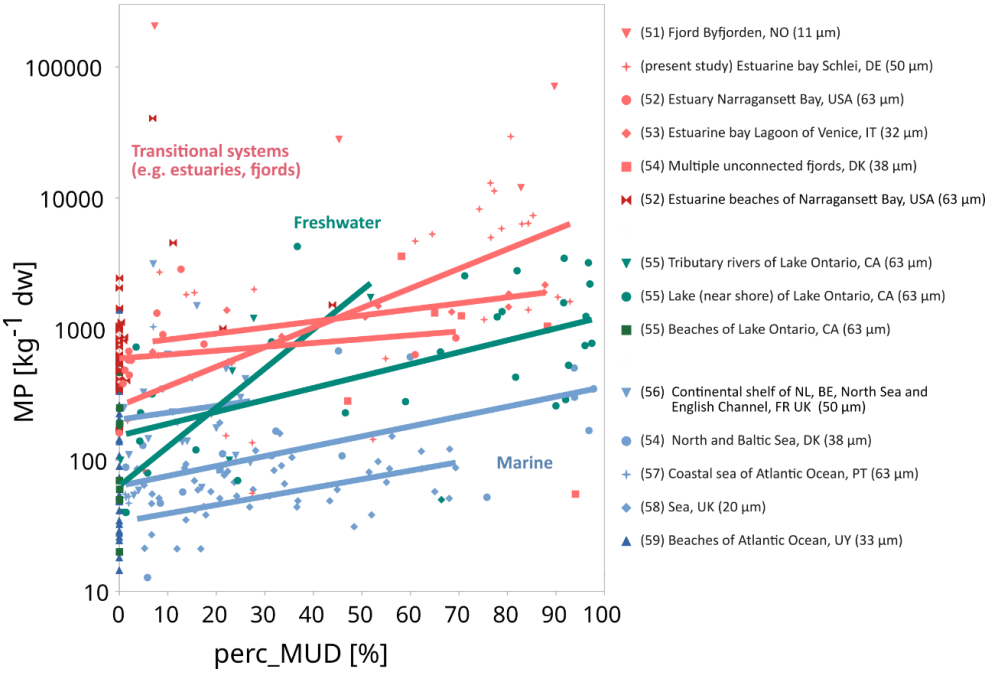


Figure 4. Meta-analysis of granulometric normalized MP concentrations of various representations of worldwide aquatic sediments [9–11,70–75]***.*** *Transitional systems at the fluvial-marine interface (red), freshwater (rivers, lakes, and their beaches, green) and marine systems (open and coastal seas and their beaches, blue) are compared. Beaches of the*

individual compartments are shown in opaque color. To allow comparability only studies with a lower size limit of MP ≤ 63 µm which reported grain size as perc_MUD (most common proxy for grain size) were included in the analysis. For studies with less than 5 stations per connected compartment or negligible variation in perc_MUD no regression line is displayed.

Limitations and uncertainties in inventory estimation and sediment layer depth

As NIXVEGS is an empirical predictive- and not a process-driven model, it estimates the state of an unknown variable based on the available input without a time component. It may be continuously re-run with new input (e.g., when a repeated monitoring campaign would provide new data) obtaining time series of MP distributions, however, it will by itself not allow a projection of the response variable's evolution into the future.

The choice of sediment depth horizon significantly influences MP inventory estimates. Here, we opted to calculate the inventory to a depth of 15 cm, based on sedimentation and granulometric data. The onset of widespread global plastic production around 1950 coincides with observations of increasing MP deposits in the sedimentary record [20]. Known sedimentation rates in the Schlei (2.2 mm a^{-1}, increasing up to 4.2 mm a^{-1} pre-1980 [46]) suggest that this period corresponds roughly to the lower boundary of 10–20 cm.

To evaluate this assumption practically, we collected additional sediment samples from deeper layers (10-15 cm) at selected locations. Interestingly, MP concentrations and sediment grain sizes at these depths closely resembled those from the surface layer (0-5 cm) in sample S02 and S04, indicating vertical sediment mixing. Such mixing in the Schlei sediments foremost results from wind-driven hydrodynamic reworking and anthropogenic disturbances, both of which obscure distinct sedimentary chronologies. The intensity and depth of mixing may vary significantly throughout different locations of the Schlei. Station S10, located near the WWTP outlet showed inverse MP concentrations of 1200 and 11267 MP kg^{-1} dw for the 0-5 cm and 10-15 cm layers, respectively.

An analysis of particle sizes (MP, organic matter, and sediment grains) demonstrated distinct patterns related to sediment type. In fine sediments, MP particle sizes were typically about one order of magnitude larger than the median sediment grain size, aligning with previous findings [5] as we elaborate in the SI (including Fig. S6). However, coarser sediments exhibit similar sizes of MPs and sediment grains, supporting observations of significant vertical mixing processes which trap MP intergranular. Infiltration, however, appears not to play a relevant role (for details see SI, Fig. S6). This granulometric complexity highlights the inherent difficulties in precisely defining an optimal sediment depth for MP inventory assessments.

Thus, while selecting 15 cm as a sedimentary depth horizon provides a pragmatic estimate of the MP legacy in the Schlei, we acknowledge inherent limitations. On the one hand, the limited number of deeper samples (10-15 cm) introduces uncertainties about sediment mixing intensity across the entire Schlei estuary. On the other hand, due to strong local differences in mixing, MP inventories could extend even deeper, implying that our reported

MP inventories may represent conservative estimates. Therefore, the presented inventory estimate based on a 0-15 cm sediment layer constitutes a workable approximation, balancing practical feasibility, empirical evidence, and historical context. Future studies focusing explicitly on deeper sediment sampling and higher vertically resolved profile analyses would help refine sedimentary MP inventories and provide stronger constraints on the vertical distribution of MPs.

Conclusion

Limited data availability remains a key challenge in accurately quantifying sedimentary MP. By using sediment properties as proxy variables, the predictive modeling approach presented here significantly improves the spatial data coverage of MP concentration estimates without requiring extensive direct MP analyses. For future studies, sampling strategies that combine a few MP-measured sites strategically chosen to represent local sedimentological diversity with numerous sediment-only samples targeted to maximize spatial coverage, can significantly reduce systemic uncertainties and enable the quantification of regional MP inventories. This combined methodological approach, presented as a fully open-source pipeline NIXVEGS, facilitates robust MP assessments, supports targeted management strategies, ultimately advancing our understanding of the role sedimentary environments play in the global MP budget.

Acknowledgments

We are grateful to the IOW workshop team for the operation of boat Klaashahn and technical customizations in the laboratory, municipal and port authorities for facilitation of the sampling campaign, Karl Walther (schleiinfozentrum.de) for local Schlei expertise, Svenja Papenmeier, Mischa Schönke, Peter Feldens and Helge Arz for access and knowledge exchange on grain size analysis, Thomas Leipe and Ines Scherff for assistance with Hg, TIC and CSN analysis, Julian Decker and Linnea Dawo for lab assistance, Franziska Klaeger for project coordination, Julia Lötsch, Anne Rödiger and Melinda Arnold for Raman analysis, Elisavet Kanaki, Robert Ohnmacht and Josef Brandt for assistance on the improvements of the GEPARD code, Christiane Hassenrück and Theodor Sperlea for helpful ML knowledge exchange and Sonja Oberbeckmann for project management.

Funding: M.L. and D.F. were supported by the German BMBF research program “Plastics in the environment”: MicroCatch_Balt “Investigation of Sinks and Sources of Microplastics from a Typical Catchment Area to the Open Baltic Sea”, grant number 03F0788A. D.F. and M.L. were supported by the EU-BONUS Programme “Blue Baltic“: MICROPOLL “Multilevel assessment of microplastics and associated pollutants in the Baltic Sea“, grant number 03F0775A

Author contributions: Conceptualization: K.E., R.L., M.L. - Funding: D.F., M.L. - Method development: K.E., R.L. - Data acquisition and analysis: K.E., R.L., F.F., K.S. - Interpretation and modeling (NIXVEGS): R.L., K.E. – Modeling (PARTRACE, UnTRIM): G.S. -Writing: All authors contributed to writing the manuscript.

Competing interests: The authors declare no competing interests.

Data and materials availability:

Supplementary Information file

EDA app (https://robna.github.io/MPSchleiSediments)

Code repository (*https://github.com/robna/MPSchleiSediments/*)

References

(1) van Sebille, E.; Aliani, S.; Law, K. L.; Maximenko, N.; Alsina, J. M.; Bagaev, A.; Bergmann, M.; Chapron, B.; Chubarenko, I.; Cózar, A.; Delandmeter, P.; Egger, M.; Fox-Kemper, B.; Garaba, S. P.; Goddijn-Murphy, L.; Hardesty, B. D.; Hoffman, M. J.; Isobe, A.; Jongedijk, C. E.; Kaandorp, M. L. A.; Khatmullina, L.; Koelmans, A. A.; Kukulka, T.; Laufkötter, C.; Lebreton, L.; Lobelle, D.; Maes, C.; Martinez-Vicente, V.; Morales Maqueda, M. A.; Poulain-Zarcos, M.; Rodríguez, E.; Ryan, P. G.; Shanks, A. L.; Shim, W. J.; Suaria, G.; Thiel, M.; van den Bremer, T. S.; Wichmann, D. The Physical Oceanography of the Transport of Floating Marine Debris. *Environmental Research Letters* **2020**, *15* (2), 023003. https://doi.org/10.1088/1748-9326/ab6d7d.

(2) Bagaev, A.; Mizyuk, A.; Khatmullina, L.; Isachenko, I.; Chubarenko, I. Anthropogenic Fibres in the Baltic Sea Water Column: Field Data, Laboratory and Numerical Testing of Their Motion. *Science of The Total Environment* **2017**, *599–600*, 560–571. https://doi.org/10.1016/j.scitotenv.2017.04.185.

(3) Canals, M.; Pham, C. K.; Bergmann, M.; Gutow, L.; Hanke, G.; van Sebille, E.; Angiolillo, M.; Buhl-Mortensen, L.; Cau, A.; Ioakeimidis, C.; Kammann, U.; Lundsten, L.; Papatheodorou, G.; Purser, A.; Sanchez-Vidal, A.; Schulz, M.; Vinci, M.; Chiba, S.; Galgani, F.; Langenkämper, D.; Möller, T.; Nattkemper, T. W.; Ruiz, M.; Suikkanen, S.; Woodall, L.; Fakiris, E.; Molina Jack, M. E.; Giorgetti, A. The Quest for Seafloor Macrolitter: A Critical Review of Background Knowledge, Current Methods and Future Prospects. *Environmental Research Letters* **2021**. https://doi.org/10.1088/1748-9326/abc6d4.

(4) Koelmans, A. A.; Kooi, M.; Law, K. L.; van Sebille, E. All Is Not Lost: Deriving a Top-down Mass Budget of Plastic at Sea. *Environmental Research Letters* **2017**, *12* (11), 114028. https://doi.org/10.1088/1748-9326/aa9500.

(5) Enders, K.; Käppler, A.; Biniasch, O.; Feldens, P.; Stollberg, N.; Lange, X.; Fischer, D.; Eichhorn, K.-J.; Pollehne, F.; Oberbeckmann, S.; Labrenz, M. Tracing Microplastics in Aquatic Environments Based on Sediment Analogies. *Scientific Reports* **2019**, *9* (1), 15207. https://doi.org/10.1038/s41598-019-50508-2.

(6) Klein, S.; Worch, E.; Knepper, T. P. Occurrence and Spatial Distribution of Microplastics in River Shore Sediments of the Rhine-Main Area in Germany. *Environmental Science & Technology* **2015**, *49* (10), 6070–6076. https://doi.org/10.1021/acs.est.5b00492.

(7) Kersten, M.; Smedes, F. Normalization Procedures for Sediment Contaminants in Spatial and Temporal Trend Monitoring. *Journal of Environmental Monitoring* **2002**, *4* (1), 109–115. https://doi.org/10.1039/b108102k.

(8) Soulsby, R. *Dynamics of Marine Sands : A Manual for Practical Applications*; Telford: London, 1997.

(9) Strand, J.; Lassen, P.; Shashoua, Y.; Andersen, J. H. Microplastic Particles in Sediments from Danish Waters.

(10) Vianello, A.; Boldrin, A.; Guerriero, P.; Moschino, V.; Rella, R.; Sturaro, A.; Da Ros, L. Microplastic Particles in Sediments of Lagoon of Venice, Italy: First Observations on

Occurrence, Spatial Patterns and Identification. *Estuarine, Coastal and Shelf Science* **2013**, *130*, 54–61. https://doi.org/10.1016/j.ecss.2013.03.022.
(11) Ballent, A.; Corcoran, P. L.; Madden, O.; Helm, P. A.; Longstaffe, F. J. Sources and Sinks of Microplastics in Canadian Lake Ontario Nearshore, Tributary and Beach Sediments. *Marine Pollution Bulletin* **2016**, *110* (1), 383–395. https://doi.org/10.1016/j.marpolbul.2016.06.037.
(12) Thompson, R. C.; Olsen, Y.; Mitchell, R. P.; Davis, A.; Rowland, S. J.; John, A. W. G.; McGonigle, D.; Russell, A. E. Lost at Sea: Where Is All the Plastic? *Science* **2004**, *304* (5672), 838–838. https://doi.org/10.1126/science.1094559.
(13) Eriksen, M.; Cowger, W.; Erdle, L. M.; Coffin, S.; Villarrubia-Gómez, P.; Moore, C. J.; Carpenter, E. J.; Day, R. H.; Thiel, M.; Wilcox, C. A Growing Plastic Smog, Now Estimated to Be over 170 Trillion Plastic Particles Afloat in the World's Oceans—Urgent Solutions Required. *PLOS ONE* **2023**, *18* (3), e0281596. https://doi.org/10.1371/journal.pone.0281596.
(14) Law, K. L.; Morét-Ferguson, S.; Maximenko, N. A.; Proskurowski, G.; Peacock, E. E.; Hafner, J.; Reddy, C. M. Plastic Accumulation in the North Atlantic Subtropical Gyre. *Science* **2010**, *329* (5996), 1185–1188. https://doi.org/10.1126/science.1192321.
(15) Beer, S.; Garm, A.; Huwer, B.; Dierking, J.; Nielsen, T. G. No Increase in Marine Microplastic Concentration over the Last Three Decades – A Case Study from the Baltic Sea. *Science of The Total Environment* **2018**, *621*, 1272–1279. https://doi.org/10.1016/j.scitotenv.2017.10.101.
(16) Galgani, F.; Brien, A. S.; Weis, J.; Ioakeimidis, C.; Schuyler, Q.; Makarenko, I.; Griffiths, H.; Bondareff, J.; Vethaak, D.; Deidun, A.; Sobral, P.; Topouzelis, K.; Vlahos, P.; Lana, F.; Hassellov, M.; Gerigny, O.; Arsonina, B.; Ambulkar, A.; Azzaro, M.; Bebianno, M. J. Are Litter, Plastic and Microplastic Quantities Increasing in the Ocean? *Microplastics and Nanoplastics* **2021**, *1* (1), 2. https://doi.org/10.1186/s43591-020-00002-8.
(17) Stubbins, A.; Law, K. L.; Muñoz, S. E.; Bianchi, T. S.; Zhu, L. Plastics in the Earth System. *Science* **2021**, *373* (6550), 51–55. https://doi.org/10.1126/science.abb0354.
(18) Lebreton, L. C. M.; Van Der Zwet, J.; Damsteeg, J.-W.; Slat, B.; Andrady, A.; Reisser, J. River Plastic Emissions to the World's Oceans. *Nat Commun* **2017**, *8* (1), 15611. https://doi.org/10.1038/ncomms15611.
(19) Koelmans, A. A.; Redondo-Hasselerharm, P. E.; Nor, N. H. M.; de Ruijter, V. N.; Mintenig, S. M.; Kooi, M. Risk Assessment of Microplastic Particles. *Nature Reviews Materials* **2022**, *7* (2), 138–152. https://doi.org/10.1038/s41578-021-00411-y.
(20) Brandon, J. A.; Jones, W.; Ohman, M. D. Multidecadal Increase in Plastic Particles in Coastal Ocean Sediments. *Science Advances* **2019**, *5* (9), eaax0587. https://doi.org/10.1126/sciadv.aax0587.
(21) Dong, M.; Luo, Z.; Jiang, Q.; Xing, X.; Zhang, Q.; Sun, Y. The Rapid Increases in Microplastics in Urban Lake Sediments. *Scientific Reports* **2020**, *10* (1), 848. https://doi.org/10.1038/s41598-020-57933-8.
(22) Turner, S.; Horton, A. A.; Rose, N. L.; Hall, C. A Temporal Sediment Record of Microplastics in an Urban Lake, London, UK. *Journal of Paleolimnology* **2019**, *61* (4), 449–462. https://doi.org/10.1007/s10933-019-00071-7.
(23) Khatmullina, L.; Chubarenko, I. Transport of Marine Microplastic Particles: Why Is It so Difficult to Predict? *Anthropocene Coasts* **2019**, *2* (1), 293–305. https://doi.org/10.1139/anc-2018-0024.

(24) Waldschläger, K.; Brückner, M. Z. M.; Carney Almroth, B.; Hackney, C. R.; Adyel, T. M.; Alimi, O. S.; Belontz, S. L.; Cowger, W.; Doyle, D.; Gray, A.; Kane, I.; Kooi, M.; Kramer, M.; Lechthaler, S.; Michie, L.; Nordam, T.; Pohl, F.; Russell, C.; Thit, A.; Umar, W.; Valero, D.; Varrani, A.; Warrier, A. K.; Woodall, L. C.; Wu, N. Learning from Natural Sediments to Tackle Microplastics Challenges: A Multidisciplinary Perspective. *Earth-Science Reviews* **2022**, *228*, 104021. https://doi.org/10.1016/j.earscirev.2022.104021.
(25) Alimi, O. S.; Farner Budarz, J.; Hernandez, L. M.; Tufenkji, N. Microplastics and Nanoplastics in Aquatic Environments: Aggregation, Deposition, and Enhanced Contaminant Transport. *Environmental Science & Technology* **2018**, *52* (4), 1704–1724. https://doi.org/10.1021/acs.est.7b05559.
(26) Hurley, R.; Woodward, J.; Rothwell, J. J. Microplastic Contamination of River Beds Significantly Reduced by Catchment-Wide Flooding. *Nature Geoscience* **2018**, *11* (4), 251–257. https://doi.org/10.1038/s41561-018-0080-1.
(27) Kooi, M.; Primpke, S.; Mintenig, S. M.; Lorenz, C.; Gerdts, G.; Koelmans, A. A. Characterizing the Multidimensionality of Microplastics across Environmental Compartments. *Water Research* **2021**, *202*, 117429. https://doi.org/10.1016/j.watres.2021.117429.
(28) Martin, J. L.; McCutcheon, S. C.; Schottman, R. W. *Hydrodynamics and Transport for Water Quality Modeling*; Lewis Publishers: Boca Raton, 1999.
(29) Besseling, E.; Quik, J. T. K.; Sun, M.; Koelmans, A. A. Fate of Nano- and Microplastic in Freshwater Systems: A Modeling Study. *Environmental Pollution* **2017**, *220*, 540–548. https://doi.org/10.1016/j.envpol.2016.10.001.
(30) Zhang, W. Sediment Dynamics. In *Encyclopedia of Marine Geosciences*; Harff, J., Meschede, M., Petersen, S., Thiede, J., Eds.; Springer Netherlands: Dordrecht, 2014; pp 1–6. https://doi.org/10.1007/978-94-007-6644-0_175-1.
(31) Jambeck, J. R.; Geyer, R.; Wilcox, C.; Siegler, T. R.; Perryman, M.; Andrady, A.; Narayan, R.; Law, K. L. Plastic Waste Inputs from Land into the Ocean. *Science* **2015**, *347* (6223), 768–771. https://doi.org/10.1126/science.1260352.
(32) Mai, L.; Sun, X.-F.; Xia, L.-L.; Bao, L.-J.; Liu, L.-Y.; Zeng, E. Y. Global Riverine Plastic Outflows. *Environ. Sci. Technol.* **2020**, *54* (16), 10049–10056. https://doi.org/10.1021/acs.est.0c02273.
(33) Strokal, M.; Vriend, P.; Bak, M. P.; Kroeze, C.; Van Wijnen, J.; Van Emmerik, T. River Export of Macro- and Microplastics to Seas by Sources Worldwide. *Nature Communications* **2023**, *14* (1), 4842. https://doi.org/10.1038/s41467-023-40501-9.
(34) Shiravani, G.; Oberrecht, D.; Roscher, L.; Kernchen, S.; Halbach, M.; Gerriets, M.; Scholz-Böttcher, B. M.; Gerdts, G.; Badewien, T. H.; Wurpts, A. Numerical Modeling of Microplastic Interaction with Fine Sediment under Estuarine Conditions. *Water Research* **2023**, *231*, 119564. https://doi.org/10.1016/j.watres.2022.119564.
(35) Osinski, R. D.; Enders, K.; Gräwe, U.; Klingbeil, K.; Radtke, H. Model Uncertainties of a Storm and Their Influence on Microplastics and Sediment Transport in the Baltic Sea. *Ocean Science* **2020**, *16* (6), 1491–1507. https://doi.org/10.5194/os-16-1491-2020.
(36) Čerkasova, N.; Enders, K.; Lenz, R.; Oberbeckmann, S.; Brandt, J.; Fischer, D.; Fischer, F.; Labrenz, M.; Schernewski, G. A Public Database for Microplastics in the Environment.
(37) NABU Schleswig-Holstein. *Plastic in the Schlei - Wastewater Treatment Plant Releases 5 Tonnes to the Environment (Original: Plastik in Der Schlei - Klärwerk Entlässt Fünf Tonnen*

Müll in Die Umwelt); 2018. https://schleswig-holstein.nabu.de/news/2018/24614.html.
(38) Bergen, K. J.; Johnson, P. A.; De Hoop, M. V.; Beroza, G. C. Machine Learning for Data-Driven Discovery in Solid Earth Geoscience. *Science* **2019**, *363* (6433), eaau0323. https://doi.org/10.1126/science.aau0323.
(39) Zhen, Y.; Wang, L.; Sun, H.; Liu, C. Prediction of Microplastic Abundance in Surface Water of the Ocean and Influencing Factors Based on Ensemble Learning. *Environmental Pollution* **2023**, *331*, 121834. https://doi.org/10.1016/j.envpol.2023.121834.
(40) Brandt, J.; Mattsson, K.; Hassellöv, M. Deep Learning for Reconstructing Low-Quality FTIR and Raman Spectra-A Case Study in Microplastic Analyses. *Analytical Chemistry* **2021**, *93* (49), 16360–16368. https://doi.org/10.1021/acs.analchem.1c02618.
(41) Ramanna, S.; Morozovskii, D.; Swanson, S.; Bruneau, J. Machine Learning of Polymer Types from the Spectral Signature of Raman Spectroscopy Microplastics Data. *Advances in Artificial Intelligence and Machine Learning* **2023**, *03* (01), 647–668. https://doi.org/10.54364/AAIML.2023.1144.
(42) Phan, S.; Torrejon, D.; Furseth, J.; Mee, E.; Luscombe, C. Exploiting Weak Supervision to Facilitate Segmentation, Classification, and Analysis of Microplastics (<100 Mm) Using Raman Microspectroscopy Images. *Science of The Total Environment* **2023**, *886*, 163786. https://doi.org/10.1016/j.scitotenv.2023.163786.
(43) Hu, B.; Dai, Y.; Zhou, H.; Sun, Y.; Yu, H.; Dai, Y.; Wang, M.; Ergu, D.; Zhou, P. Using Artificial Intelligence to Rapidly Identify Microplastics Pollution and Predict Microplastics Environmental Behaviors. *Journal of Hazardous Materials* **2024**, *474*, 134865. https://doi.org/10.1016/j.jhazmat.2024.134865.
(44) Pedregosa, F.; Varoquaux, G.; Gramfort, A.; Michel, V.; Thirion, B.; Grisel, O.; Blondel, M.; Prettenhofer, P.; Weiss, R.; Dubourg, V.; Vanderplas, J.; Passos, A.; Cournapeau, D. Scikit-Learn: Machine Learning in Python. *MACHINE LEARNING IN PYTHON*.
(45) Chen, T.; Guestrin, C. XGBoost: A Scalable Tree Boosting System. In *Proceedings of the 22nd ACM SIGKDD International Conference on Knowledge Discovery and Data Mining*; ACM: San Francisco California USA, 2016; pp 785–794. https://doi.org/10.1145/2939672.2939785.
(46) Schwarzer, K.; Ricklefs, K.; Höft, D. *Sediment Inventory and Hydromorphology of the Schlei, (Original: Sedimentinventar Und Hydromorphologie Der Schlei)*; Institute of Geosciences, Kiel University, 2019; p 114. https://www.schleswig-holstein.de/DE/fachinhalte/M/meeresschutz/Downloads/Bericht_SedimentinventarHydromorphologieSchlei.pdf.
(47) Enders, K.; Lenz, R.; Ivar do Sul, J. A.; Tagg, A. S.; Labrenz, M. When Every Particle Matters: A QuEChERS Approach to Extract Microplastics from Environmental Samples. *MethodsX* **2020**, *7*, 100784. https://doi.org/10.1016/j.mex.2020.100784.
(48) Brandt, J.; Bittrich, L.; Fischer, F.; Kanaki, E.; Tagg, A.; Lenz, R.; Labrenz, M.; Brandes, E.; Fischer, D.; Eichhorn, K.-J. High-Throughput Analyses of Microplastic Samples Using Fourier Transform Infrared and Raman Spectrometry. *Applied Spectroscopy* **2020**, *74* (9), 1185–1197. https://doi.org/10.1177/0003702820932926.
(49) Käppler, A.; Windrich, F.; Löder, M. G. J.; Malanin, M.; Fischer, D.; Labrenz, M.; Eichhorn, K.-J.; Voit, B. Identification of Microplastics by FTIR and Raman Microscopy: A Novel Silicon Filter Substrate Opens the Important Spectral Range below 1300 Cm-1 for FTIR

Transmission Measurements. *Analytical and Bioanalytical Chemistry* **2015**, *407* (22), 6791–6801. https://doi.org/10.1007/s00216-015-8850-8.
(50) Bittrich, L.; Brandt, J. GEPARD - Gepard-Enabled PARticle Detection for Raman Microscopes. https://gitlab.ipfdd.de/gepard/gepard.
(51) Käppler, A.; Fischer, D.; Oberbeckmann, S.; Schernewski, G.; Labrenz, M.; Eichhorn, K.-J.; Voit, B. Analysis of Environmental Microplastics by Vibrational Microspectroscopy: FTIR, Raman or Both? *Analytical and Bioanalytical Chemistry* **2016**, *408* (29), 8377–8391. https://doi.org/10.1007/s00216-016-9956-3.
(52) Kreyling, O.; Kölbl, A.; Spielvogel, S.; Rennert, T.; Kaiser, K.; Kögel-Knabner, I. Density Fractionation of Organic Matter in Dolomite-Derived Soils. *Journal of Plant Nutrition and Soil Science* **2013**, *176* (4), 509–519. https://doi.org/10.1002/jpln.201200276.
(53) Wakeham, S. G.; Canuel, E. A. The Nature of Organic Carbon in Density-Fractionated Sediments in the Sacramento-San Joaquin River Delta (California). *Biogeosciences* **2016**, *13* (2), 567–582. https://doi.org/10.5194/bg-13-567-2016.
(54) Wilkinson, M. D.; Dumontier, M.; Aalbersberg, Ij. J.; Appleton, G.; Axton, M.; Baak, A.; Blomberg, N.; Boiten, J.-W.; Da Silva Santos, L. B.; Bourne, P. E.; Bouwman, J.; Brookes, A. J.; Clark, T.; Crosas, M.; Dillo, I.; Dumon, O.; Edmunds, S.; Evelo, C. T.; Finkers, R.; Gonzalez-Beltran, A.; Gray, A. J. G.; Groth, P.; Goble, C.; Grethe, J. S.; Heringa, J.; 'T Hoen, P. A. C.; Hooft, R.; Kuhn, T.; Kok, R.; Kok, J.; Lusher, S. J.; Martone, M. E.; Mons, A.; Packer, A. L.; Persson, B.; Rocca-Serra, P.; Roos, M.; Van Schaik, R.; Sansone, S.-A.; Schultes, E.; Sengstag, T.; Slater, T.; Strawn, G.; Swertz, M. A.; Thompson, M.; Van Der Lei, J.; Van Mulligen, E.; Velterop, J.; Waagmeester, A.; Wittenburg, P.; Wolstencroft, K.; Zhao, J.; Mons, B. The FAIR Guiding Principles for Scientific Data Management and Stewardship. *Sci Data* **2016**, *3* (1), 160018. https://doi.org/10.1038/sdata.2016.18.
(55) Blott, S. J.; Pye, K. GRADISTAT: A Grain Size Distribution and Statistics Package for the Analysis of Unconsolidated Sediments. *Earth Surface Processes and Landforms* **2001**, *26* (11), 1237–1248. https://doi.org/10.1002/esp.261.
(56) Bray, J. R.; Curtis, J. T. An Ordination of the Upland Forest Communities of Southern Wisconsin. *Ecological Monographs* **1957**, *27* (4), 325–349. https://doi.org/10.2307/1942268.
(57) Seiß, G. Hydrodynamic Numerical Models Suitable for Application to the German Fairways and Ports at the Baltic Sea Coast. **2014**.
(58) BAWiki. Mathematical Model UNTRIM.
(59) BAWiki. PARTRACE.DAT.
(60) Stone, M. Cross-Validatory Choice and Assessment of Statistical Predictions. *Journal of the Royal Statistical Society: Series B (Methodological)* **1974**, *36* (2), 111–133. https://doi.org/10.1111/j.2517-6161.1974.tb00994.x.
(61) Varma, S.; Simon, R. Bias in Error Estimation When Using Cross-Validation for Model Selection. *BMC Bioinformatics* **2006**, *7* (1), 91. https://doi.org/10.1186/1471-2105-7-91.
(62) Krstajic, D.; Buturovic, L. J.; Leahy, D. E.; Thomas, S. Cross-Validation Pitfalls When Selecting and Assessing Regression and Classification Models. *Journal of Cheminformatics* **2014**, *6* (1), 10. https://doi.org/10.1186/1758-2946-6-10.
(63) Breiman, L. Random Forests. *Machine Learning* **2001**, *45* (1), 5–32. https://doi.org/10.1023/A:1010933404324.

(64) Cawley, G. C.; Talbot, N. L. C. On Over-Fitting in Model Selection and Subsequent Selection Bias in Performance Evaluation. *Journal of Machine Learning Research* **2010**, *11* (70), 2079–2107. https://doi.org/10.5555/1756006.1859921.
(65) Sperlea, T.; Kreuder, N.; Beisser, D.; Hattab, G.; Boenigk, J.; Heider, D. Quantification of the Covariation of Lake Microbiomes and Environmental Variables Using a Machine Learning-Based Framework. *Molecular Ecology* **2021**, *30* (9), 2131–2144. https://doi.org/10.1111/mec.15872.
(66) Li, J. Predicting the Spatial Distribution of Seabed Gravel Content Using Random Forest, Spatial Interpolation Methods and Their Hybrid Methods. In *Piantadosi, J., Anderssen, R.S. and Boland J. (Eds) MODSIM2013, 20th International Congress on Modelling and Simulation*; Modelling and Simulation Society of Australia and New Zealand, 2013. https://doi.org/10.36334/modsim.2013.A9.li.
(67) Harris, P. T. The Fate of Microplastic in Marine Sedimentary Environments: A Review and Synthesis. *Marine Pollution Bulletin* **2020**, *158*, 111398. https://doi.org/10.1016/j.marpolbul.2020.111398.
(68) McLusky, D. S.; Elliott, M. Transitional Waters: A New Approach, Semantics or Just Muddying the Waters? *Estuarine, Coastal and Shelf Science* **2007**, *71* (3–4), 359–363. https://doi.org/10.1016/j.ecss.2006.08.025.
(69) Woodward, J.; Li, J.; Rothwell, J.; Hurley, R. Acute Riverine Microplastic Contamination Due to Avoidable Releases of Untreated Wastewater. *Nature Sustainability* **2021**, *4* (9), 793–802. https://doi.org/10.1038/s41893-021-00718-2.
(70) Haave, M.; Lorenz, C.; Primpke, S.; Gerdts, G. Different Stories Told by Small and Large Microplastics in Sediment - First Report of Microplastic Concentrations in an Urban Recipient in Norway. *Marine Pollution Bulletin* **2019**, *141*, 501–513. https://doi.org/10.1016/j.marpolbul.2019.02.015.
(71) Fulfer, V. M.; Walsh, J. P. Extensive Estuarine Sedimentary Storage of Plastics from City to Sea: Narragansett Bay, Rhode Island, USA. *Sci Rep* **2023**, *13* (1), 10195. https://doi.org/10.1038/s41598-023-36228-8.
(72) Maes, T.; Van Der Meulen, M. D.; Devriese, L. I.; Leslie, H. A.; Huvet, A.; Frère, L.; Robbens, J.; Vethaak, A. D. Microplastics Baseline Surveys at the Water Surface and in Sediments of the North-East Atlantic. *Frontiers in Marine Science* **2017**, *4*, 135. https://doi.org/10.3389/fmars.2017.00135.
(73) Rodrigues, D.; Antunes, J.; Pais, J.; Pequeno, J.; Caetano, P. S.; Rocha, F.; Sobral, P.; Costa, M. H. Distribution Patterns of Microplastics in Subtidal Sediments from the Sado River Estuary and the Arrábida Marine Park, Portugal. *Front. Environ. Sci.* **2022**, *10*, 998513. https://doi.org/10.3389/fenvs.2022.998513.
(74) Bakir, A.; Doran, D.; Silburn, B.; Russell, J.; Archer-Rand, S.; Barry, J.; Maes, T.; Limpenny, C.; Mason, C.; Barber, J.; Nicolaus, E. E. M. A Spatial and Temporal Assessment of Microplastics in Seafloor Sediments: A Case Study for the UK. *Front. Mar. Sci.* **2023**, *9*, 1093815. https://doi.org/10.3389/fmars.2022.1093815.
(75) Vermeiren, P.; Lercari, D.; Muñoz, C. C.; Ikejima, K.; Celentano, E.; Jorge-Romero, G.; Defeo, O. Sediment Grain Size Determines Microplastic Exposure Landscapes for Sandy Beach Macroinfauna. *Environmental Pollution* **2021**, *286*, 117308. https://doi.org/10.1016/j.envpol.2021.117308.

This is the end of the publication

Mapping the plastic legacy: Machine-learning enabled microplastic inventory prediction in aquatic sedimentary systems

by Kristina Enders, Robin Lenz, Franziska Fischer, Klaus Schwarzer, Guntram Seiß, Matthias Labrenz

You might want to continue reading the synopsis at page 26, or jump back to the start of this publication at page 208.

Appendix

Acknowledgements

Diving nose first into microplastics during my master's thesis felt like an exciting, useful and self-directed endeavour. So much, that I stubbornly turned down the offer of a PhD position to work on a different topic, bravely convinced that I could do it my own way. Or in fact, our own way, as Kristina and I had the - for some people perhaps strange or naive - attitude that working closely together as a couple, yet each on their own PhD project, must be a great idea. And in many ways it was. So here we are, not without some mental scars and scratches from the journey, from academic publishing, from ourselves and each other, but I am so grateful that you were there, helping me often enough to get on track and see the bigger picture when getting a bit too excited about some details, and most importantly that we made it through together. Love rocks. May the people think and say what they want, this experience is ours now. And as everything is connected with everything else, looking back on how life has unfolded over the past years, I am happy we have taken this route and can also take the next turn together.

Thanks to an invitation by Dieter and Klaus to present our master's thesis at the ESOPS conference, we met Matthias. Offering one, then two PhD positions got us to the IOW. Matthias, thank you for this atmosphere of trust and freedom you created, for a support which felt like I could choose to work independently when I'd prefer to, but always come to you with any question or problem when needed. And of course for the certainty that no scientific conversation can be had without also learning something about bee keeping, mushroom hunting, raising children or academic life in general.

There are many people at the IOW who have supported me in various ways, and I am grateful for all of them. In particular, I would like to thank Ju and Alex for the great lab, office, field and beach time we had together. Together with Franzi K., who did amazing project coordination and communication work, and with the wider microplastics crew at IOW there was a strong sense of community and collaboration that made the work enjoyable. The technical staff, especially Kristian (to whom, I think, we owe that our sampling device is now called "Rocket") and Sascha have been very helpful on all practical matters, from the design and construction of sampling and laboratory devices, support out in the field, to assistance with electron microscopy. Thanks to Jakob I could have a guest stay at the Risø labs of Aarhus University to work on some of my samples.

A pandemic came and went, Lotta came and changed our lives forever. Thank you for being that little magnet for time and attention, which takes my energy and converts it into love, joy and more often than not, pure wonder. Biology at work. Pretty awesome. Now I am looking forward to you getting even more of my time as this thesis no longer gets any. Speaking of family, I thank my parents for all their support, encouragement, a feeling of being home and being loved the way I am. It has been a great comfort that helped me retaining sanity, no matter how challenging the journey became or for how long one can actually *just finish* a thesis. And, of course, thank you for all the

practical support, helping us with childcare and so many other daily matters. Also to my wider family, thanks for being a great support network.

The second phase it took me before finishing this thesis was at the IPF. Thank you, Dieter, for relentlessly looking for funding for everyone in the group and always trusting in whatever us young researchers wanted to try out. Again, a great team spirit with Franzi F., Julia, Melinda, Anne, Lilly, Elisa and Mareike made the workdays interesting and meaningful. Josef, thank you for your openness to sharing coding ideas and helping out many times on technical matters. Marco and Lars, thank you for helpful discussions on data science and machine learning topics, which I could apply to my work.

Last but not least, I want to thank Karl, who I luckily got to know at our Schlei sampling campaign. Karl, your expertise and helpfulness were invaluable. I am sure there would have been no better guide for us to explore the depths of the Schlei for microplastics. I learnt a lot and collected many impressions from how you are. I am pretty sure now that age is, above all, a deliberate choice. So long, and thanks for all the fish!

Use of Tools

This thesis was written using Quarto, an open-source framework for scientific writing in Markdown. To facilitate the rendering process, I created several scripts to automatically embed PDF files of published papers, generate paper cover pages and include custom figure styles and citations, among other things. Anyone interested can find and reuse all the necessary files to recreate a document using my setup in the accompanying data deposit [44].

The writing of this thesis coincided with the period in which humans began to explore artificial intelligence tools for an increasing number of knowledge work applications. As the implications of this development is still unclear, with the potential to fundamentally change the way we work, large ethical and legal questions remain. With an avid interest in technological developments, I have been following the progress of artificial intelligence tools closely to gain a better understanding of how they transform my scientific work. At its core, I regard the use of such tools as a form of automation. For transparency it would be great to be able to fully record what tools I used in which way. I realise, however, that for certain tasks such a documentation is practically impossible without an administrative overhead that would stall the work as a whole. This is especially the case for small interactive text-transformative work such as translations, rephrasing, or stylistic improvements. In such cases, I can only name the tools I used without detailing the specific inputs and outputs. Other, more conversational interactions, I documented by keeping a full record of the prompts and responses through log files. Because of their length they are not reproduced here, but they are available in the accompanying data deposit [44].

With the following list I attempt to provide a comprehensive overview of software tools that I used directly in the creation of this thesis. If not stated otherwise, the tools were used in their latest available version at the time of writing.

Tools acknowledged for their help in the creation of this thesis:

- System:
  - Operation system:
    - Manjaro Linux with Gnome
  - Editor:
    - Visual Studio Code
    - Github Copilot extension for code completion and suggestions
  - Writing framework:
    - Quarto for writing this thesis as a Quarto book project
    - Document format of the raw writing file: Markdown
    - Enhanced by LaTeX for typesetting
    - Rendered with Pandoc via LuaTeX engine LuaHBTeX for conversion to PDF
  - Coding:
    - Lua for custom code execution in the rendering process, Lua code creation is assisted by the Lua language server extension for Visual Studio Code as a formatter and linter
    - Jupyter notebooks as an interactive code and visualisation development environment
    - Python is used for data analysis and visualisation
    - Vega-Altair, Seaborn and Matplotlib as visualisation libraries
    - Pandas, Scipy and Numpy for data processing and analysis
    - uv for environment management
    - ruff for code formatting and linting
  - Version control: Git for versioning all files in this project
    - Gitkraken / Gitlens for managing the Git repository
    - Nextcloud additional automated backup and cross-device synchronisation of project

files

- Literature management:
  - Library and citation management:
    - Zotero for reference management
    - Better BibTeX for citation key generation
    - Citation Style Language using the style of NIST Technical Publications - Journal of Research of NIST for citation formatting
  - Literature search and retrieval:
    - OpenAlex for literature search and metadata crawling
    - Semantic Scholar, DimensionsAI and Research Rabbit for literature discovery
    - ScienceOS, SciSpace and scite_ for experimental testing of literature data extraction (no logs collected as output was not satisfactory and therefore not used in the thesis)
- Writing assistance:
  - Spelling assistance:
    - British English Code Spell Checker extension in Visual Studio Code spelling correction in code and text files
    - Translation tasks:
      - dict.cc, Linguee and DeepL Translate for German-English translation
    - Style editing:
      - Linguee for idiomatic expressions and phrase researching
      - DeepL Write for stylistic improvements and rephrasing
- Conversational assistance:
  - Text-based conversations with "Large Language Models" were used mostly for coding related tasks, but also as a general conversational sparrings partner to facilitate thinking processes or to seek assistance on topics such as literature and information search, or phrasing advice
  - The following models were used as documented in the logged conversations available in the accompanying data deposit [44]:
    - Claude-Sonnet-3.5, -3.7, -3.7-thinking and -4 by Anthropic for coding assistance, research support and text rephrasing tasks accessed through the interface of Github Copilot Chat
    - Gemini-2.5-pro by Google for coding assistance, research support and text rephrasing tasks accessed through the interface of Github Copilot Chat
    - GPT-4.1, -4o, -o3 and -o4-mini by OpenAI for coding assistance, research support and text rephrasing tasks accessed either through the interface of ChatGPT or Github Copilot Chat
- Additional tools:
  - Spreadsheet editing:
    - LibreOffice
  - Vector graphics editing:
    - Inkscape

Declaration of Authenticity

Ich versichere hiermit an Eides statt, dass ich die vorliegende Arbeit selbstständig angefertigt und ohne fremde Hilfe verfasst habe, keine außer den von mir angegebenen Hilfsmitteln und Quellen dazu verwendet habe und die den benutzten Werken inhaltlich und wörtlich entnommenen Stellen als solche kenntlich gemacht habe.

Rostock, den January 23, 2026.